GE Hitachi Nuclear Energy

26A6642AL
Revision 6
June 2009

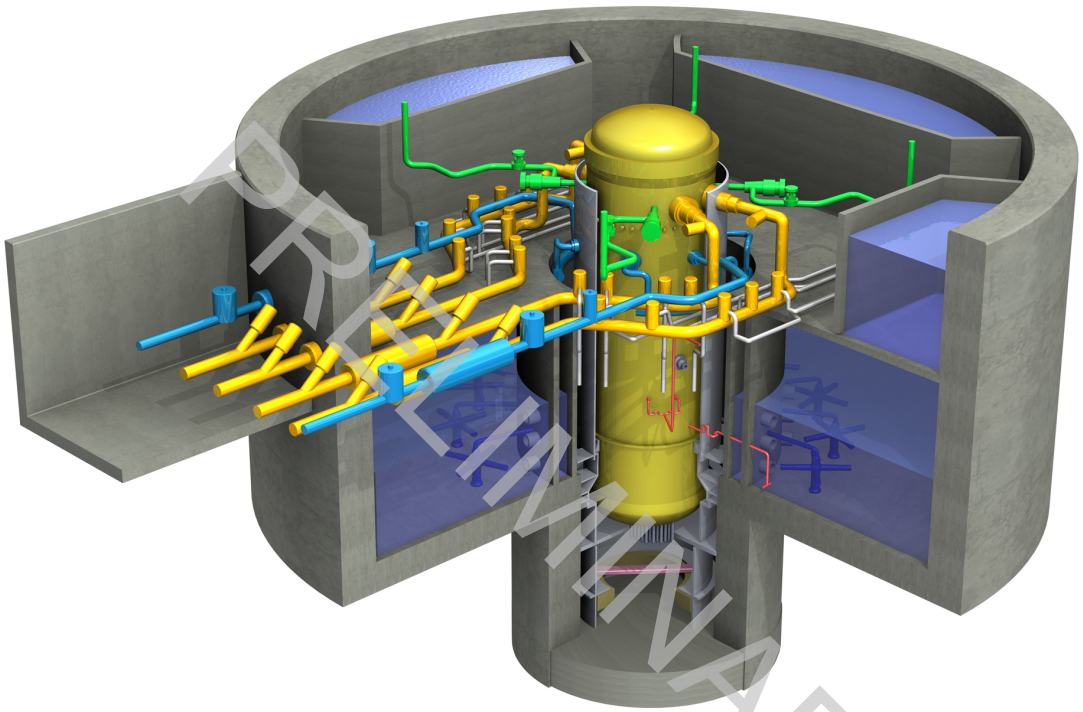

ESBWR Design Control Document
Tier 2

Chapter 3
Design of Structures, Components, Equipment, and Systems
Appendices 3A – 3F

Contents

List of Tables

List of Illustrations

3A. SEISMIC SOIL-STRUCTURE INTERACTION ANALYSIS

3A.1 INTRODUCTION

This appendix presents Soil-Structure Interaction (SSI) analysis performed for two site conditions, generic site and North Anna Early Site Permit (ESP) site-specific, adopted to establish seismic design loads for the Reactor Building (RB), Fuel Building (FB), Control Building (CB) and Firewater Service Complex (FWSC) of the ESBWR Standard Plant under safe shutdown earthquake (SSE) excitation. The RB and FB are integrated and founded on a common basemat. They are termed RB/FB hereafter. The FWSC is composed of two Firewater Storage Tanks (FWS) and a Fire Pump Enclosure (FPE), which are founded on a common basemat. The SSE design ground motion at the foundation level for both site conditions is described in Subsection 3.7.1. The SSI analysis results are presented here in the form of site-enveloped seismic responses at key locations in the RB/FB, CB and FWSC. The structural adequacy calculations for the RB, FB, CB and FWSC are shown in Appendix 3G.

For a standard plant design, the analysis must be performed over a range of site parameters. The site parameters considered and their ranges together form the generic site conditions. The generic site conditions are selected to provide an adequate seismic design margin for the standard plant located at any site with site parameters within the range of parameters considered in this study. In addition, the North Anna ESP site-specific condition is also considered in this study. When actual sites for these facilities are selected, site-specific geotechnical data is developed and submitted to the Nuclear Regulatory Commission (NRC) demonstrating compatibility with the site enveloping parameters considered in the standard design.

This appendix details the basis for selecting the site conditions and analysis cases, and the method of the seismic SSI analysis. Descriptions of the input motion and damping values, the structural model, and the soil model are included. The parametric study SSI results as well as the enveloping seismic responses are also presented.

To demonstrate the seismic adequacy of the standard ESBWR design, 34 RB/FB cases, 14 CB cases and 7 FWSC cases are analyzed for the uniform site cases using the sway-rocking stick model for the SSE condition. In addition, 6 RB/FB cases, 6 CB cases and 5 FWSC cases are analyzed for the layered site cases using the SASSI2000 SSI model. The enveloped results reported in this appendix form the design SSE loads.

3A.2 ESBWR STANDARD PLANT SITE PLAN

The typical site plan of the ESBWR Standard Plant is shown in Figure 1.1-1. The plan orientations are identified by 0°–180° (NS) and 90°–270° (EW) directions. The RB/FB complex, CB and FWSC are rectangular in plan with dimensions and embedment depths shown in Table 3A.2-1.

In modeling the building, the 0°–180° (NS) and 90°–270° (EW) directions are designated as X- and Y-axes, respectively. The Z-axis is in the vertical direction.

Table 3A.2-1

Standard ESBWR Building Dimensions

	RB/FB Complex Dimensions (m)	CB Dimension (m)	FWSC Dimension (m)
0°–180° (NS) width	70.0	30.3	52.0
90°–270° (EW) width	49.0	23.8	20.0
Embedment depth	20	14.9	2.35

3A.3 SITE CONDITIONS

This section describes the generic site conditions and the North Anna ESP site-specific conditions used in the SSI analysis.

3A.3.1 Generic Site Conditions

The design philosophy of the standard plant stipulates that the design should be applicable to as many practical sites as possible, which are suitable for nuclear plant construction. To implement this philosophy, the effects of a wide range of subsurface conditions are considered in the seismic design. To evaluate these effects, a series of seismic SSI analyses in various subsurface conditions are performed. However, performing SSI analysis for combinations of all possible site properties and conditions where a nuclear power plant may be sited would be a formidable task. The purpose of this section is to define a limited number of bounding subsurface conditions selected according to experience gained from previous generic SSI studies. Three subsurface conditions are finally selected to encompass a wide range of applicable site properties and conditions. They are classified as soft, medium and hard sites. The soft site is intended to cover a spectrum of soft soil conditions. The medium site is for medium stiff soil and soft rock conditions, and the hard site for competent rock conditions. For hard sites a fixed-base case is also considered to account for very stiff sites. These sites are considered to be uniform half-space with final enveloping properties provided in Table 3A.3-1 for SSI analysis. These values are considered to be compatible with the strain level expected during SSE. They are used directly in computing soil spring and damper properties.

In addition to these uniform sites, four layered sites are also considered. They are composed of soft, medium and hard soil layers of varying depths as shown in Table 3A.3-3, taking into account variation of shear wave velocity with depth so that the effect of impedance mismatches between layers can be captured.

3A.3.2 North Anna ESP Site Conditions

As described in Subsection 3.7.1, the North Anna ESP site-specific conditions are also considered for the ESBWR design for the RB/FB and CB. North Anna is a rock site. The foundation properties considered in the SSI analysis are presented in Table 3A.3-2.

Table 3A.3-1

Generic Site Properties for SSI Analysis

	Soft	Medium	Hard	Fixed Base
Shear wave velocity (m/s)	300	800	1700	>1700
Mass density (kg/m^3)	2000	2200	2500	Not Applicable
Poisson's ratio	0.478	0.40	0.35	Not Applicable
Material damping (%)	5	4	3	Not Applicable

(1) The shear wave velocity and material damping specified above are used as strain compatible values.

(2) The maximum ground water table is 0.61 m (2 ft) below grade. The effect of ground water on SSI analysis is considered in the selected values for the Poisson's ratio, resulting in the P-wave velocity no less than the minimum P-wave velocity of water (1460 m/sec).

Table 3A.3-2

North Anna Site-specific Properties for SSI Analysis

	RB/FB Complex			Control Building		
	(BE)	(UB)	(LB)	(BE)	(UB)	(LB)
Low strain shear modulus (kg/m^2)	G 6.70E+08	1.5G 1.00E+09	G/1.5 4.47E+08	G 4.97E+08	1.5G 7.46E+08	G/1.5 3.31E+08
Shear wave velocity (m/s)	1589	1946	1297	1369	1677	1118
Mass density (kg/m^3)	2606	2606	2606	2606	2606	2606
Poisson's ratio	0.33	0.33	0.33	0.33	0.33	0.33
Material damping (%)	2	2	2	2	2	2

Note: The rock properties are provided for three conditions, G, 1.5G, & G/1.5, which are considered as best-estimate (BE), upper bound (UB) and lower bound (LB) cases.

Table 3A.3-3

Layered Site Cases

Layer	Shear Wave Velocity (m/s)/Depth (m)			
	CASE 1	CASE 2	CASE 3	CASE 4
Top	300/20	300/20	300/20	300/20
Middle	300/20	800/20	300/40	800/40
Bedrock	1700	1700	1700	1700

(1) The 20 m depth of the middle layer corresponds to the embedded depth of the RB/FB and the 40 m depth corresponds to about one-half the largest plan dimension of the RB/FB foundation.

(2) Properties of the three layers of soils are the same as the generic site properties for soft, medium, and hard soils in Table 3A.3-1.

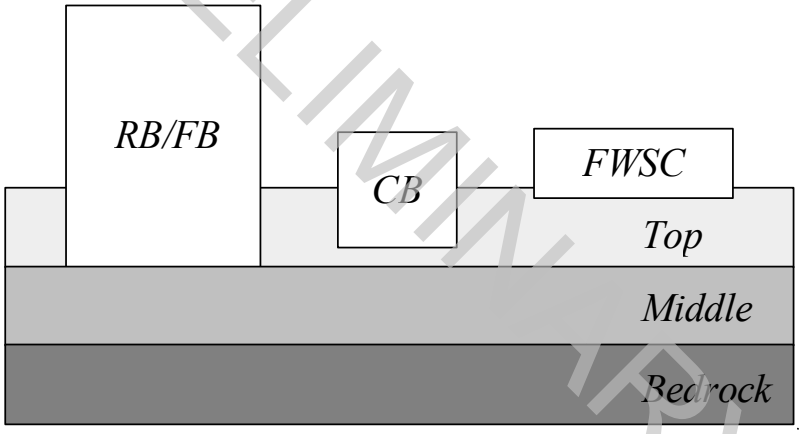

3A.4 INPUT MOTION AND DAMPING VALUES

3A.4.1 Input Motion

The time-history method is used in performing the seismic SSI analysis. Earthquake input motions in the form of synthetic acceleration time histories are generated as described in Subsection 3.7.1 for three orthogonal components designated as H_1, H_2, and V. The H_1 and H_2 are the two horizontal components mutually perpendicular to each other. In the SSI analyses, H_1 and H_2 components are used in the horizontal X-(0°) and Y-(90°) directions, respectively. The V component is used in the vertical Z-direction.

Depending on the soil characteristics at the site and subject to availability of appropriate recorded ground-motion data, the control motion is defined on the soil surface at the top of finished grade or on an outcrop or a hypothetical outcrop at a location on the top of the competent material in accordance with the NRC Standard Review Plan 3.7.1. For the generic sites defined in Subsection 3A.3.1, the design response spectra are conservatively applied at the level of foundation (bottom of the base slab) in the free field. The input motion for North Anna ESP site is also defined at the foundation level (bottom of the base slab).

For the layered site cases, the input ground motion is defined as an outcrop motion at the RB/FB foundation level for the RB/FB and CB. The corresponding surface motion is generated for use as input to the SASSI2000 calculation for each site.

For the FWSC, which is essentially a ground surface founded structure, the input ground motion is taken to be 1.35 times the RB/FB/CB foundation input motion and is applied directly at the foundation level (bottom of the base slab).

Vertically propagating plane seismic shear waves for the horizontal components and compression waves for the vertical component are assumed to generate the input motion.

3A.4.2 Damping Values

The structural components damping values used in the seismic analysis are in accordance with those specified in Regulatory Guide (RG) 1.61. These values for the SSE are summarized in Table 3.7-1.

3A.5 SOIL-STRUCTURE INTERACTION ANALYSIS METHOD

The seismic analysis for uniform sites is performed using the program DAC3N with the sway-rocking SSI model without embedment. The seismic analysis for layered sites is performed using the program SASSI2000 with the finite elements for modeling the SSI with embedment. SASSI2000 analysis is also performed for uniform sites with embedment for the purpose of obtaining more realistic interface loads with the foundation medium for use in the foundation stability evaluation.

3A.5.1 DAC3N Analysis Method

The analysis model is a lumped mass-beam model with soil springs. The structural models are described in Subsection 3.7.2, and in Section 3A.7 in more detail.

To account for SSI effect, sway-rocking base soil springs are attached to the structural model. The base spring is evaluated from vibration admittance theory, based on three-dimensional wave propagation theory for uniform half space soil. For this evaluation, soil material damping values are conservatively neglected. Though the spring values consist of frequency dependent real and imaginary parts, they are simplified and replaced with frequency independent soil spring K_c, and damping coefficient C_c, respectively, for the time history analysis solved in time domain. The method used to obtain the equivalent frequency-independent soil stiffness and damping is illustrated in Figure 3A.5-1. The calculated K_c and C_c values are tabulated in Tables 3A.5-1 through 3A.5-3 for the RB/FB complex, CB and FWSC, respectively.

The effect of lateral soil/backfill on embedded foundations is conservatively accounted for by applying the control motion directly at the foundation level. Dynamic lateral soil pressures are calculated separately and considered in the design of external walls, using the elastic solution procedures in Subsection 3.5.3.2 of ASCE 4-98.

Because the three component ground motion time histories are statistically independent as described in Subsections 3.7.1.1.2 and 3.7.1.1.3, they are input simultaneously in the response analysis using the time history method of analysis solved by direct integration. The numerical integration time step is 0.002 sec. for the RG 1.60 input motion and 0.001 sec. for the North Anna site input motion and the single envelope input motion. Structural responses in terms of accelerations, forces, and moments are computed directly. Floor response spectra (FRS) are obtained from the calculated response acceleration time histories (Subsection 3.7.2.5).

3A.5.2 SASSI2000 Analysis Method

For the seismic analysis of layered and uniform sites, the linear finite element computer program SASSI2000 is used. The program uses finite elements with complex moduli for modeling the structure and foundation properties and is based on the subtraction method and the frequency domain complex response method. The lumped mass-beam model described in Subsection 3A.5.1 is coupled with finite element soil model. The model details are described in Section 3A.7. Structural responses in terms of accelerations, forces and moments are computed directly. FRS are obtained from the calculated response acceleration time histories.

The SSI analyses for the three directional earthquake components are performed separately. The maximum co-directional responses to each of the three earthquake components are combined using algebraic sum in the time domain.

Table 3A.5-1

Soil Spring and Damping Coefficient for RB/FB complex

			Generic Site			North Anna Site		
			Soft 300 m/s	Medium 800 m/s	Hard 1700 m/s	BE 1589 m/s	UB 1946 m/s	LB 1297 m/s
Soil Spring Kc	X-dir	MN/m	2.910E+04	2.178E+05	1.087E+06	9.676E+05	1.451E+06	6.447E+05
	Y-dir	MN/m	3.085E+04	2.281E+05	1.131E+06	1.001E+06	1.501E+06	6.670E+05
	Z-dir	MN/m	4.366E+04	2.972E+05	1.408E+06	1.245E+06	1.868E+06	8.297E+05
	X-X Rot.	MN•m/rad	2.466E+07	1.678E+08	7.950E+08	6.871E+08	1.030E+09	4.578E+08
	Y-Y Rot.	MN•m/rad	4.280E+07	2.913E+08	1.379E+09	1.145E+09	1.717E+09	7.627E+08
	Z-Z Rot.	MN•m/rad	9.804E+15	9.804E+15	9.804E+15	9.804E+15	9.804E+15	9.804E+15
Damping coefficient Cc	X-dir	MN•sec/m	1.708E+03	4.837E+03	1.143E+04	1.083E+04	1.324E+04	8.870E+03
	Y-dir	MN•sec/m	1.910E+03	5.294E+03	1.236E+04	1.159E+04	1.416E+04	9.484E+03
	Z-dir	MN•sec/m	3.852E+03	9.740E+03	2.114E+04	2.011E+04	2.437E+04	1.663E+04
	X-X Rot.	MN•m•sec/rad	2.512E+05	4.378E+05	4.626E+05	4.631E+05	4.235E+05	4.877E+05
	Y-Y Rot.	MN•m•sec/rad	8.432E+05	1.590E+06	1.694E+06	1.567E+06	1.444E+06	1.643E+06
	Z-Z Rot.	MN•m•sec/rad	0.0	0.0	0.0	0.0	0.0	0.0

Table 3A.5-2

Soil Spring and Damping Coefficient for CB

			Generic Site			North Anna Site		
			Soft	Medium	Hard	BE	UB	LB
			300 m/sec	800 m/sec	1700 m/sec	1369 m/sec	1677 m/sec	1188 m/sec
Soil Spring Kc	X-dir	MN/m	1.323E+04	9.879E+04	4.926E+05	3.298E+05	4.949E+05	2.200E+05
	Y-dir	MN/m	1.372E+04	1.017E+05	5.050E+05	3.375E+05	5.065E+05	2.251E+05
	Z-dir	MN/m	1.964E+04	1.336E+05	6.330E+05	4.158E+05	6.239E+05	2.773E+05
	X-X Rot.	MN·m/rad	2.509E+06	1.707E+07	8.088E+07	5.312E+07	7.971E+07	3.543E+07
	Y-Y Rot.	MN·m/rad	3.544E+06	2.412E+07	1.142E+08	7.503E+07	1.126E+08	5.004E+07
	Z-Z Rot.	MN·m/rad	9.804E+15	9.804E+15	9.804E+15	9.804E+15	9.804E+15	9.804E+15
Damping Coefficient Cc	X-dir	MN·sec/m	3.493E+02	9.914E+02	2.344E+03	1.970E+03	2.407E+03	1.614E+03
	Y-dir	MN·sec/m	3.768E+02	1.052E+03	2.464E+03	2.064E+03	2.521E+03	1.691E+03
	Z-dir	MN·sec/m	7.768E+02	1.968E+03	4.275E+03	3.527E+03	4.279E+03	2.907E+03
	X-X Rot.	MN·m·sec/rad	1.217E+04	2.252E+04	2.338E+04	2.578E+04	2.409E+04	2.650E+04
	Y-Y Rot.	MN·m·sec/rad	2.410E+04	4.667E+04	5.111E+04	5.551E+04	5.260E+04	5.620E+04
	Z-Z Rot.	MN·m·sec/rad	0.0	0.0	0.0	0.0	0.0	0.0

Table 3A.5-3

Soil Spring and Damping Coefficient for FWSC

			Generic Site		
			Soft 300 m/sec	Medium 800 m/sec	Hard 1700 m/sec
Soil Spring Kc	X-dir	MN/m	1.591E+04	1.200E+05	6.018E+05
	Y-dir	MN/m	1.829E+04	1.340E+05	6.611E+05
	Z-dir	MN/m	2.481E+04	1.688E+05	7.997E+05
	X-X Rot.	MN·m/rad	2.765E+06	1.881E+07	8.912E+07
	Y-Y Rot.	MN·m/rad	1.102E+07	7.503E+07	3.554E+08
	Z-Z Rot.	MN·m/rad	9.804E+15	9.804E+15	9.804E+15
Damping Coefficient Cc	X-dir	MN·sec/m	5.151E+02	1.494E+03	3.556E+03
	Y-dir	MN·sec/m	6.974E+02	1.919E+03	4.381E+03
	Z-dir	MN·sec/m	1.316E+03	3.362E+03	7.412E+03
	X-X Rot.	MN·m·sec/rad	2.258E+04	5.296E+04	8.130E+04
	Y-Y Rot.	MN·m·sec/rad	2.077E+05	5.217E+05	9.027E+05
	Z-Z Rot.	MN·m·sec/rad	0.0	0.0	0.0

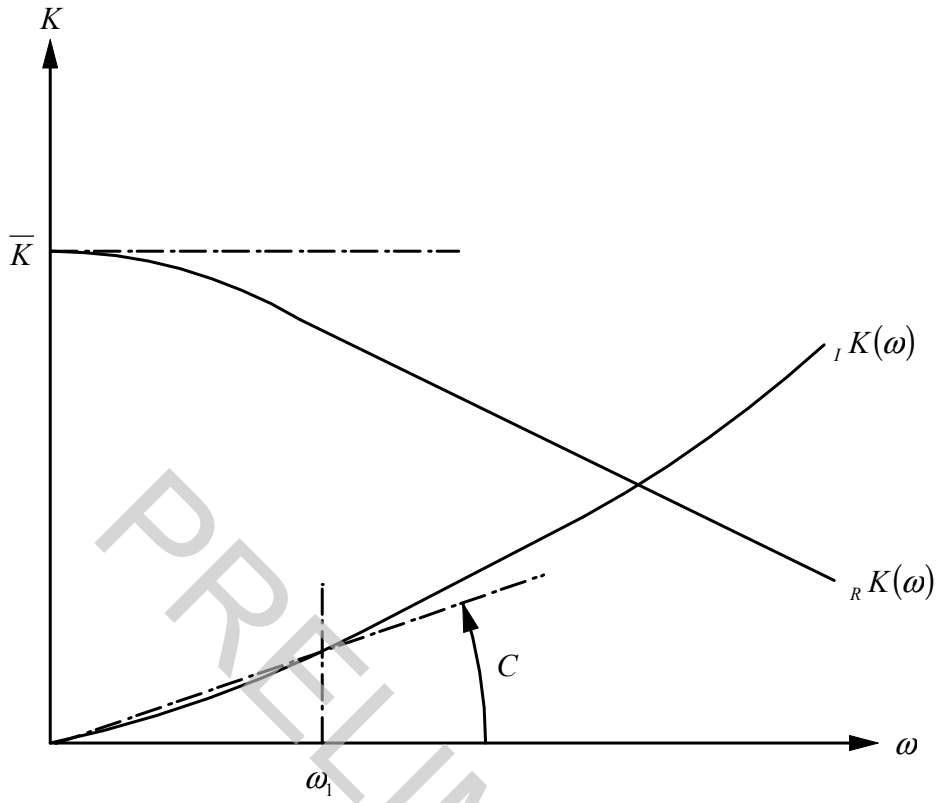

Notes:

(1) The translational and rotational components of the soil springs $(\overline{K_S}, \overline{K_R})$ are represented by the static theoretical solutions of the elastic wave theory with frequency $(\omega = 0)$.

(2) The damping constants (h_{S1}, h_{R1}) of the translational and rotational components of the soil springs corresponding to the fundamental frequency (ω_1) of the soil/building coupled system are calculated as follows:

$$h_{S1} = \frac{{}_I K_S(\omega_1)}{2_R K_S(\omega_1)}, \qquad h_{R1} = \frac{{}_I K_R(\omega_1)}{2_R K_R(\omega_1)}$$

(3) The damping constants (h_S, h_R) of the soil spring is approximated linearly as follows:

$$h_S(\omega) = \frac{h_{S1}}{\omega_1}\omega, \qquad h_R(\omega) = \frac{h_{R1}}{\omega_1}\omega$$

(4) The viscous damping coefficient is derived as follows:

$$C_S = \frac{2h_{S1}}{\omega_1}\overline{K_S} \qquad C_R = \frac{2h_{R1}}{\omega_1}\overline{K_R}$$

Figure 3A.5-1. Method for Frequency-Independent Soil Properties

3A.6 SOIL-STRUCTURE INTERACTION ANALYSIS CASES

To establish design envelopes of seismic responses of the RB/FB complex, SSI analyses are performed for 34 cases of uniform sites and 6 cases of layered sites, as summarized in Table 3A.6-1. Similarly for the CB, SSI analyses are performed for 14 cases of uniform sites and 6 cases of layered sites. SSI analyses for the FWSC are performed for 7 cases of uniform sites and 5 cases of layered sites.

The enveloping results are obtained from the responses of all SSI cases to cover a wide range of conditions.

Table 3A.6-1

Seismic SSI Analysis Cases

Building	No.	Model	Input Motion	Uniform Soil Condition						
				Generic Site				North Anna ESP Site		
				Soft	Medium	Hard	Fixed	NA-BE	NA-UB	NA-LB
RB/FB	RU-1	Base	RG 1.60 (0.3g)	*	*	*	*			
	RU-2	Base	NA site spectra					*	*	*
	RU-3	Base	Single envelope spectra	*	*	*	*			
	RU-4	Updated[1]	Single envelope spectra	*	*	*	*			
	RU-5	50% Infill Concrete Stiffness[2]	Single envelope spectra	*	*	*	*			
	RU-5a	100% Infill Concrete Stifness[3]	Single envelope spectra	*	*	*	*			
	RU-6	LOCA flooding[4]	Single envelope spectra	*	*	*	*			
	RU-7	Wall Out-of-plane[5]	Single envelope spectra	*	*	*	*			
	RU-8	Base[6]	Single envelope spectra	*	*	*				
CB	CU-1	Base	RG 1.60 (0.3g)	*	*	*	*			
	CU-2	Base	NA site spectra					*	*	*
	CU-3	Base	Single envelope spectra	*	*	*	*			
	CU-4	Base[6]	Single envelope spectra	*	*	*				
FWSC	FU-1	Base	Single envelope spectra	*	*	*	*			
	FU-2	Base[6]	Single envelope spectra	*	*	*				

NA North Anna
BE best-estimate
UB upper bound
LB lower bound

Notes:

(1) Updated model for RSW, VW and D/F properties with 0% infill concrete stiffness

(2) Updated model + VW D/F 50% infill concrete stiffness

(3) Updated model + VW D/F 100% infill concrete stiffness

(4) Updated model + LOCA flooding condition

(5) Wall out-of-plane oscillator model

(6) SASSI2000 analysis with embedment for RB/FB and CB and without embedment for surface founded FWSC.

Table 3A.6-1

Seismic SSI Analysis Cases (Continued)

Building	No.	Model	Input Motion	Layered Soil Conditions			
				case1	case2	case3	case4
RBFB	RL-1	Base	Single envelope spectra	*			
	RL-2	Base	Single envelope spectra		*		
	RL-3	Base	Single envelope spectra			*	
	RL-4	Base	Single envelope spectra				*
	RL-5	Cracked (1)	Single envelope spectra	(critical case from RL-1 to RL-4)			
	RL-6	Cracked wall out-of-plane (2)	Single envelope spectra	(critical case from RL-1 to RL-4)			
CB	CL-1	Base	Single envelope spectra	*			
	CL-2	Base	Single envelope spectra		*		
	CL-3	Base	Single envelope spectra			*	
	CL-4	Base	Single envelope spectra				*
	CL-5	Cracked (1)	Single envelope spectra	(critical case from CL-1 to CL-4)			
	CL-6	Structure-structure interaction effect (3)	Single envelope spectra	(critical case from CL-1 to CL-4)			
FWSC	FL-1	Base	Single envelope spectra	*			
	FL-2	Base	Single envelope spectra		*		
	FL-3	Base	Single envelope spectra			*	
	FL-4	Base	Single envelope spectra				*
	FL-5	Structure-structure interaction effect (4)	Single envelope spectra	(critical case from CL-1 to CL-4)			
FWSC	FC-1	Cracked (1)	Single envelope spectra	(critical case from FU-1 and FL-1 to FL-4)			

(1) Concrete stiffness 50% reduced model considering crack effect
(2) Wall out-of-plane oscillator model considering crack effect
(3) Soil response obtained from the RB/FB analysis is used as input motion for the CB model
(4) The input motion for the coupled CB-FWSC interaction analysis is the CSDRS applied at the CB foundation level.

3A.7 ANALYSIS MODELS

The analysis model is a three-dimensional lumped mass-beam model that considers shear, bending, torsion and axial deformations. The structural elements of the RB outside containment and the FB are reduced to one set of stick models. The containment and the containment internal structures including the reactor pressure vessel (RPV) are modelled as separate interconnected sticks. The CB is modelled with a single stick.

3A.7.1 Method of Dynamic Structural Model Development

Evaluation of stiffness for the seismic model is done according to the following assumptions.

- Exterior walls and those inner walls that are continuous up from the basemat and have 500 mm or more in thickness are treated as seismic walls.
- Those openings that have 2.0 m^2 (21.53 ft^2) or larger area are explicitly considered in the stiffness evaluation.

Effective Shear Area (Sx, Sy):

As effective shear area, seismic walls parallel to each of two earthquake directions are considered. When openings exist in a wall, equivalent shear area is calculated so that shear displacements of two walls, with and without openings, are equal.

Moment of Inertia (Iyy, Ixx):

Moment of inertia of seismic walls is calculated according to the following procedures.

- Moment of inertia in each direction is calculated around a horizontal axis that goes through the centroid.
- When openings exist in a wall, equivalent moment of inertia is calculated so that angles of rotation of two walls, with and without openings, are equal.
- The effective flange length is taken to be eight times the flange wall thickness, and it is limited to one-half of the flange wall length.

Torsional Constant (Izz):

Torsional constant of seismic walls is calculated around the vertical axis that goes through the center of rigidity.

Vertical Axial Area (S_a):

Vertical axial area of each element is equal to the summation of effective shear areas that are evaluated in two directions for the horizontal analysis. However, the overlap area at the corner of box walls is subtracted from the summation.

The locations (X_c and Y_c) of centroid of axial area for various sections define the locations of center of rigidity of the equivalent beam stick model in the vertical direction.

Because the stick model has different center-of-rigidity locations in the horizontal and the vertical directions, the lumped mass-beam model comprises two stick models. One stick consists of elements with axial areas located at the centers of rigidity for axial area, and another stick consists of elements with all other remaining sectional properties (i.e., excluding axial area)

located at the centers of rigidity for shear and torsional deformations. Both sticks are connected at common centers of mass at various floor elevations.

As described above, the RB/FB complex is represented by several stick models. These stick models are interconnected by horizontal links representing the floor diaphragm at respective elevations. These links are modeled as rigid springs for floor in-plane translational displacement and having no stiffness for all other deformations.

The vertical floor frequencies are obtained at major floor locations by independent modal analysis of the respective floor finite element model. These frequencies are included in the stick model by a series of vertical single degree-of-freedom oscillators at the corresponding floor elevations.

The out-of-plane vibrations frequencies of walls are evaluated by using finite element model in the same manner as the slab frequencies. These frequencies are included in the stick model by a series of horizontal single degree-of-freedom oscillators at the corresponding wall elevations to obtain design loads of these walls and design FRS for the components attached to these walls.

To obtain the mass properties for the stick model, the dead load, 25% of the live load, 100% of the roof snow load and an additional 2394 Pa (50 psf) load for piping and cable trays, etc. are used to compute the lumped mass properties following the steps described below.

(1) Depending on whether the floor has a regular or an irregular layout, hand calculations or floor finite element models are used to obtain the total mass (M_x, M_y, M_z), the mass moments of inertia (M_{xx}, M_{yy}, M_{zz}) and the center of mass of each floor. Similar calculations are performed for the tributary areas of the walls above and below the floors.

(2) These properties are subsequently reduced to one center of mass with its associated properties at each floor elevation. The water masses in the pools are also included in this calculation.

(3) The bending mass moment of inertia at various floor elevations are also added to each floor mass.

Based on the methodology described above, the lumped mass-beam stick model for SSI is developed as described in Subsection 3A.7.2.

3A.7.2 Lumped Mass-Beam Stick Model for SSI Analysis

The lumped mass-beam stick models for the RB/FB complex in the XZ- and YZ-planes are shown in Figures 3A.7-1. Similarly, the stick models corresponding to the Reinforced Concrete Containment Vessel (RCCV) and pedestal wall are shown in Figures 3A.7-2 and 3A.7-3. The overall integrated building model is shown in Figure 3A.7-4. As shown in the figure, the building model is also coupled to the vent wall (VW), the reactor shield wall (RSW) and the RPV. They are symmetric in both horizontal directions.

The stick models are interconnected at floor elevations by horizontal links. These links are rigid for floor in-plane displacements and have no stiffness for out-of-plane displacement and rotations.

The lumped mass-beam stick models for the CB in the XZ- and YZ-planes are shown in Figures 3A.7-5. The overall CB seismic model is shown in Figure 3A.7-6.

The overall seismic model for the FWSC is shown in Figure 3A.7-7.

To account for SSI effect, sway-rocking base soil springs are attached to this structural model, as described in Section 3A.5. Natural frequencies of the seismic model at all site conditions are shown in Tables 3A.7-1 through 3A.7-7 for the RB/FB model, Tables 3A.7-8 through 3A.7-14 for the CB model, and Tables 3A.7-15 through 3A.7-18 for the FWSC model.

3A.7.3 SSI Model for SASSI2000 Analysis

In the SASSI2000 SSI model, the exterior walls below grade and the foundation basemat along with the supporting soil medium are modeled. For this reason, the sectional properties of the stick model below grade are modified to subtract the stiffness properties corresponding to subgrade outer walls. In this model, the basemat and the exterior walls are modeled by plate elements.

For the RB/FB complex, the basemat plate elements are shown in Figure 3A.7-8. The thickness of basemat is 4.0 m (13.12 ft). The side wall plate elements are shown in Figures 3A.7-9. The thickness of the modeled side wall is 2.0 m (6.56 ft) between EL –11.5 m to 4.5 m and set as a quarter of basemat width between EL –11.5 m to –15.5m.

The RB/FB stick model is connected to the basemat and side walls at floor EL –11.5 m, 6.4 m, -1.0 m and 4.5 m by a set of rigid links. At the base of the model at EL –11.5 m, a rigid link is used to connect all the stick models to the middle of the basemat. The overall RB/FB SASSI2000 model is shown in Figure 3A.7-10.

For the CB, the basemat plate elements are shown in Figure 3A.7-11. The thickness of basemat is 3.0 m (9.84 ft). The side wall plate elements are shown in Figure 3A.7-12. The thickness of the modeled side wall is 0.9 m (2.95 ft) between EL –7.4 m to 4.5 m and set as a quarter of basemat width between EL –7.4 m to –10.4 m.

The CB stick model is connected to the basemat and side walls at floor EL –10.4 m, 6.4 m, -2.0 m and 4.5 m by a set of rigid links. At the base of the model at EL -7.4 m, a rigid link is used to connect all the stick models to the middle of the basemat. The overall CB SASSI2000 model is shown in Figure 3A.7-13.

For the FWSC, the basemat plate elements are shown in Figure 3A.7-14. The thickness of basemat is 2.5 m (8.20 ft).

The FWS stick models and the FPE stick model are connected to the basemat. Rigid links are located along the footprint of walls of the FWS and the FPE. The overall FWSC SASSI2000 model is shown in Figure 3A.7-15.

Table 3A.7-1

Eigenvalue Analysis Results for RB/FB model at Soft Site

Mode No.	Frequency (Hz)	Period (sec)	Participation Factor					
			X dir.	Y dir.	Z dir.	X rot	Y rot	Z rot
1	1.19	0.84	-0.02	1.56	-0.01	-1032	-19	-38
2	1.43	0.70	1.43	0.02	0.10	-8	738	3
3	2.09	0.48	-0.21	0.02	2.34	3	204	0
4	2.78	0.36	-0.20	-0.10	-1.40	-193	604	0
5	2.90	0.34	0.00	0.63	-0.01	1321	16	16
6	3.20	0.31	-0.45	0.00	-0.10	-7	1887	7
7	3.81	0.26	0.00	-0.18	0.00	243	21	-256
8	3.81	0.26	-0.14	-0.01	0.02	10	-498	-8
9	5.23	0.19	0.11	0.00	-0.05	16	-1055	-74
10	5.26	0.19	-0.06	0.01	-0.23	15	615	90
11	5.94	0.17	0.00	-0.05	0.00	1359	189	-13034
12	5.99	0.17	-0.11	0.01	-0.01	31	700	-72
13	5.99	0.17	-0.01	-0.08	0.00	-1899	-164	12881
14	6.76	0.15	-0.05	0.00	-0.13	41	411	-158
15	8.73	0.11	0.00	-0.11	0.01	-564	-64	298
16	9.77	0.10	0.02	0.00	-0.05	-227	7713	139
17	10.11	0.10	-0.19	0.00	0.07	528	-5566	-48
18	10.27	0.10	-0.03	0.02	0.01	-5566	-1230	-2631
19	10.57	0.09	0.00	0.00	-0.02	151	-4336	17
20	10.86	0.09	-0.10	0.00	-0.01	-63	27	-130

Notes: (1) The participation factors are calculated for mode vectors normalized by the maximum mode displacement.

(2) Modal information shown is not used in the response analysis performed by the direct integration method.

Table 3A.7-2

Eigenvalue Analysis Results for RB/FB model at Medium Site

Mode No.	Frequency (Hz)	Period (sec)	Participation Factor					
			X dir.	Y dir.	Z dir.	X rot	Y rot	Z rot
1	2.58	0.39	-0.02	1.68	0.01	-1170	-13	-251
2	2.73	0.37	0.99	-0.11	1.49	58	875	34
3	2.95	0.34	1.95	0.02	0.08	-15	1336	29
4	3.81	0.26	0.00	-0.29	-0.04	1023	-2	-46
5	3.81	0.26	-0.86	0.00	-0.20	0	-1337	-34
6	4.93	0.20	-0.56	-0.17	5.93	-201	700	98
7	5.22	0.19	-0.90	0.00	0.04	4	1374	-76
8	5.47	0.18	1.07	0.19	-5.09	270	-1835	-101
9	5.96	0.17	-0.13	4.00	0.64	9794	788	-26998
10	5.98	0.17	1.54	-0.15	1.17	212	-3545	-3213
11	6.00	0.17	-0.09	0.87	-0.08	-2801	-388	29807
12	6.22	0.16	0.25	-4.53	-0.36	-6638	-489	-2842
13	6.58	0.15	4.40	0.23	1.53	360	-10263	52
14	6.79	0.15	-4.00	-0.15	-2.77	-213	9480	-140
15	9.79	0.10	0.00	-0.74	0.04	-690	-25	696
16	10.30	0.10	-0.91	0.01	-0.25	20	6097	103
17	10.30	0.10	0.04	-0.37	-0.08	-4311	336	-1353
18	10.53	0.09	1.39	-0.05	-0.80	-128	5121	311
19	10.92	0.09	-1.16	-0.01	0.36	222	-7359	-216
20	11.21	0.09	0.12	0.01	0.18	317	-4118	29

Notes: (1) The participation factors are calculated for mode vectors normalized by the maximum mode displacement.

(2) Modal information shown is not used in the response analysis performed by the direct integration method.

Table 3A.7-3

Eigenvalue Analysis Results for RB/FB model at Hard Site

Mode No.	Frequency (Hz)	Period (sec)	Participation Factor					
			X dir.	Y dir.	Z dir.	X rot	Y rot	Z rot
1	2.74	0.37	0.12	0.03	1.16	-38	197	-3
2	3.52	0.28	-0.11	3.75	0.07	-2594	-77	-1458
3	3.81	0.26	8.25	0.23	0.38	-142	4886	231
4	3.81	0.26	0.07	-2.65	-0.08	2560	70	1185
5	3.95	0.25	-7.16	-0.20	-0.39	137	-4812	-242
6	5.20	0.19	0.07	-0.11	1.87	-72	-19	238
7	5.22	0.19	-0.68	0.00	-0.14	15	297	-128
8	5.98	0.17	0.09	0.62	-0.16	2664	131	-12494
9	5.99	0.17	0.56	-0.03	-0.16	9	-1021	-301
10	6.05	0.17	-0.08	0.29	0.09	-1693	-166	12891
11	6.75	0.15	0.17	-0.26	2.37	-211	-228	-659
12	7.64	0.13	0.12	1.25	-0.48	1676	-276	911
13	8.09	0.12	1.38	-0.33	-2.16	-463	-3023	-214
14	9.09	0.11	1.11	0.14	2.86	169	-1897	-72
15	10.31	0.10	0.00	0.52	-0.29	-2402	-258	-1429
16	10.45	0.10	-1.14	-0.02	-2.10	-83	5436	165
17	10.71	0.09	0.72	0.03	-2.27	80	-1818	1
18	11.22	0.09	0.00	-0.68	0.07	310	57	832
19	11.26	0.09	0.25	-0.01	0.31	6	-1539	-36
20	11.64	0.09	0.00	-2.94	0.07	-2245	24	2090

Notes:

(1) The participation factors are calculated for mode vectors normalized by the maximum mode displacement.

(2) Modal information shown is not used in the response analysis performed by the direct integration method.

Table 3A.7-4

Eigenvalue Analysis Results for RB/FB model in Fixed-base Case

Mode No.	Frequency (Hz)	Period (sec)	Participation Factor					
			X dir.	Y dir.	Z dir.	X rot	Y rot	Z rot
1	2.74	0.37	0.07	0.02	1.10	-31	144	-2
2	3.81	0.26	-0.31	6.84	0.15	-3936	-179	-3818
3	3.81	0.26	2.33	0.11	0.06	-45	856	33
4	3.95	0.25	0.25	-5.78	-0.16	3912	172	3528
5	4.40	0.23	1.66	0.07	0.08	-48	1038	70
6	5.21	0.19	0.11	-0.12	1.59	-53	-2	317
7	5.22	0.19	-0.80	0.00	-0.23	24	92	-174
8	5.98	0.17	0.07	0.50	-0.10	1922	100	-8354
9	5.99	0.17	0.45	-0.03	-0.09	11	-794	-212
10	6.09	0.16	-0.06	0.26	0.06	-1204	-118	8782
11	6.75	0.15	0.24	-0.15	1.41	-62	-306	-604
12	8.03	0.12	0.04	1.35	-0.23	1930	-130	1287
13	8.74	0.11	1.55	-0.11	-1.11	-145	-3709	-165
14	10.25	0.10	0.66	0.23	3.65	-582	1260	-368
15	10.32	0.10	-0.12	0.35	-1.18	-1876	-1037	-1037
16	10.65	0.09	1.36	0.06	2.08	7	-4236	-190
17	11.17	0.09	-0.47	-0.09	-2.93	258	-130	206
18	11.23	0.09	0.05	-0.25	0.44	347	234	459
19	11.33	0.09	-0.79	-0.04	-3.61	262	1472	199
20	12.03	0.08	-0.33	-0.06	-1.35	-81	374	22

Notes:

(1) The participation factors are calculated for mode vectors normalized by the maximum mode displacement.

(2) Modal information shown is not used in the response analysis performed by the direct integration method.

Table 3A.7-5

Eigenvalue Analysis Results for RB/FB model at Best-estimate North Anna Site

Mode No.	Frequency (Hz)	Period (sec)	Participation Factor					
			X dir.	Y dir.	Z dir.	X rot	Y rot	Z rot
1	2.74	0.37	0.13	0.03	1.17	-39	209	-3
2	3.46	0.29	-0.09	3.26	0.06	-2271	-65	-1201
3	3.81	0.26	14.37	0.38	0.73	-251	9204	418
4	3.81	0.26	0.05	-2.17	-0.07	2237	57	929
5	3.89	0.26	-13.28	-0.35	-0.75	245	-9127	-429
6	5.20	0.19	0.07	-0.11	1.92	-74	-19	230
7	5.22	0.19	-0.68	0.00	-0.13	15	320	-124
8	5.98	0.17	0.10	0.64	-0.17	2802	139	-13290
9	5.99	0.17	0.58	-0.03	-0.17	8	-1063	-306
10	6.05	0.17	-0.08	0.30	0.10	-1789	-176	13684
11	6.75	0.15	0.14	-0.29	2.60	-247	-184	-681
12	7.58	0.13	0.14	1.21	-0.56	1613	-325	854
13	7.98	0.13	-0.95	0.30	1.68	421	2075	182
14	8.93	0.11	1.15	0.14	2.54	179	-2064	-62
15	10.30	0.10	0.01	0.54	-0.26	-2431	-240	-1466
16	10.44	0.10	-1.08	-0.01	-1.86	-83	5493	158
17	10.70	0.09	0.83	0.05	-1.99	80	-1898	-11
18	11.21	0.09	0.00	-0.84	0.07	213	54	943
19	11.25	0.09	0.25	-0.01	0.28	8	-1586	-34
20	11.55	0.09	0.00	-3.07	0.07	-2371	17	2099

Notes:

(1) The participation factors are calculated for mode vectors normalized by the maximum mode displacement.

(2) Modal information shown is not used in the response analysis performed by the direct integration method.

Table 3A.7-6

Eigenvalue Analysis Results for RB/FB model at Upper-bound North Anna Site

Mode No.	Frequency (Hz)	Period (sec)	Participation Factor					
			X dir.	Y dir.	Z dir.	X rot	Y rot	Z rot
1	2.74	0.37	0.11	0.03	1.14	-36	185	-2
2	3.61	0.28	-0.16	5.07	0.10	-3503	-115	-2164
3	3.81	0.26	5.29	0.17	0.22	-94	2902	137
4	3.81	0.26	0.11	-3.98	-0.11	3469	107	1888
5	4.04	0.25	-4.21	-0.13	-0.23	89	-2826	-149
6	5.20	0.19	0.08	-0.11	1.78	-67	-17	250
7	5.22	0.19	-0.70	0.00	-0.16	17	250	-136
8	5.98	0.17	0.08	0.58	-0.14	2470	126	-11440
9	5.99	0.17	0.53	-0.03	-0.14	9	-960	-269
10	6.06	0.16	-0.07	0.28	0.08	-1569	-155	11838
11	6.75	0.15	0.20	-0.22	2.02	-158	-278	-627
12	7.74	0.13	0.09	1.30	-0.38	1758	-218	1006
13	8.29	0.12	1.12	-0.18	-1.39	-243	-2491	-136
14	9.45	0.11	1.11	0.15	3.65	131	-1591	-103
15	10.31	0.10	-0.01	0.49	-0.35	-2352	-329	-1365
16	10.48	0.10	-1.31	-0.03	-2.76	-87	5455	185
17	10.73	0.09	0.43	0.00	-3.12	92	-1514	39
18	11.22	0.09	0.00	-0.49	0.08	400	68	697
19	11.26	0.09	0.25	-0.01	0.41	0	-1515	-40
20	11.81	0.08	0.01	-2.69	0.08	-2093	38	2071

Notes :

(1) The participation factors are calculated for mode vectors normalized by the maximum mode displacement.

(2) Modal information shown is not used in the response analysis performed by the direct integration method.

Table 3A.7-7

Eigenvalue Analysis Results for RB/FB model at Lower-bound North Anna Site

Mode No.	Frequency (Hz)	Period (sec)	Participation Factor					
			X dir.	Y dir.	Z dir.	X rot	Y rot	Z rot
1	2.73	0.37	0.17	0.04	1.21	-47	252	-4
2	3.27	0.31	-0.05	2.35	0.03	-1651	-40	-713
3	3.68	0.27	9.03	0.20	0.52	-137	6322	252
4	3.81	0.26	0.02	-1.25	-0.05	1620	31	446
5	3.81	0.26	-7.93	-0.17	-0.54	130	-6249	-261
6	5.19	0.19	0.04	-0.11	2.21	-88	-11	209
7	5.22	0.19	-0.67	0.00	-0.09	12	426	-112
8	5.98	0.17	0.12	0.74	-0.25	3372	150	-16376
9	5.99	0.17	0.67	-0.04	-0.27	0	-1254	-335
10	6.04	0.17	-0.09	0.32	0.13	-2155	-208	16783
11	6.74	0.15	-0.18	-0.56	4.60	-568	378	-919
12	7.29	0.14	0.52	1.18	-1.87	1547	-1089	785
13	7.50	0.13	-0.40	0.61	1.02	831	831	337
14	8.36	0.12	1.22	0.11	1.47	164	-2418	-39
15	10.30	0.10	0.02	0.66	-0.20	-2465	-150	-1630
16	10.41	0.10	-0.95	0.01	-1.17	-65	5645	142
17	10.67	0.09	1.11	0.12	-1.38	114	-1642	-42
18	11.10	0.09	0.00	-1.80	0.05	-1072	6	1282
19	11.25	0.09	0.27	-0.02	0.19	0	-1694	-26
20	11.27	0.09	0.00	-1.84	0.01	-2250	-10	804

Notes:

(1) The participation factors are calculated for mode vectors normalized by the maximum mode displacement.

(2) Modal information shown is not used in the response analysis performed by the direct integration method.

Table 3A.7-8

Eigenvalue Analysis Results for CB Model at Soft Site

Mode No.	Frequency (Hz)	Period (sec)	Participation Factor					
			X dir.	Y dir.	Z dir.	X rot	Y rot	Z rot
1	2.84	0.35	0.02	1.31	0.00	-333	6	-1
2	3.04	0.33	1.27	-0.02	0.00	4	405	1
3	4.90	0.20	0.00	0.00	1.12	-1	-1	0
4	6.81	0.15	0.52	0.03	0.00	28	-751	0
5	6.96	0.14	-0.03	0.61	0.00	574	45	0
6	14.83	0.07	0.00	0.00	0.00	0	0	24
7	16.54	0.06	0.00	0.00	-0.12	1	0	0
8	18.51	0.05	0.00	0.00	-0.12	4	-2	0
9	21.96	0.05	-0.02	-0.01	0.00	243	-457	-8
10	22.55	0.04	0.01	-0.01	0.00	396	267	20

Notes:

(1) The participation factors are calculated for mode vectors normalized by the maximum mode displacement.

(2) Modal information shown is not used in the response analysis performed by the direct integration method.

Table 3A.7-9

Eigenvalue Analysis Results for CB Model at Medium Site

Mode No.	Frequency (Hz)	Period (sec)	Participation Factor					
			X dir.	Y dir.	Z dir.	X rot	Y rot	Z rot
1	6.00	0.17	0.08	1.36	0.01	-323	27	-6
2	6.44	0.16	1.33	-0.08	0.00	17	409	9
3	11.32	0.09	-0.01	-0.02	1.99	-8	6	0
4	14.83	0.07	0.00	0.00	0.00	0	1	-24
5	15.61	0.06	0.43	0.17	0.01	121	-504	-15
6	15.96	0.06	-0.17	0.49	0.01	353	201	13
7	16.70	0.06	-0.01	-0.04	-0.87	-28	10	0
8	18.87	0.05	0.00	-0.01	-0.88	-4	3	0
9	24.94	0.04	0.09	0.07	0.00	-255	285	1
10	25.59	0.04	0.08	-0.07	0.00	259	307	12

Notes:

(1) The participation factors are calculated for mode vectors normalized by the maximum mode displacement.

(2) Modal information shown is not used in the response analysis performed by the direct integration method.

Table 3A.7-10

Eigenvalue Analysis Results for CB Model at Hard Site

Mode No.	Frequency (Hz)	Period (sec)	Participation Factor					
			X dir.	Y dir.	Z dir.	X rot	Y rot	Z rot
1	7.92	0.13	0.15	1.33	0.01	-263	46	-12
2	8.51	0.12	1.30	-0.16	0.00	27	340	21
3	14.83	0.07	0.00	0.00	0.00	0	0	-35
4	15.31	0.07	-0.04	-0.05	3.45	-40	37	-4
5	17.26	0.06	0.03	0.04	-1.58	35	-33	1
6	20.56	0.05	0.46	0.54	-1.07	554	-731	-2
7	20.85	0.05	-0.46	-0.46	-0.79	-464	738	4
8	21.43	0.05	-0.21	0.22	0.02	220	343	9
9	30.28	0.03	0.12	0.26	-0.01	-445	170	-7
10	31.47	0.03	-0.30	0.11	0.00	-195	-540	-18

Notes:

(1) The participation factors are calculated for mode vectors normalized by the maximum mode displacement.

(2) Modal information shown is not used in the response analysis performed by the direct integration method.

Table 3A.7-11

Eigenvalue Analysis Results for CB Model in Fixed-base Case

Mode No.	Frequency (Hz)	Period (sec)	Participation Factor					
			X dir.	Y dir.	Z dir.	X rot	Y rot	Z rot
1	8.98	0.11	0.19	1.28	0.01	-202	48	-16
2	9.58	0.10	1.26	-0.19	0.01	25	267	30
3	15.19	0.07	0.00	0.00	0.00	0	0	-43
4	15.94	0.06	-0.03	-0.04	2.52	-35	33	-2
5	17.66	0.06	-0.02	-0.04	1.60	-37	35	-1
6	21.97	0.05	0.14	0.21	-0.12	272	-272	1
7	22.92	0.04	0.10	0.12	1.12	158	-199	0
8	22.99	0.04	0.18	-0.14	-0.01	-175	-373	-8
9	33.18	0.03	-0.09	-0.17	0.00	415	-186	8
10	34.02	0.03	0.01	0.02	-0.19	-45	26	-1

Notes:

(1) The participation factors are calculated for mode vectors normalized by the maximum mode displacement.

(2) Modal information shown is not used in the response analysis performed by the direct integration method.

Table 3A.7-12

Eigenvalue Analysis Results for CB Model at Best-estimate North Anna Site

Mode No.	Frequency (Hz)	Period (sec)	Participation Factor					
			X dir.	Y dir.	Z dir.	X rot	Y rot	Z rot
1	7.57	0.13	0.14	1.34	0.01	-280	43	-11
2	8.13	0.12	1.31	-0.14	0.00	25	362	18
3	14.80	0.07	-0.03	-0.05	3.44	-35	30	47
4	14.83	0.07	0.00	0.00	0.00	0	1	-48
5	17.09	0.06	0.03	0.04	-1.71	38	-35	0
6	19.95	0.05	0.63	0.65	-1.11	603	-921	-5
7	20.14	0.05	-0.65	-0.55	-0.79	-503	950	6
8	20.68	0.05	-0.23	0.28	0.02	248	337	9
9	29.02	0.03	0.13	0.27	-0.01	-439	180	-6
10	30.11	0.03	0.29	-0.11	0.00	186	494	15

Notes:

(1) The participation factors are calculated for mode vectors normalized by the maximum mode displacement.

(2) Modal information shown is not used in the response analysis performed by the direct integration method.

Table 3A.7-13

Eigenvalue Analysis Results for CB Model at Upper-bound North Anna Site

Mode No.	Frequency (Hz)	Period (sec)	Participation Factor					
			X dir.	Y dir.	Z dir.	X rot	Y rot	Z rot
1	7.92	0.13	0.15	1.33	0.01	-264	46	-12
2	8.50	0.12	1.30	-0.15	0.00	27	342	21
3	14.83	0.07	0.00	0.00	0.00	0	0	-35
4	15.30	0.07	-0.04	-0.05	3.45	-40	36	-4
5	17.26	0.06	0.03	0.04	-1.59	35	-33	1
6	20.55	0.05	0.46	0.53	-1.15	549	-722	-2
7	20.84	0.05	-0.46	-0.45	-0.72	-460	728	4
8	21.43	0.05	-0.21	0.22	0.02	221	344	9
9	30.27	0.03	0.12	0.26	-0.01	-447	169	-7
10	31.47	0.03	-0.31	0.11	0.00	-195	-543	-18

Notes:

(1) The participation factors are calculated for mode vectors normalized by the maximum mode displacement.

(2) Modal information shown is not used in the response analysis performed by the direct integration method.

Table 3A.7-14

Eigenvalue Analysis Results for CB Model at Lower-bound North Anna Site

Mode No.	Frequency (Hz)	Period (sec)	Participation Factor					
			X dir.	Y dir.	Z dir.	X rot	Y rot	Z rot
1	7.11	0.14	0.12	1.35	0.01	-298	38	-9
2	7.65	0.13	1.32	-0.12	0.00	23	384	15
3	13.90	0.07	-0.02	-0.04	3.03	-23	20	1
4	14.83	0.07	0.00	0.00	0.00	0	0	-28
5	16.92	0.06	0.03	0.05	-1.55	38	-36	0
6	19.00	0.05	0.29	0.21	-0.01	176	-377	-3
7	19.46	0.05	-0.69	0.69	-1.26	557	921	23
8	19.52	0.05	0.49	-0.82	-0.38	-660	-653	-20
9	27.51	0.04	0.12	0.21	-0.01	-376	194	-4
10	28.41	0.04	0.23	-0.10	0.00	191	432	13

Notes:

(1) The participation factors are calculated for mode vectors normalized by the maximum mode displacement.

(2) Modal information shown is not used in the response analysis performed by the direct integration method.

Table 3A.7-15

Eigenvalue Analysis Results for FWSC Model at Soft Site

Mode No.	Frequency (Hz)	Period (sec)	Participation Factor					
			X dir.	Y dir.	Z dir.	X rot	Y rot	Z rot
1	0.24	4.15	0.00	1.00	0.00	0	0	0
2	0.24	4.15	1.00	0.00	0.00	0	0	0
3	4.73	0.21	0.00	1.46	0.00	-119	0	0
4	4.76	0.21	1.19	0.00	0.00	0	124	0
5	6.05	0.17	0.00	0.00	1.05	0	1	0
6	8.30	0.12	-0.19	0.00	0.00	0	628	0
7	10.53	0.09	0.00	-0.47	0.00	-579	0	-1
8	21.01	0.05	-0.08	0.00	0.00	0	-313	0
9	22.67	0.04	0.00	-0.01	0.00	402	0	-143
10	34.80	0.03	0.01	0.00	-0.05	3	-1075	-3
11	35.46	0.03	0.00	0.00	0.00	4	0	87
12	40.55	0.02	0.01	0.00	0.00	0	82	2
13	40.77	0.02	0.00	0.02	0.00	63	0	101
14	50.16	0.02	-0.01	0.00	0.00	4	-75	84
15	55.13	0.02	0.00	-0.01	0.00	41	16	-312

Notes:

(1) The participation factors are calculated for mode vectors normalized by the maximum mode displacement.

(2) Modal information shown is not used in the response analysis performed by the direct integration method.

Table 3A.7-16

Eigenvalue Analysis Results for FWSC Model at Medium Site

Mode No.	Frequency (Hz)	Period (sec)	Participation Factor					
			X dir.	Y dir.	Z dir.	X rot	Y rot	Z rot
1	0.24	4.14	0.00	1.00	0.00	0	0	0
2	0.24	4.14	1.00	0.00	0.00	0	0	0
3	11.76	0.09	0.00	2.02	0.00	-187	0	-4
4	12.20	0.08	1.82	0.00	0.01	0	221	0
5	15.67	0.06	-0.01	0.00	1.40	0	11	0
6	20.77	0.05	-0.66	0.00	-0.06	0	931	0
7	21.39	0.05	0.00	-1.17	0.00	-264	1	-101
8	22.82	0.04	-0.25	0.00	0.05	0	-892	0
9	29.85	0.03	0.00	-0.25	0.00	-642	-1	169
10	35.09	0.03	0.07	0.00	-0.38	6	-1518	-11
11	35.51	0.03	0.00	0.00	0.00	-7	0	-57
12	40.72	0.02	0.09	0.00	0.00	0	23	3
13	42.15	0.02	0.00	0.19	0.00	301	0	77
14	50.27	0.02	-0.12	0.00	0.00	4	-70	83
15	55.18	0.02	0.00	-0.07	0.00	38	18	-327

Notes:

(1) The participation factors are calculated for mode vectors normalized by the maximum mode displacement.

(2) Modal information shown is not used in the response analysis performed by the direct integration method.

Table 3A.7-17

Eigenvalue Analysis Results for FWSC Model at Hard Site

Mode No.	Frequency (Hz)	Period (sec)	Participation Factor					
			X dir.	Y dir.	Z dir.	X rot	Y rot	Z rot
1	0.24	4.14	0.00	1.00	0.00	0	0	0
2	0.24	4.14	1.00	0.00	0.00	0	0	0
3	17.05	0.06	0.00	2.01	0.00	-189	0	-59
4	17.63	0.06	2.01	0.00	0.01	0	214	0
5	31.13	0.03	0.78	0.00	5.35	2	570	-1
6	32.66	0.03	0.02	-1.31	-0.01	59	1	-180
7	32.80	0.03	-1.60	-0.03	0.38	1	-61	-6
8	35.44	0.03	0.00	-0.09	0.00	-15	0	231
9	36.29	0.03	-0.37	0.00	-4.88	-4	716	-4
10	38.76	0.03	0.00	0.16	0.01	-364	-1	80
11	40.51	0.02	-0.35	0.00	0.02	0	-726	-4
12	45.34	0.02	0.55	0.00	0.21	0	-979	6
13	51.25	0.02	-0.95	-0.01	-0.06	1	134	78
14	55.43	0.02	-0.02	-0.25	-0.03	205	35	-435
15	61.42	0.02	0.00	0.31	0.00	404	0	-65

Notes:

(1) The participation factors are calculated for mode vectors normalized by the maximum mode displacement.

(2) Modal information shown is not used in the response analysis performed by the direct integration method.

Table 3A.7-18

Eigenvalue Analysis Results for FWSC Model in Fixed-base Case

Mode No.	Frequency (Hz)	Period (sec)	Participation Factor					
			X dir.	Y dir.	Z dir.	X rot	Y rot	Z rot
1	0.24	4.14	0.00	1.00	0.00	0	0	0
2	0.24	4.14	1.00	0.00	0.00	0	0	0
3	18.31	0.05	0.00	1.49	0.00	-115	0	-89
4	18.62	0.05	1.52	0.00	0.00	0	113	0
5	33.90	0.03	0.01	0.00	1.73	0	52	0
6	35.40	0.03	0.00	0.01	0.00	-3	0	112
7	39.06	0.03	0.00	-0.43	0.00	-243	0	73
8	39.59	0.03	-0.58	0.00	0.00	0	237	0
9	49.06	0.02	1.07	0.01	0.02	0	44	83
10	54.07	0.02	0.00	1.20	0.06	-99	0	62
11	55.41	0.02	0.03	0.00	1.04	0	96	-1
12	67.34	0.01	0.00	-0.15	0.00	324	0	-84
13	67.72	0.01	-0.04	0.00	0.01	0	-311	1
14	69.94	0.01	-0.01	0.66	0.00	-24	-1	777
15	89.60	0.01	0.07	0.17	0.00	-35	10	-40

Notes:

(1) The participation factors are calculated for mode vectors normalized by the maximum mode displacement.

(2) Modal information shown is not used in the response analysis performed by the direct integration method.

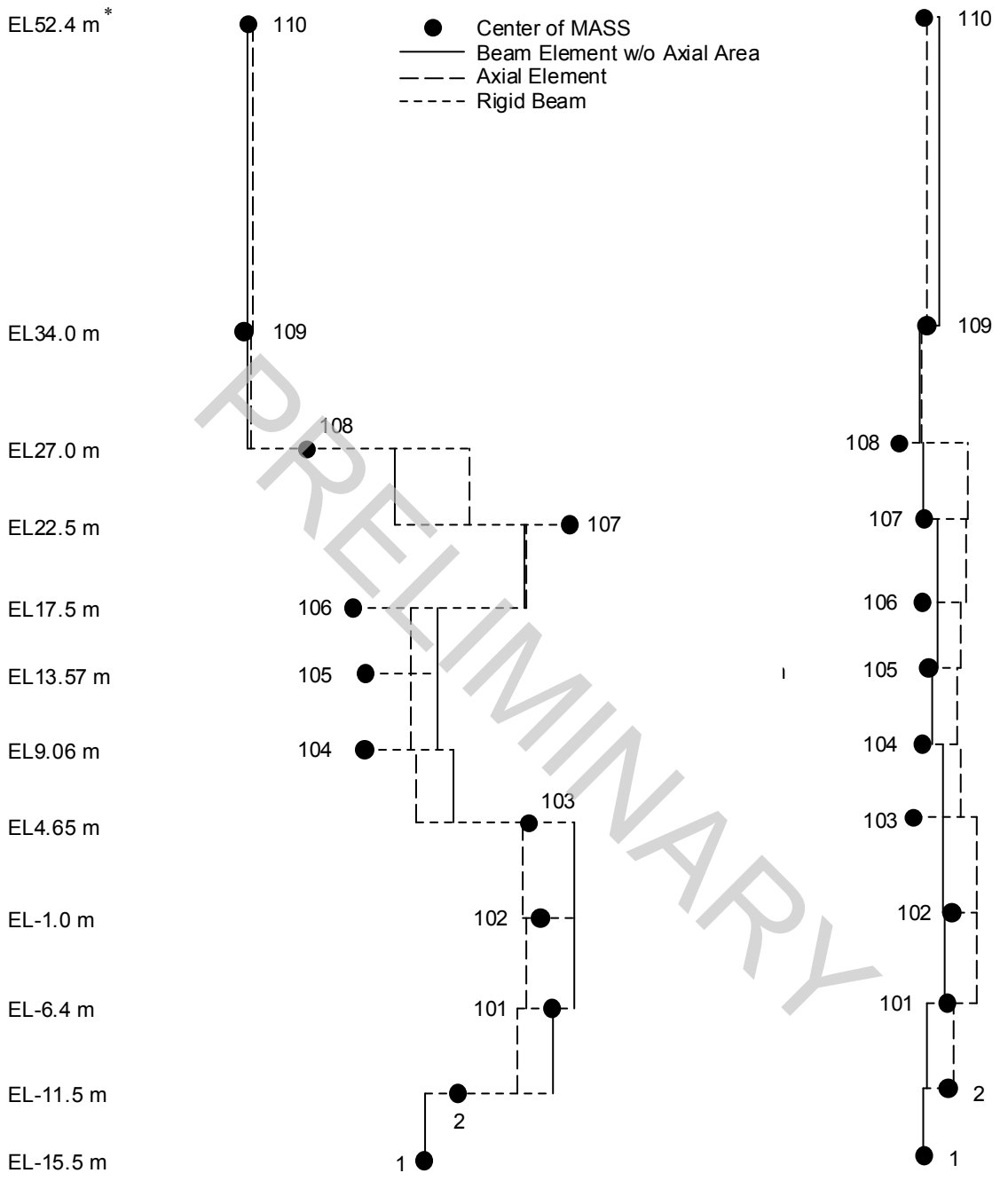

*: The difference between the modeled elevation 52.4 m and the actual elevation 52.7 m at the RB roof is negligibly small.

Figure 3A.7-1. RB/FB Stick Model

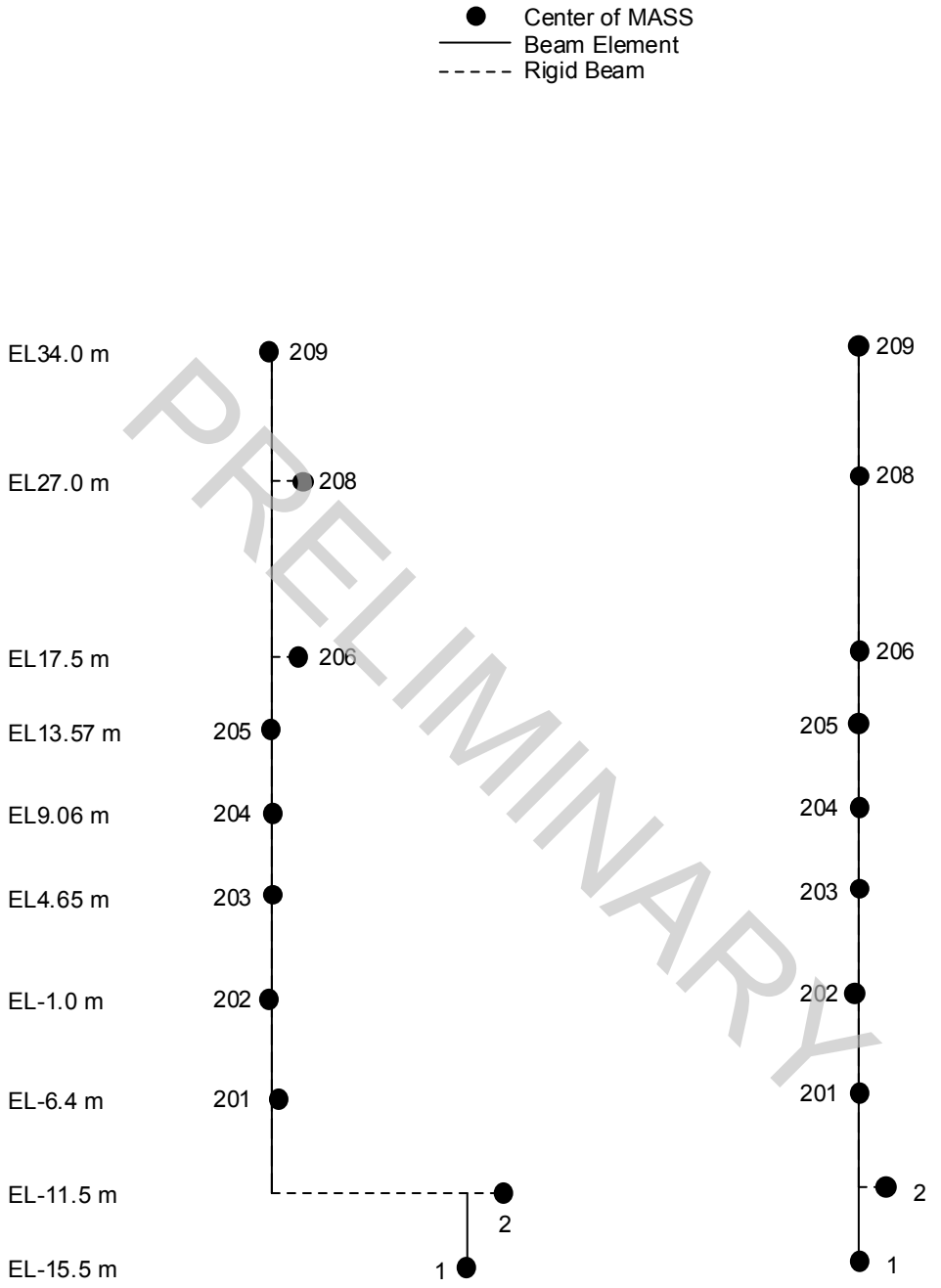

(a) XZ Plane **(b) YZ Plane**

Figure 3A.7-2. RCCV Stick Model

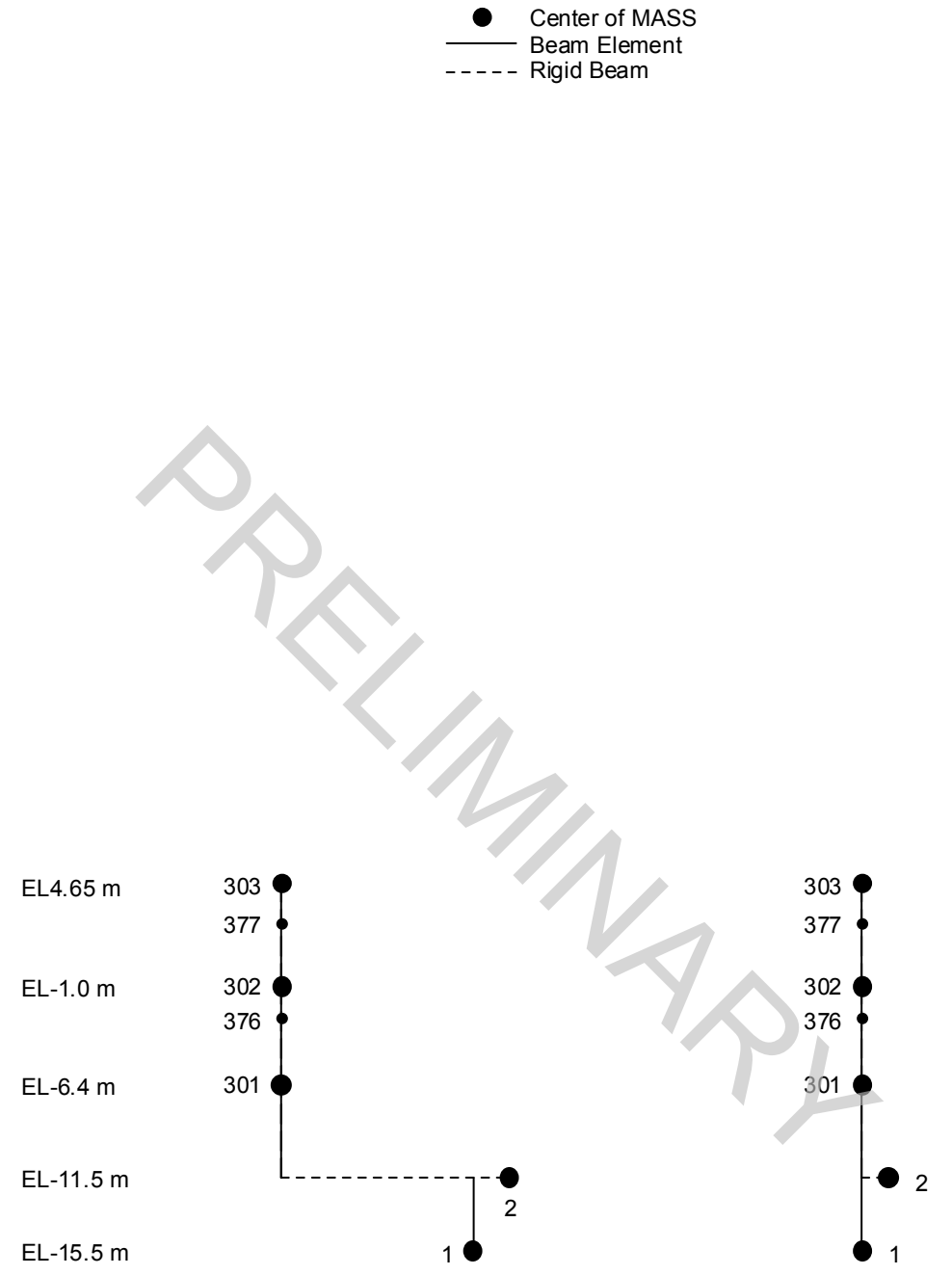

(a) XZ Plane **(b) YZ Plane**

Figure 3A.7-3. Pedestal Stick Model

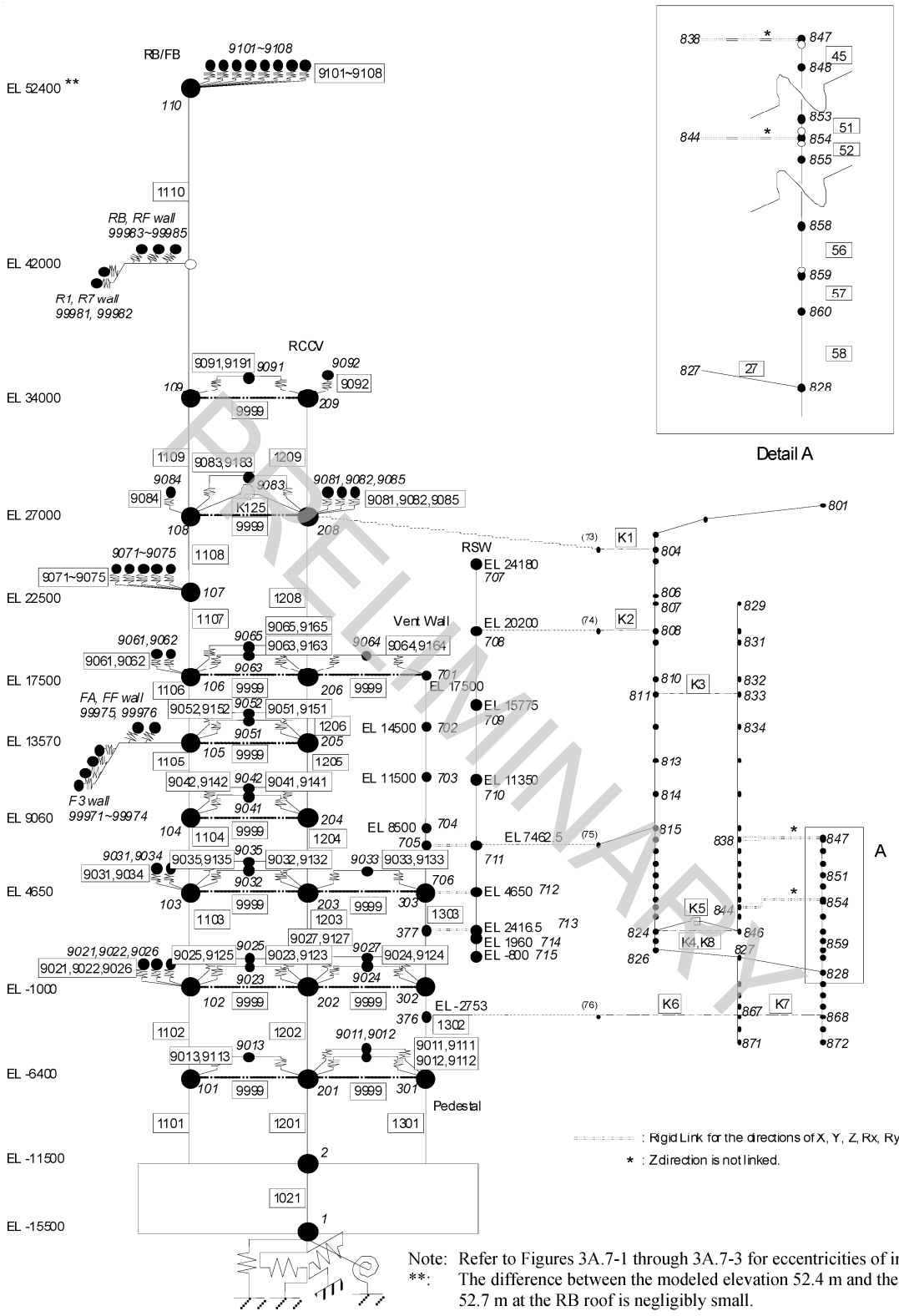

Note: Refer to Figures 3A.7-1 through 3A.7-3 for eccentricities of individual sticks.
**: The difference between the modeled elevation 52.4 m and the actual elevation 52.7 m at the RB roof is negligibly small.

Figure 3A.7-4. RB/FB Complex Seismic Model

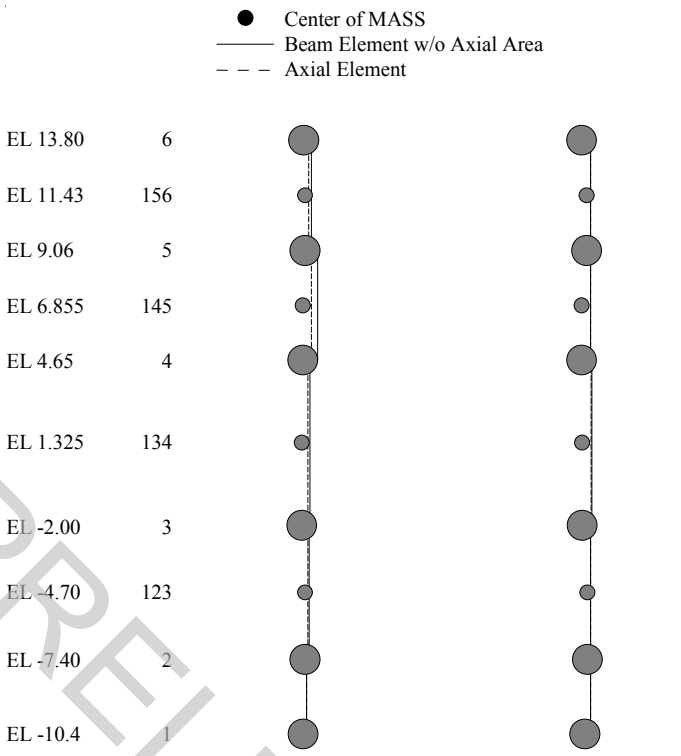

Figure 3A.7-5. Control Building Stick Model

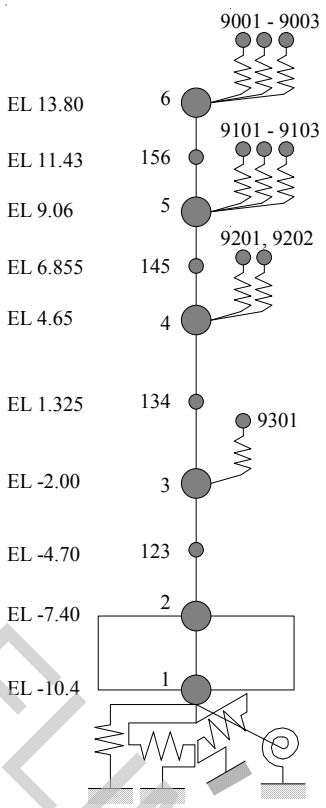

Figure 3A.7-6. Control Building Seismic Model

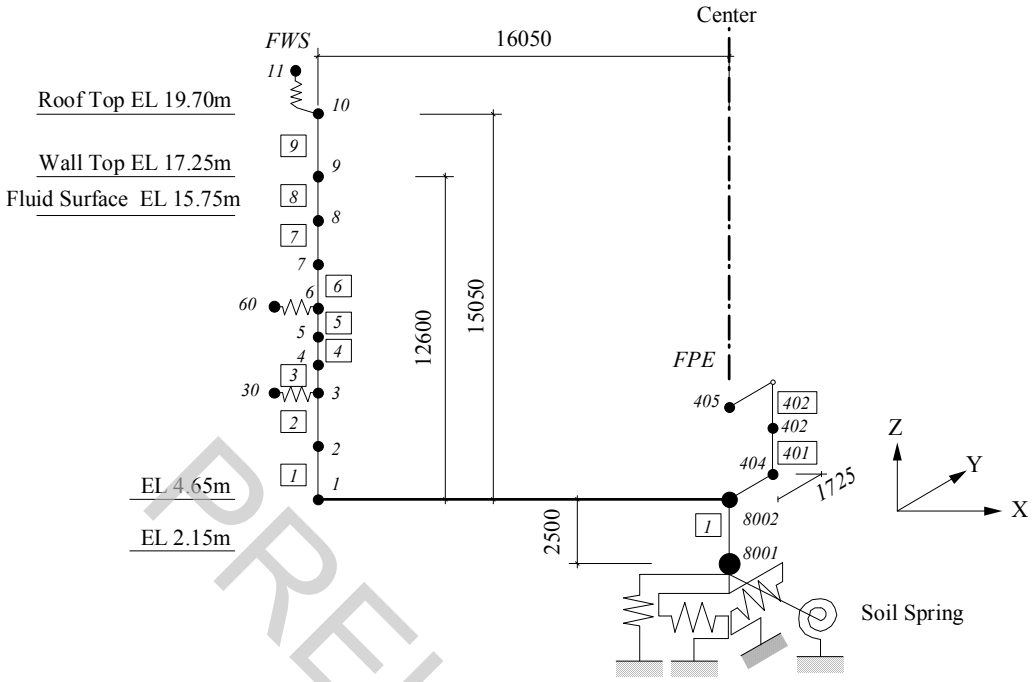

Mass at Node 30 represents the impulsive mode.
Mass at Node 60 represents the fundamental sloshing (convective) mode.
The model is assumed to be symmetric about YZ-plane including the center line.

Figure 3A.7-7. FWSC Seismic Model

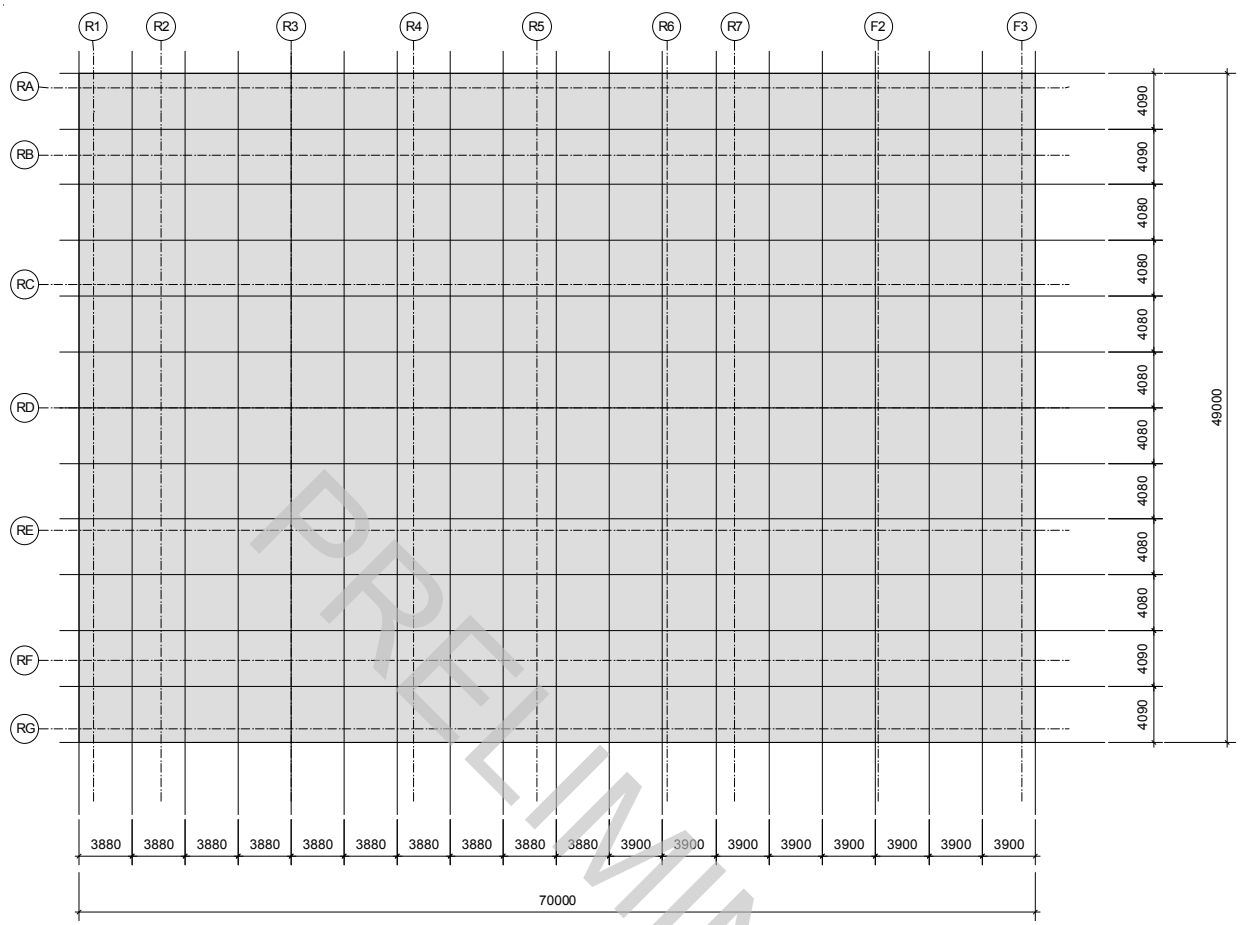

Figure 3A.7-8. SASSI2000 Plate Elements for RB/FB Basemat

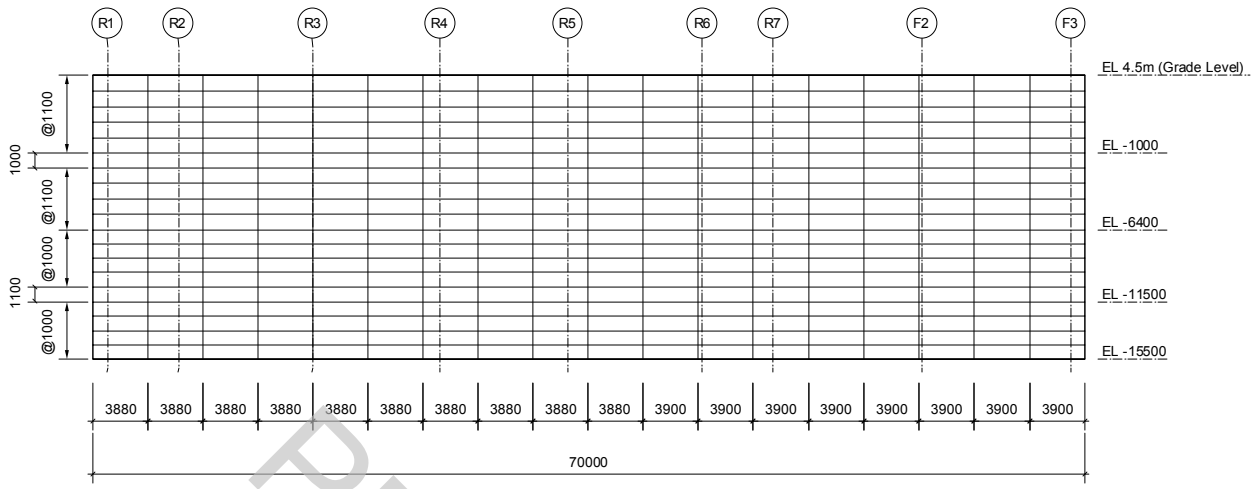

(a) Walls on Column Rows RA and RG

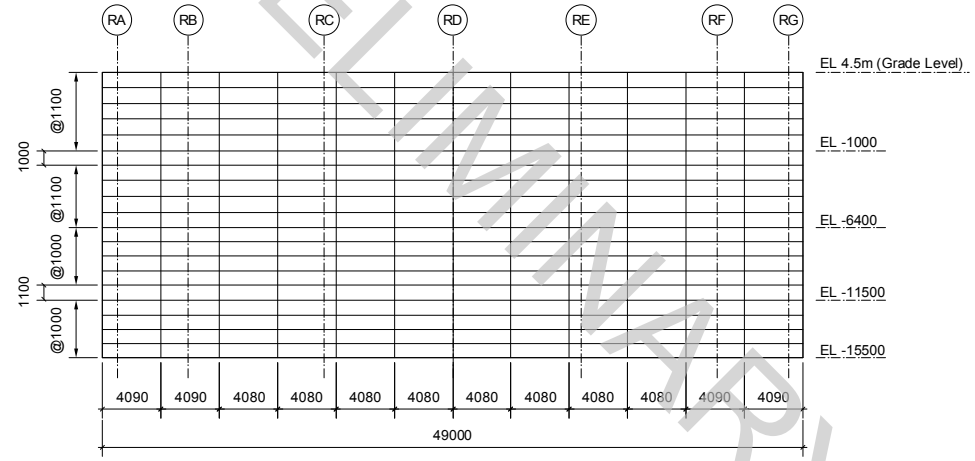

(b) Walls on Column Rows R1 and F3

Figure 3A.7-9. SASSI2000 Plate Elements for RB/FB Exterior Walls

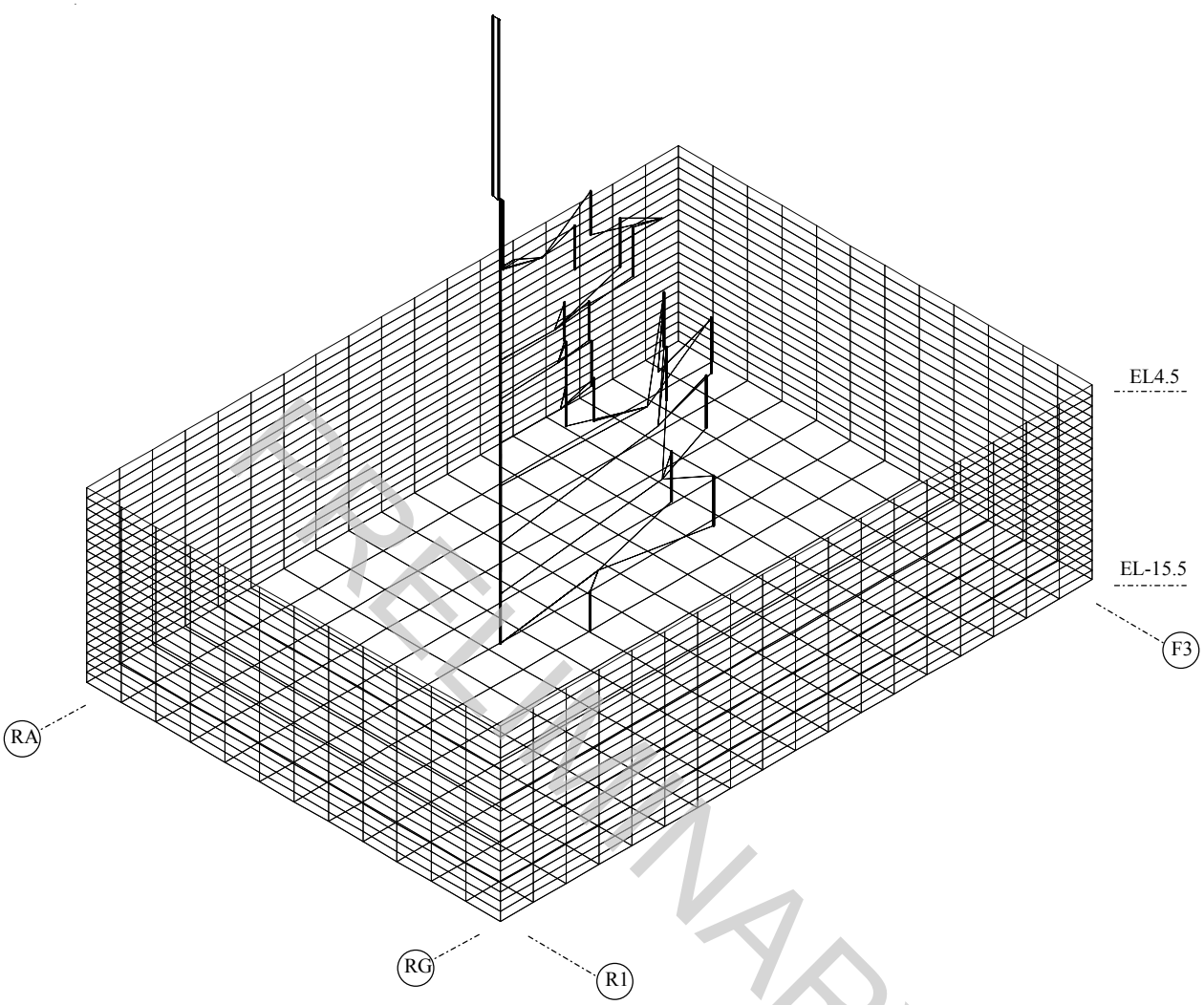

Figure 3A.7-10. Overview of RB/FB SASSI2000 Model

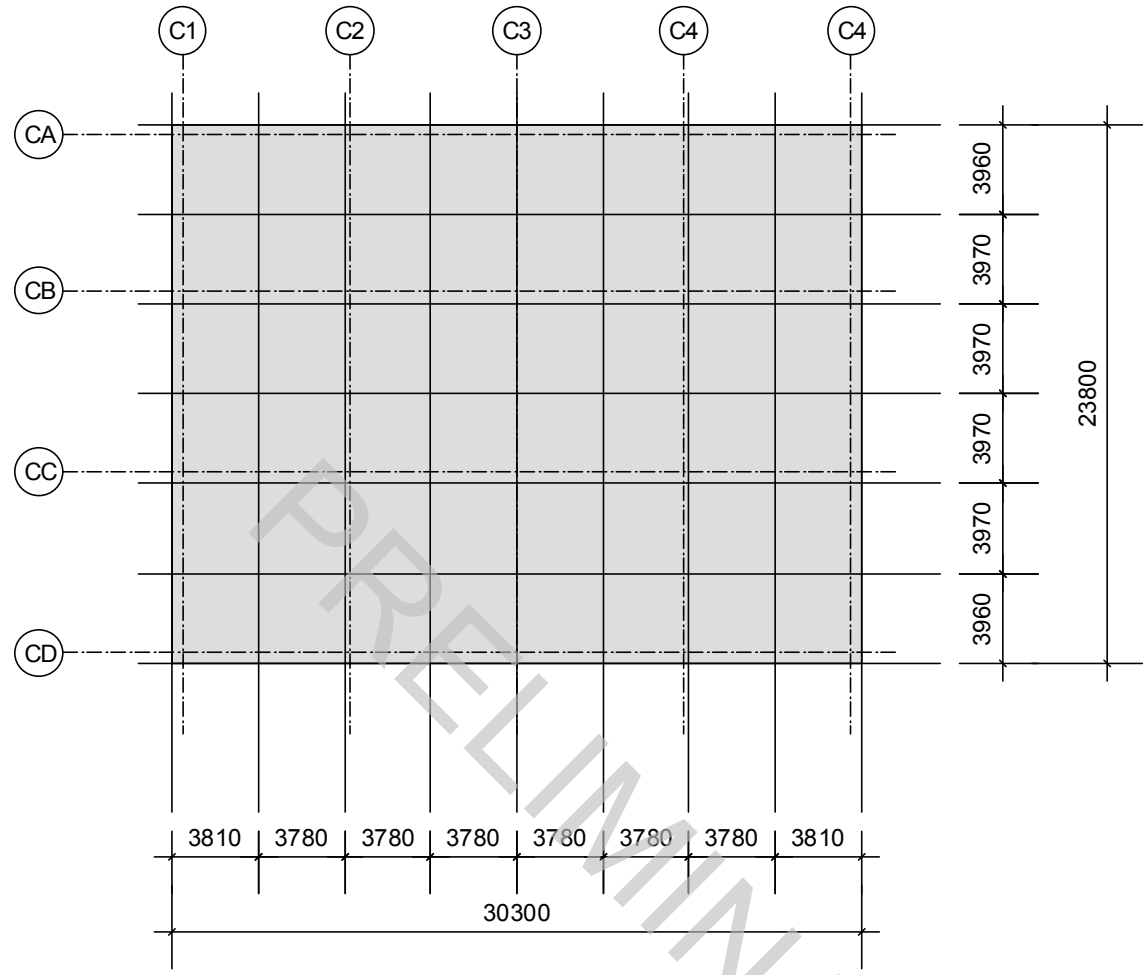

Figure 3A.7-11. SASSI2000 Plate Elements for CB Basemat

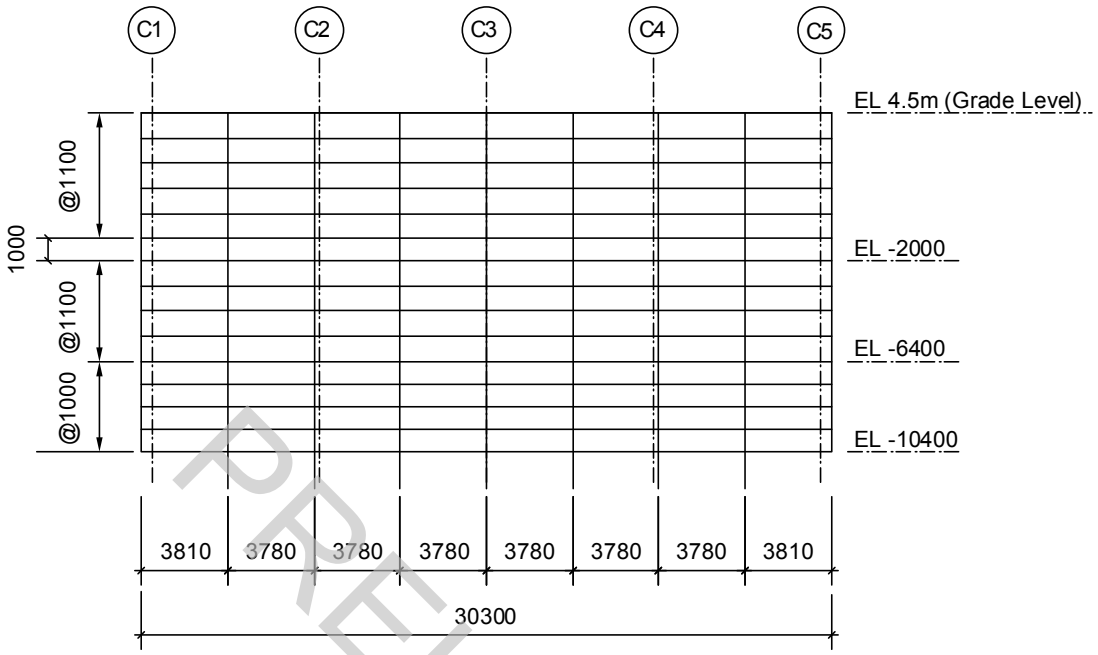

(a) Walls on Column Rows CA and CD

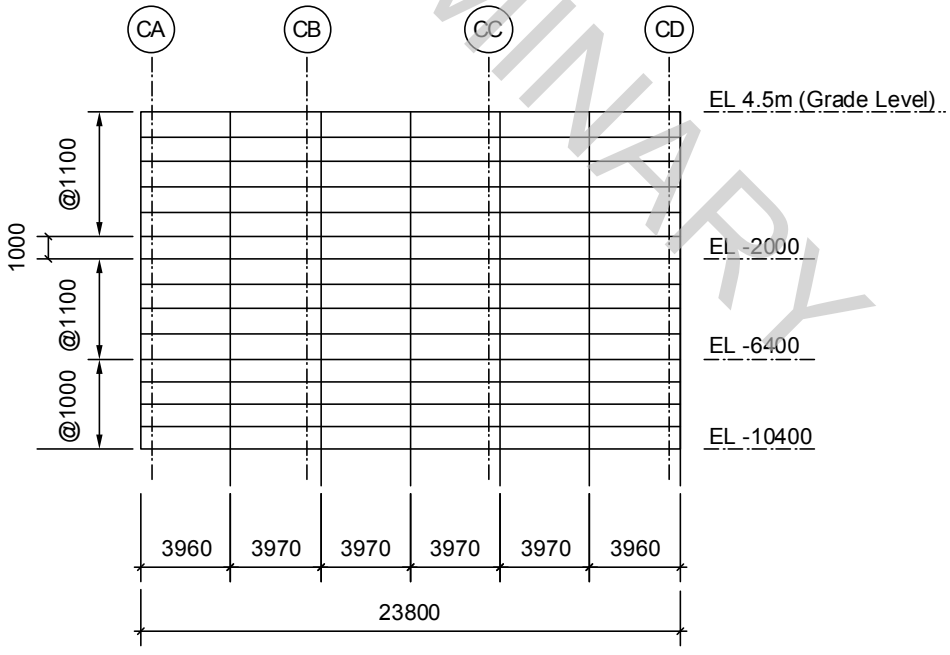

(b) Walls on Column Rows C1 and C5

Figure 3A.7-12. SASSI2000 Plate Elements for CB Exterior Walls

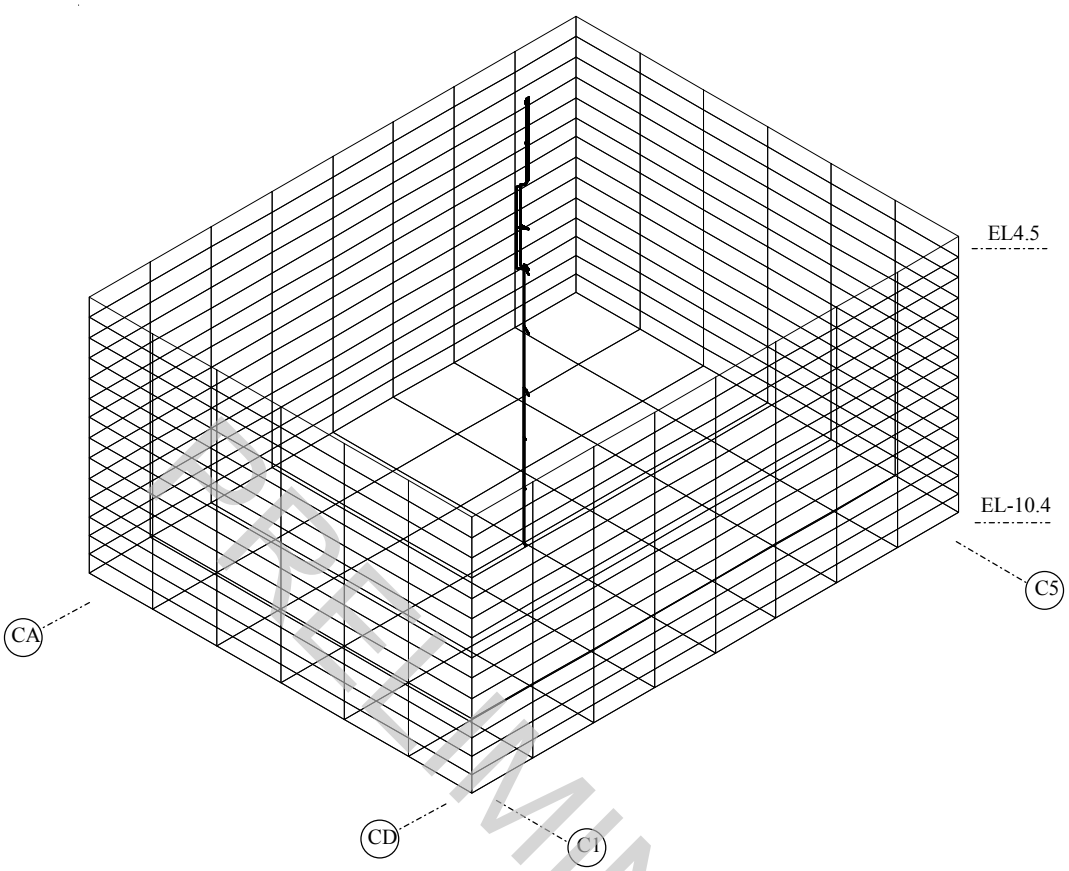

Figure 3A.7-13. Overview of CB SASSI2000 Model

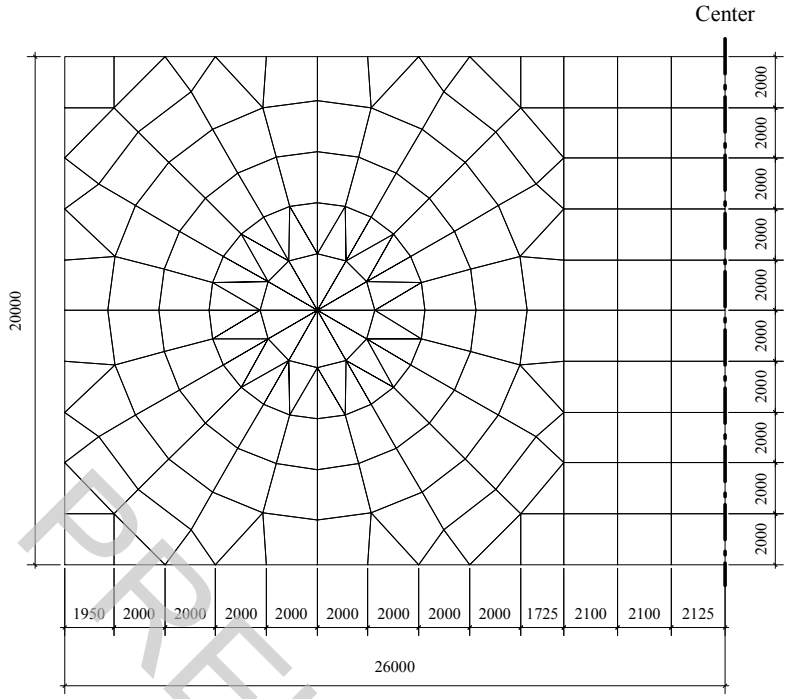

Figure 3A.7-14. SASSI2000 Plate Elements for FWSC Basemat

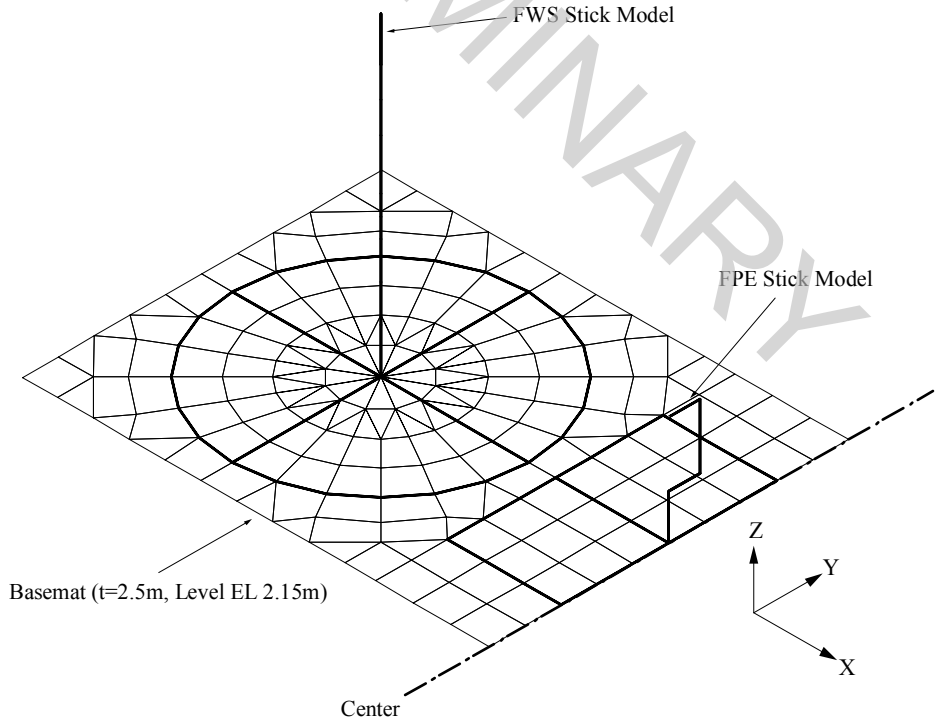

The model is assumed to be symmetric about YZ-plane including the center line.

Figure 3A.7-15. Overview of FWSC SASSI2000 Model

3A.8 ANALYSIS RESULTS

In this section, typical SSI results are presented to show the effect of different soil properties on seismic responses at selected locations in terms of acceleration response spectra and seismic forces. The site-envelope seismic responses are presented in Section 3A.9.

For comparison study, the acceleration response spectra at 5% damping are shown for the following locations:

Location	Node Number
RB/FB Refueling Floor	109
RCCV Top Slab	208
Vent Wall Top	701
RSW Top	707
RPV Top	801
RB/FB Basemat	2
CB Top	6
CB Basemat	2
FWS Wall Top	9
FWS Basemat	1
FPE Top	405
FPE Basemat	404

For each soil case analyzed, the calculated co-directional FRS in X, Y and Z directions are combined by the Square Root of the Sum of the Squares (SRSS) method to obtain FRS at the building edges considering the coupling effects between vertical and rocking and between lateral and torsion motions.

The seismic forces are presented at the following locations:

Location	Connecting Nodes
RPV Support	815 – 711
RSW Base	710 – 711
Vent Wall Base	704 – 705
Pedestal Base	301 – 2
RCCV Base	201 – 2
RB/FB Base	101 – 2
CB Base	3 –2

Location	Connecting Nodes
FWS Base	2-1
FPE Base	405-404

3A.8.1 Effect of Soil Stiffness

For the RG 1.60 (RU-1 and CU-1) and North Anna site (RU-2 and CU-2) spectra motion cases of the RB/FB and CB, the horizontal response spectra in the X-direction are shown in Figures 3A.8.1-1a through 3A.8.1-1h. The response spectra in the Y-direction are shown in Figures 3A.8.1-2a through 3A.8.1-2h. The vertical response spectra (Z-direction) are shown in Figures 3A.8.1-3a through 3A.8.1-3h. The results of the North Anna cases are the envelopes of the three soil conditions, Best-estimate, Upper-bound, and Lower-bound. Generic site responses are higher at frequencies below 10 Hz, whereas North Anna responses are generally more dominant in the higher frequency range above 10 Hz.

The results in terms of seismic forces of the RB/FB and CB are compared in Tables 3A.8.1-1 and 3A.8.1-2, respectively for X direction and Y direction. As shown in these tables, the results of generic medium or stiffer sites govern the seismic responses of the RB/FB complex structure, except for relatively stiff structures such as the RPV support for which the moment response is controlled by the North Anna site, due to the high-frequency content in its input ground motion. The results of generic hard rock or North Anna sites govern the seismic responses of the CB structure.

For the FWSC, response results using single envelope input motion (FU-1) are compared. The horizontal response spectra in the X-direction are shown in Figures 3A.8.1-4a through 3A.8.1-4d. The response spectra in the Y-direction are shown in Figures 3A.8.1-5a through 3A.8.1-5d. The vertical response spectra (Z-direction) are shown in Figures 3A.8.1-6a through 3A.8.1-6d. Fixed base condition is dominant in the higher frequency range above 20 Hz, while soft soil condition is dominant in the lower frequency range.

The results in terms of seismic forces of the FWSC are compared in Table 3A.8.1-3 and Table 3A.8.1-4, respectively for X direction and Y direction. As shown in these tables, the results are mostly enveloped by the fixed base case.

The results of all soil cases shown are used to obtain the enveloping results (Section 3A.9).

3A.8.2 Effect of Single Envelope Ground Motion

The effect of single envelope ground motion is evaluated by comparing the results of single envelope input motion (RU-3/CU-3) with the envelope results of two separate input motions described in Subsection 3A.8.1 (RU-1and RU-2/ CU-1and CU-2) for the RB/FB/CB.

Comparisons of FRS at the selected locations are shown in Figures 3A.8.2-1a through 3A.8.2-1h, Figures 3A.8.2-2a through 3A.8.2-2h, and Figures 3A.8.2-3a through 3A.8.2-3h, respectively for X direction, Y direction, and Z direction.

It is found from the results that the responses due to the single envelope input motion are generally bounded by the envelope responses of RG 1.60 input motion and North Anna site input motion. However, when analyzed separately, in the lower frequency range the fixed case and

hard site case exceed the envelope responses of RG 1.60 input motion and North Anna site input motion in the higher frequency range. This is because the effect of the high-frequency component of the ground motion is more pronounced for stiffer sites. The fixed case is analyzed only for 0.3 g RG 1.60 input motion but not for North Anna site input motion.

The results in terms of seismic forces are compared in Tables 3A.8.2-1 and 3A.8.2-2, respectively for X direction and Y direction. As shown in these tables, there are some locations where the seismic forces are governed by the results of single envelop input motion. Thus, the results of single envelope spectra input motion are used with the RG 1.60 spectra motion and North Anna site spectra motion to obtain the enveloping results (Section 3A.9).

3A.8.3 Effect of Updated Design of RSW and VW

In the design process, the section of the RSW and VW is slightly changed from the originally assumed section. To evaluate the effect of this updated design on the seismic responses, seismic analysis of the updated model for the RSW and VW (RU-4) are performed compared with those of the original model (RU-3) in the case of single envelope input motion.

The results of the updated model are shown in Figures 3A.8.3-1a through 3A.8.3-1f, Figures 3A.8.3-2a through 3A.8.3-2f, and Figures 3A.8.3-3a through 3A.8.3-3f, respectively for X direction, Y direction, and Z direction, compared with the broadened envelope results of RU-3. The seismic shear forces and moments are compared in Table 3A.8.3-1 and Table 3A.8.3-2.

The comparison indicates that the effects on the seismic responses of building stick models are insignificant. However, there are some effects on the internal structure, such as RSW and VW. Thus, the responses from this case are included to obtain the enveloping results (Section 3A.9).

3A.8.4 Effect of Infill Concrete Stiffness of VW and D/F

To evaluate the effect of infill concrete on the frequency shift for the VW and D/F, the stiffness properties of the two structures in the seismic model are adjusted to include contribution of 50% concrete stiffness (RU-5) and 100% concrete stiffness (RU-5a).

The results of the RU-5 are shown in Figures 3A.8.4-1a through 3A.8.4-1f, Figures 3A.8.4-2a through 3A.8.4-2f, and Figures 3A.8.4-3a through 3A.8.4-3f, respectively for X direction, Y direction, and Z direction, compared with the broadened envelope results of RU-3. The seismic shear forces and moments are compared in Table 3A.8.4-1 and Table 3A.8.4-2.

The results of the RU-5a are shown in Figures 3A.8.4-4a through 3A.8.4-4f, Figures 3A.8.4-5a through 3A.8.4-5f and Figures 3A.8.4-6a through 3A.8.4-6f, respectively for X direction, Y direction and Z direction, compared with the broadened envelope results of RU-3. The seismic shear forces and moments are compared in Tables 3A.8.4-3 and 3A.8.4-4.

The comparison indicates that the results of the RU-5 and RU-5a, which consider infill concrete stiffness, are not completely bounded by the broadened envelope results of RU-3, which does not consider the infill concrete stiffness. Thus, the responses from all three infill concrete stiffness cases (0%, 50% and 100%) are included to obtain the enveloping results (Section 3A.9).

3A.8.5 Effect of Loss-of-Coolant-Accident (LOCA) Flooding

To account for the plant condition after a LOCA, a LOCA flooding model is constructed and seismic analyses are performed (RU-6).

The LOCA model results are compared with the broadened envelope results of the normal model RU-3 in terms of acceleration spectra as shown in Figures 3A.8.5-1a through 3A.8.5-1f, Figures 3A.8.5-2a through 3A.8.5-2f, and Figures 3A.8.5-3a through 3A.8.5-3f, respectively for X direction, Y direction, and Z direction. The responses from the LOCA model are included to obtain the enveloping response spectra (Section 3A.9).

The seismic shear forces and moments are compared in Table 3A.8.5-1 and Table 3A.8.5-2. The obtained seismic forces are used for the load combinations including the LOCA flooding condition (Section 3A.9).

3A.8.6 Effect of Layered Sites

The effect of layered sites is evaluated by comparing the results of layered site cases (RL-1 through RL-4/CL-1 through CL-4/FL-1 through FL-4) with the broadened envelope results of uniform site cases (RU-3/CU-3/FU-1) for the RB/FB, CB, and FWSC.

Comparisons of response spectra are shown in Figures 3A.8.6-1a through 3A.8.6-1l, Figures 3A.8.6-2a through 3A.8.6-2l, and Figures 3A.8.6-3a through 3A.8.6-3l, respectively for X direction, Y direction, and Z direction.

As for the case of the RB/FB and CB, it is found from the results that the responses for the layered site cases are bounded by the broadened envelope responses of uniform site cases in the whole frequency range.

As for the case of the FWSC, the responses for the layered site cases are essentially bounded by the broadened envelope responses of uniform site cases except at around 5 Hz.

Thus the effect of layered sites is included to obtain the enveloping design loads (Section 3A.9).

3A.8.7 Effect of Embedment

It is shown in Subsection 3A.8.6 that the responses for the layered site cases are bounded by the broadened envelope responses of uniform site cases in the whole frequency range. One of reasons for this difference is considered to be the effect of embedment.

As explained in Subsection 3A.5.1, for uniform sites, the SSI analysis method follows the lumped soil spring approach using the program DAC3N. This model neglects the effect of embedment. On the other hand, for layer sites, the finite element method using the program SASSI2000 is employed for SSI analysis including the effect of embedment.

Table 3A.8.7-1 shows the comparisons of the RB/FB basemat reaction shear forces between Case RU-3 (Soft uniform site) and Case RL-3 (Soft layered site) and between Case RU-3 (Medium uniform site) and Case RL-4 (Medium layered site). Please note that Case RL-3 has a deeper soft soil layer (40 m [131.23 ft]) supporting the basemat and that Case RL-4 has a deeper medium soil layer (40 m [131.23 ft]) supporting the basemat.

It is found from the results that the effect of embedment works to reduce basemat reaction shear forces. It is considered to be because the building shear force is partially transferred to the lateral

soil layers. Regarding the lateral soil pressure, the analysis results are shown in Subsection 3A.8.8.

As shown in Table 3A.8.7-1 the basemat reaction shear forces calculated by DAC3N for case RU-3 without the embedment effect are conservative. To better predict interface loads with the supporting foundation medium, uniform sites are further analyzed using SASSI2000 with embedment included for RB/FB and CB and without embedment for surface founded FWSC. These SASSI2000 cases are designated as RU-8, CU-4 and FU-2 in Table 3A.6-1. The results of case RU-8 are also shown in Table 3A.8.7-1 and they are lower than RU-3 results as expected. The basemat interface loads for uniform sites considered in the foundation stability evaluation are those calculated by SASSI2000.

The SASSI2000 results of uniform sites are also compared with the DAC3N results for floor response spectra as discussed below.

Comparisons of response spectra are shown in Figures 3A.8.7-1a through 3A.8.7-1l, Figures 3A.8.7-2a through 3A.8.7-2l, and Figures 3A.8.7-3a through 3A.8.7-3l, respectively for X direction, Y direction, and Z direction.

As for the case of the RB/FB, it is found from the results that the responses for SASSI2000 cases are bounded by the broadened envelope responses of DAC3N cases in the whole frequency range. The responses of RU-8 hard site at vent wall top X direction (Figure 3A.8.7-1c) and refueling floor Z direction (Figure 3A.8.7-3a) are slightly higher around 20 Hz but the exceedance is negligibly small. Furthermore, the slightly higher responses at these two locations are bounded by the design envelope response spectra after the spectral valleys are filled-in as described in Section 3A.9.

On the other hand, the response spectra of a portion of the CB above ground and the FPE in the FWSC exceeded greater than 10% at the broadened envelope responses of the DAC3N cases in the higher frequency range.

Thus the SASSI2000 uniform site results of the CB and FWSC are included to obtain the enveloping design spectra (Section 3A.9).

The uniform site SASSI2000 results for seismic forces of building structural members are less than the DAC3N results, thus there is no impact on the design envelope loads.

3A.8.8 Effect of Lateral Soil Pressures

The lateral pressure computed from the equivalent static pressure analysis listed in ASCE 4-98 is used for the design soil pressure. To confirm that the ASCE 4-98 method is conservative, the soil pressures calculated from the SASSI2000 analysis for the layered sites described in Subsection 3A.8.6 are compared with the ASCE 4-98 method soil pressures in Figures 3A.8.8-1 through 3A.8.8-4.

It is found from the results that the SASSI2000 soil pressures are generally bounded by the ASCE 4-98 soil pressures; however, at the elevation close to the ground surface and the basemat elevation, the SASSI2000 soil pressure exceeds the ASCE 4-98 soil pressure. The design soil pressure loads for the exterior walls are calculated by averaging soil pressures which each wall is subjected to. The calculated design soil pressures are summarized in Tables 3A.8.8-1 and 3A.8.8-2, comparing the SASSI2000 soil pressures and the ASCE 4-98 soil pressures. The

embedded walls are designed for the worst soil pressures resulting from either SASSI2000 analysis or ASCE 4-98 methodology.

3A.8.9 Effect of Concrete Cracking

In order to address the effect of the cracked concrete stiffness, an additional evaluation is performed using SASSI2000, assuming that the cracked concrete stiffness is 50% of the uncracked value in accordance with ASCE 43-05.

For the comparison, Case RL-2/CL-2 is selected for the RB/FB/CB, because they show the largest responses among various layered sites. Case RL-5/CL-5 is the RB/FB/CB cracked case, which has the same layered site as Case RL-2/CL-2.

For the comparison of the FWSC, Fixed-base Case FU-1 is selected, because it shows the largest responses among various analysis cases. Case FC-1 is the FWSC cracked case, which is also the Fixed-base case.

Comparisons of response spectra at the selected locations are shown in Figures 3A.8.9-1a through 3A.8.9-1l and Figures 3A.8.9-2a through 3A.8.9-2l, respectively for X direction and Y direction. The broadened envelope results of Case RU-3/CU-3/FU-1 (uniform site, single envelope input motion case) are also shown in the figures for comparison.

It is found from the results that the FRS peaks move to lower frequencies by concrete cracking in all the buildings. As for the case of the RB/FB and CB, FRS of uncracked and cracked cases are bounded by the broadened envelope responses of uniform site cases in the whole frequency range. As for the upper portion of the FWSC, FRS of cracked cases exceed the broadened envelope responses of uniform site cases.

Thus the effect of concrete cracking is included to obtain the enveloping design loads (Section 3A.9).

3A.8.10 Effect of Wall Out-of-plane Vibration

It is found from the review of the out-of-plane vibration frequencies of walls that the RB walls above the refueling floor at EL 34.0 m and the FB walls at EL 4.65 m have some vibration modes lower than 50 Hz. To obtain design loads and FRS for these walls, seismic analysis is performed using wall oscillators evaluated in the same manner as floor oscillators. The calculated wall oscillators are shown in the seismic analysis model of Figure 3A.7-4.

The maximum horizontal acceleration of the wall out-of-plane oscillators are shown for each site condition of Case RU-7 in Table 3A.8.10-1. The results for the cracked Case RL-6 are shown in Table 3A.8.10-2. The design loads and FRS for these walls are determined by enveloping these response results (Section 3A.9).

3A.8.11 Effect of Structure-Structure Interaction

The RB/FB effects on the CB are more significant than the CB effects on the RB/FB because the size of the RB/FB is much larger than the CB. To evaluate the RB/FB effects on the CB, the analyses are performed by the following two steps:

(1) Perform the RB/FB SASSI2000 analysis to obtain the ground surface response at the CB location.

(2) Perform the CB SASSI2000 analysis using the input motion obtained in Step 1.

For the comparison of without and with structure-structure interaction effect, Case CL-2 layered site is selected, because the CB shows the largest responses at Case CL-2 site among various layered sites. The corresponding RB/FB case is Case RL-2. The CB case considering structure-structure interaction effect is called Case CL-6.

Comparisons of FRS at the top and basemat of the CB are shown in Figures 3A.8.11-1 through 3A.8.11-6. The broadened envelope results of Case CU-3 (uniform site, single envelope input motion case) are also shown in the figures for comparison.

It is found from the results that the effect of structure-structure interaction is the largest in the Y direction (East-West) FRS, however, both FRS without and with structure-structure interaction effect are bounded by the broadened envelope responses of uniform site cases in the whole frequency range. Thus the effect of structure-structure interaction between the RB/FB and CB is included in the enveloping design loads (Section 3A.9).

In addition to the through-soil interaction between the RB/FB and CB described above, the structure-structure interaction analysis is also performed for the FWSC with CB for the same layered site Case 2 (CL-2 for CB and FL-2 for FWSC). The analysis model is composed of these two independent structures coupled through soil using the SASSI2000 computer code. The input motion for the coupled SSI model is the Certified Seismic Design Response Spectra (CSDRS) applied at the CB foundation level. This analysis case is named Case FL-5.

Figures 3A.8.11-7 through 3A.8.11-24 show comparisons of FRS with the design envelope spectra at the top of the structure and basemat for the CB and FWSC. The FRS for the corresponding analysis Cases CL-2 and FL-2 without the structure-structure interaction effect are also shown in the figures for comparison. It is confirmed from the results that the FRS with the structure-structure interaction effect are bounded by the design envelope spectra in all frequency ranges. Thus the effect of structure-structure interaction between the CB and FWSC is included in the enveloping design loads (Section 3A.9).

Table 3A.8.1-1

Maximum Forces - X Direction (RU-1 and RU-2/CU-1 and CU-2)

Locations	Response Types	Soil Stiffness				
		SOFT	MEDIUM	HARD	FIX	North Anna
RPV Support	Shear	6	14	14	17	9
	Moment	24	65	108	117	120
RSW Base	Shear	5	13	17	20	10
	Moment	52	146	201	236	146
Vent Wall Base	Shear	8	16	16	19	11
	Moment	54	127	143	167	92
Pedestal Base	Shear	48	102	96	95	38
	Moment	712	1590	1494	1485	567
RCCV Base	Shear	119	255	240	237	92
	Moment	5148	10836	10483	9836	4039
RB/FB Base	Shear	427	922	868	856	335
	Moment	16554	31489	32235	26978	9856
CB Base	Shear	85	80	88	80	91
	Moment	1331	1395	1537	1247	1570

Units: Shear Forces in MN; Moment in MN-m

Table 3A.8.1-2

Maximum Forces - Y Direction (RU-1 and RU-2/CU-1 and CU-2)

Locations	Response Types	Soil Stiffness				
		SOFT	MEDIUM	HARD	FIX	North Anna
RPV	Shear	6	12	11	12	11
Support	Moment	30	54	69	66	117
RSW Base	Shear	6	11	11	10	11
	Moment	66	122	128	116	136
Vent Wall	Shear	10	20	17	16	13
Base	Moment	77	165	148	126	79
Pedestal	Shear	55	121	97	88	41
Base	Moment	898	1963	1616	1455	580
RCCV	Shear	137	304	244	220	99
Base	Moment	6942	14200	11797	10876	4342
RB/FB	Shear	477	1030	804	704	350
Base	Moment	17623	35275	28459	25566	8843
CB Base	Shear	96	96	84	81	67
	Moment	1454	1525	1289	1261	1141

Units: Shear Forces in MN; Moment in MN-m

Table 3A.8.1-3

Maximum Forces – X Direction (FU-1)

Locations	Response Types	Soil Stiffness			
		SOFT	MEDIUM	HARD	FIX
FWS Base	Shear	24	26	42	45
	Moment	165	234	344	366
FPE Base	Shear	4	5	7	7
	Moment	12	16	25	25

Units: Shear Forces in MN; Moment in MN-m

Table 3A.8.1-4

Maximum Forces – Y Direction (FU-1)

Locations	Response Types	Soil Stiffness			
		SOFT	MEDIUM	HARD	FIX
FWS Base	Shear	21	30	43	48
	Moment	143	257	375	373
FPE Base	Shear	3	5	6	7
	Moment	13	15	23	23

Units: Shear Forces in MN; Moment in MN-m

Table 3A.8.2-1

Maximum Forces - X Direction (RU-3/ CU-3)

Locations	Response Types	Soil Stiffness			
		SOFT	MEDIUM	HARD	FIX
RPV Support	Shear	8	13	18	18
	Moment	35	64	101	128
RSW Base	Shear	7	11	15	16
	Moment	78	121	167	195
Vent Wall Base	Shear	10	18	17	22
	Moment	60	122	146	148
Pedestal Base	Shear	63	104	103	103
	Moment	931	1478	1521	1522
RCCV Base	Shear	157	256	260	258
	Moment	6243	10268	10170	9508
RB/FB Base	Shear	563	917	930	921
	Moment	18839	31774	29695	26645
CB Base	Shear	95	81	84	91
	Moment	1442	1232	1376	1353
FWT Base	Shear	17	19	31	34
	Moment	123	174	255	271
FPE Base	Shear	3	4	5	6
	Moment	9	12	18	19

Units: Shear Forces in MN; Moment in MN-m

Table 3A.8.2-2

Maximum Forces - Y Direction (RU-3/ CU-3)

Locations	Response Types	Soil Stiffness			
		SOFT	MEDIUM	HARD	FIX
RPV Support	Shear	7	12	16	18
	Moment	41	73	124	122
RSW Base	Shear	6	11	15	14
	Moment	72	131	181	158
Vent Wall Base	Shear	12	19	20	23
	Moment	92	142	171	162
Pedestal Base	Shear	55	107	90	92
	Moment	944	1620	1451	1480
RCCV Base	Shear	138	267	223	229
	Moment	7671	12474	10856	10934
RB/FB Base	Shear	474	907	736	790
	Moment	19908	30116	28273	25733
CB Base	Shear	87	85	93	78
	Moment	1320	1356	1268	1268
FWT Base	Shear	15	22	32	36
	Moment	106	190	278	277
FPE Base	Shear	2	4	5	5
	Moment	10	11	17	17

Units: Shear Forces in MN; Moment in MN-m

Table 3A.8.3-1

Maximum Forces - X Direction (RU-4)

Locations	Response Types	Soil Stiffness				Envelope
		SOFT	MEDIUM	HARD	FIX	RU-1, 2 and 3
RPV Support	Shear	8	13	17	19	18
	Moment	34	64	100	129	128
RSW Base	Shear	7	11	15	16	20
	Moment	77	122	165	189	236
Vent Wall Base	Shear	10	19	18	23	22
	Moment	65	136	160	159	167
Pedestal Base	Shear	63	104	104	103	104
	Moment	936	1492	1531	1523	1590
RCCV Base	Shear	157	257	261	258	260
	Moment	6245	10317	10238	9605	10836
RB/FB Base	Shear	564	921	934	921	930
	Moment	18888	31921	29920	26409	32235

Units: Shear Forces in MN; Moment in MN-m

Table 3A.8.3-2

Maximum Forces - Y Direction (RU-4)

Locations	Response Types	Soil Stiffness				Envelope
		SOFT	MEDIUM	HARD	FIX	RU-1, 2 and 3
RPV	Shear	7	12	16	18	18
Support	Moment	42	71	123	122	124
RSW Base	Shear	6	11	15	14	15
	Moment	73	132	183	157	181
Vent Wall	Shear	13	21	21	24	23
Base	Moment	101	154	187	177	171
Pedestal	Shear	55	107	90	92	121
Base	Moment	953	1640	1463	1489	1963
RCCV	Shear	138	268	224	230	304
Base	Moment	7692	12513	10925	11013	14200
RB/FB	Shear	477	911	737	793	1030
Base	Moment	19957	30244	28420	25929	35275

Units: Shear Forces in MN; Moment in MN-m

Table 3A.8.4-1

Maximum Forces - X Direction (RU-5)

Locations	Response Types	Soil Stiffness				Envelope
		SOFT	MEDIUM	HARD	FIX	RU-1, 2 and 3
RPV	Shear	9	14	17	18	18
Support	Moment	35	60	100	141	128
RSW Base	Shear	7	12	17	19	20
	Moment	78	135	186	210	236
Vent Wall	Shear	16	29	30	30	22
Base	Moment	129	243	284	307	167
Pedestal	Shear	62	102	102	104	104
Base	Moment	962	1558	1592	1638	1590
RCCV	Shear	157	257	261	262	260
Base	Moment	6233	10356	10238	9473	10836
RB/FB	Shear	563	919	931	930	930
Base	Moment	18888	31921	29665	26870	32235

Units: Shear Forces in MN; Moment in MN-m

Table 3A.8.4-2

Maximum Forces - Y Direction (RU-5)

Locations	Response Types	Soil Stiffness				Envelope
		SOFT	MEDIUM	HARD	FIX	RU-1, 2 and 3
RPV Support	Shear	6	12	15	17	18
	Moment	43	66	128	133	124
RSW Base	Shear	7	10	16	16	15
	Moment	77	121	185	188	181
Vent Wall Base	Shear	20	33	35	35	23
	Moment	182	272	352	319	171
Pedestal Base	Shear	55	106	88	94	121
	Moment	1002	1690	1520	1485	1963
RCCV Base	Shear	138	268	224	233	304
	Moment	7682	12484	10925	10964	14200
RB/FB Base	Shear	477	913	740	801	1030
	Moment	19937	30214	28233	25645	35275

Units: Shear Forces in MN; Moment in MN-m

Table 3A.8.4-3

Maximum Forces – X Direction (RU-5a)

Locations	Response Types	Soil Stiffness				Envelope
		SOFT	MEDIUM	HARD	FIX	RU-1, 2 and 3
RPV Support	Shear	9	13	17	18	18
	Moment	32	57	92	120	128
RSW Base	Shear	7	12	17	19	20
	Moment	75	136	188	211	236
Vent Wall Base	Shear	20	37	38	37	22
	Moment	169	313	365	379	167
Pedestal Base	Shear	62	101	101	104	104
	Moment	977	1600	1600	1655	1590
RCCV Base	Shear	157	257	261	262	260
	Moment	6225	10346	10238	9467	10836
RB/FB Base	Shear	563	920	931	928	930
	Moment	18878	31882	29704	26870	32235

Unit: Shear Forces in MN; Moment in MN-m

Table 3A.8.4-4

Maximum Forces – Y Direction (RU-5a)

Locations	Response Types	Soil Stiffness				Envelope
		SOFT	MEDIUM	HARD	FIX	RU-1, 2 and 3
RPV Support	Shear	7	12	16	17	18
	Moment	42	67	136	137	124
RSW Base	Shear	7	10	17	16	15
	Moment	76	120	194	199	181
Vent Wall Base	Shear	25	41	43	45	23
	Moment	236	356	438	404	171
Pedestal Base	Shear	54	105	87	94	121
	Moment	1033	1734	1564	1503	1963
RCCV Base	Shear	139	268	223	234	304
	Moment	7673	12464	10954	10993	14200
RB/FB Base	Shear	477	913	738	804	1030
	Moment	19917	30195	28165	25566	35275

Units: Shear Forces in MN; Moment in MN-m

Table 3A.8.5-1

Maximum Forces - X Direction (RU-6)

Locations	Response Types	Soil Stiffness				Envelope
		SOFT	MEDIUM	HARD	FIX	RU-1, 2 and 3
RPV	Shear	8	13	17	18	18
Support	Moment	35	66	107	122	128
RSW Base	Shear	7	12	16	17	20
	Moment	80	130	174	194	236
Vent Wall	Shear	11	21	19	22	22
Base	Moment	65	132	157	148	167
Pedestal	Shear	61	105	104	104	104
Base	Moment	920	1491	1556	1553	1590
RCCV	Shear	153	258	263	260	260
Base	Moment	6175	10336	10189	9463	10836
RB/FB	Shear	550	924	939	928	930
Base	Moment	19162	31989	29744	26762	32235

Units: Shear Forces in MN; Moment in MN-m

Table 3A.8.5-2

Maximum Forces - Y Direction (RU-6)

Locations	Response Types	Soil Stiffness				Envelope
		SOFT	MEDIUM	HARD	FIX	RU-1, 2 and 3
RPV	Shear	7	13	16	18	18
Support	Moment	42	74	127	130	124
RSW Base	Shear	7	12	16	14	15
	Moment	75	136	190	164	181
Vent Wall	Shear	13	22	22	26	23
Base	Moment	98	148	173	166	171
Pedestal	Shear	55	107	90	92	121
Base	Moment	951	1630	1482	1484	1963
RCCV	Shear	138	269	225	230	304
Base	Moment	7657	12464	10885	10934	14200
RB/FB	Shear	476	915	742	792	1030
Base	Moment	19908	30136	28263	25694	35275

Units: Shear Forces in MN; Moment in MN-m

Table 3A.8.7-1

Comparisons of RB/FB Basemat Reaction Shear Force

Analysis Method	Effect of Embedment	Soft site (Vs 300m/s) (MN)			Medium site (Vs 800m/s) (MN)			Hard site (Vs 1700m/s) (MN)		
		Case	NS	EW	Case	NS	EW	Case	NS	EW
DAC3N	Neglect	RU-3	900	760	RU-3	1450	1500	RU-3	1470	1160
SASSI2000	Consider	RL-3	560	490	RL-4	1380	1310	-	-	-
		RU-8	490	480	RU-8	650	590	RU-8	590	590

Table 3A.8.8-1

Lateral Soil Pressure – RB/FB

Floor Level	R1 and F3 Wall Soil Pressure (MPa)					RA and RG Wall Soil Pressure (MPa)					ASCE 4-98	Envelope (MPa)	
(m)	RL-1	RL-2	RL-3	RL-4	RL-5	RL-1	RL-2	RL-3	RL-4	RL-5	(MPa)	R1 and F3 Wall	RA and RG Wall
4.65													
Slab													
3.65													
	0.20	0.19	0.24	0.19	0.21	0.27	0.17	0.33	0.19	0.22	0.30	0.30	0.33
-1.00													
Slab													
-2.00													
	0.15	0.21	0.20	0.21	0.26	0.17	0.19	0.21	0.19	0.20	0.29	0.29	0.29
-6.40													
Slab													
-7.40													
	0.19	0.21	0.20	0.21	0.25	0.18	0.19	0.18	0.20	0.20	0.23	0.25	0.23
-11.50													
Basemat	0.29	0.24	0.28	0.25	0.23	0.25	0.24	0.25	0.26	0.20	0.16	0.29	0.26

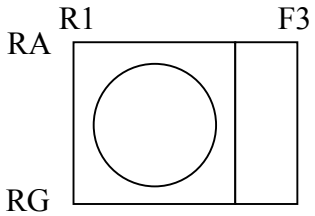

Table 3A.8.8-2

Lateral Soil Pressure - CB

Floor Level	C1 and C5 Wall Soil Pressure (MPa)						CA and CD Wall Soil Pressure (MPa)						ASCE 4-98	Envelope (MPa)	
(m)	CL-1	CL-2	CL-3	CL-4	CL-5	CL-6	CL-1	CL-2	CL-3	CL-4	CL-5	CL-6	(MPa)	C1 and C5 Wall	CA and CD Wall
4.65															
Slab															
3.95 -2.00	0.08	0.15	0.08	0.15	0.12	0.14	0.10	0.13	0.09	0.13	0.11	0.12	0.22	0.22	0.22
Slab															
-2.50 -7.40	0.10	0.14	0.09	0.14	0.14	0.13	0.10	0.13	0.10	0.13	0.14	0.13	0.18	0.18	0.18
Basemat	0.14	0.19	0.13	0.19	0.17	0.18	0.14	0.19	0.13	0.19	0.16	0.17	0.12	0.19	0.19

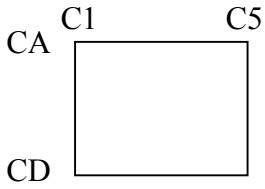

Table 3A.8.10-1

Maximum Horizontal Acceleration RB/FB Wall Out-of-plane Oscillators (RU-7)

Locations	Wall Oscillator	Frequency (Hz)	Soil Stiffness			
			SOFT	MEDIUM	HARD	FIX
RB above EL34000 X direction	R1 and R7 wall (1)	15.87	0.69	1.14	1.54	1.53
	R1 and R7 wall (2)	35.22	0.62	1.23	1.22	1.30
	Node in RB/FB Stick		0.61	1.11	1.12	1.19
RB above EL34000 Y direction	RB and RF wall (1)	14.14	0.74	1.22	1.54	1.71
	RB and RF wall (2)	24.51	0.76	1.29	1.47	1.56
	RB and RF wall (3)	43.36	0.75	1.22	1.25	1.14
	Node in RB/FB Stick		0.74	1.21	1.22	1.08
FB above EL4650 X direction	F3 wall (1)	12.73	0.49	0.69	1.01	1.38
	F3 wall (2)	18.34	0.51	0.88	1.08	1.37
	F3 wall (3)	35.36	0.47	0.75	1.00	1.15
	F3 wall (4)	42.50	0.48	0.72	0.86	0.99
	Node in RB/FB Stick		0.45	0.66	0.85	0.97
FB above EL4650 Y direction	FA and FF wall (1)	13.27	0.45	0.92	1.18	1.28
	FA and FF wall (2)	40.73	0.39	0.75	0.82	0.98
	Node in RB/FB Stick		0.37	0.69	0.71	0.72

Unit: Acceleration in g.

Table 3A.8.10-2

Maximum Horizontal Acceleration RB/FB Cracked Wall Out-of-plane Oscillators (RL-6)

Locations	Wall Oscillator	Frequency (Hz)	Site Case 2
RB above EL34000 X direction	R1 and R7 wall (1)	15.87	1.14
	R1 and R7 wall (2)	35.22	1.11
	Node in RB/FB Stick		1.03
RB above EL34000 Y direction	RB and RF wall (1)	14.14	1.07
	RB and RF wall (2)	24.51	1.08
	RB and RF wall (3)	43.36	1.02
	Node in RB/FB Stick		0.98
FB above EL4650 X direction	F3 wall (1)	12.73	0.67
	F3 wall (2)	18.34	0.72
	F3 wall (3)	35.36	0.68
	F3 wall (4)	42.50	0.63
	Node in RB/FB Stick		0.61
FB above EL4650 Y direction	FA and FF wall (1)	13.27	0.61
	FA and FF wall (2)	40.73	0.67
	Node in RB/FB Stick		0.55

Unit: Acceleration in g.

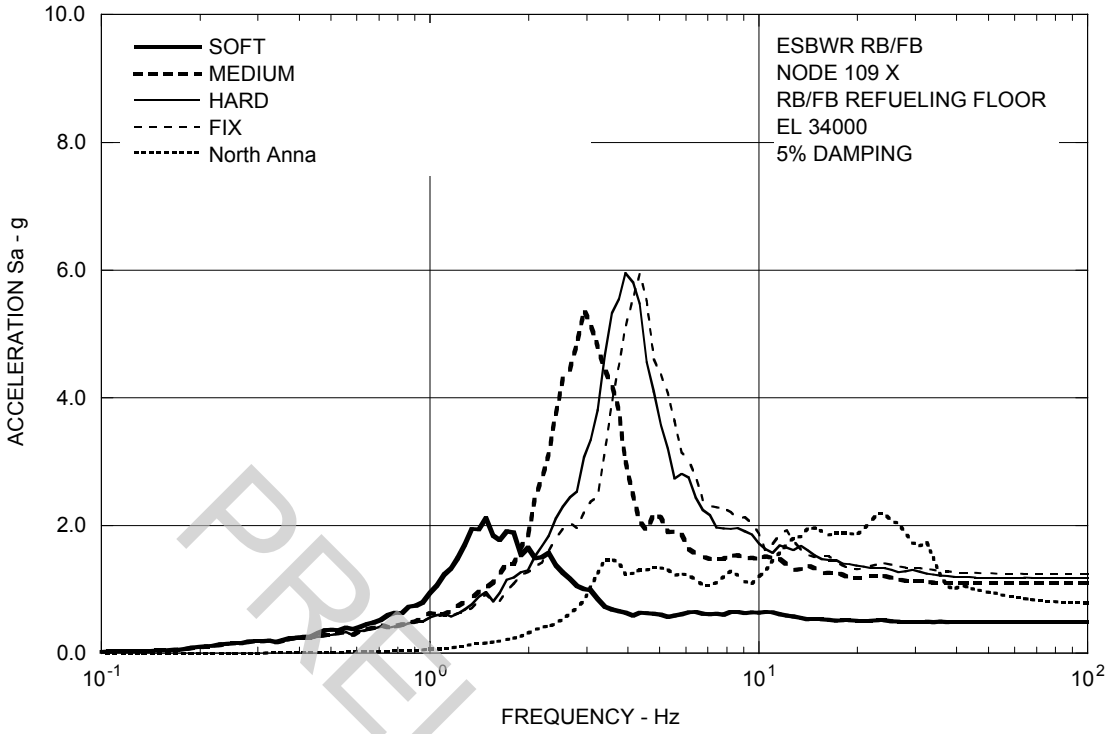

Figure 3A.8.1-1a. FRS (Effect of Soil Stiffness) – RB/FB Refueling Floor X

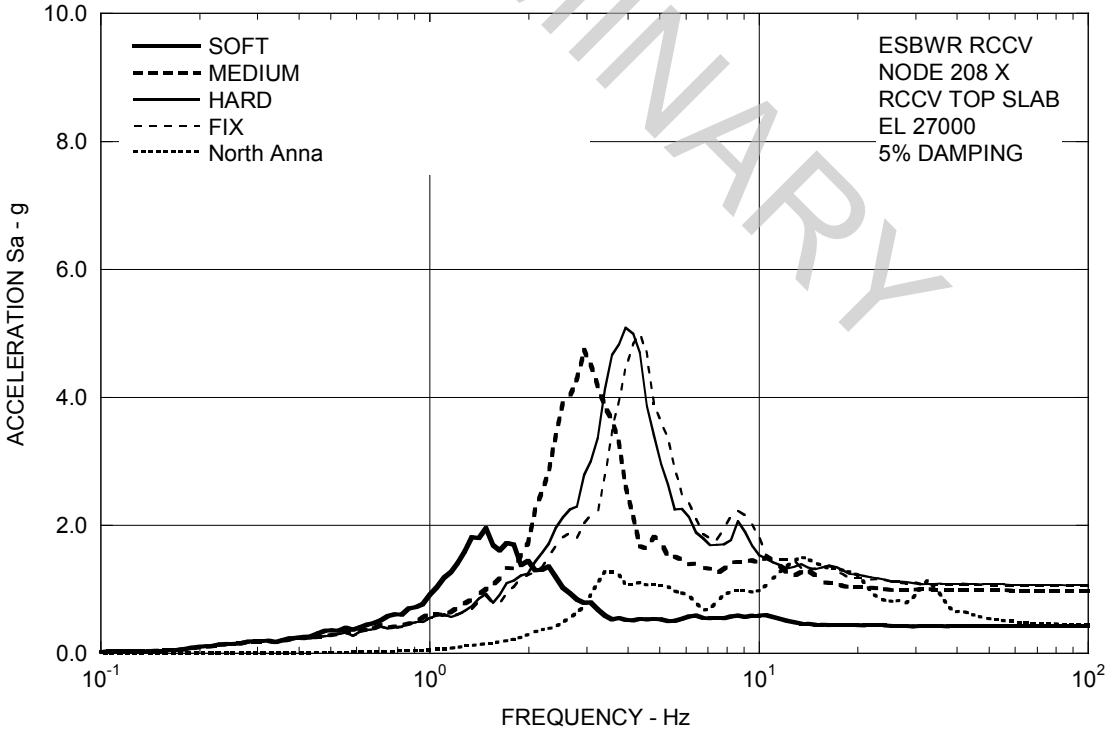

Figure 3A.8.1-1b. FRS (Effect of Soil Stiffness) – RCCV Top Slab X

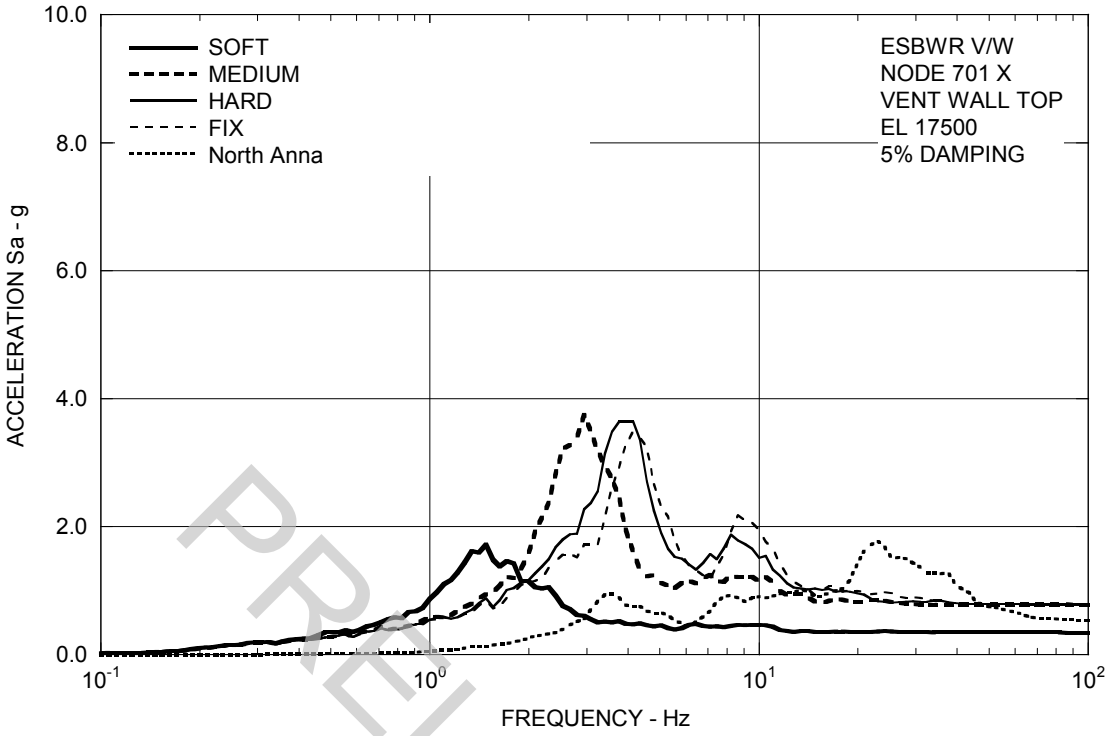

Figure 3A.8.1-1c. FRS (Effect of Soil Stiffness) – Vent Wall Top X

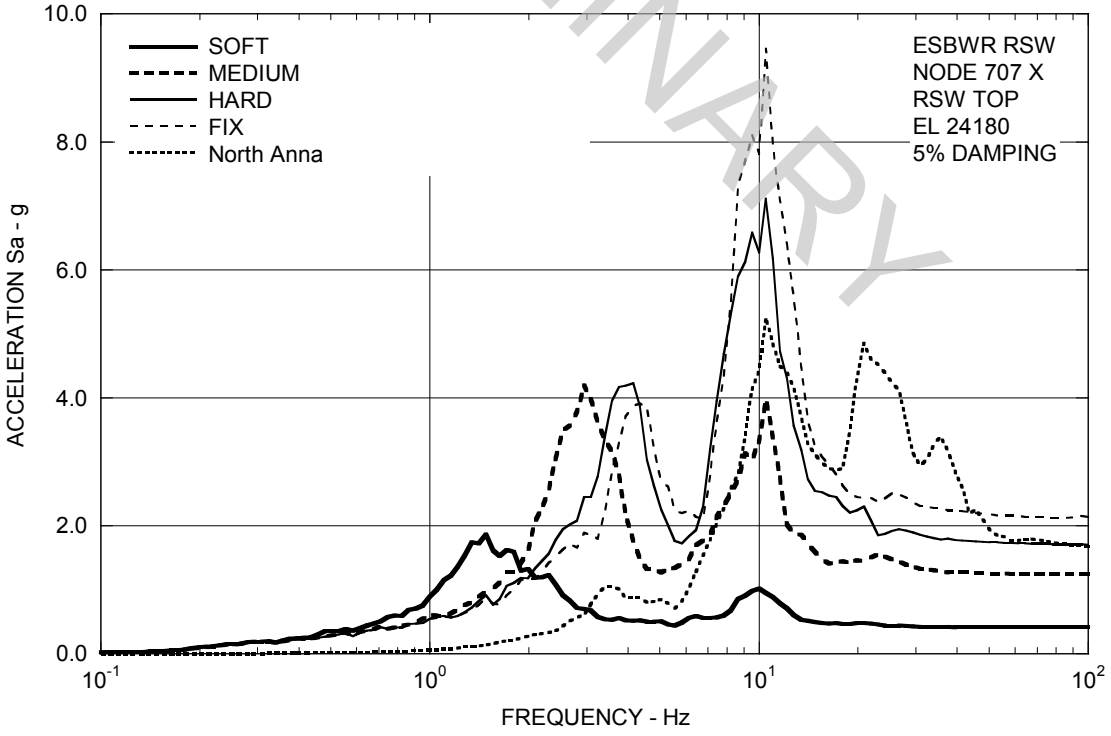

Figure 3A.8.1-1d. FRS (Effect of Soil Stiffness) – RSW Top X

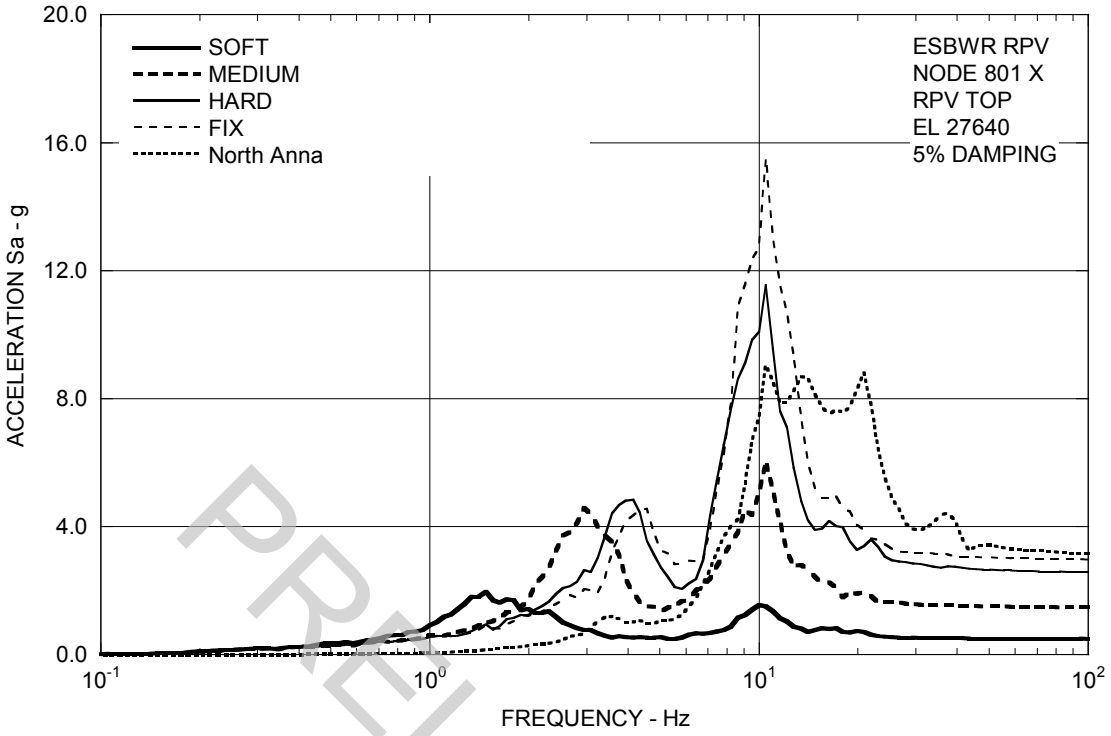

Figure 3A.8.1-1e. FRS (Effect of Soil Stiffness) – RPV Top X

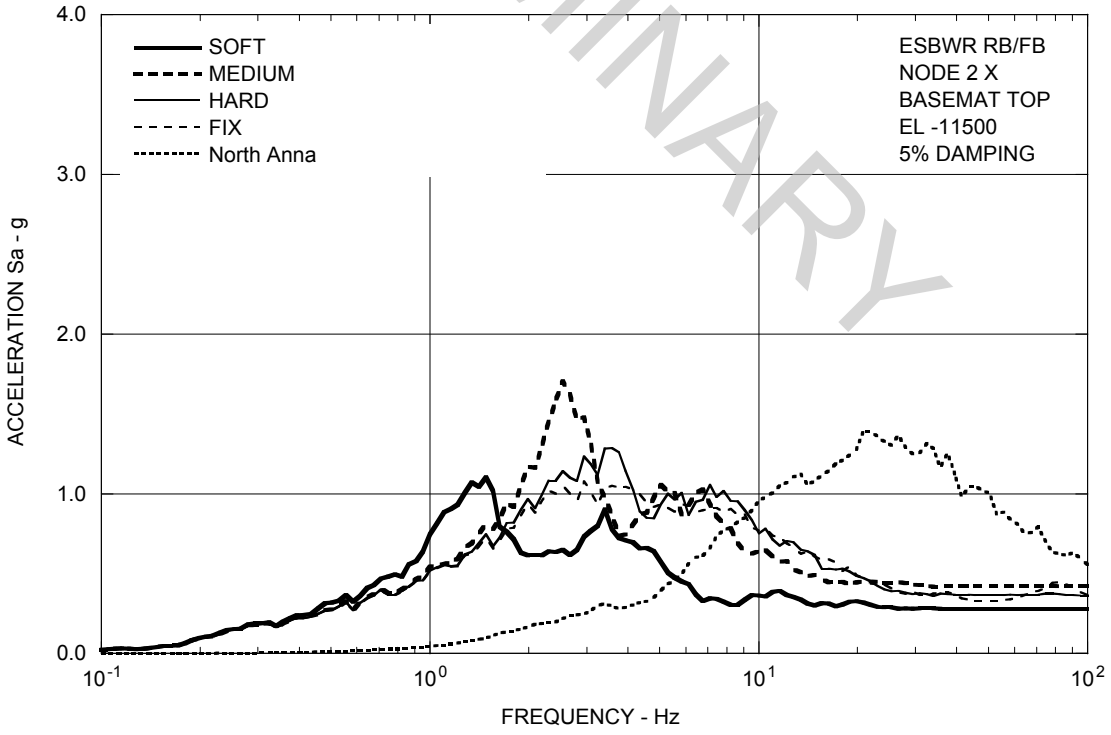

Figure 3A.8.1-1f. FRS (Effect of Soil Stiffness) – RB/FB Basemat X

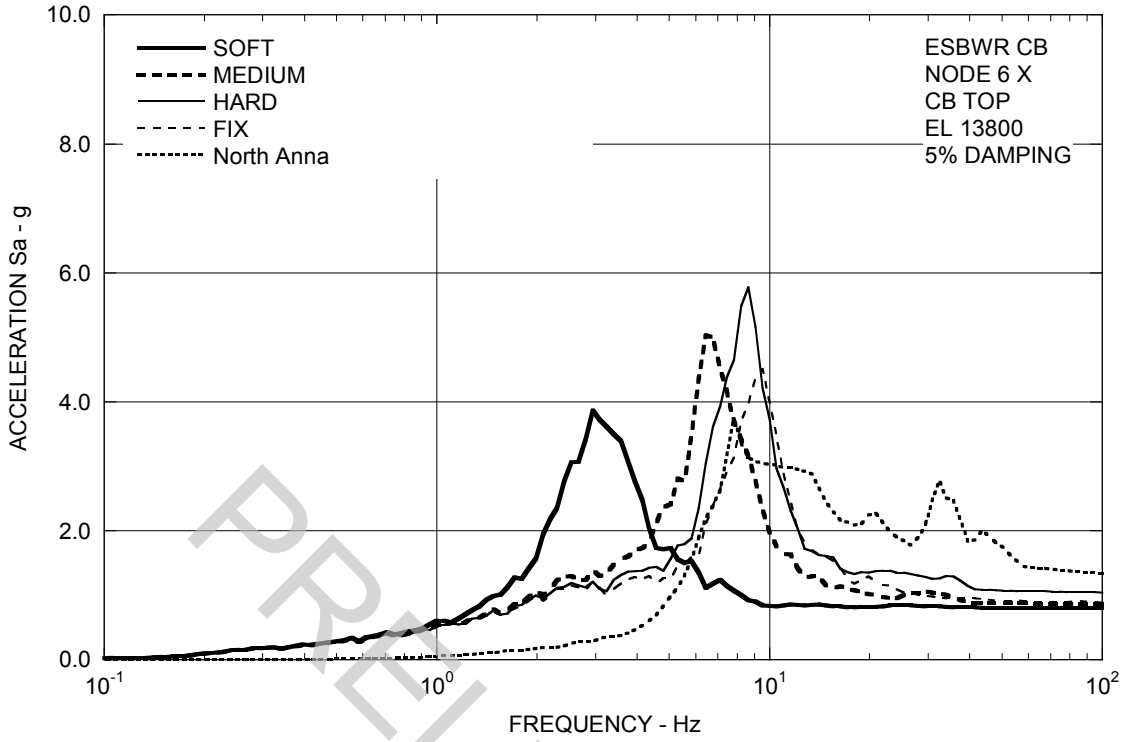

Figure 3A.8.1-1g. FRS (Effect of Soil Stiffness) – CB Top X

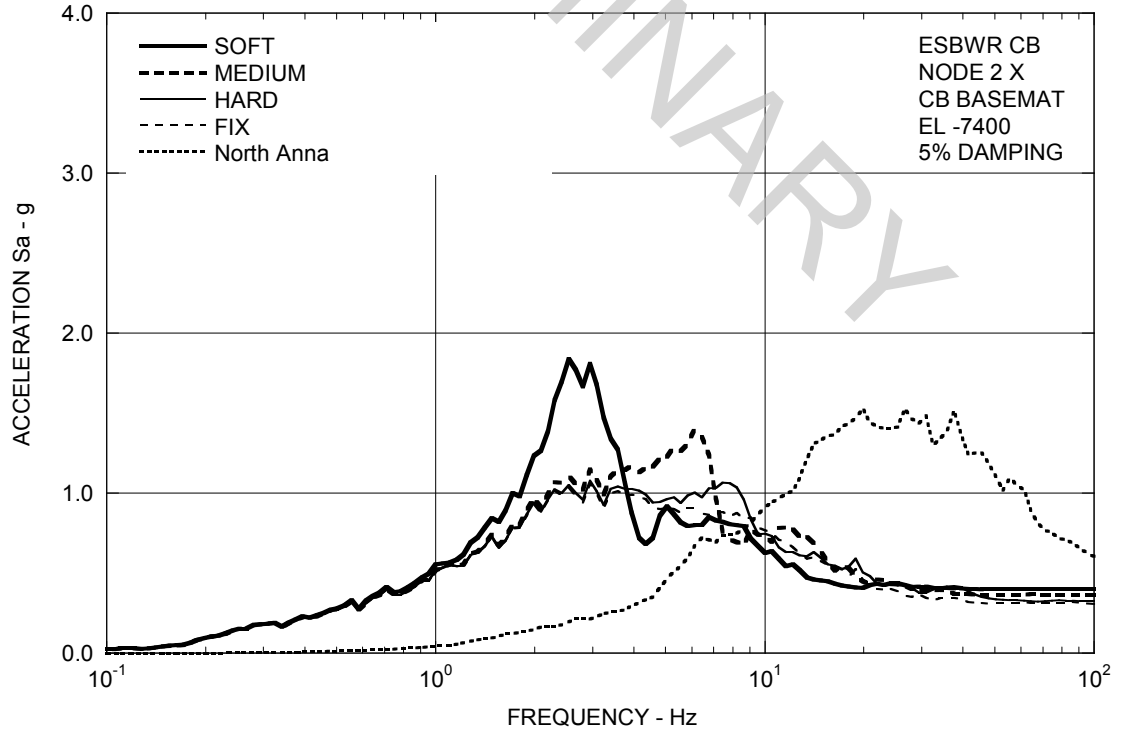

Figure 3A.8.1-1h. FRS (Effect of Soil Stiffness) – CB Basemat X

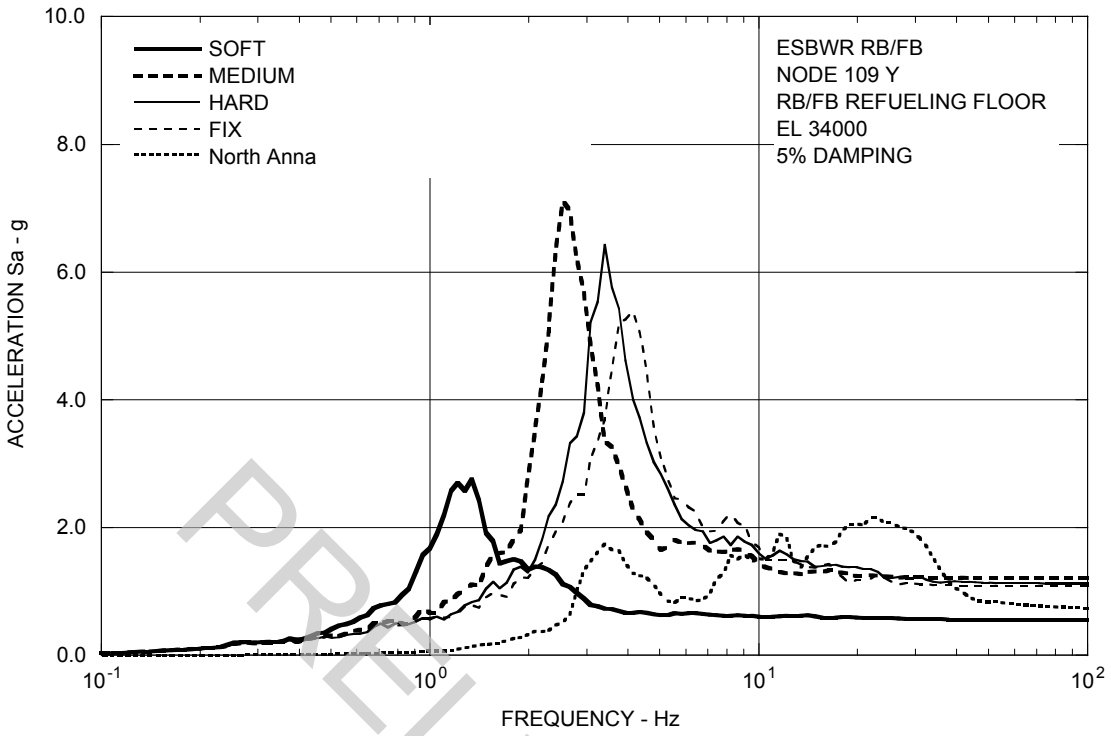

Figure 3A.8.1-2a. FRS (Effect of Soil Stiffness) – RB/FB Refueling Floor Y

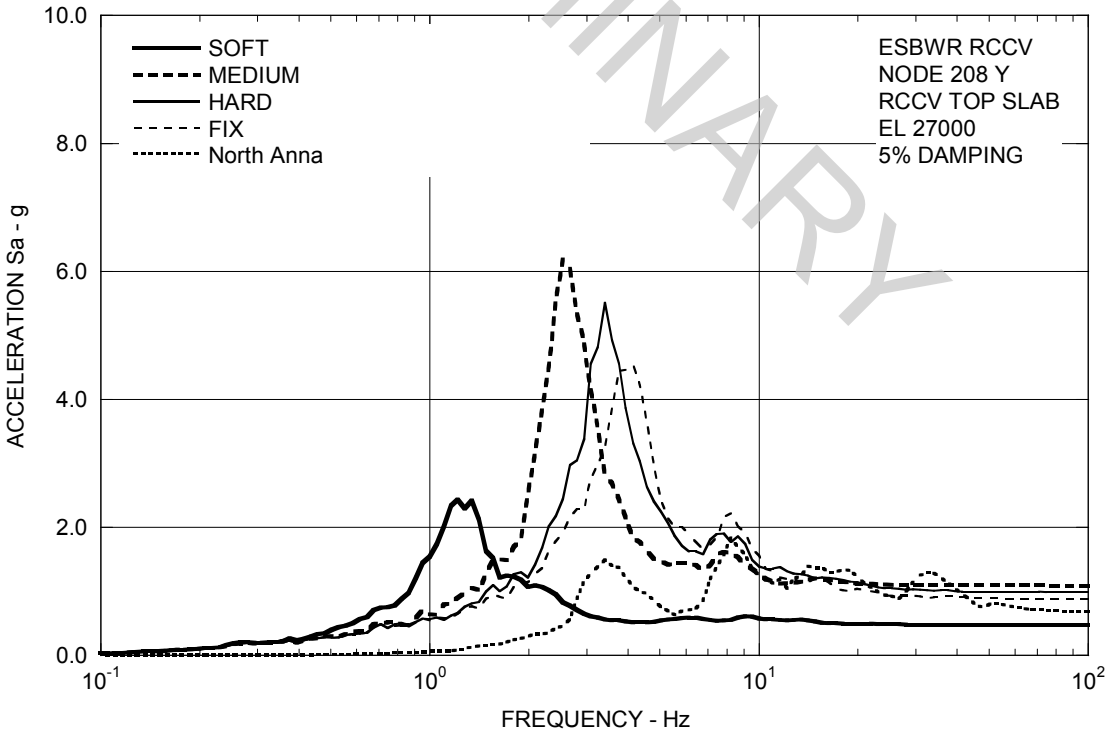

Figure 3A.8.1-2b. FRS (Effect of Soil Stiffness) – RCCV Top Slab Y

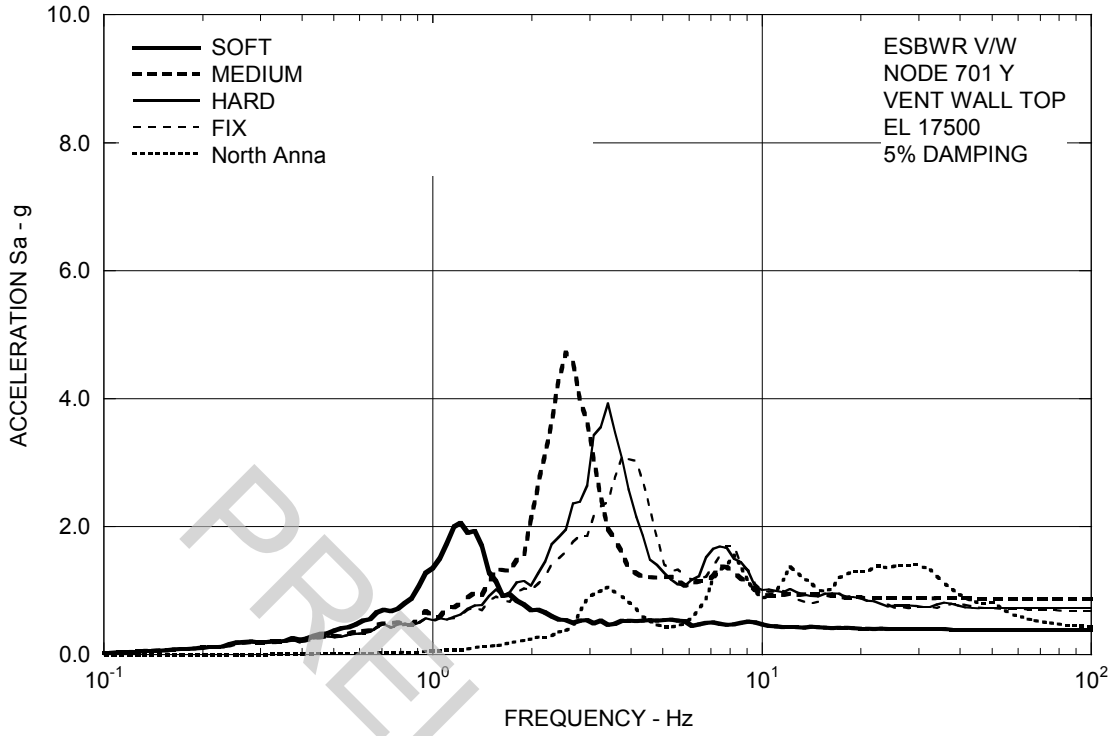

Figure 3A.8.1-2c. FRS (Effect of Soil Stiffness) – Vent Wall Top Y

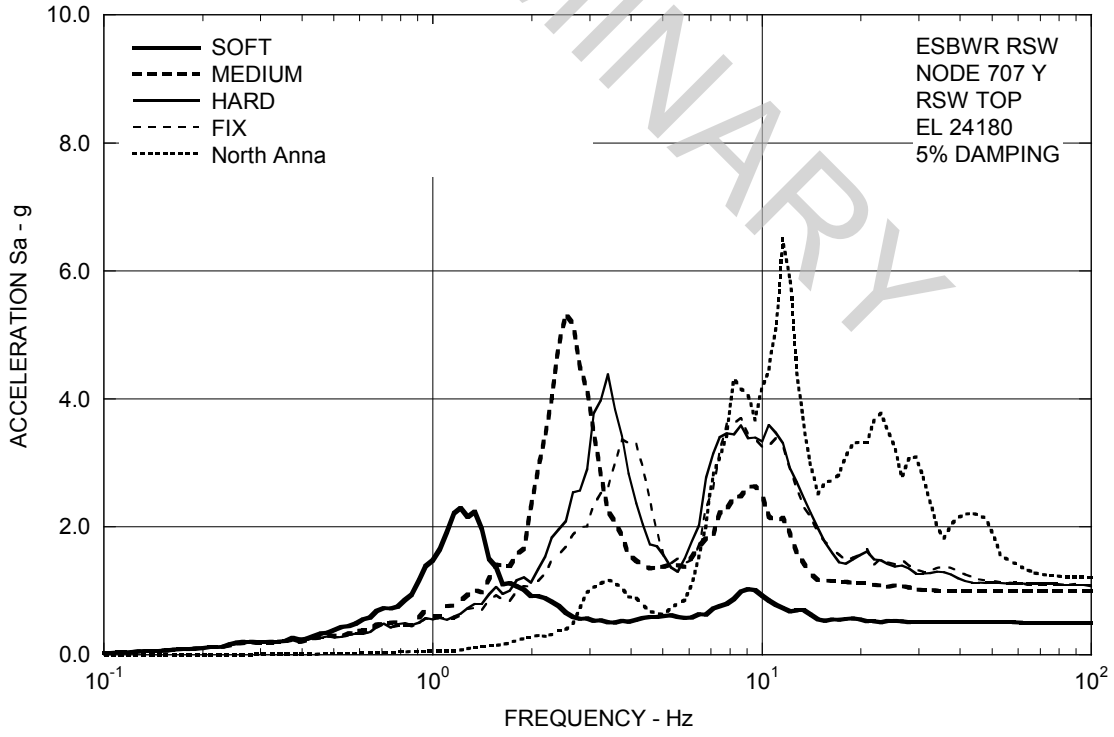

Figure 3A.8.1-2d. FRS (Effect of Soil Stiffness) – RSW Top Y

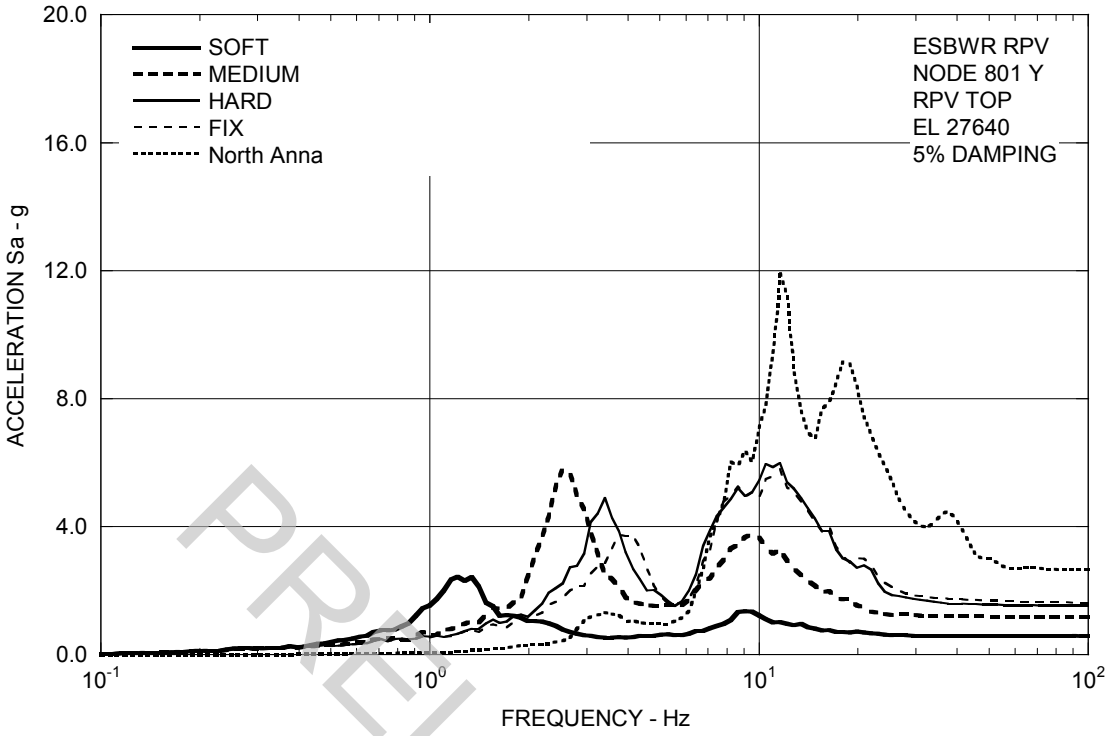

Figure 3A.8.1-2e. FRS (Effect of Soil Stiffness) – RPV Top Y

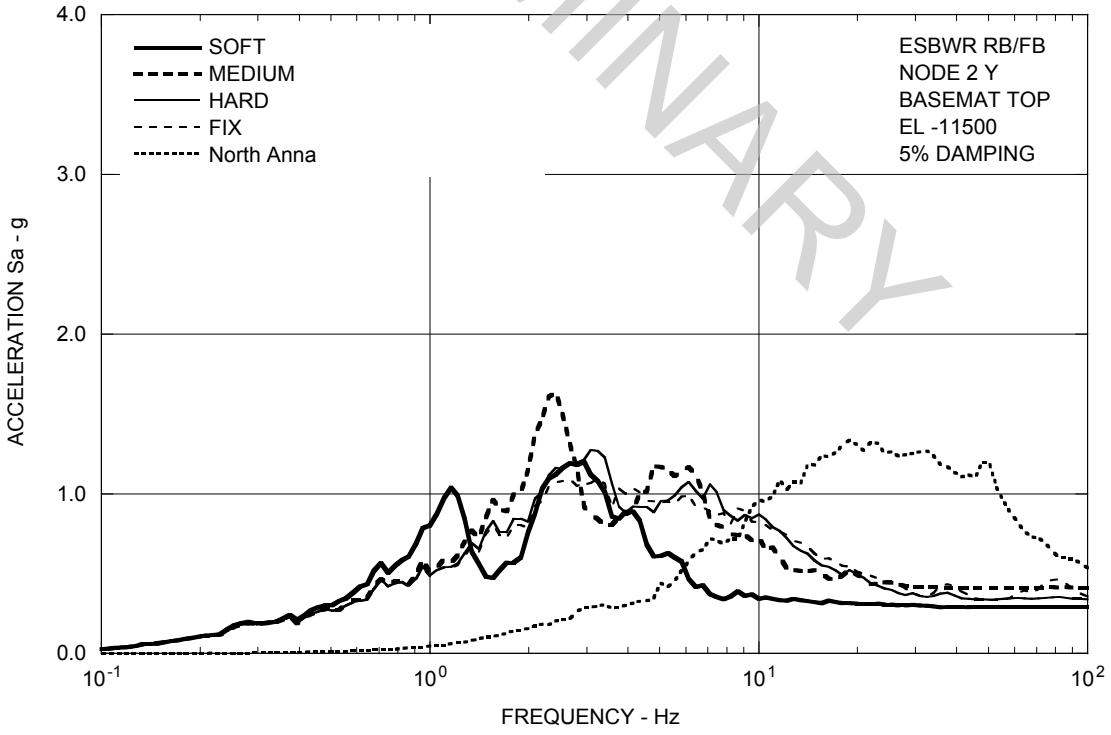

Figure 3A.8.1-2f. FRS (Effect of Soil Stiffness) – RB/FB Basemat Y

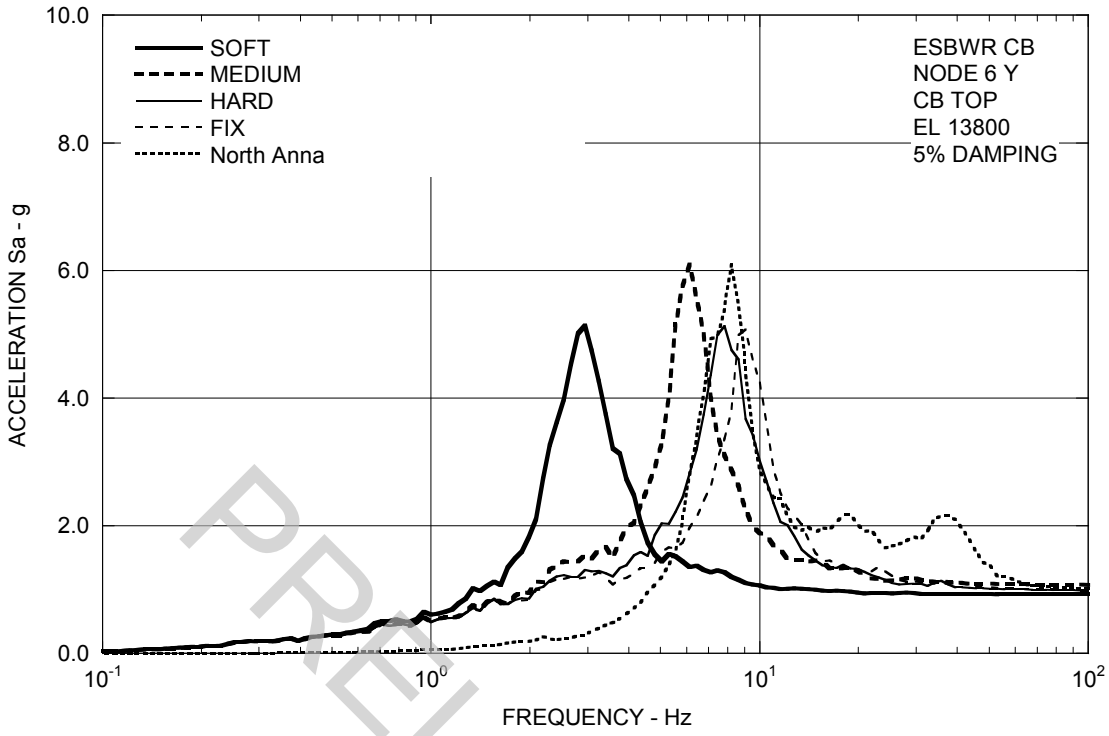

Figure 3A.8.1-2g. FRS (Effect of Soil Stiffness) – CB Top Y

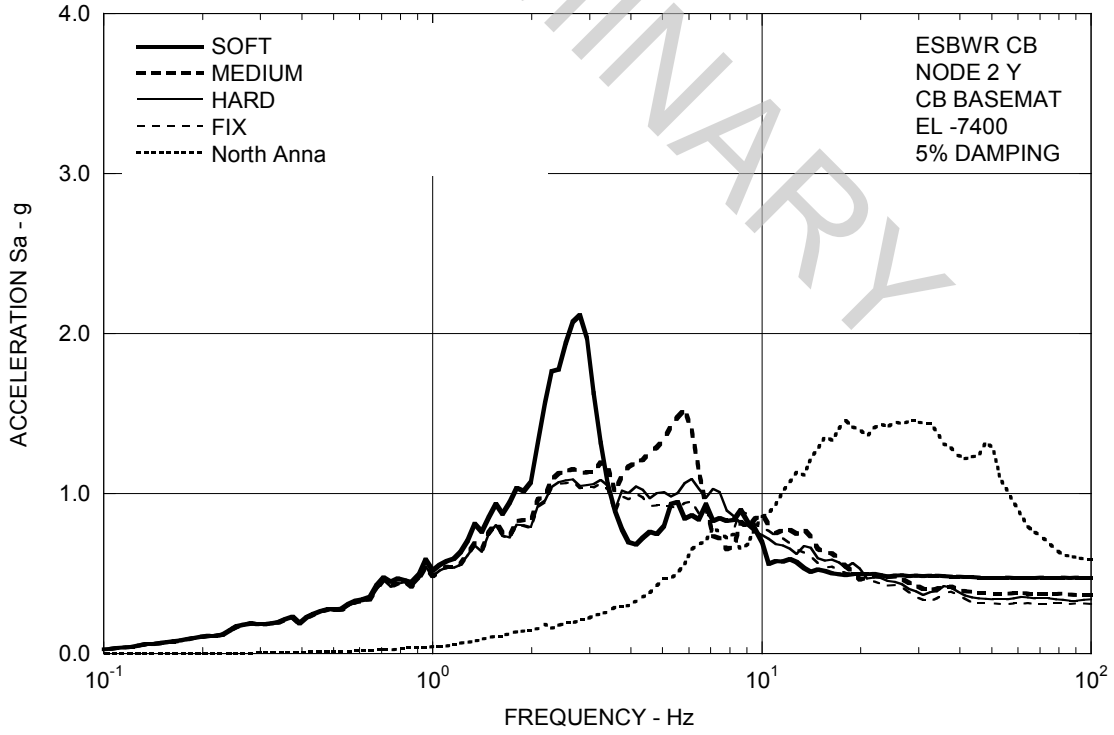

Figure 3A.8.1-2h. FRS (Effect of Soil Stiffness) – CB Basemat Y

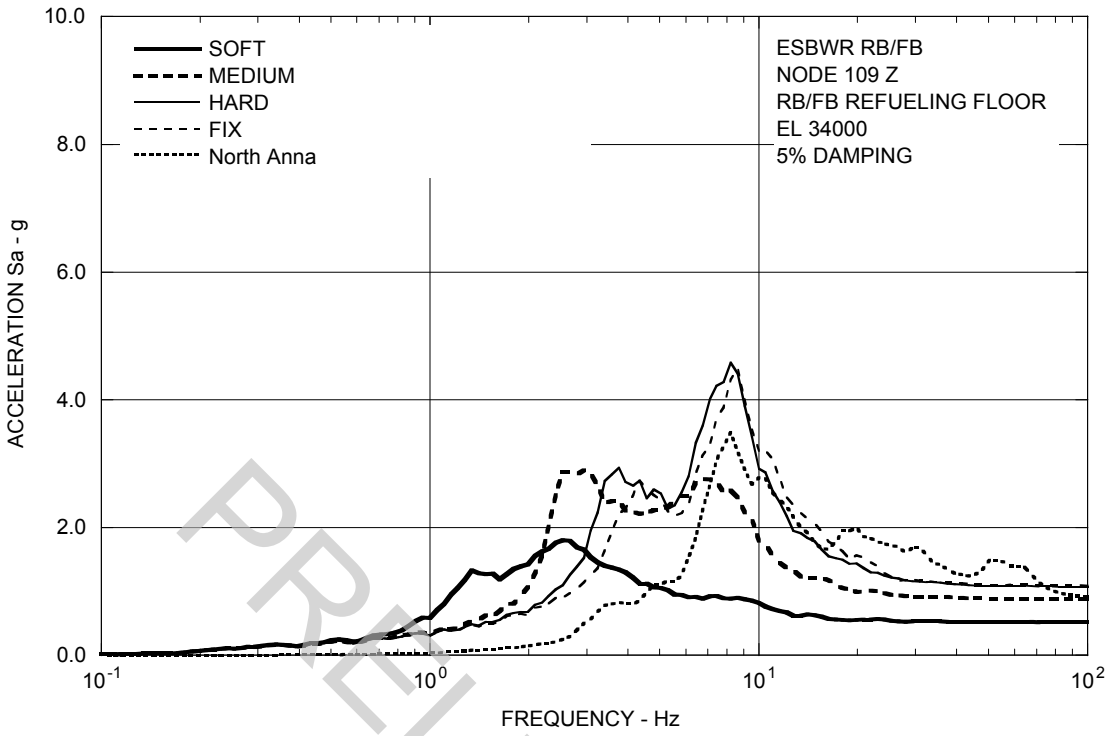

Figure 3A.8.1-3a. FRS (Effect of Soil Stiffness) – RB/FB Refueling Floor Z

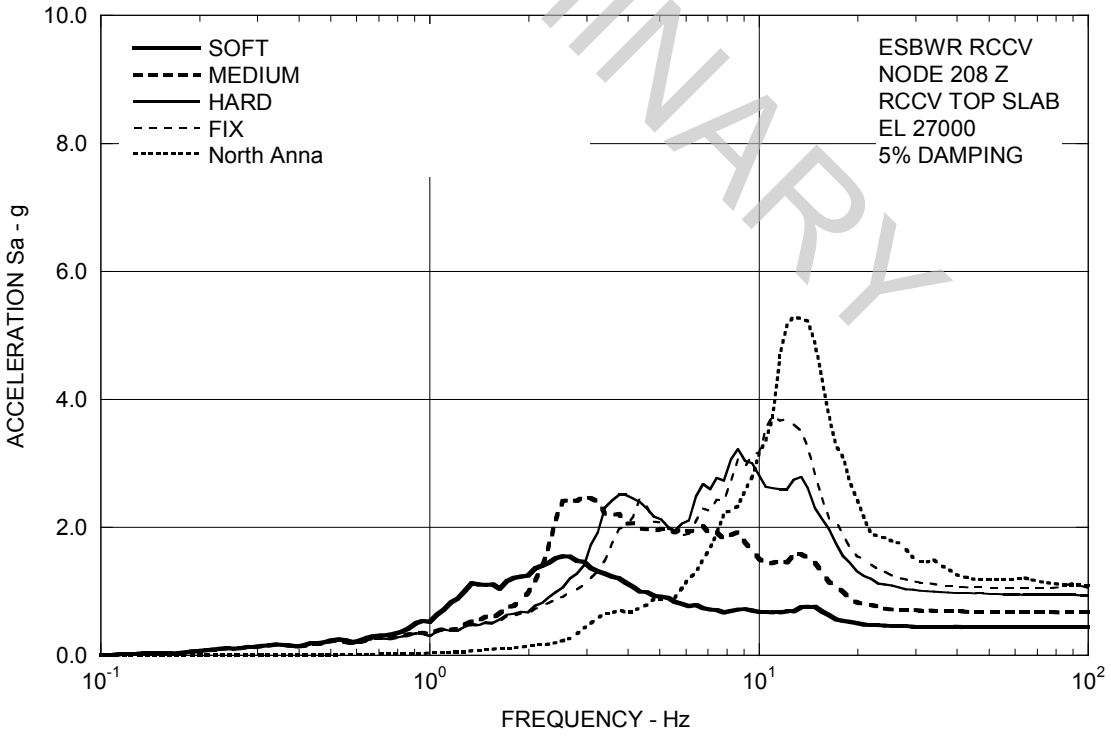

Figure 3A.8.1-3b. FRS (Effect of Soil Stiffness) – RCCV Top Slab Z

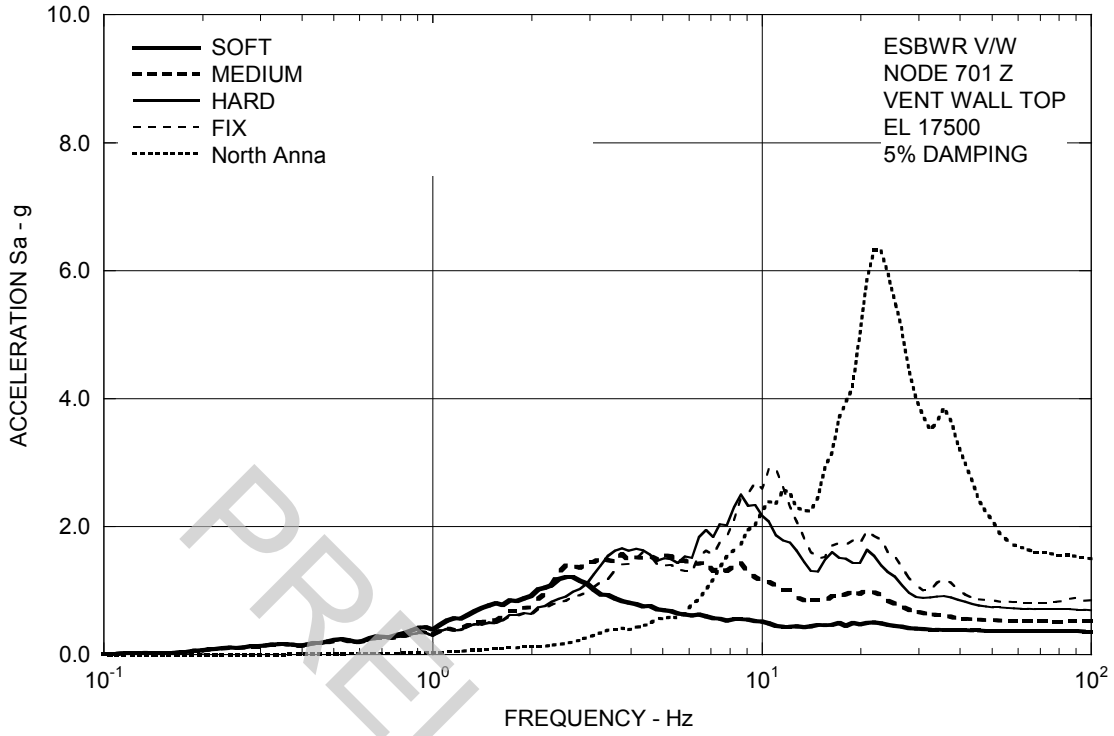

Figure 3A.8.1-3c. FRS (Effect of Soil Stiffness) – Vent Wall Top Z

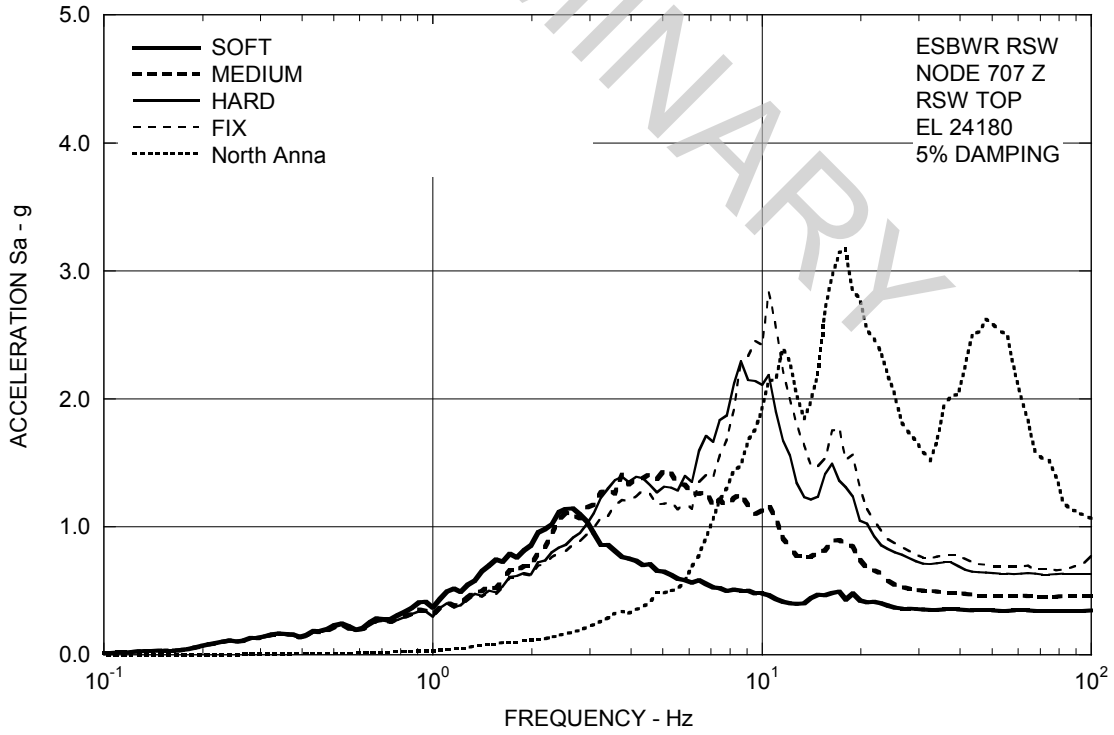

Figure 3A.8.1-3d. FRS (Effect of Soil Stiffness) – RSW Top Z

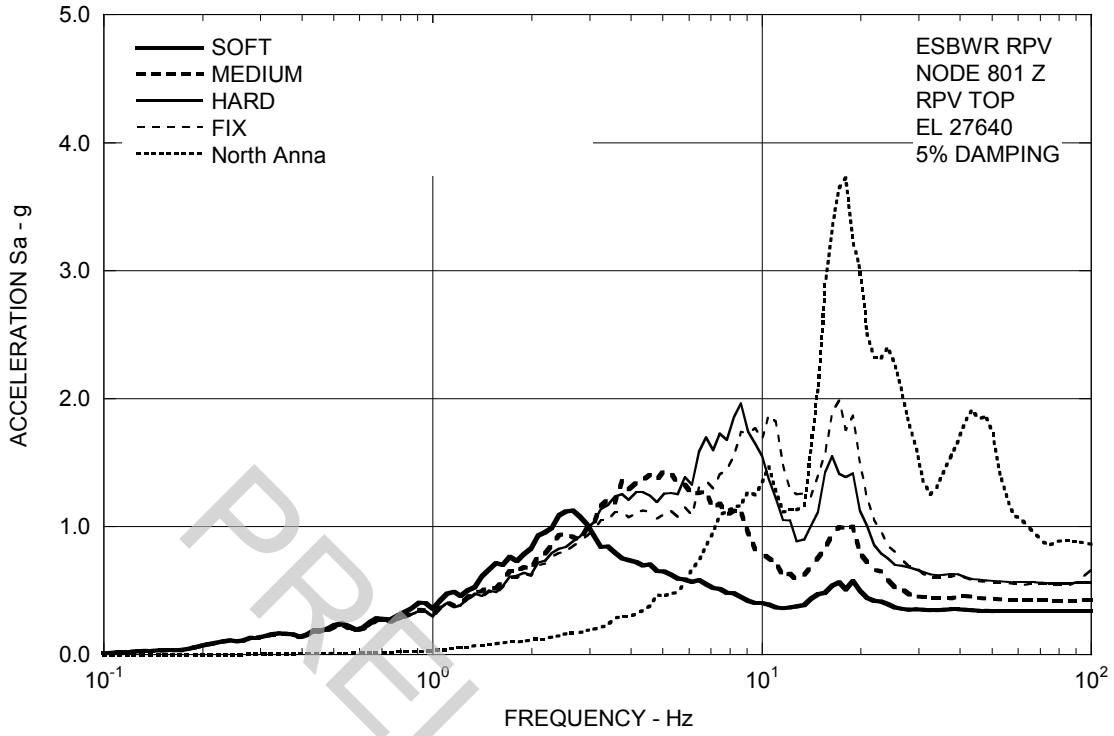

Figure 3A.8.1-3e. FRS (Effect of Soil Stiffness) – RPV Top Z

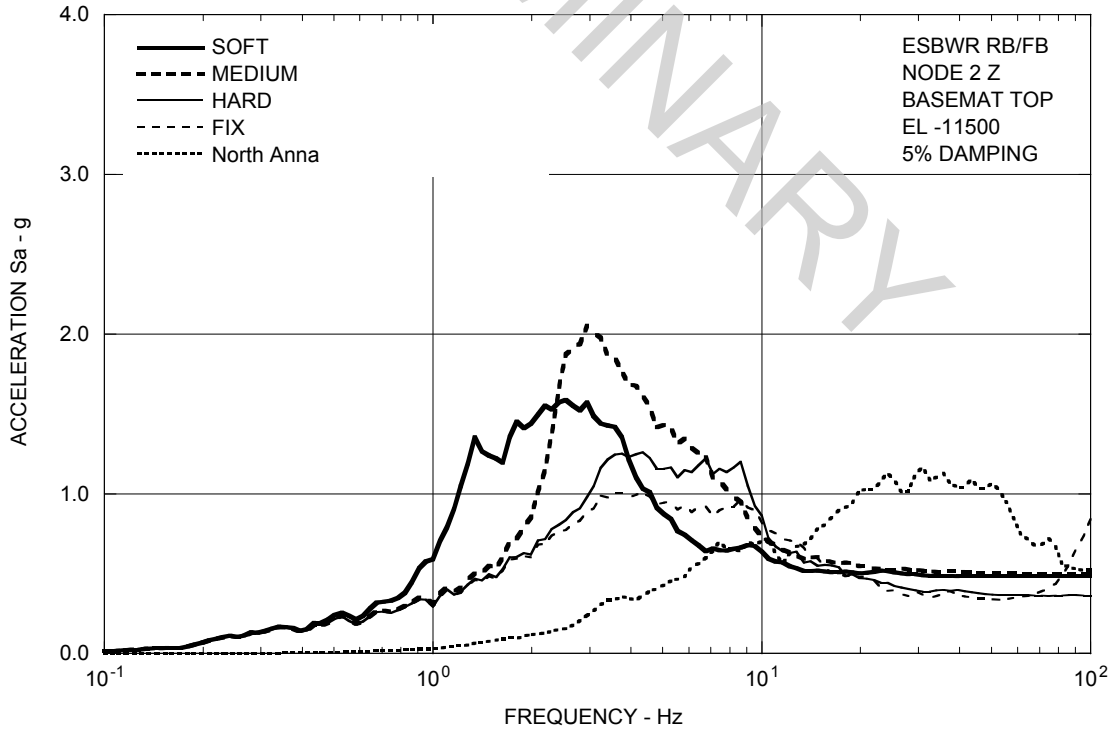

Figure 3A.8.1-3f. FRS (Effect of Soil Stiffness) – RB/FB Basemat Z

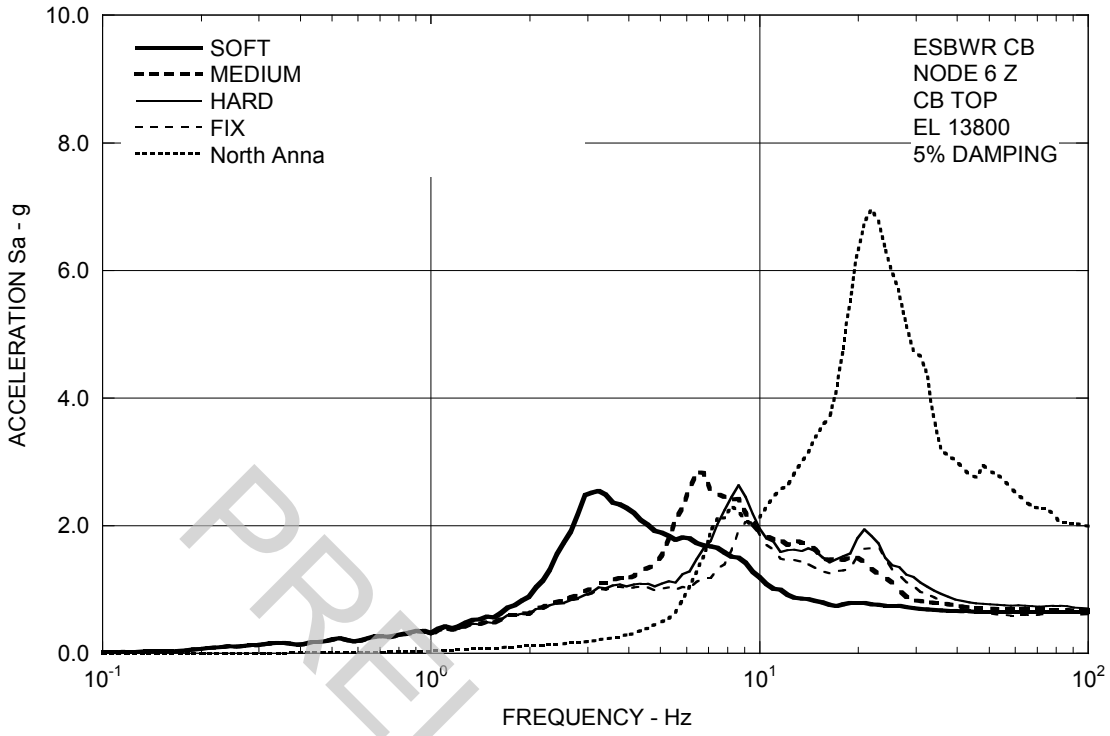

Figure 3A.8.1-3g. FRS (Effect of Soil Stiffness) – CB Top Z

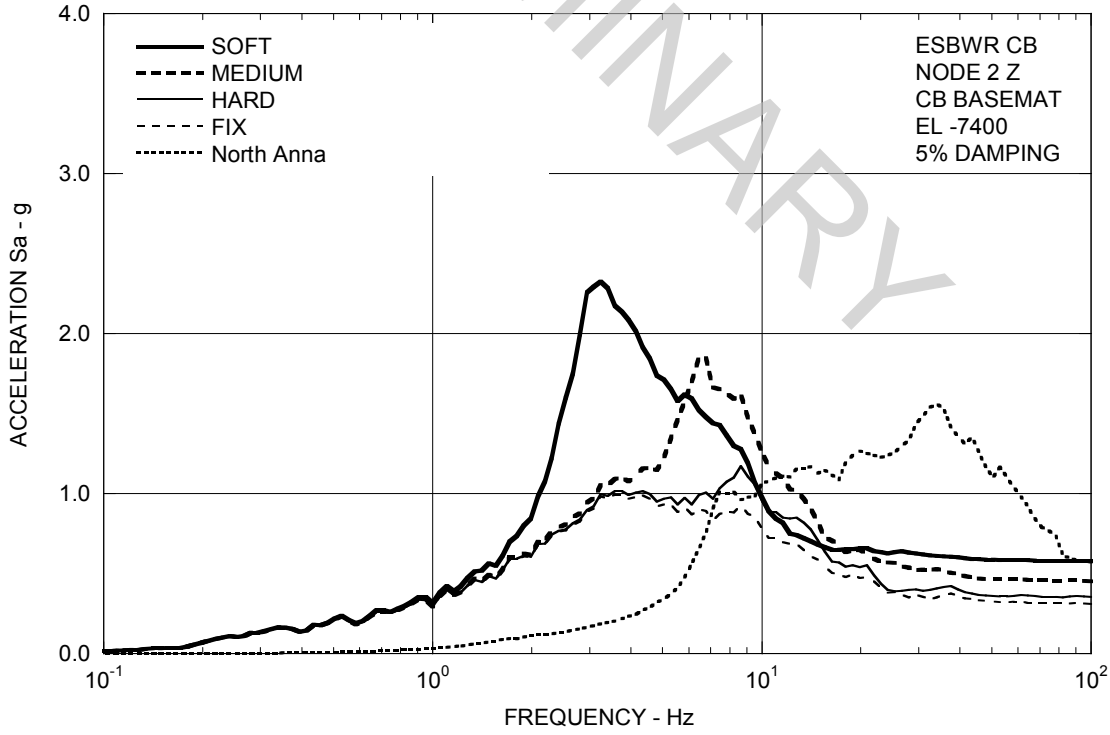

Figure 3A.8.1-3h. FRS (Effect of Soil Stiffness) – CB Basemat Z

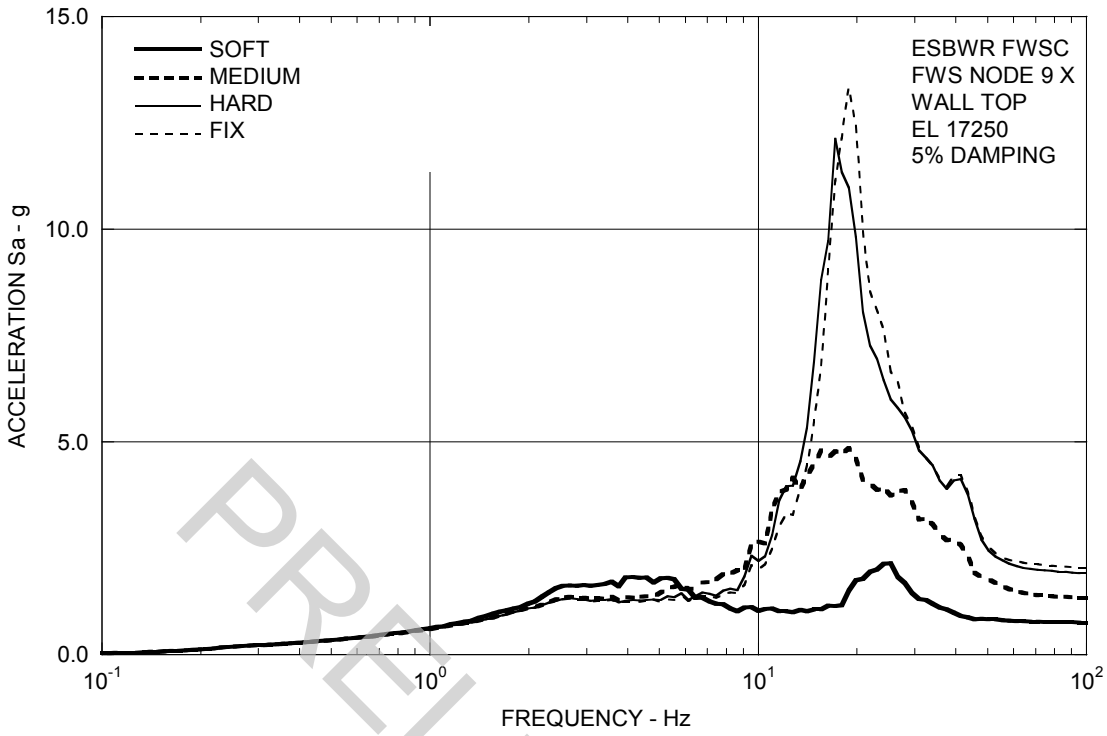

Figure 3A.8.1-4a. FRS (Effect of Soil Stiffness) – FWS Wall Top X

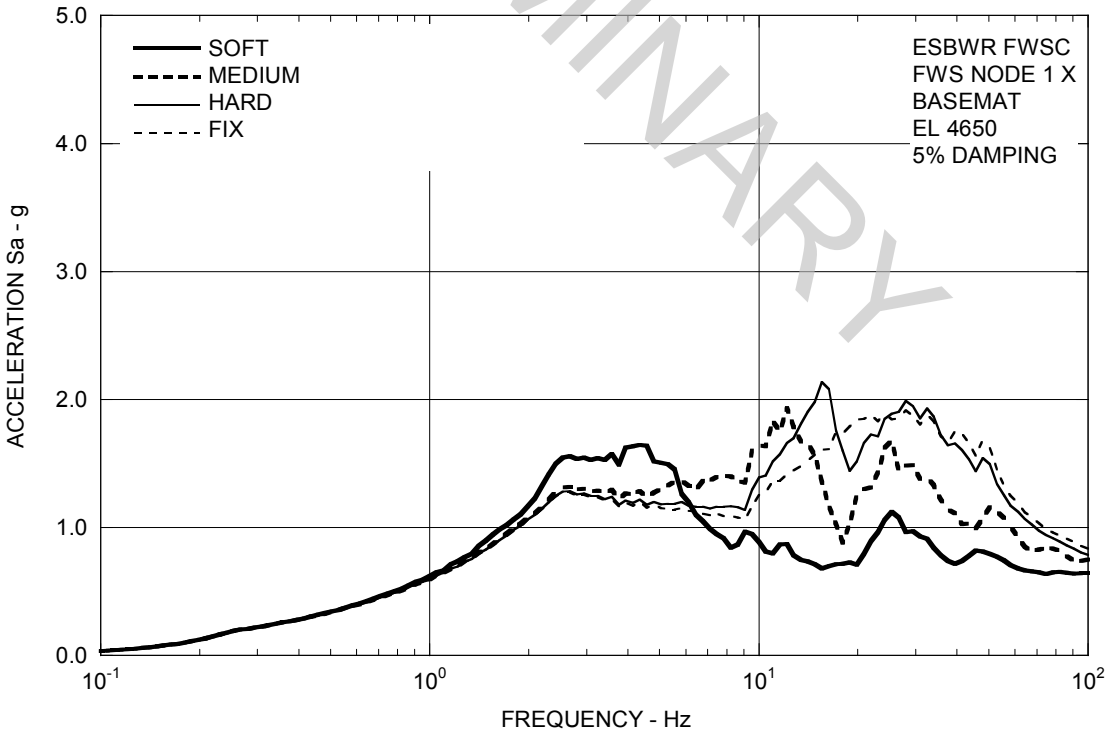

Figure 3A.8.1-4b. FRS (Effect of Soil Stiffness) – FWS Basemat X

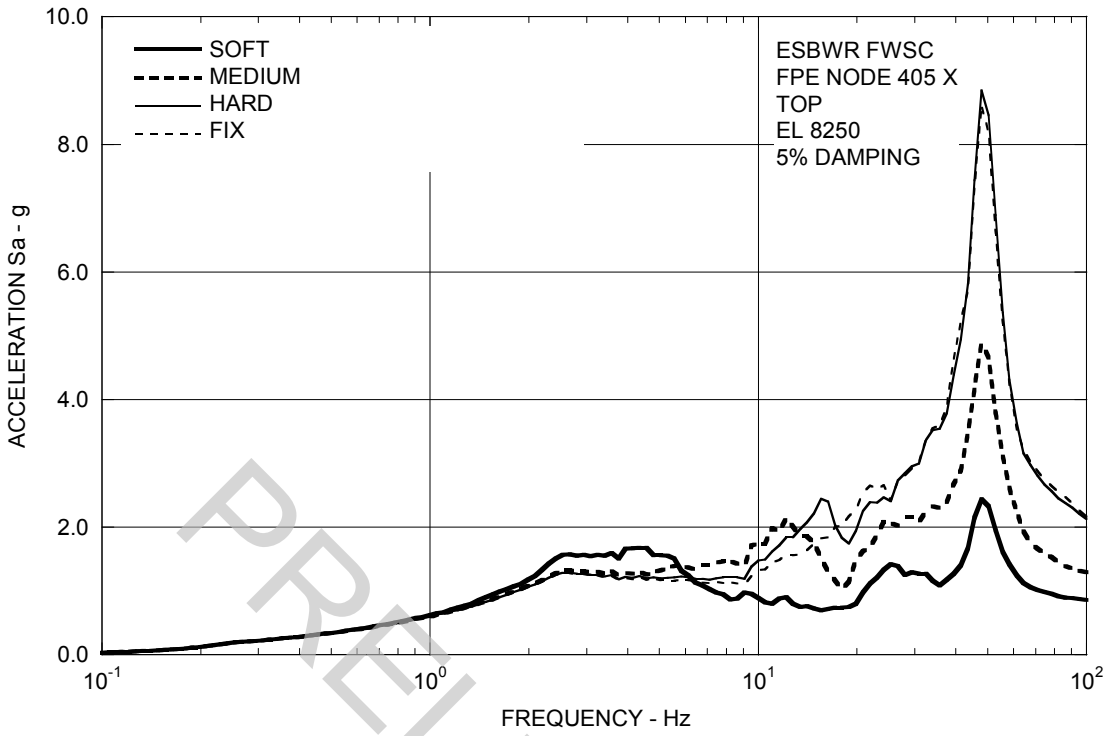

Figure 3A.8.1-4c. FRS (Effect of Soil Stiffness) – FPE Top X

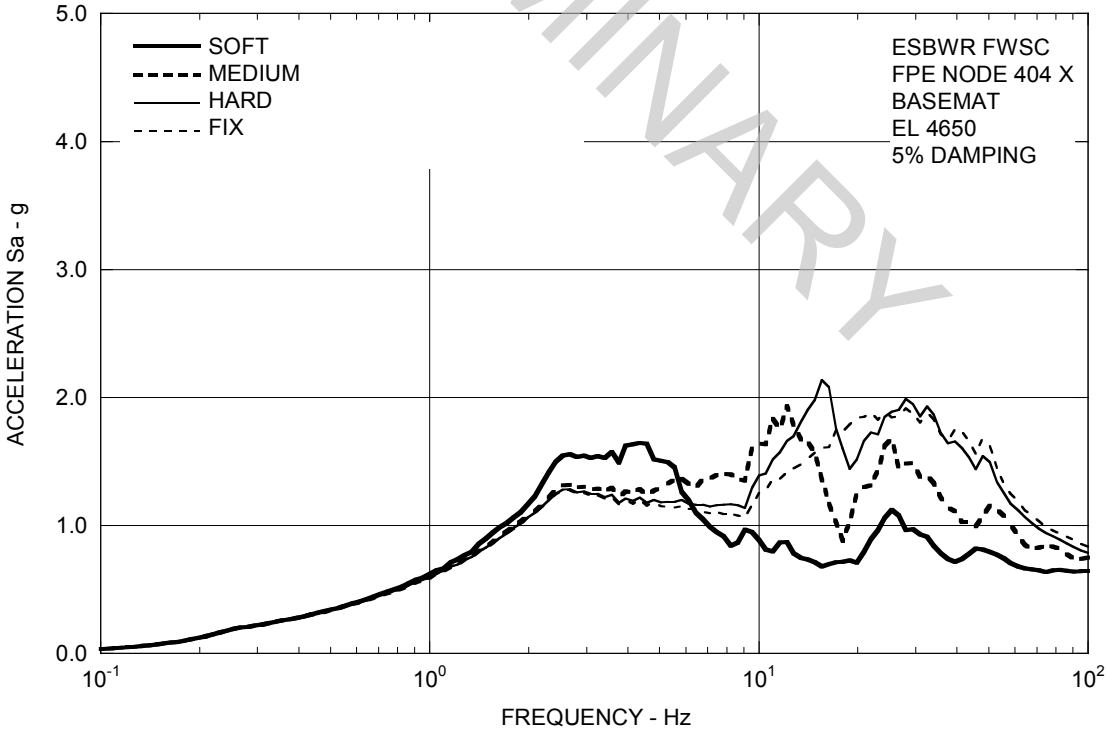

Figure 3A.8.1-4d. FRS (Effect of Soil Stiffness) – FPE Basemat X

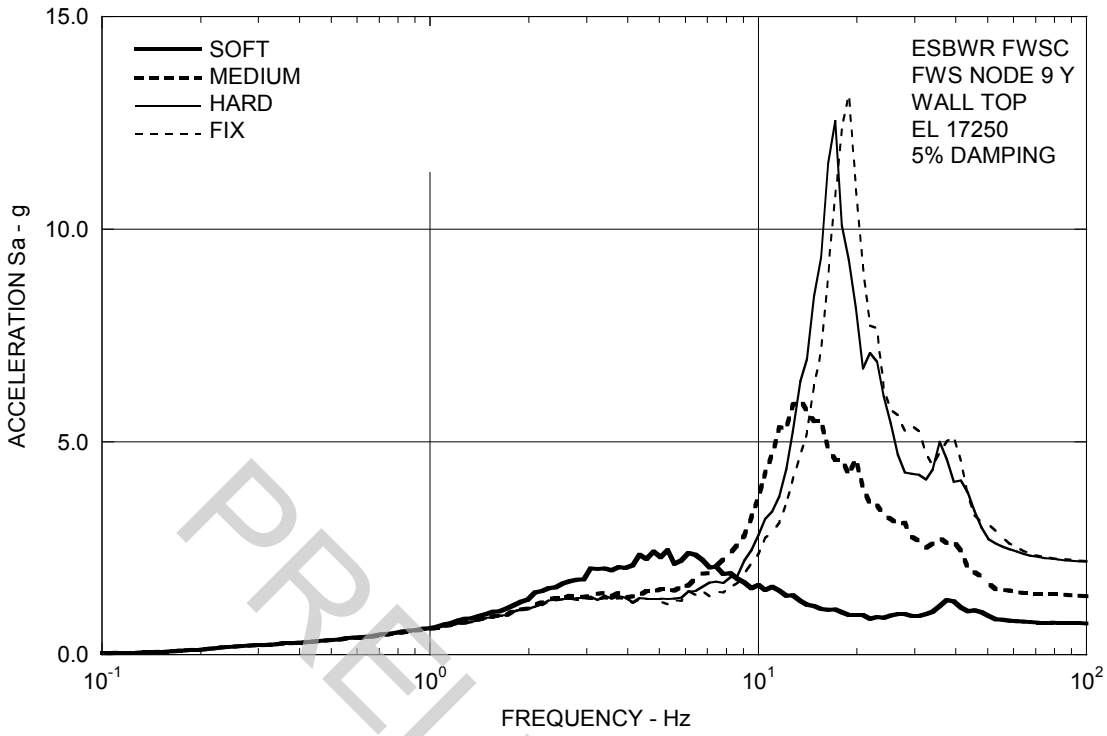

Figure 3A.8.1-5a. FRS (Effect of Soil Stiffness) – FWS Wall Top Y

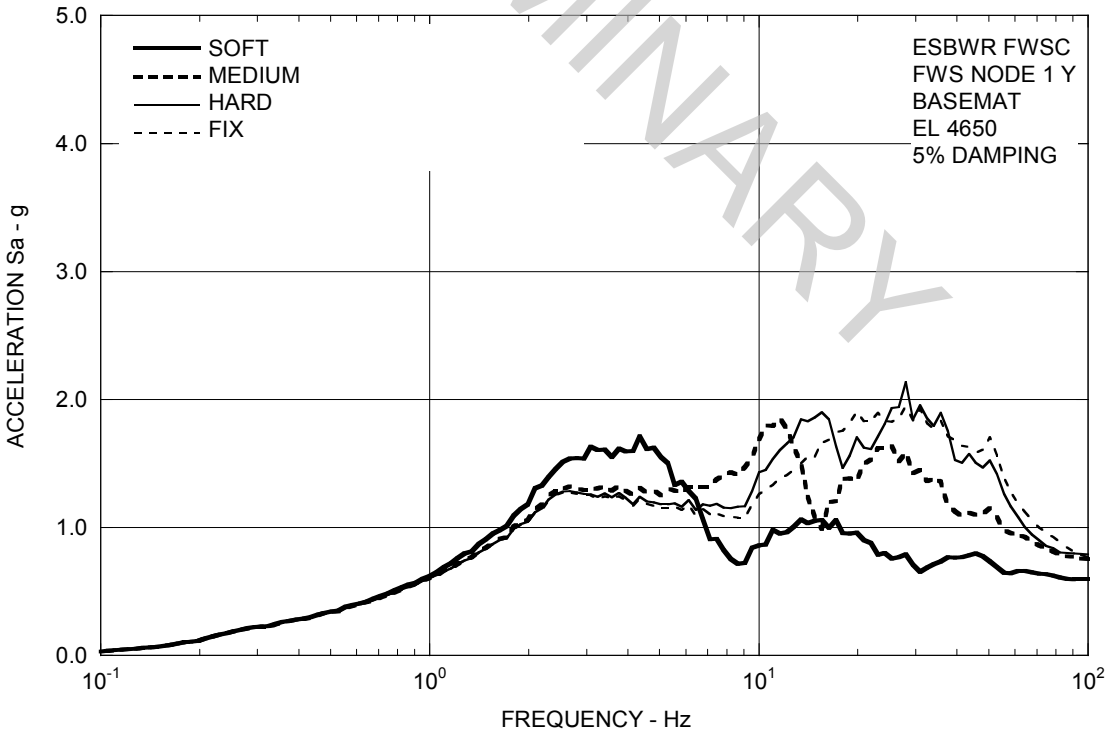

Figure 3A.8.1-5b. FRS (Effect of Soil Stiffness) – FWS Basemat Y

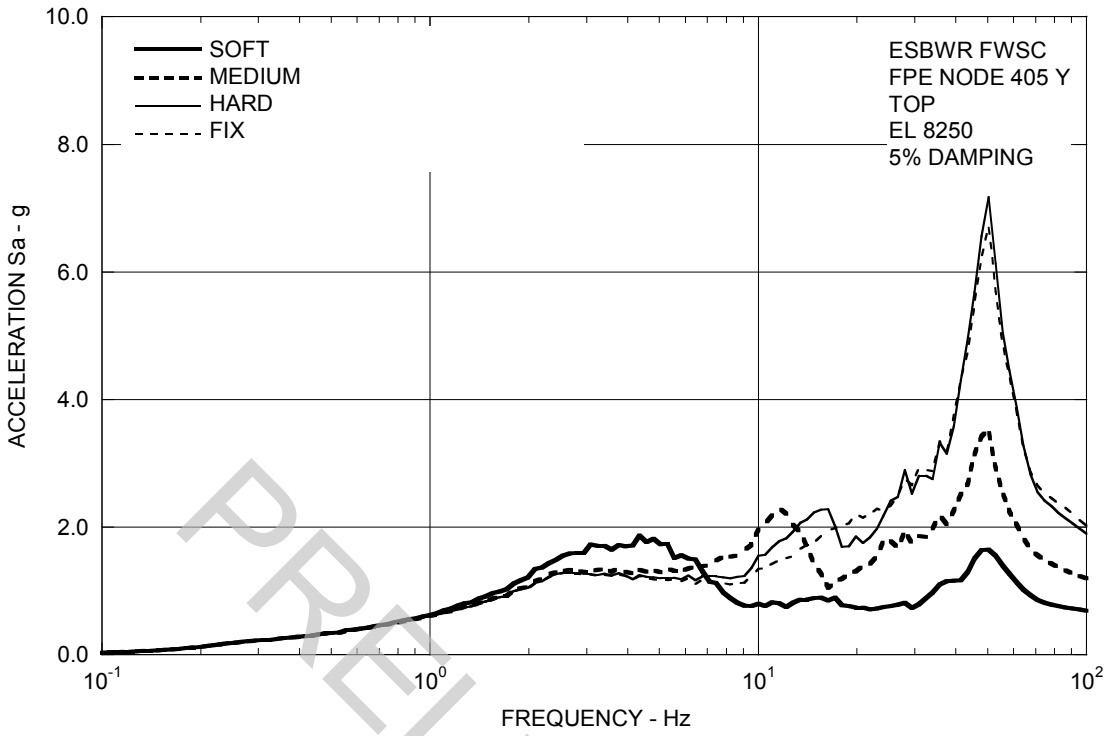

Figure 3A.8.1-5c. FRS (Effect of Soil Stiffness) – FPE Top Y

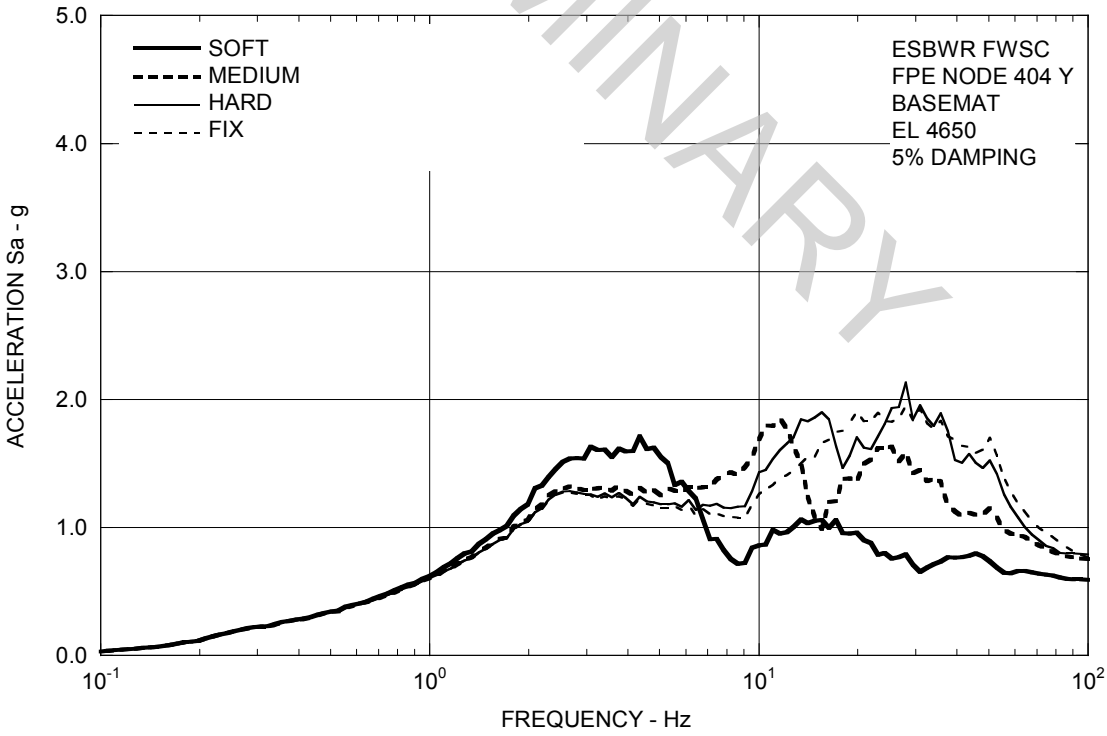

Figure 3A.8.1-5d. FRS (Effect of Soil Stiffness) – FPE Basemat Y

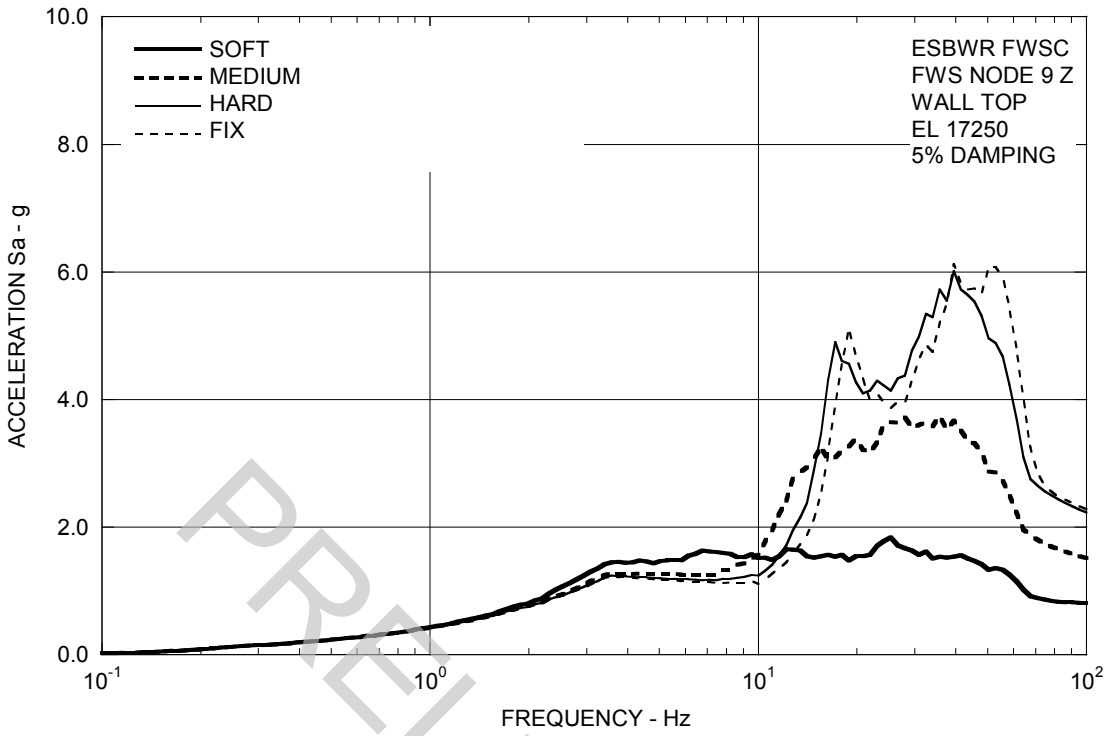

Figure 3A.8.1-6a. FRS (Effect of Soil Stiffness) – FWS Wall Top Z

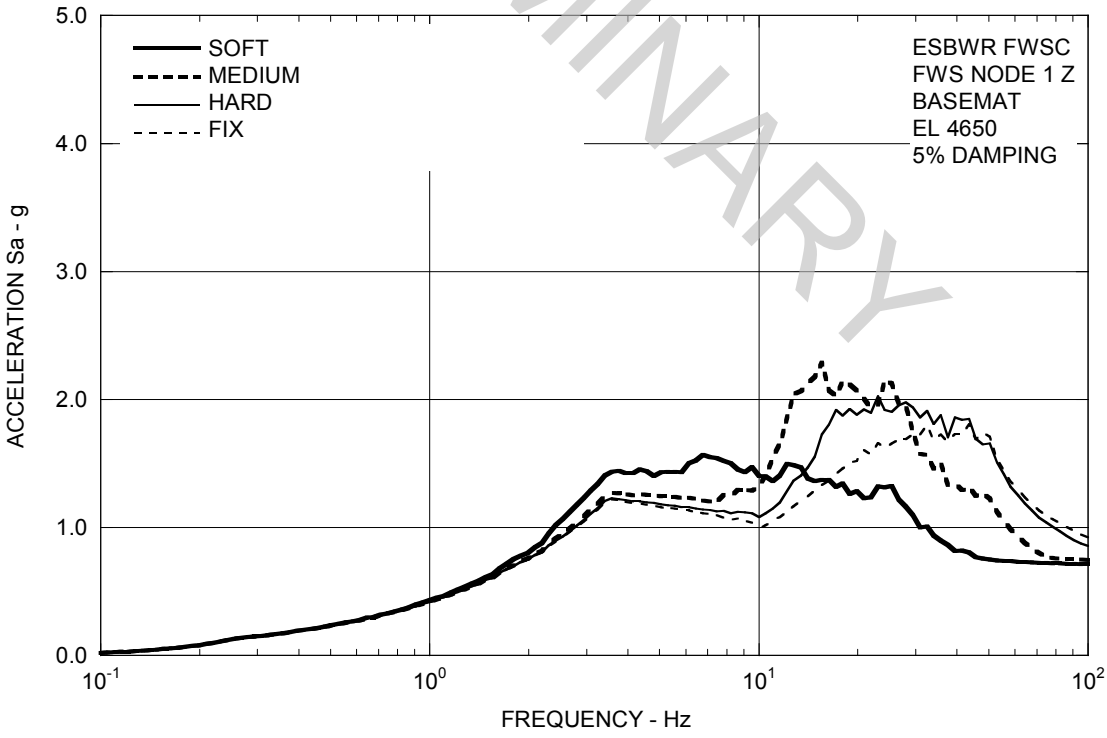

Figure 3A.8.1-6b. FRS (Effect of Soil Stiffness) – FWS Basemat Z

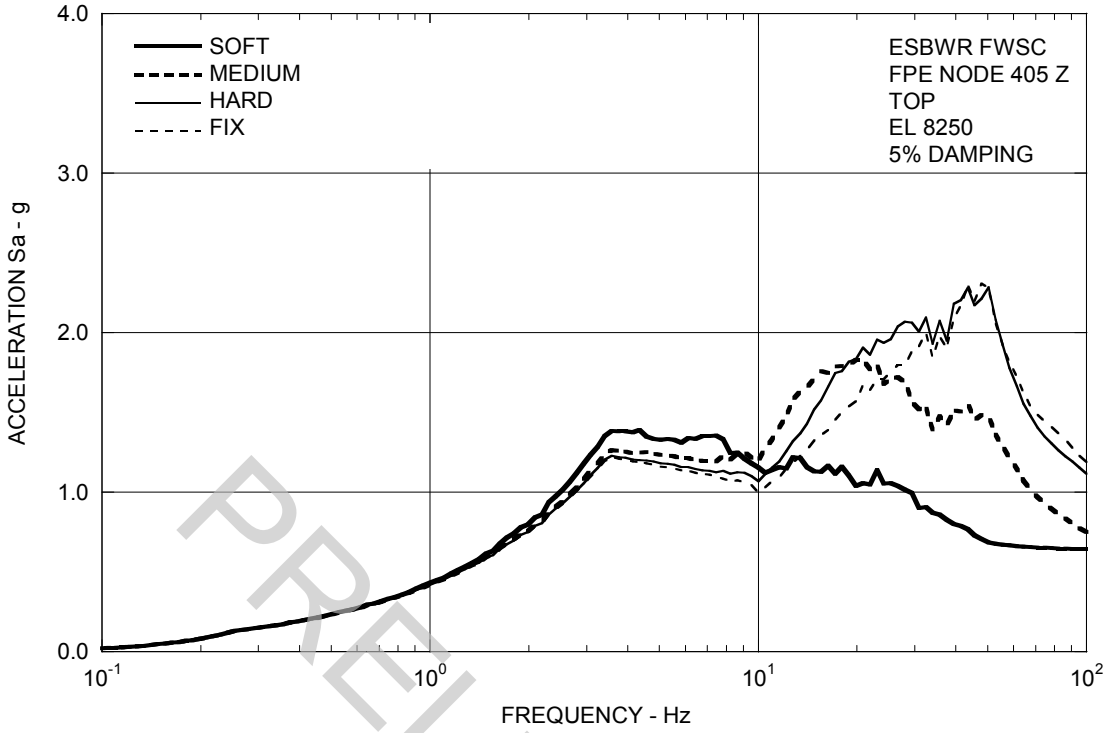

Figure 3A.8.1-6c. FRS (Effect of Soil Stiffness) – FPE Top Z

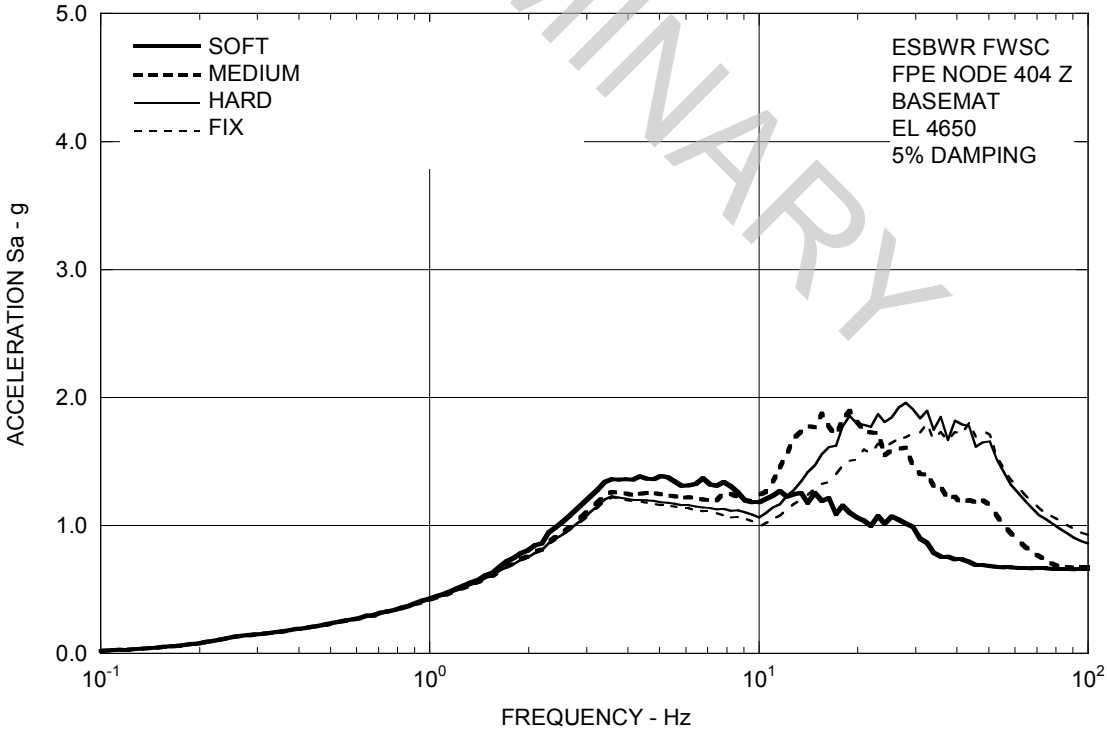

Figure 3A.8.1-6d. FRS (Effect of Soil Stiffness) – FPE Basemat Z

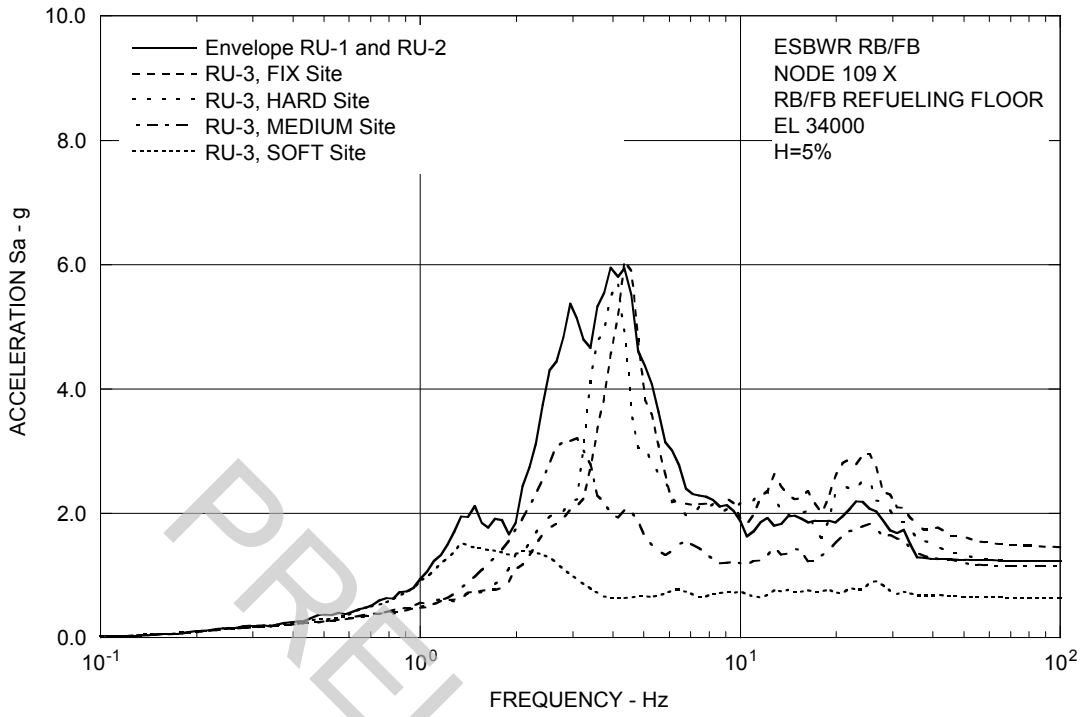

Figure 3A.8.2-1a. FRS (Effect of Single Envelope Ground Motion) – RB/FB Refueling Floor X

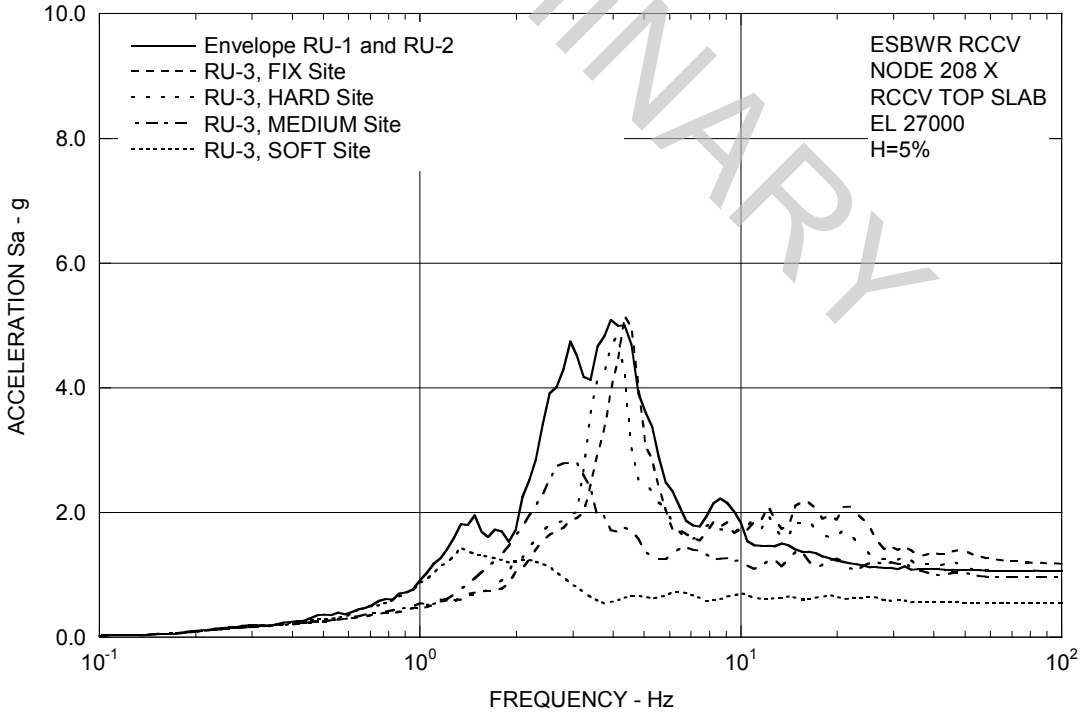

Figure 3A.8.2-1b. FRS (Effect of Single Envelope Ground Motion) – RCCV Top Slab X

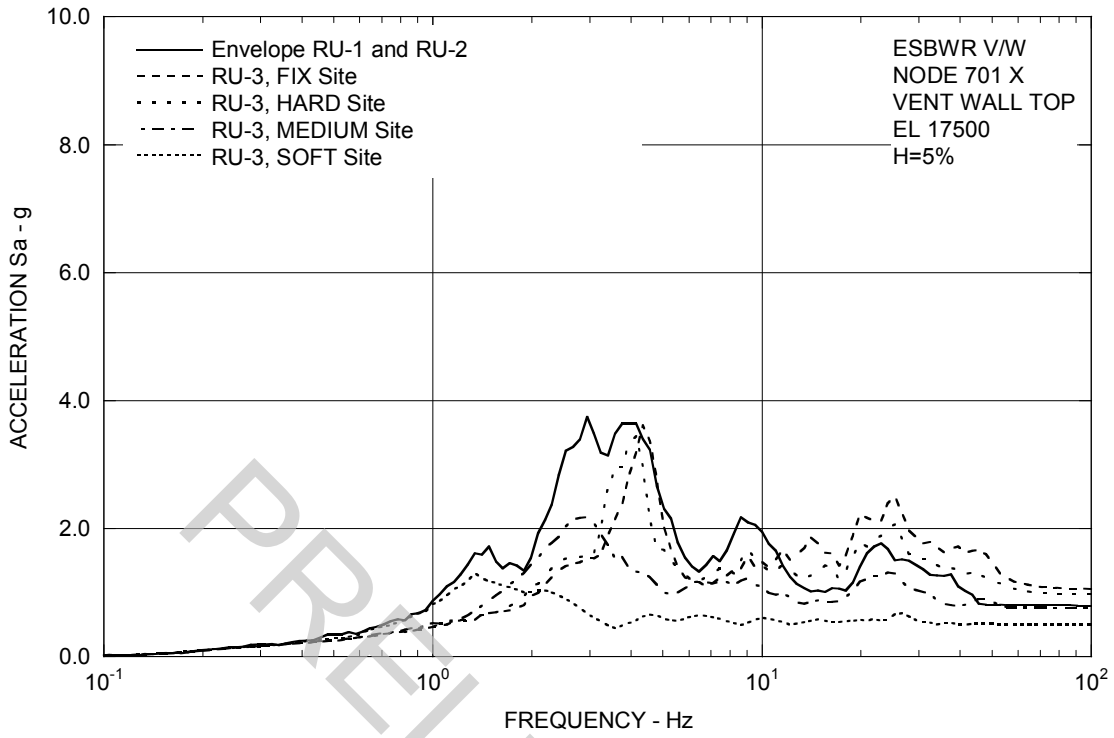

Figure 3A.8.2-1c. FRS (Effect of Single Envelope Ground Motion) – Vent Wall Top X

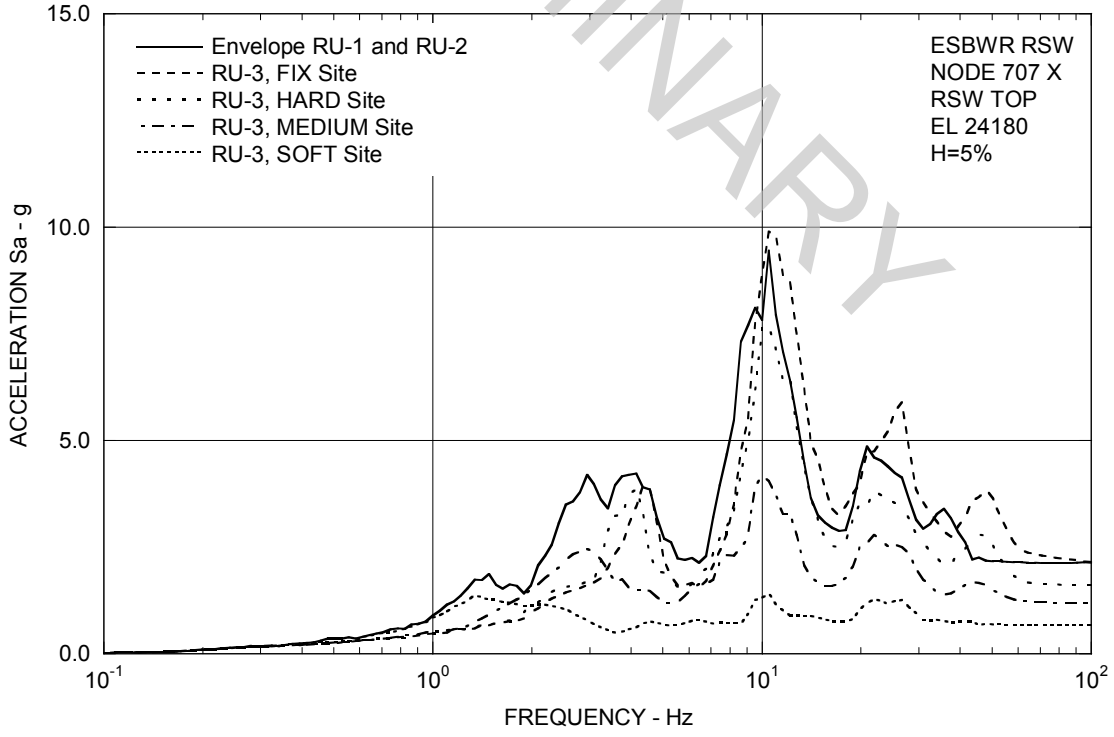

Figure 3A.8.2-1d. FRS (Effect of Single Envelope Ground Motion) – RSW Top X

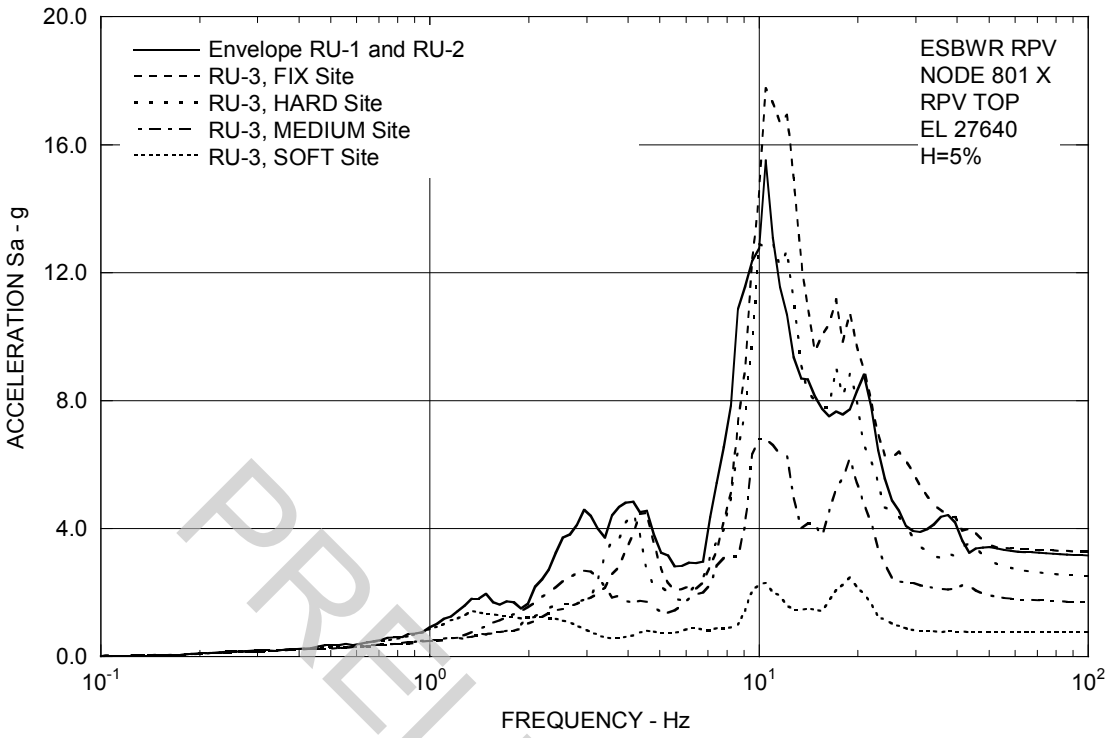

Figure 3A.8.2-1e. FRS (Effect of Single Envelope Ground Motion) – RPV Top X

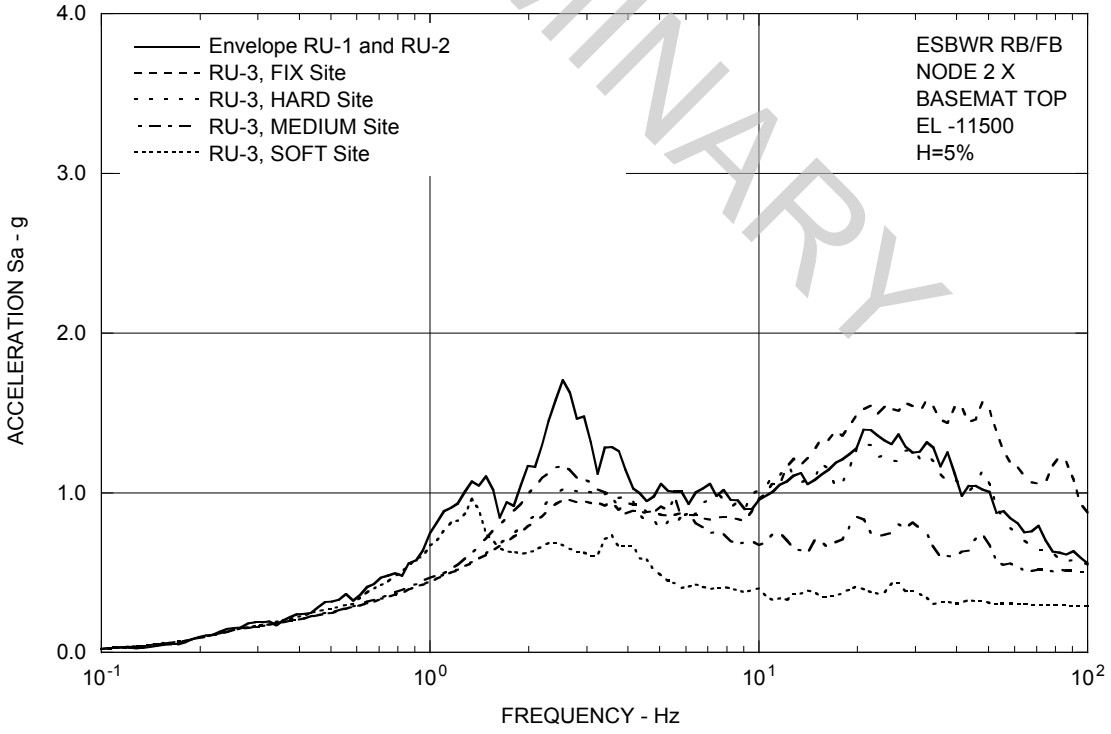

Figure 3A.8.2-1f. FRS (Effect of Single Envelope Ground Motion) – RB/FB Basemat X

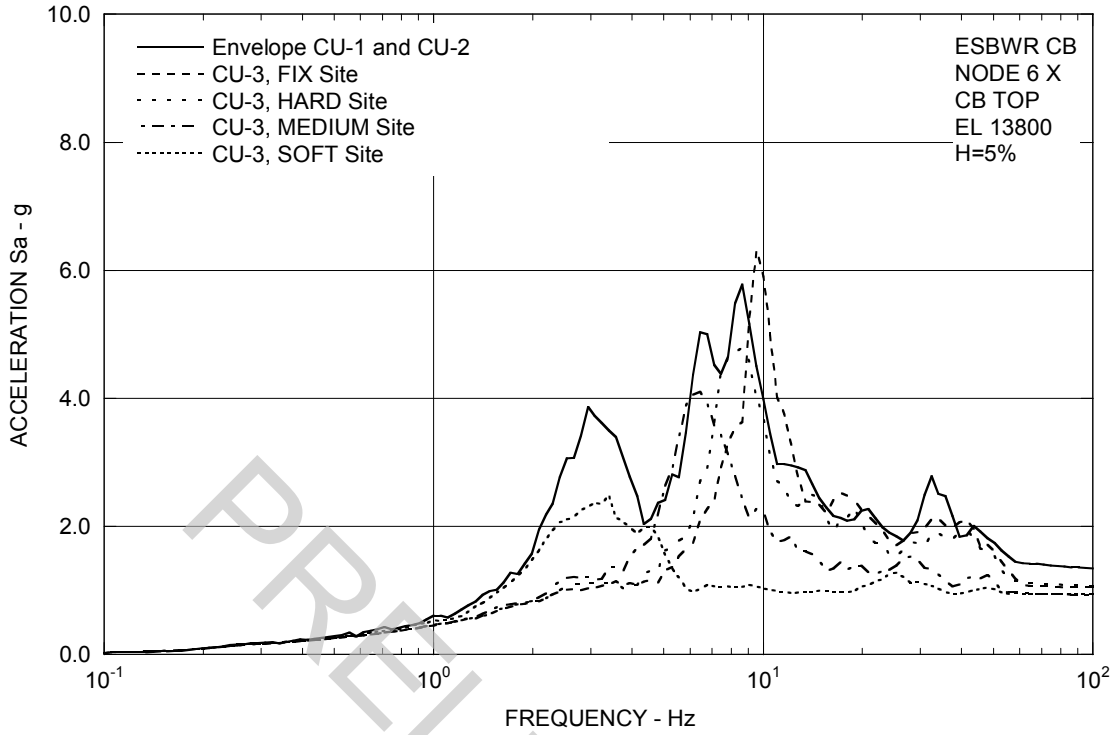

Figure 3A.8.2-1g. FRS (Effect of Single Envelope Ground Motion) – CB Top X

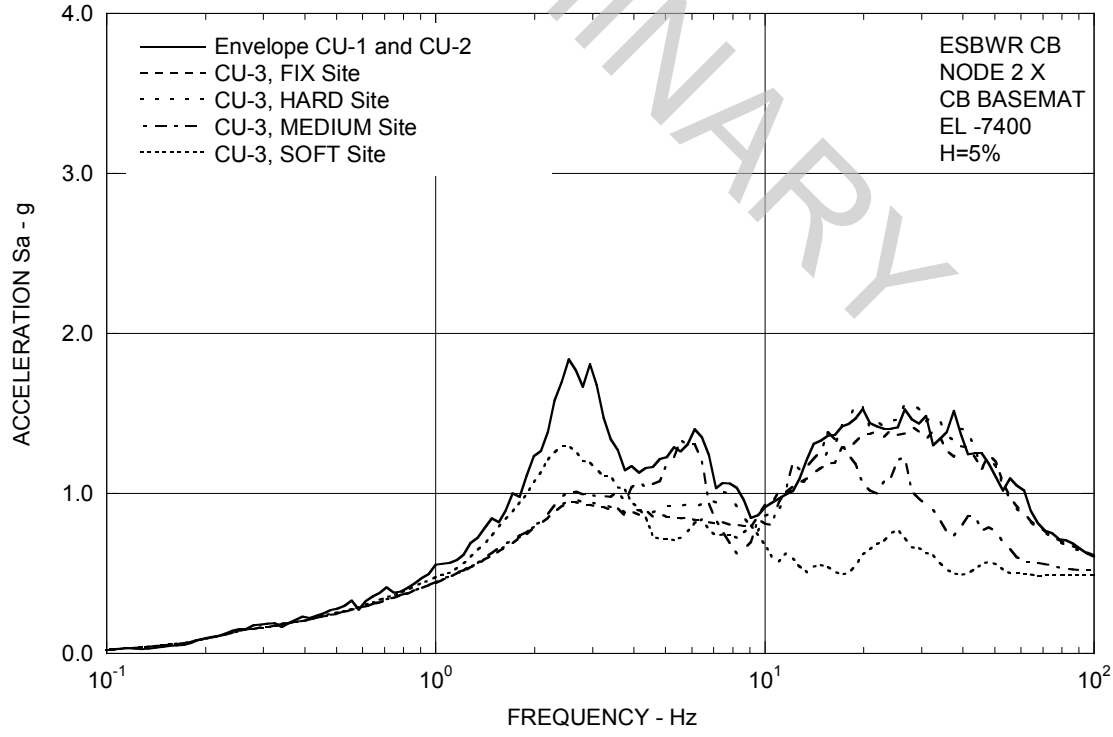

Figure 3A.8.2-1h. FRS (Effect of Single Envelope Ground Motion) – CB Basemat X

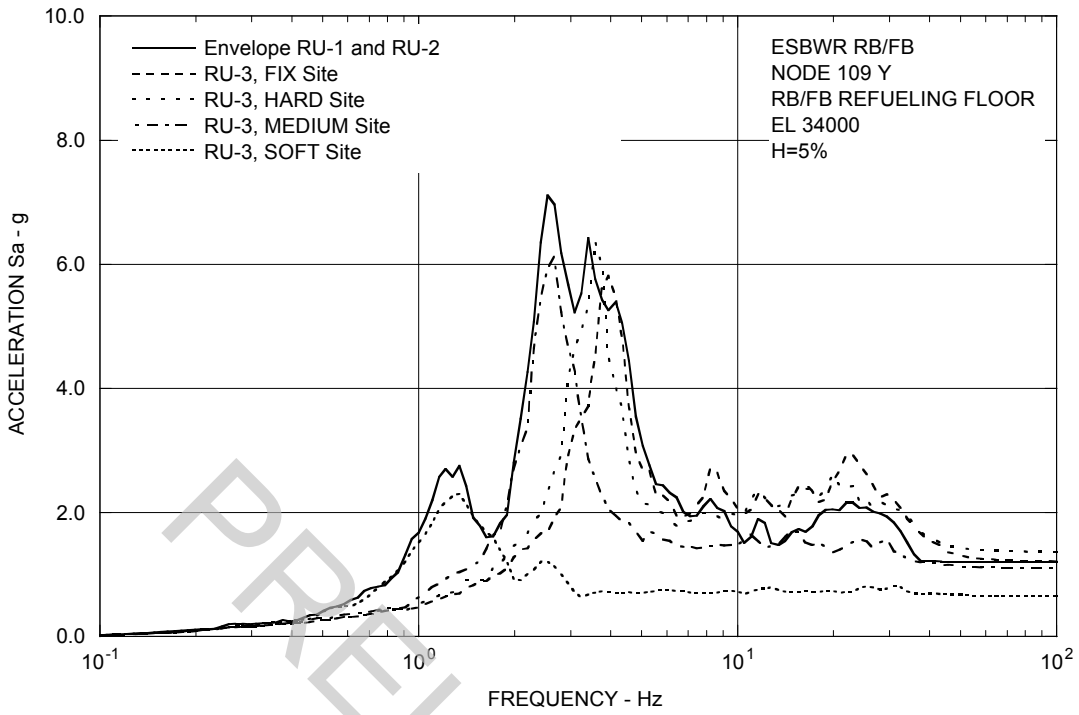

Figure 3A.8.2-2a. FRS (Effect of Single Envelope Ground Motion) – RB/FB Refueling Floor Y

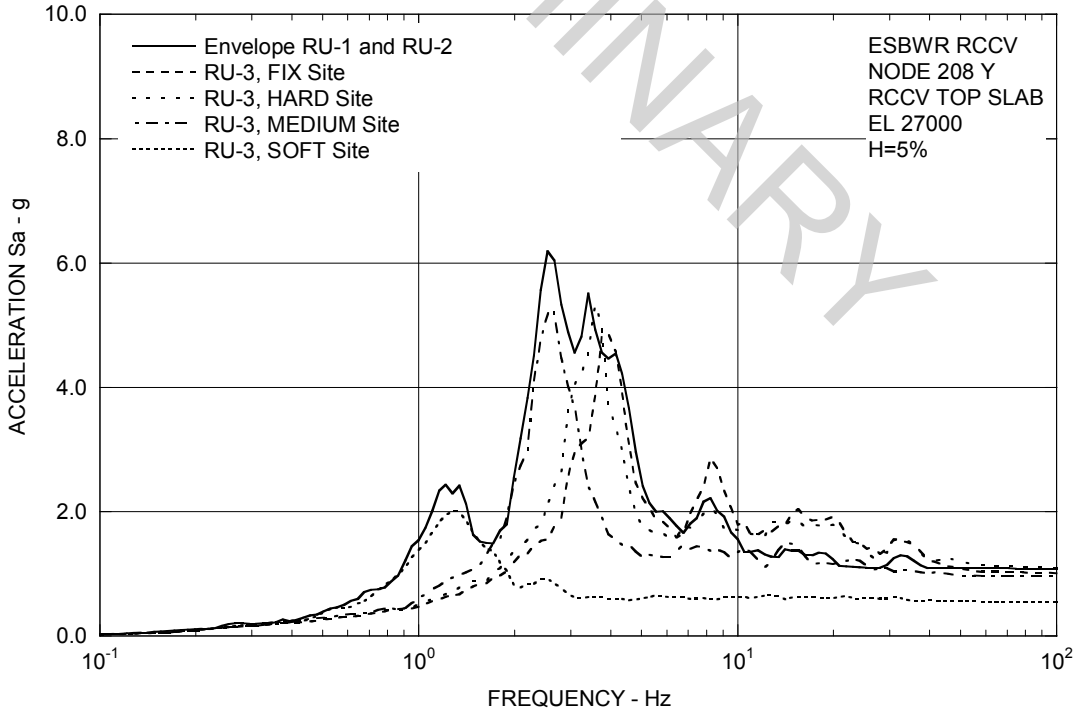

Figure 3A.8.2-2b. FRS (Effect of Single Envelope Ground Motion) – RCCV Top Slab Y

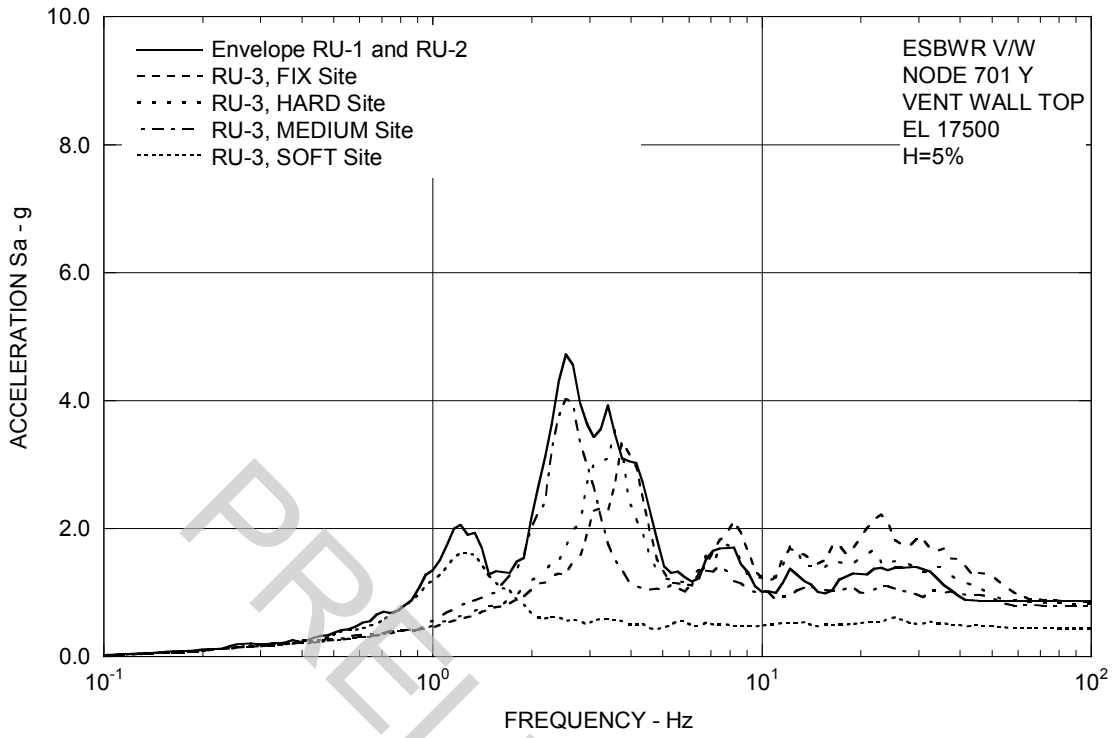

Figure 3A.8.2-2c. FRS (Effect of Single Envelope Ground Motion) – Vent Wall Top Y

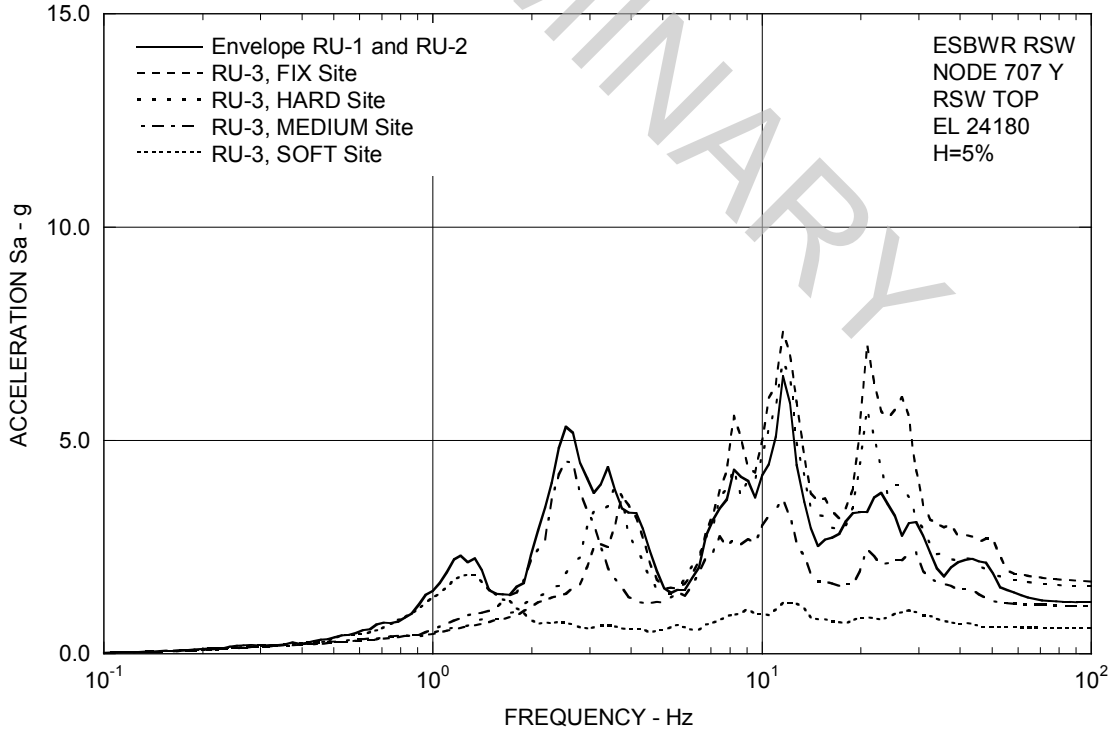

Figure 3A.8.2-2d. FRS (Effect of Single Envelope Ground Motion) – RSW Top Y

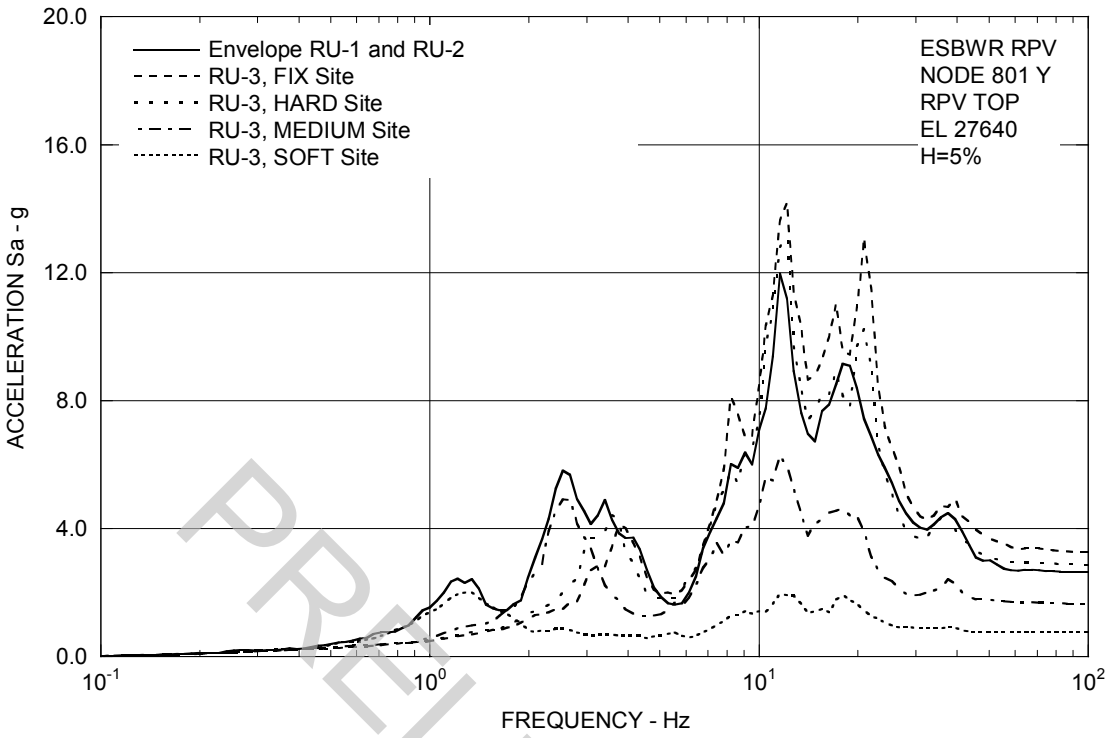

Figure 3A.8.2-2e. FRS (Effect of Single Envelope Ground Motion) – RPV Top Y

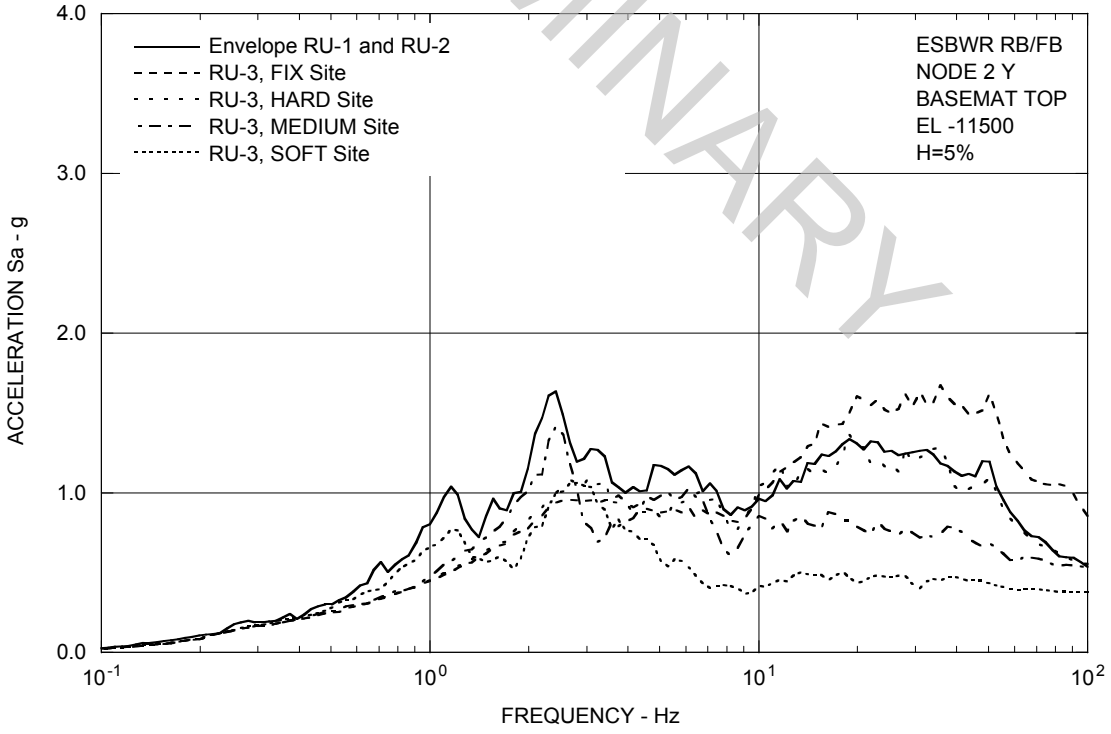

Figure 3A.8.2-2f. FRS (Effect of Single Envelope Ground Motion) – RB/FB Basemat Y

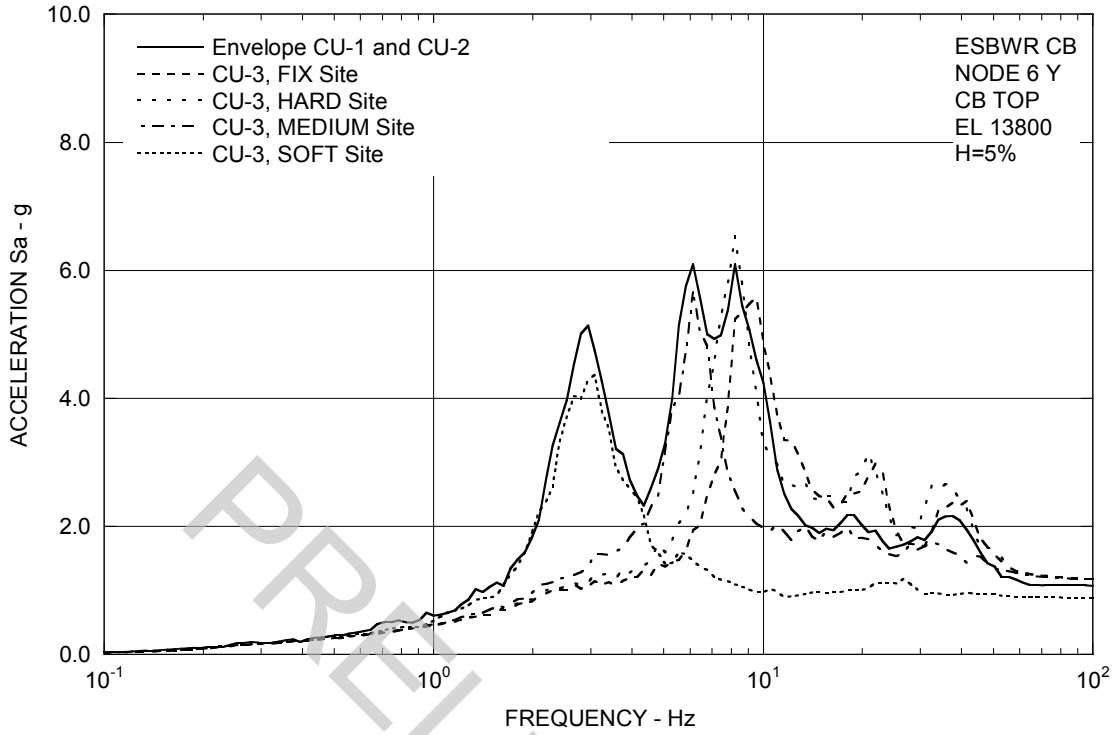

Figure 3A.8.2-2g. FRS (Effect of Single Envelope Ground Motion) – CB Top Y

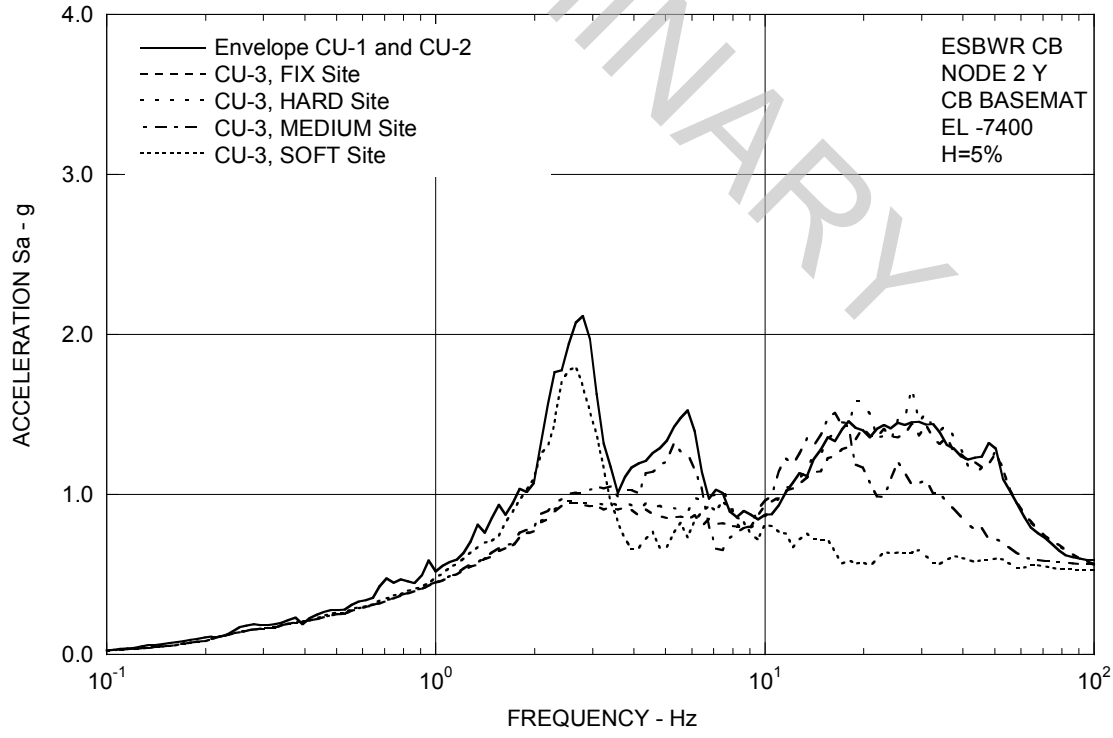

Figure 3A.8.2-2h. FRS (Effect of Single Envelope Ground Motion) – CB Basemat Y

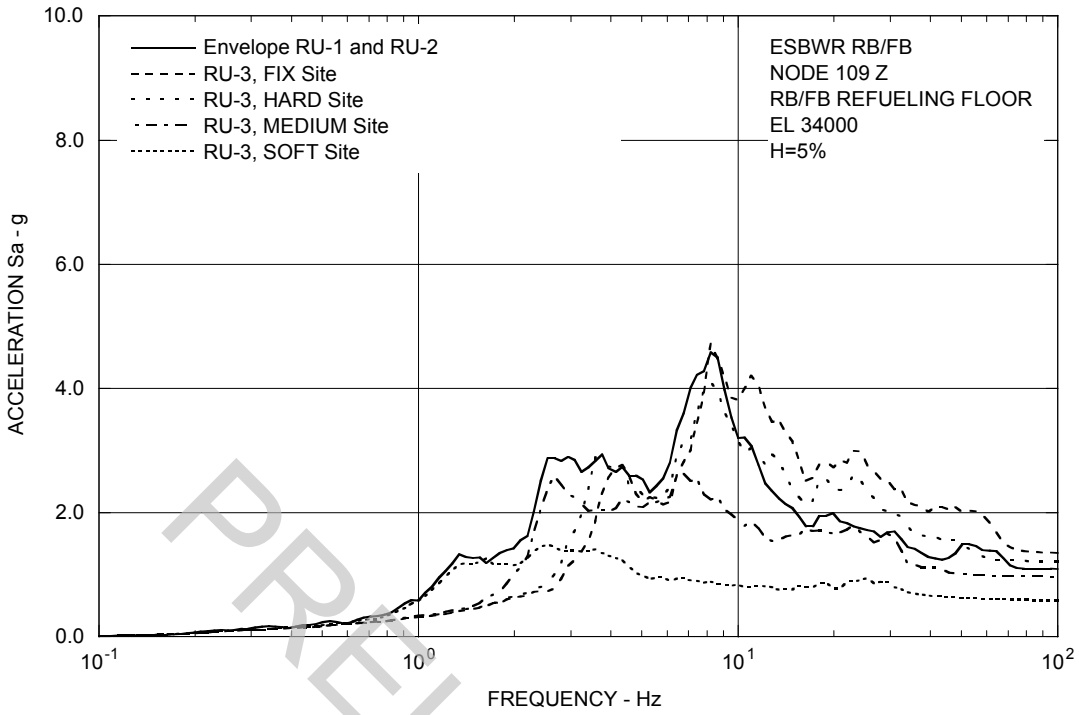

Figure 3A.8.2-3a. FRS (Effect of Single Envelope Ground Motion) – RB/FB Refueling Floor Z

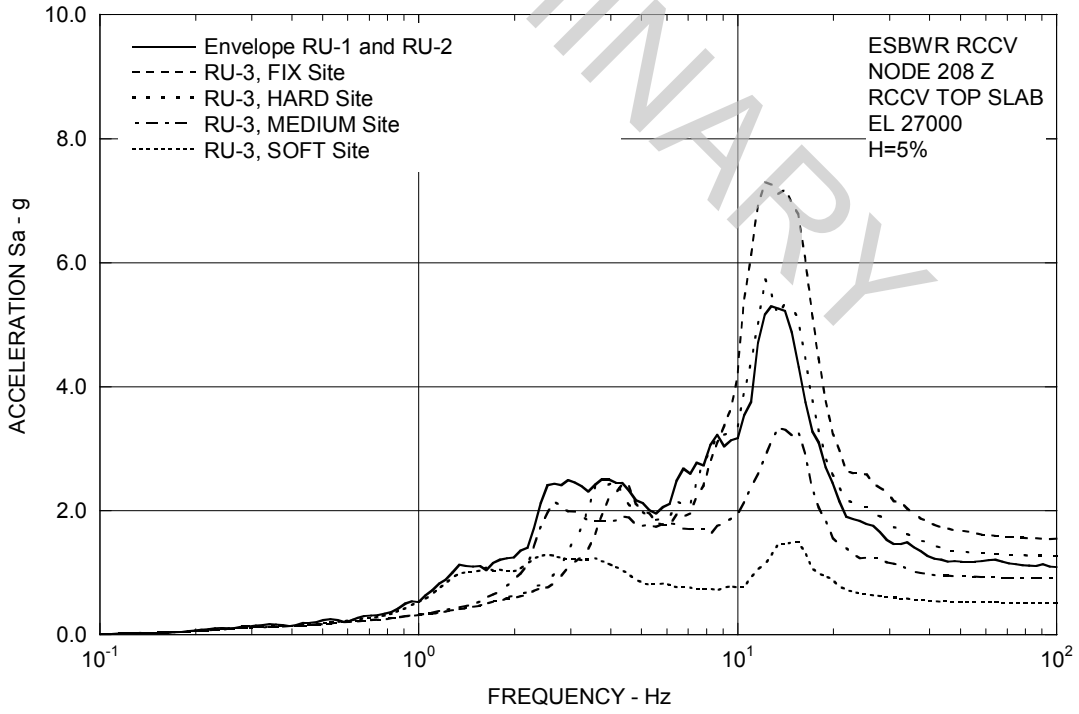

Figure 3A.8.2-3b. FRS (Effect of Single Envelope Ground Motion) – RCCV Top Slab Z

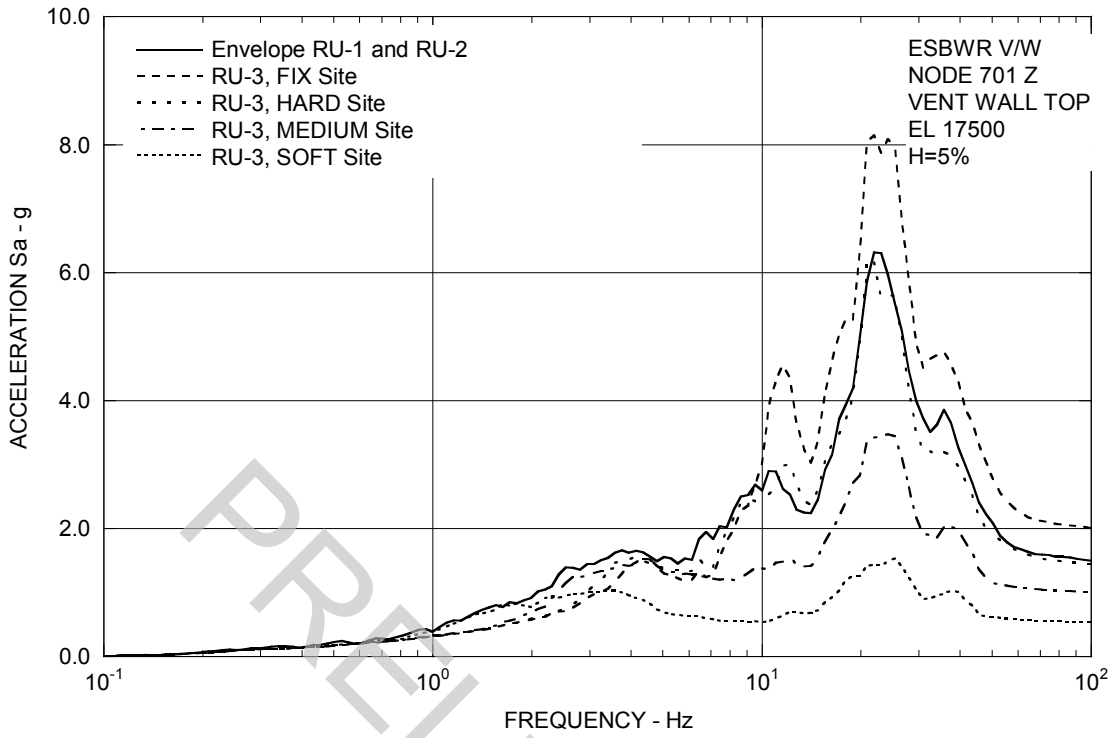

Figure 3A.8.2-3c. FRS (Effect of Single Envelope Ground Motion) – Vent Wall Top Z

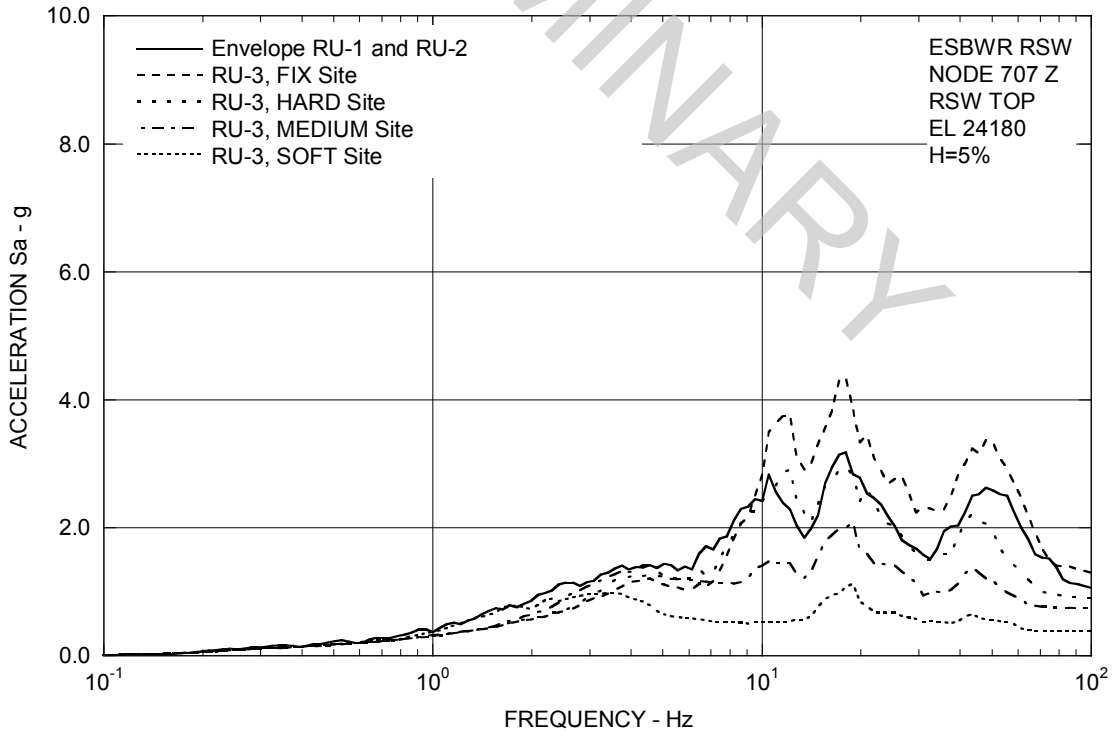

Figure 3A.8.2-3d. FRS (Effect of Single Envelope Ground Motion) – RSW Top Z

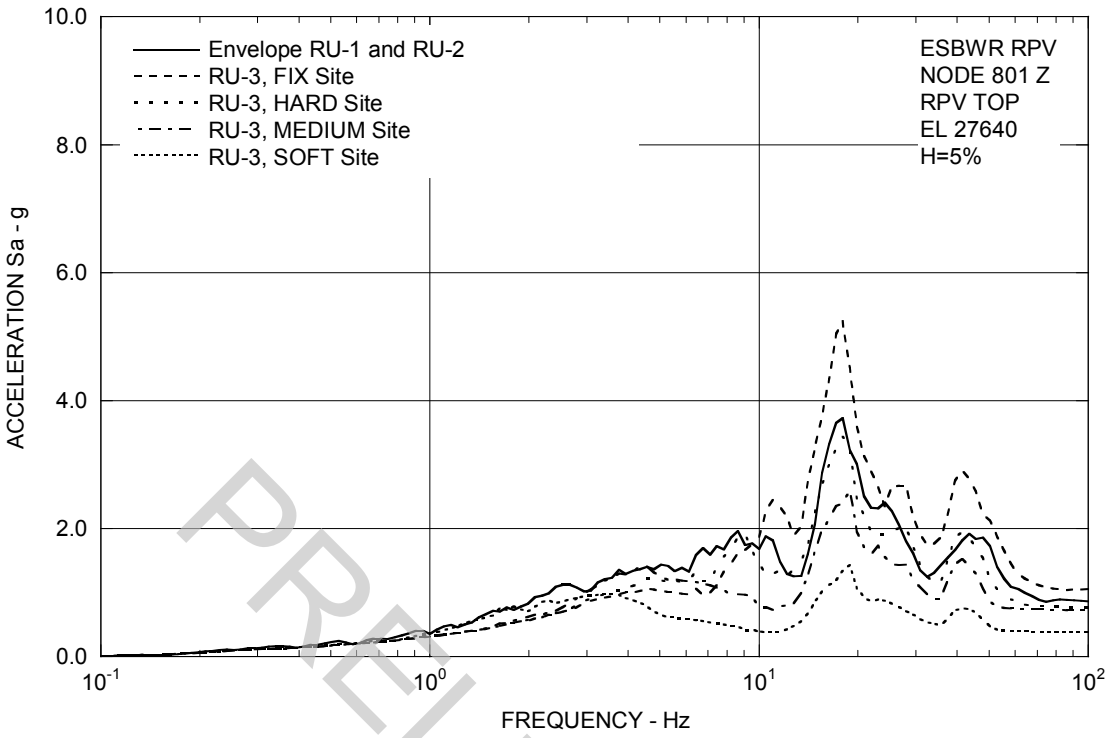

Figure 3A.8.2-3e. FRS (Effect of Single Envelope Ground Motion) – RPV Top Z

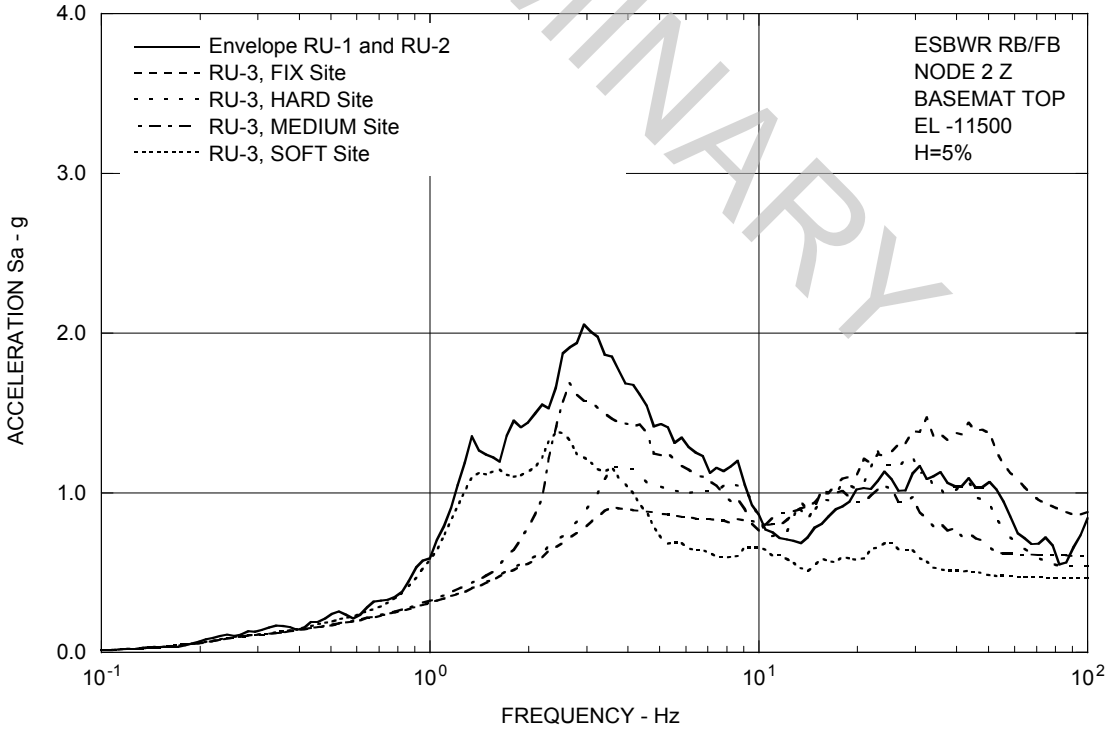

Figure 3A.8.2-3f. FRS (Effect of Single Envelope Ground Motion) – RB/FB Basemat Z

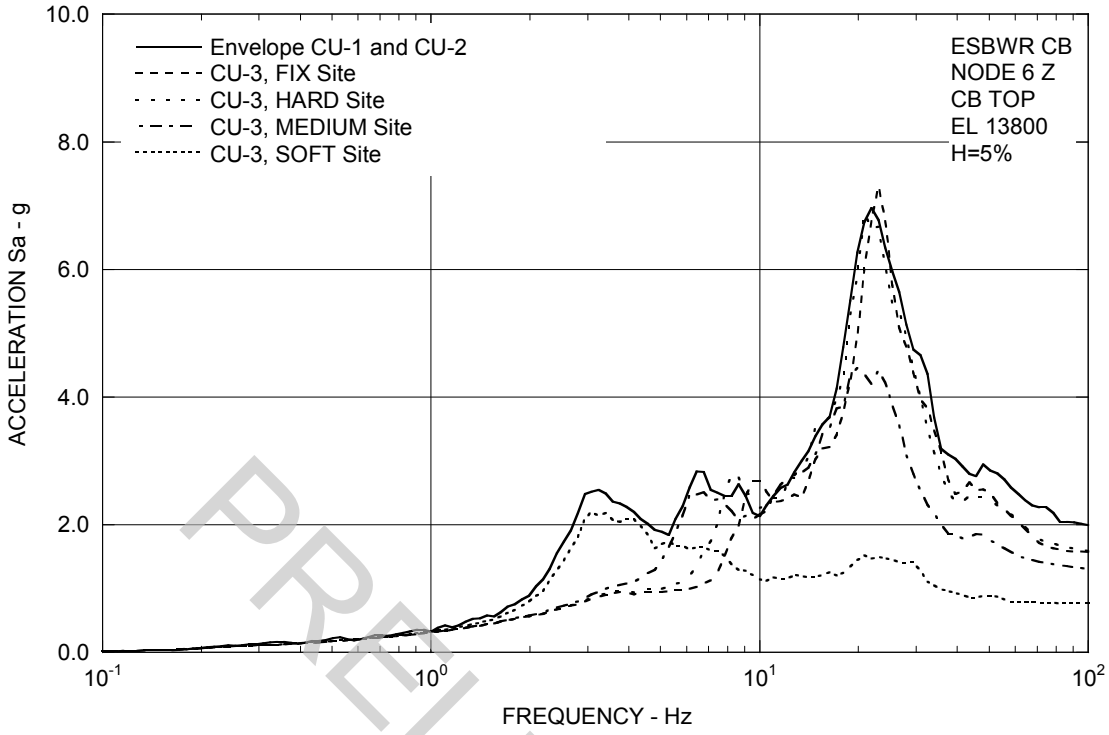

Figure 3A.8.2-3g. FRS (Effect of Single Envelope Ground Motion) – CB Top Z

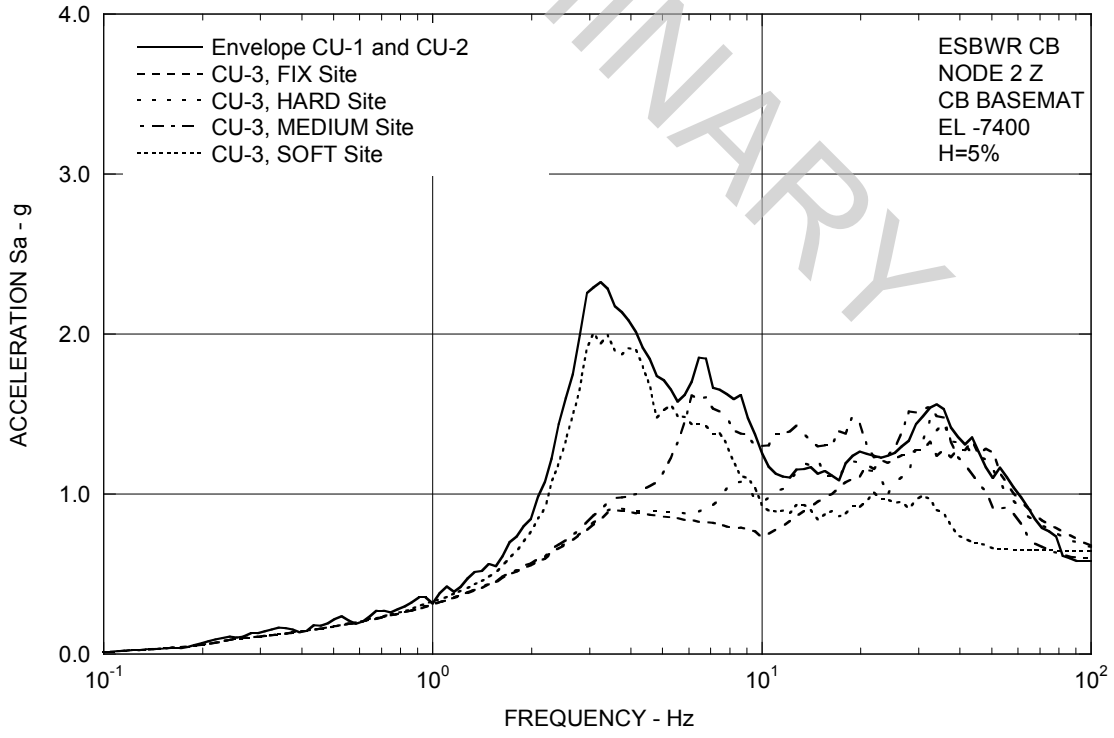

Figure 3A.8.2-3h. FRS (Effect of Single Envelope Ground Motion) – CB Basemat Z

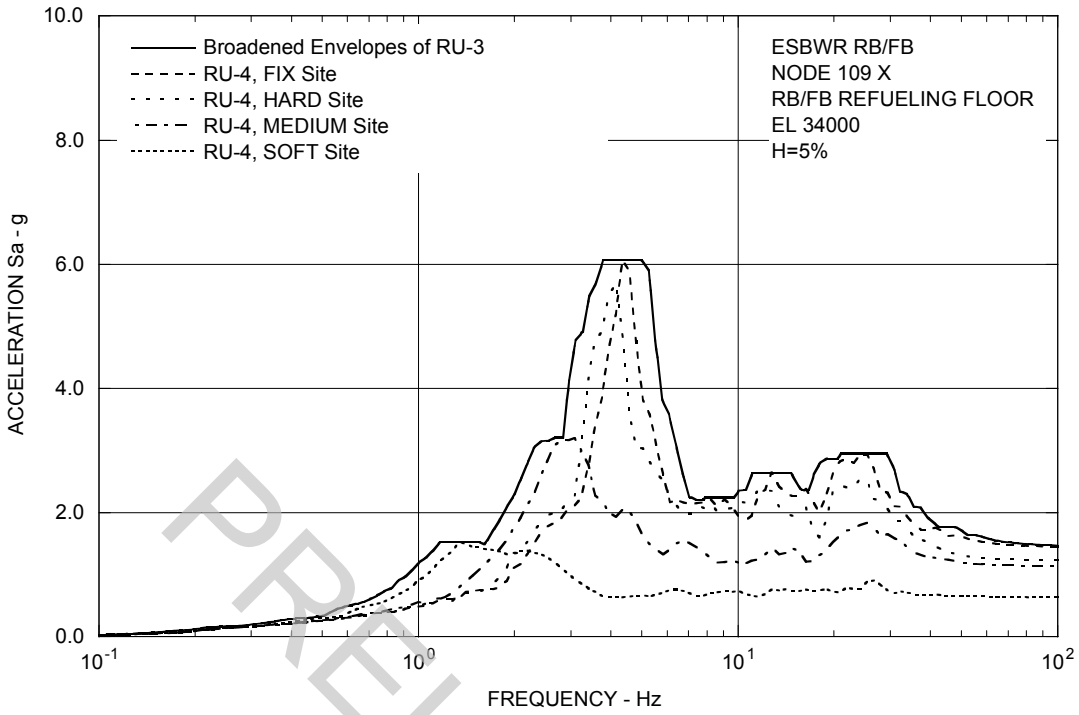

Figure 3A.8.3-1a. FRS (Effect of Updated Design of RSW and VW) – RB/FB Refueling Floor X

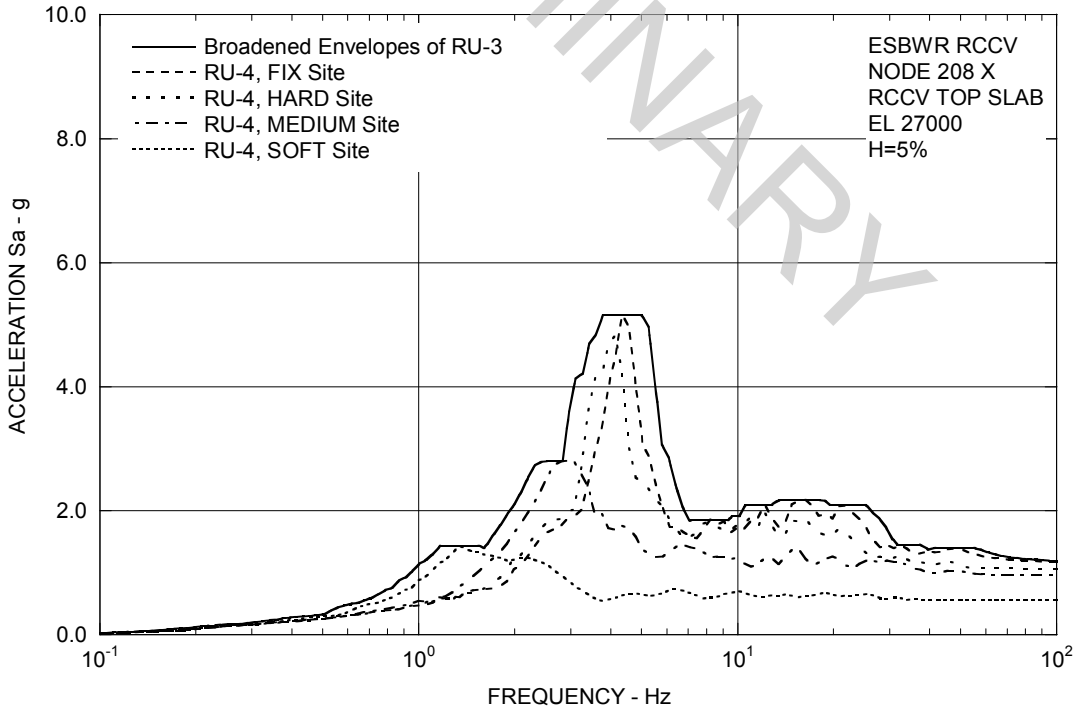

Figure 3A.8.3-1b. FRS (Effect of Updated Design of RSW and VW) – RCCV Top Slab X

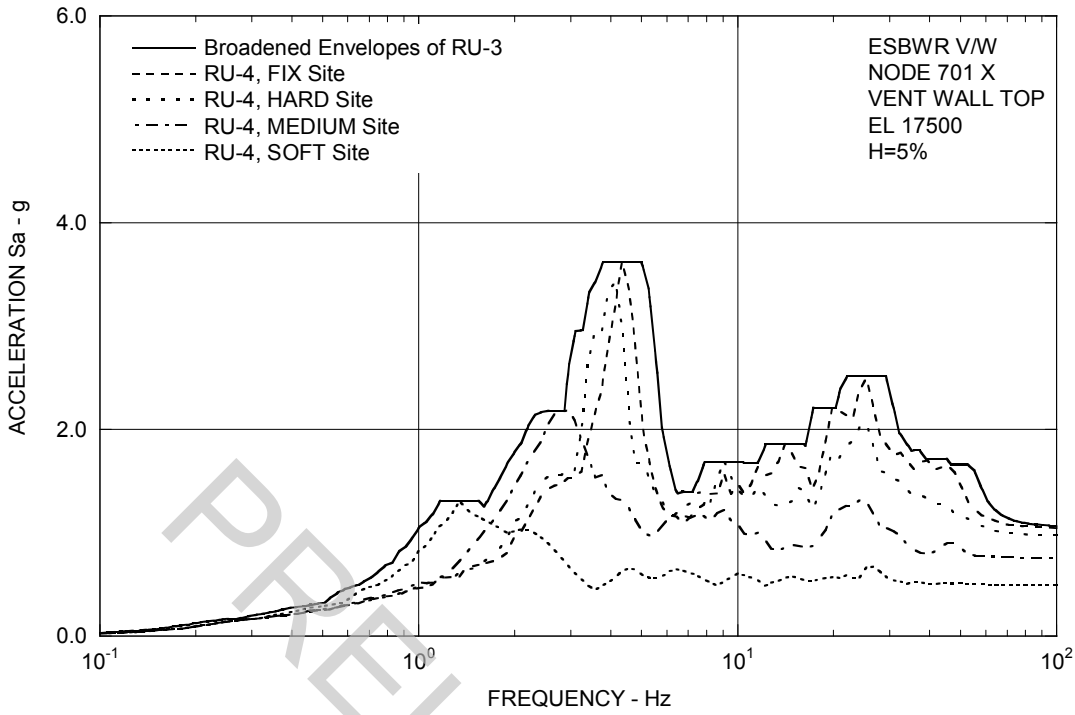

Figure 3A.8.3-1c. FRS (Effect of Updated Design of RSW and VW) – Vent Wall Top X

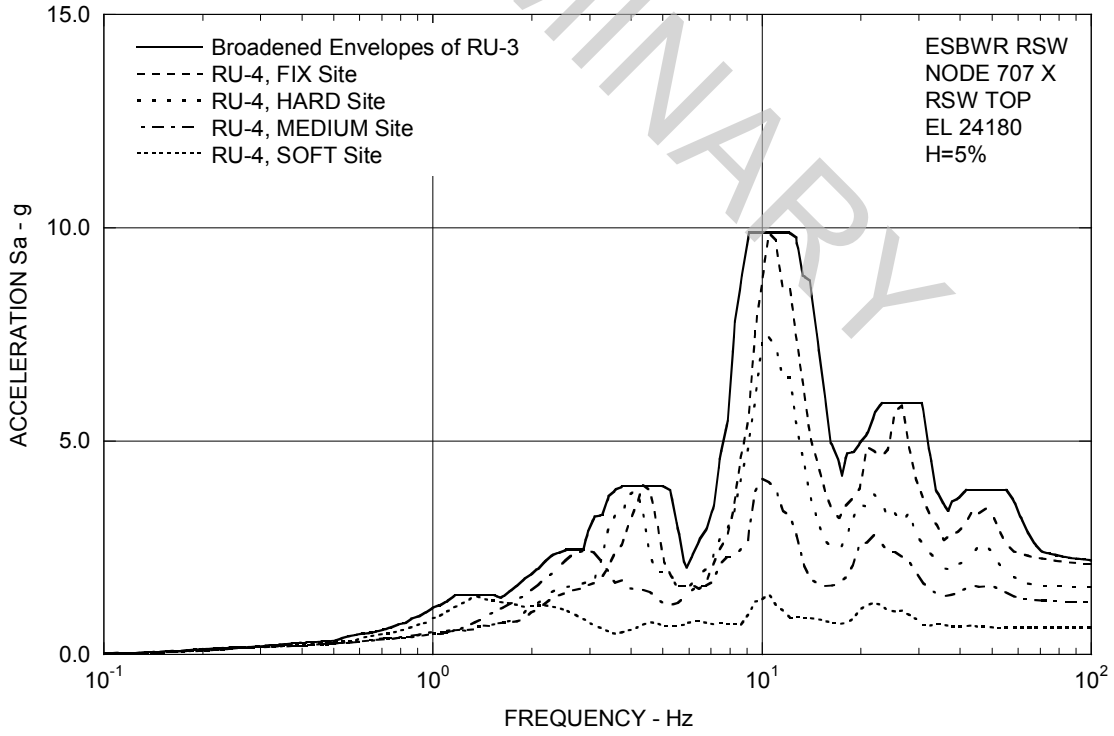

Figure 3A.8.3-1d. FRS (Effect of Updated Design of RSW and VW) – RSW Top X

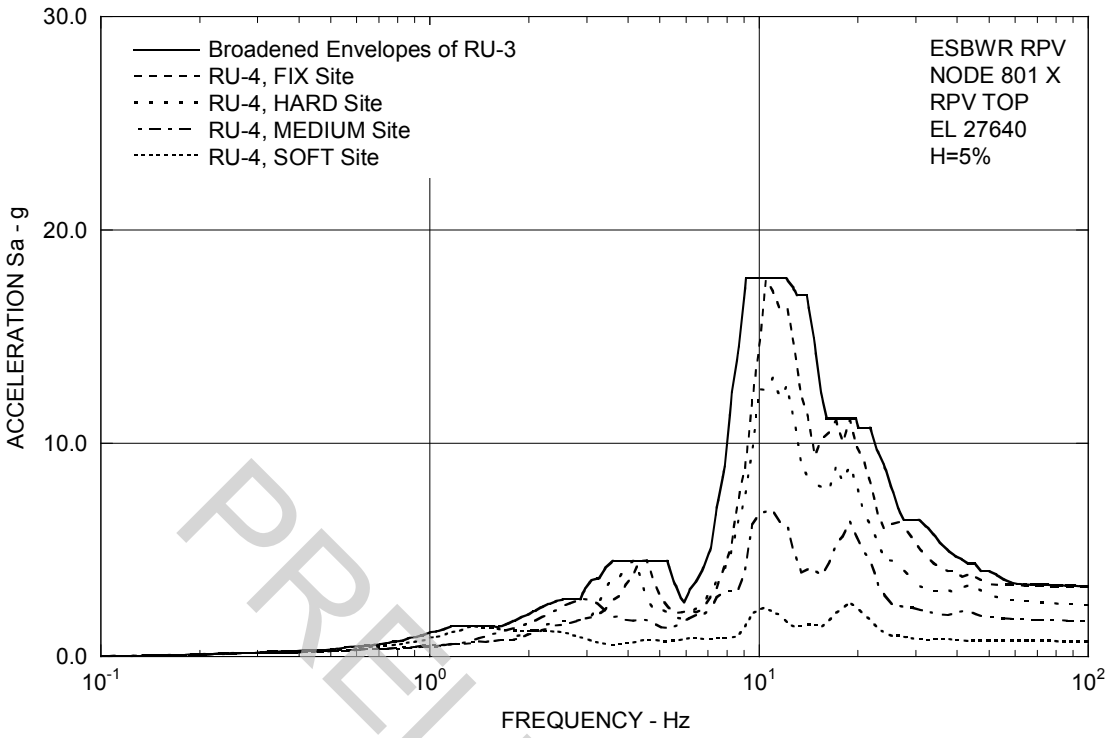

Figure 3A.8.3-1e. FRS (Effect of Updated Design of RSW and VW) – RPV Top X

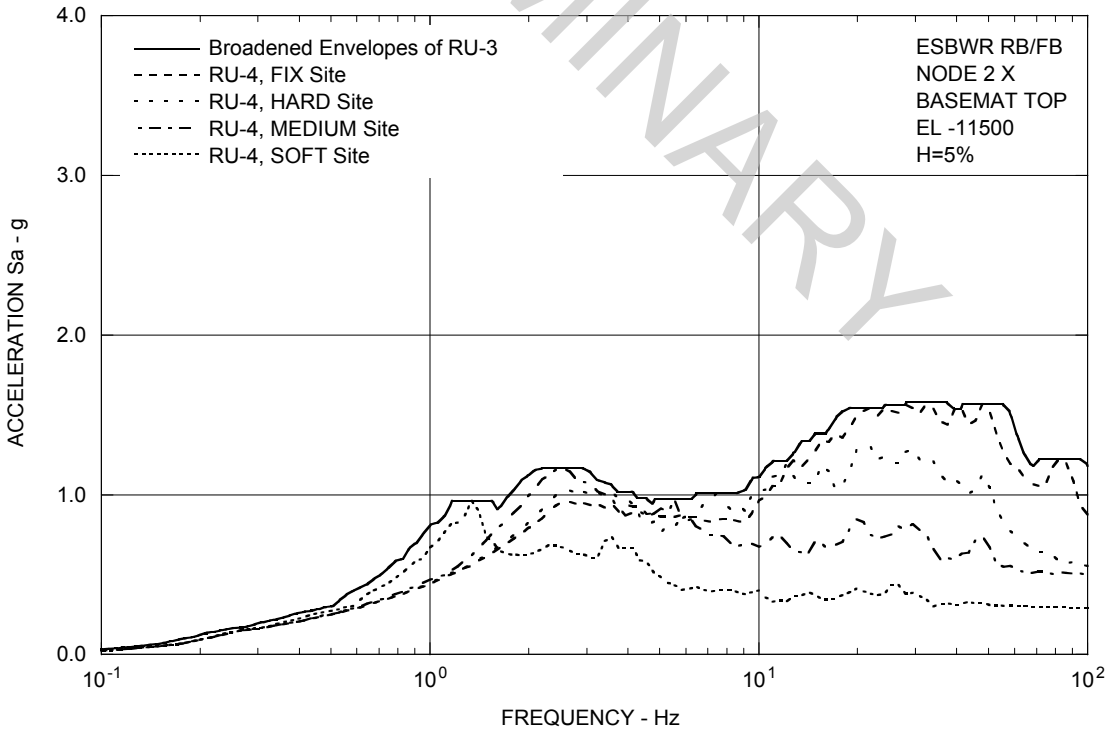

Figure 3A.8.3-1f. FRS (Effect of Updated Design of RSW and VW) – RB/FB Basemat X

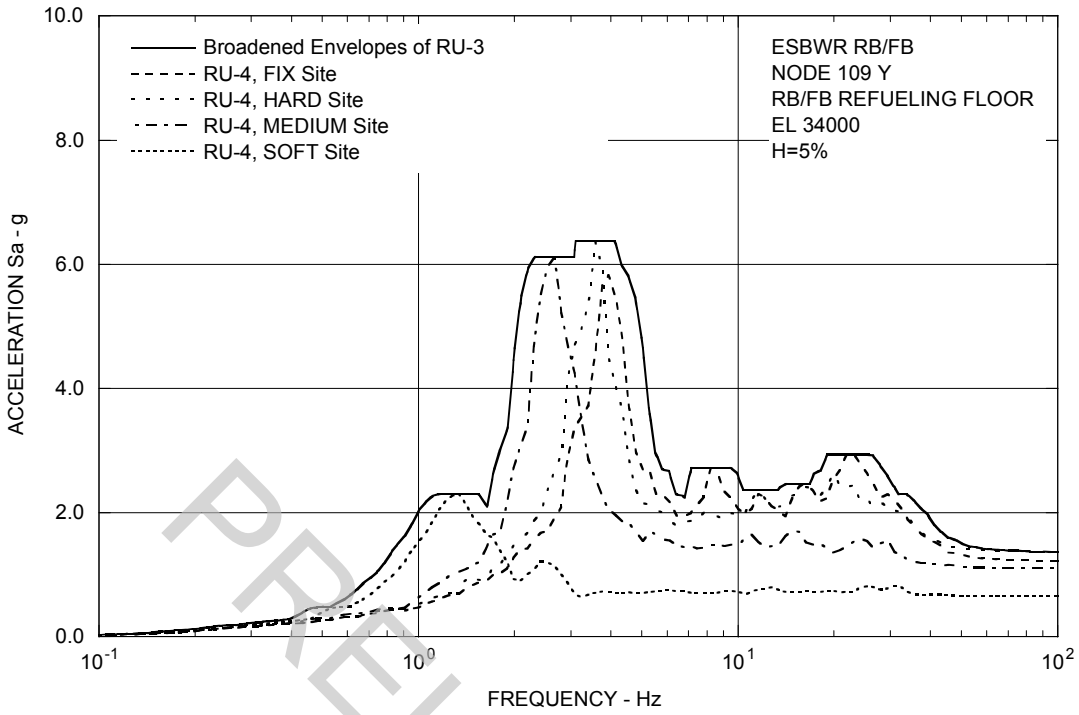

Figure 3A.8.3-2a. FRS (Effect of Updated Design of RSW and VW) – RB/FB Refueling Floor Y

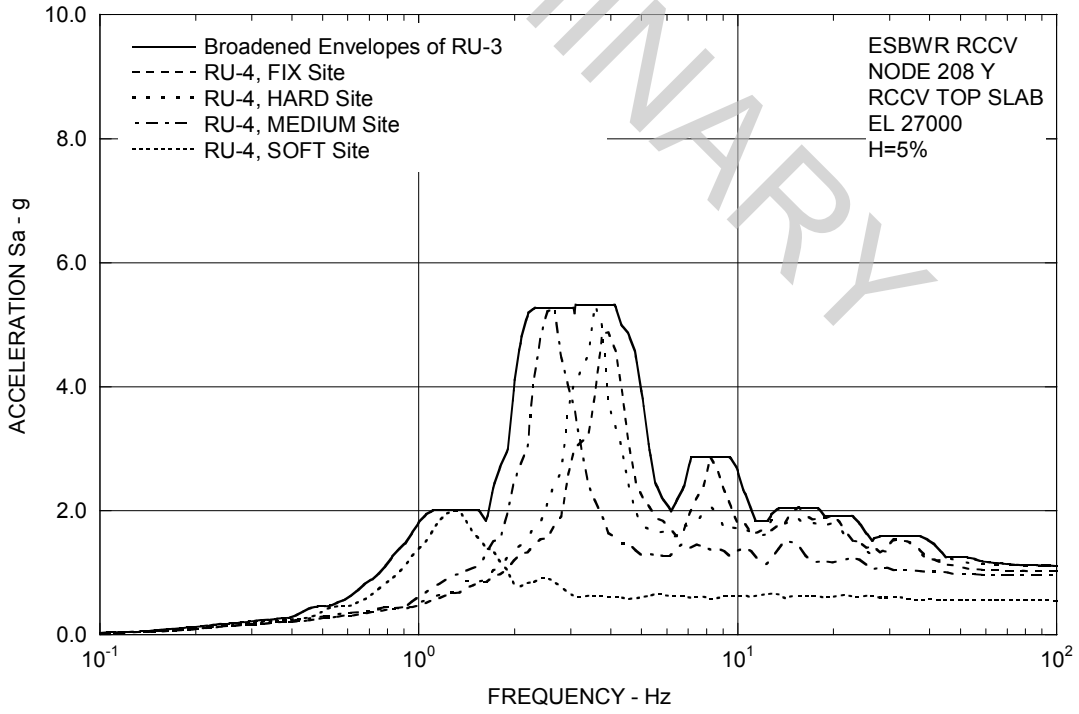

Figure 3A.8.3-2b. FRS (Effect of Updated Design of RSW and VW) – RCCV Top Slab Y

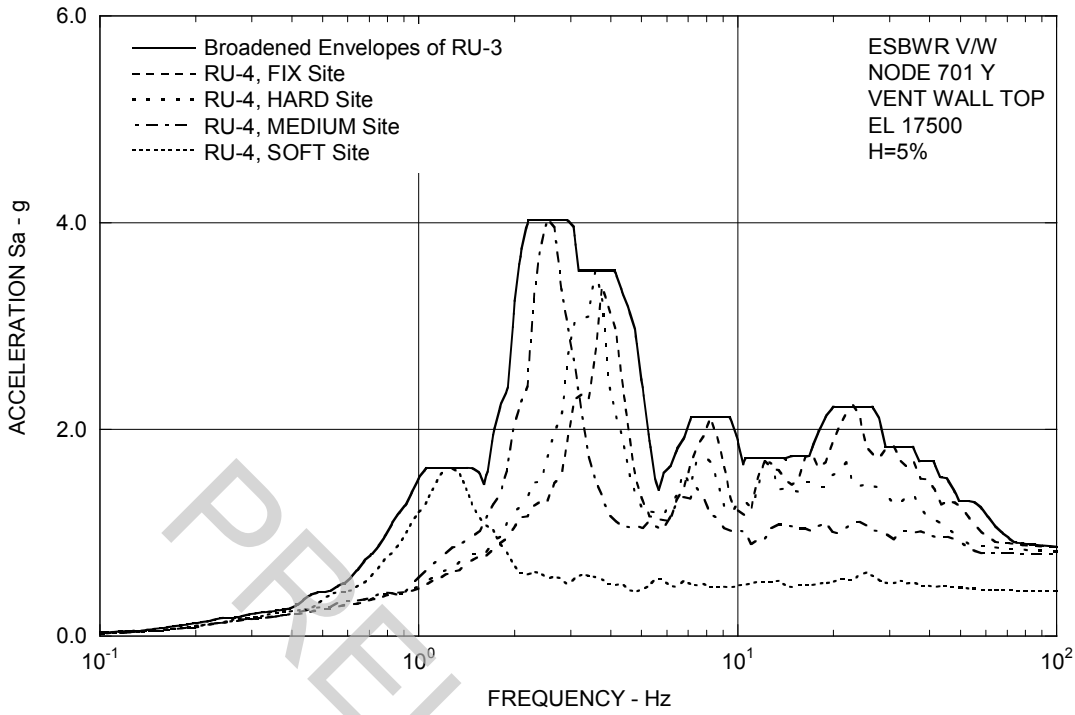

Figure 3A.8.3-2c. FRS (Effect of Updated Design of RSW and VW) – Vent Wall Top Y

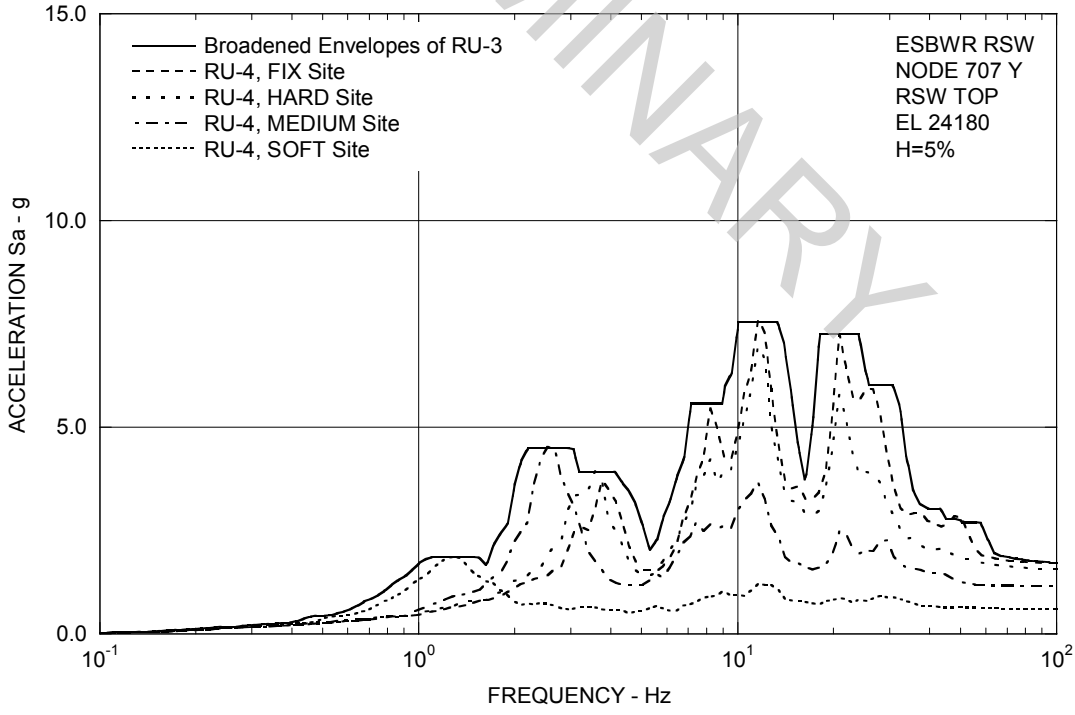

Figure 3A.8.3-2d. FRS (Effect of Updated Design of RSW and VW) – RSW Top Y

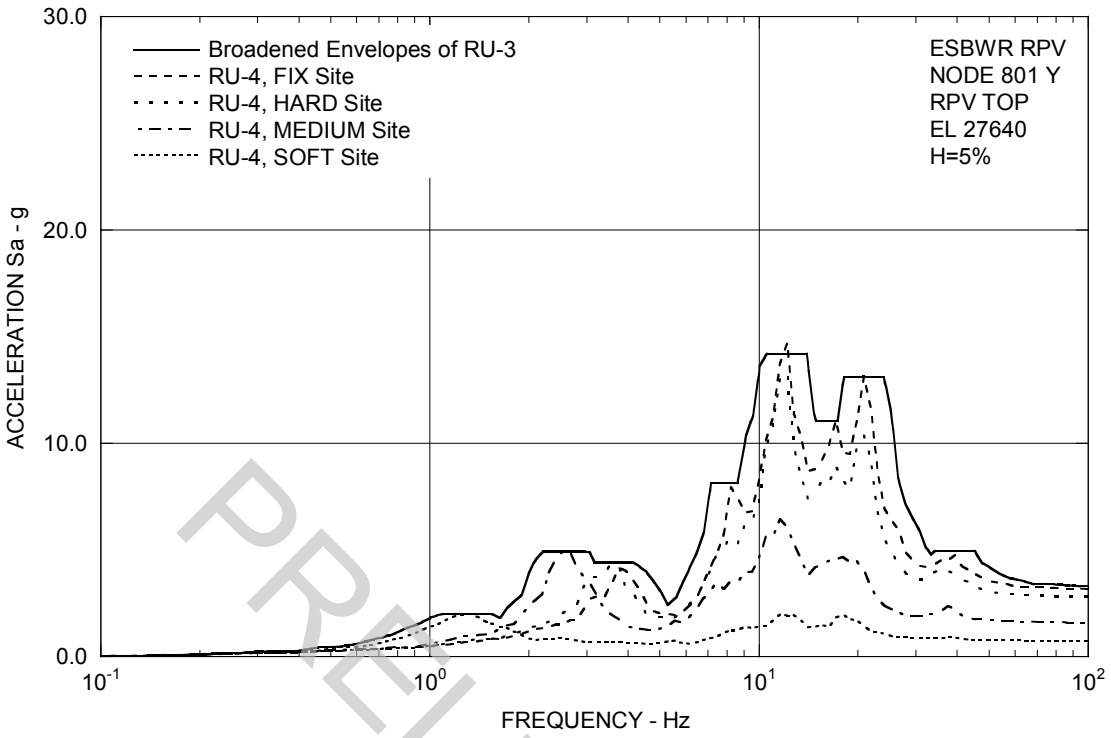

Figure 3A.8.3-2e. FRS (Effect of Updated Design of RSW and VW) – RPV Top Y

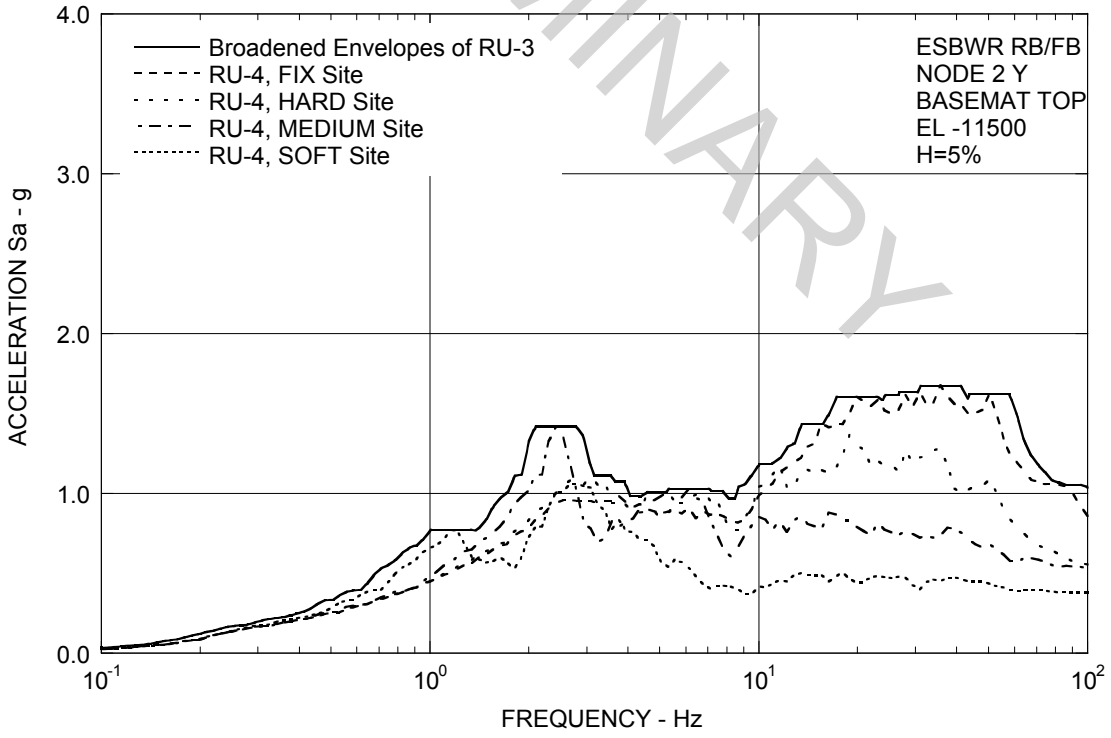

Figure 3A.8.3-2f. FRS (Effect of Updated Design of RSW and VW) – RB/FB Basemat Y

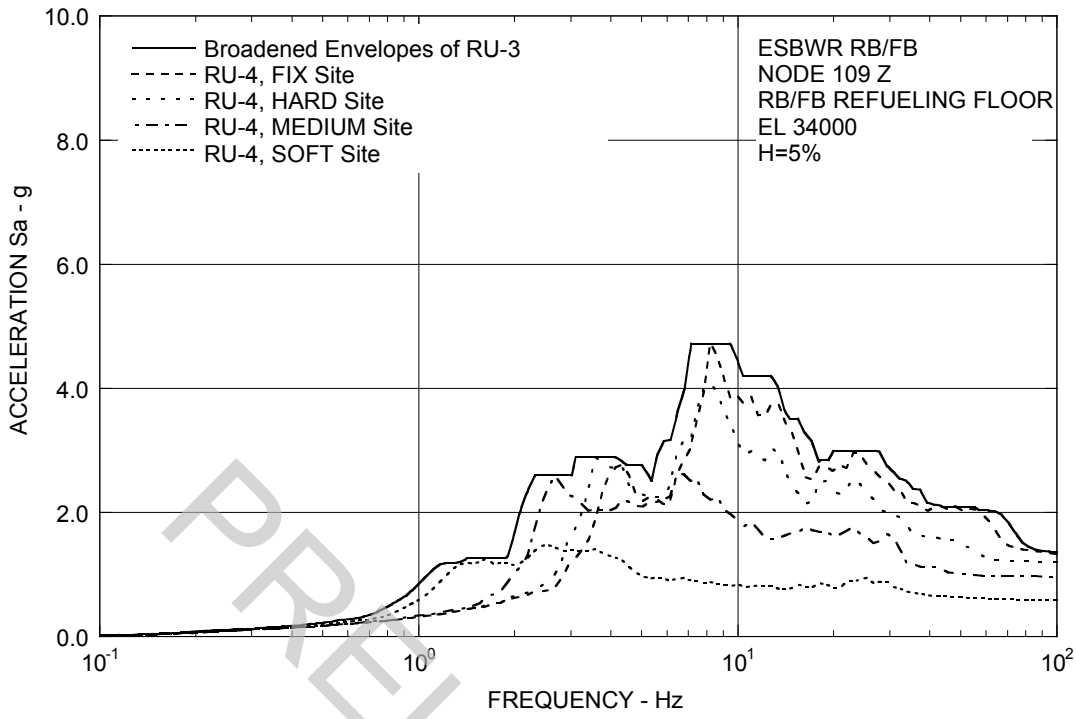

Figure 3A.8.3-3a. FRS (Effect of Updated Design of RSW and VW) – RB/FB Refueling Floor Z

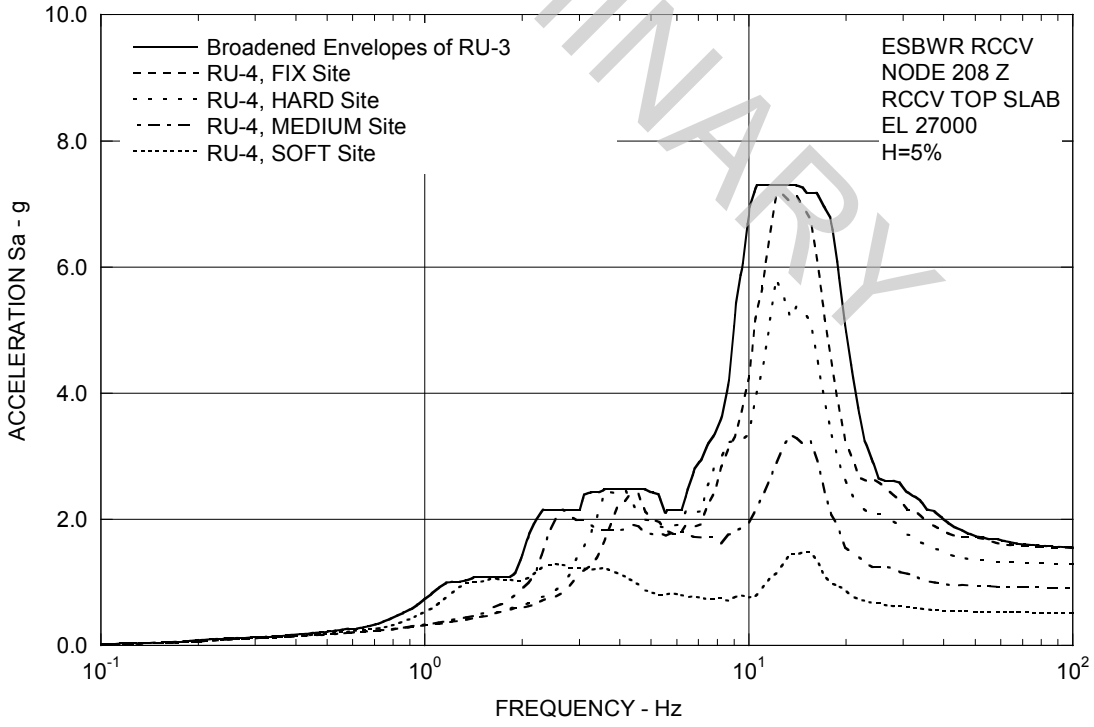

Figure 3A.8.3-3b. FRS (Effect of Updated Design of RSW and VW) – RCCV Top Slab Z

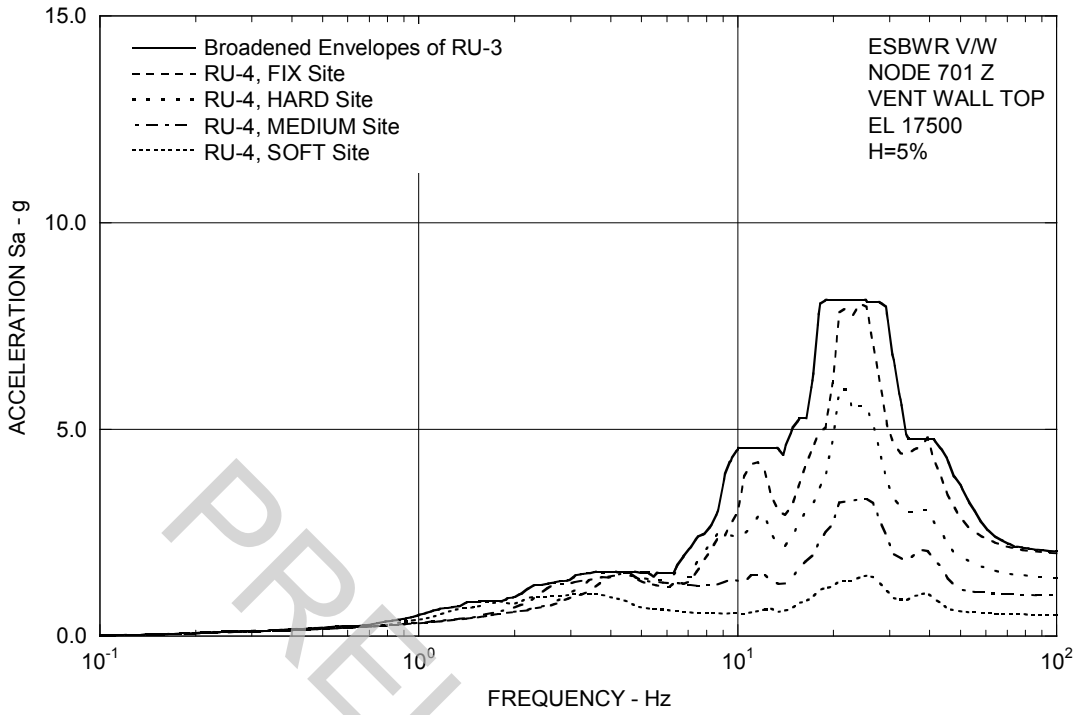

Figure 3A.8.3-3c. FRS (Effect of Updated Design of RSW and VW) – Vent Wall Top Z

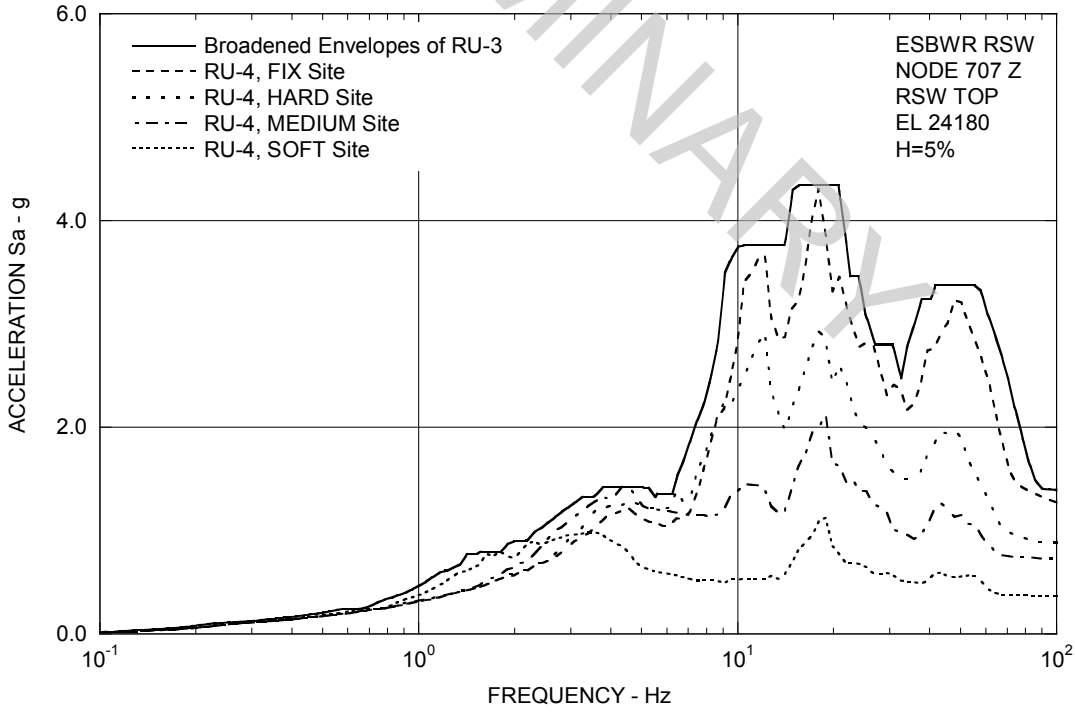

Figure 3A.8.3-3d. FRS (Effect of Updated Design of RSW and VW) – RSW Top Z

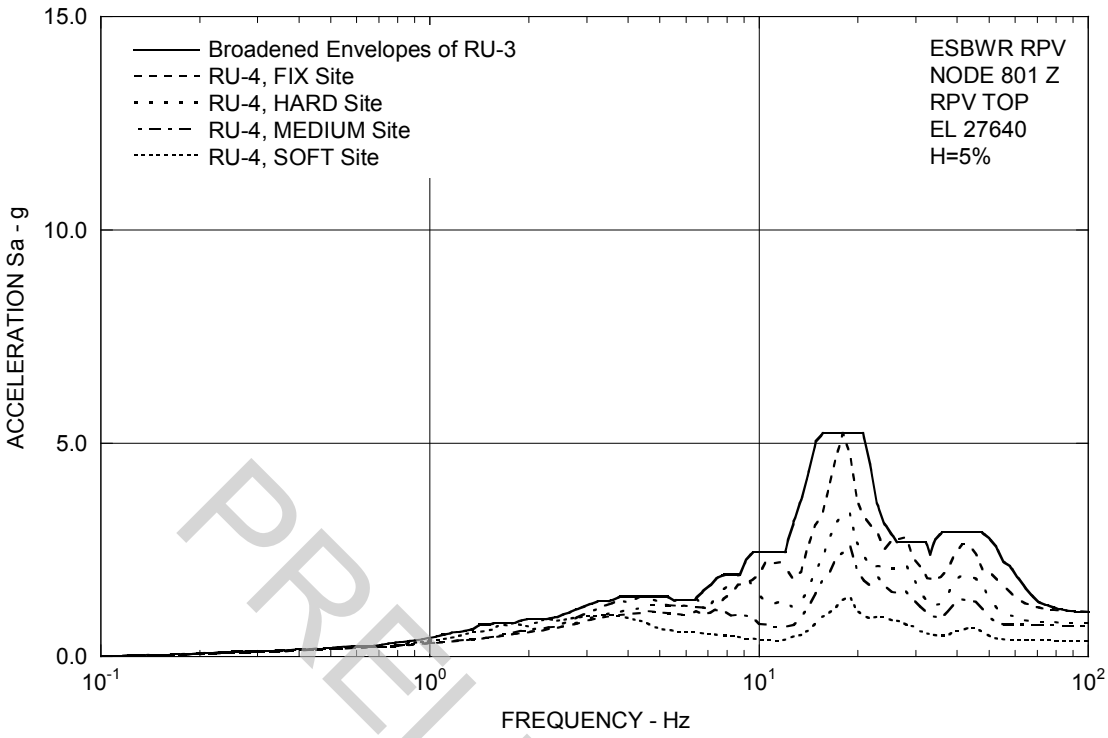

Figure 3A.8.3-3e. FRS (Effect of Updated Design of RSW and VW) – RPV Top Z

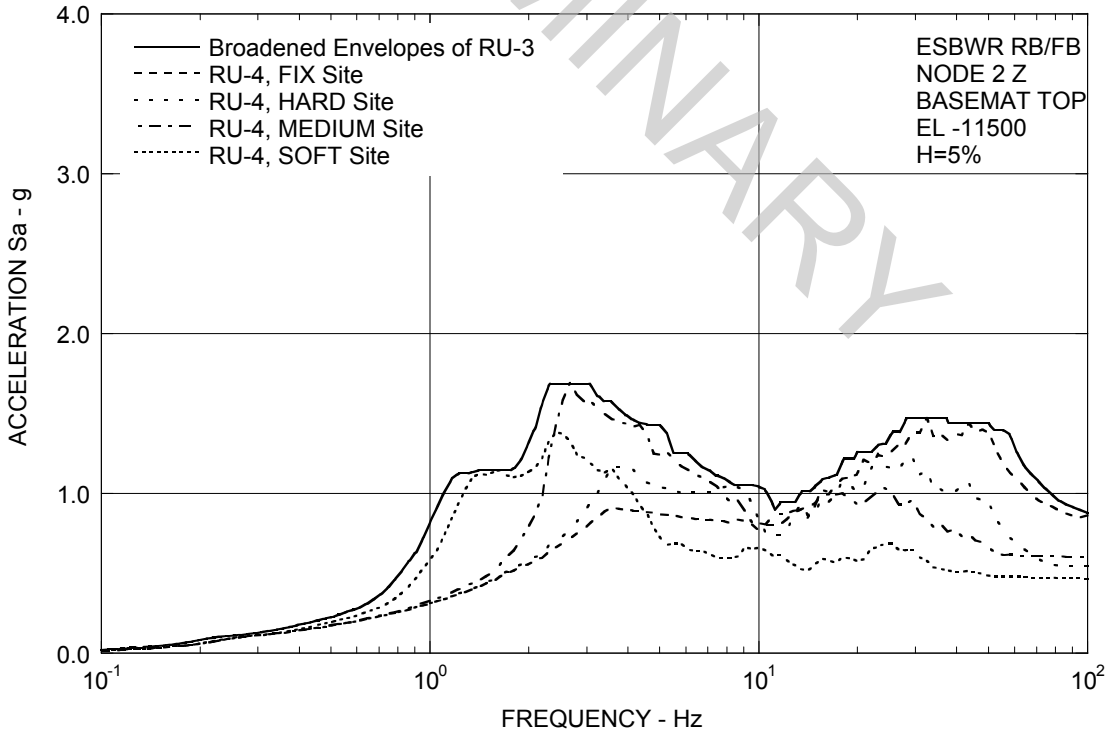

Figure 3A.8.3-3f. FRS (Effect of Updated Design of RSW and VW) – RB/FB Basemat Z

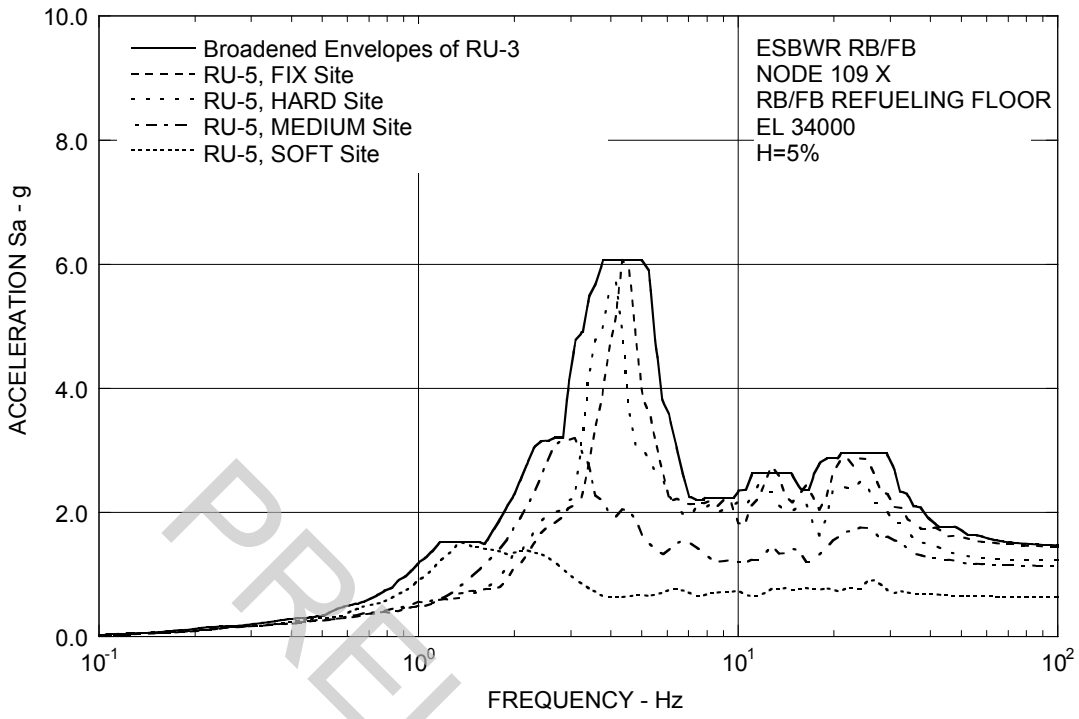

Figure 3A.8.4-1a. FRS (Effect of 50% Infill Concrete Stiffness of VW and D/F) – RB/FB Refueling Floor X

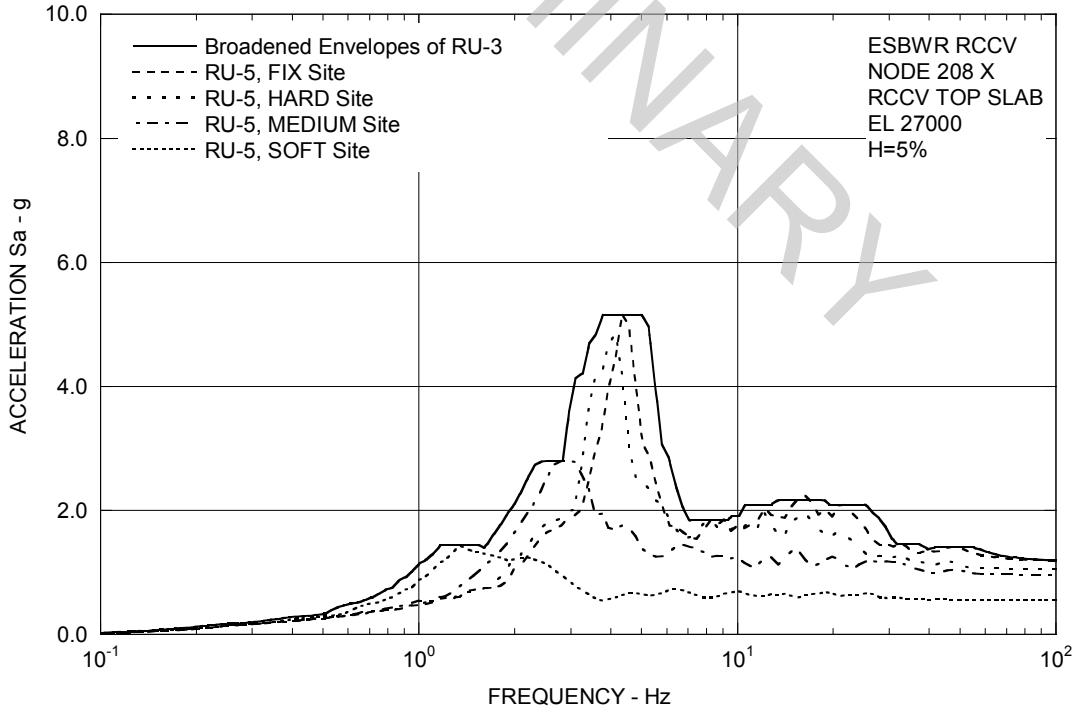

Figure 3A.8.4-1b. FRS (Effect of 50% Infill Concrete Stiffness of VW and D/F) – RCCV Top Slab X

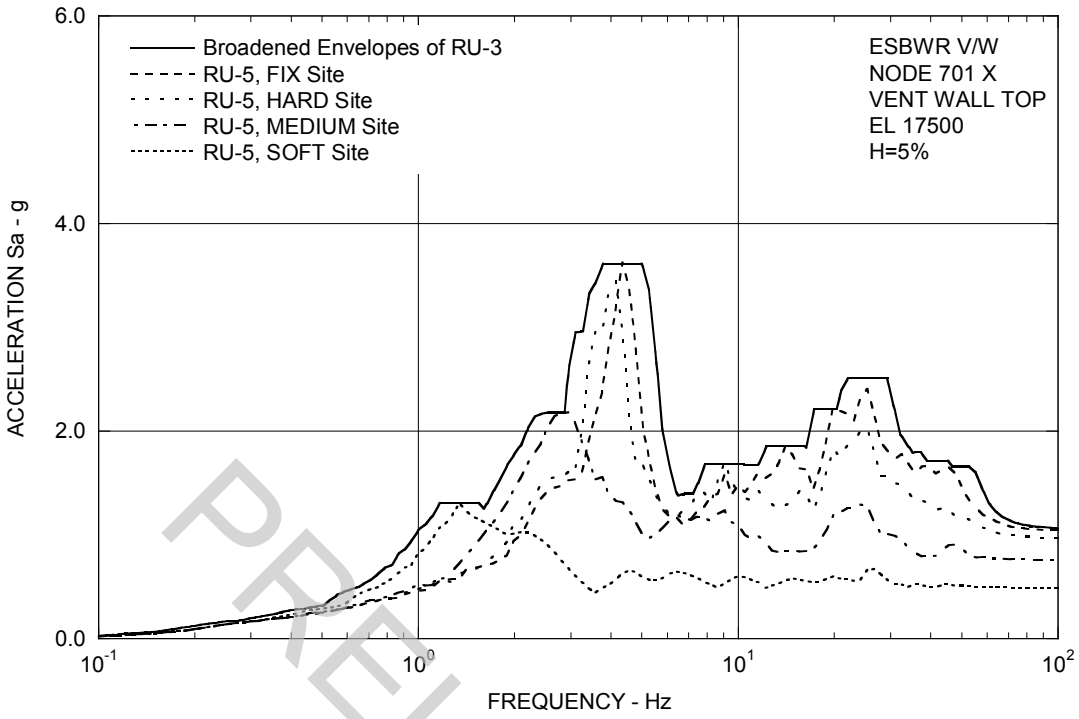

Figure 3A.8.4-1c. FRS (Effect of 50% Infill Concrete Stiffness of VW and D/F) – Vent Wall Top X

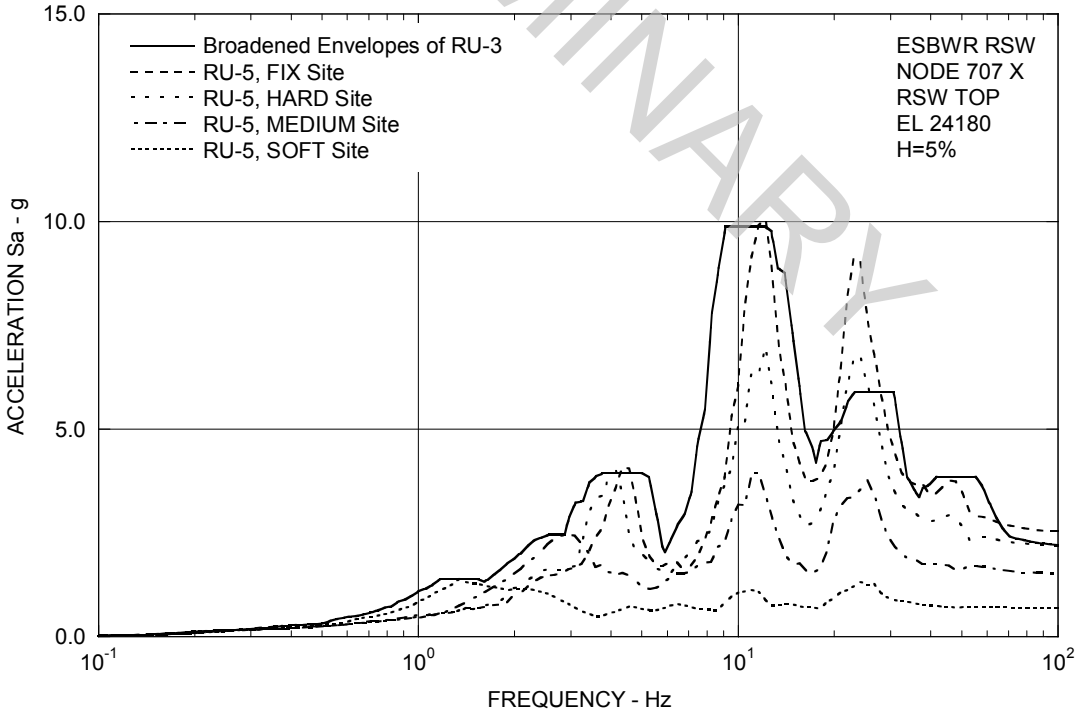

Figure 3A.8.4-1d. FRS (Effect of 50% Infill Concrete Stiffness of VW and D/F) – RSW Top X

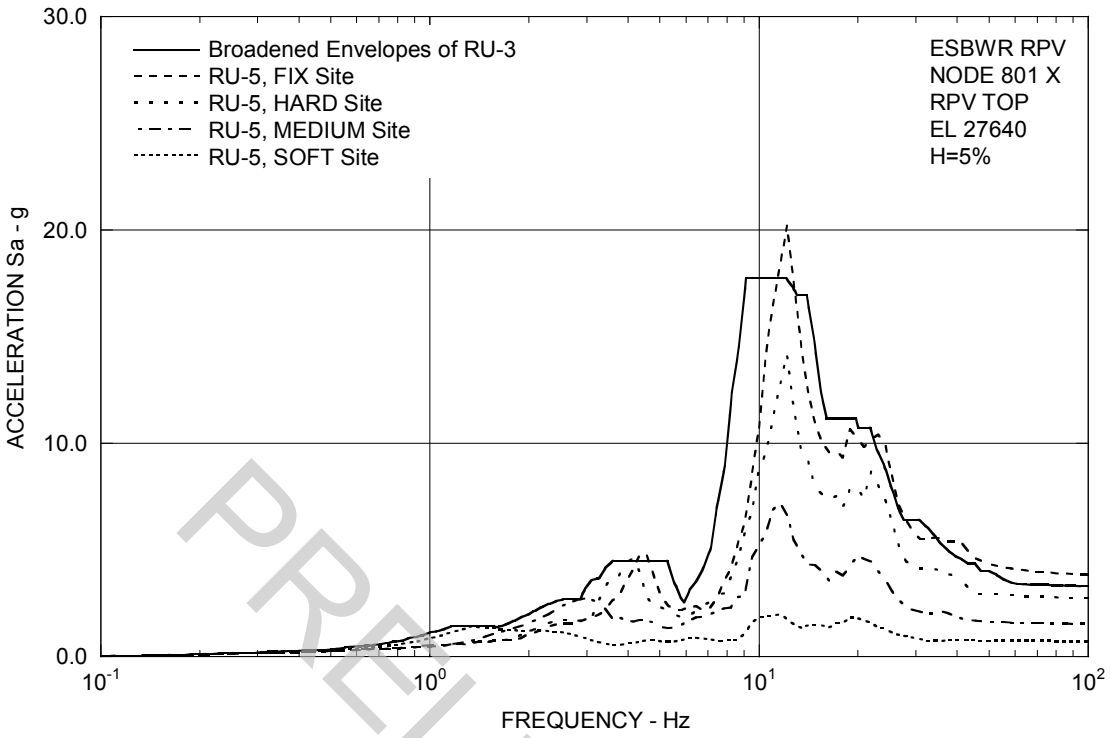

Figure 3A.8.4-1e. FRS (Effect of 50% Infill Concrete Stiffness of VW and D/F) – RPV Top X

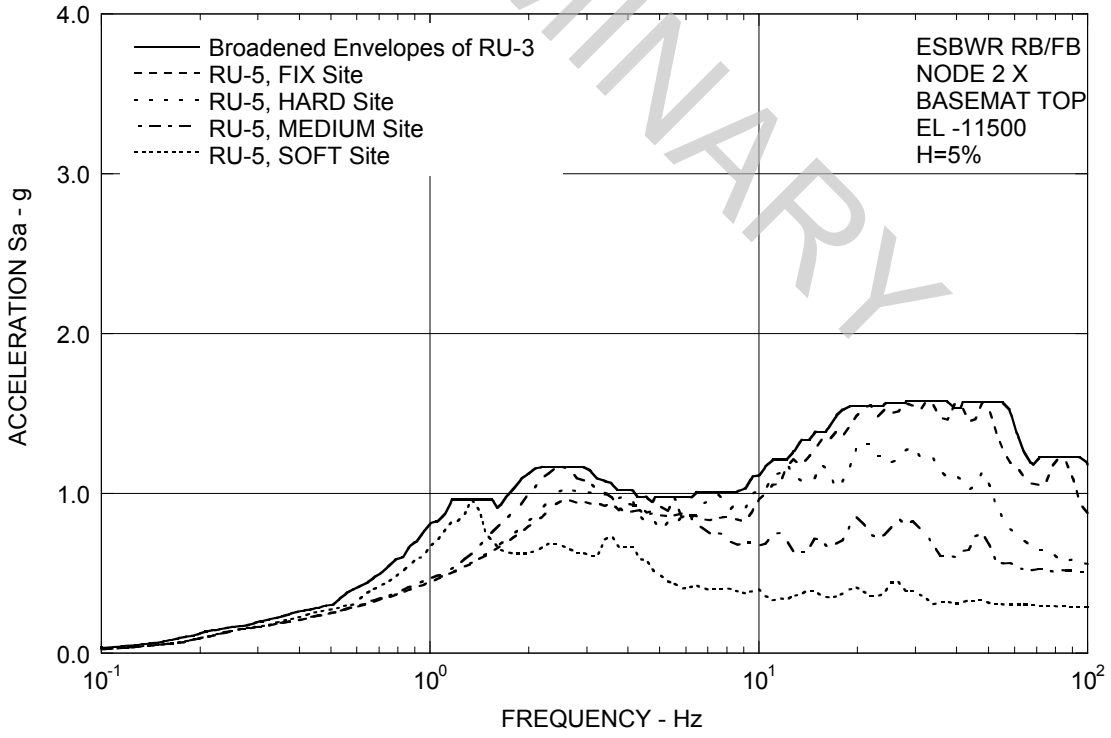

Figure 3A.8.4-1f. FRS (Effect of Infill 50% Concrete Stiffness of VW and D/F) – RB/FB Basemat X

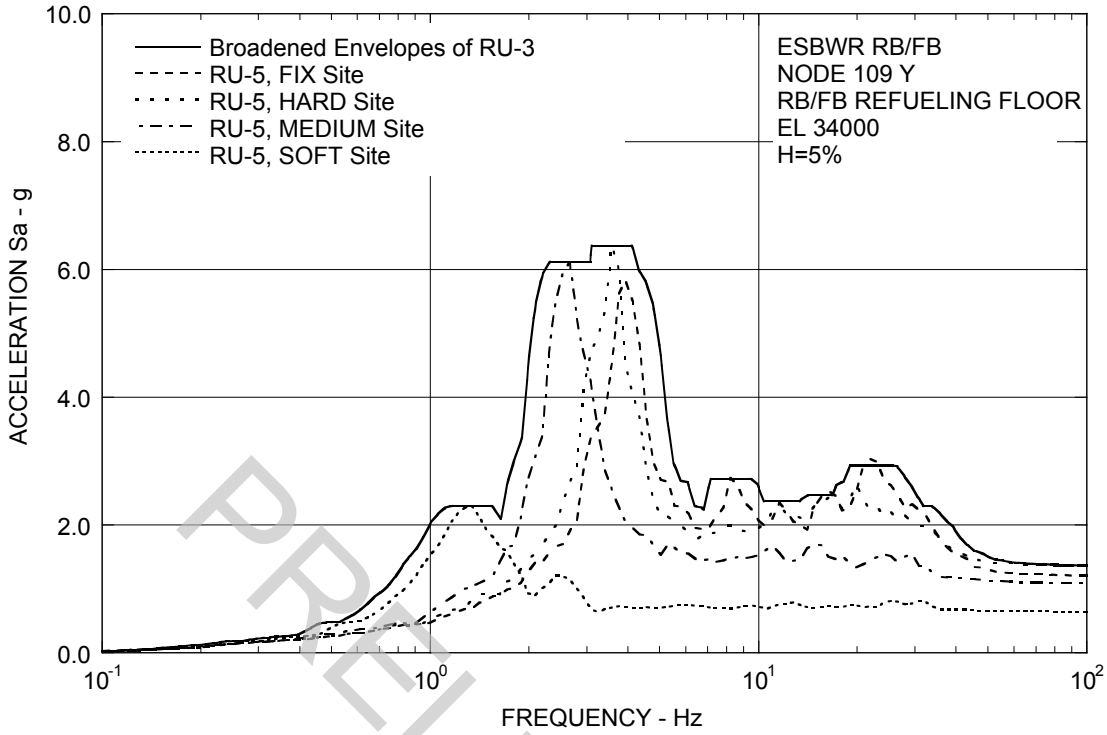

Figure 3A.8.4-2a. FRS (Effect of 50% Infill Concrete Stiffness of VW and D/F) – RB/FB Refueling Floor Y

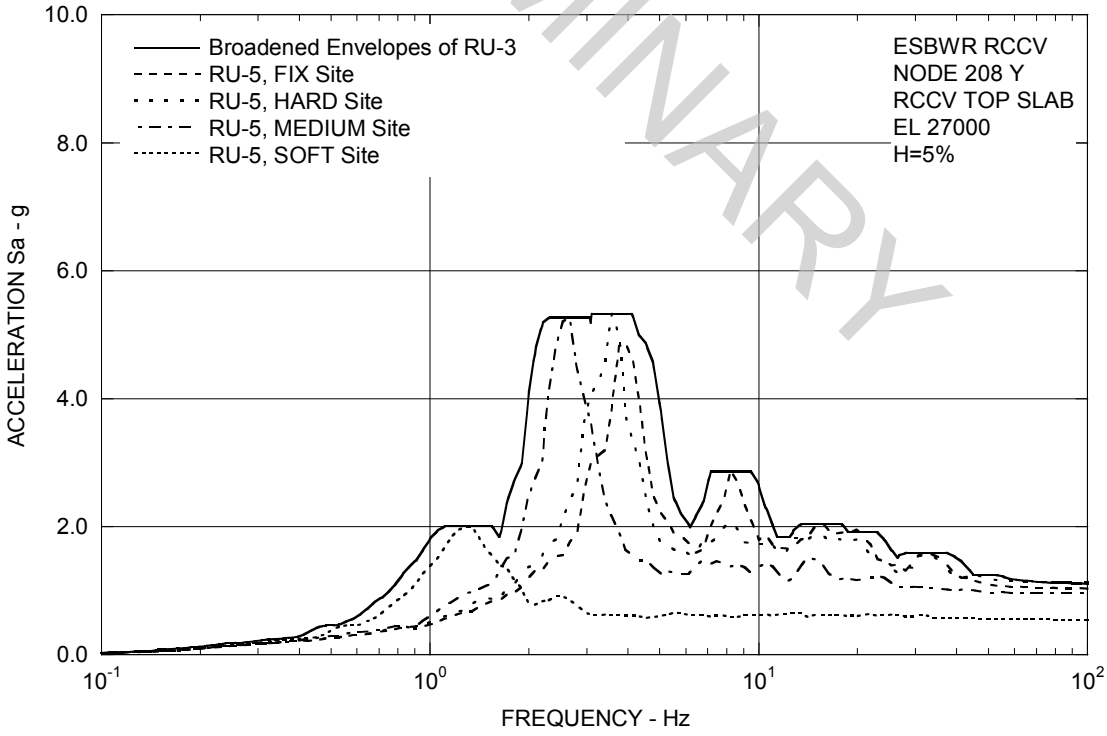

Figure 3A.8.4-2b. FRS (Effect of 50% Infill Concrete Stiffness of VW and D/F) – RCCV Top Slab Y

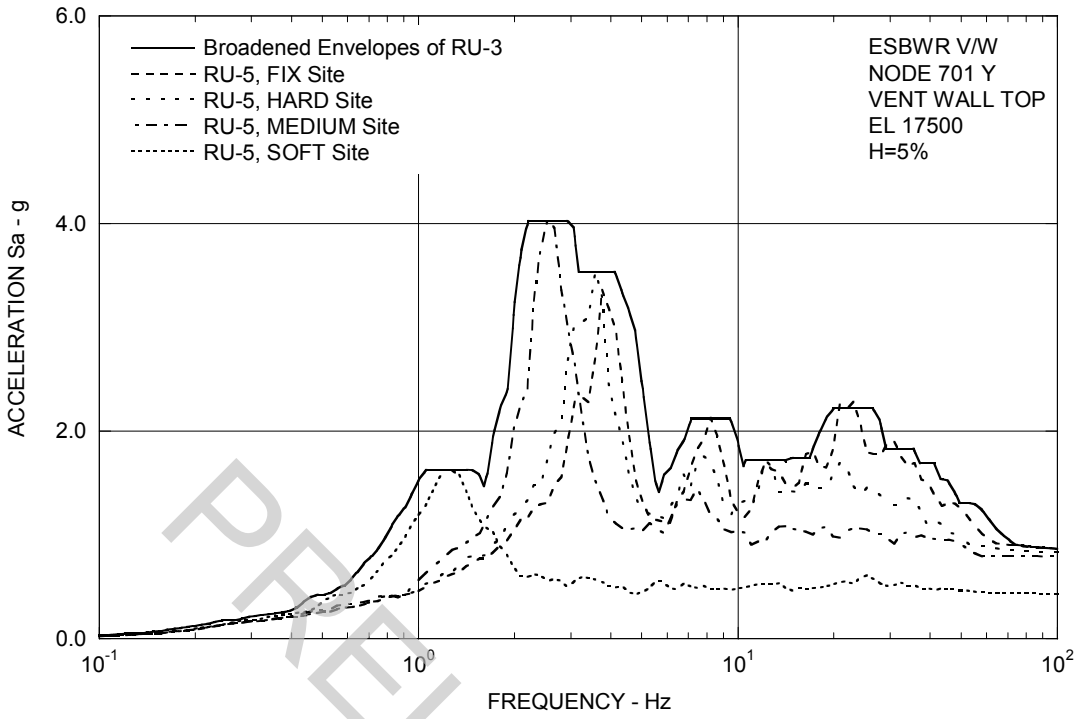

Figure 3A.8.4-2c. FRS (Effect of 50% Infill Concrete Stiffness of VW and D/F) – Vent Wall Top Y

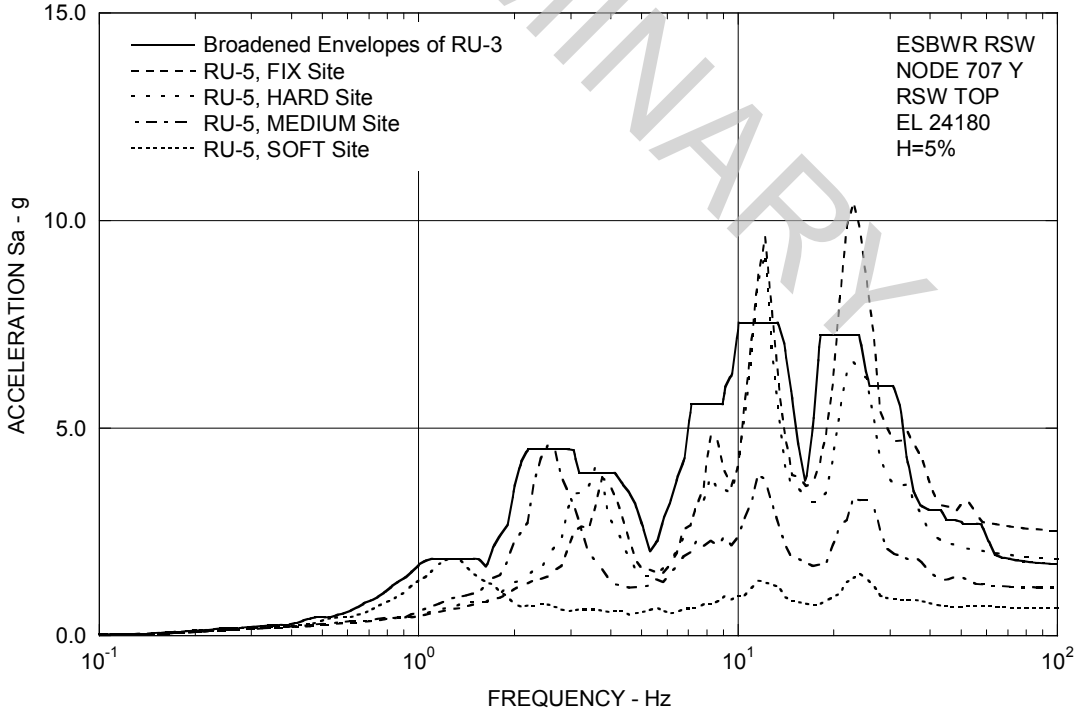

Figure 3A.8.4-2d. FRS (Effect of 50% Infill Concrete Stiffness of VW and D/F) – RSW Top Y

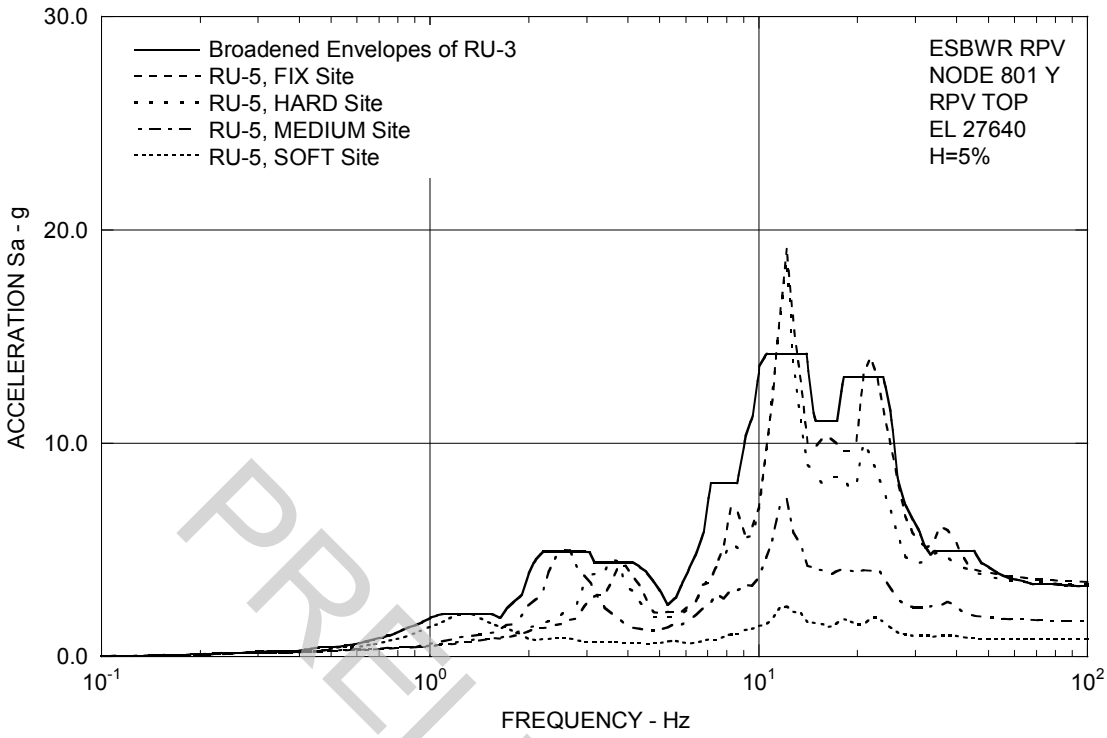

Figure 3A.8.4-2e. FRS (Effect of 50% Infill Concrete Stiffness of VW and D/F) – RPV Top Y

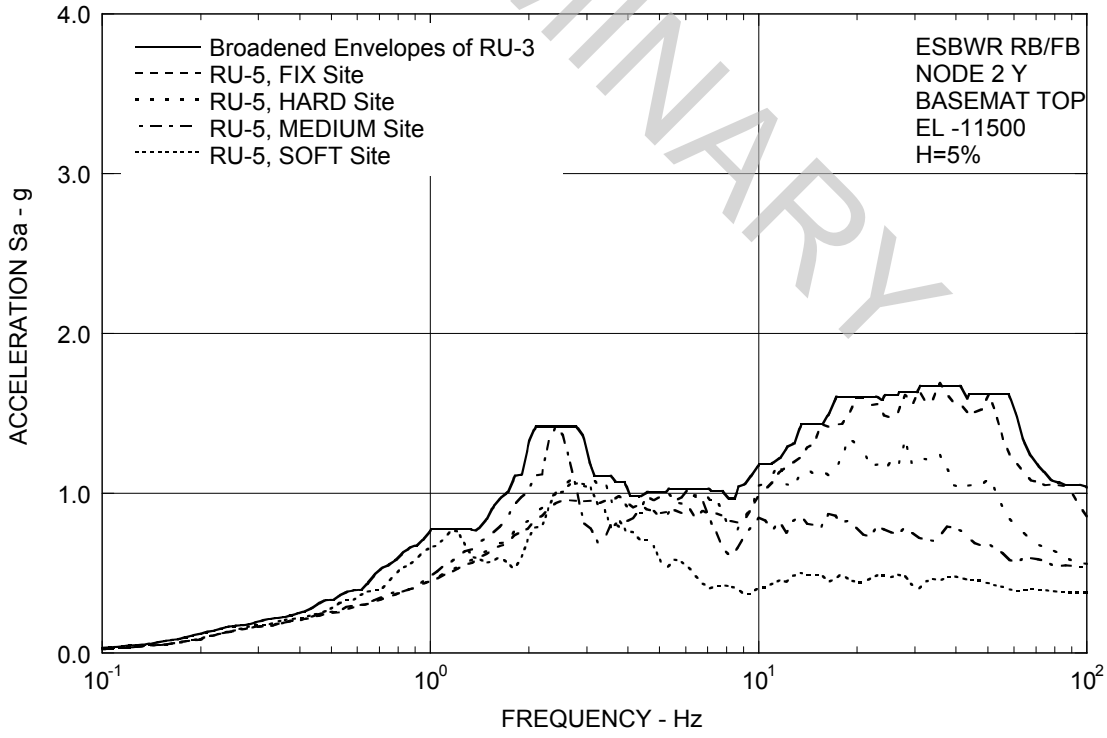

Figure 3A.8.4-2f. FRS (Effect of 50% Infill Concrete Stiffness of VW and D/F) – RB/FB Basemat Y

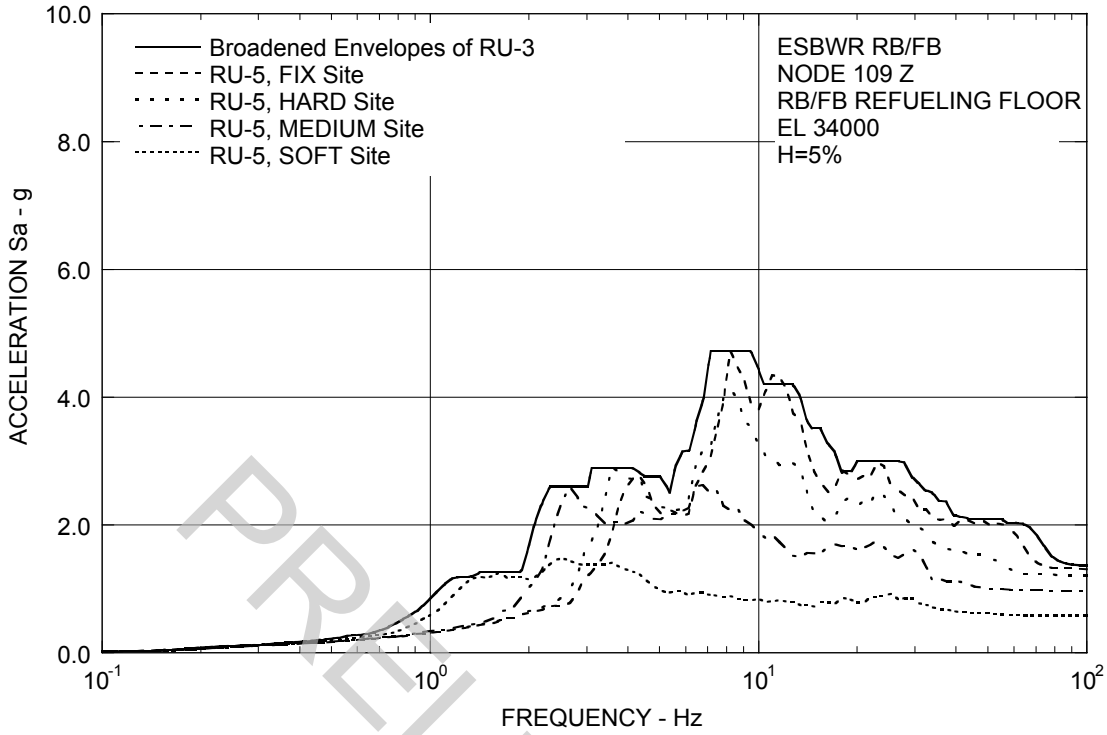

Figure 3A.8.4-3a. FRS (Effect of 50% Infill Concrete Stiffness of VW and D/F) – RB/FB Refueling Floor Z

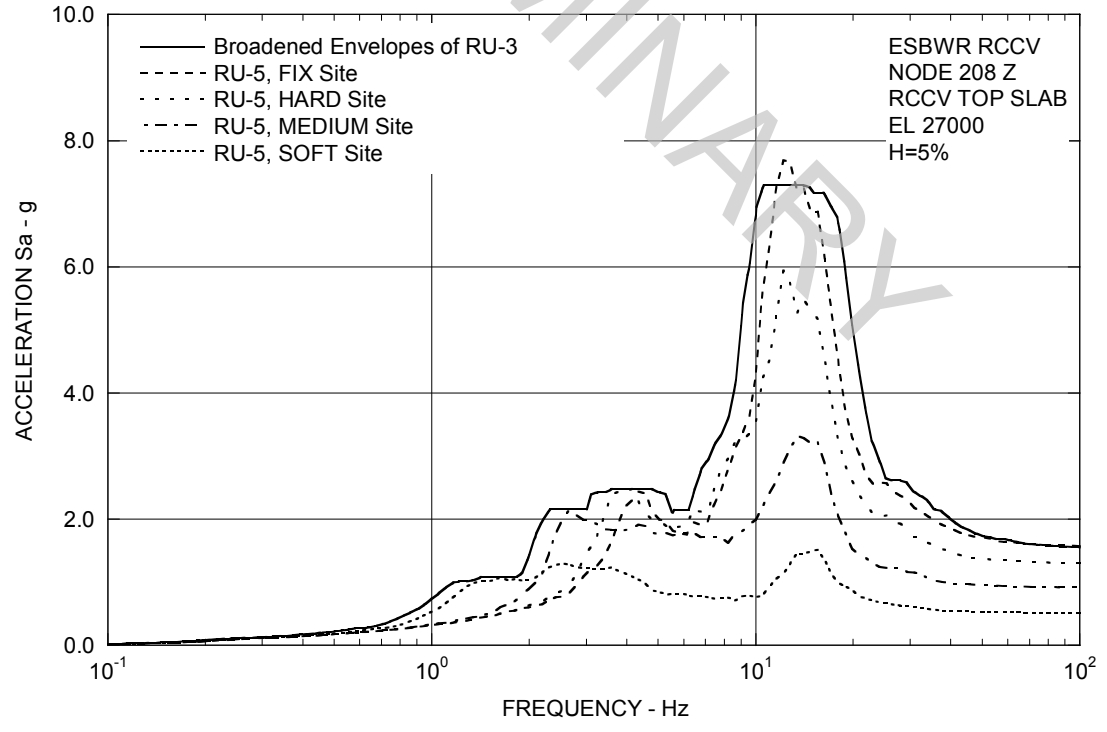

Figure 3A.8.4-3b. FRS (Effect of 50% Infill Concrete Stiffness of VW and D/F) – RCCV Top Slab Z

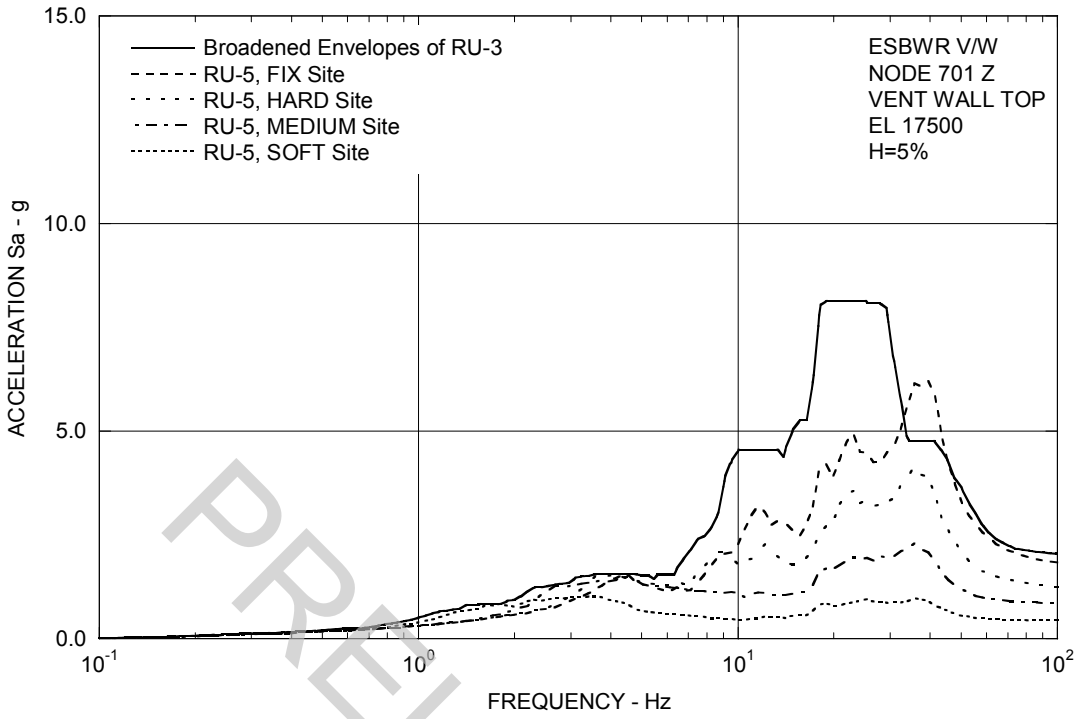

Figure 3A.8.4-3c. FRS (Effect of 50% Infill Concrete Stiffness of VW and D/F) – Vent Wall Top Z

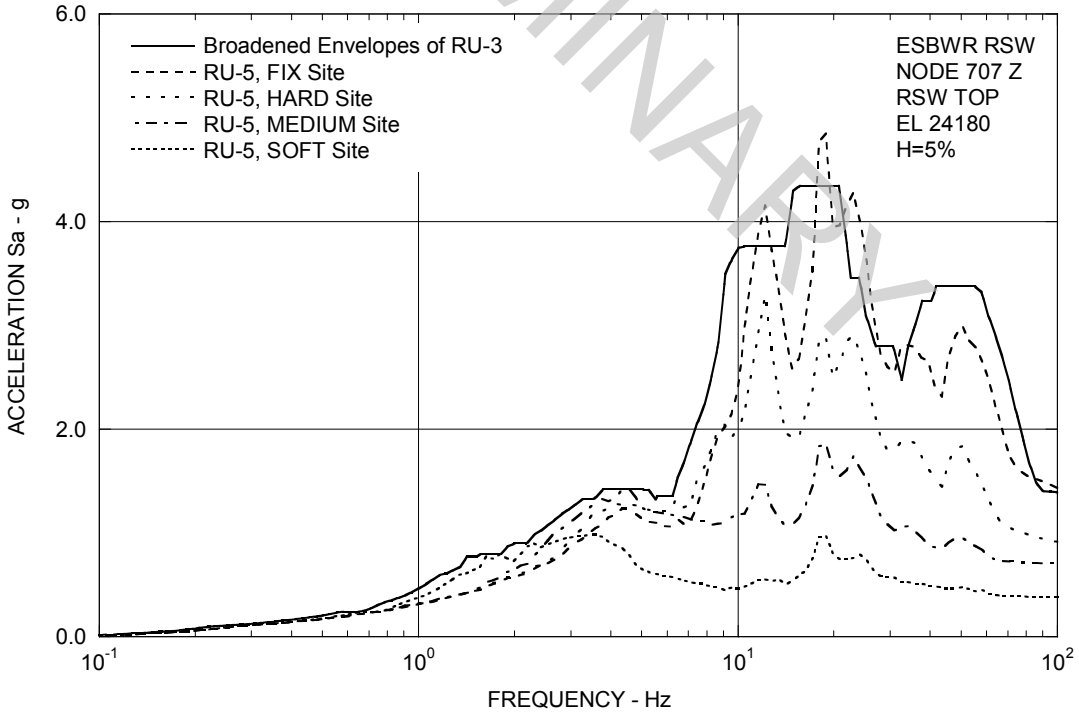

Figure 3A.8.4-3d. FRS (Effect of 50% Infill Concrete Stiffness of VW and D/F) – RSW Top Z

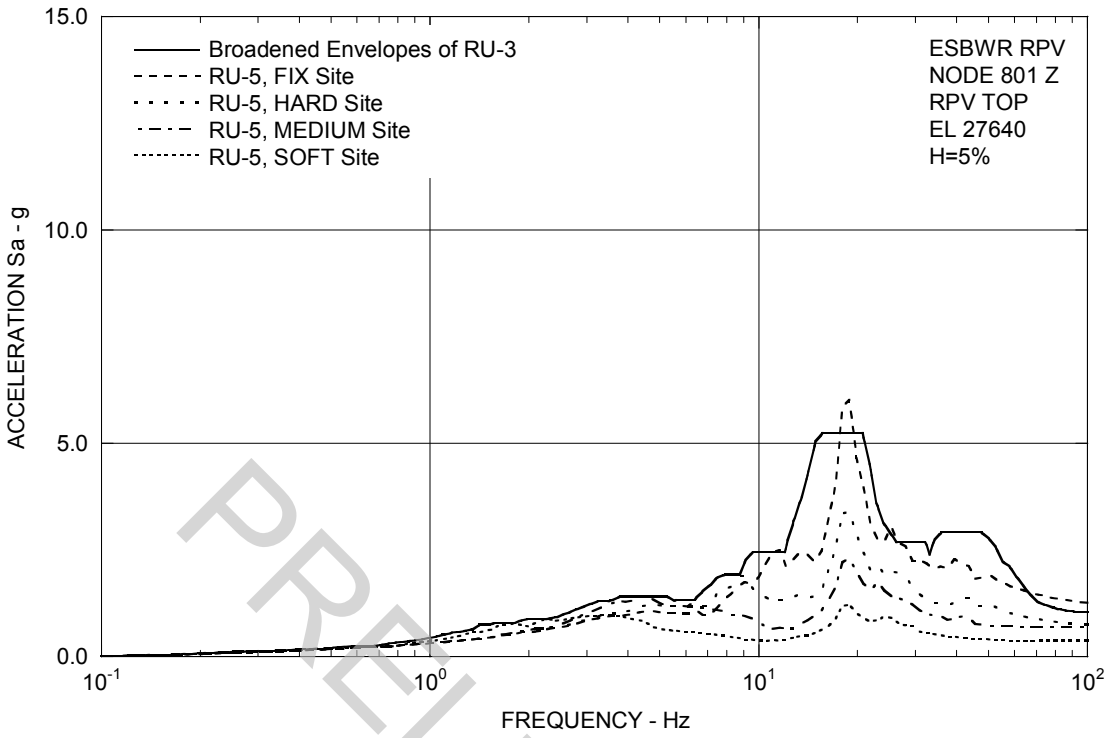

Figure 3A.8.4-3e. FRS (Effect of 50% Infill Concrete Stiffness of VW and D/F) – RPV Top Z

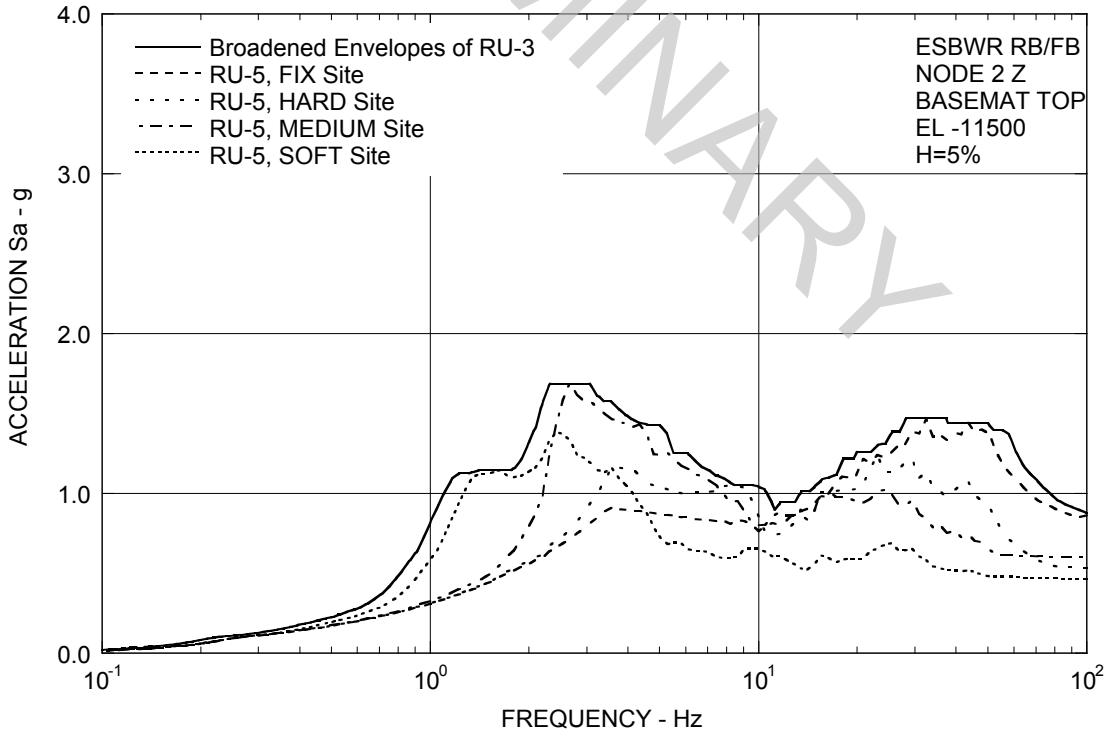

Figure 3A.8.4-3f. FRS (Effect of 50% Infill Concrete Stiffness of VW and D/F) – RB/FB Basemat Z

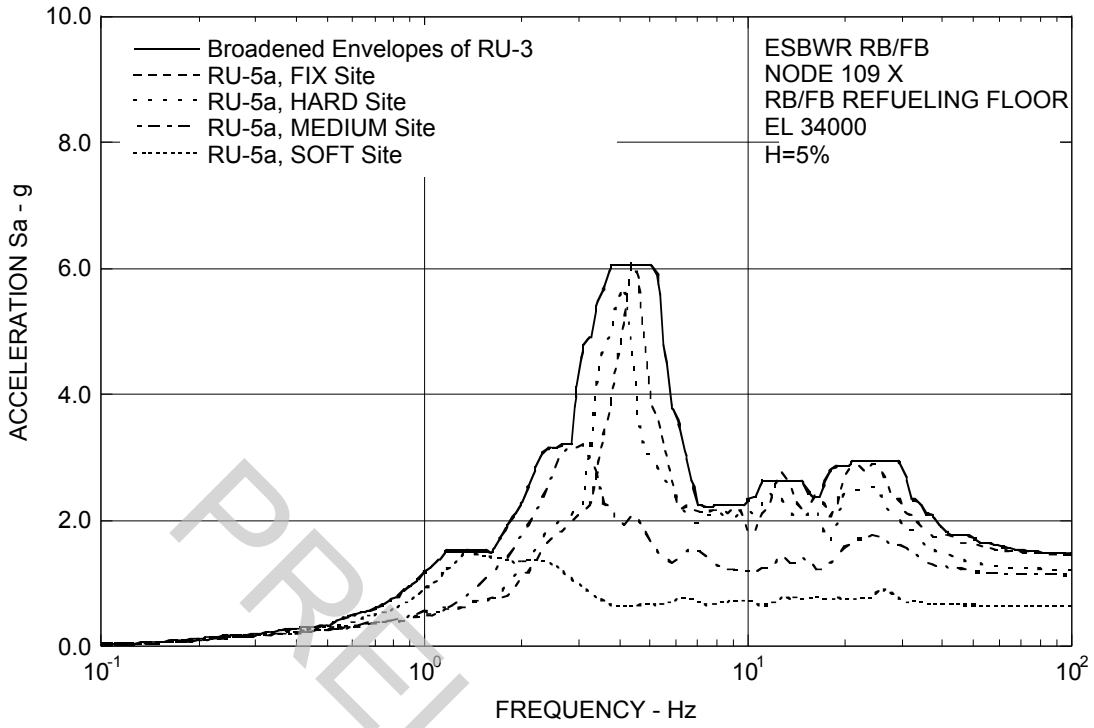

Figure 3A.8.4-4a. FRS (Effect of 100% Infill Concrete Stiffness of VW and D/F) – RB/FB Refueling Floor X

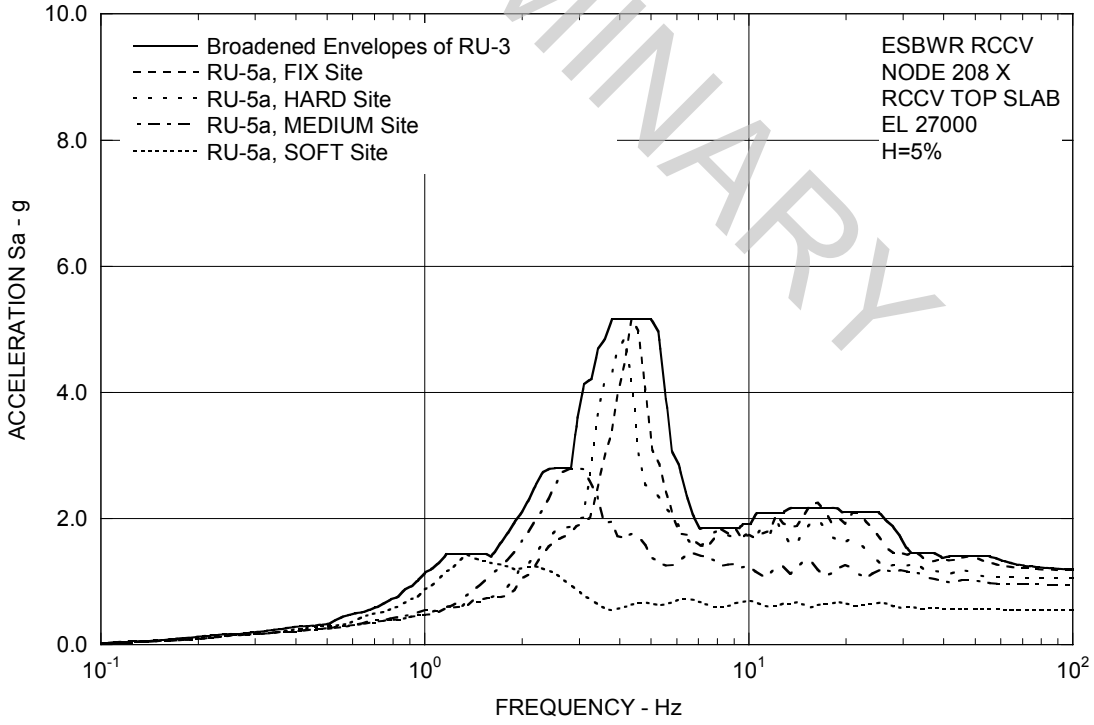

Figure 3A.8.4-4b. FRS (Effect of 100% Infill Concrete Stiffness of VW and D/F) – RCCV Top Slab X

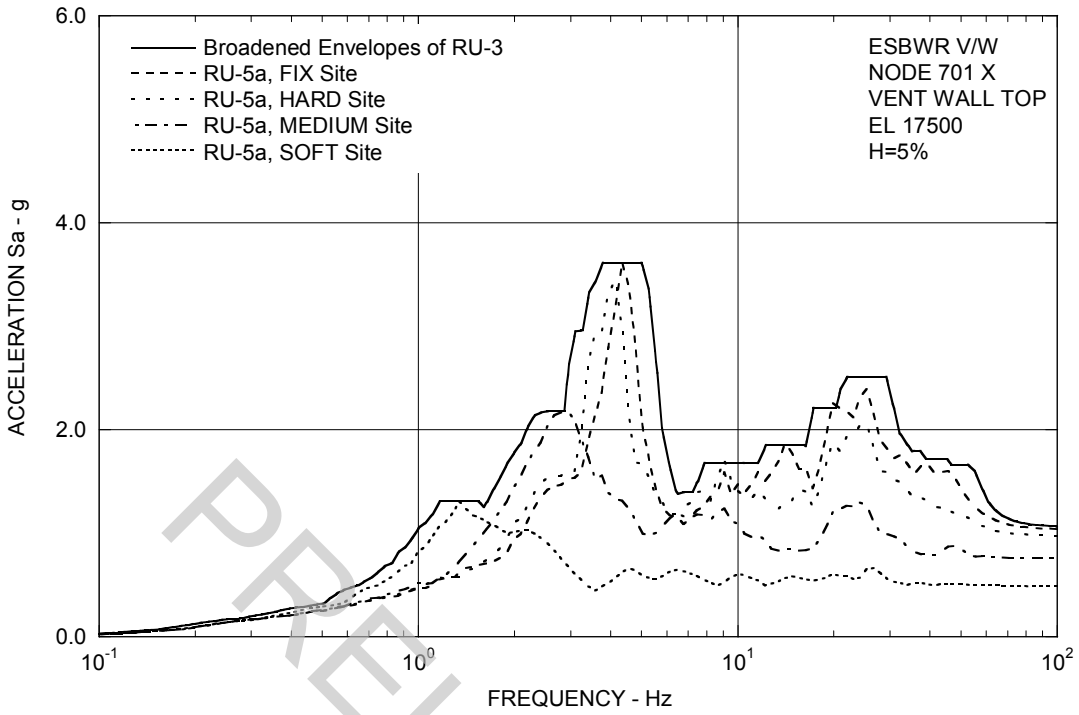

Figure 3A.8.4-4c. FRS (Effect of 100% Infill Concrete Stiffness of VW and D/F) – Vent Wall Top X

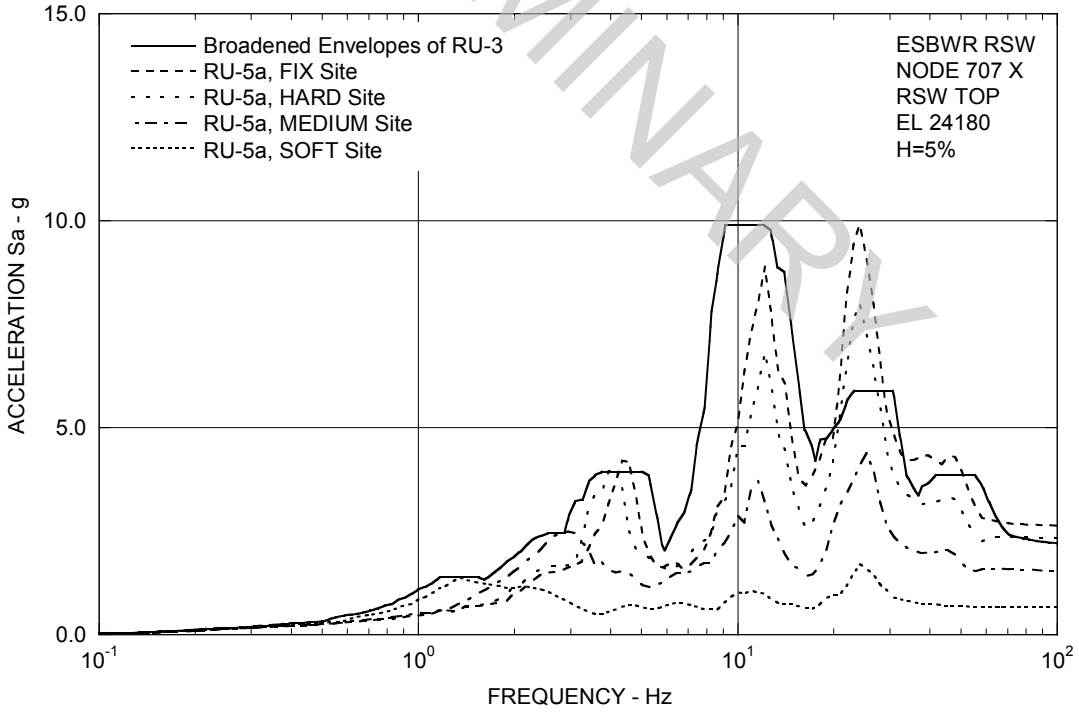

Figure 3A.8.4-4d. FRS (Effect of 100% Infill Concrete Stiffness of VW and D/F) – RSW Top X

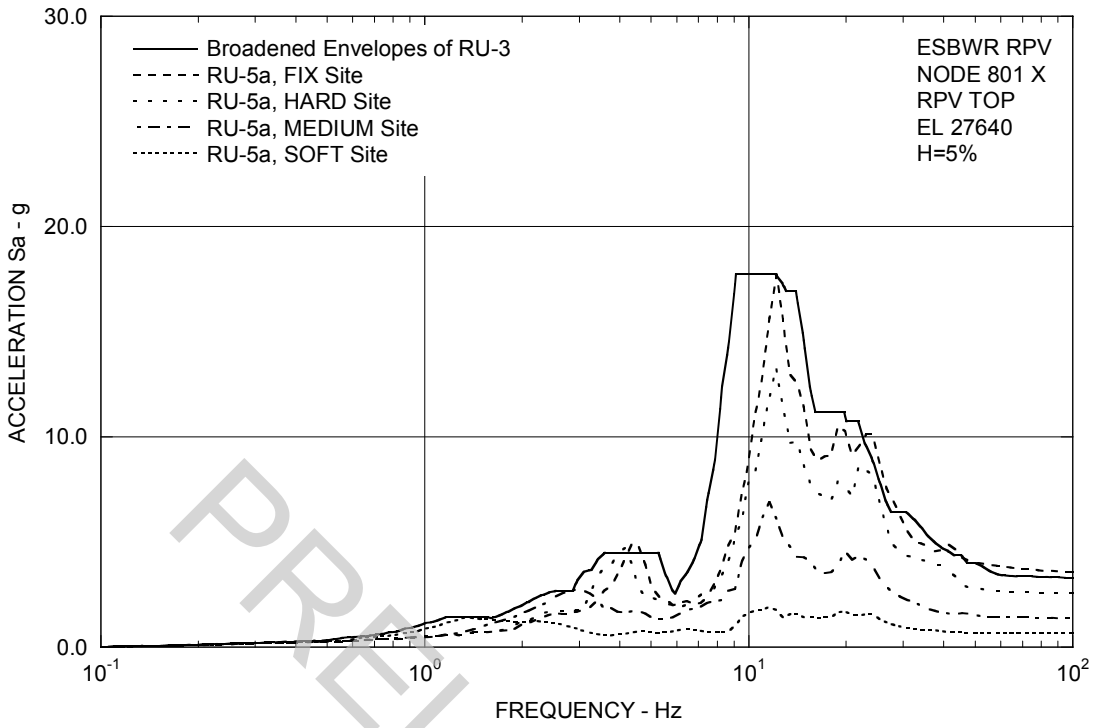

Figure 3A.8.4-4e. FRS (Effect of 100% Infill Concrete Stiffness of VW and D/F) – RPV Top X

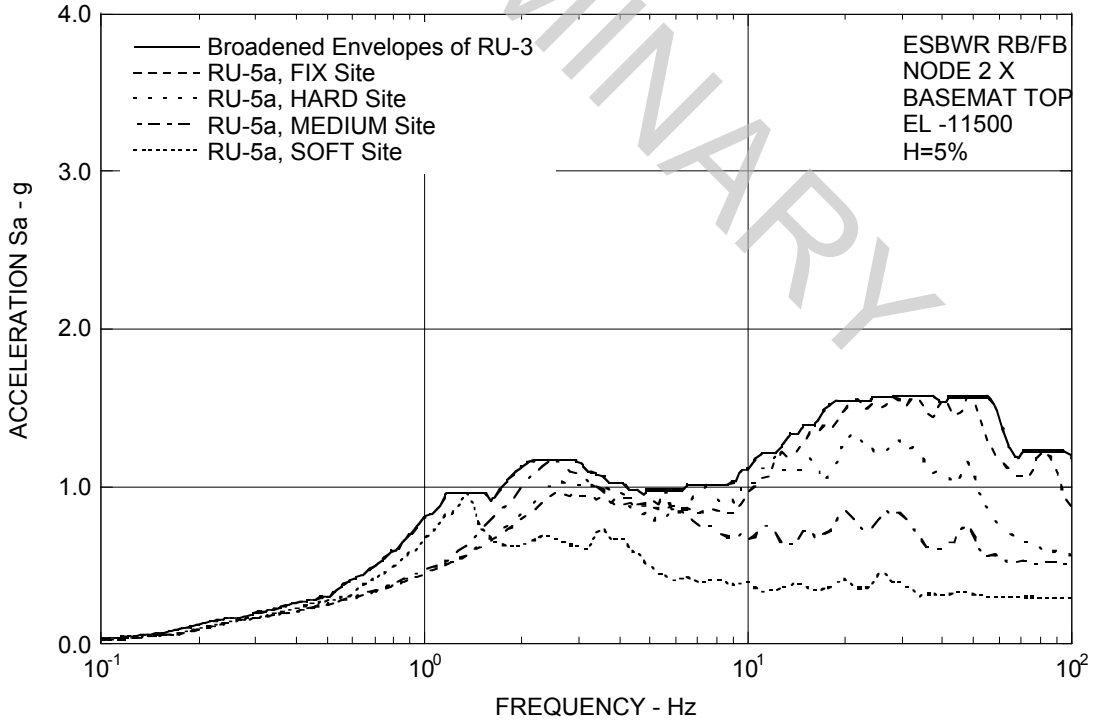

Figure 3A.8.4-4f. FRS (Effect of 100% Infill Concrete Stiffness of VW and D/F) – RB/FB Basemat X

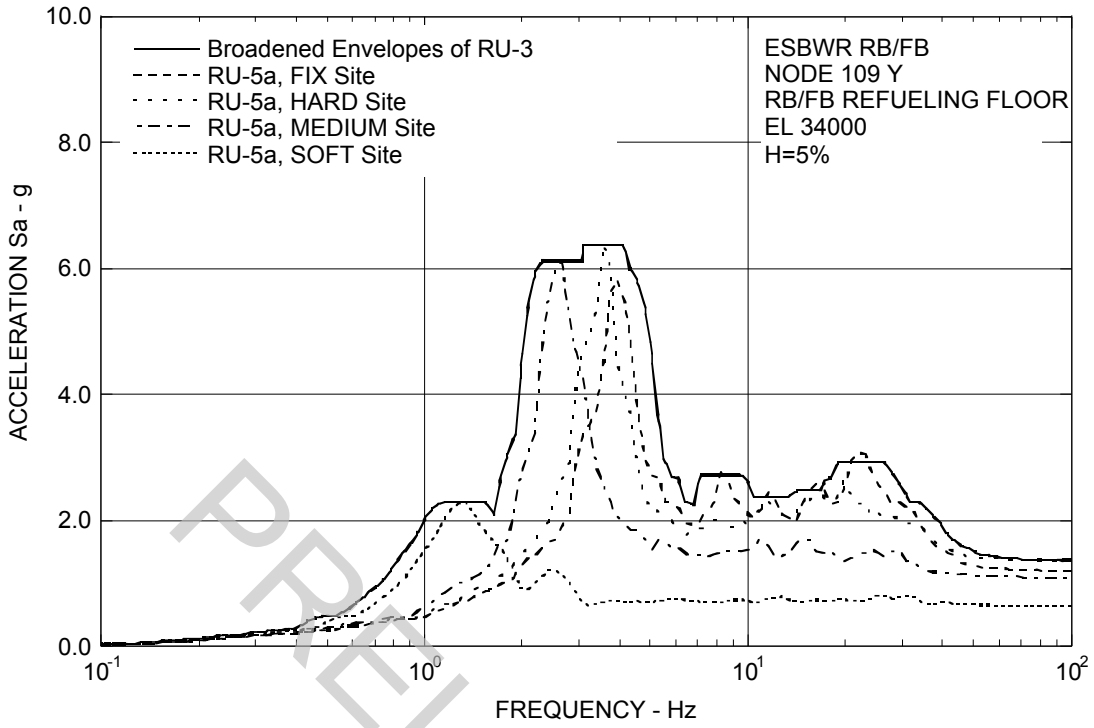

Figure 3A.8.4-5a. FRS (Effect of 100% Infill Concrete Stiffness of VW and D/F) – RB/FB Refueling Floor Y

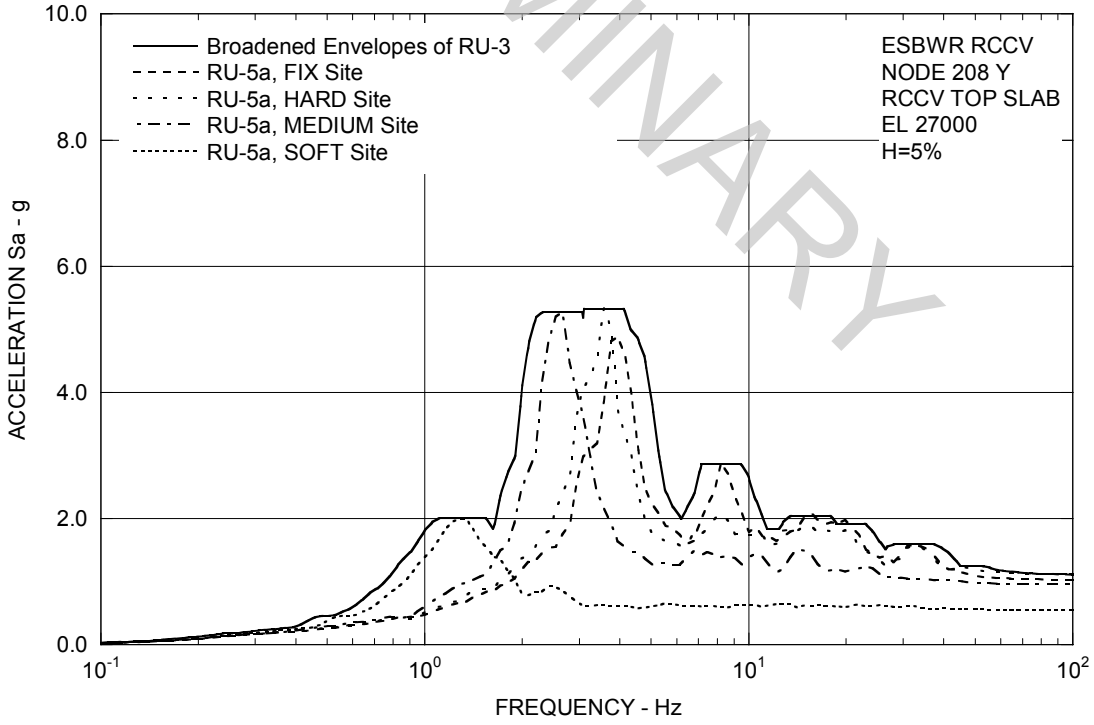

Figure 3A.8.4-5b. FRS (Effect of 100% Infill Concrete Stiffness of VW and D/F) – RCCV Top Slab Y

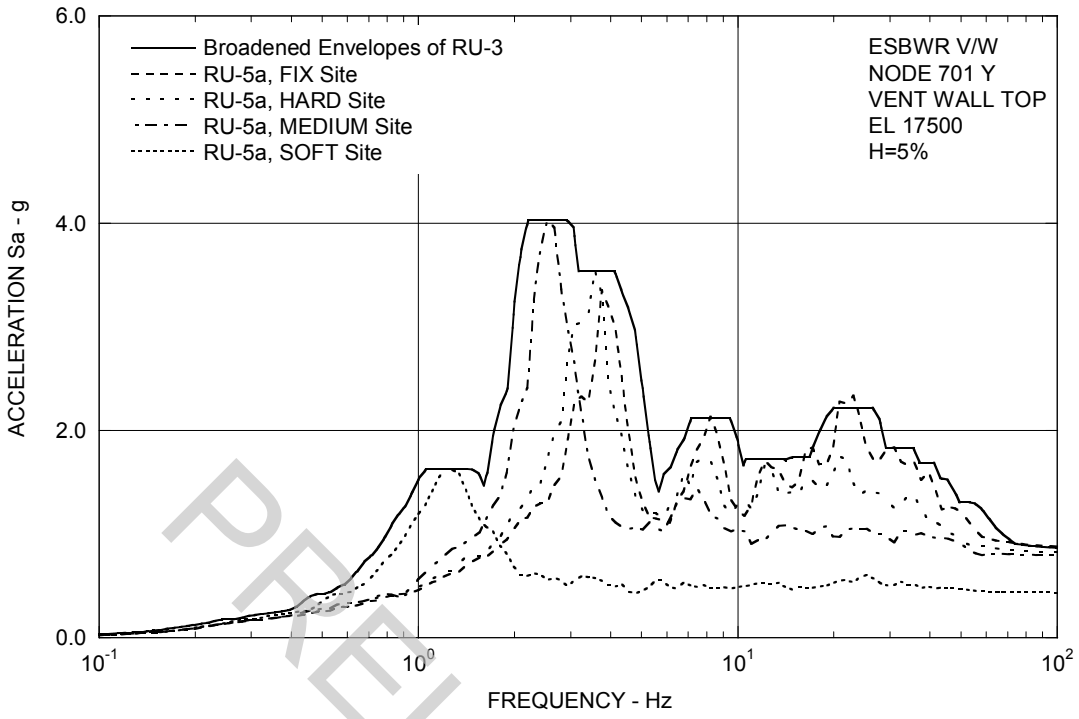

Figure 3A.8.4-5c. FRS (Effect of 100% Infill Concrete Stiffness of VW and D/F) – Vent Wall Top Y

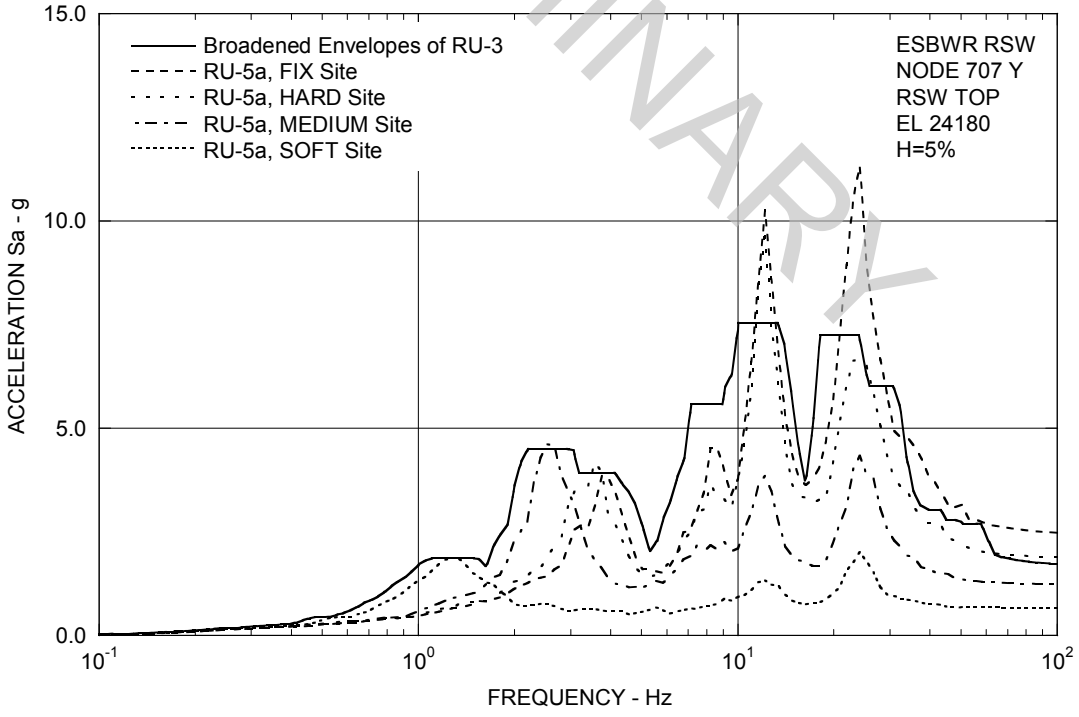

Figure 3A.8.4-5d. FRS (Effect of 100% Infill Concrete Stiffness of VW and D/F) – RSW Top Y

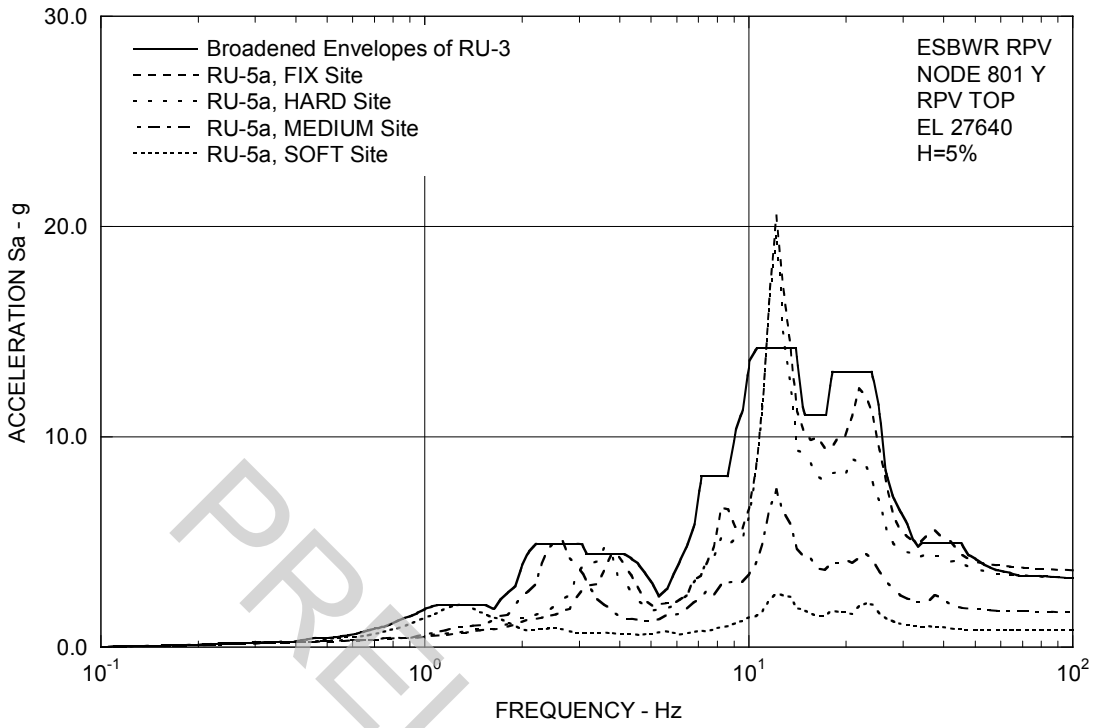

Figure 3A.8.4-5e. FRS (Effect of 100% Infill Concrete Stiffness of VW and D/F) – RPV Top Y

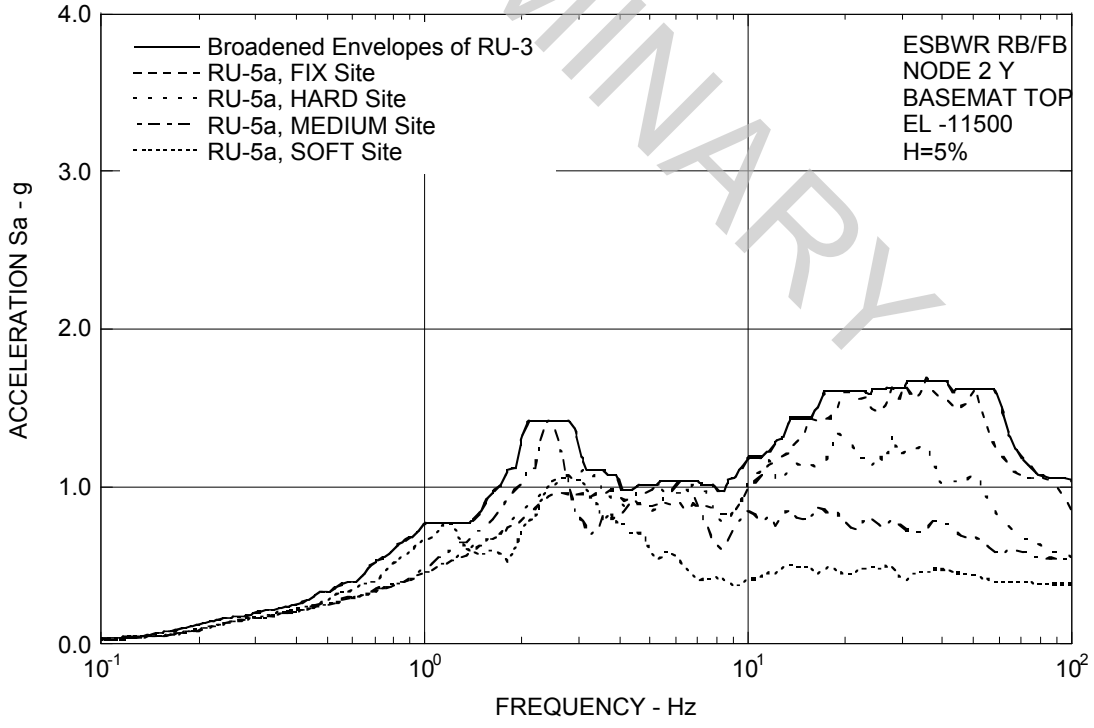

Figure 3A.8.4-5f. FRS (Effect of 100% Infill Concrete Stiffness of VW and D/F) – RB/FB Basemat Y

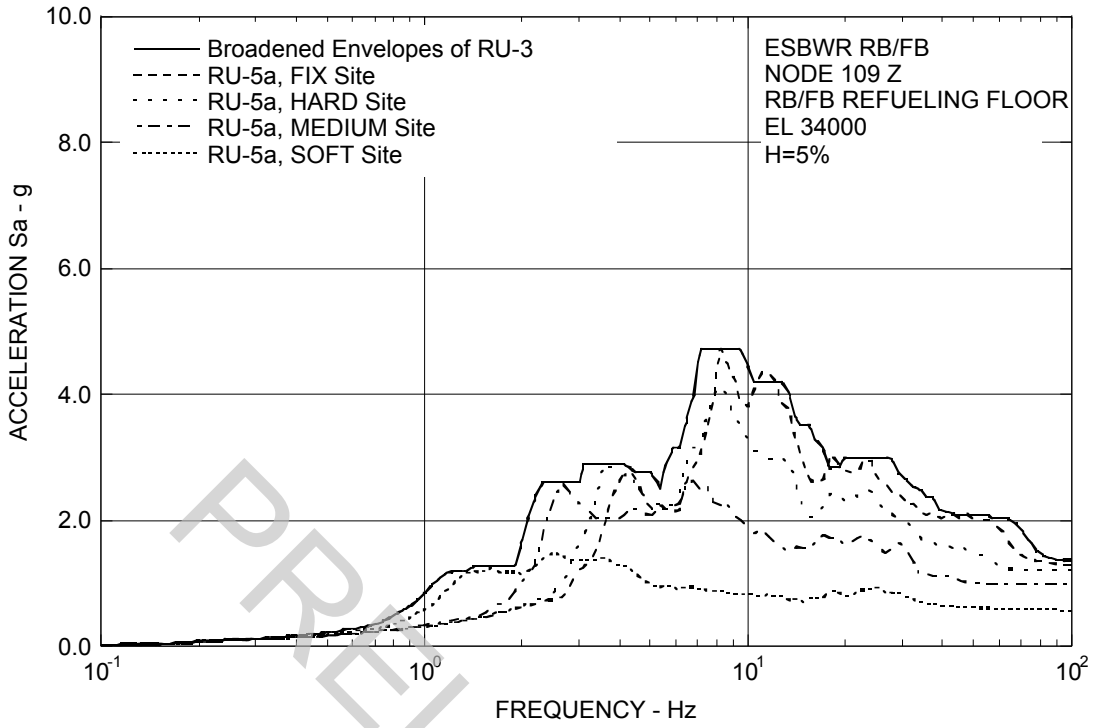

Figure 3A.8.4-6a. FRS (Effect of 100% Infill Concrete Stiffness of VW and D/F) – RB/FB Refueling Floor Z

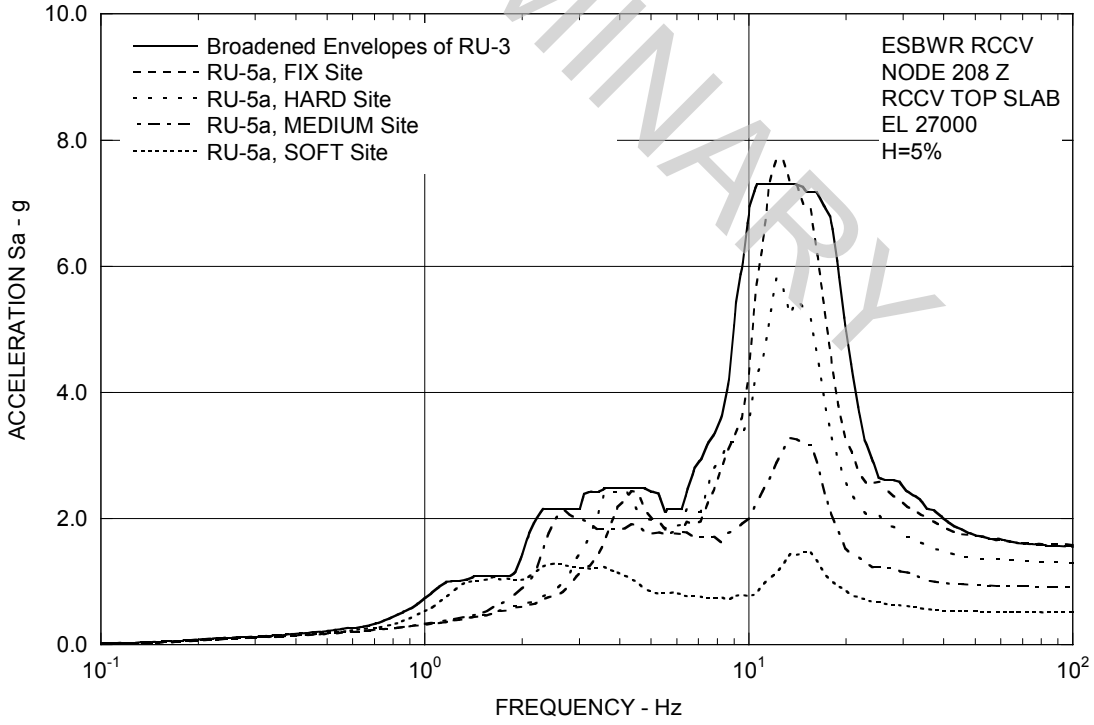

Figure 3A.8.4-6b. FRS (Effect of 100% Infill Concrete Stiffness of VW and D/F) – RCCV Top Slab Z

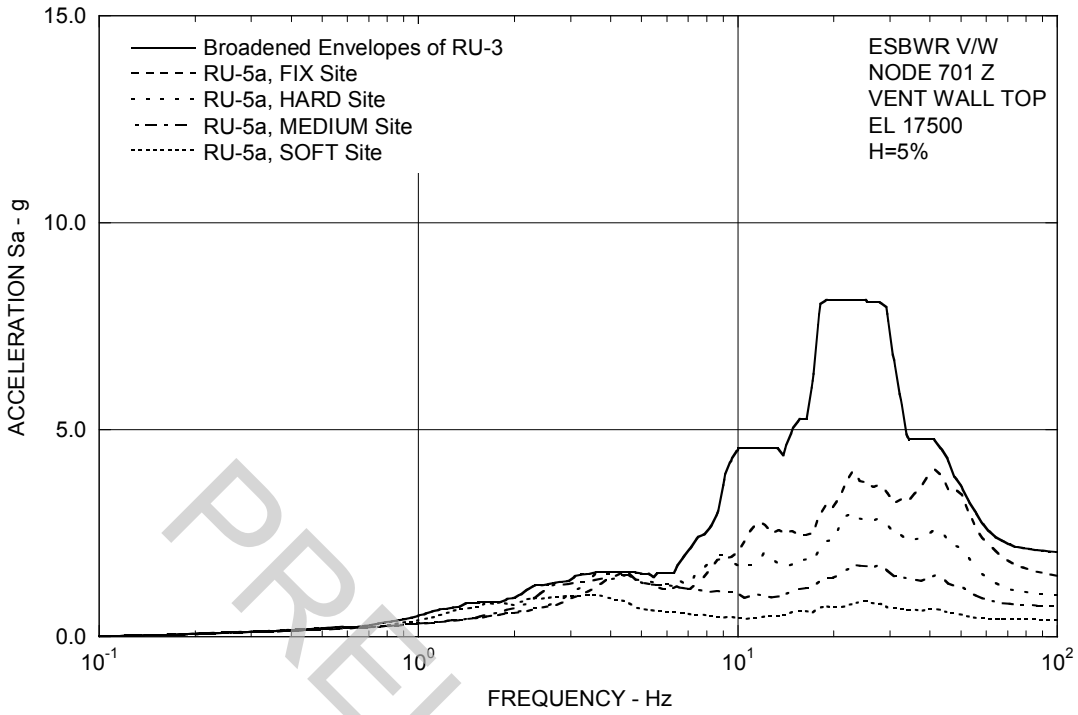

Figure 3A.8.4-6c. FRS (Effect of 100% Infill Concrete Stiffness of VW and D/F) – Vent Wall Top Z

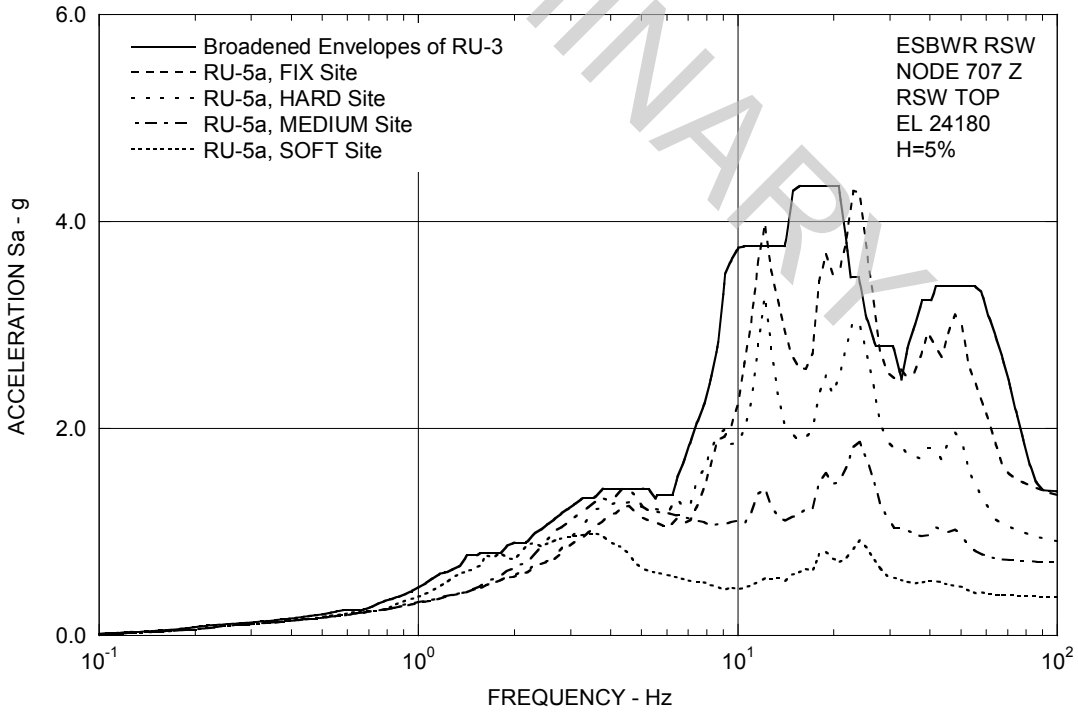

Figure 3A.8.4-6d. FRS (Effect of 100% Infill Concrete Stiffness of VW and D/F) – RSW Top Z

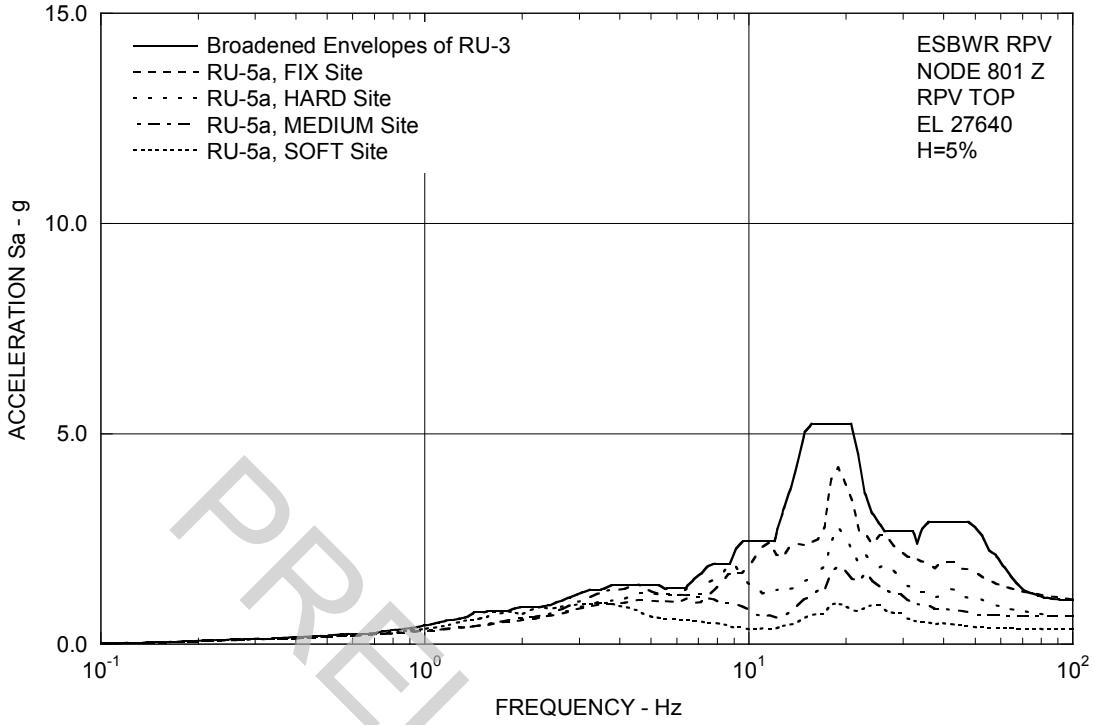

Figure 3A.8.4-6e. FRS (Effect of 100% Infill Concrete Stiffness of VW and D/F) – RPV Top Z

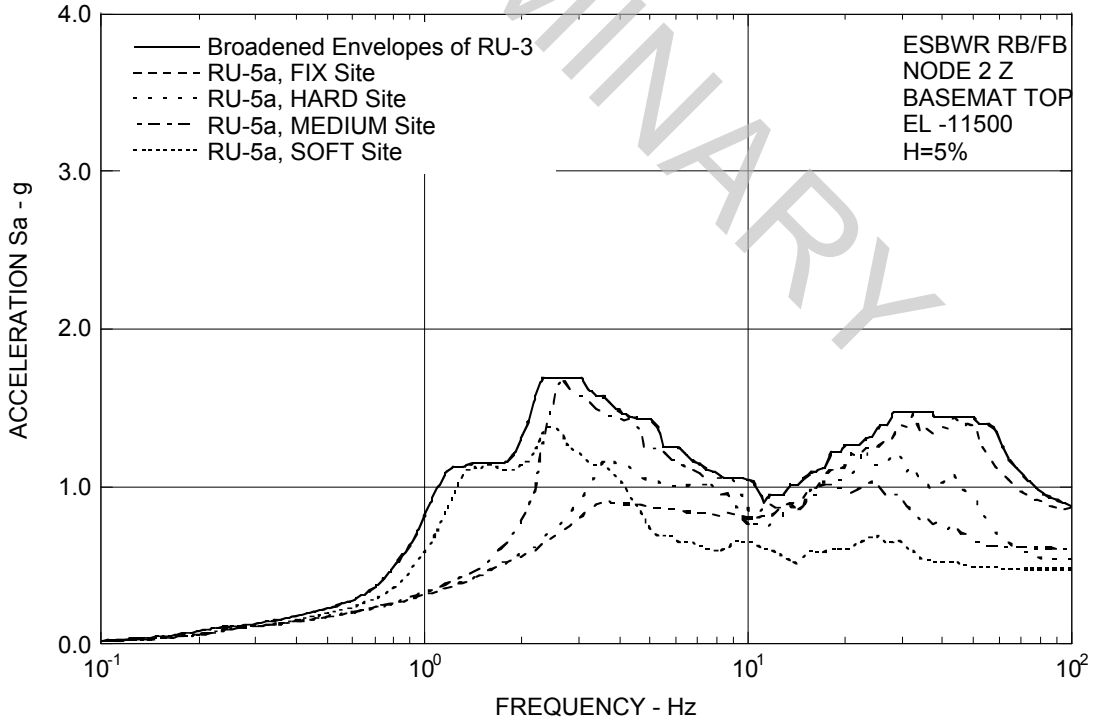

Figure 3A.8.4-6f. FRS (Effect of 100% Infill Concrete Stiffness of VW and D/F) – RB/FB Basemat Z

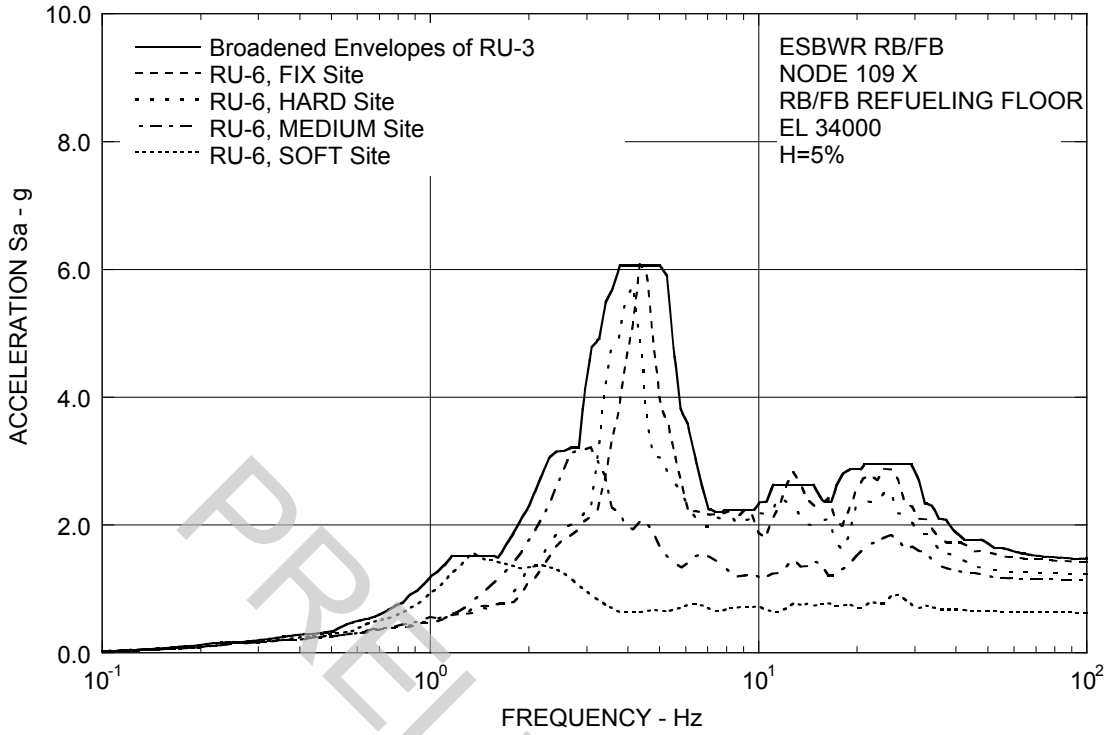

Figure 3A.8.5-1a. FRS (Effect of LOCA Flooding) – RB/FB Refueling Floor X

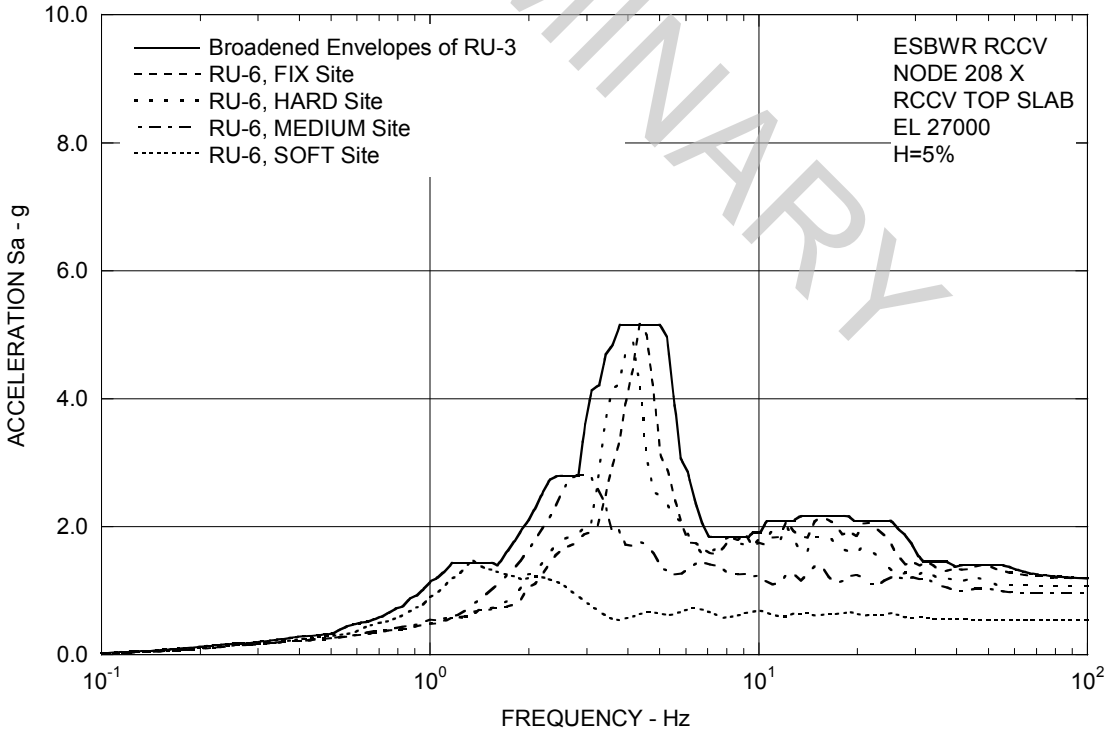

Figure 3A.8.5-1b. FRS (Effect of LOCA Flooding) – RCCV Top Slab X

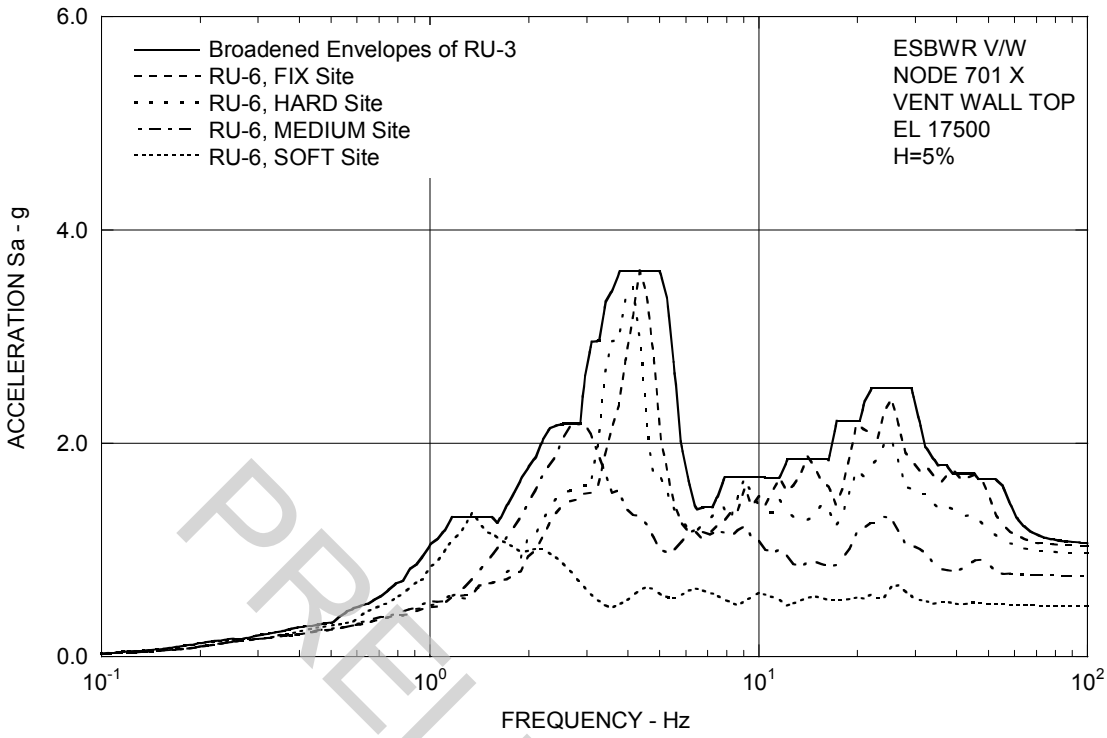

Figure 3A.8.5-1c. FRS (Effect of LOCA Flooding) – Vent Wall Top X

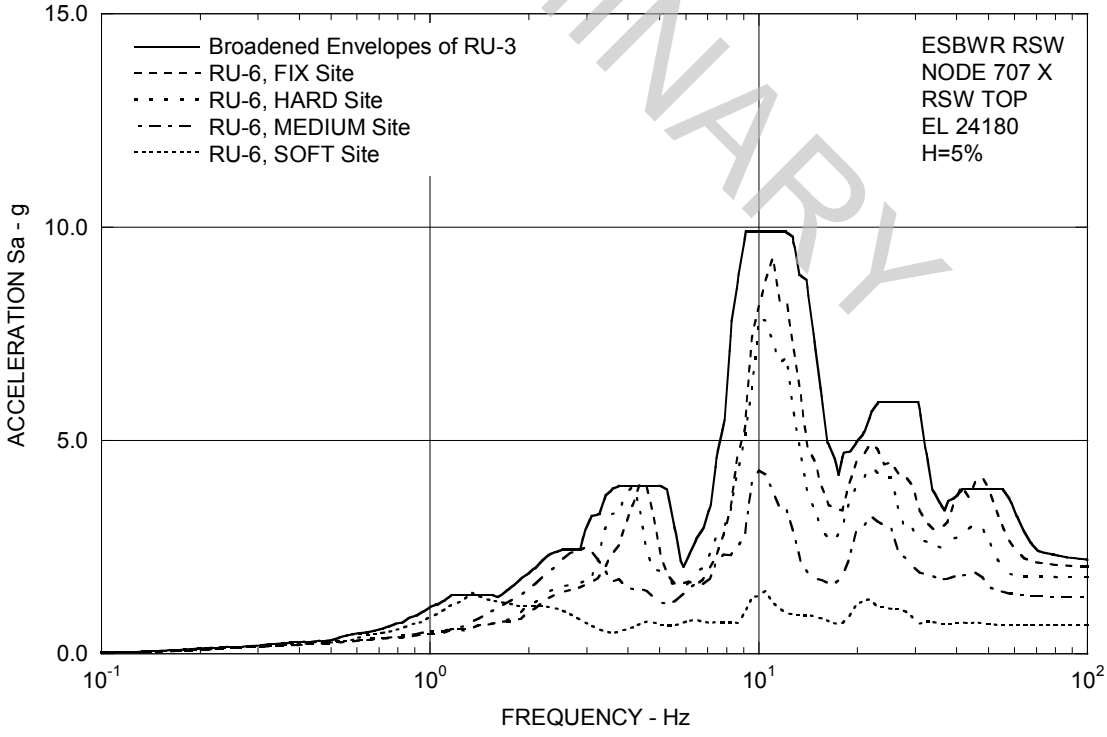

Figure 3A.8.5-1d. FRS (Effect of LOCA Flooding) – RSW Top X

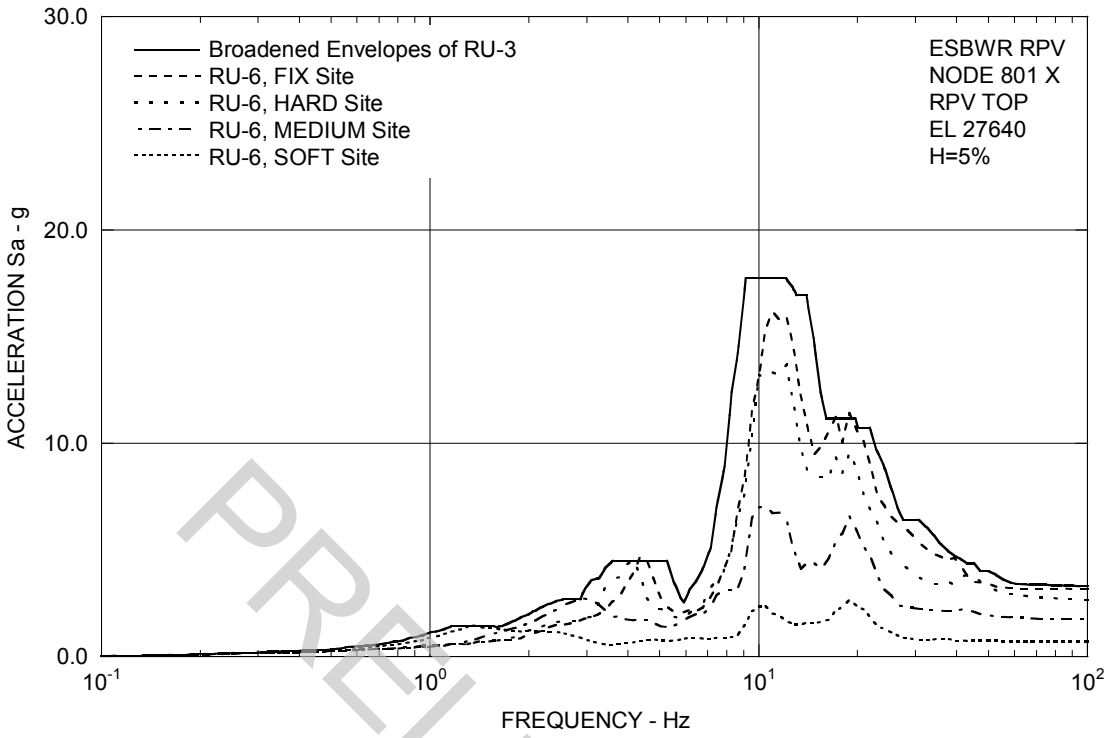

Figure 3A.8.5-1e. FRS (Effect of LOCA Flooding) – RPV Top X

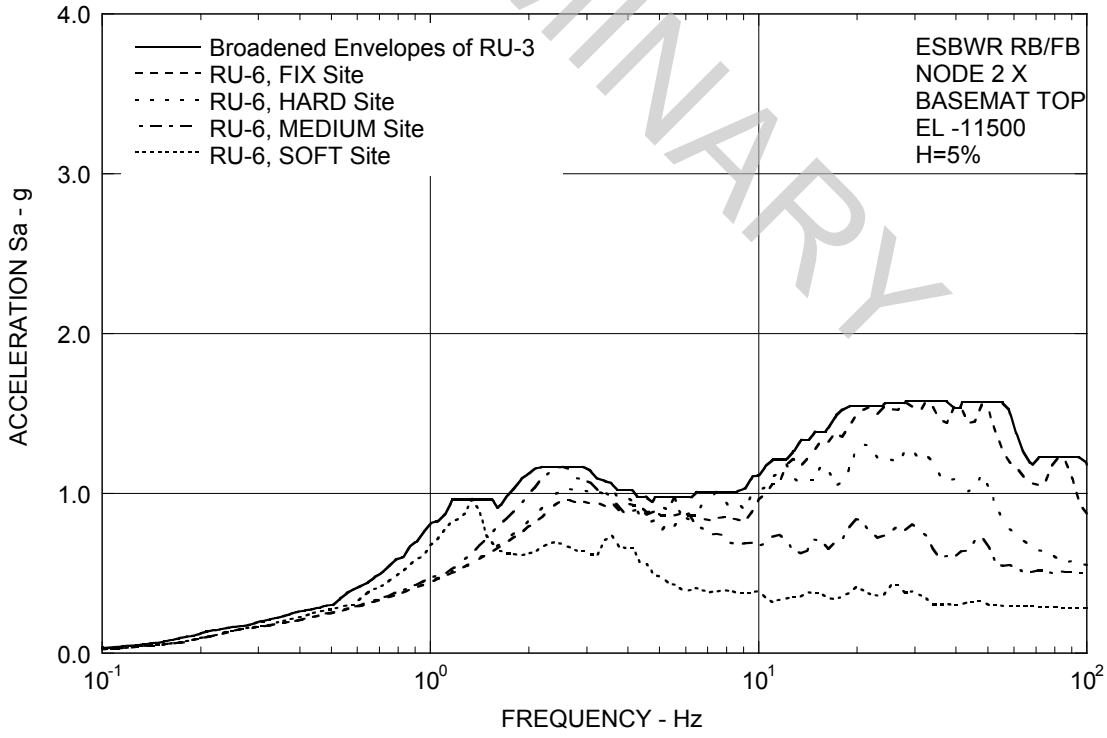

Figure 3A.8.5-1f. FRS (Effect of LOCA Flooding) – RB/FB Basemat X

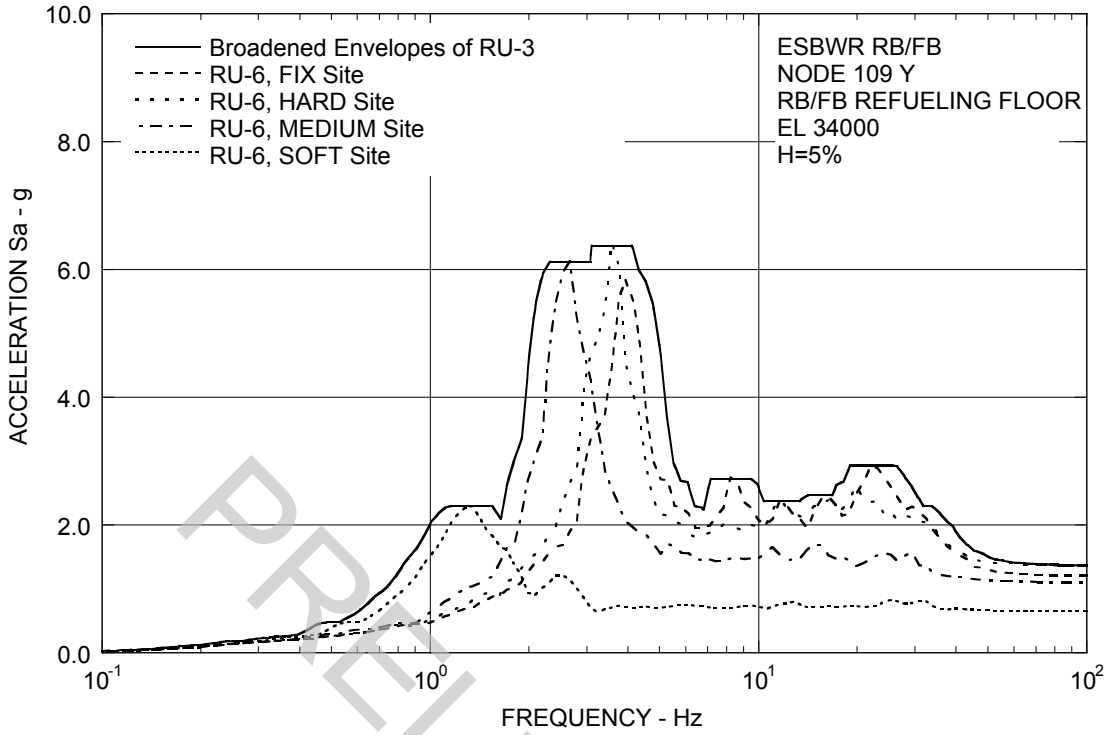

Figure 3A.8.5-2a. FRS (Effect of LOCA Flooding) – RB/FB Refueling Floor Y

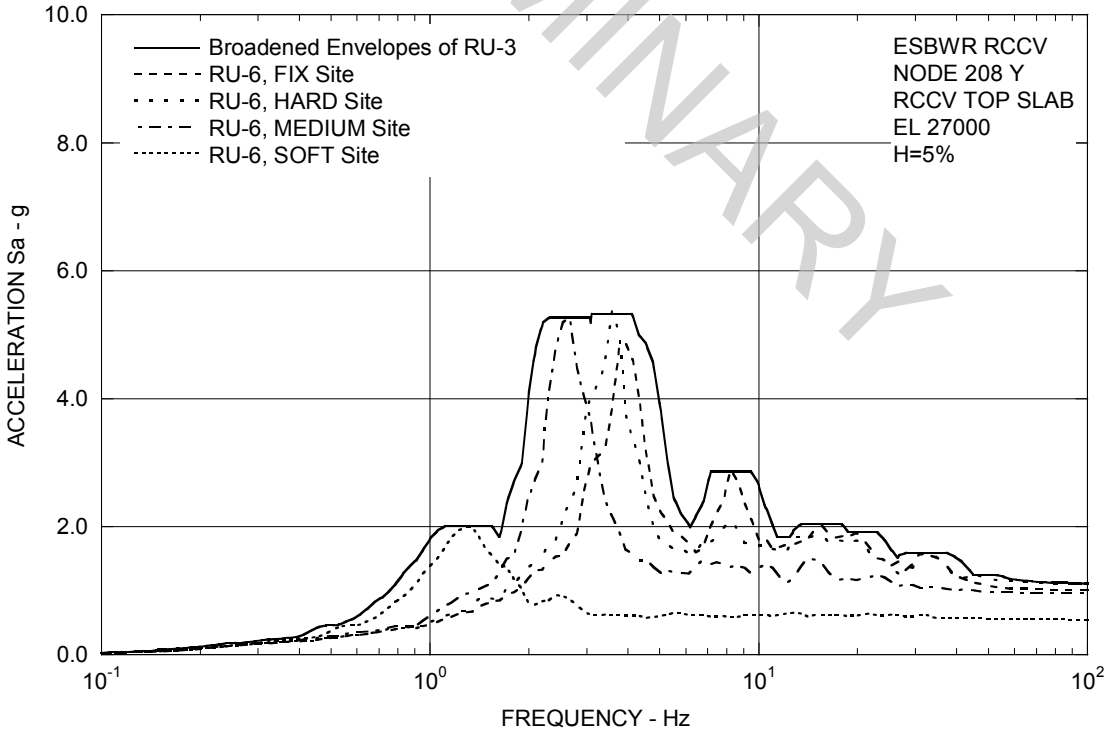

Figure 3A.8.5-2b. FRS (Effect of LOCA Flooding) – RCCV Top Slab Y

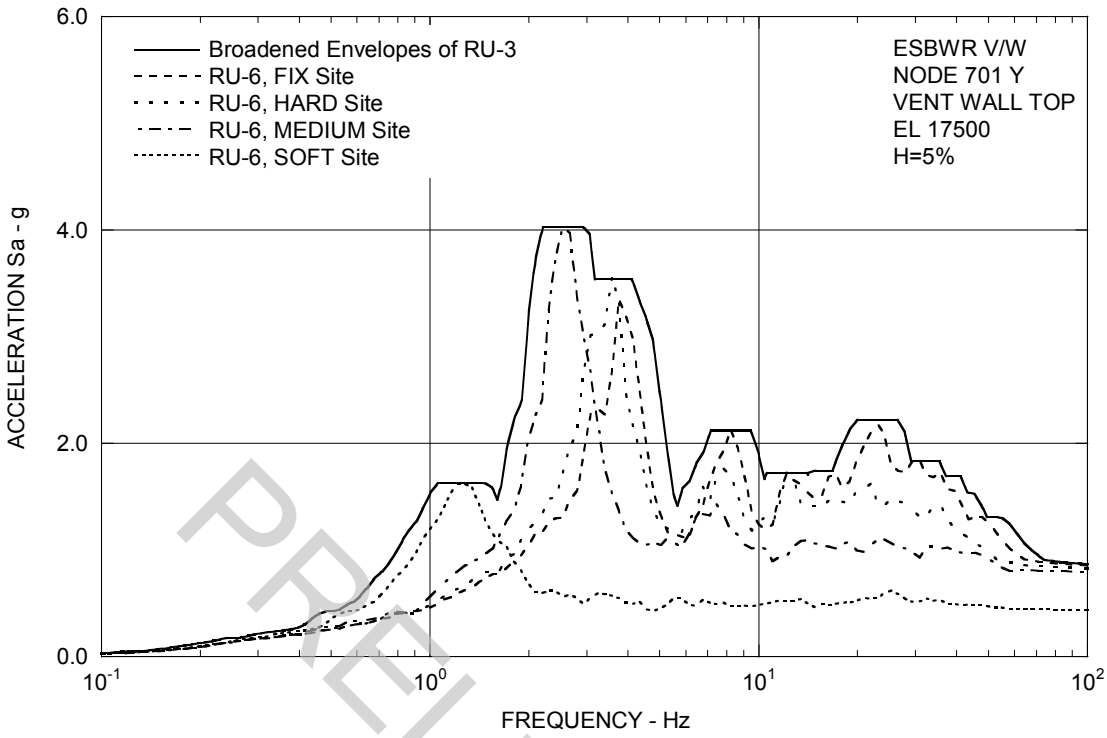

Figure 3A.8.5-2c. FRS (Effect of LOCA Flooding) – Vent Wall Top Y

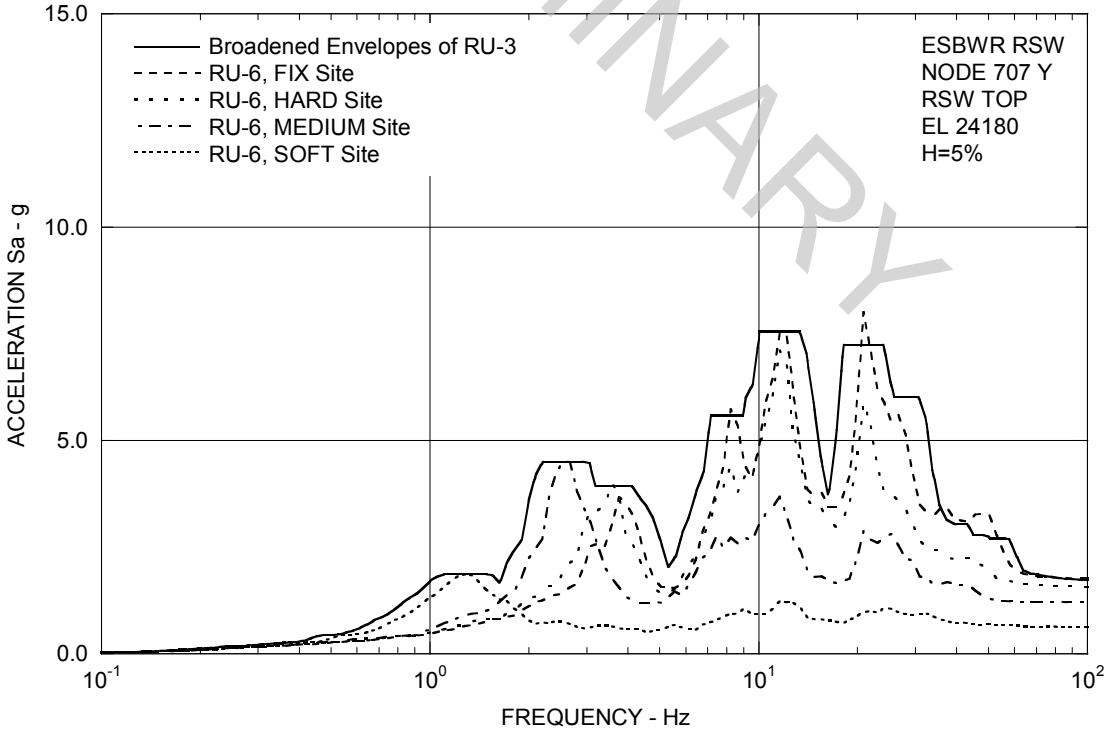

Figure 3A.8.5-2d. FRS (Effect of LOCA Flooding) – RSW Top Y

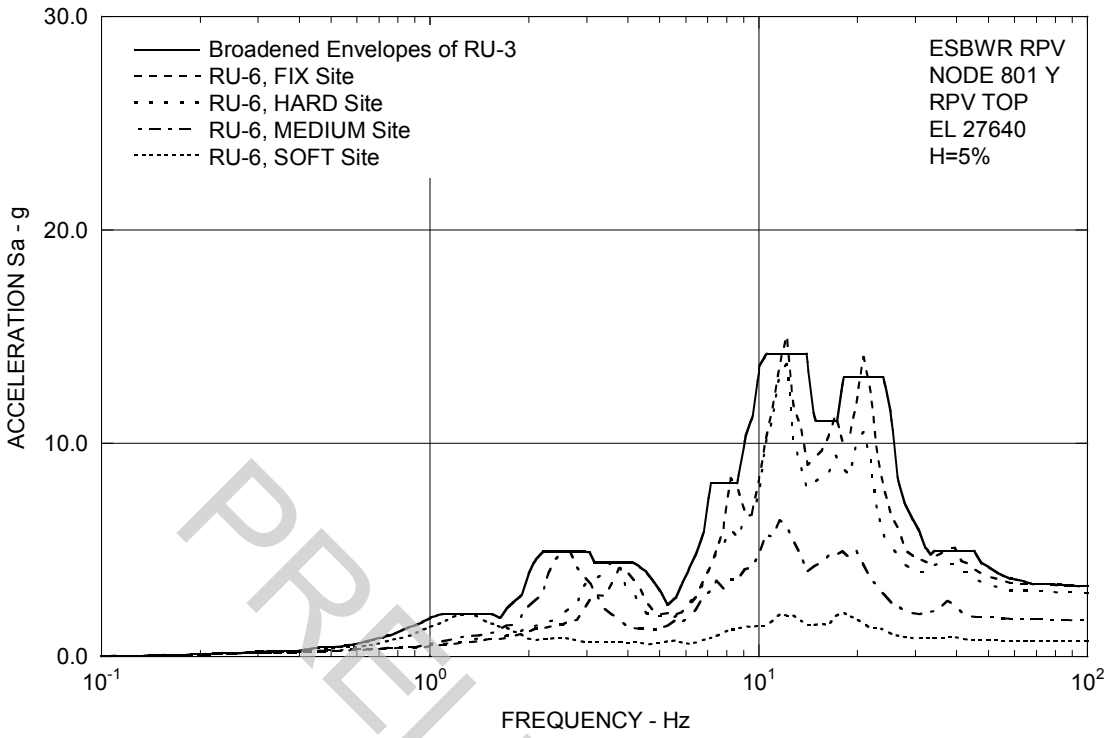

Figure 3A.8.5-2e. FRS (Effect of LOCA Flooding) – RPV Top Y

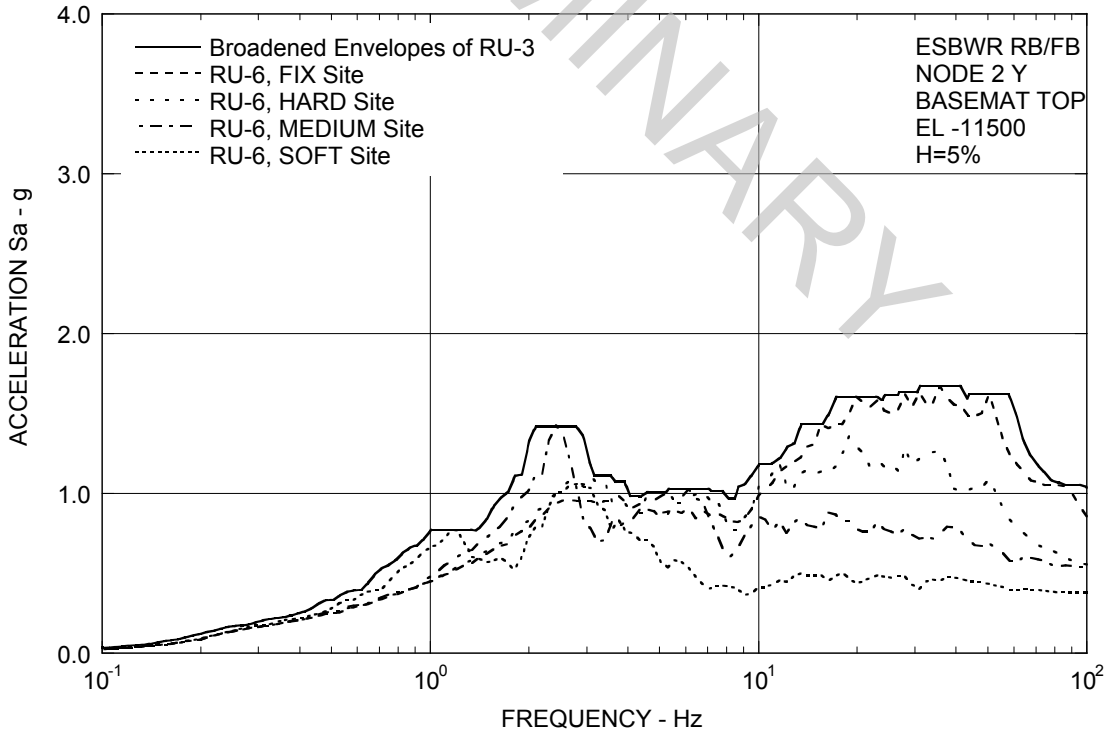

Figure 3A.8.5-2f. FRS (Effect of LOCA Flooding) – RB/FB Basemat Y

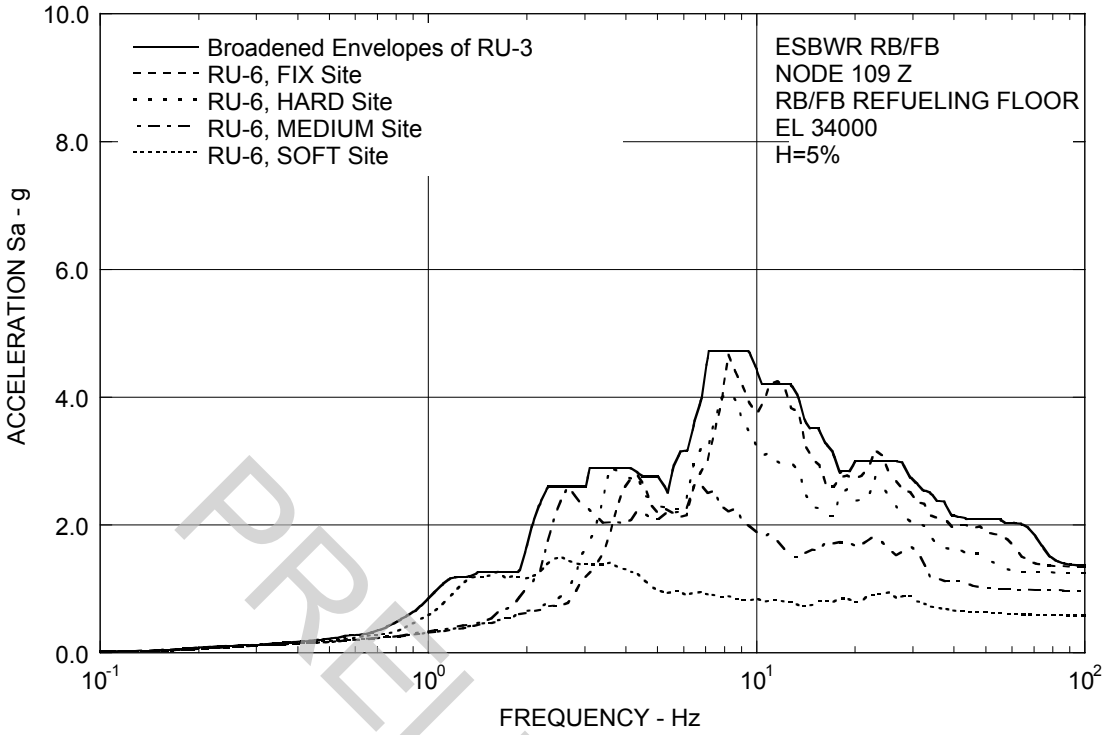

Figure 3A.8.5-3a. FRS (Effect of LOCA Flooding) – RB/FB Refueling Floor Z

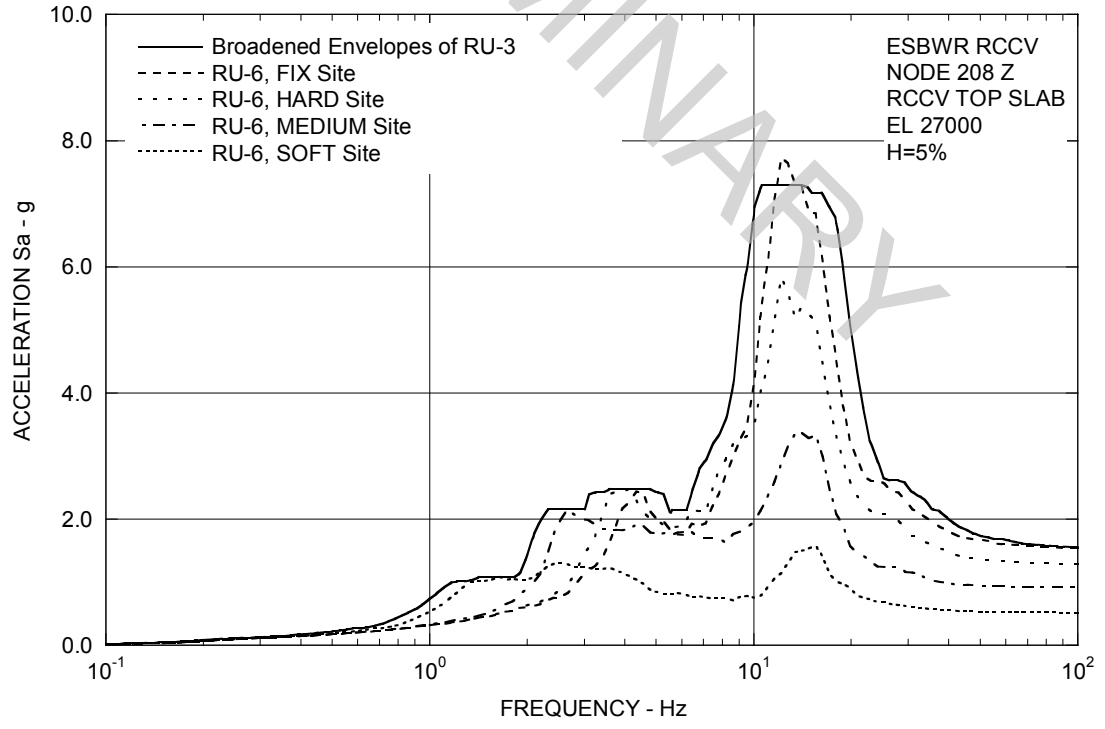

Figure 3A.8.5-3b. FRS (Effect of LOCA Flooding) – RCCV Top Slab Z

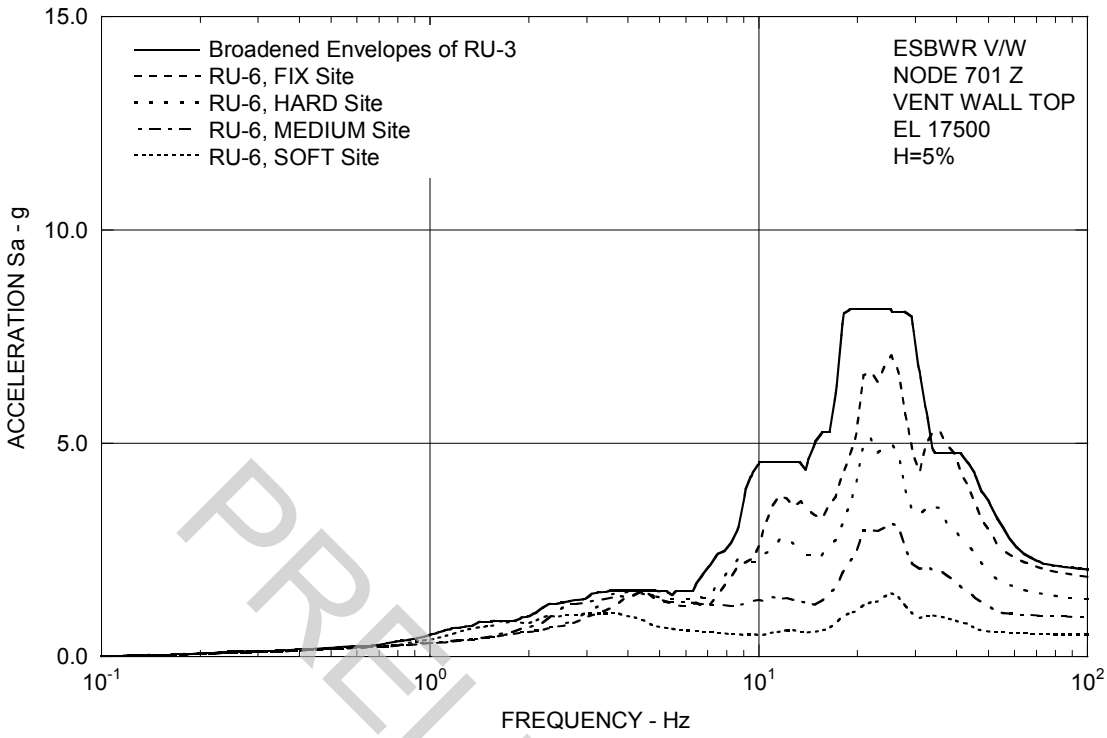

Figure 3A.8.5-3c. FRS (Effect of LOCA Flooding) – Vent Wall Top Z

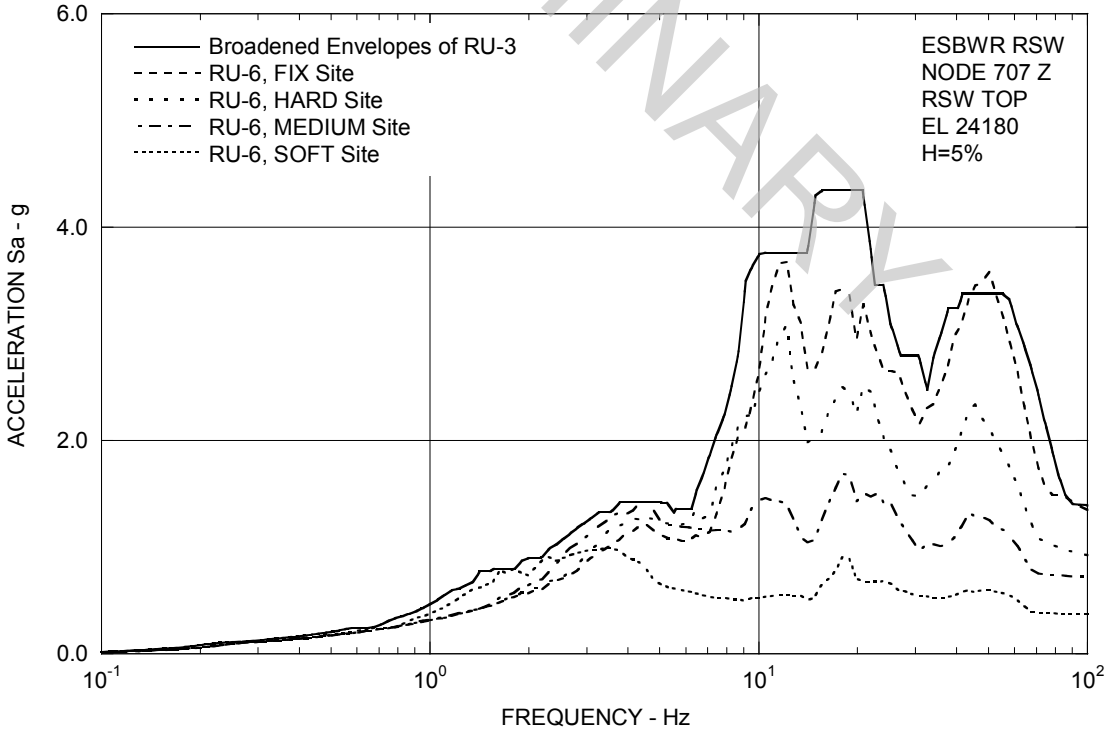

Figure 3A.8.5-3d. FRS (Effect of LOCA Flooding) – RSW Top Z

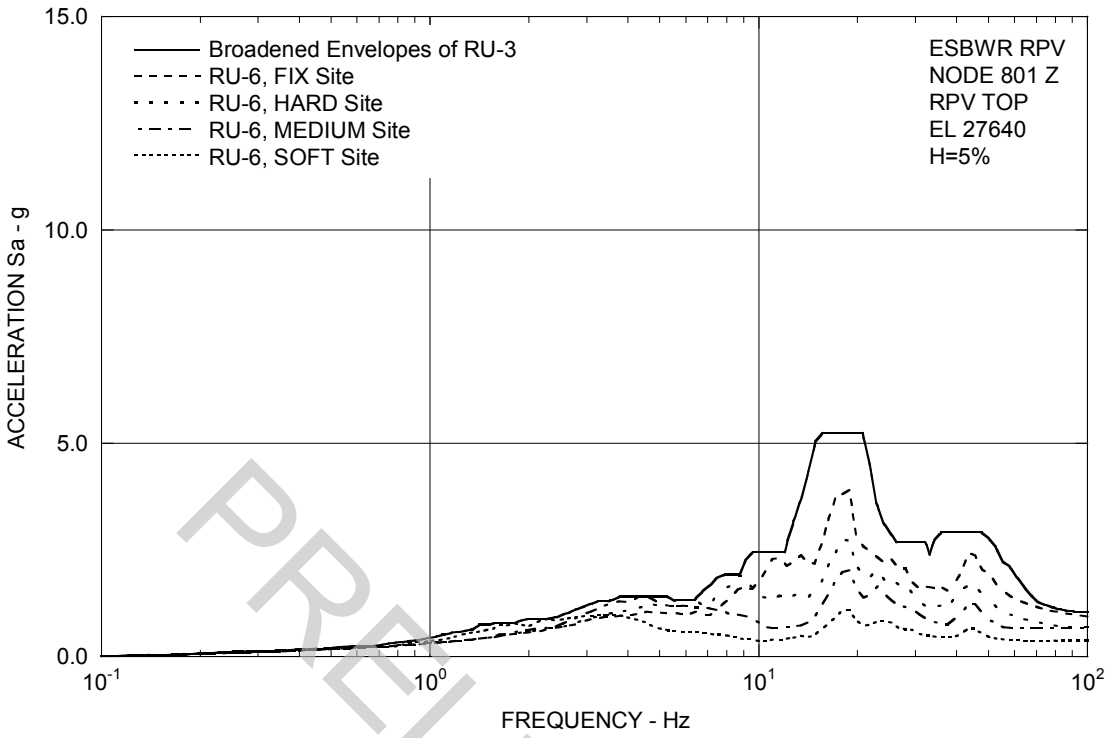

Figure 3A.8.5-3e. FRS (Effect of LOCA Flooding) – RPV Top Z

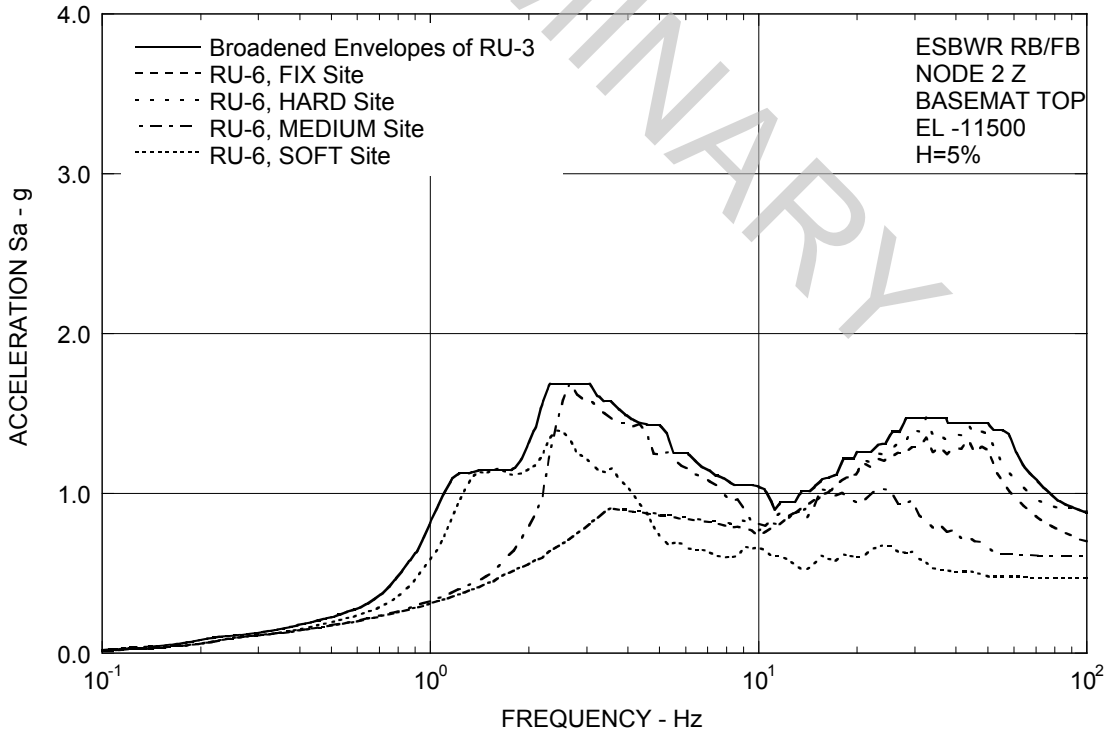

Figure 3A.8.5-3f. FRS (Effect of LOCA Flooding) – RB/FB Basemat Z

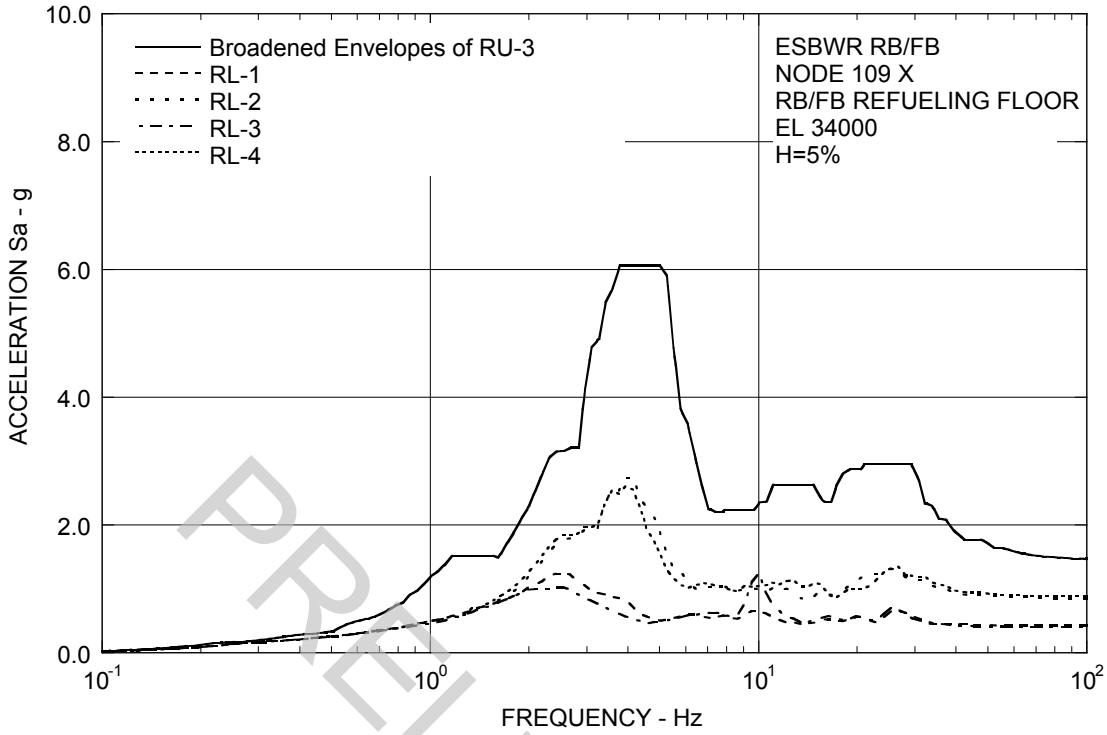

Figure 3A.8.6-1a. FRS (Effect of Layered Sites) – RB/FB Refueling Floor X

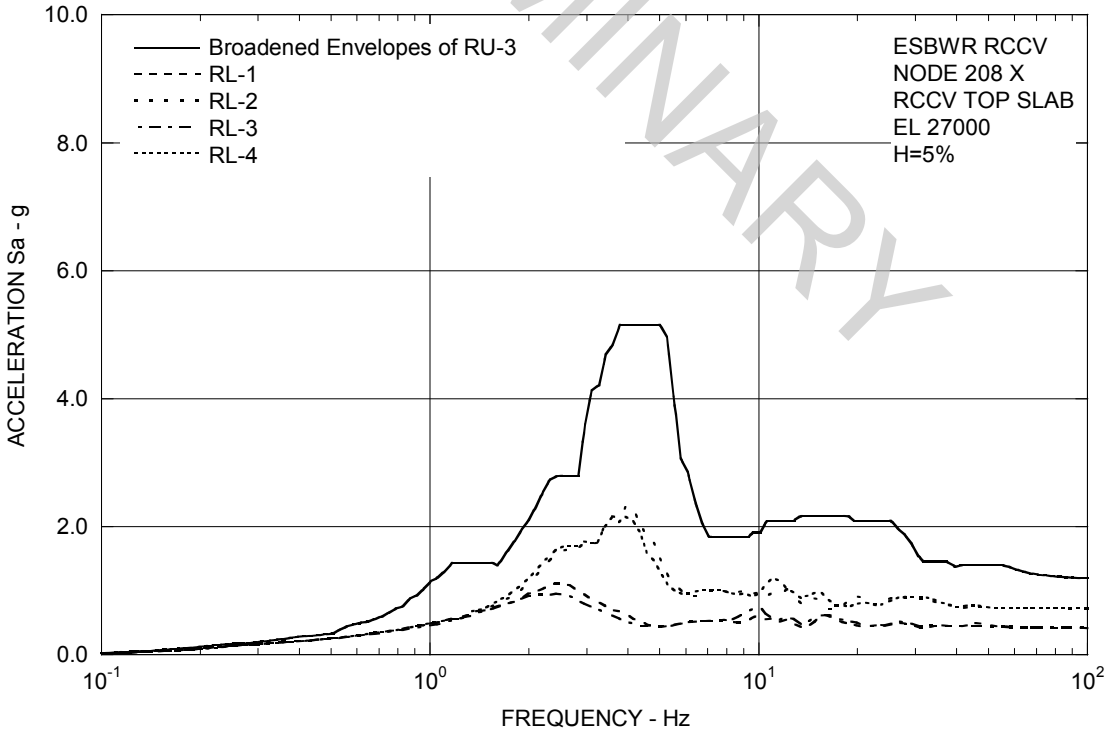

Figure 3A.8.6-1b. FRS (Effect of Layered Sites) – RCCV Top Slab X

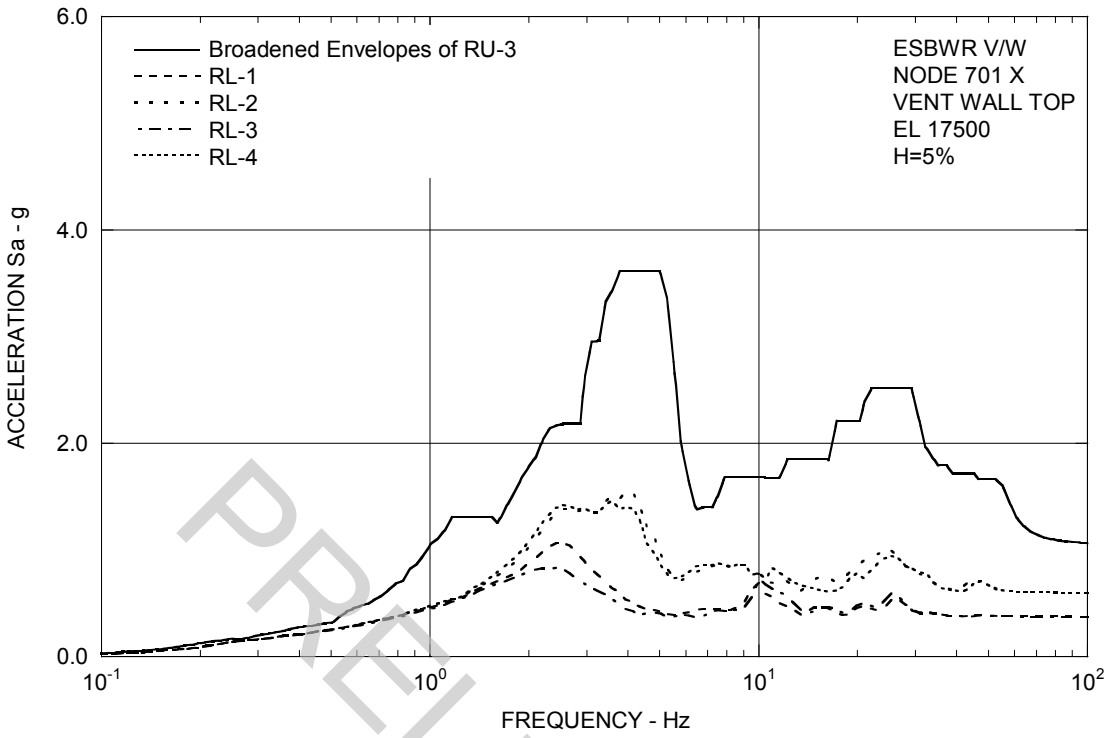

Figure 3A.8.6-1c. FRS (Effect of Layered Sites) – Vent Wall Top X

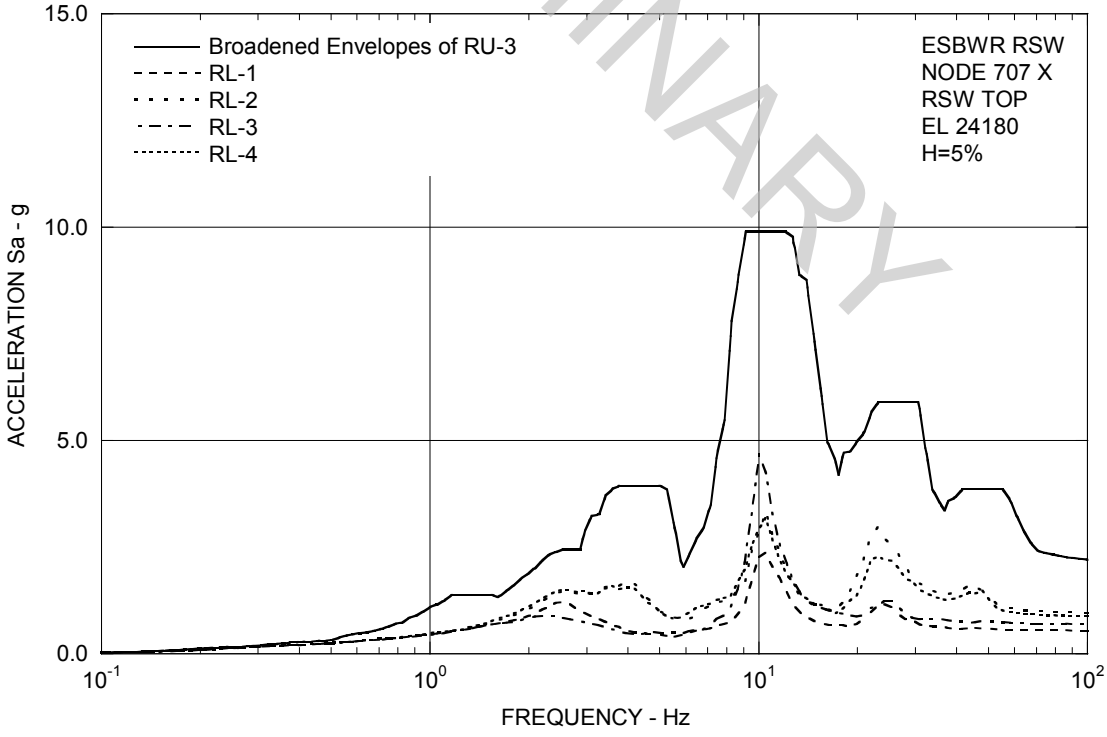

Figure 3A.8.6-1d. FRS (Effect of Layered Sites) – RSW Top X

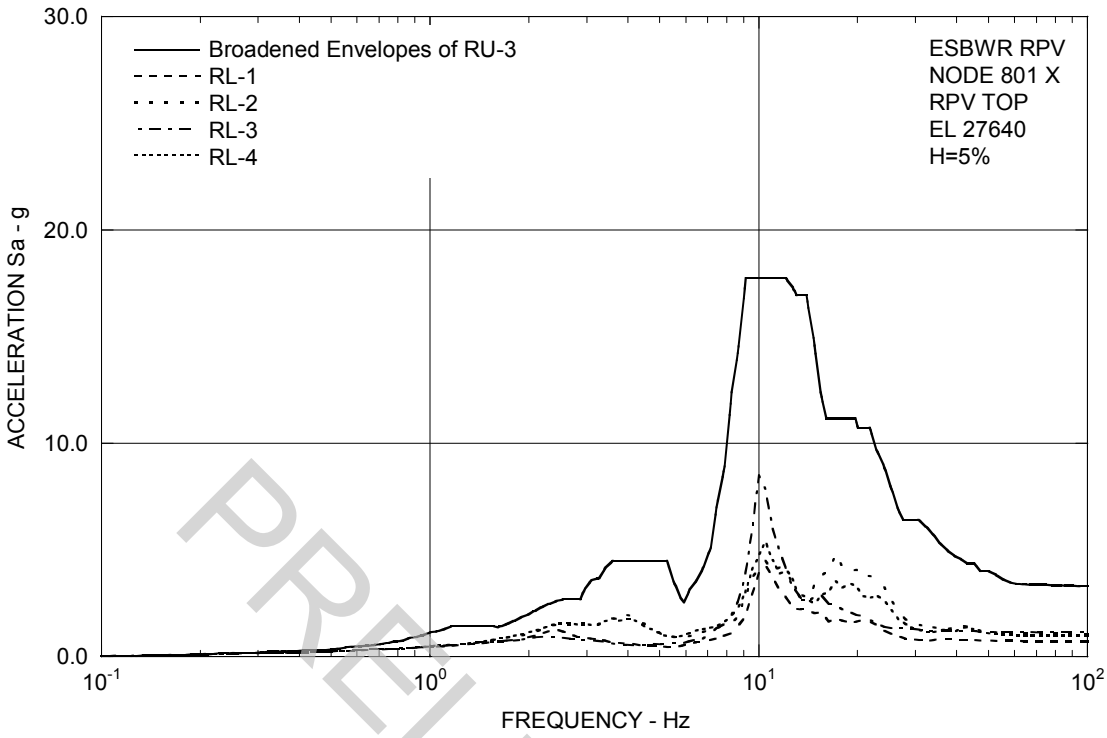

Figure 3A.8.6-1e. FRS (Effect of Layered Sites) – RPV Top X

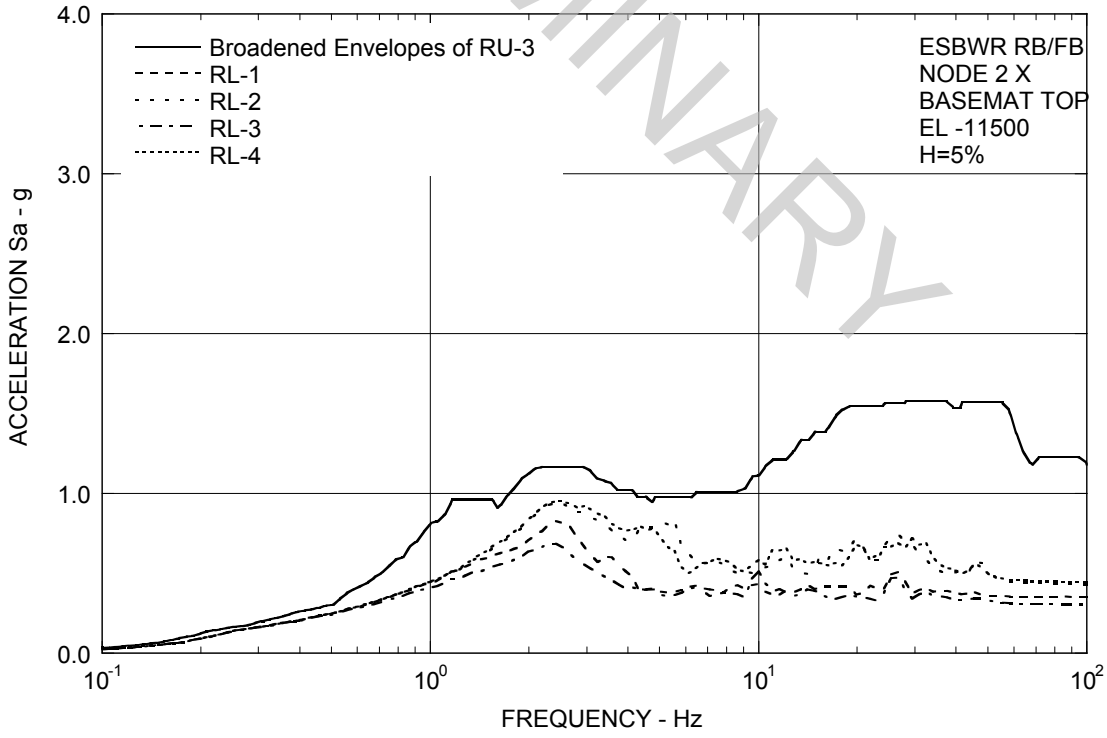

Figure 3A.8.6-1f. FRS (Effect of Layered Sites) – RB/FB Basemat X

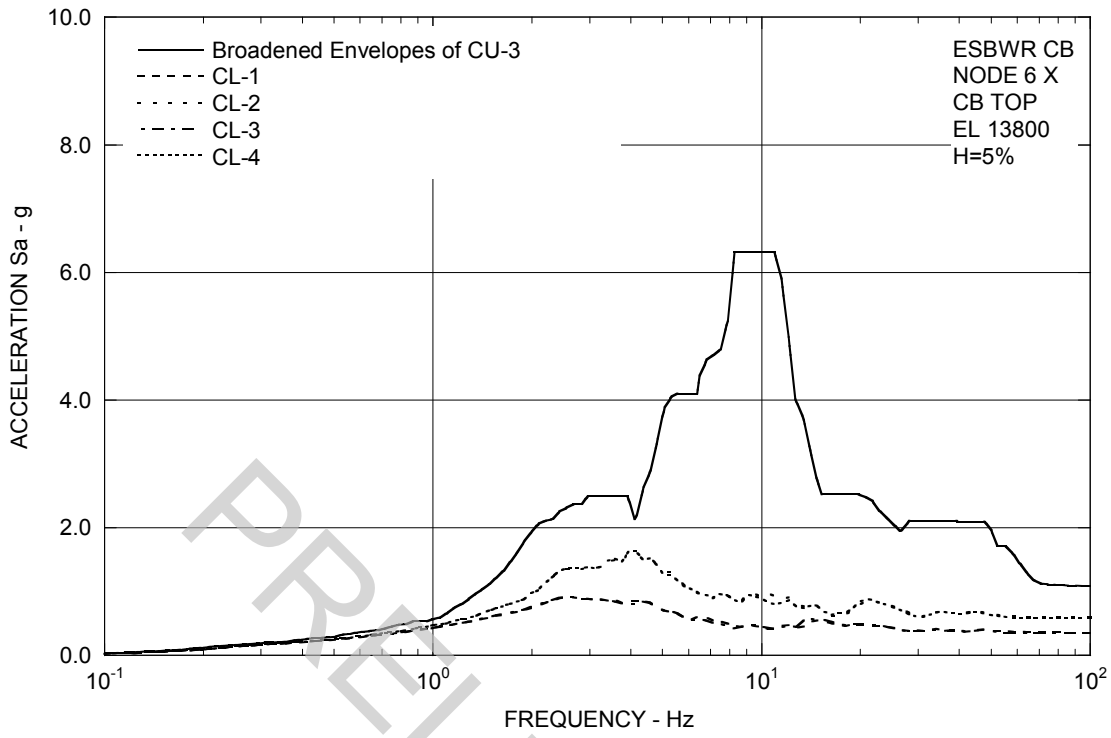

Figure 3A.8.6-1g. FRS (Effect of Layered Sites) – CB Top X

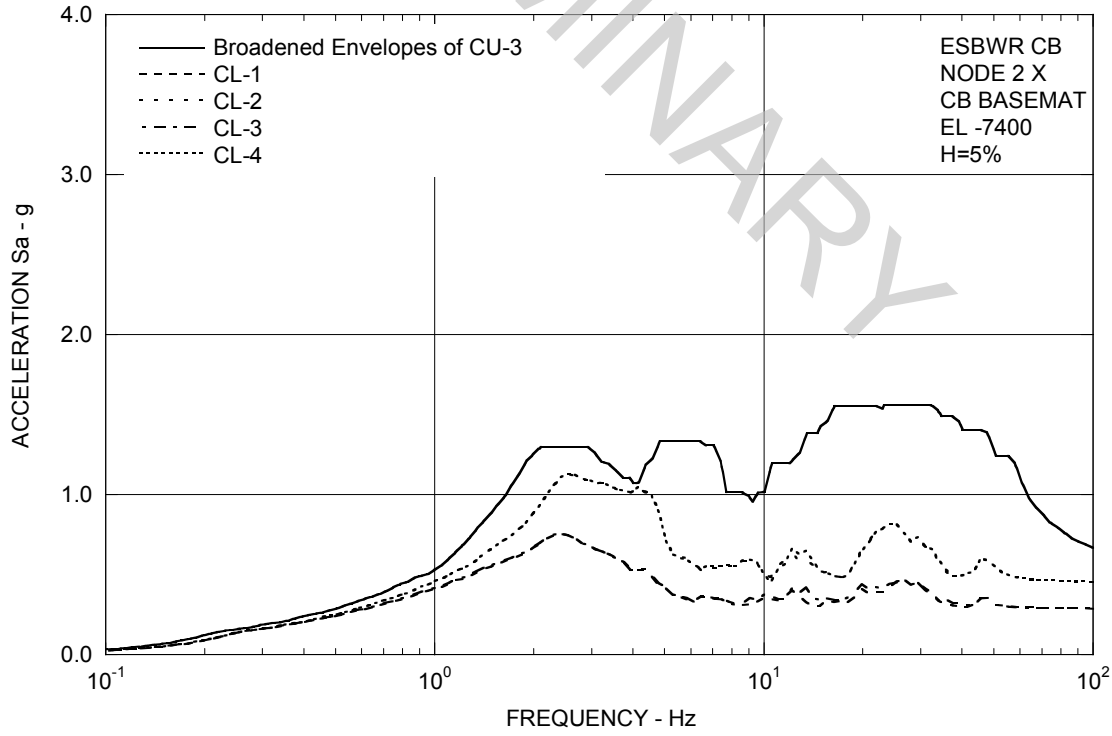

Figure 3A.8.6-1h. FRS (Effect of Layered Sites) – CB Basemat X

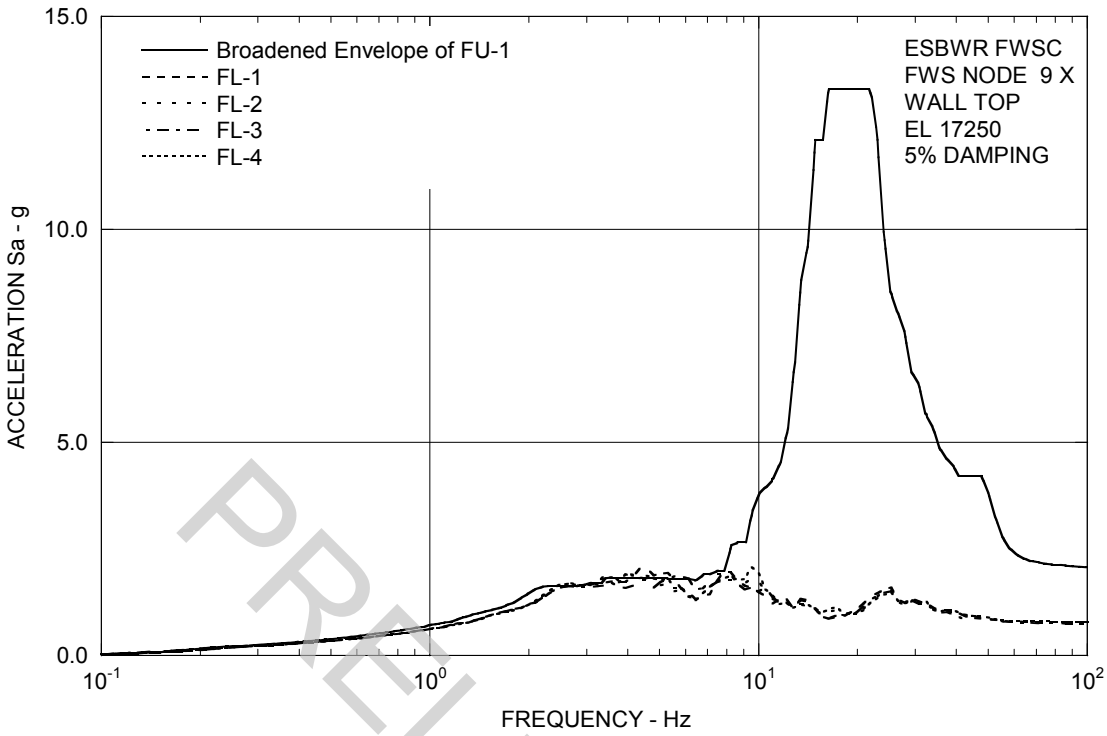

Figure 3A.8.6-1i. FRS (Effect of Layered Sites) – FWS Wall Top X

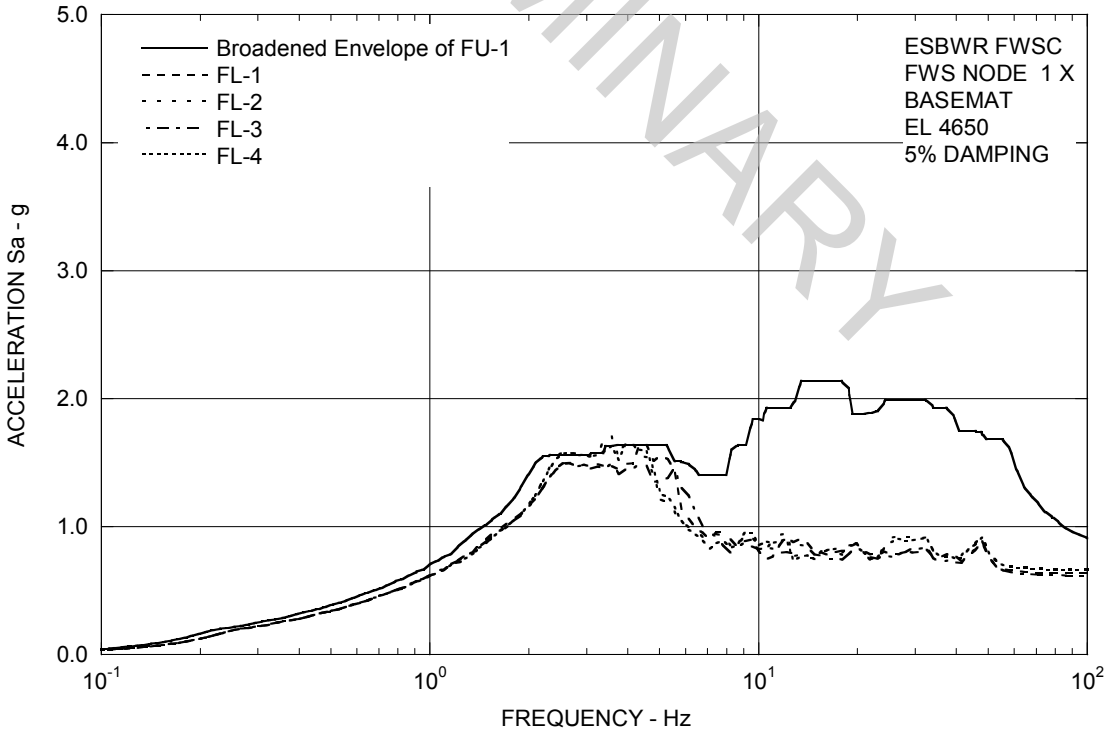

Figure 3A.8.6-1j. FRS (Effect of Layered Sites) – FWS Basemat X

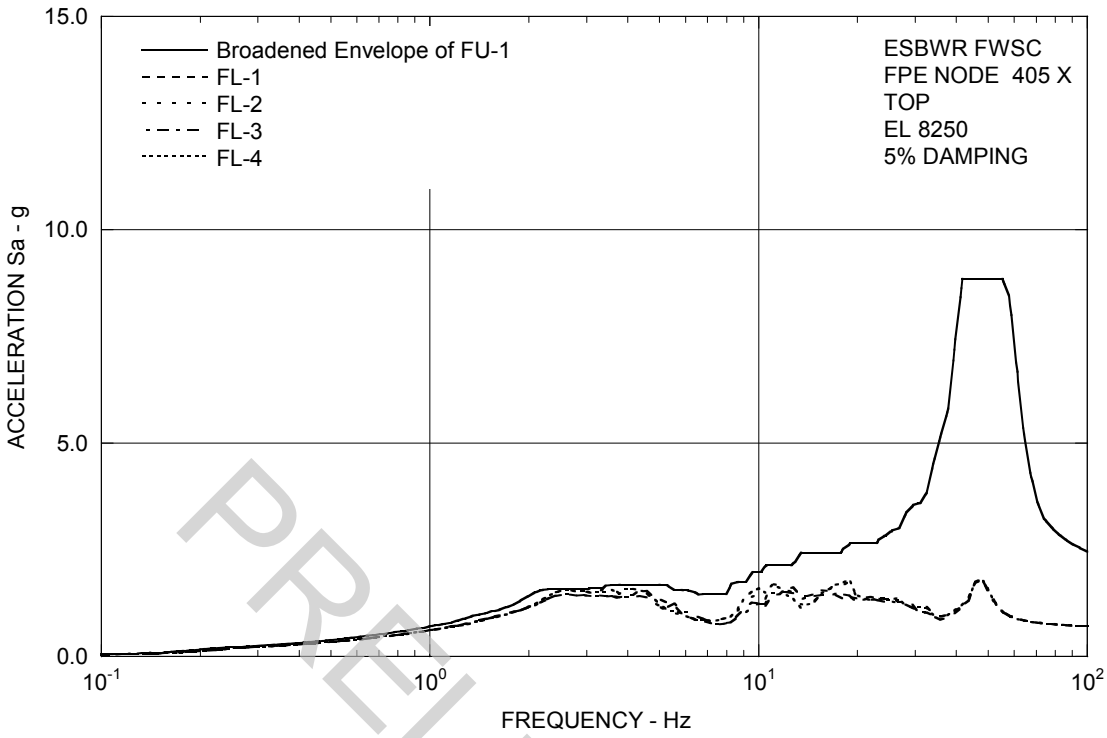

Figure 3A.8.6-1k. FRS (Effect of Layered Sites) – FPE Top X

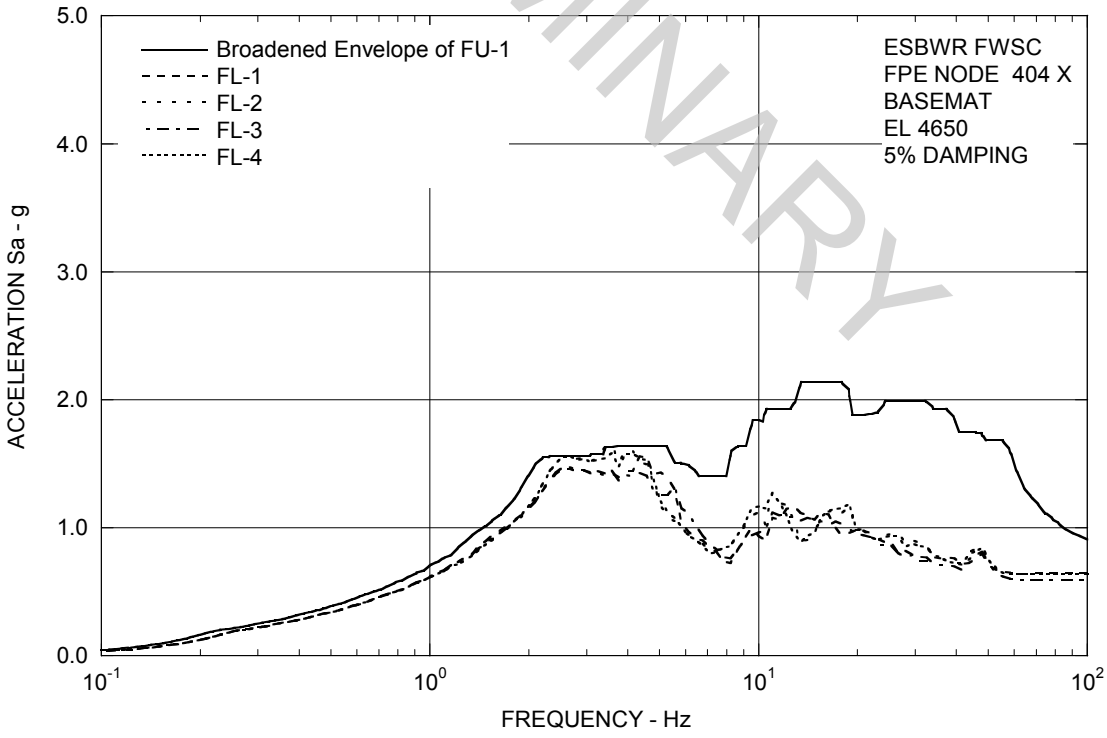

Figure 3A.8.6-1l. FRS (Effect of Layered Sites) – FPE Basemat X

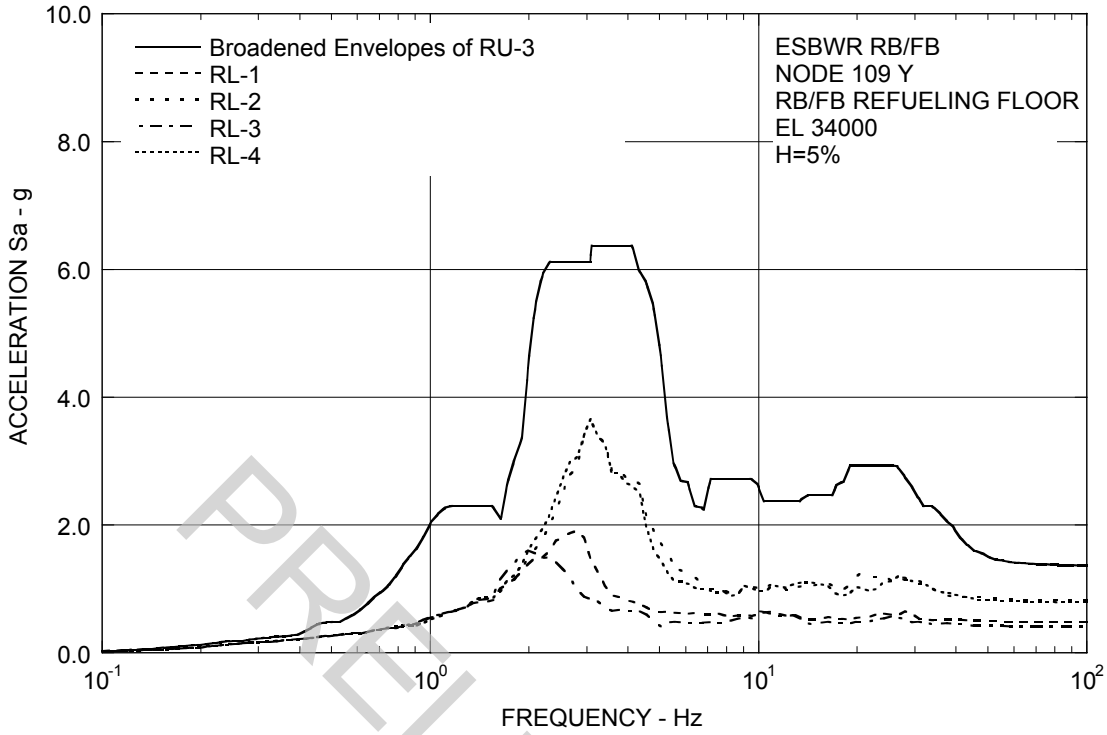

Figure 3A.8.6-2a. FRS (Effect of Layered Sites) – RB/FB Refueling Floor Y

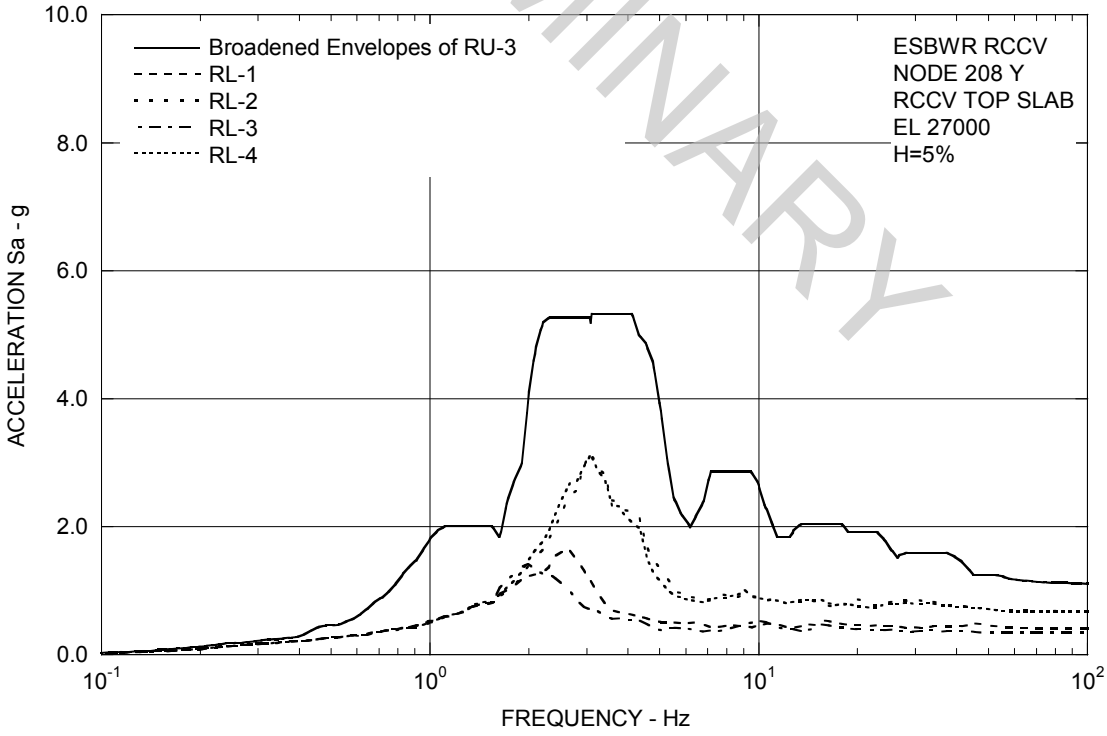

Figure 3A.8.6-2b. FRS (Effect of Layered Sites) – RCCV Top Slab Y

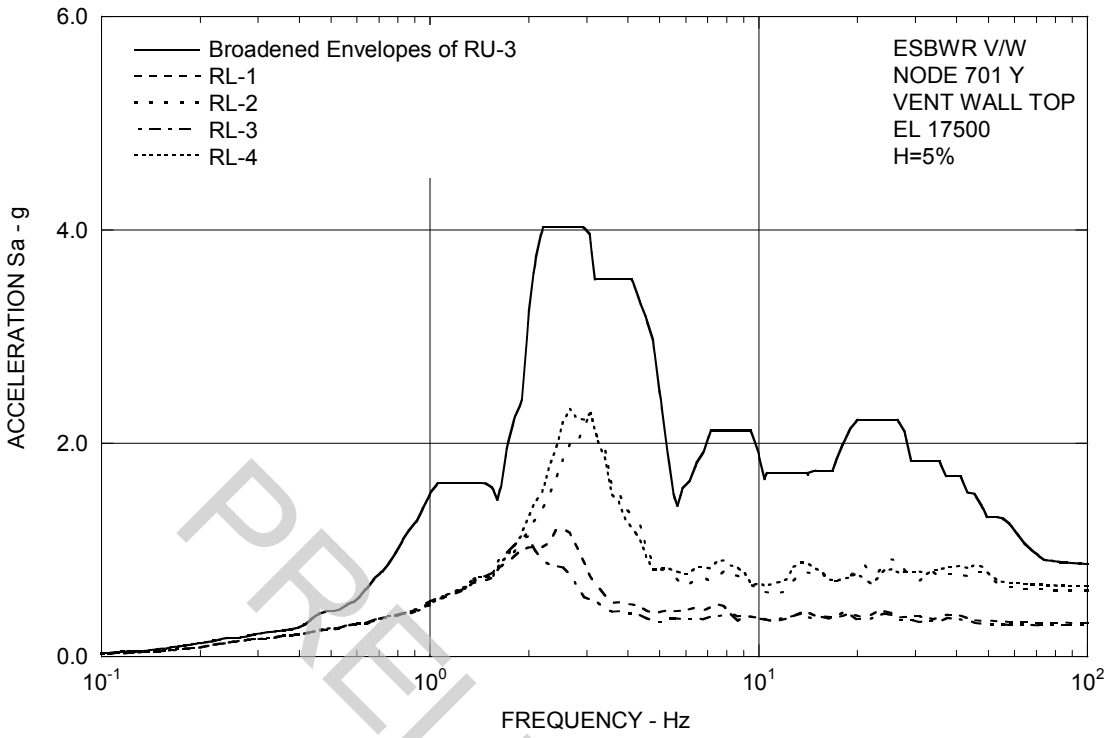

Figure 3A.8.6-2c. FRS (Effect of Layered Sites) – Vent Wall Top Y

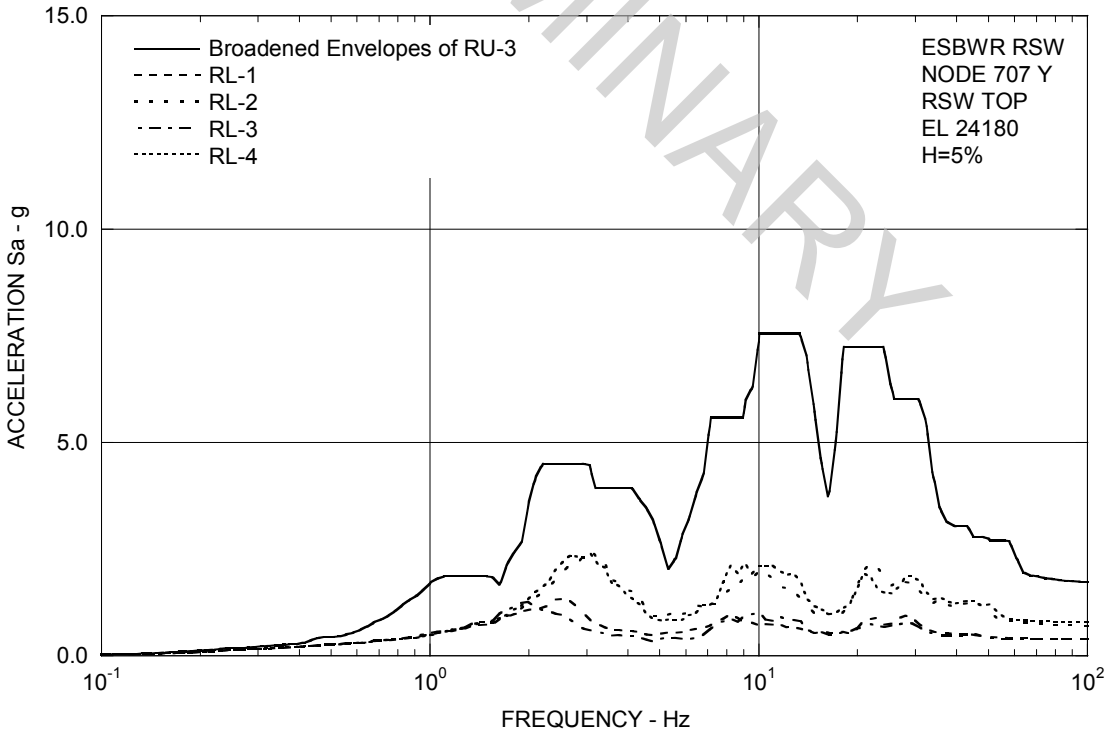

Figure 3A.8.6-2d. FRS (Effect of Layered Sites) – RSW Top Y

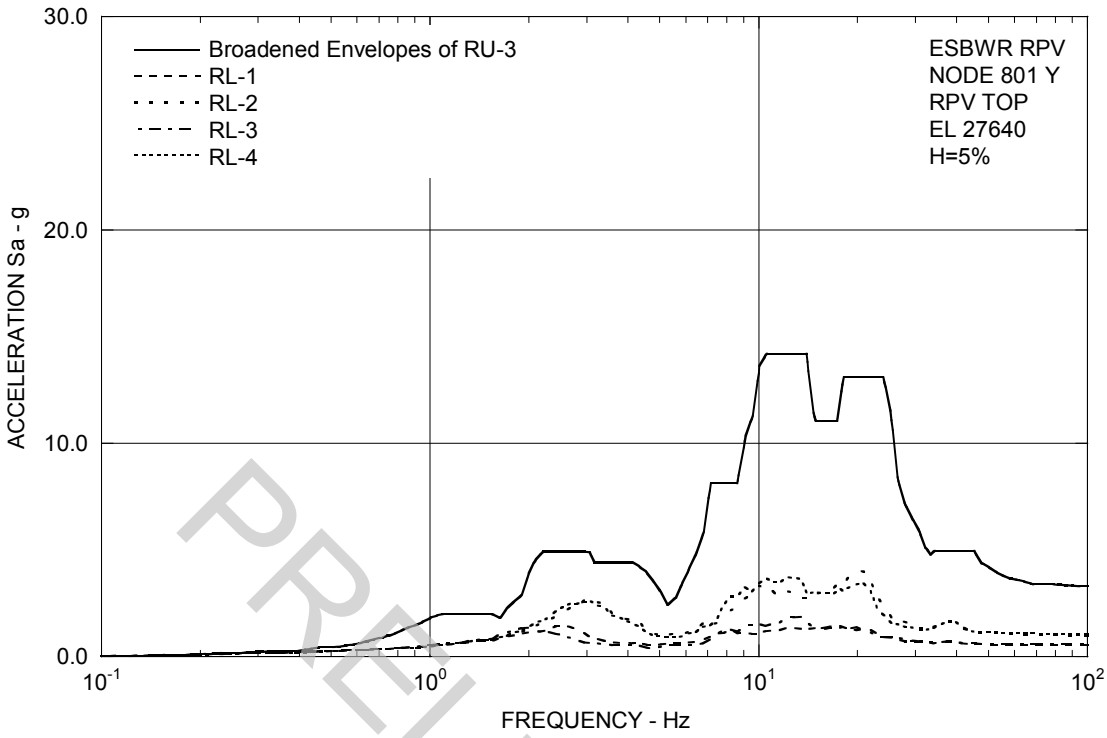

Figure 3A.8.6-2e. FRS (Effect of Layered Sites) – RPV Top Y

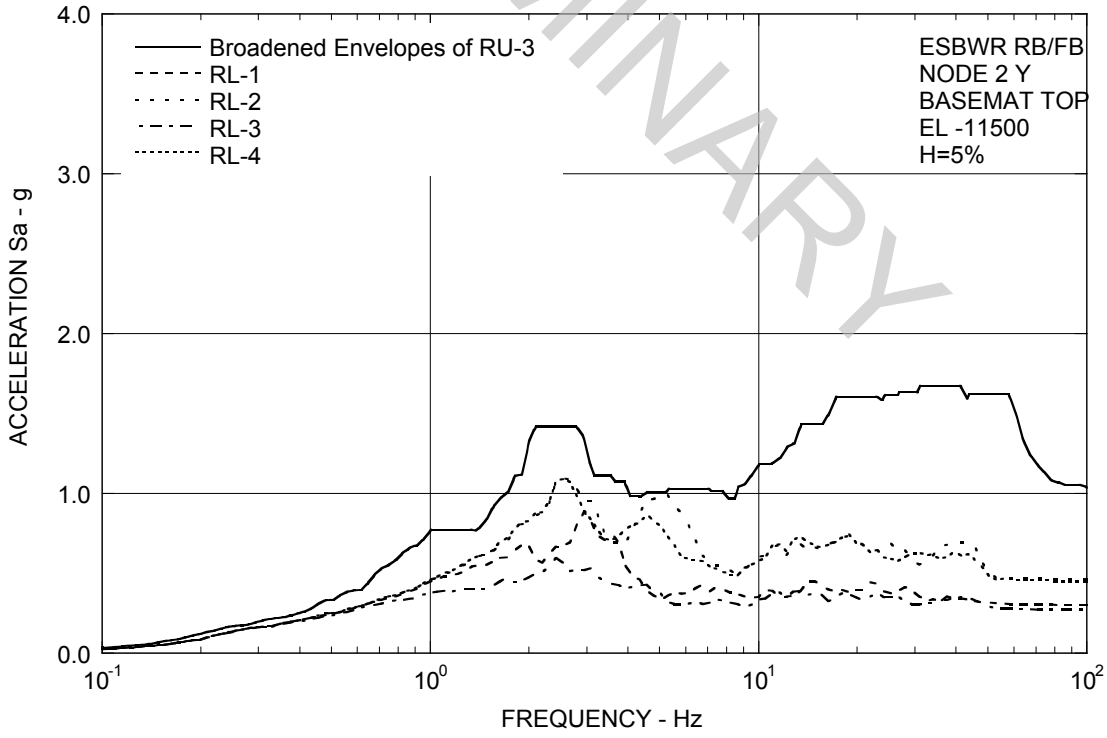

Figure 3A.8.6-2f. FRS (Effect of Layered Sites) – RB/FB Basemat Y

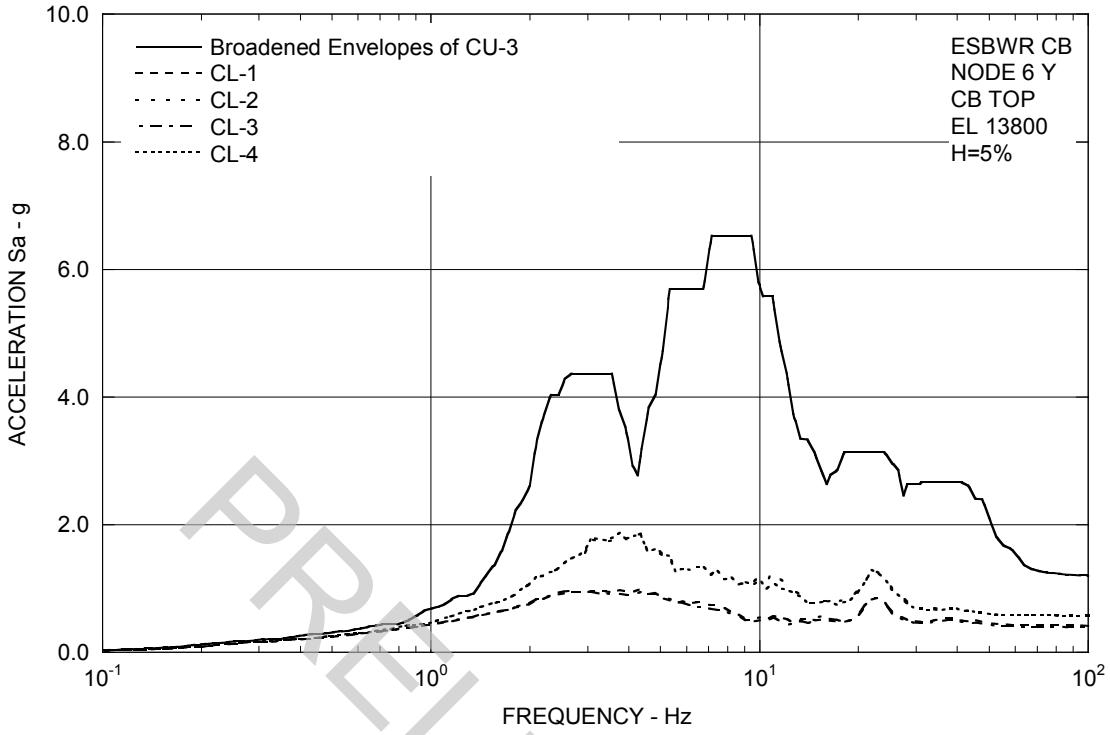

Figure 3A.8.6-2g. FRS (Effect of Layered Sites) – CB Top Y

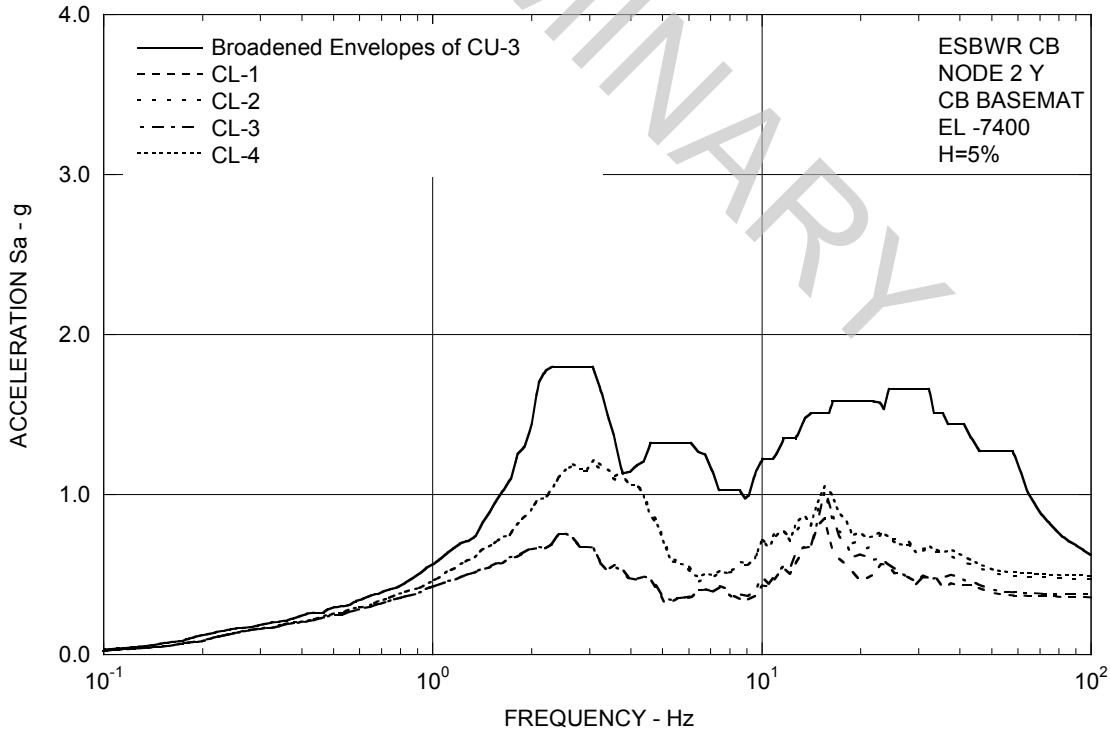

Figure 3A.8.6-2h. FRS (Effect of Layered Sites) – CB Basemat Y

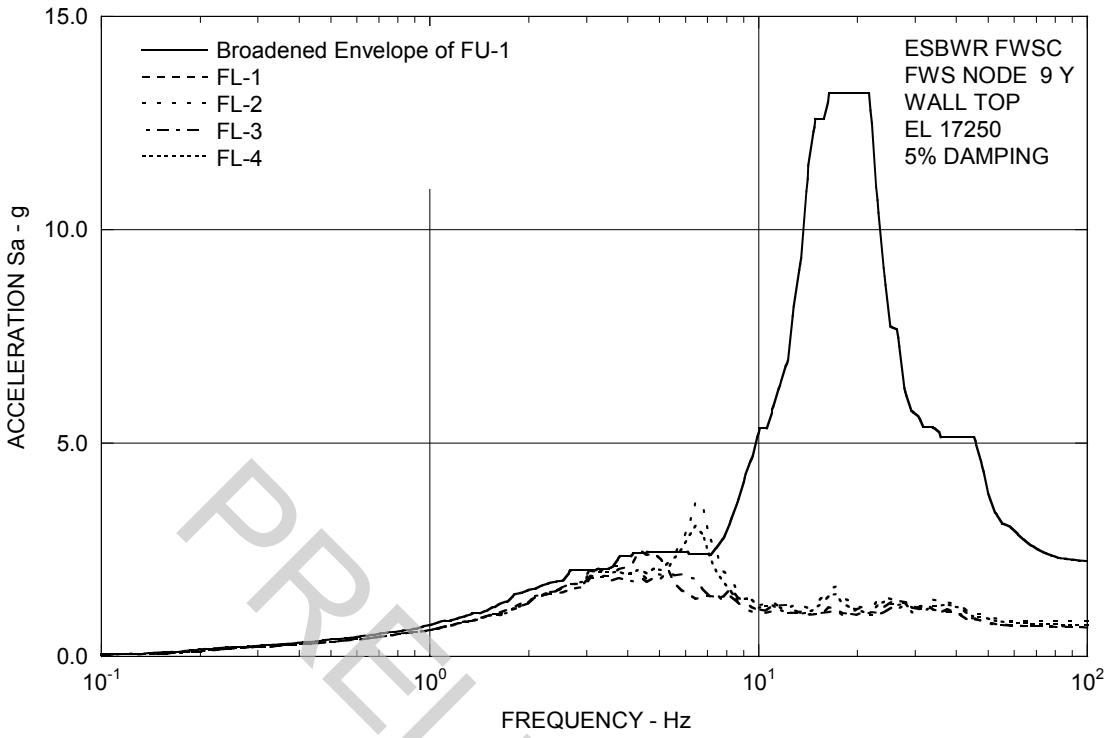

Figure 3A.8.6-2i. FRS (Effect of Layered Sites) – FWS Wall Top Y

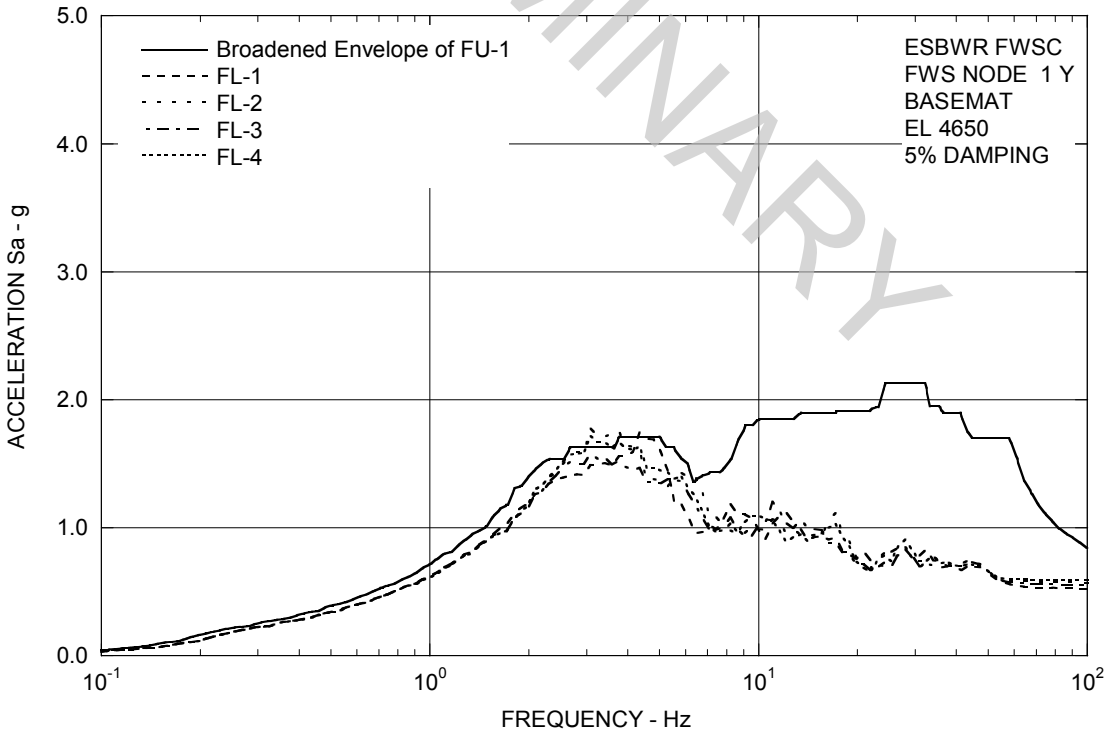

Figure 3A.8.6-2j. FRS (Effect of Layered Sites) – FWS Basemat Y

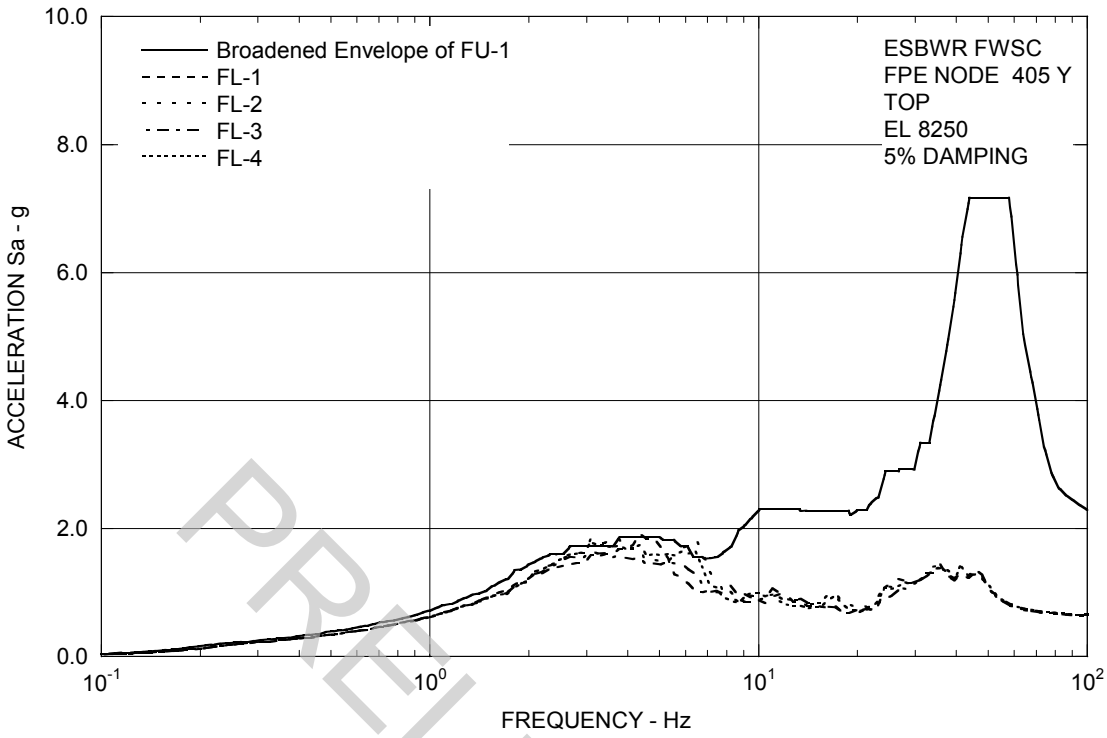

Figure 3A.8.6-2k. FRS (Effect of Layered Sites) – FPE Top Y

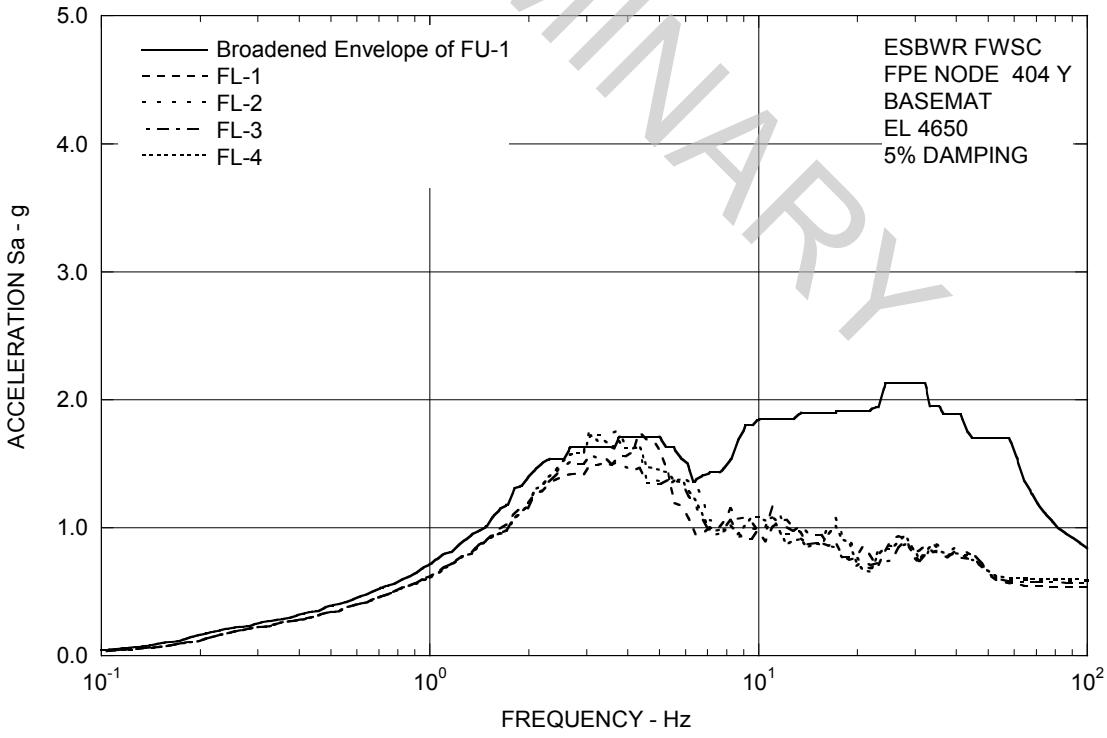

Figure 3A.8.6-2l. FRS (Effect of Layered Sites) – FPE Basemat Y

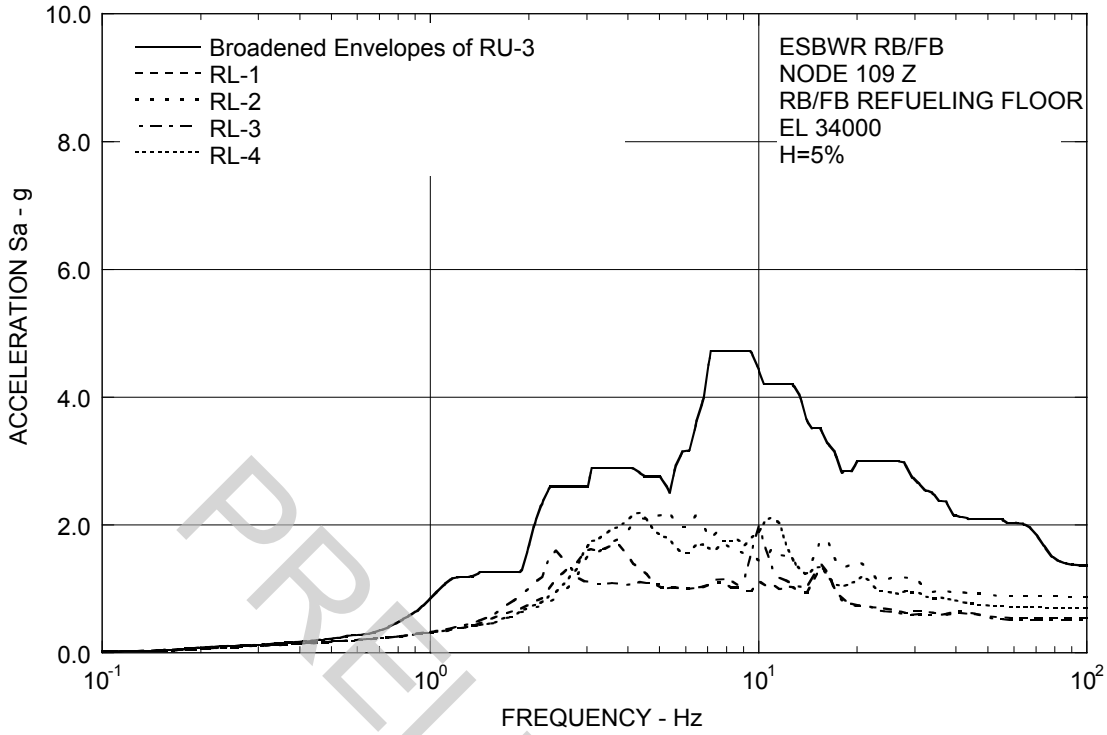

Figure 3A.8.6-3a. FRS (Effect of Layered Sites) – RB/FB Refueling Floor Z

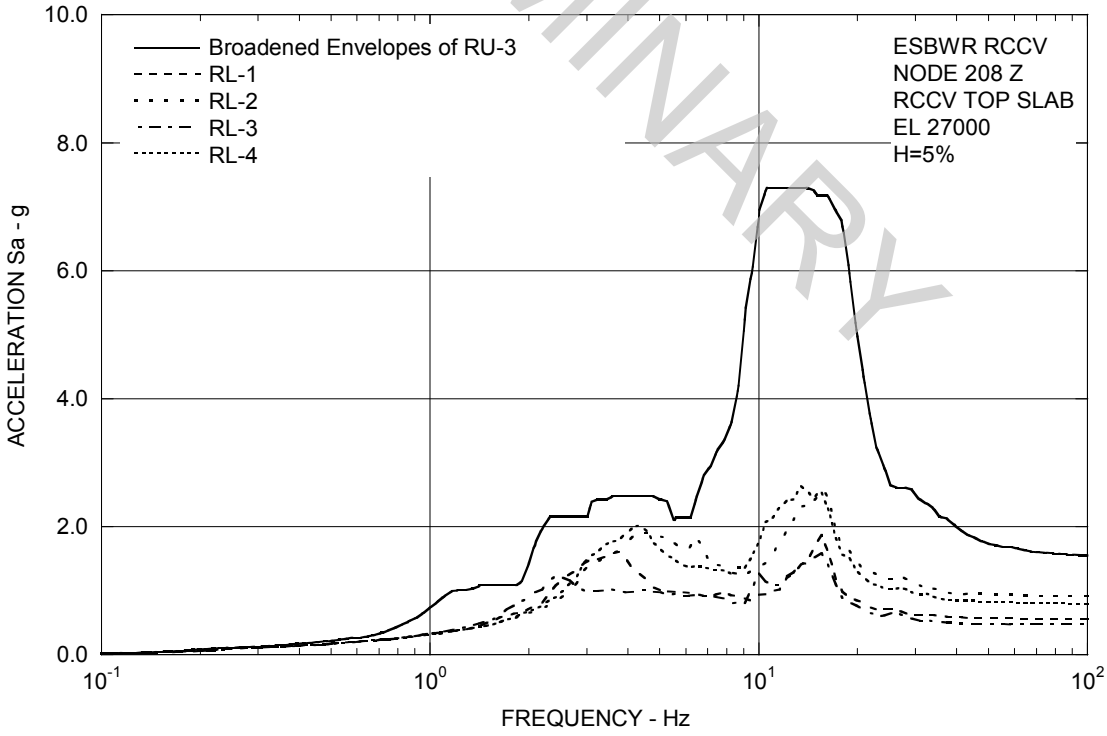

Figure 3A.8.6-3b. FRS (Effect of Layered Sites) – RCCV Top Slab Z

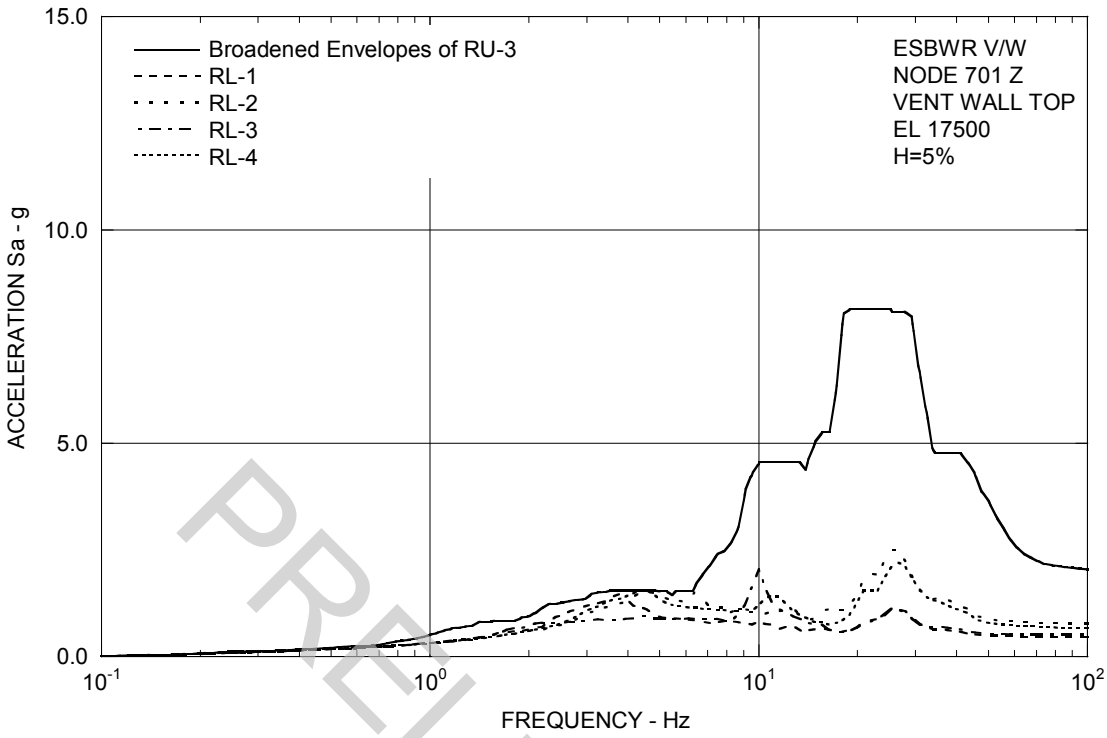

Figure 3A.8.6-3c. FRS (Effect of Layered Sites) – Vent Wall Top Z

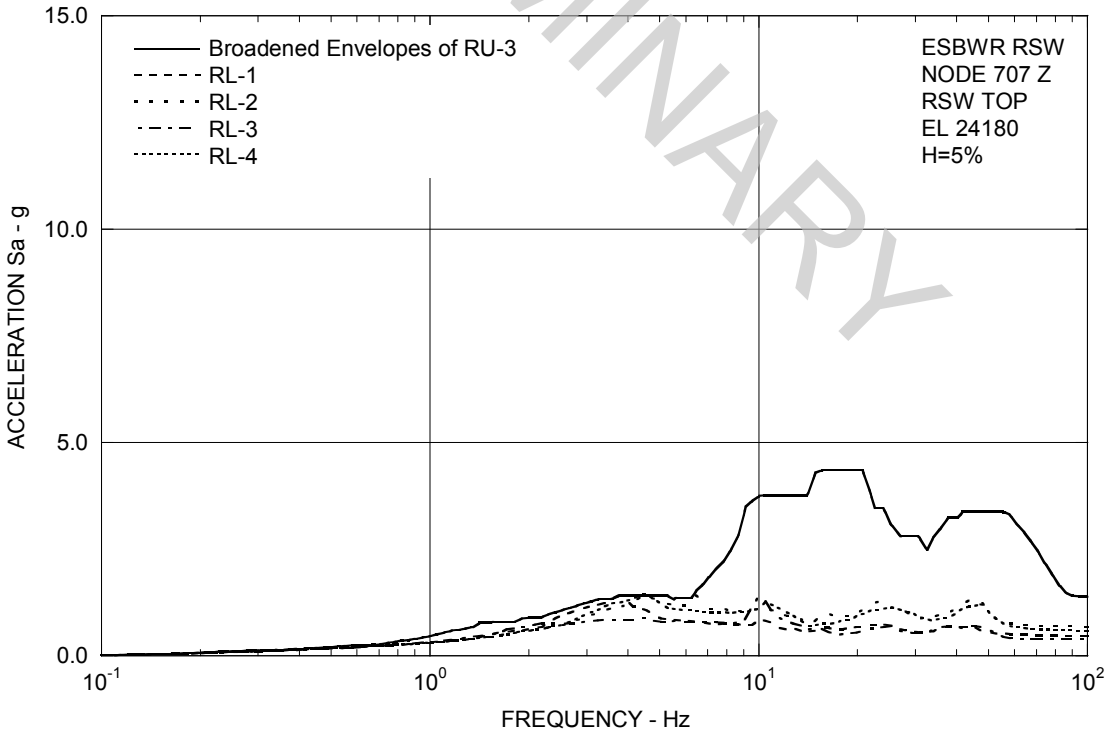

Figure 3A.8.6-3d. FRS (Effect of Layered Sites) – RSW Top Z

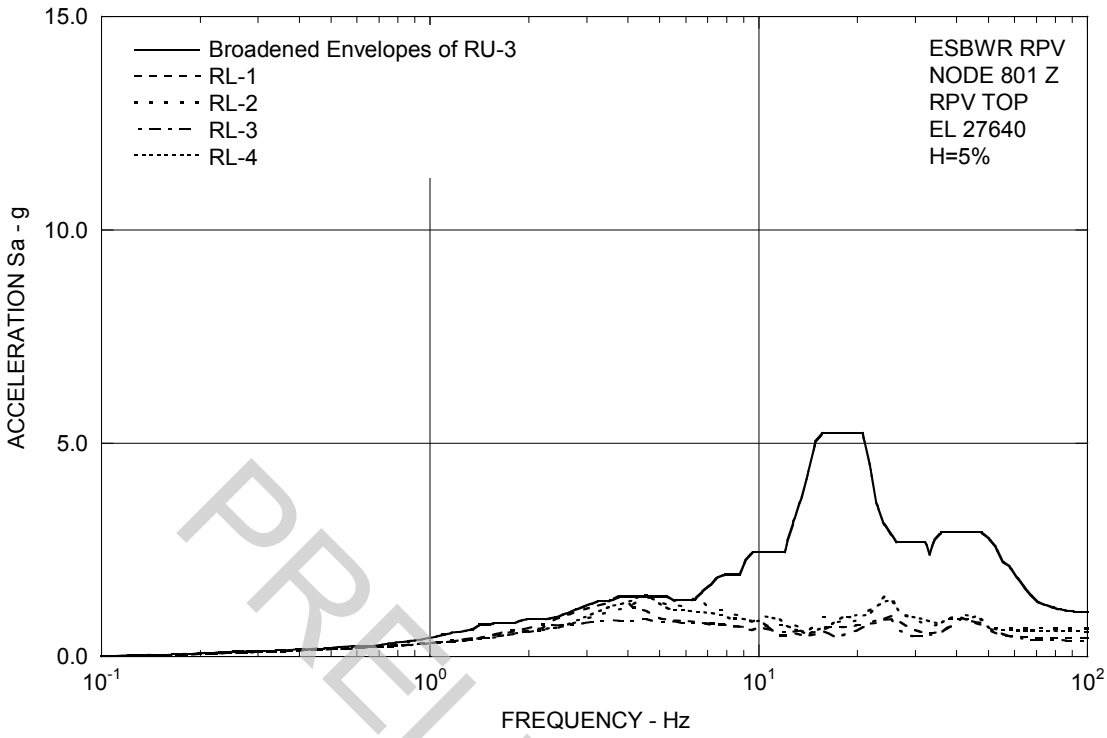

Figure 3A.8.6-3e. FRS (Effect of Layered Sites) – RPV Top Z

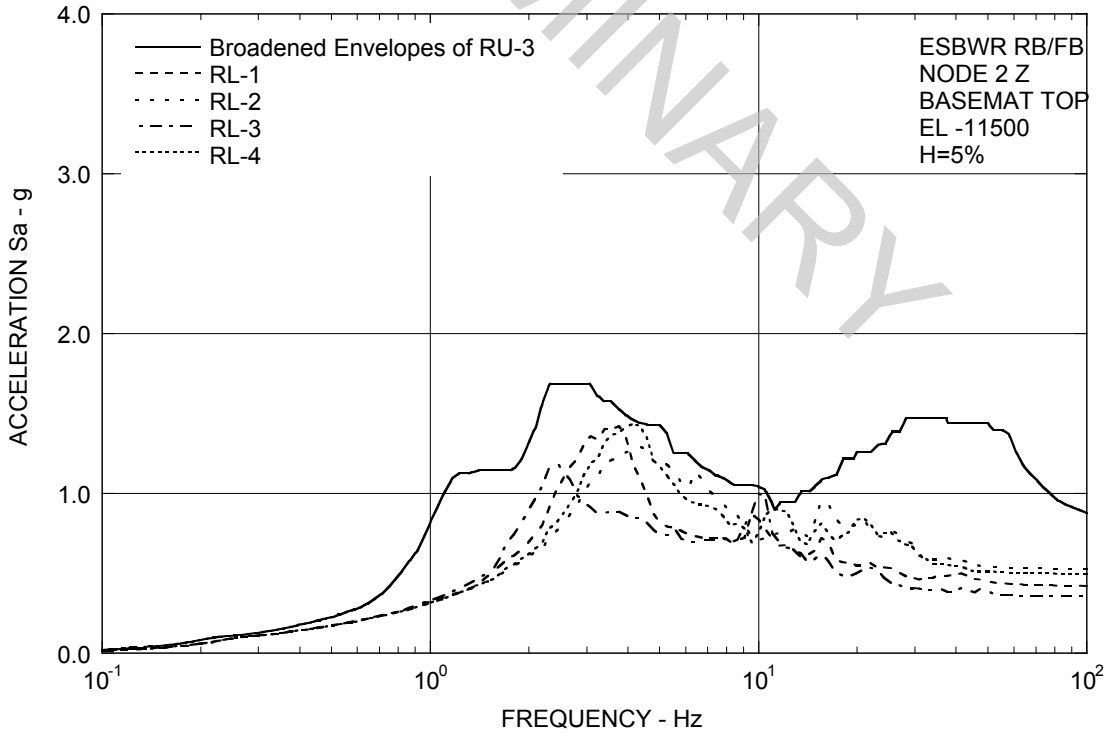

Figure 3A.8.6-3f. FRS (Effect of Layered Sites) – RB/FB Basemat Z

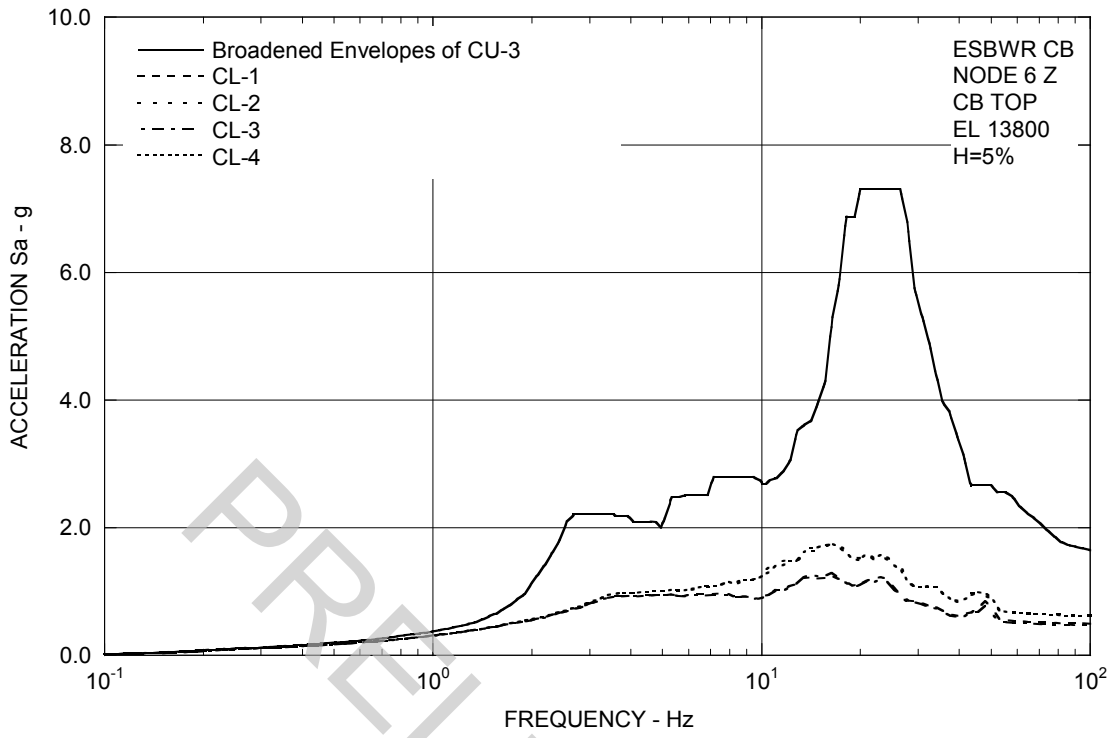

Figure 3A.8.6-3g. FRS (Effect of Layered Sites) – CB Top Z

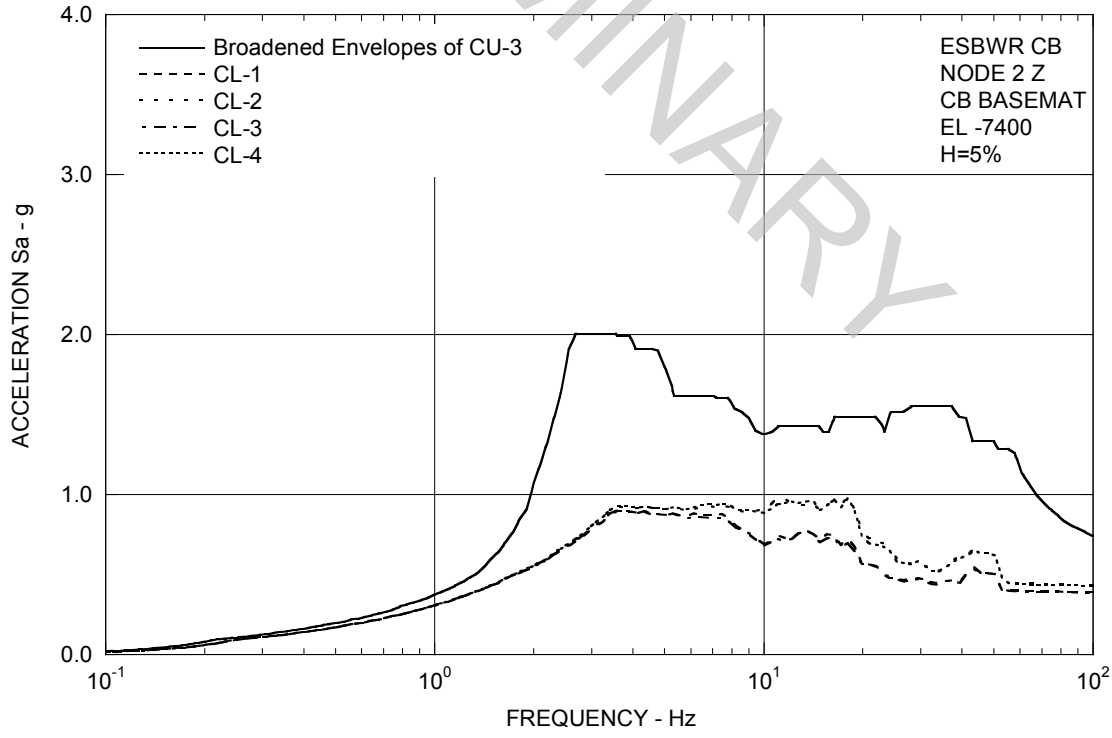

Figure 3A.8.6-3h. FRS (Effect of Layered Sites) – CB Basemat Z

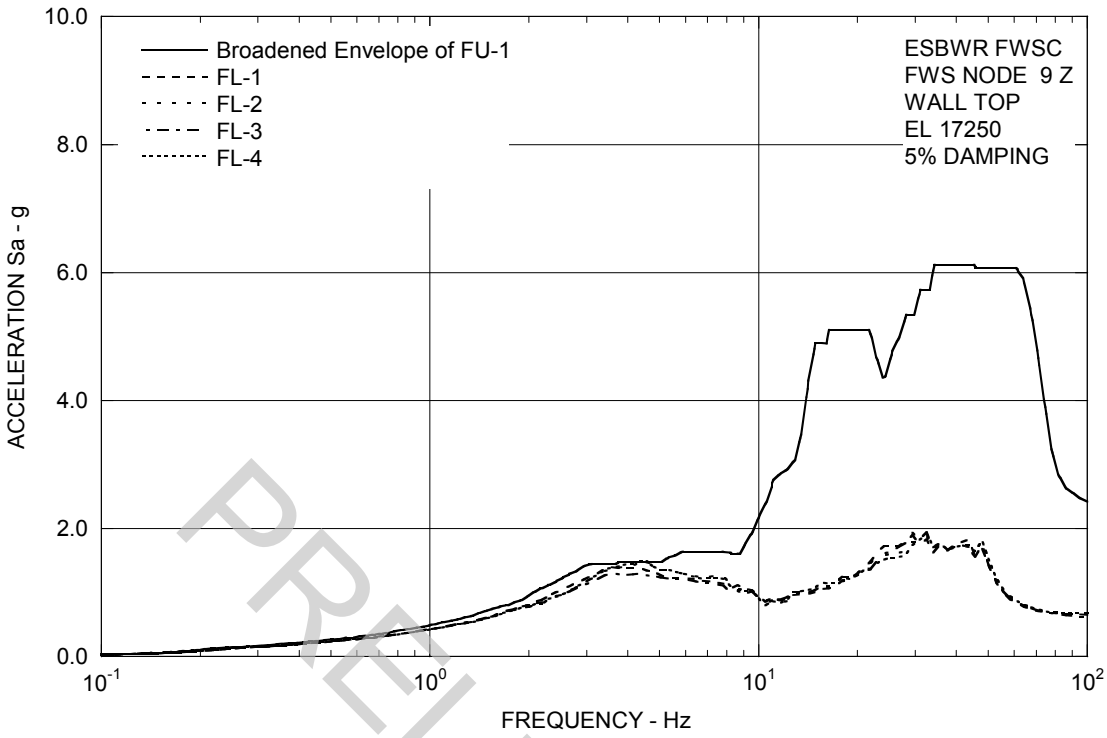

Figure 3A.8.6-3i. FRS (Effect of Layered Sites) – FWS Wall Top Z

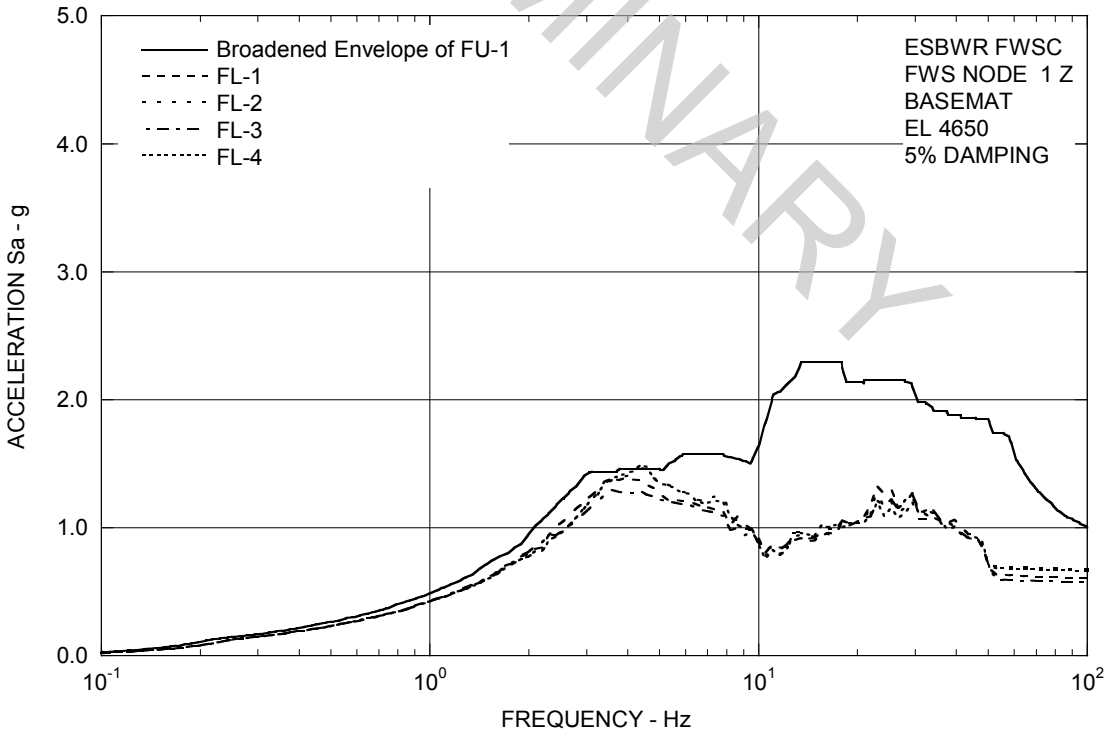

Figure 3A.8.6-3j. FRS (Effect of Layered Sites) – FWS Basemat Z

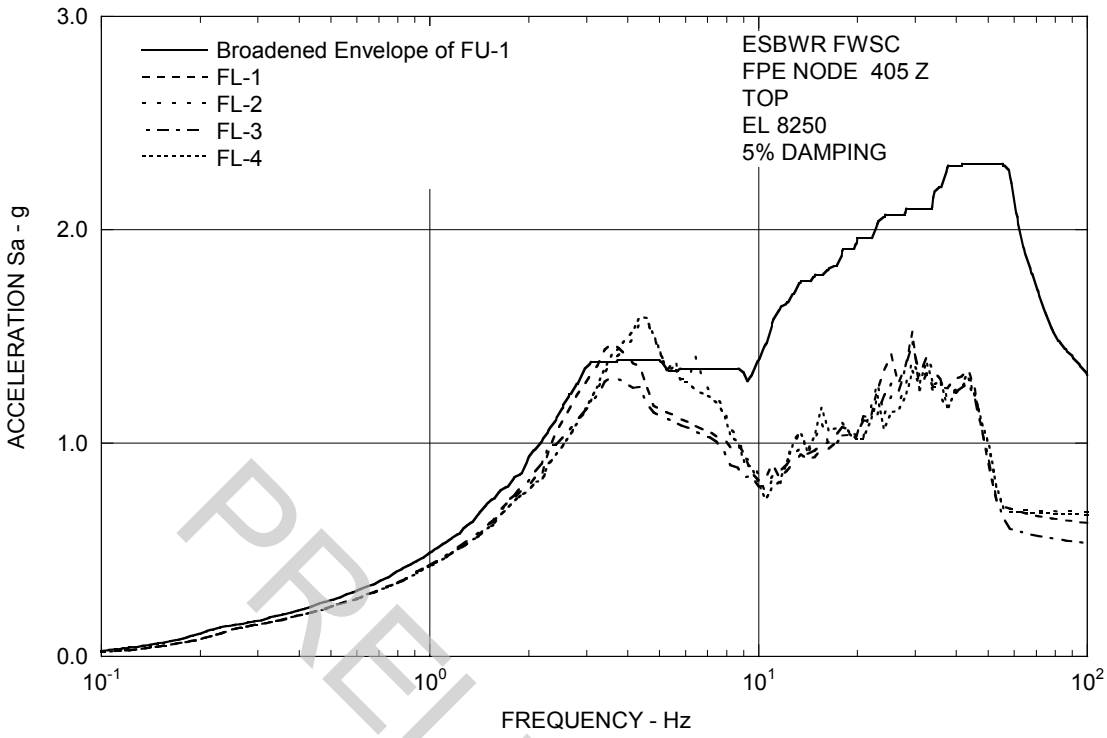

Figure 3A.8.6-3k. FRS (Effect of Layered Sites) – FPE Top Z

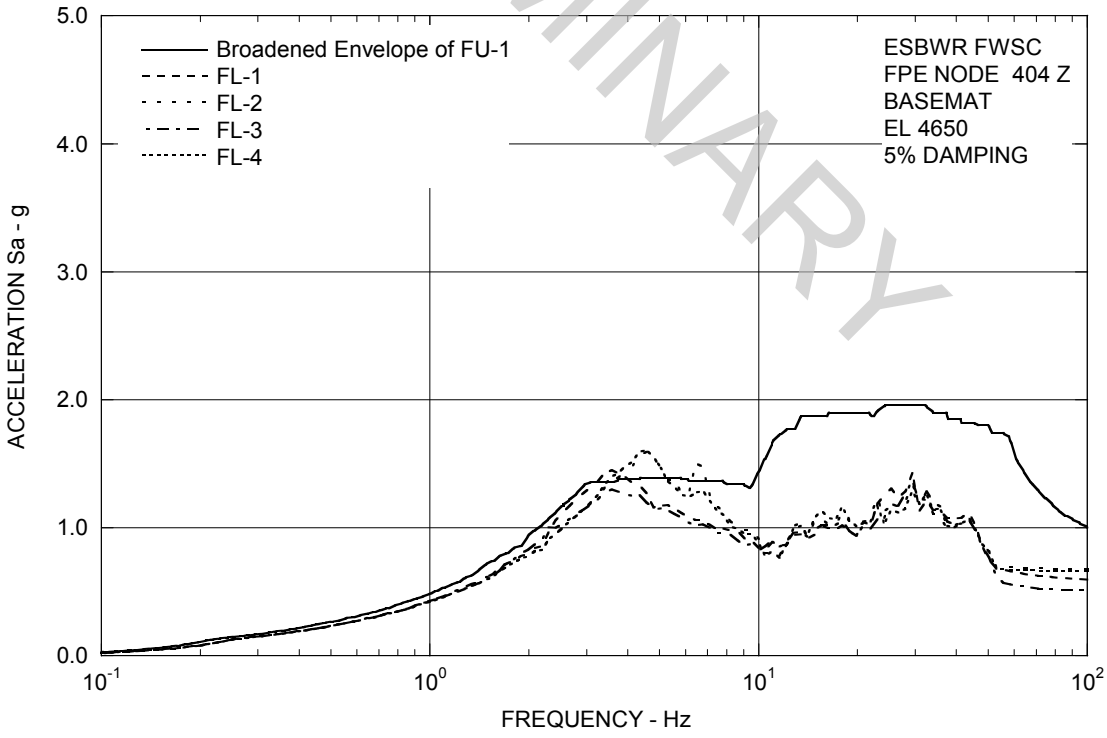

Figure 3A.8.6-3l. FRS (Effect of Layered Sites) – FPE Basemat Z

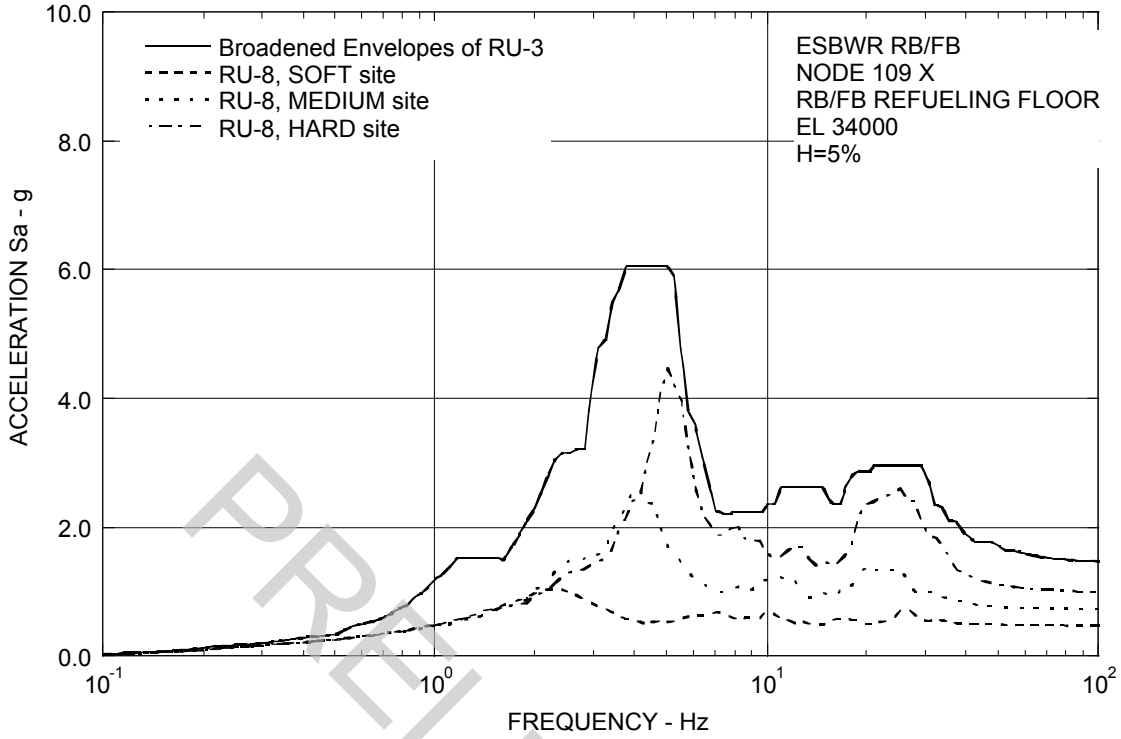

Figure 3A.8.7-1a. FRS (Effect of Embedment) – RB/FB Refueling Floor X

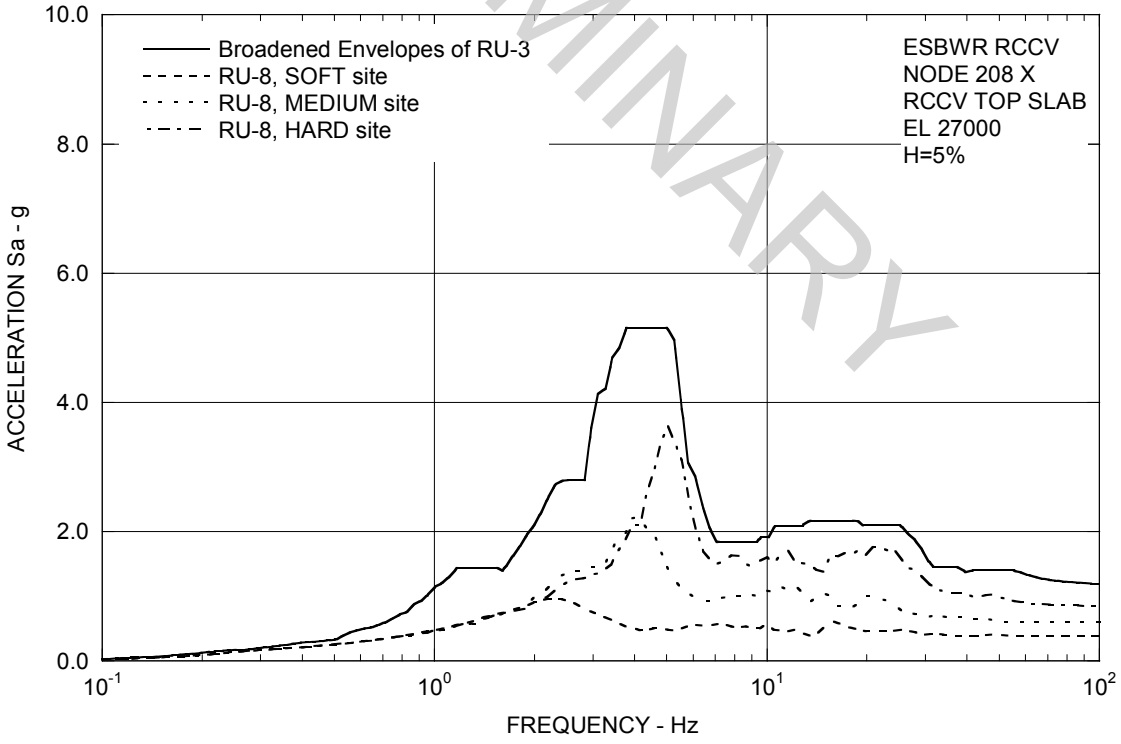

Figure 3A.8.7-1b. FRS (Effect of Embedment) – RCCV Top Slab X

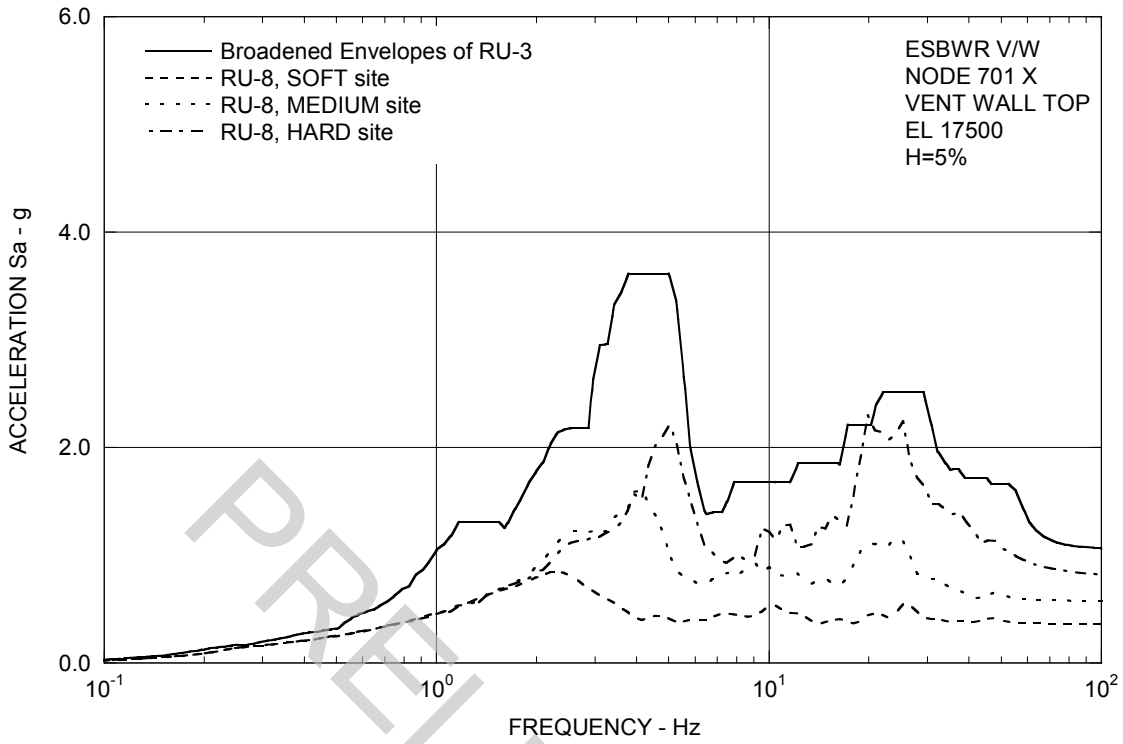

Figure 3A.8.7-1c. FRS (Effect of Embedment) – Vent Wall Top X

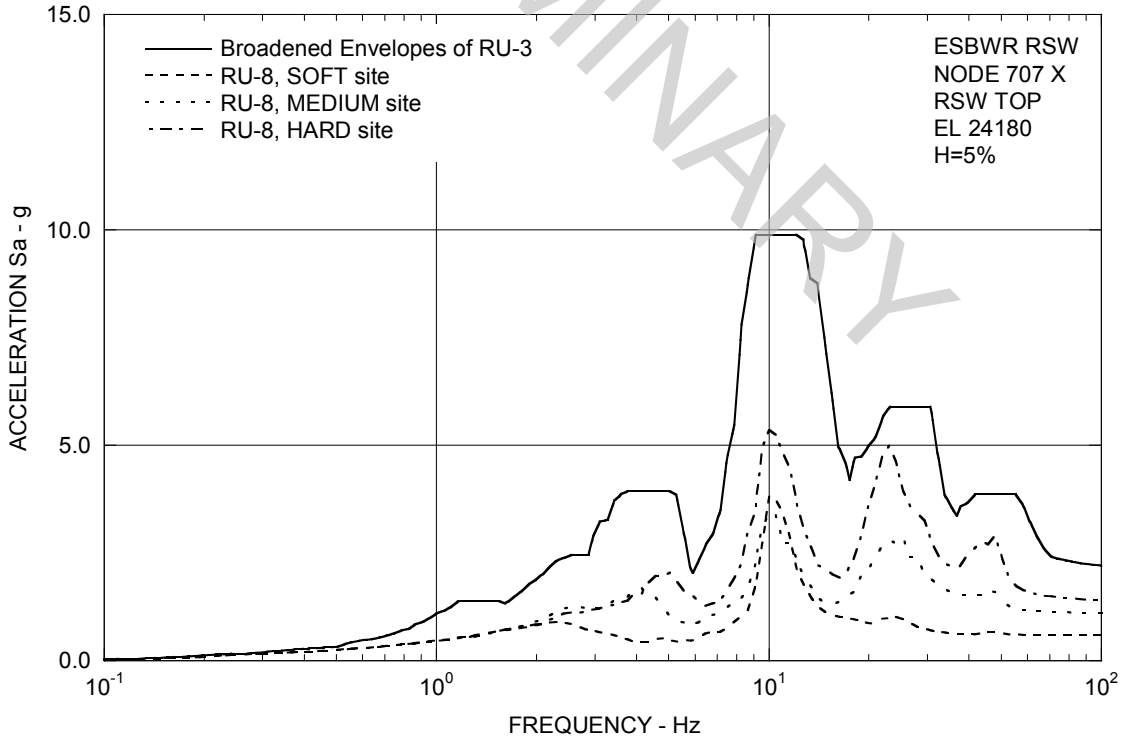

Figure 3A.8.7-1d. FRS (Effect of Embedment) – RSW Top X

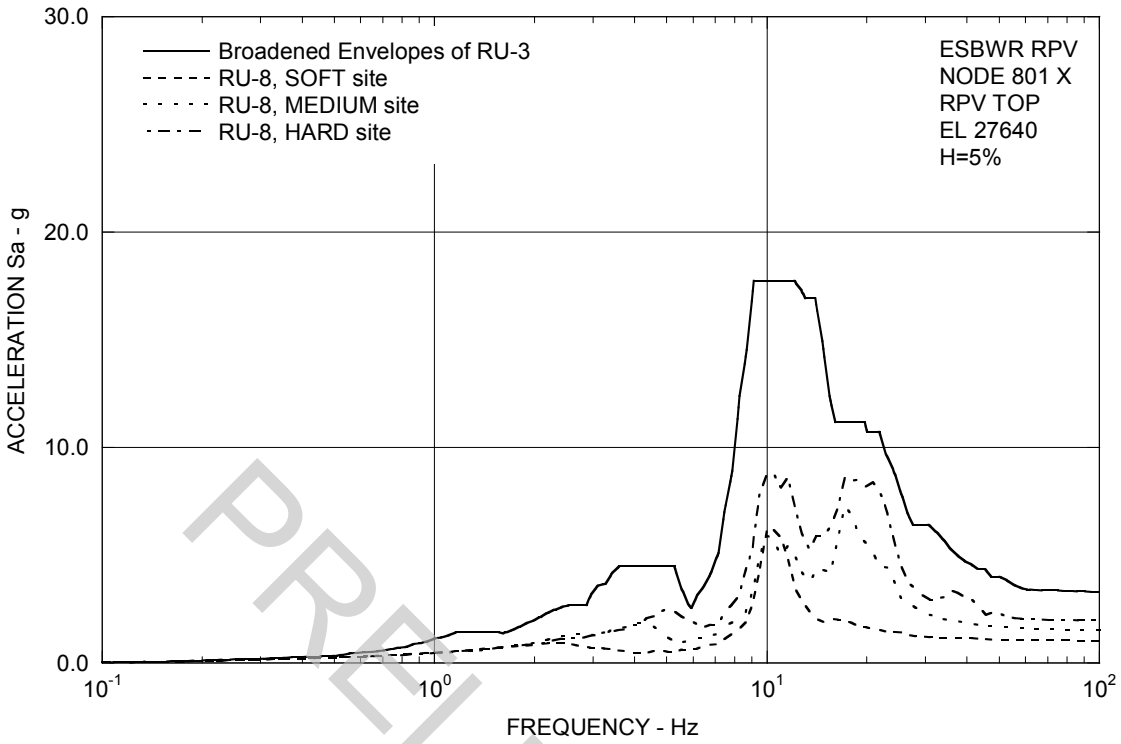

Figure 3A.8.7-1e. FRS (Effect of Embedment) – RPV Top X

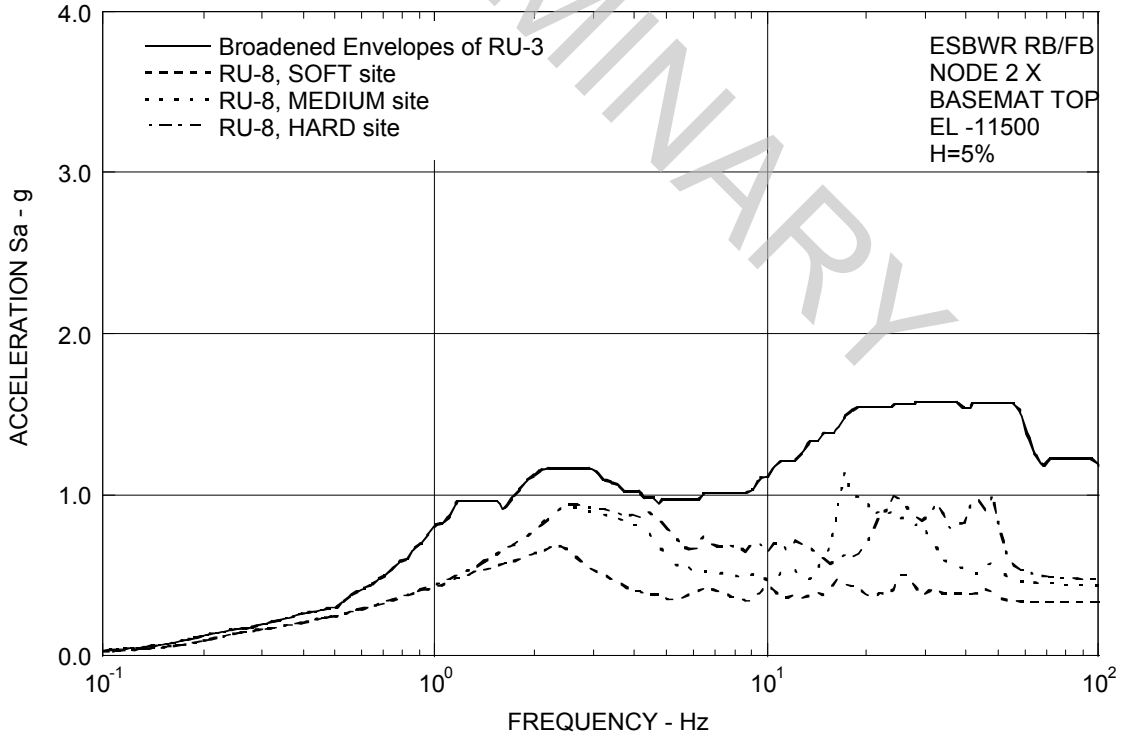

Figure 3A.8.7-1f. FRS (Effect of Embedment) – RB/FB Basemat X

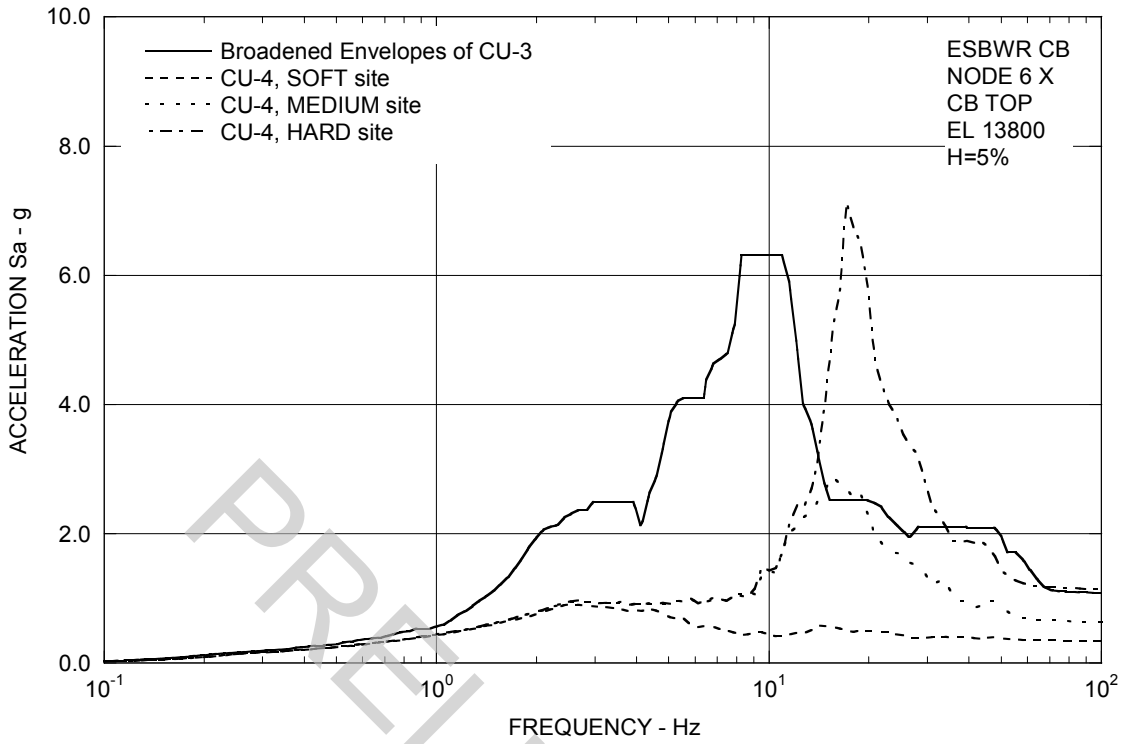

Figure 3A.8.7-1g. FRS (Effect of Embedment) – CB Top X

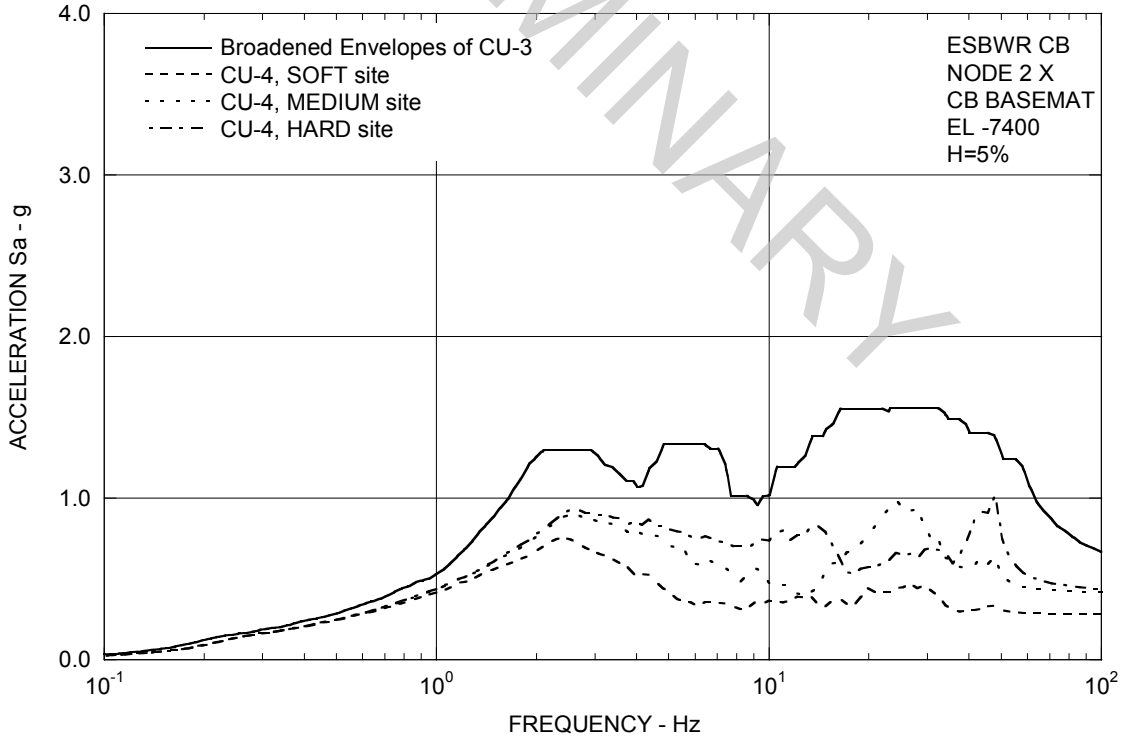

Figure 3A.8.7-1h. FRS (Effect of Embedment) – CB Basemat X

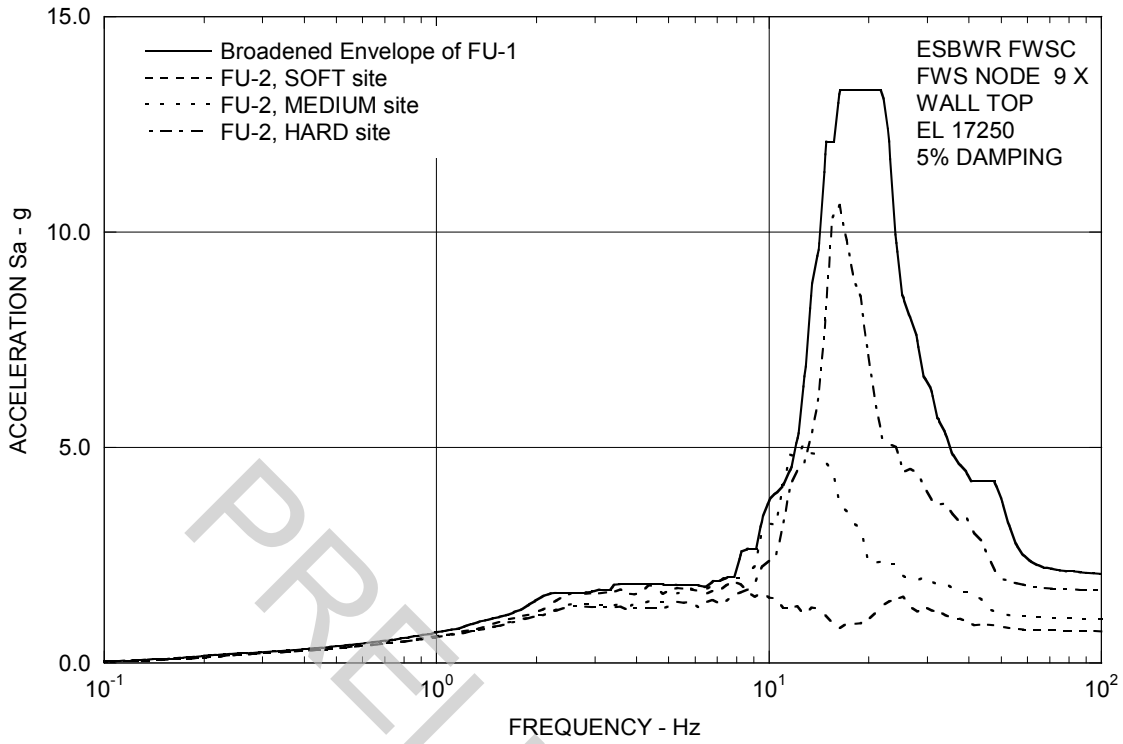

Figure 3A.8.7-1i. FRS (Effect of Embedment) – FWS Wall Top X

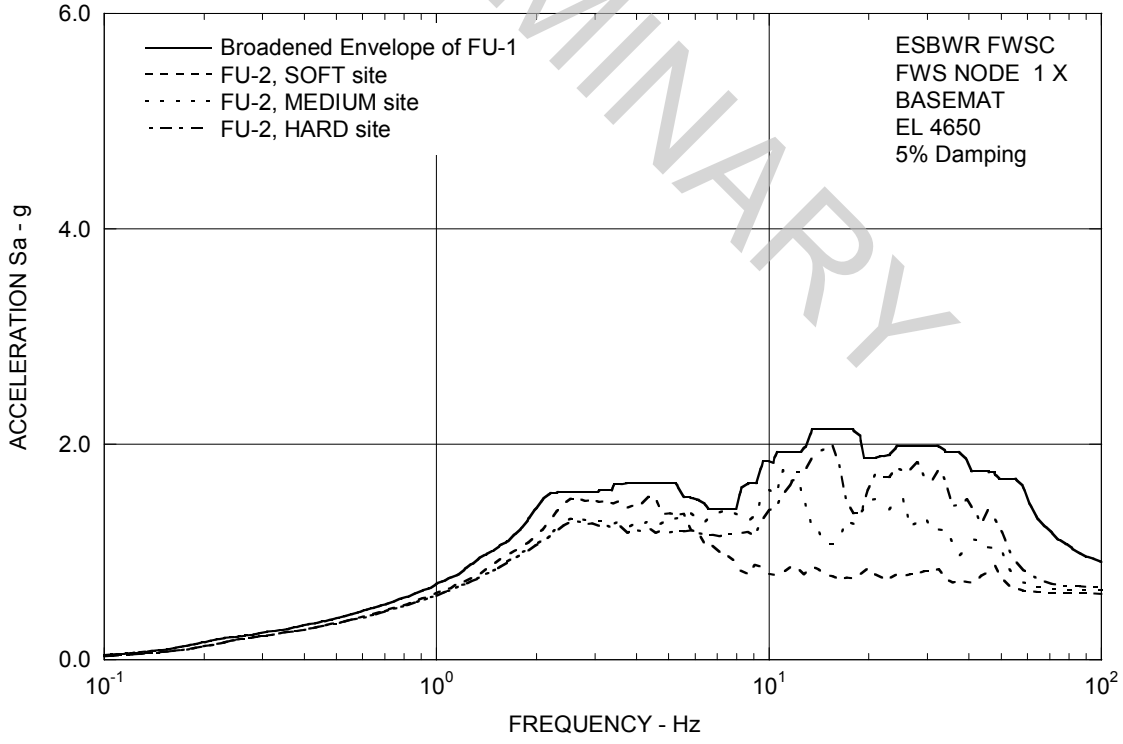

Figure 3A.8.7-1j. FRS (Effect of Embedment) – FWS Basemat X

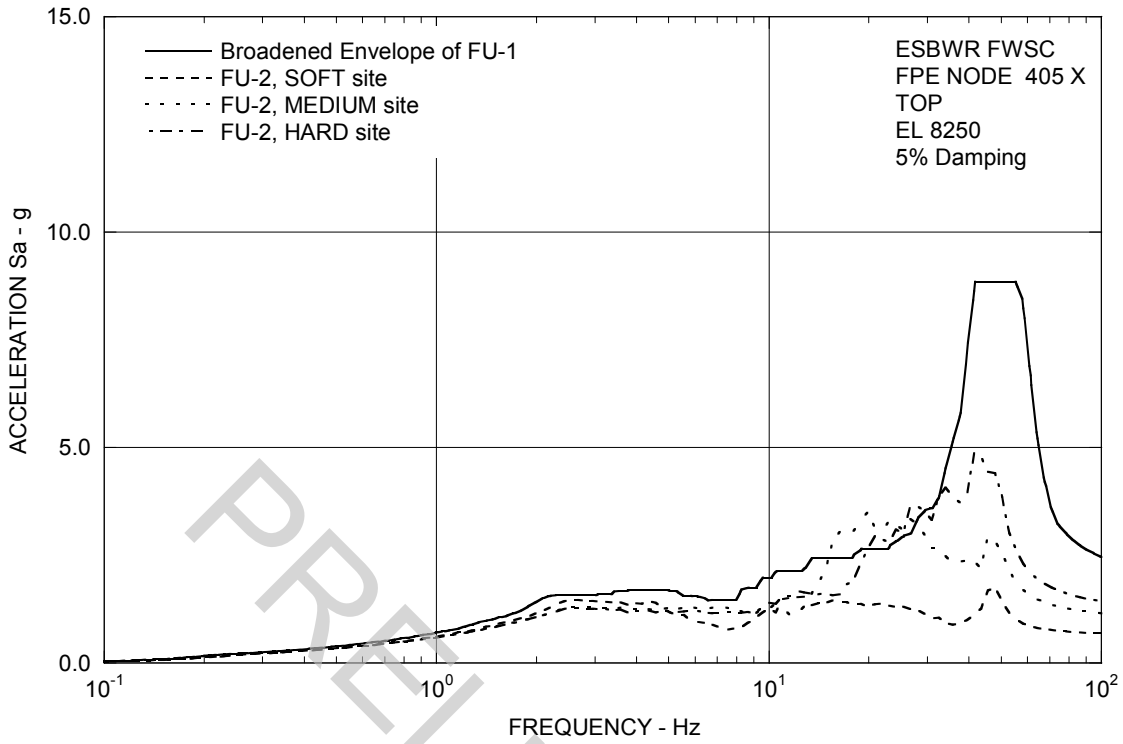

Figure 3A.8.7-1k. FRS (Effect of Embedment) – FPE Top X

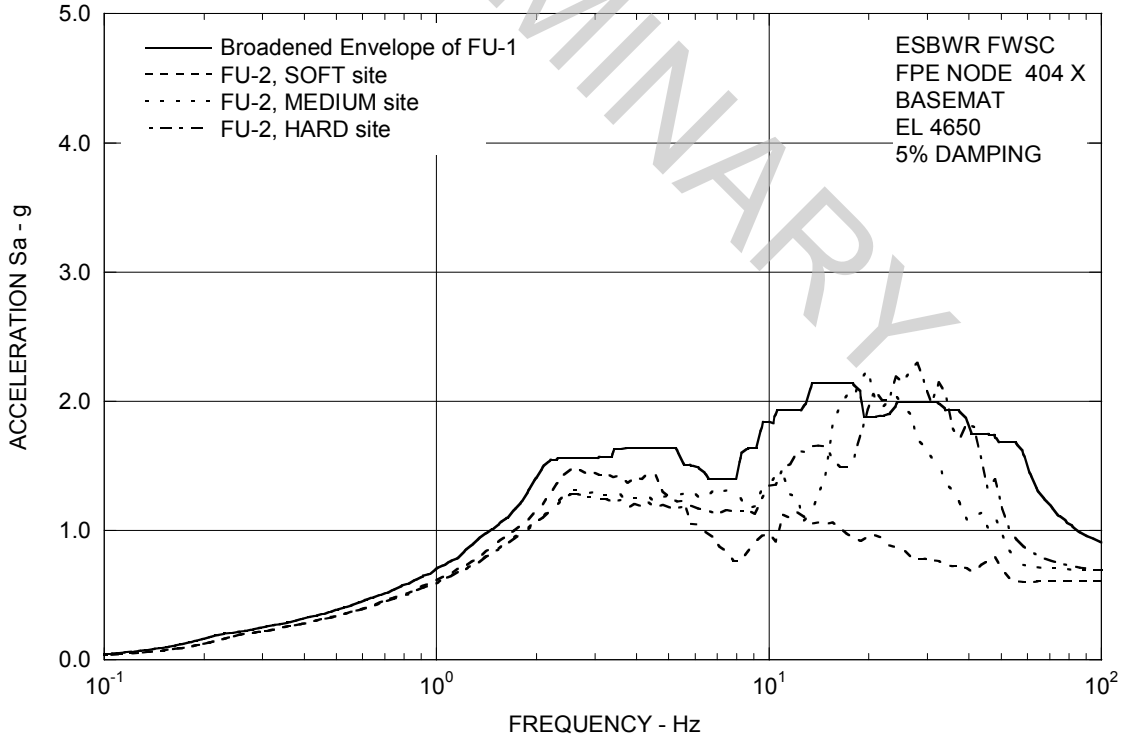

Figure 3A.8.7-1l. FRS (Effect of Embedment) – FPE Basemat X

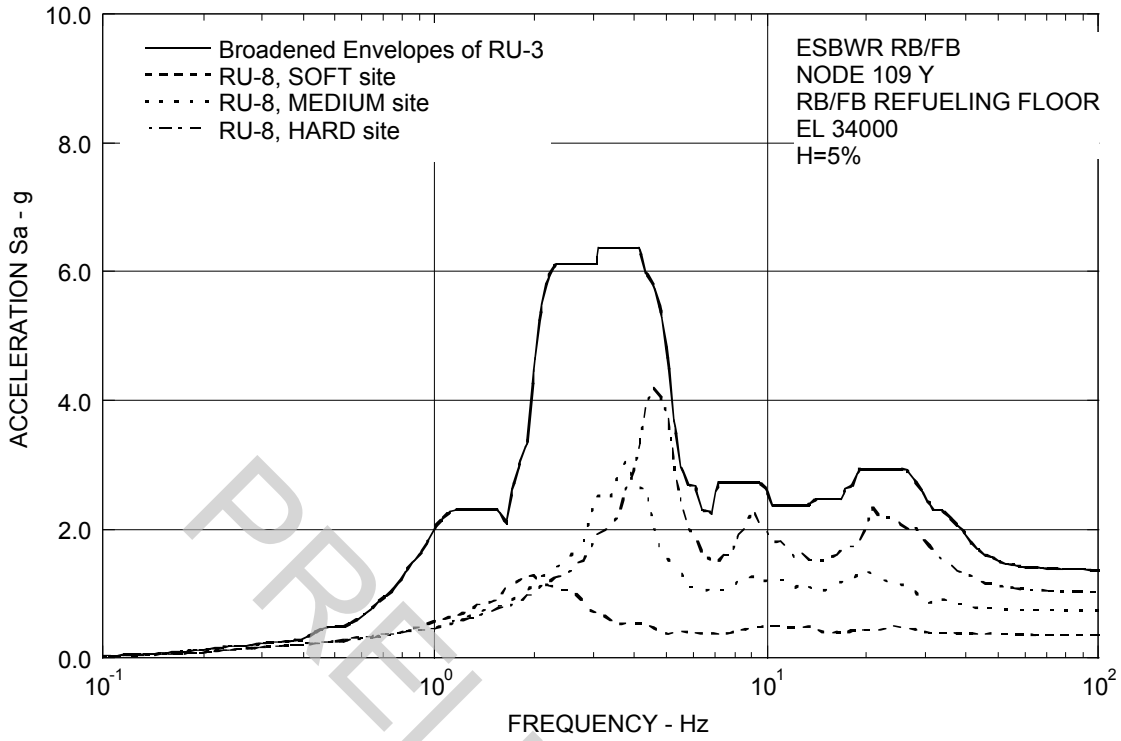

Figure 3A.8.7-2a. FRS (Effect of Embedment) – RB/FB Refueling Floor Y

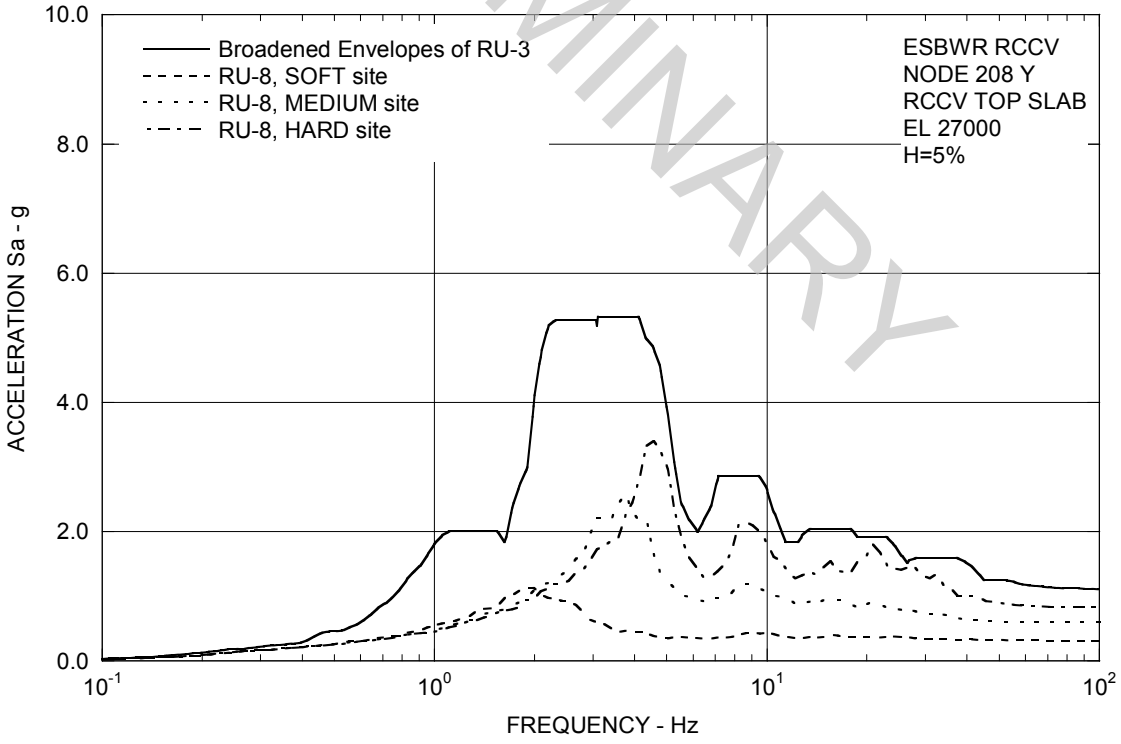

Figure 3A.8.7-2b. FRS (Effect of Embedment) – RCCV Top Slab Y

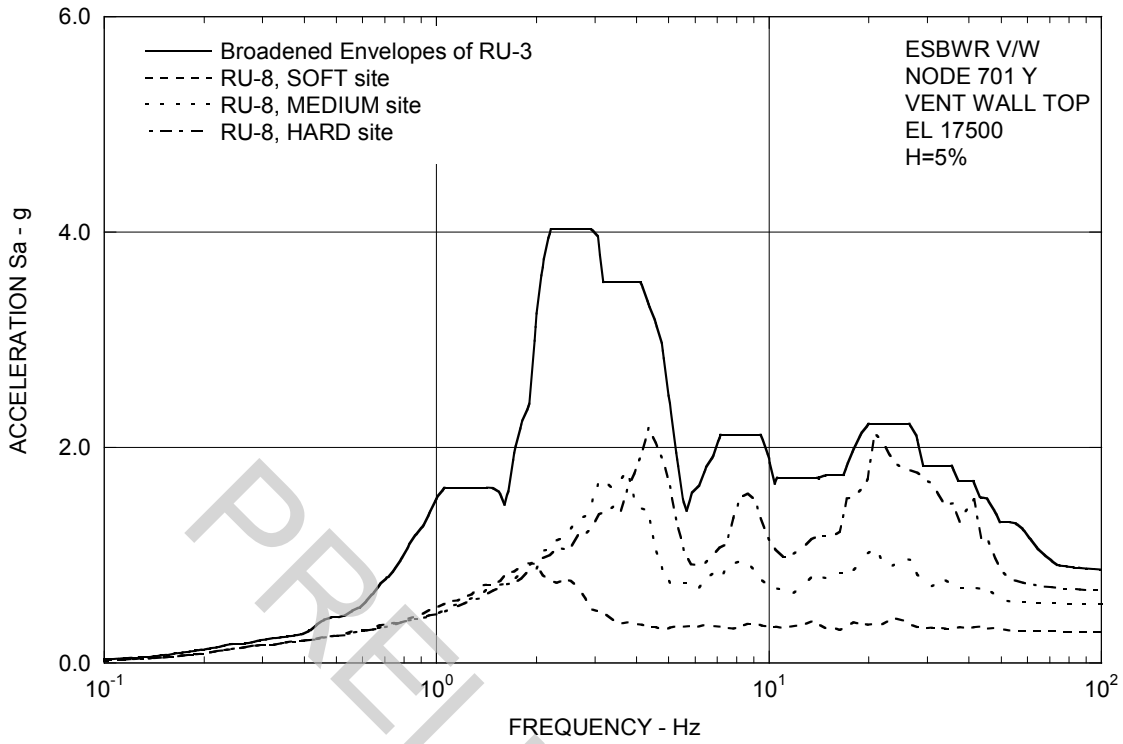

Figure 3A.8.7-2c. FRS (Effect of Embedment) – Vent Wall Top Y

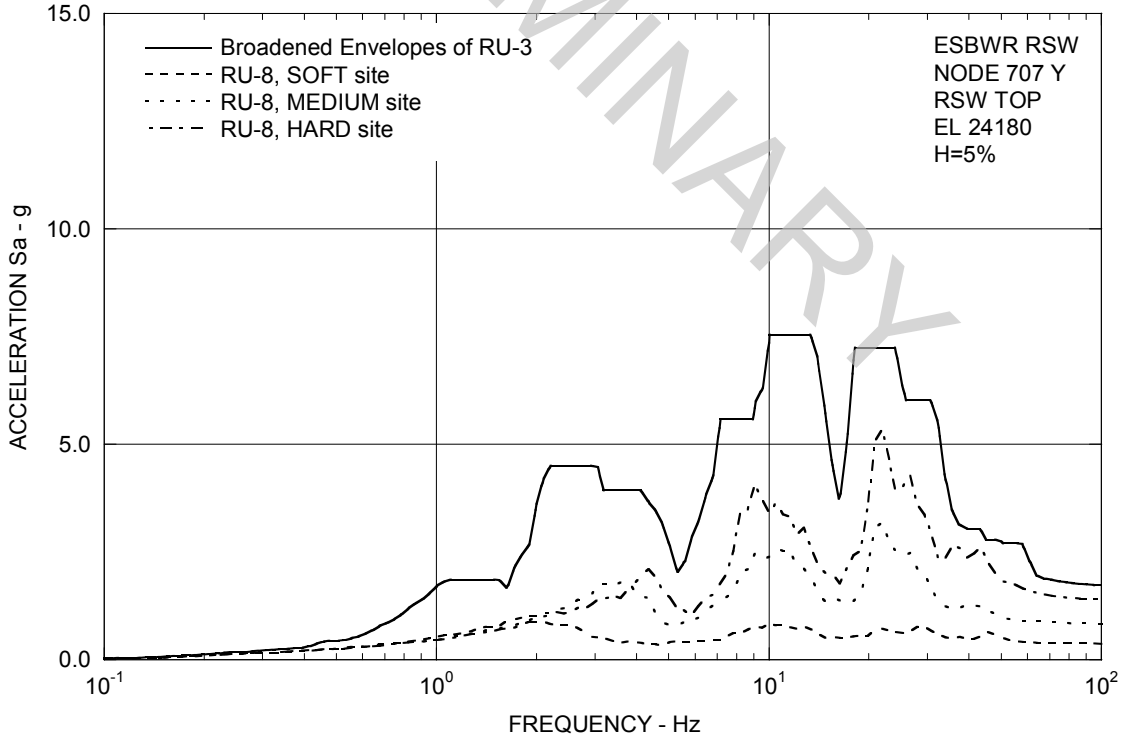

Figure 3A.8.7-2d. FRS (Effect of Embedment) – RSW Top Y

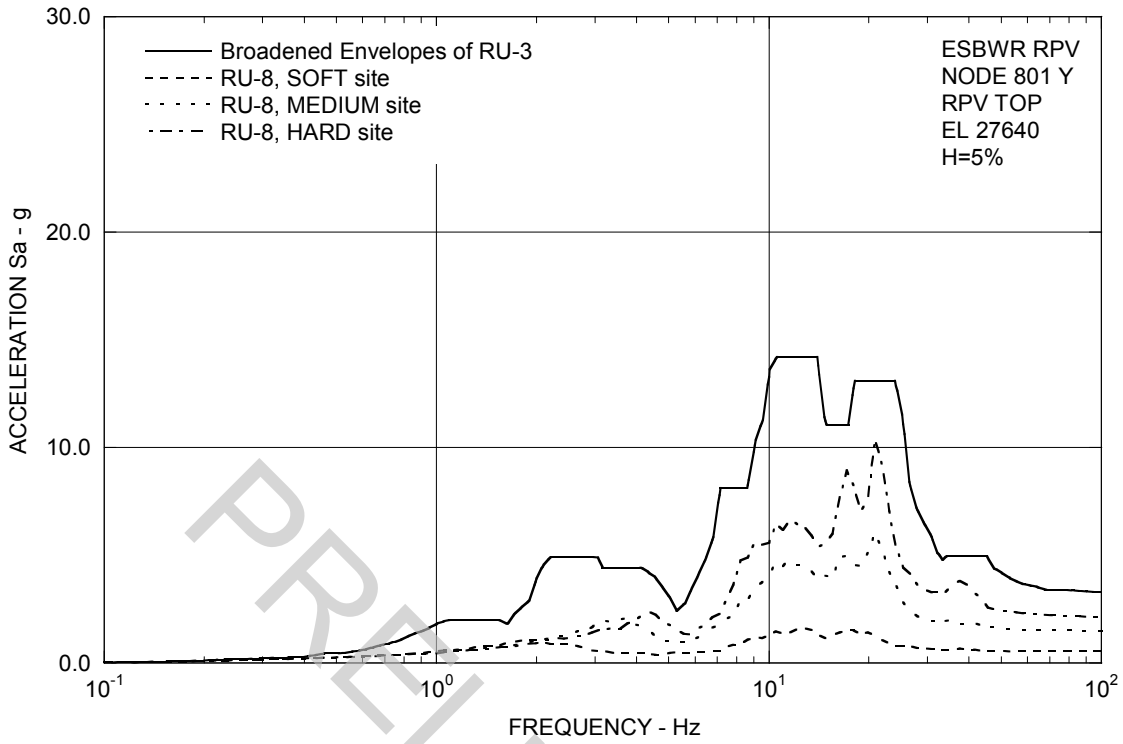

Figure 3A.8.7-2e. FRS (Effect of Embedment) – RPV Top Y

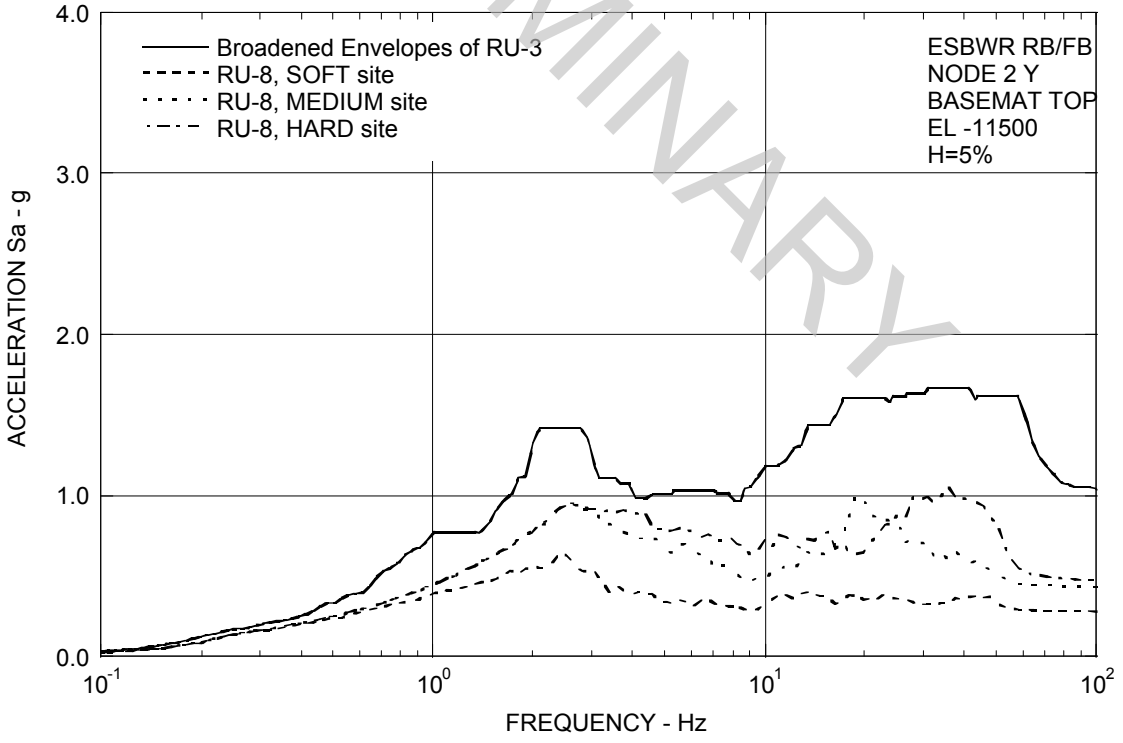

Figure 3A.8.7-2f. FRS (Effect of Embedment) – RB/FB Basemat Y

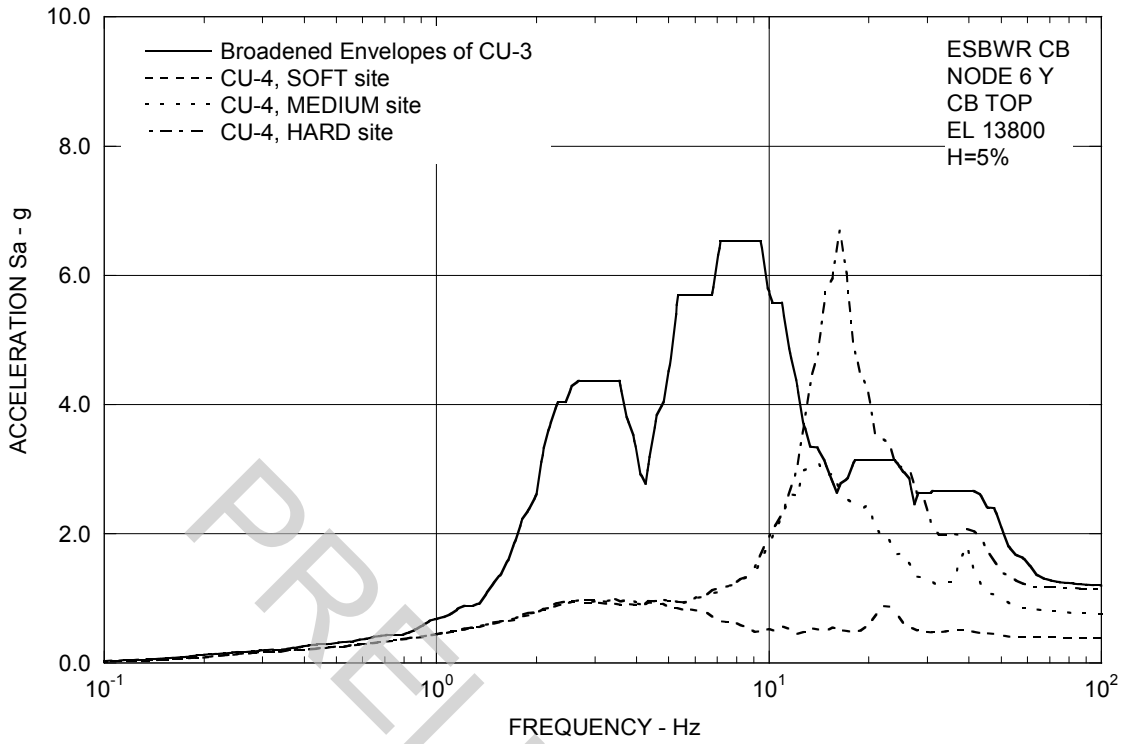

Figure 3A.8.7-2g. FRS (Effect of Embedment) – CB Top Y

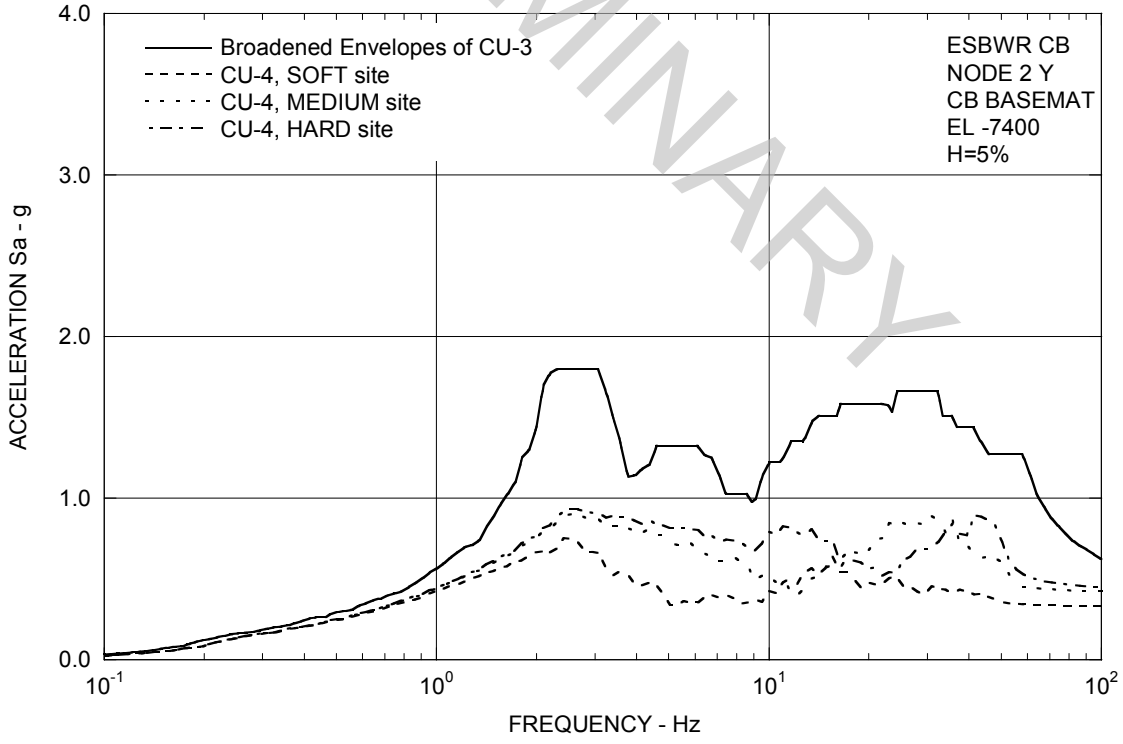

Figure 3A.8.7-2h. FRS (Effect of Embedment) – CB Basemat Y

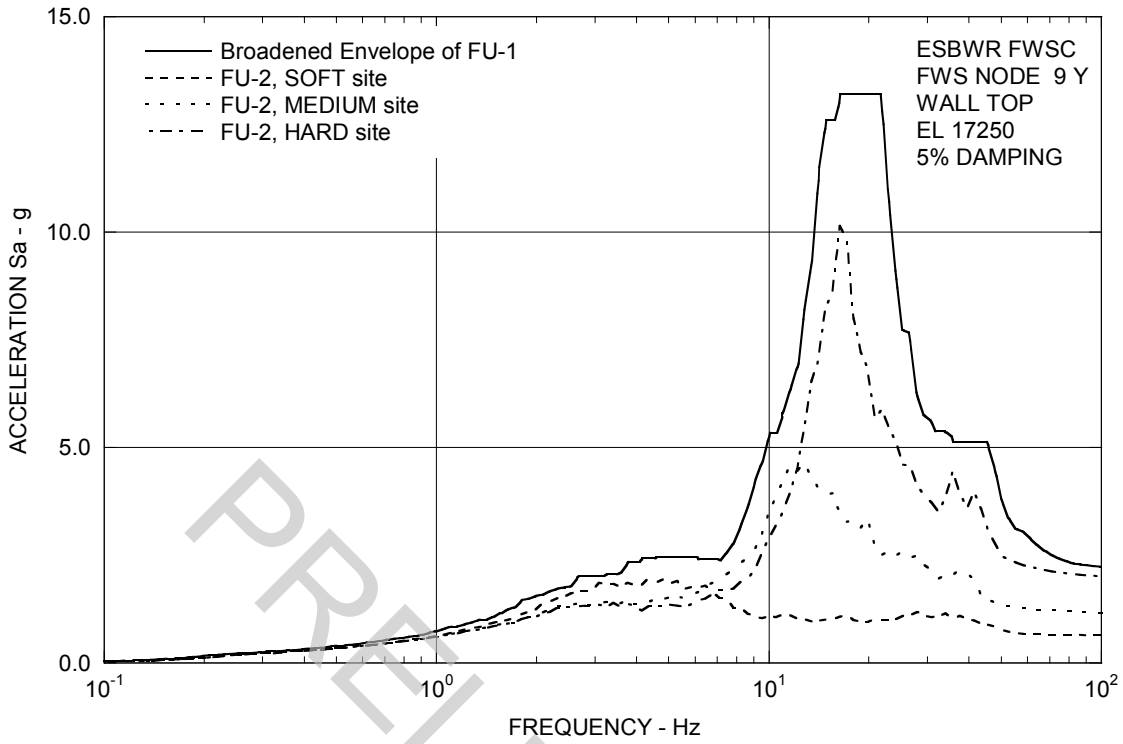

Figure 3A.8.7-2i. FRS (Effect of Embedment) – FWS Wall Top Y

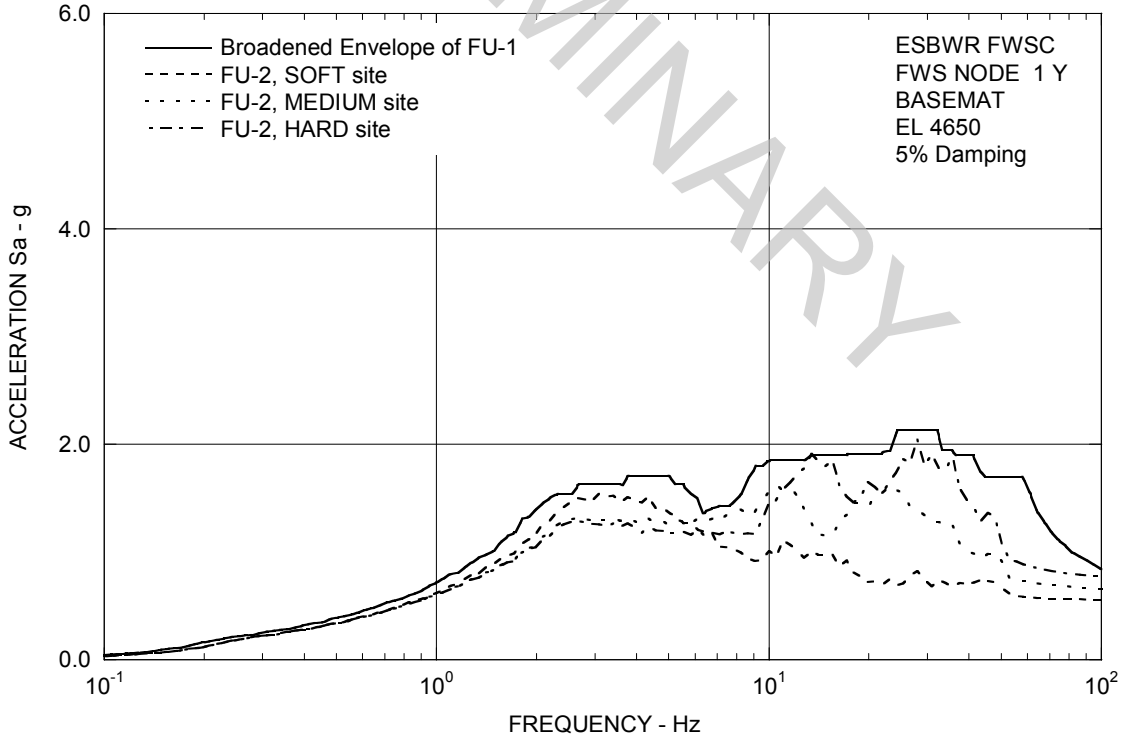

Figure 3A.8.7-2j. FRS (Effect of Embedment) – FWS Basemat Y

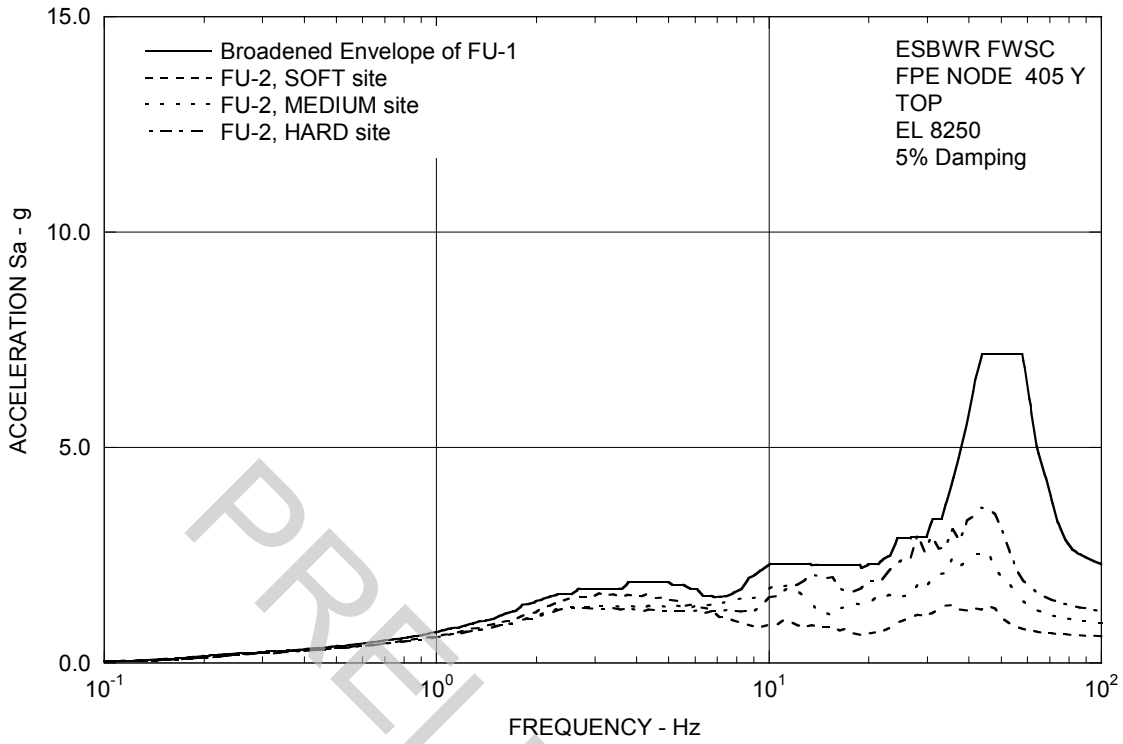

Figure 3A.8.7-2k. FRS (Effect of Embedment) – FPE Top Y

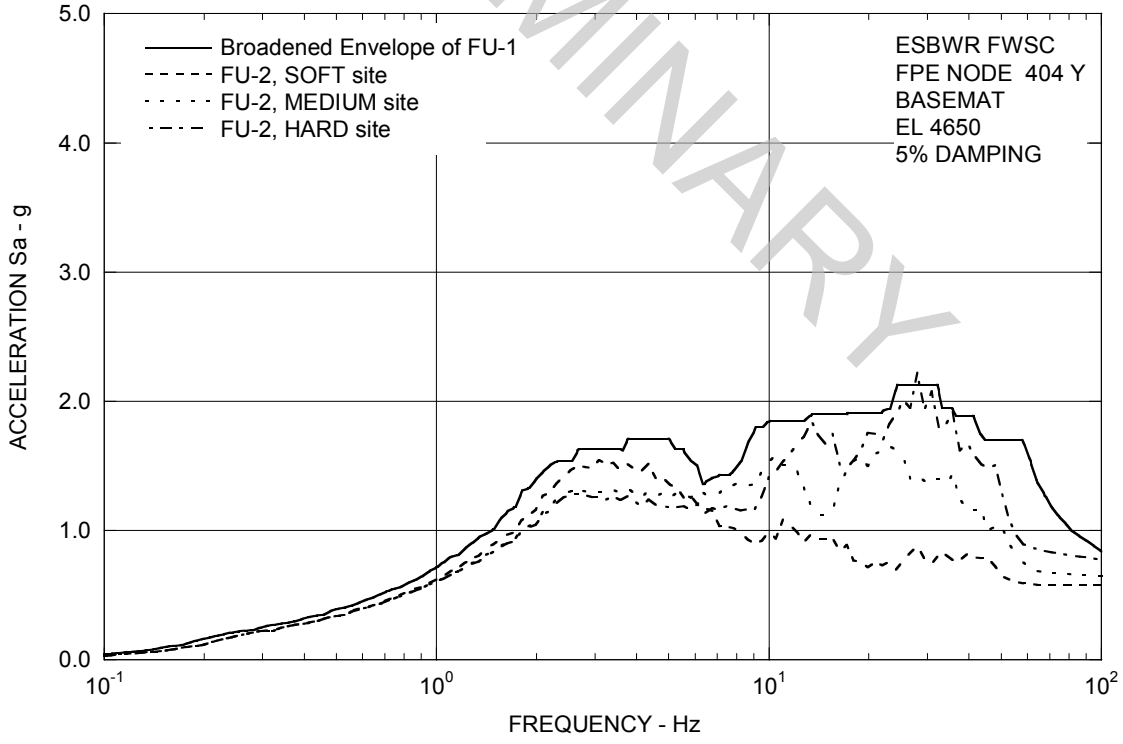

Figure 3A.8.7-2l. FRS (Effect of Embedment) – FPE Basemat Y

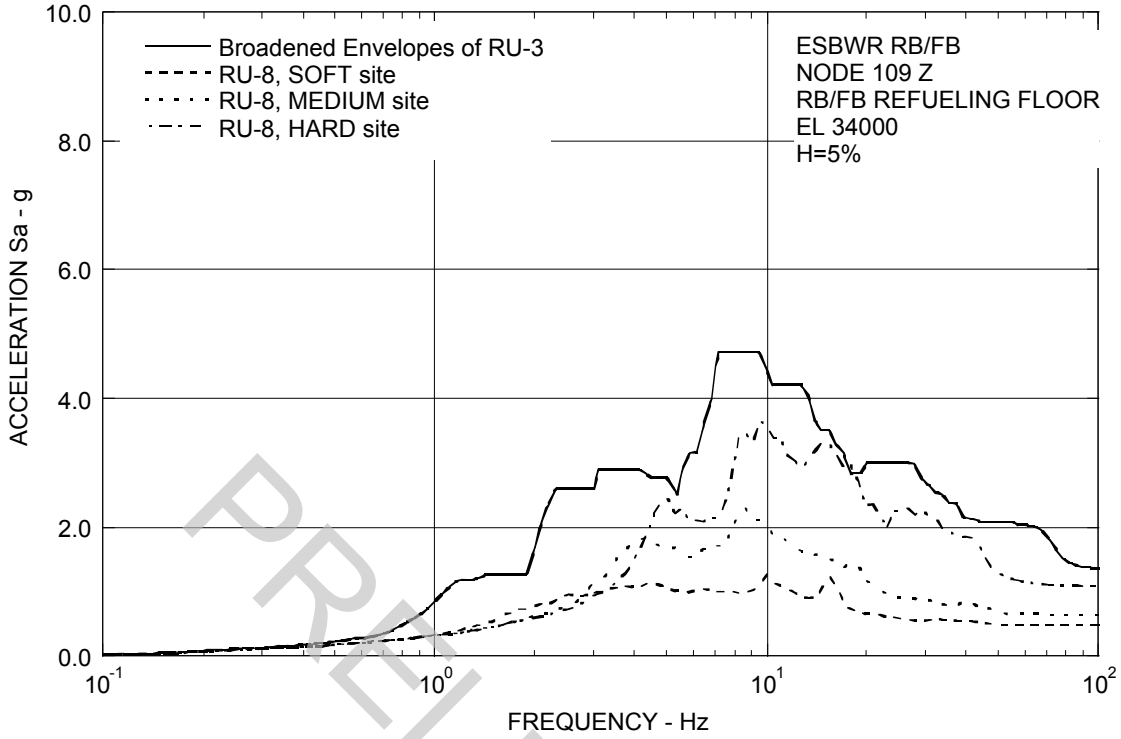

Figure 3A.8.7-3a. FRS (Effect of Embedment) – RB/FB Refueling Floor Z

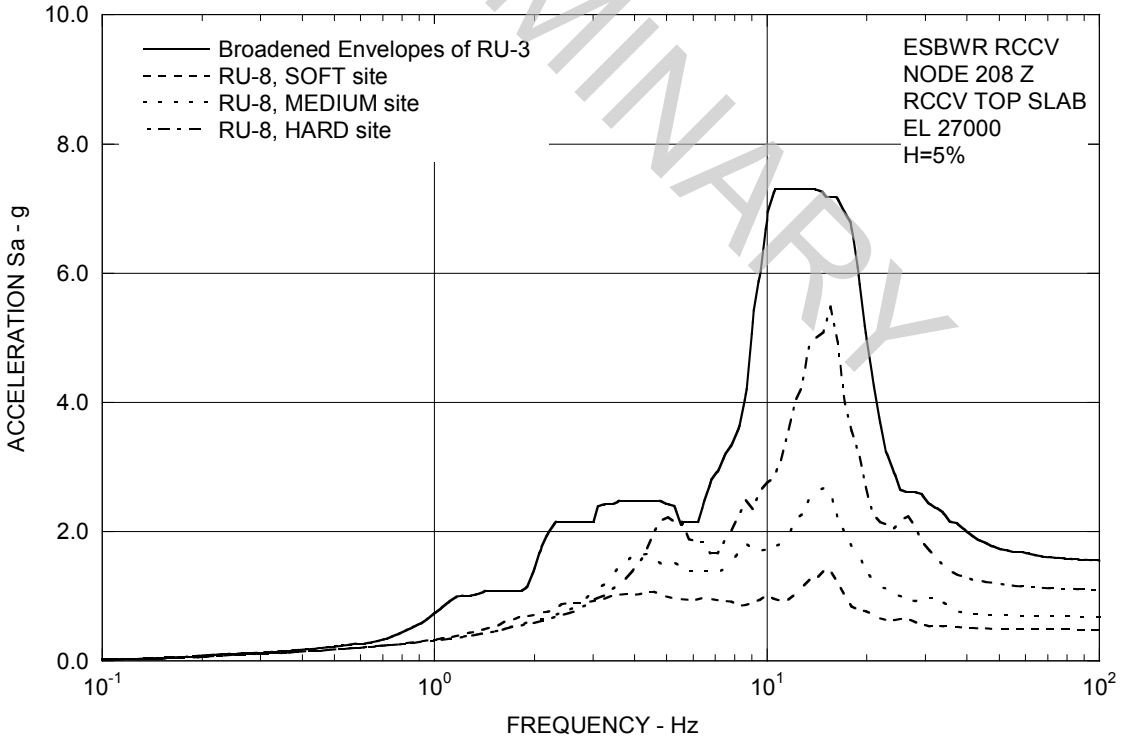

Figure 3A.8.7-3b. FRS (Effect of Embedment) – RCCV Top Slab Z

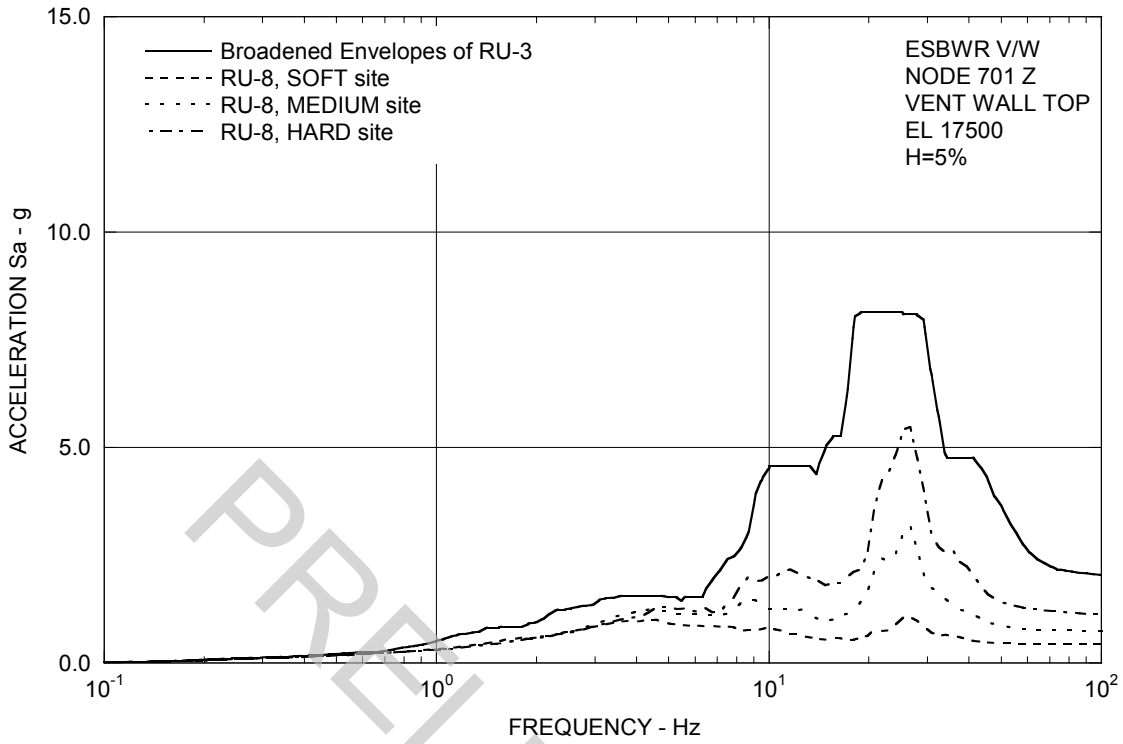

Figure 3A.8.7-3c. FRS (Effect of Embedment) – Vent Wall Top Z

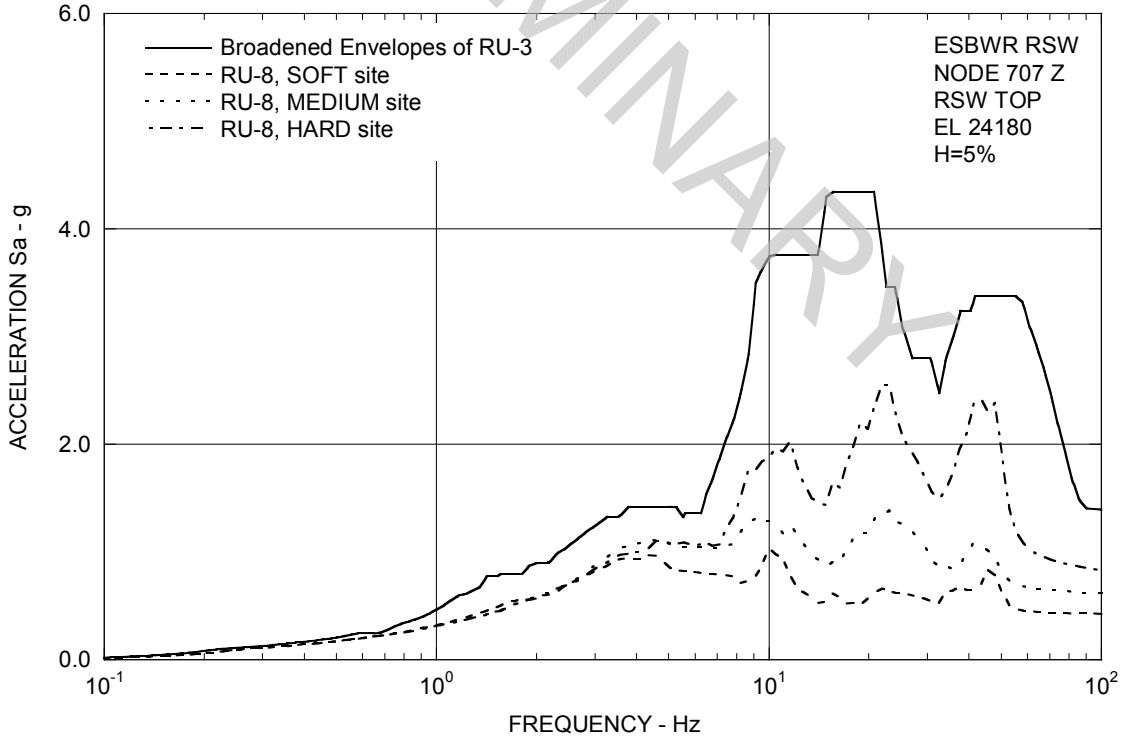

Figure 3A.8.7-3d. FRS (Effect of Embedment) – RSW Top Z

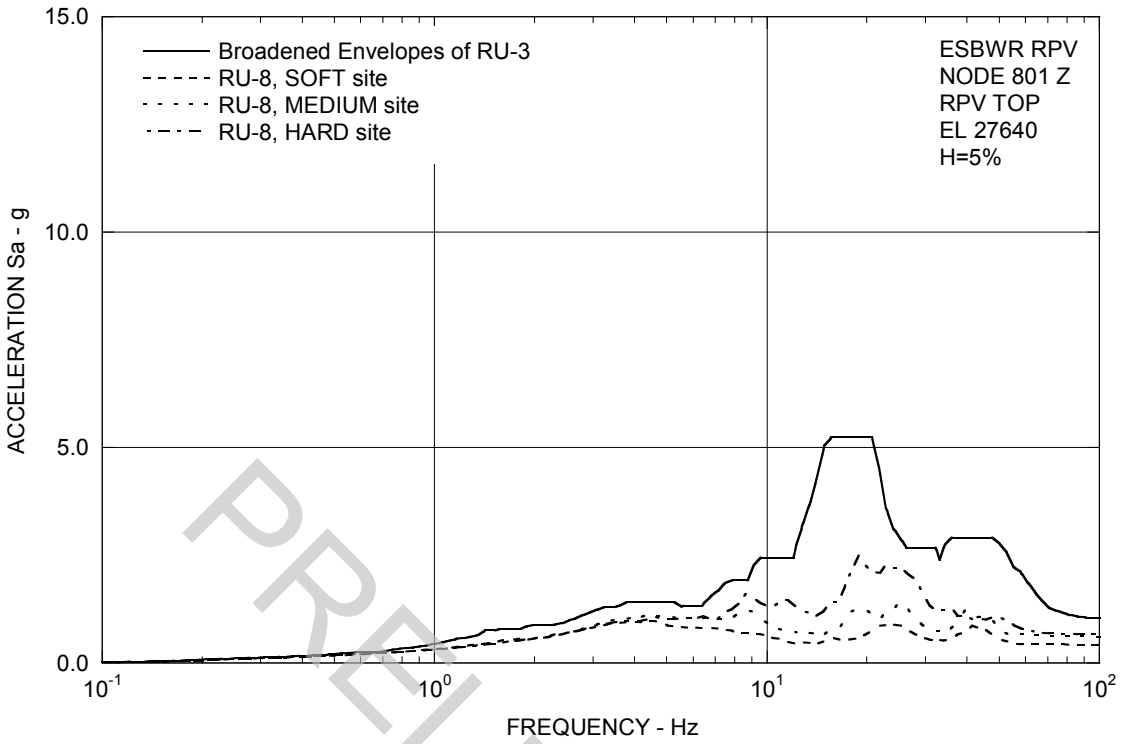

Figure 3A.8.7-3e. FRS (Effect of Embedment) – RPV Top Z

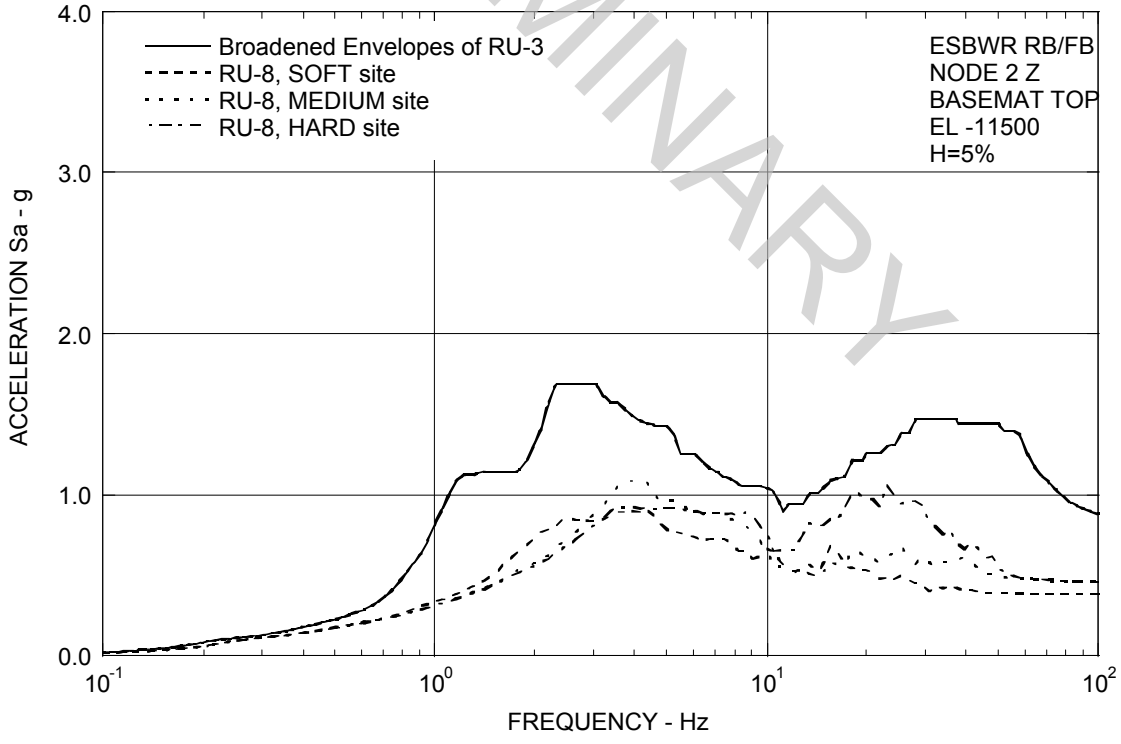

Figure 3A.8.7-3f. FRS (Effect of Embedment) – RB/FB Basemat Z

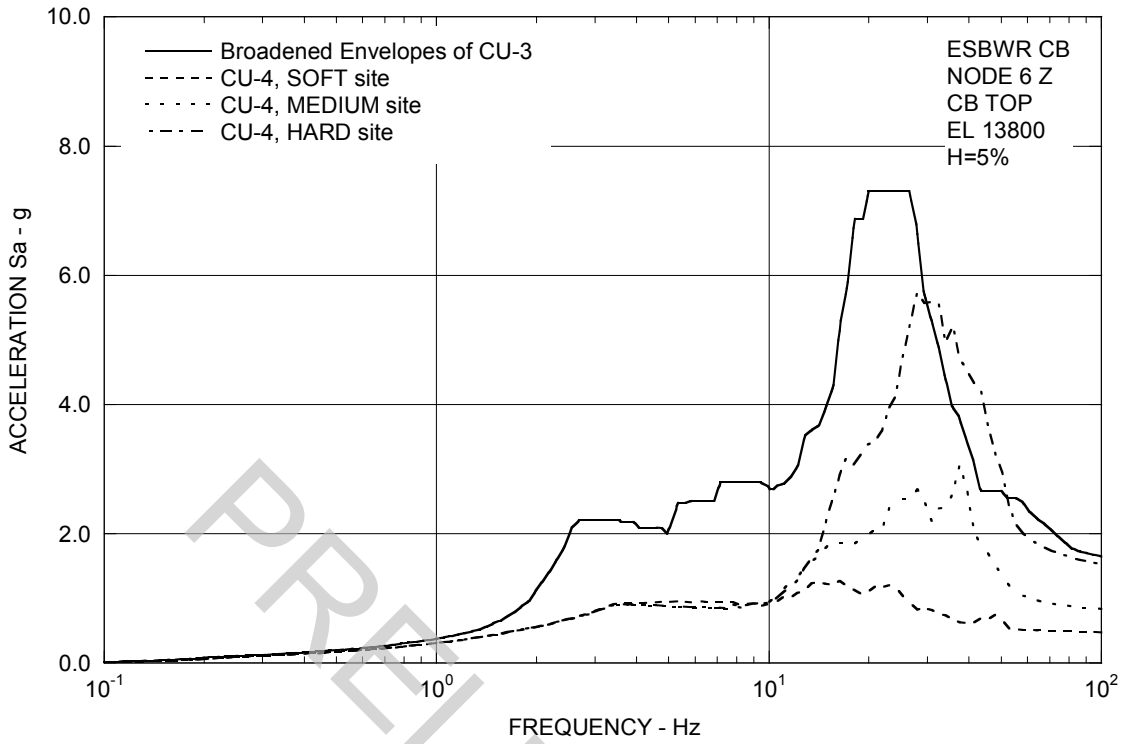

Figure 3A.8.7-3g. FRS (Effect of Embedment) – CB Top Z

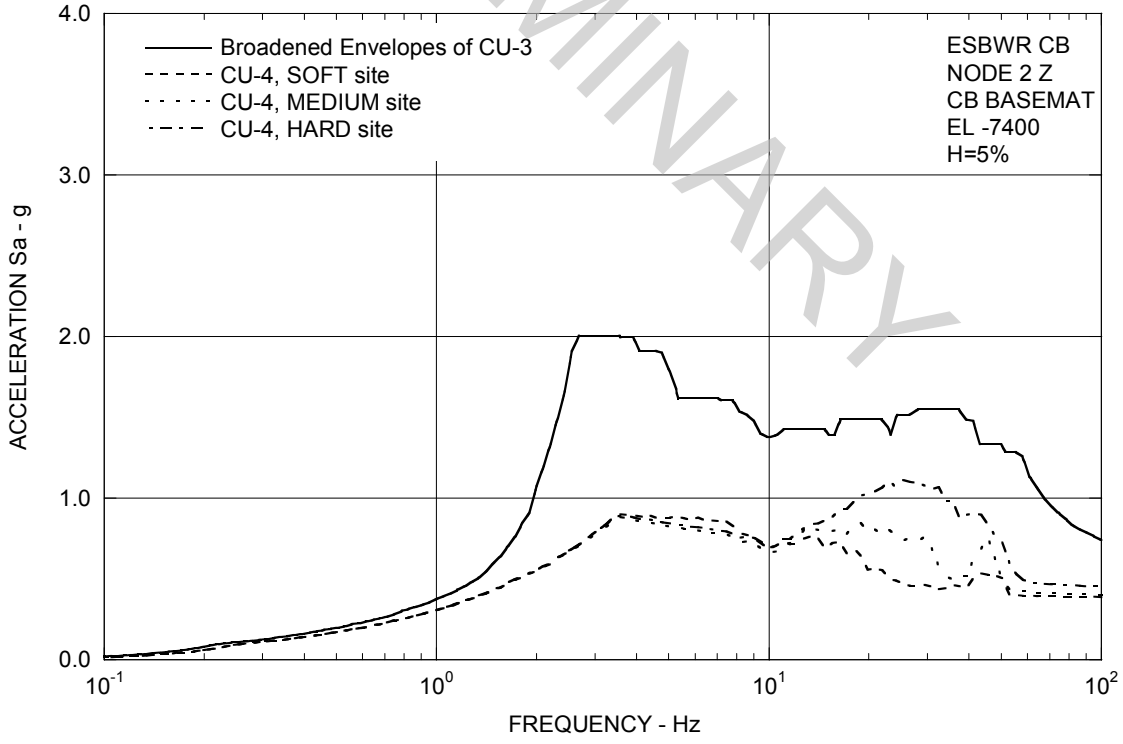

Figure 3A.8.7-3h. FRS (Effect of Embedment) – CB Basemat Z

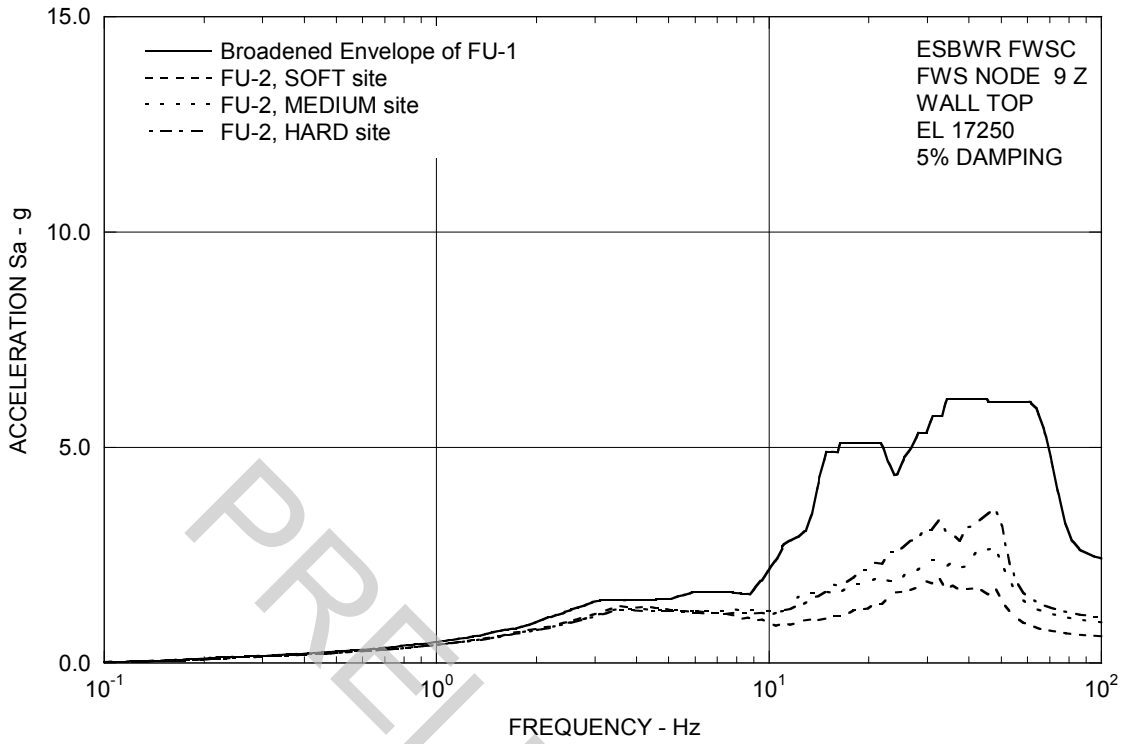

Figure 3A.8.7-3i. FRS (Effect of Embedment) – FWS Wall Top Z

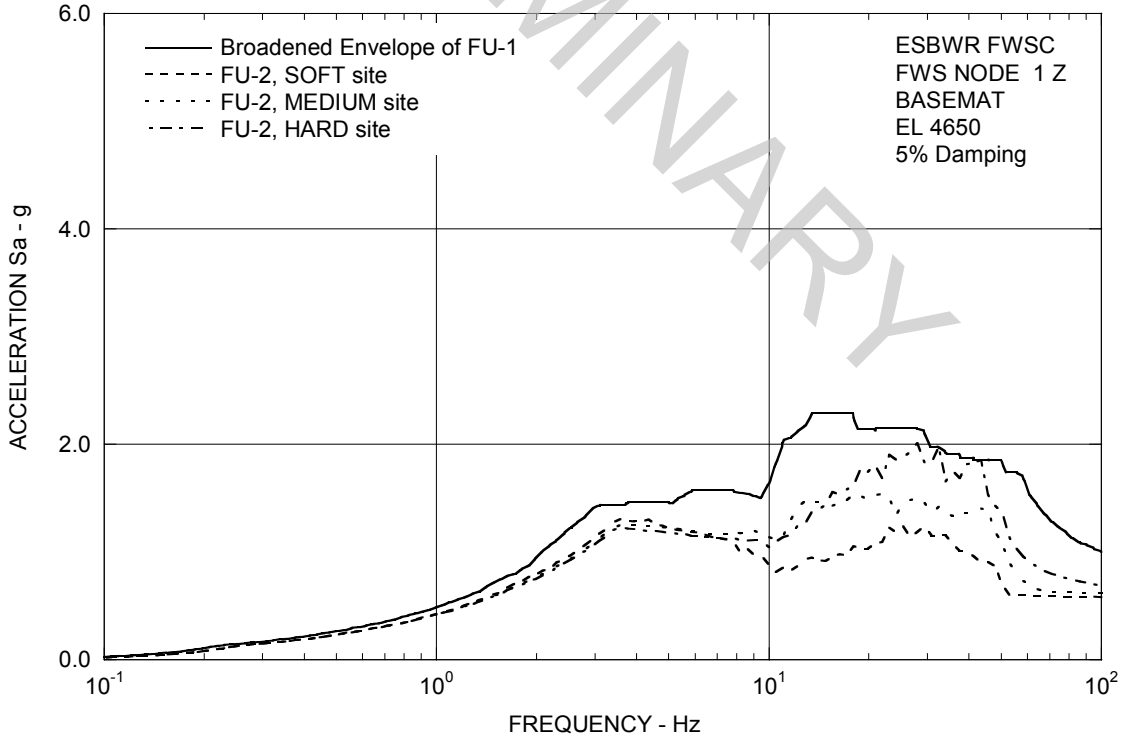

Figure 3A.8.7-3j. FRS (Effect of Embedment) – FWS Basemat Z

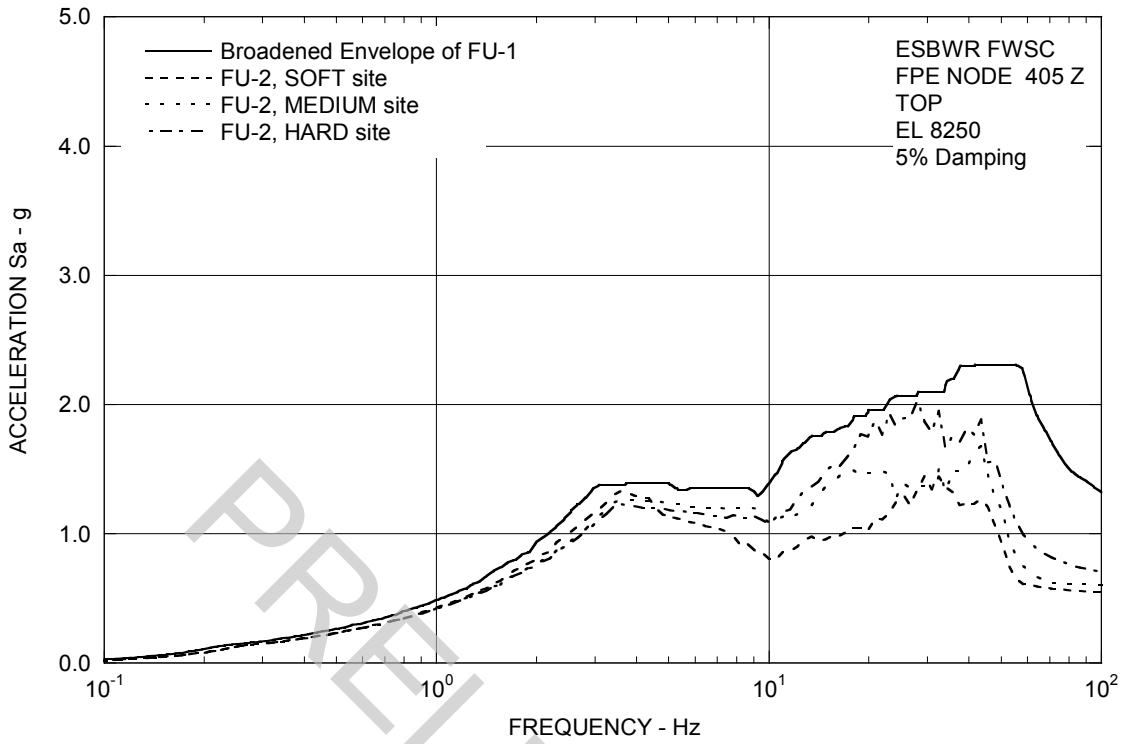

Figure 3A.8.7-3k. FRS (Effect of Embedment) – FPE Top Z

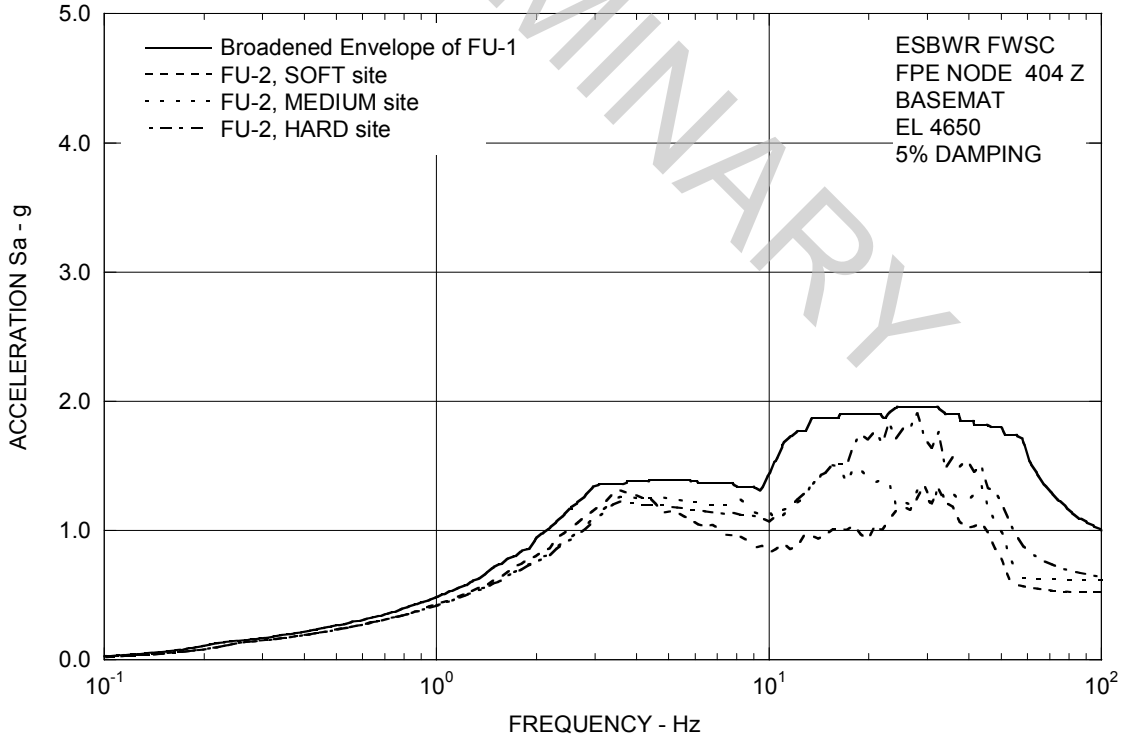

Figure 3A.8.7-3l. FRS (Effect of Embedment) – FPE Basemat Z

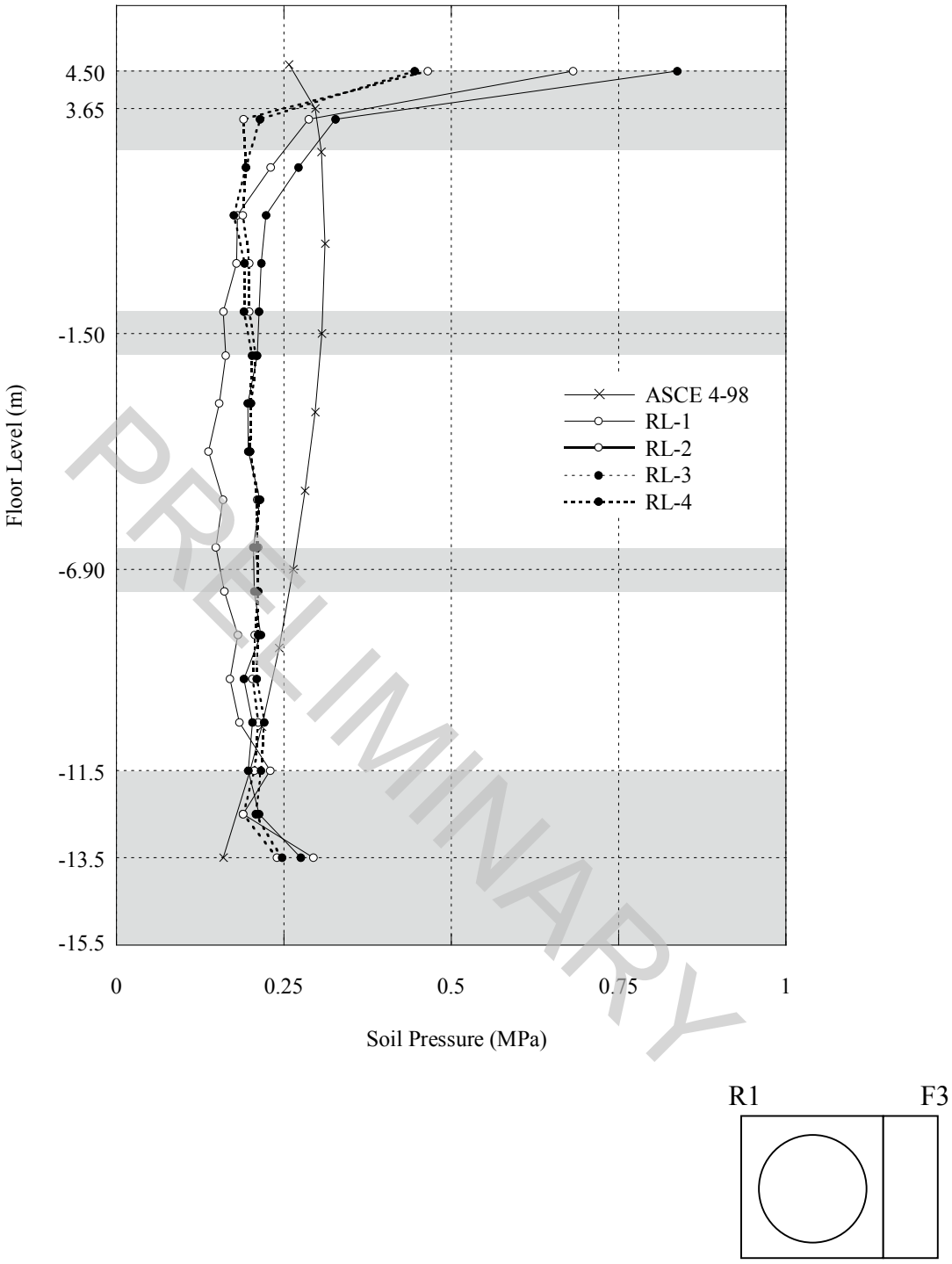

Note: The shaded area shows thickness of the floor slabs and basemat.

Figure 3A.8.8-1. Lateral Soil Pressure – RB/FB R1 and F3 Wall

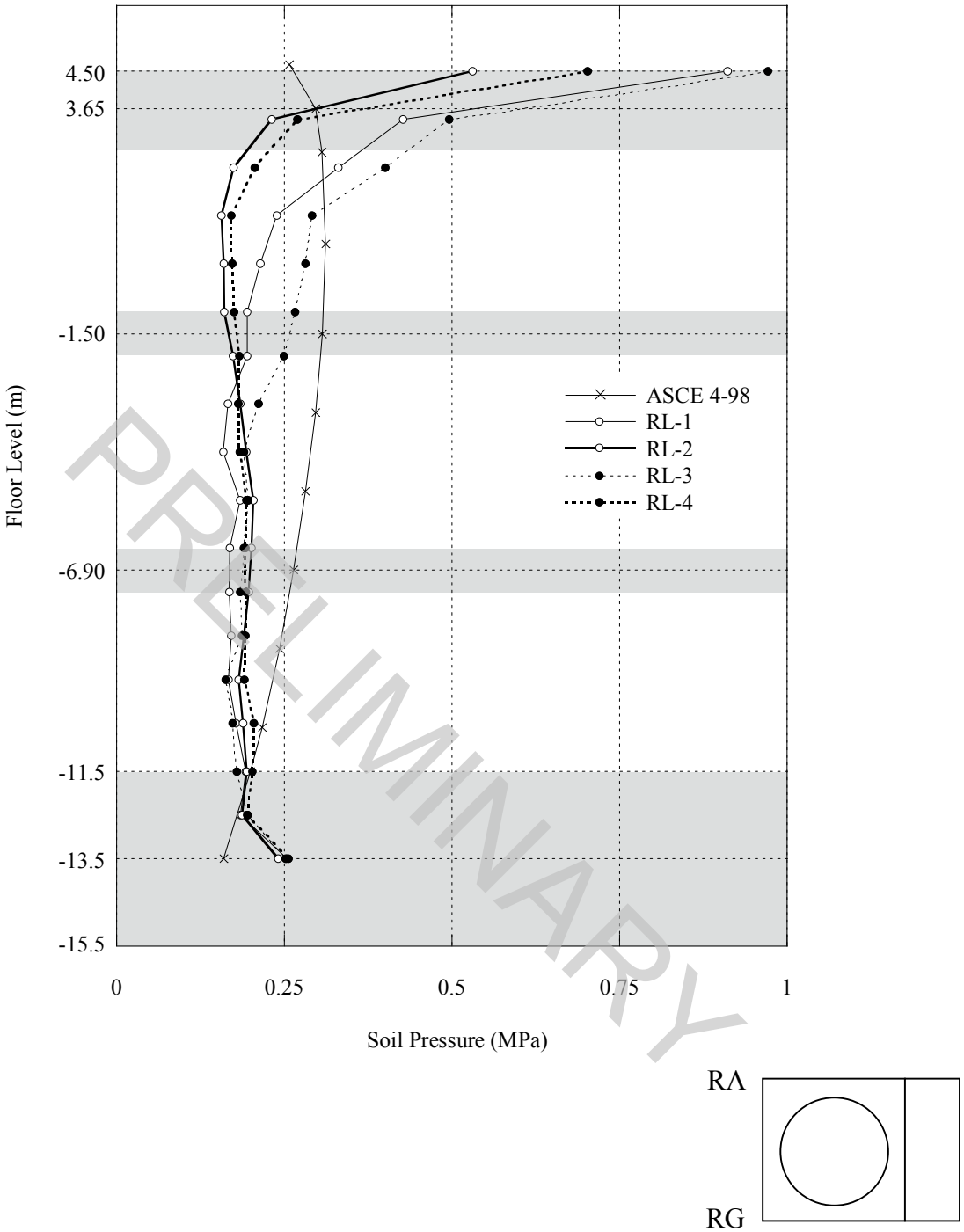

Note: The shaded area shows thickness of the floor slabs and basemat.

Figure 3A.8.8-2. Lateral Soil Pressure – RB/FB RA and RG Wall

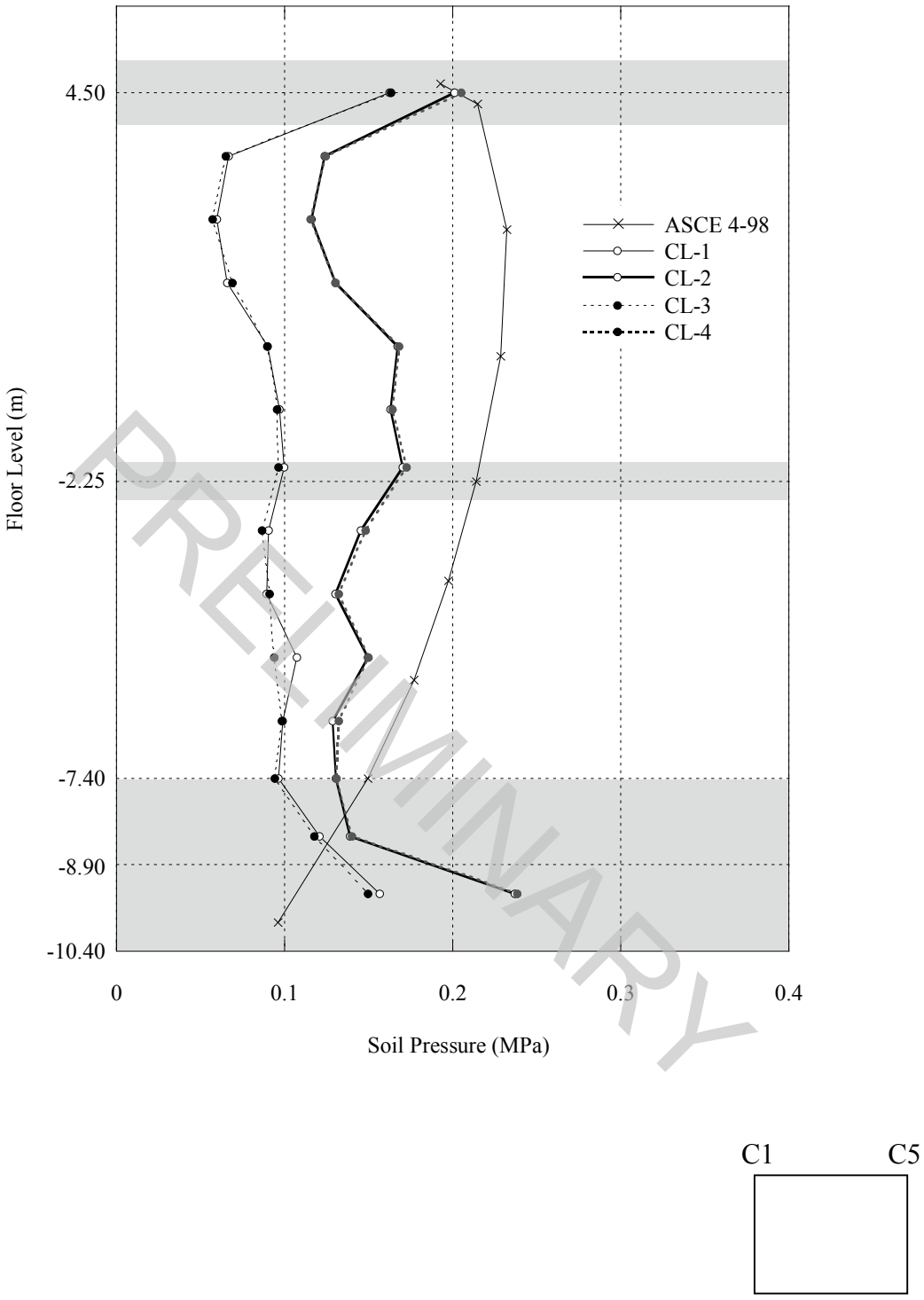

Note: The shaded area shows thickness of the floor slabs and basemat.

Figure 3A.8.8-3. Lateral Soil Pressure - CB C1 and C5 Wall

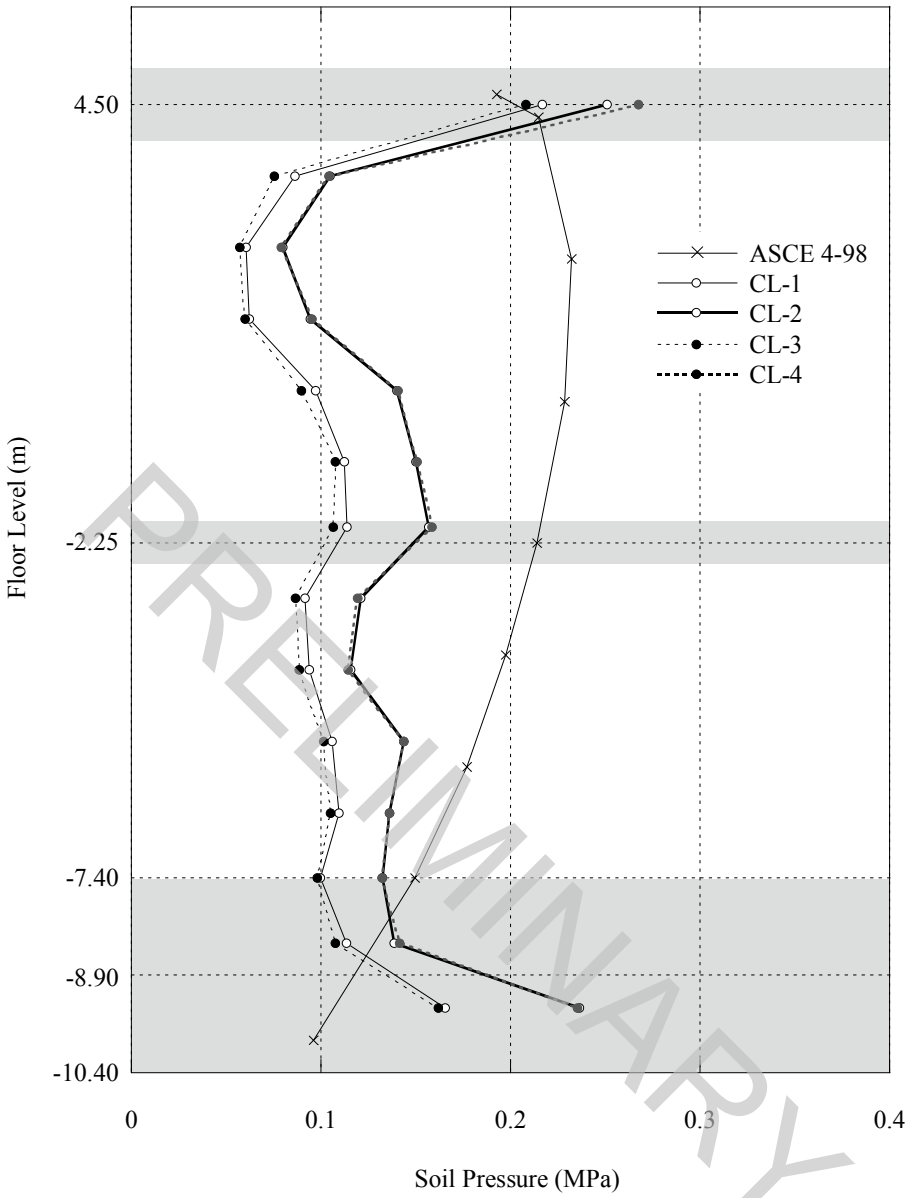

Note: The shaded area shows thickness of the floor slabs and basemat.

Figure 3A.8.8-4. Lateral Soil Pressure - CB CA and CD Wall

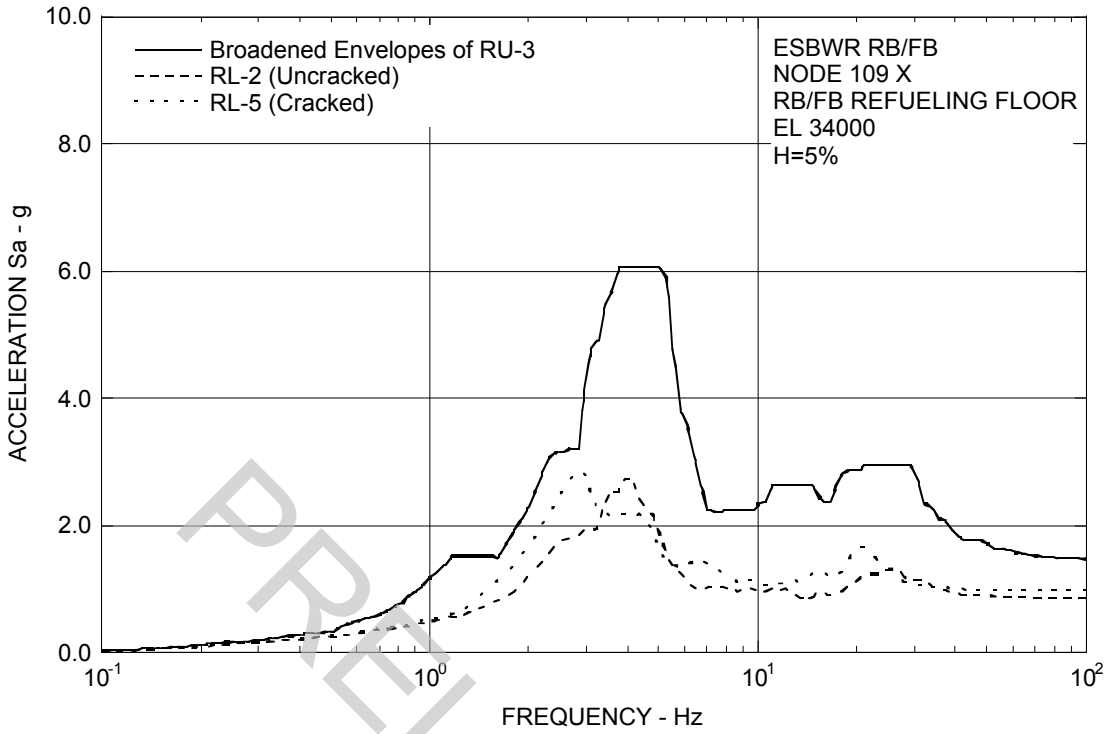

Figure 3A.8.9-1a. FRS (Effect of Concrete Cracking) – RB/FB Refueling Floor X

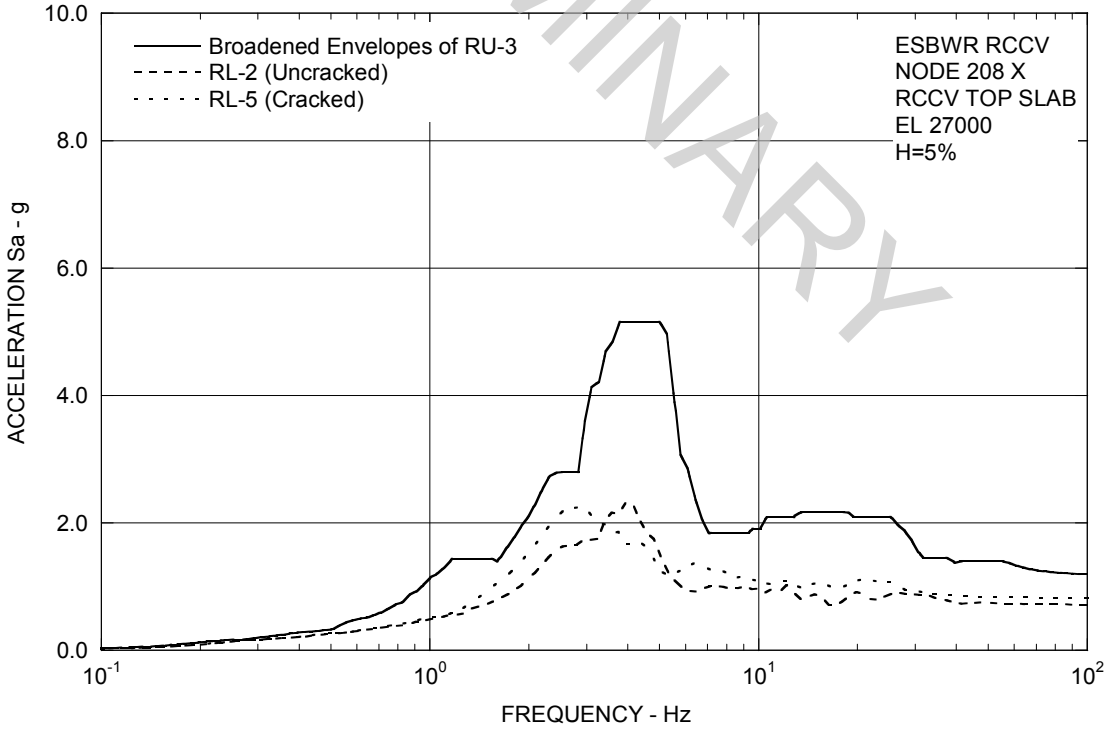

Figure 3A.8.9-1b. FRS (Effect of Concrete Cracking) – RCCV Top Slab X

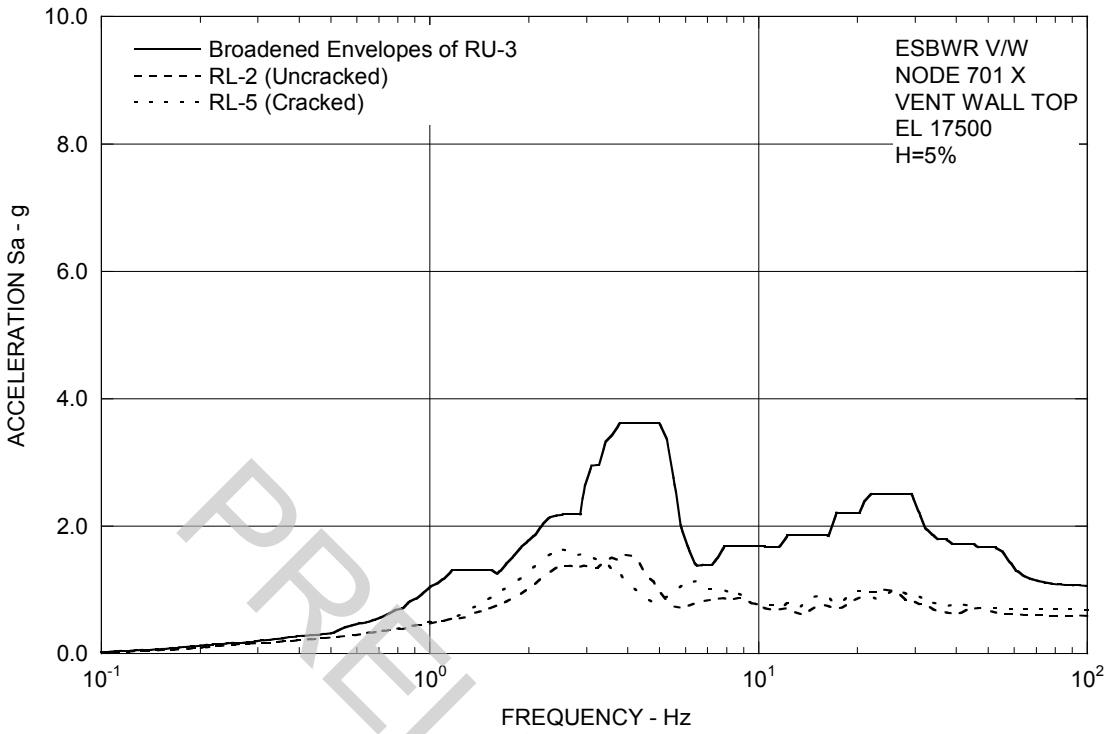

Figure 3A.8.9-1c. FRS (Effect of Concrete Cracking) – Vent Wall Top X

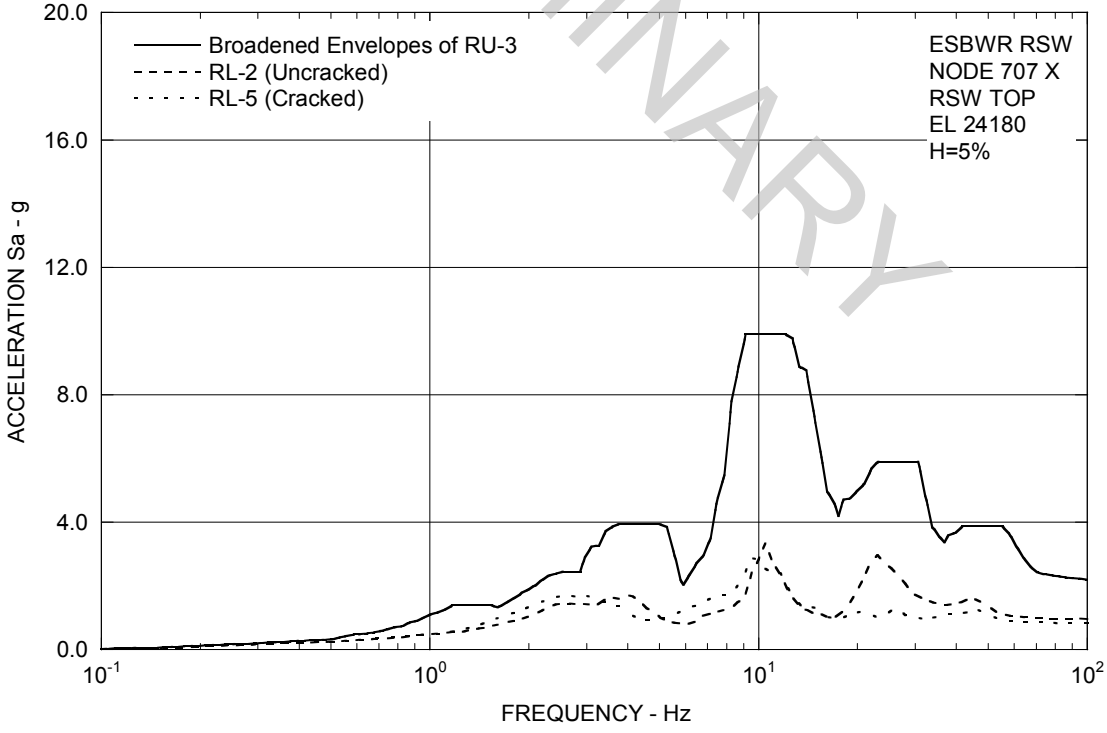

Figure 3A.8.9-1d. FRS (Effect of Concrete Cracking) – RSW Top X

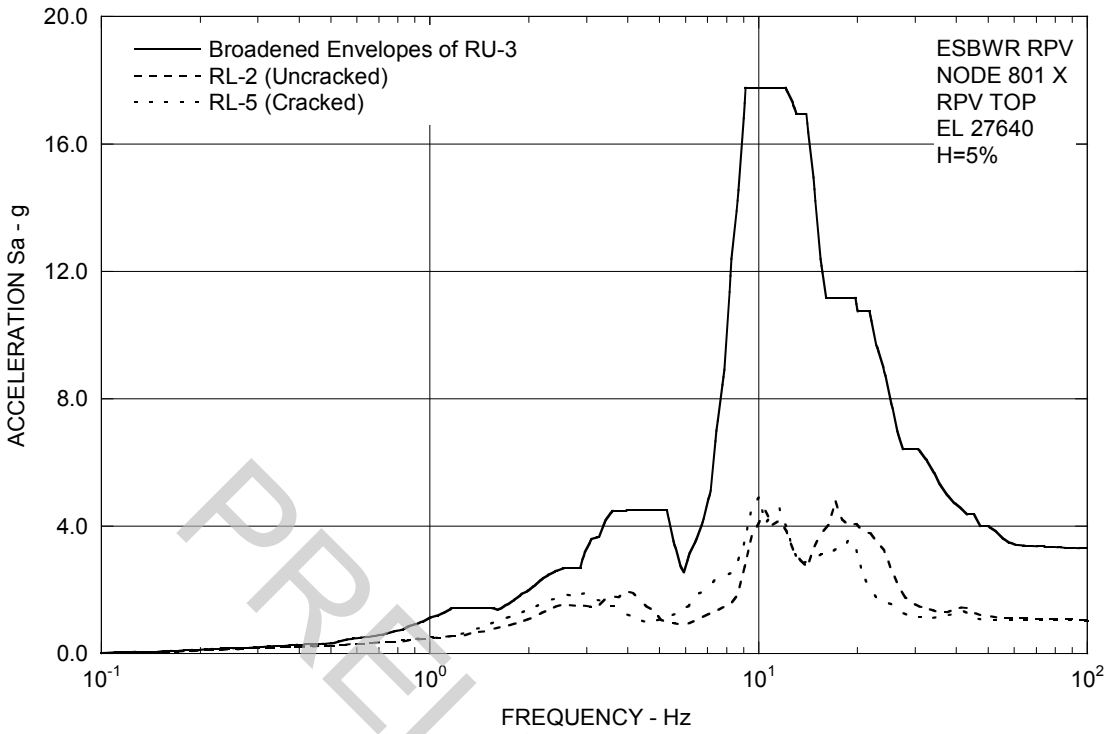

Figure 3A.8.9-1e. FRS (Effect of Concrete Cracking) – RPV Top X

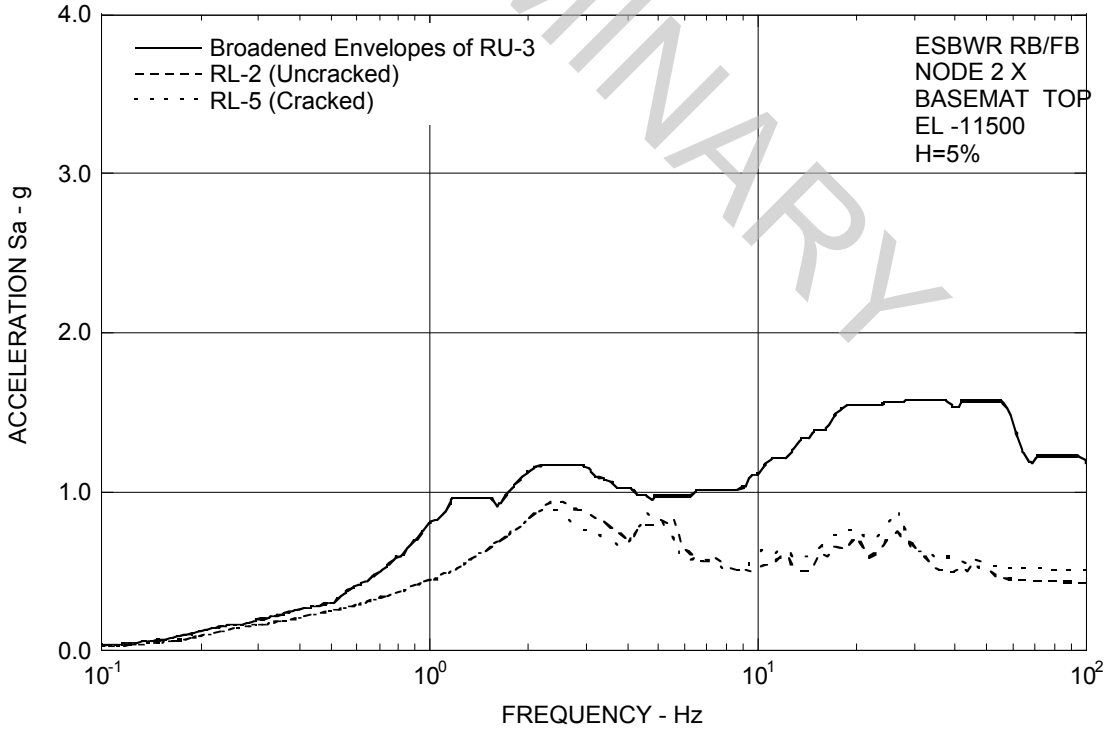

Figure 3A.8.9-1f. FRS (Effect of Concrete Cracking) – RB/FB Basemat X

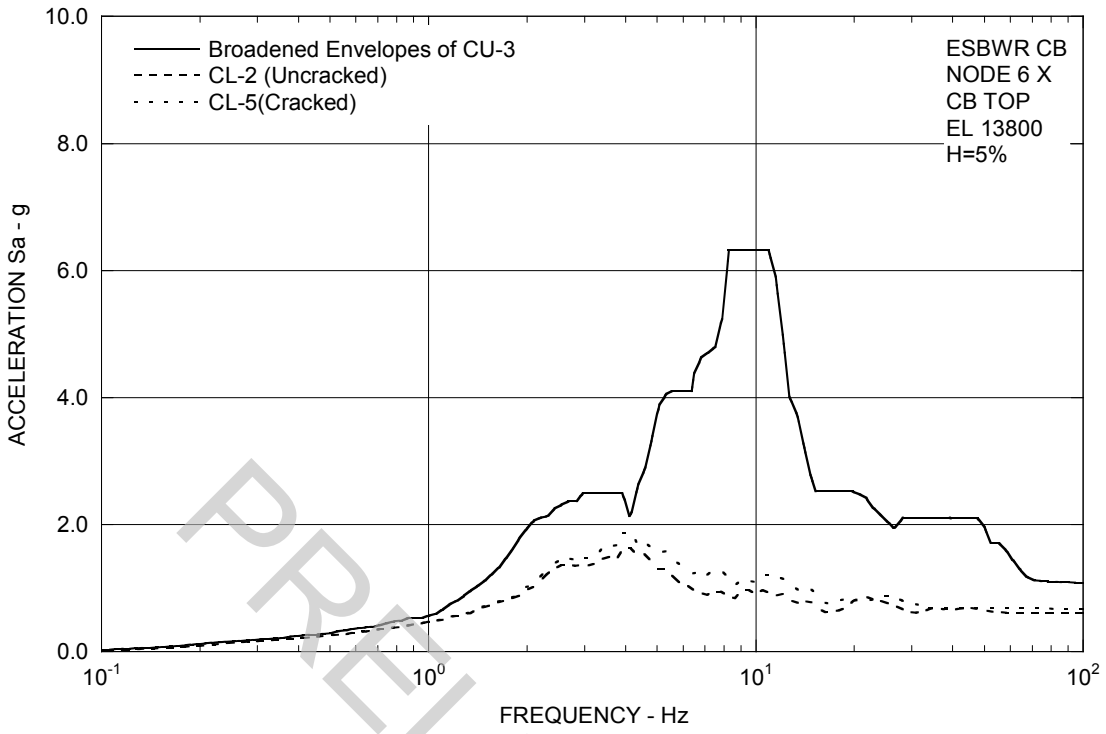

Figure 3A.8.9-1g. FRS (Effect of Concrete Cracking) – CB Top X

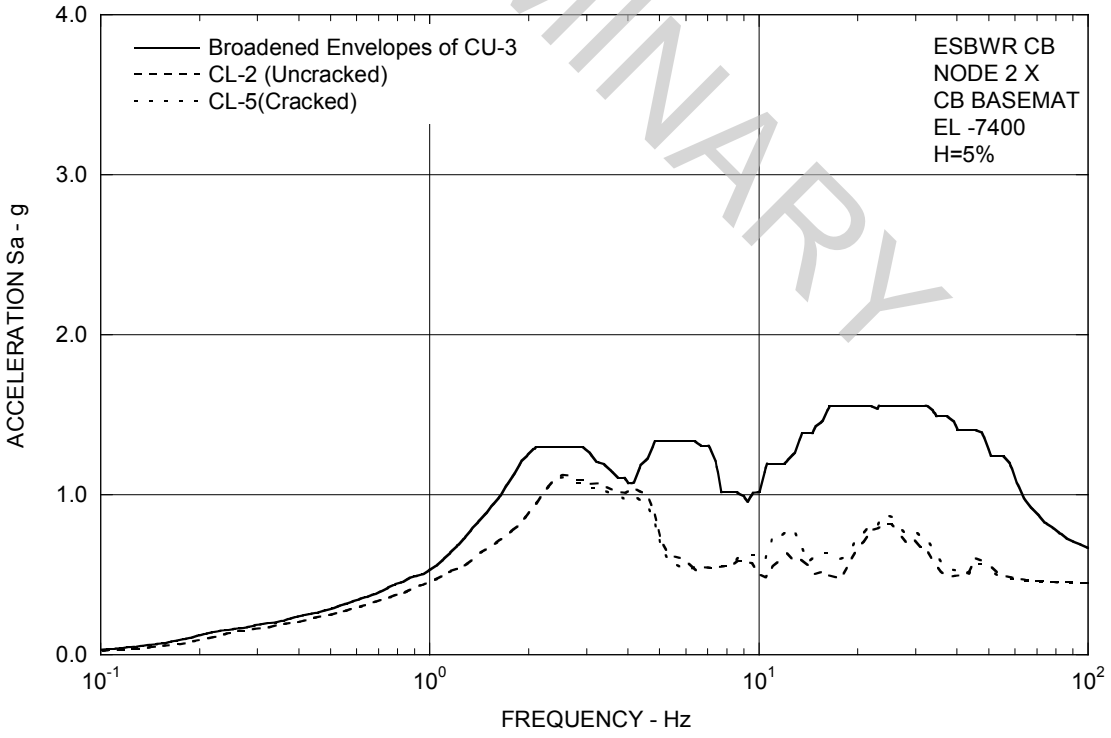

Figure 3A.8.9-1h. FRS (Effect of Concrete Cracking) – CB Basemat X

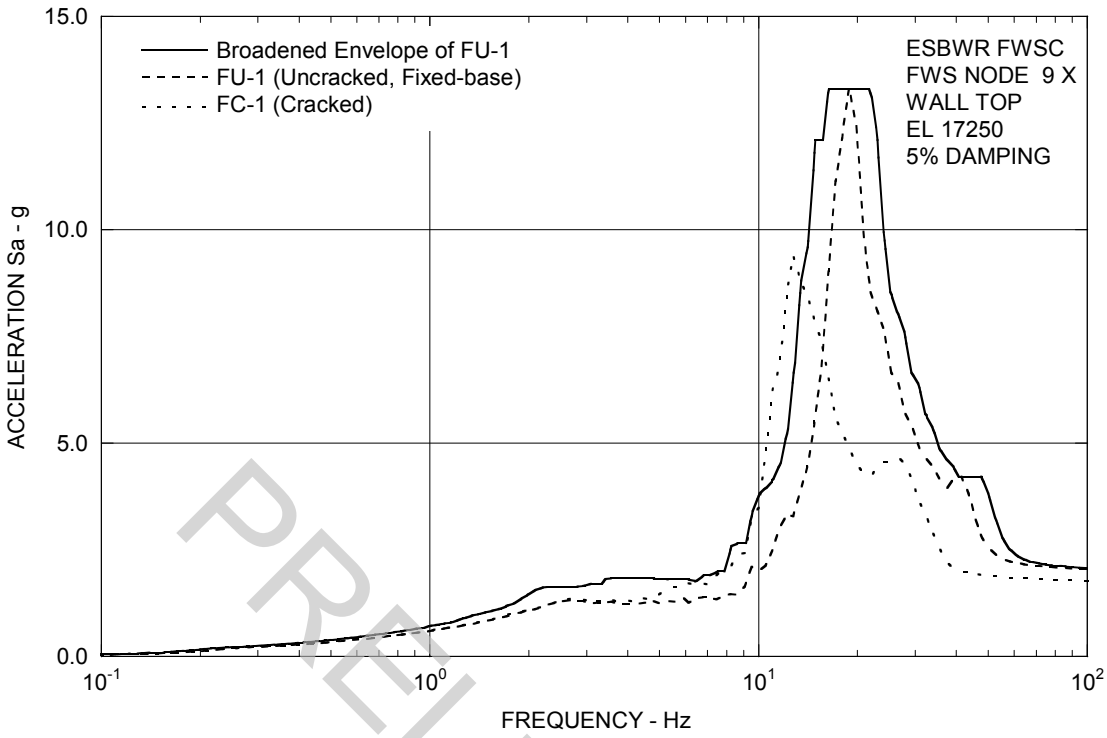

Figure 3A.8.9-1i. FRS (Effect of Concrete Cracking) – FWS Wall Top X

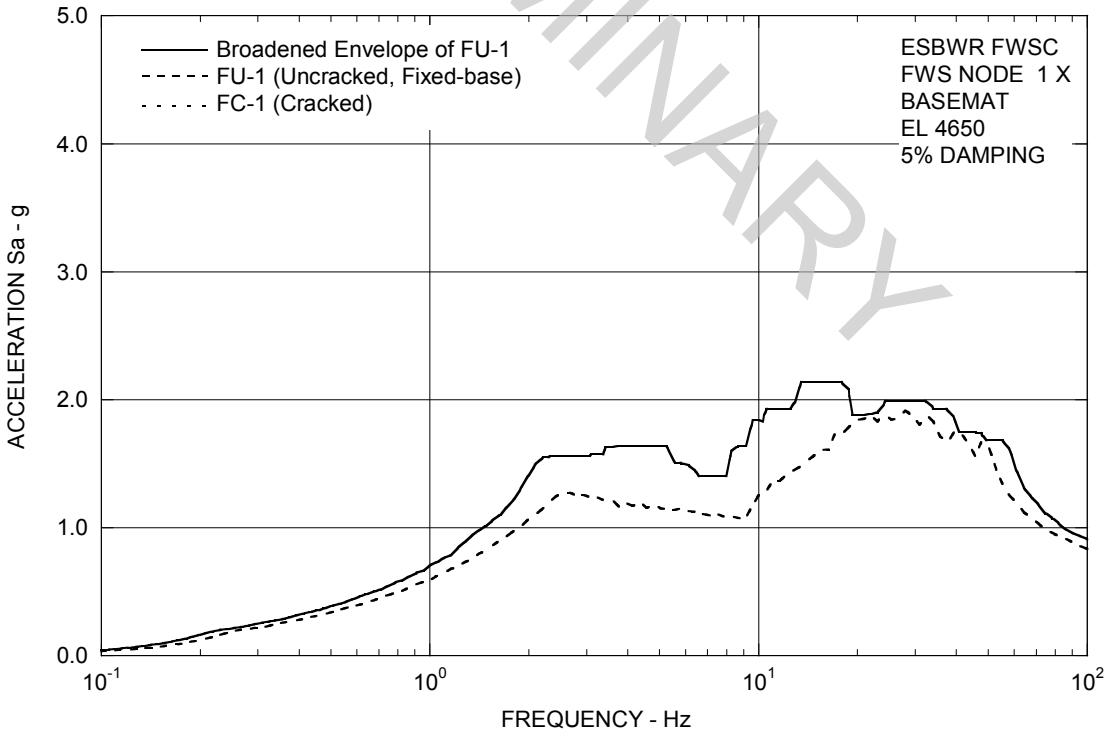

Figure 3A.8.9-1j. FRS (Effect of Concrete Cracking) – FWS Basemat X

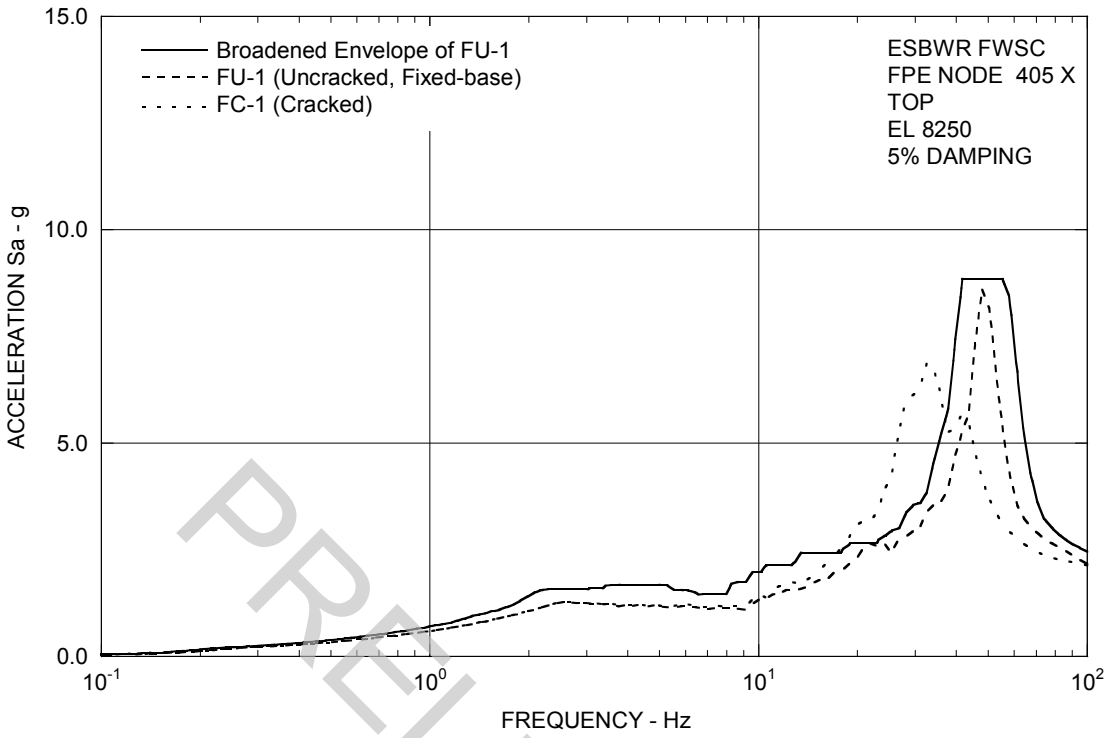

Figure 3A.8.9-1k. FRS (Effect of Concrete Cracking) – FPE Top X

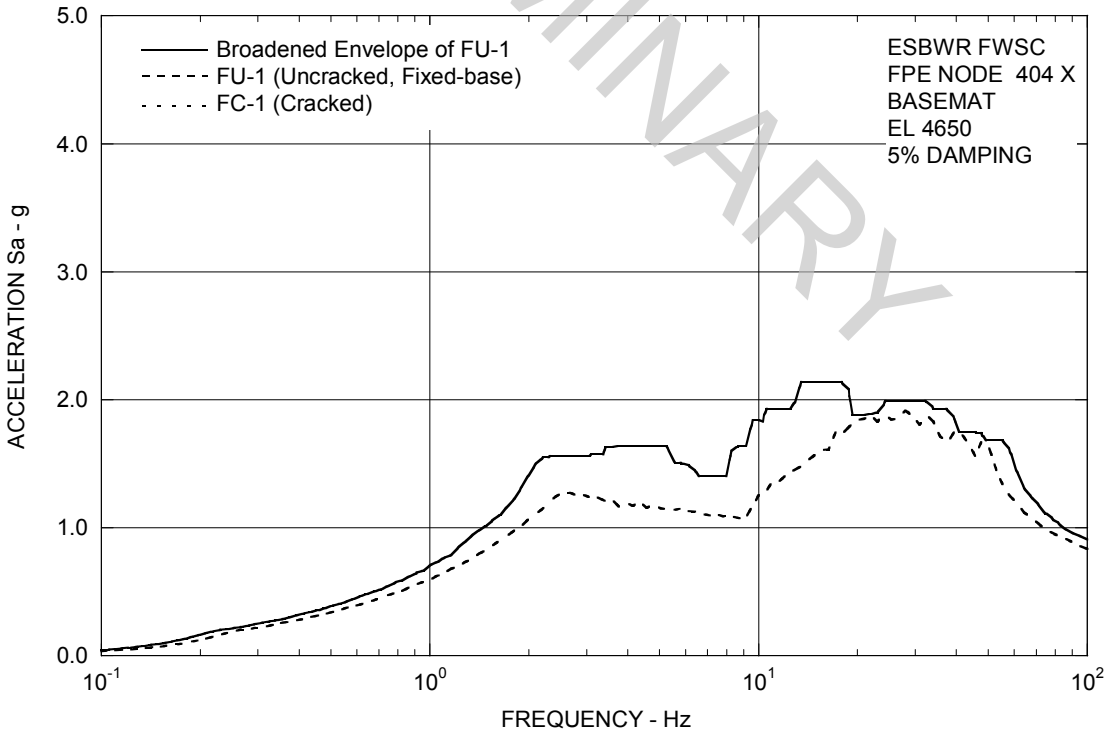

Figure 3A.8.9-1l. FRS (Effect of Concrete Cracking) – FPE Basemat X

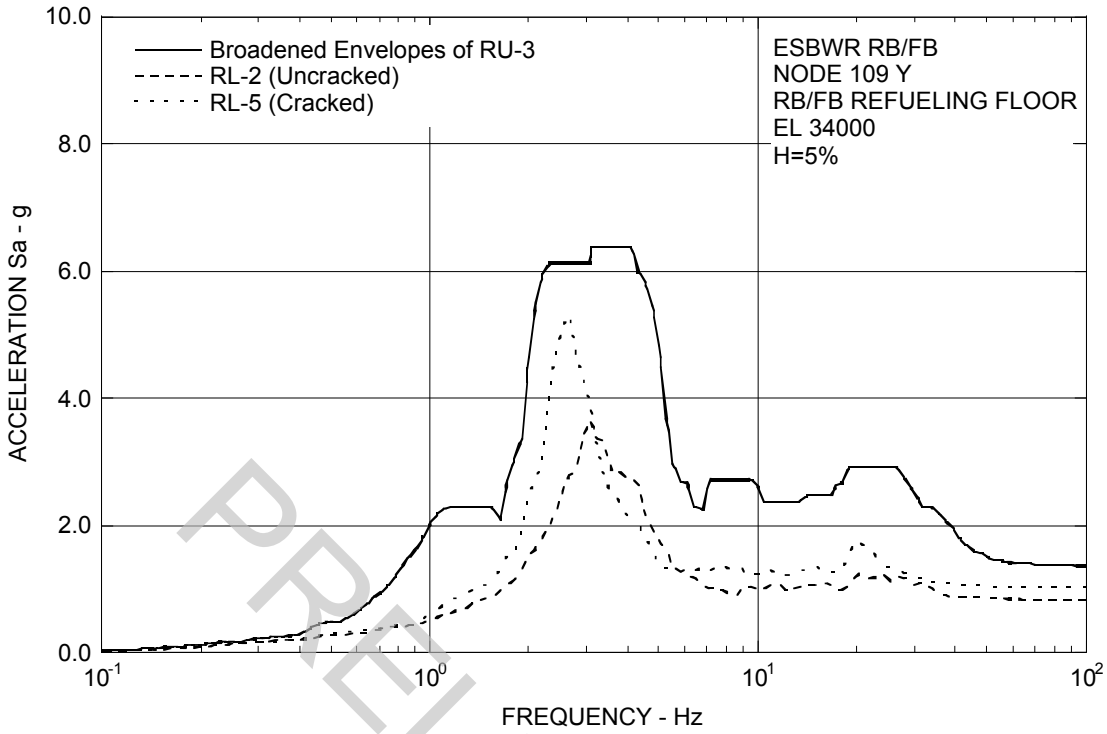

Figure 3A.8.9-2a. FRS (Effect of Concrete Cracking) – RB/FB Refueling Floor Y

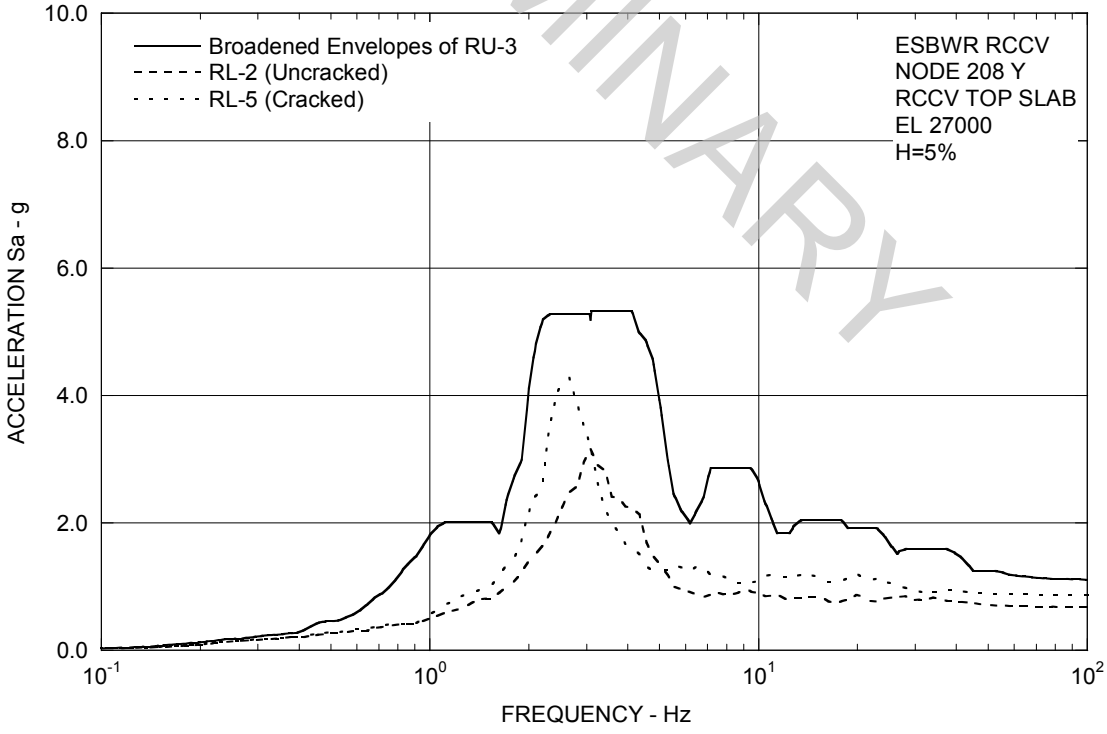

Figure 3A.8.9-2b. FRS (Effect of Concrete Cracking) – RCCV Top Slab Y

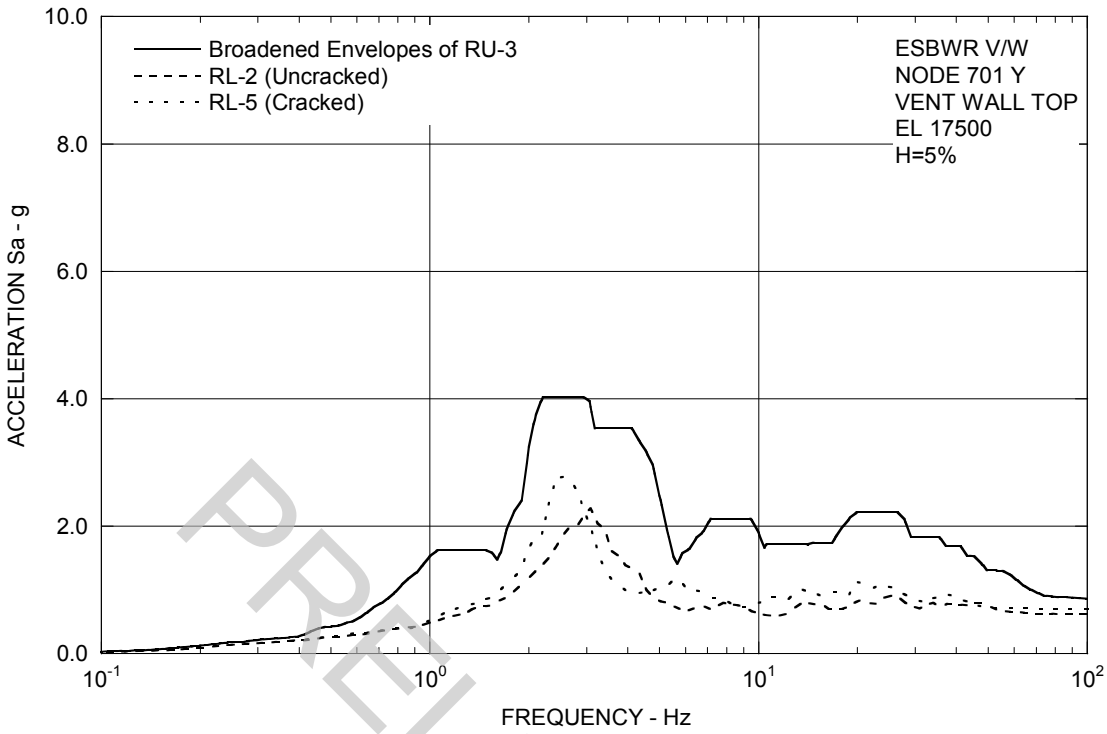

Figure 3A.8.9-2c. FRS (Effect of Concrete Cracking) – Vent Wall Top Y

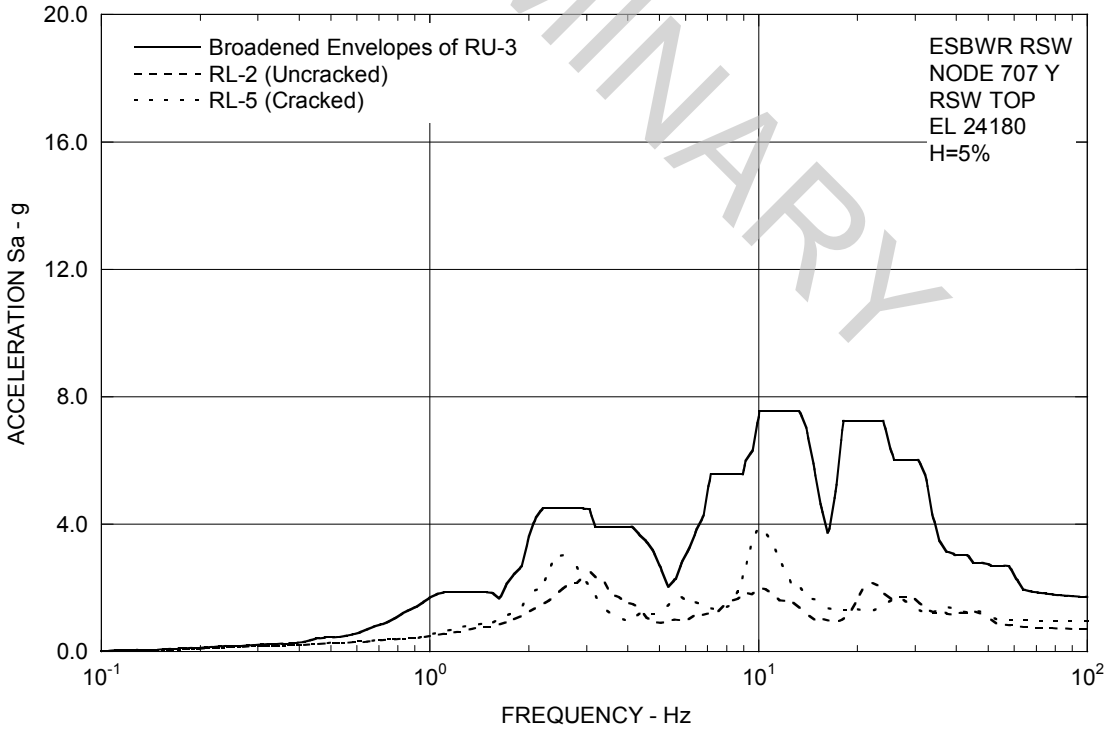

Figure 3A.8.9-2d. FRS (Effect of Concrete Cracking) – RSW Top Y

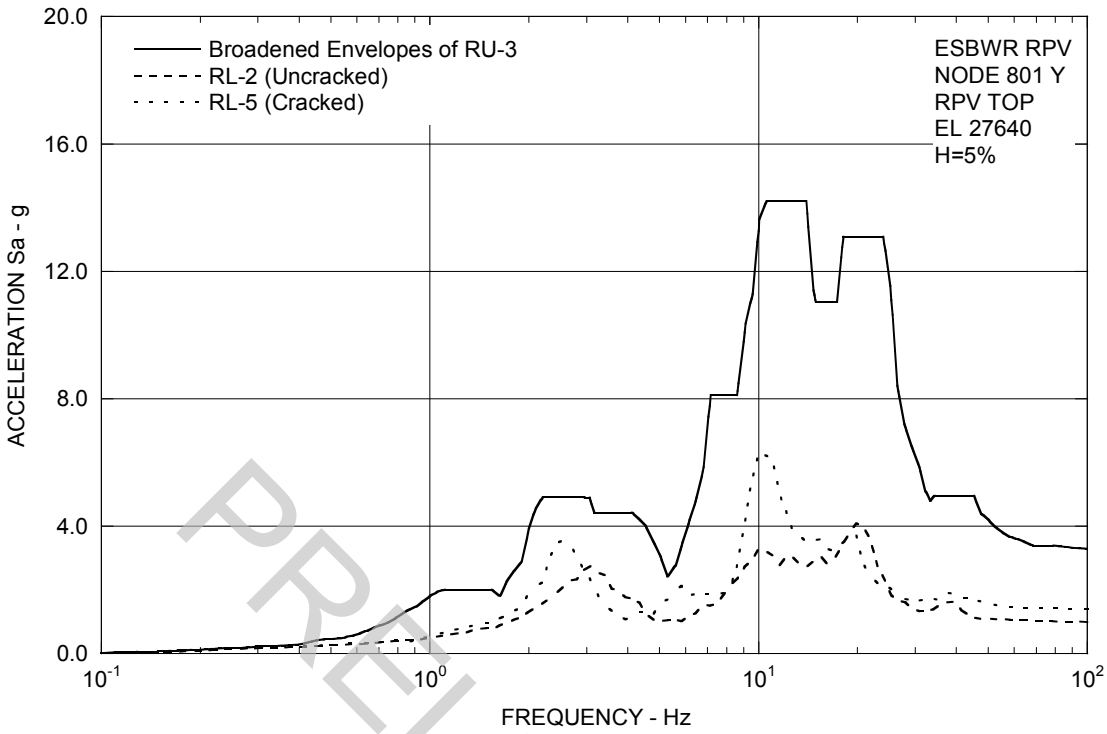

Figure 3A.8.9-2e. FRS (Effect of Concrete Cracking) – RPV Top Y

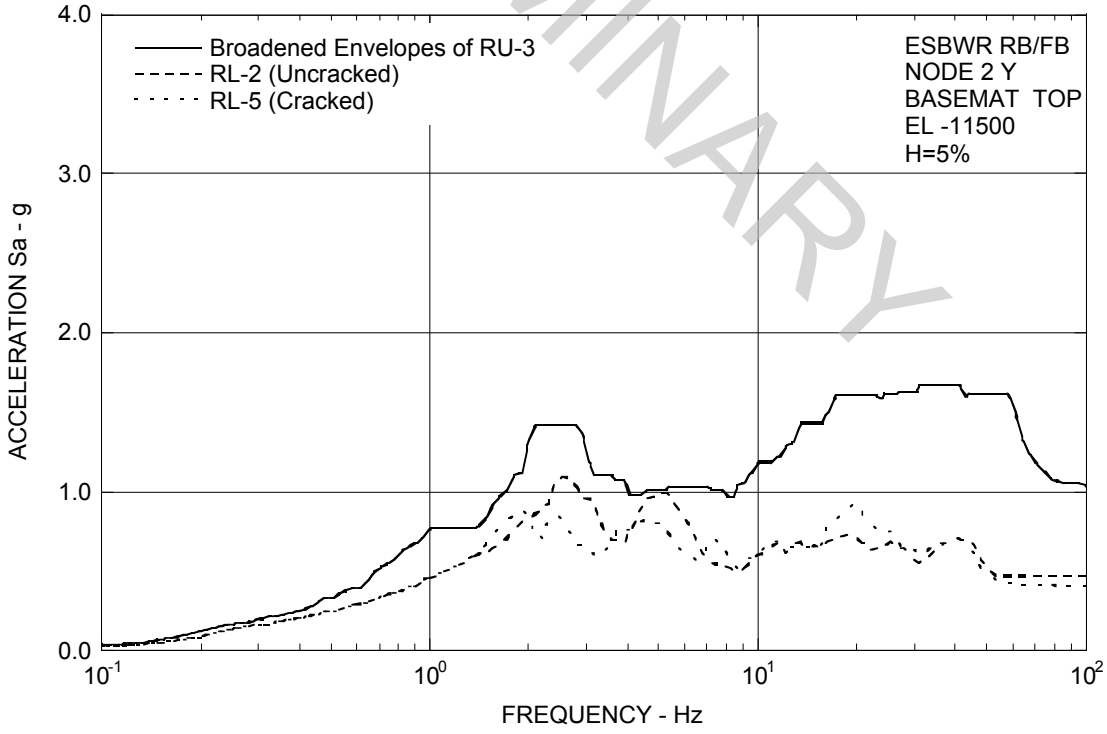

Figure 3A.8.9-2f. FRS (Effect of Concrete Cracking) – RB/FB Basemat Y

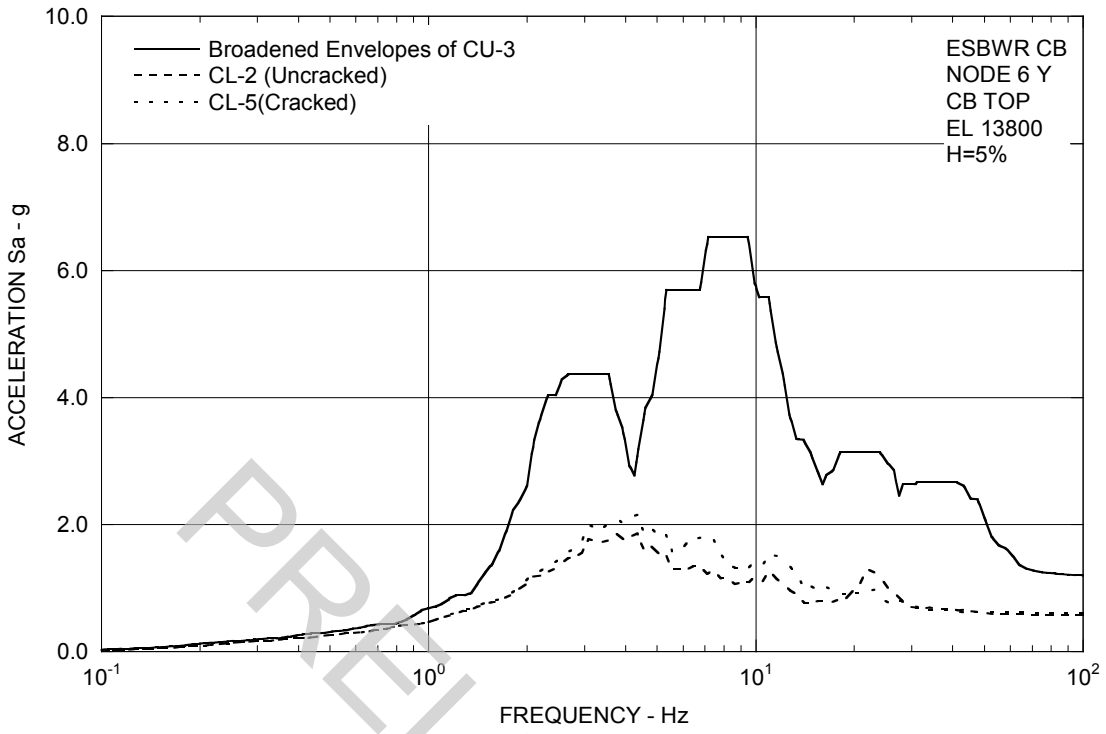

Figure 3A.8.9-2g. FRS (Effect of Concrete Cracking) – CB Top Y

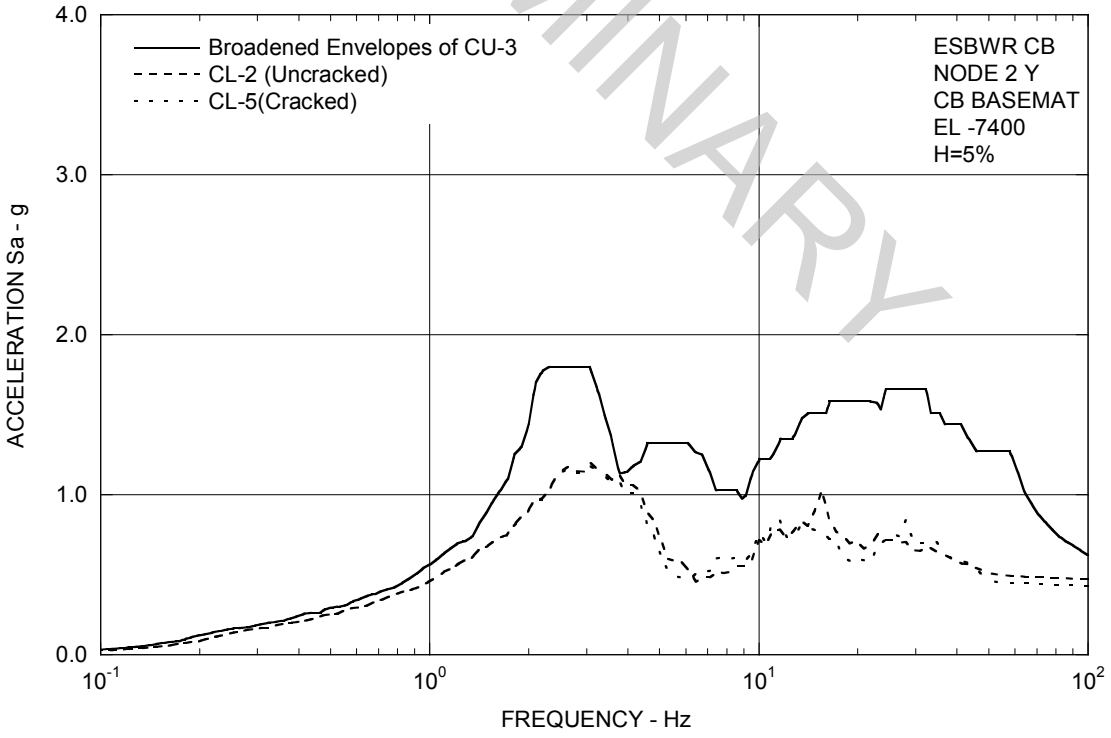

Figure 3A.8.9-2h. FRS (Effect of Concrete Cracking) – CB Basemat Y

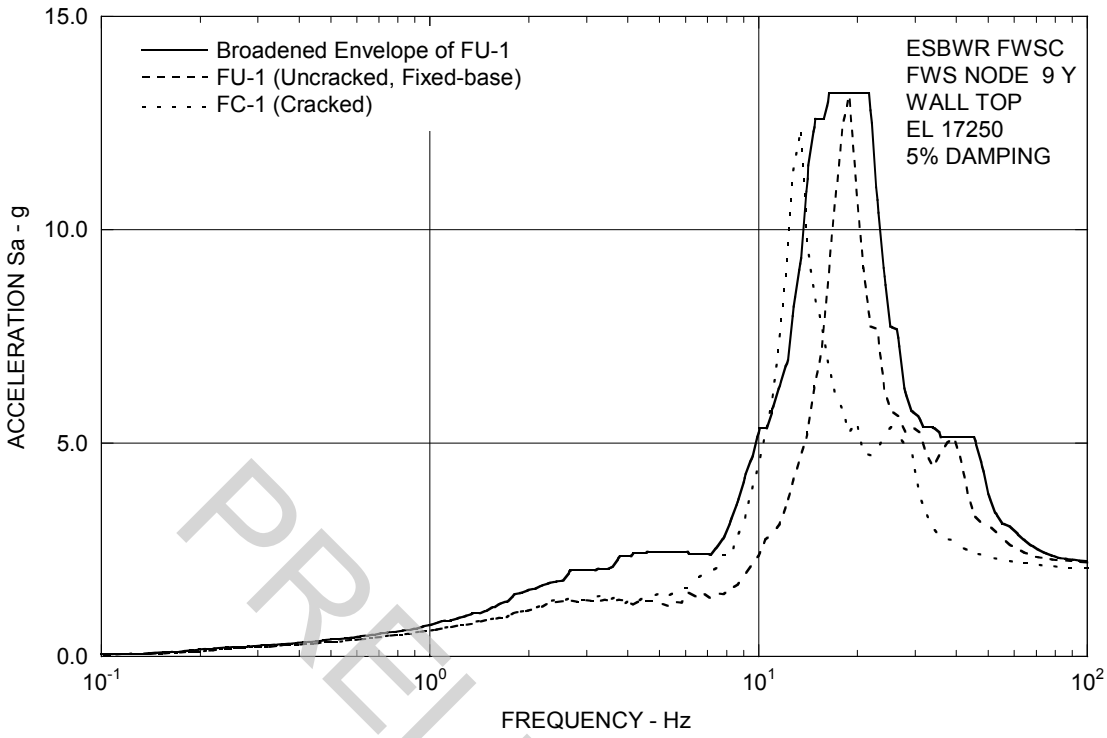

Figure 3A.8.9-2i. FRS (Effect of Concrete Cracking) – FWS Wall Top Y

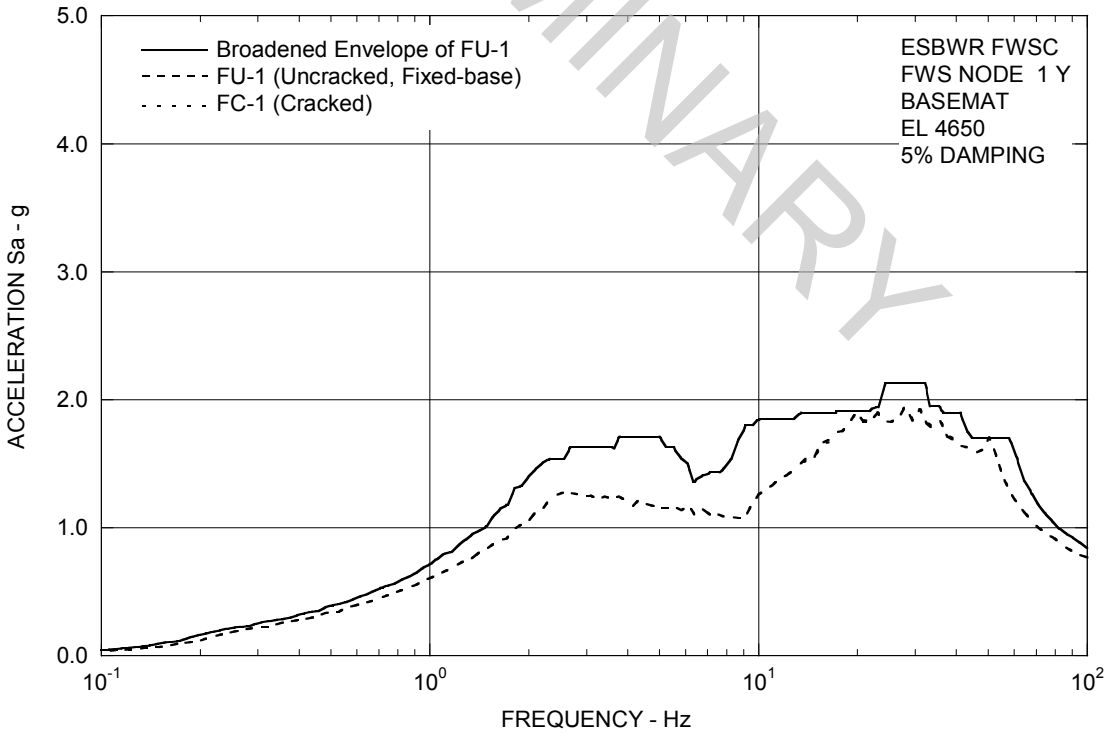

Figure 3A.8.9-2j. FRS (Effect of Concrete Cracking) – FWS Basemat Y

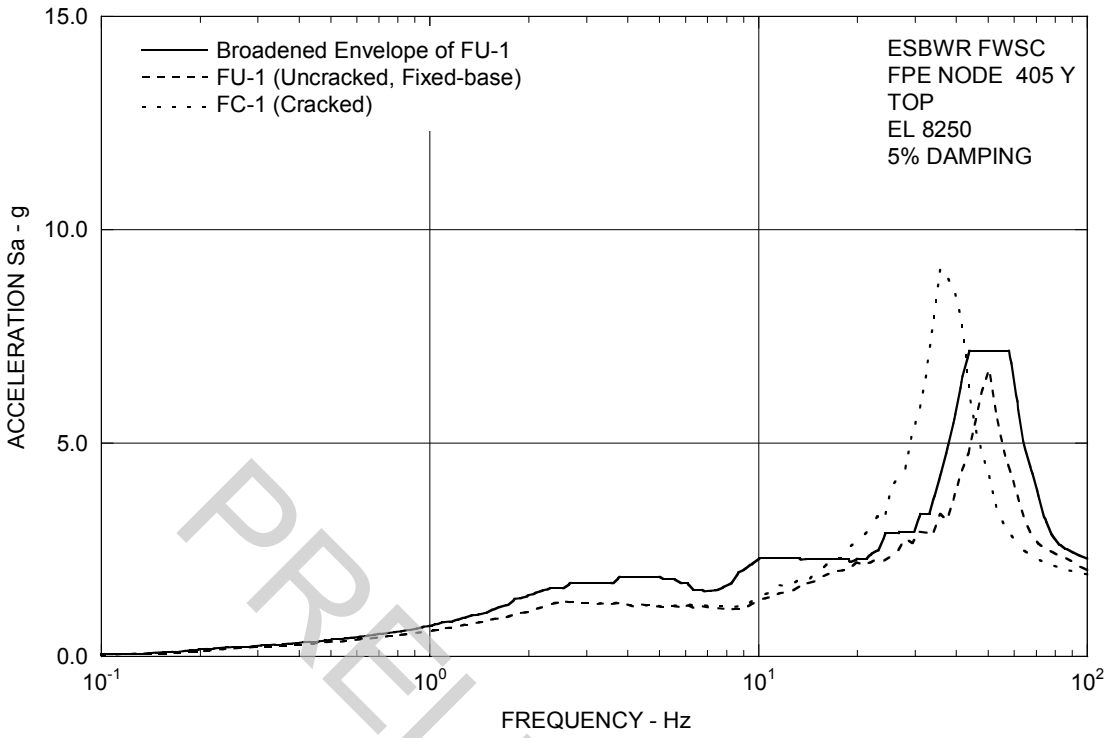

Figure 3A.8.9-2k. FRS (Effect of Concrete Cracking) – FPE Top Y

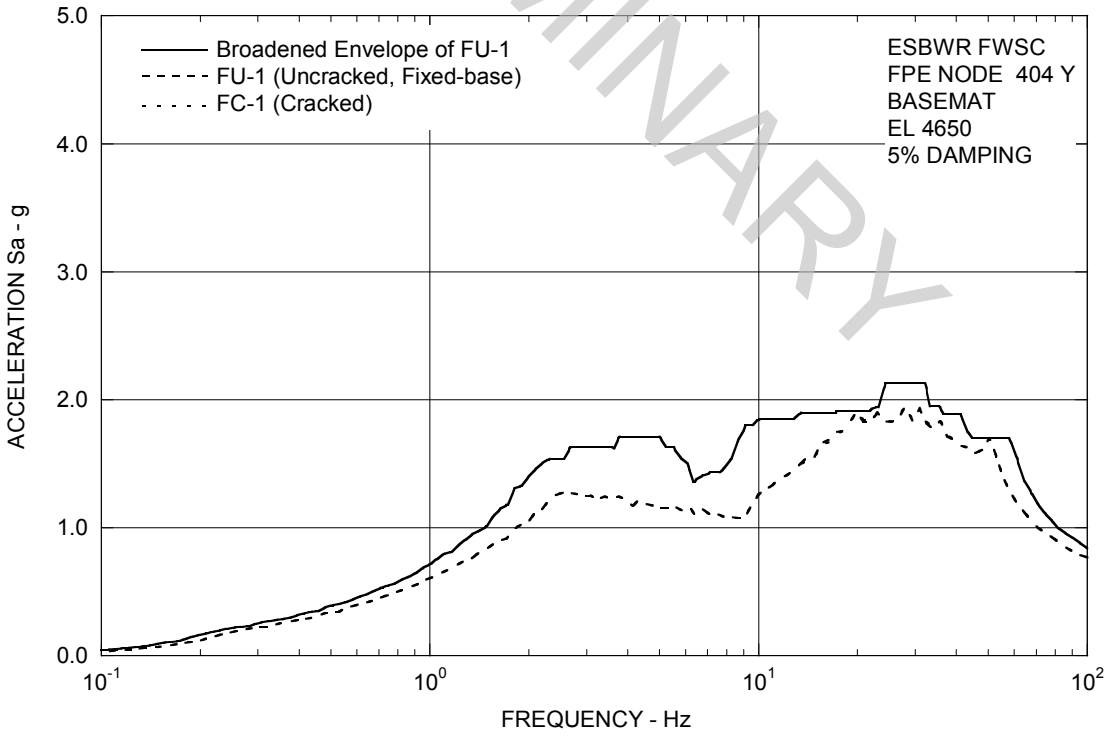

Figure 3A.8.9-2l. FRS (Effect of Concrete Cracking) – FPE Basemat Y

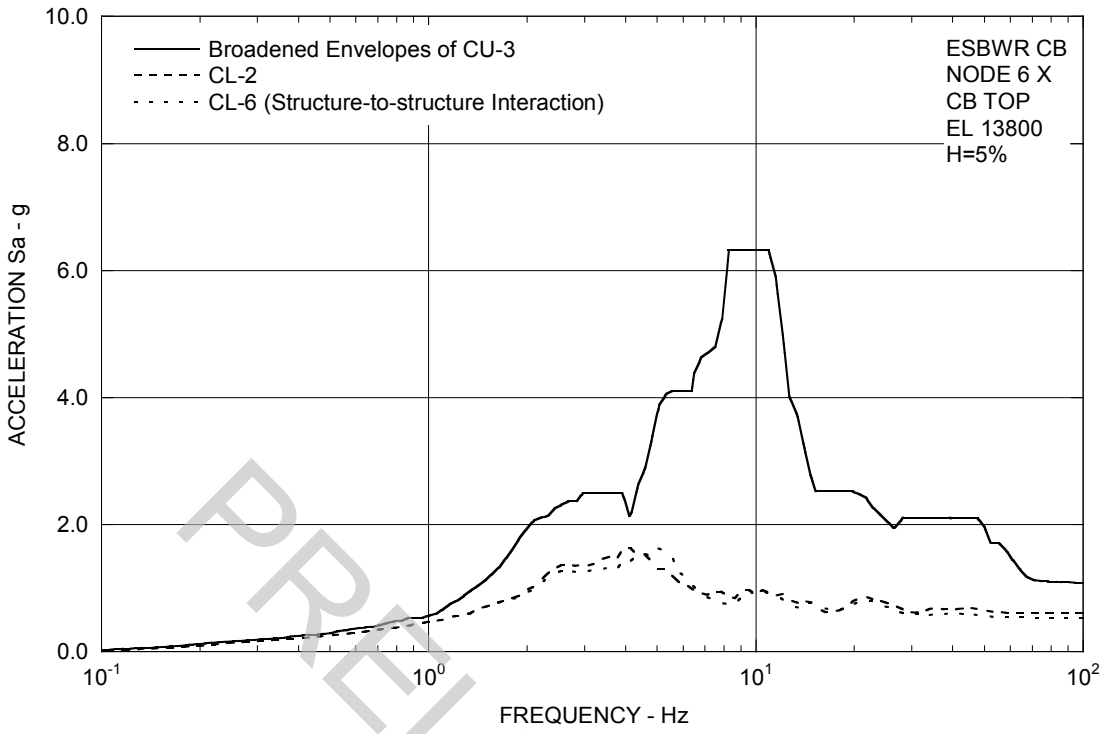

Figure 3A.8.11-1. FRS (Effect of Structure-Structure Interaction) – CB Top X

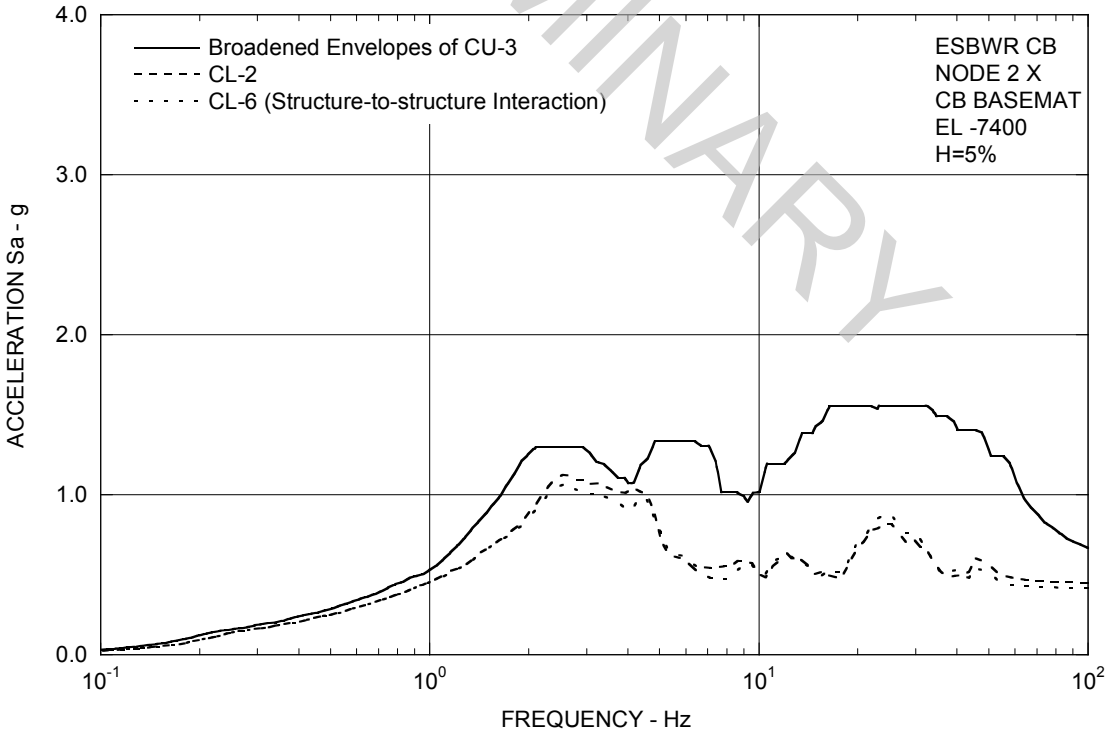

Figure 3A.8.11-2. FRS (Effect of Structure-Structure Interaction) – CB Basemat X

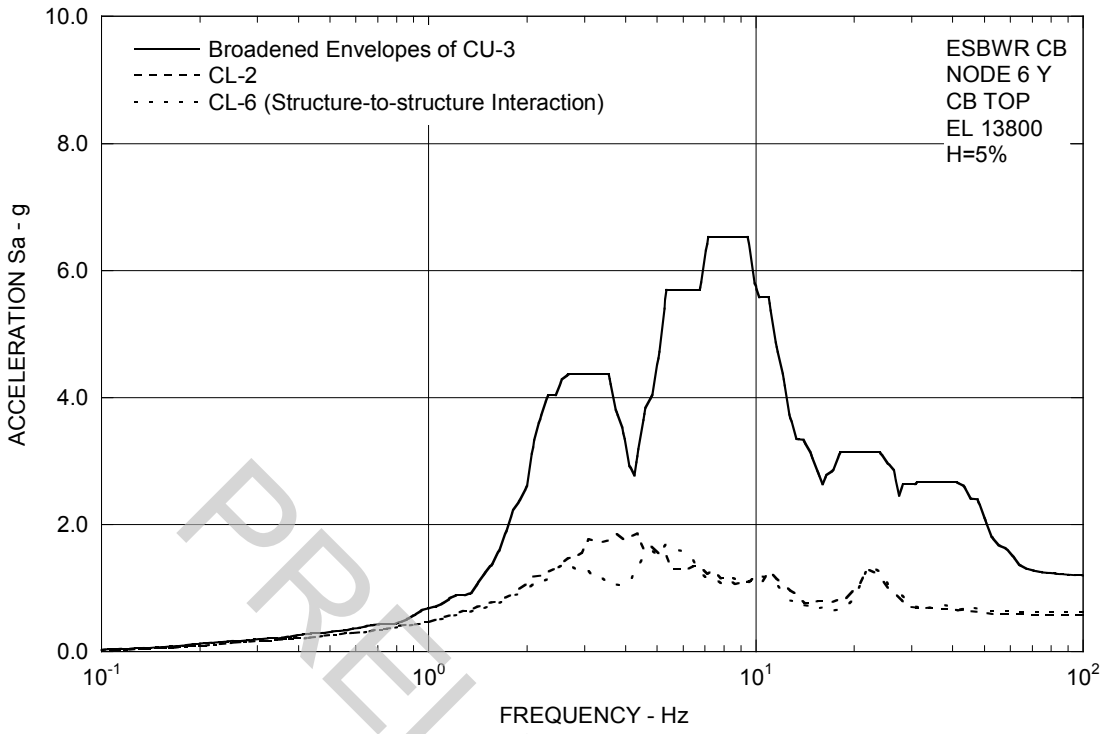

Figure 3A.8.11-3. FRS (Effect of Structure-Structure Interaction) – CB Top Y

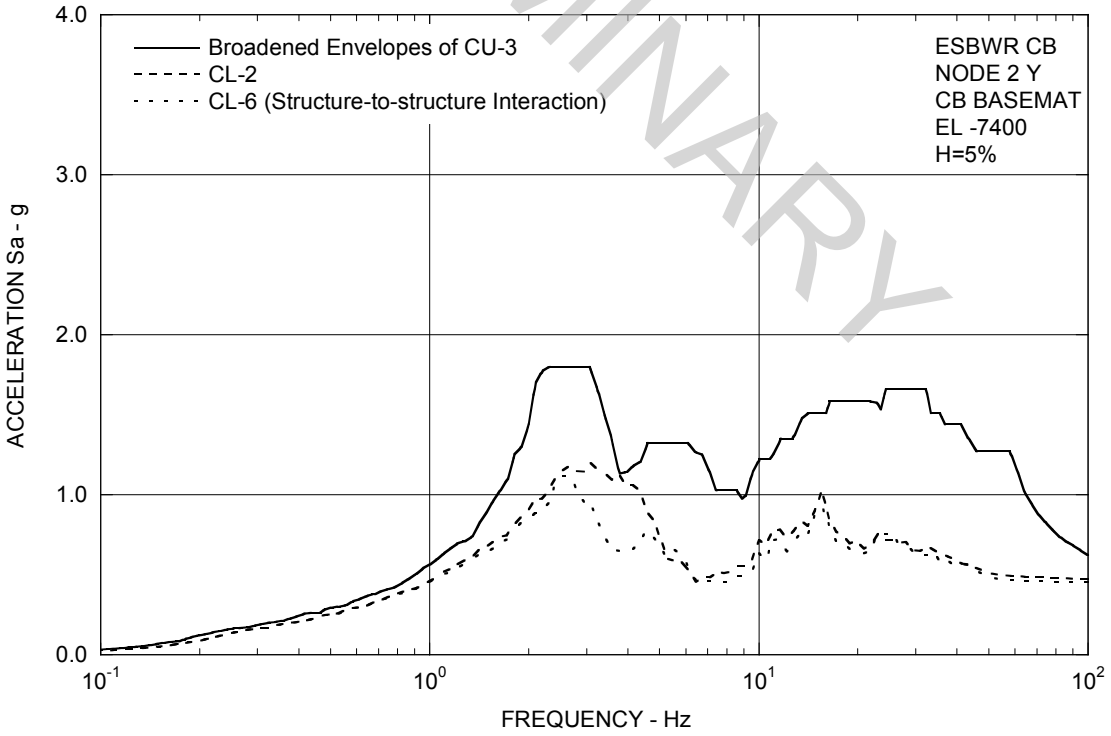

Figure 3A.8.11-4. FRS (Effect of Structure-Structure Interaction) – CB Basemat Y

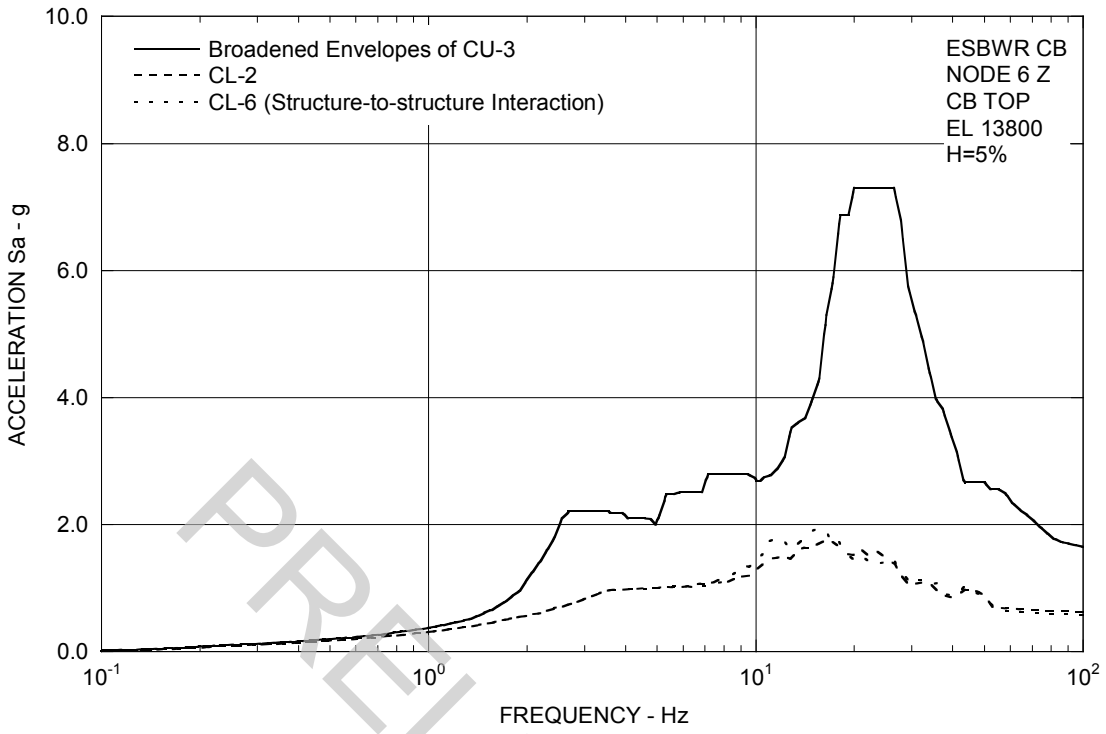

Figure 3A.8.11-5. FRS (Effect of Structure-Structure Interaction) – CB Top Z

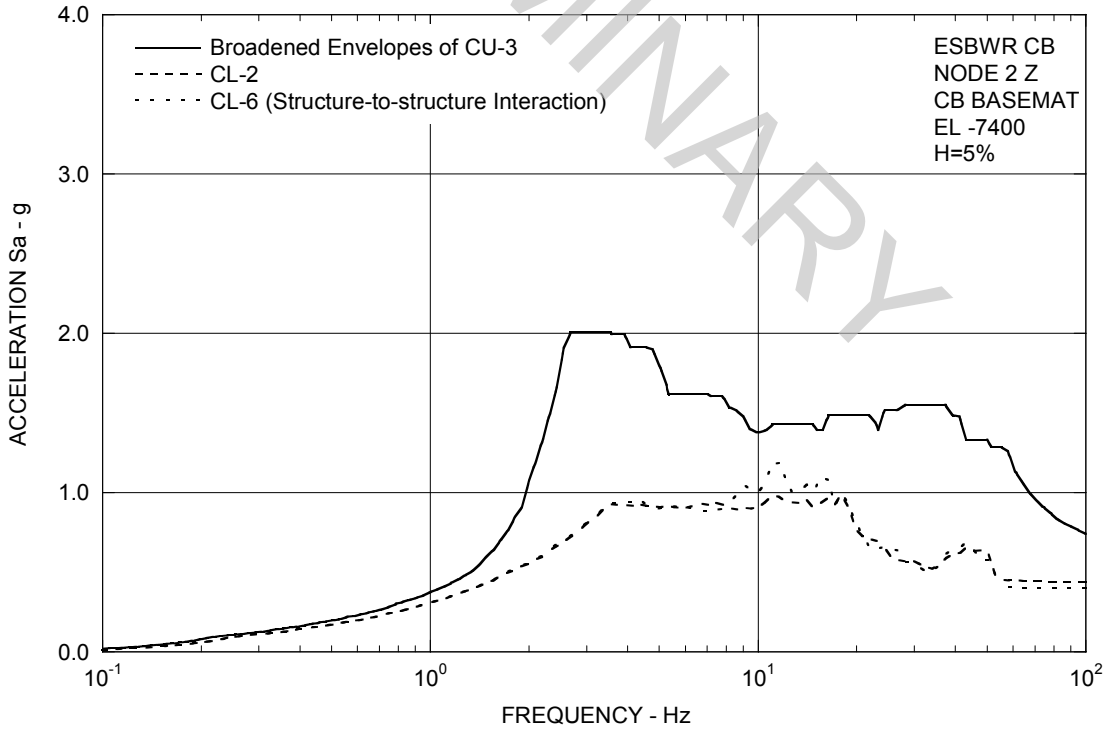

Figure 3A.8.11-6. FRS (Effect of Structure-Structure Interaction) – CB Basemat Z

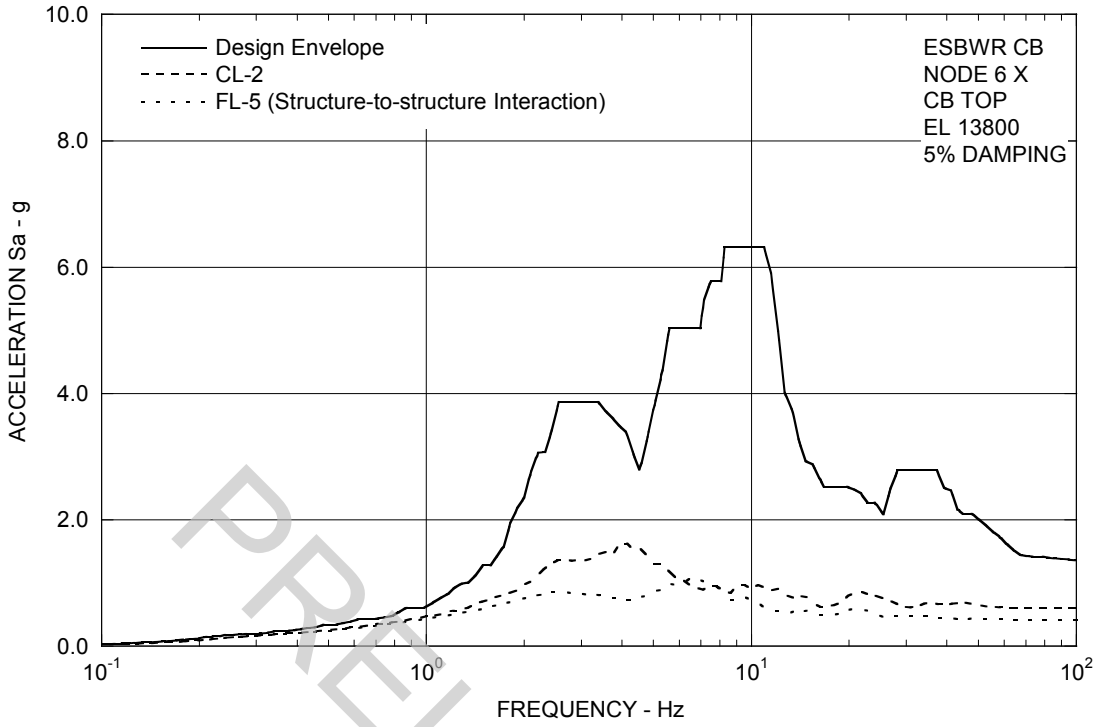

Figure 3A.8.11-7. FRS (Effect of Structure-Structure Interaction) – CB Top X

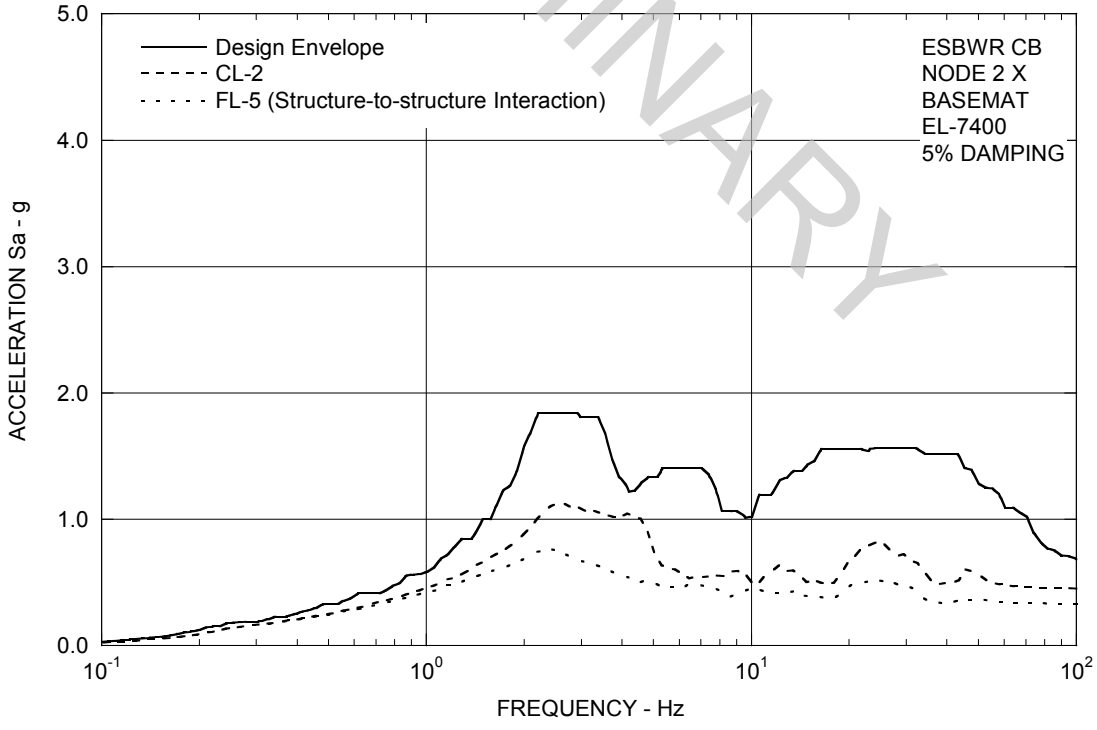

Figure 3A.8.11-8. FRS (Effect of Structure-Structure Interaction) – CB Basemat X

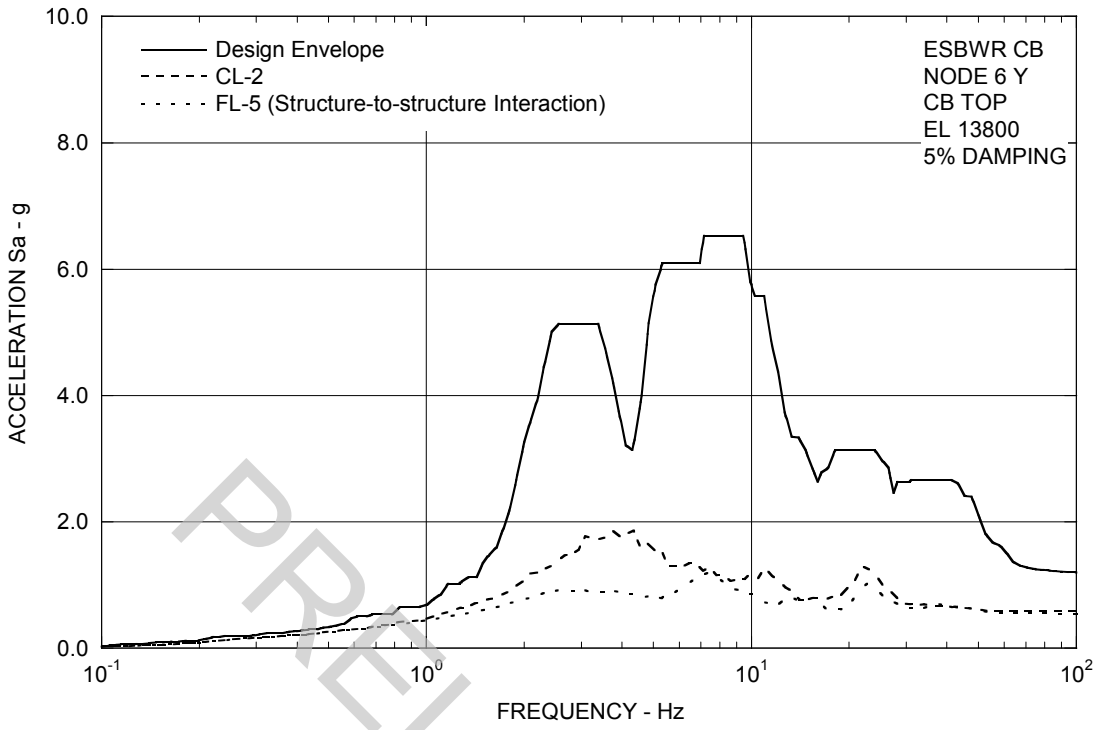

Figure 3A.8.11-9. FRS (Effect of Structure-Structure Interaction) – CB Top Y

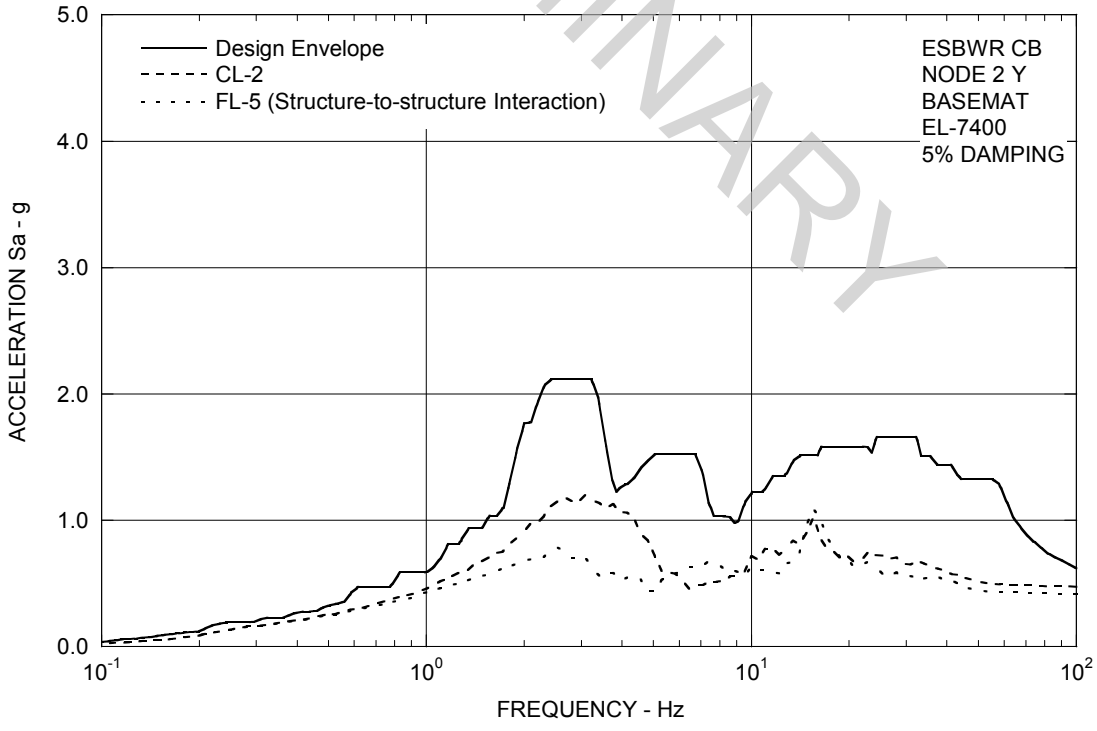

Figure 3A.8.11-10. FRS (Effect of Structure-Structure Interaction) – CB Basemat Y

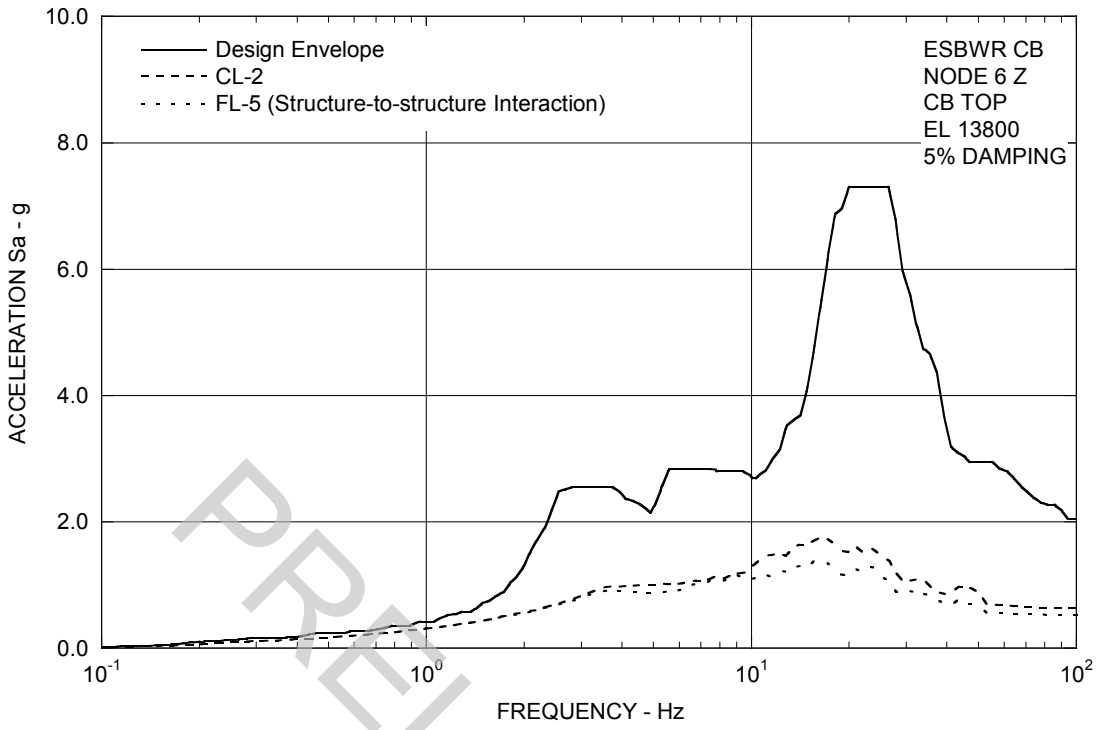

Figure 3A.8.11-11. FRS (Effect of Structure-Structure Interaction) – CB Top Z

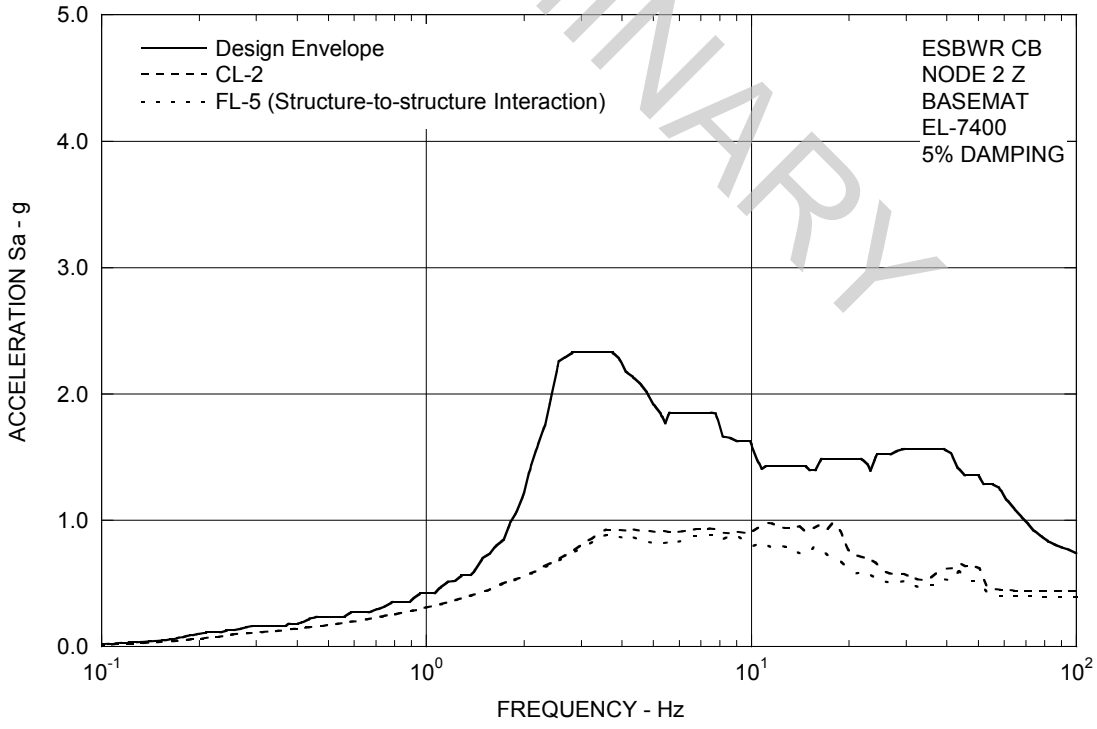

Figure 3A.8.11-12. FRS (Effect of Structure-Structure Interaction) – CB Basemat Z

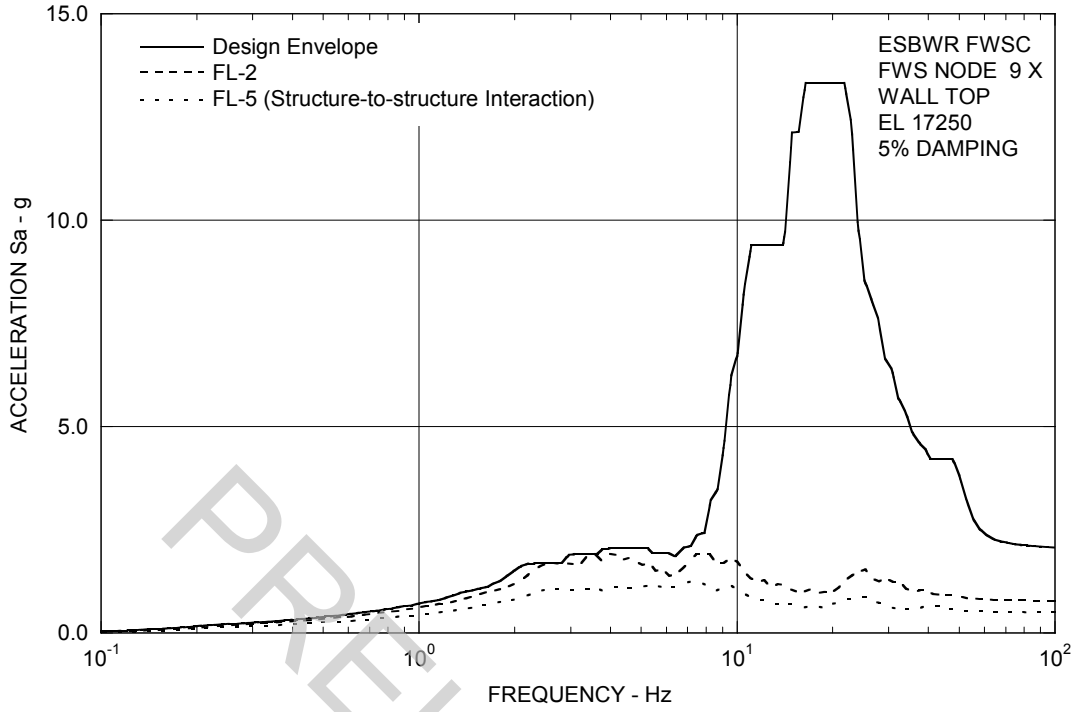

Figure 3A.8.11-13. FRS (Effect of Structure-Structure Interaction) – FWS Wall Top X

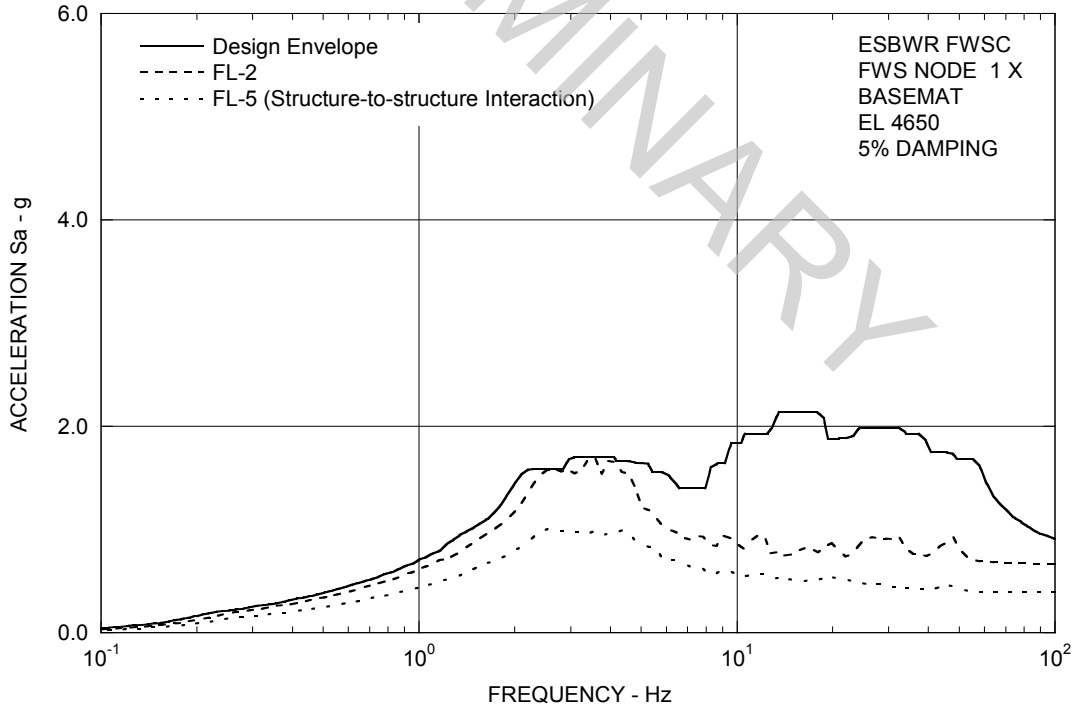

Figure 3A.8.11-14. FRS (Effect of Structure-Structure Interaction) – FWS Basemat X

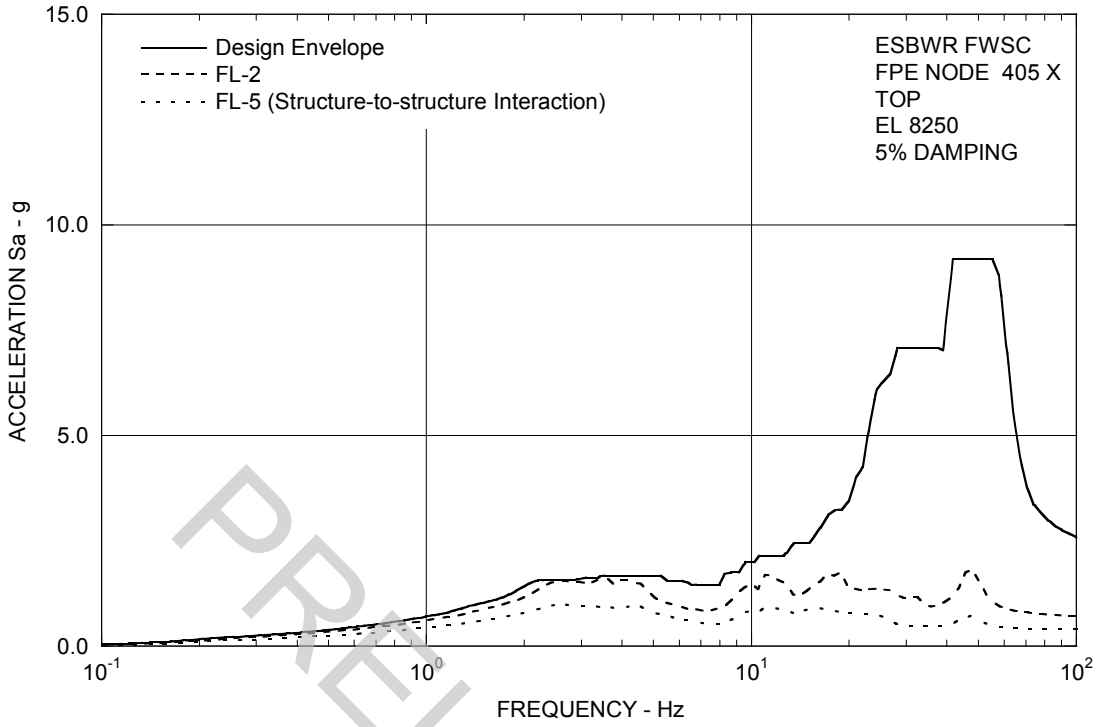

Figure 3A.8.11-15. FRS (Effect of Structure-Structure Interaction) – FPE Top X

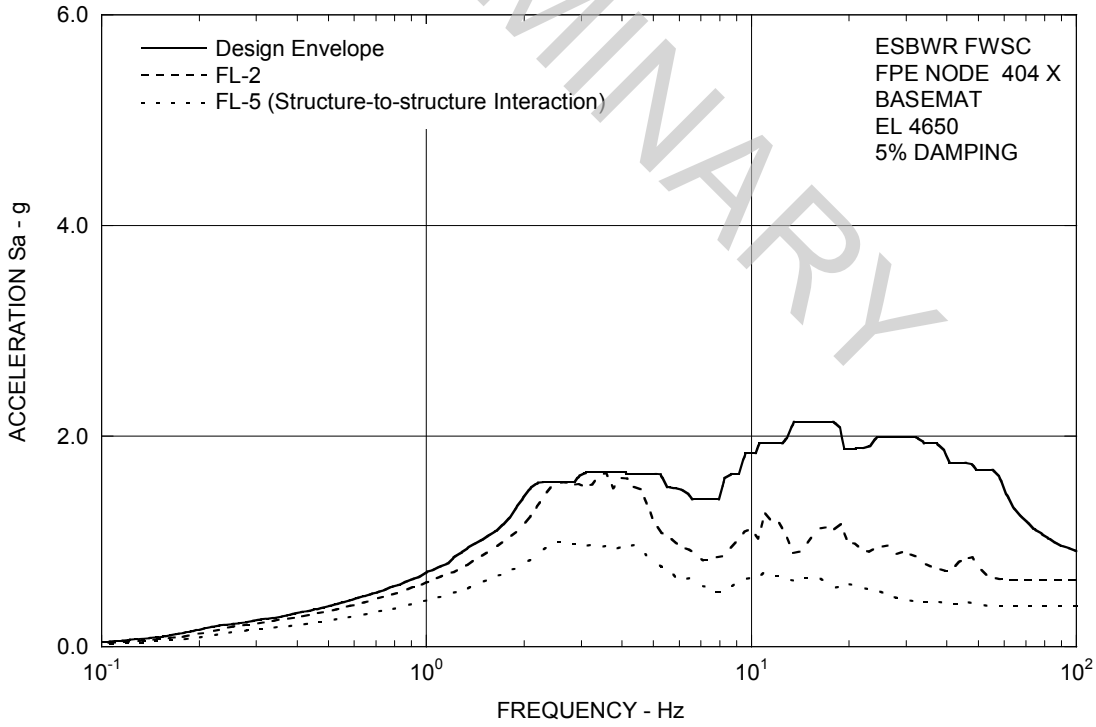

Figure 3A.8.11-16. FRS (Effect of Structure-Structure Interaction) – FPE Basemat X

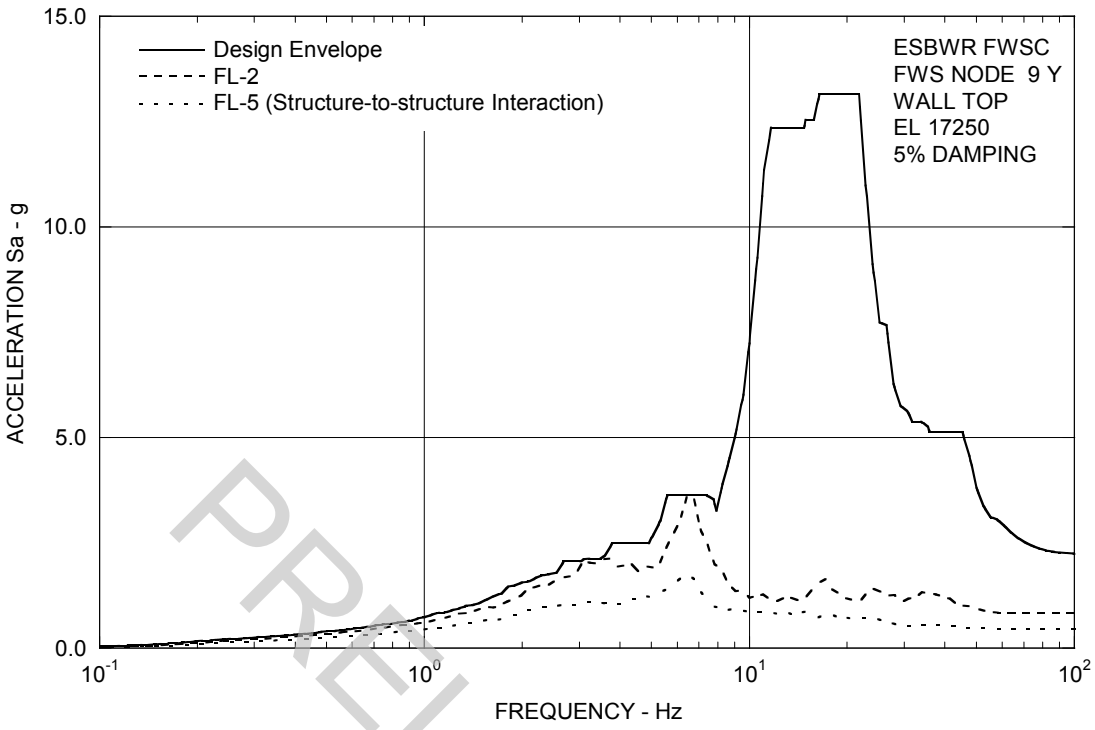

Figure 3A.8.11-17. FRS (Effect of Structure-Structure Interaction) – FWS Wall Top Y

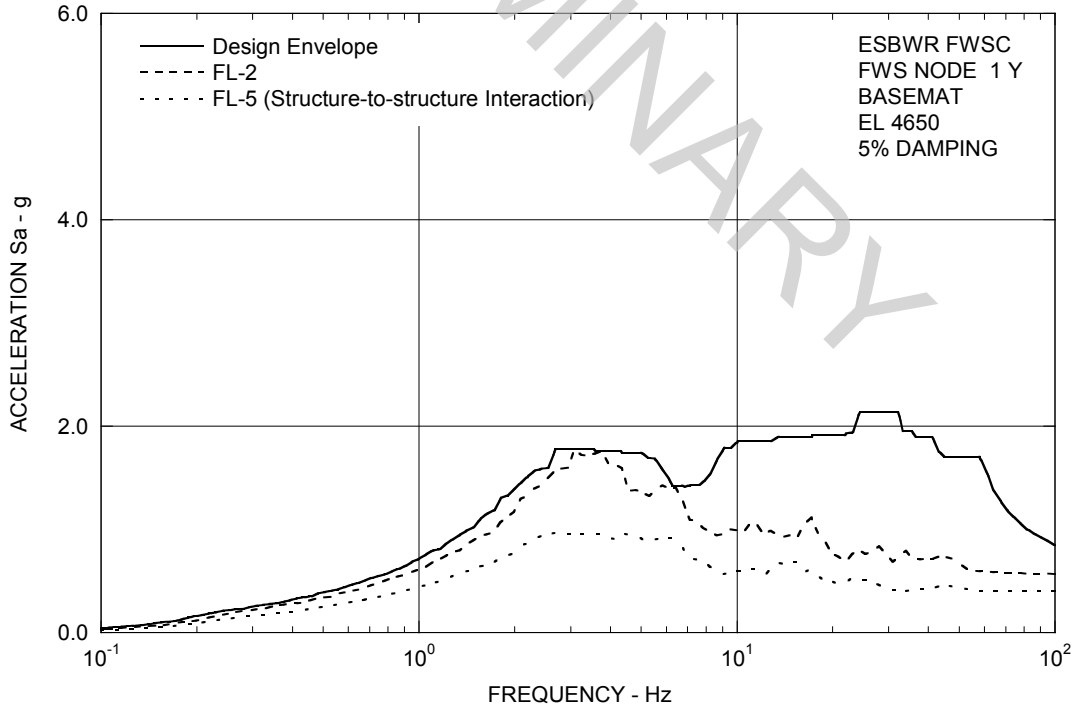

Figure 3A.8.11-18. FRS (Effect of Structure-Structure Interaction) – FWS Basemat Y

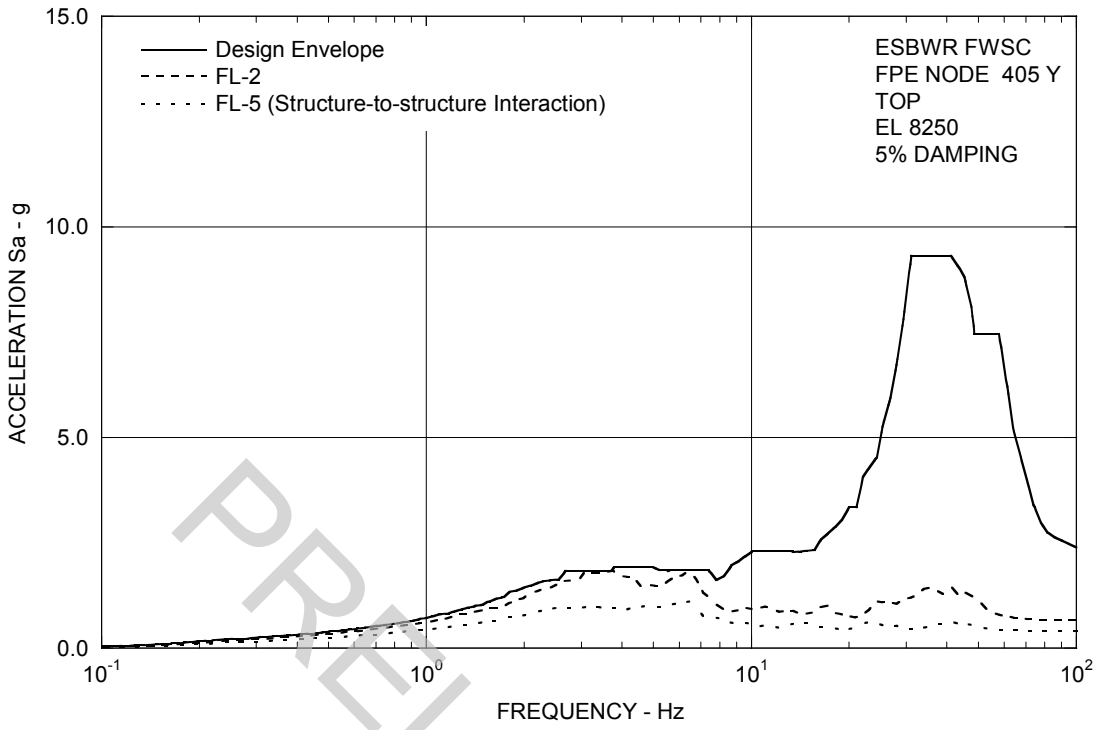

Figure 3A.8.11-19. FRS (Effect of Structure-Structure Interaction) – FPE Top Y

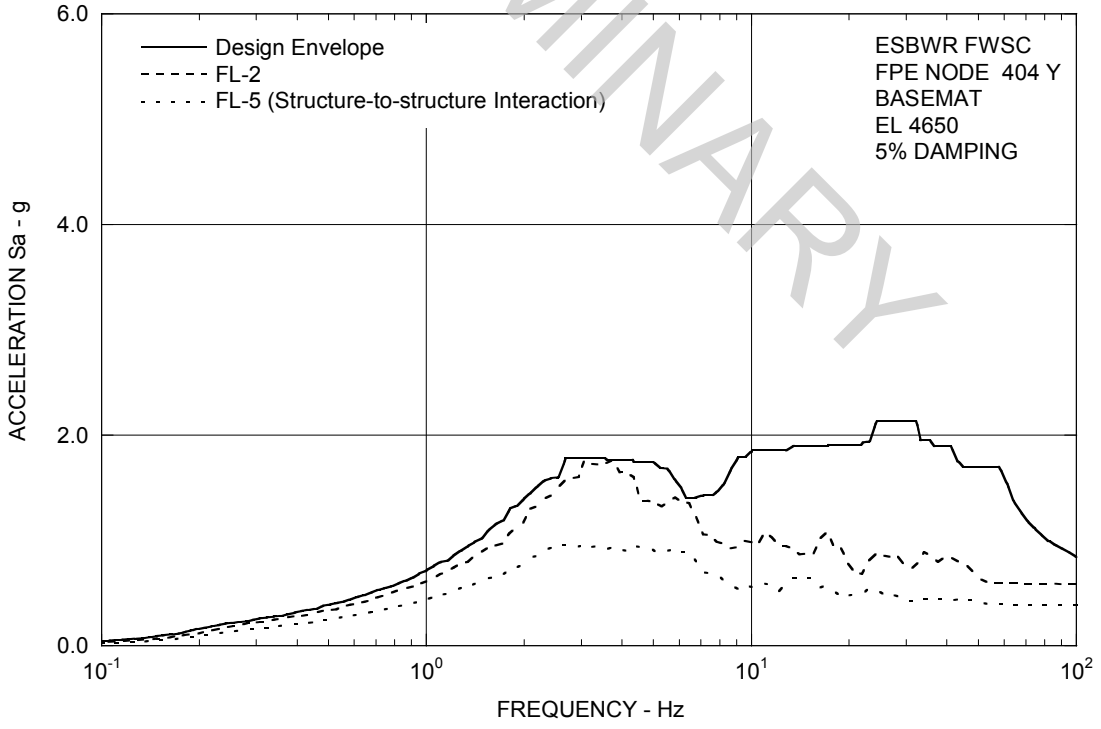

Figure 3A.8.11-20. FRS (Effect of Structure-Structure Interaction) – FPE Basemat Y

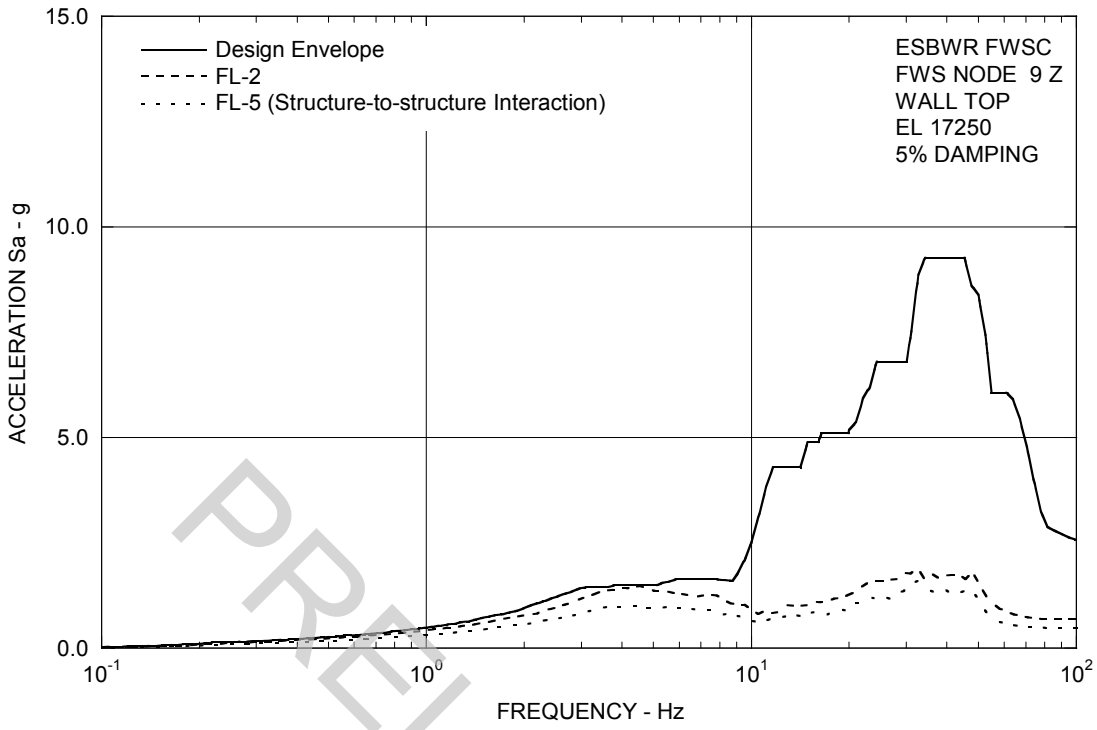

Figure 3A.8.11-21. FRS (Effect of Structure-Structure Interaction) – FWS Wall Top Z

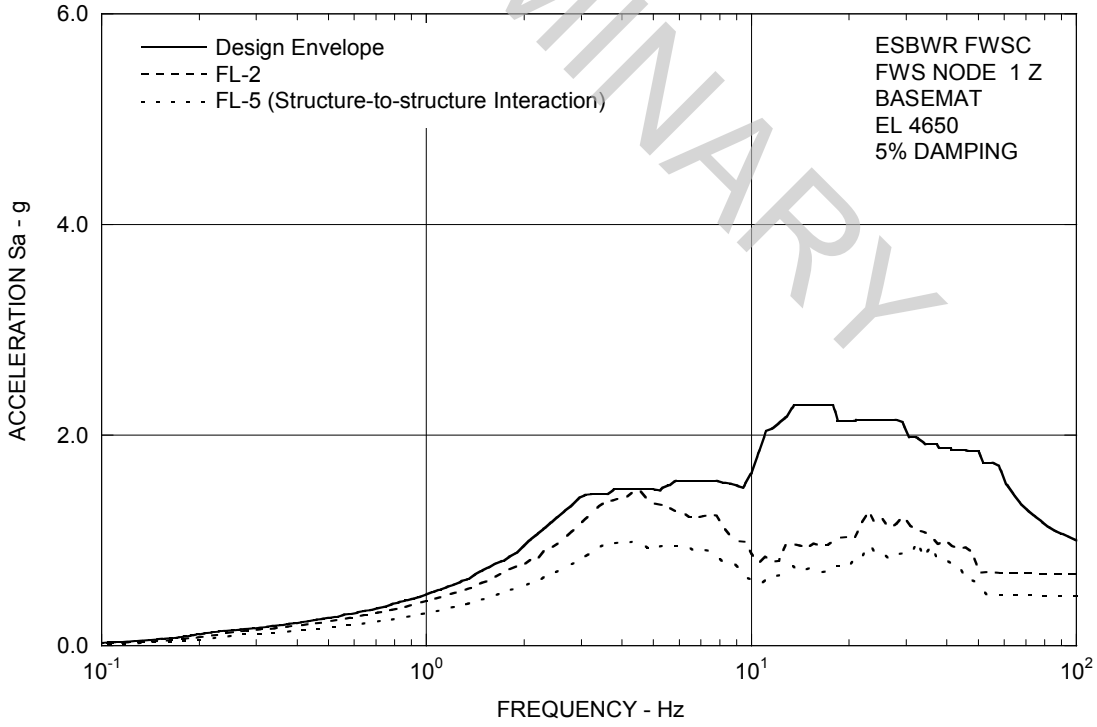

Figure 3A.8.11-22. FRS (Effect of Structure-Structure Interaction) – FWS Basemat Z

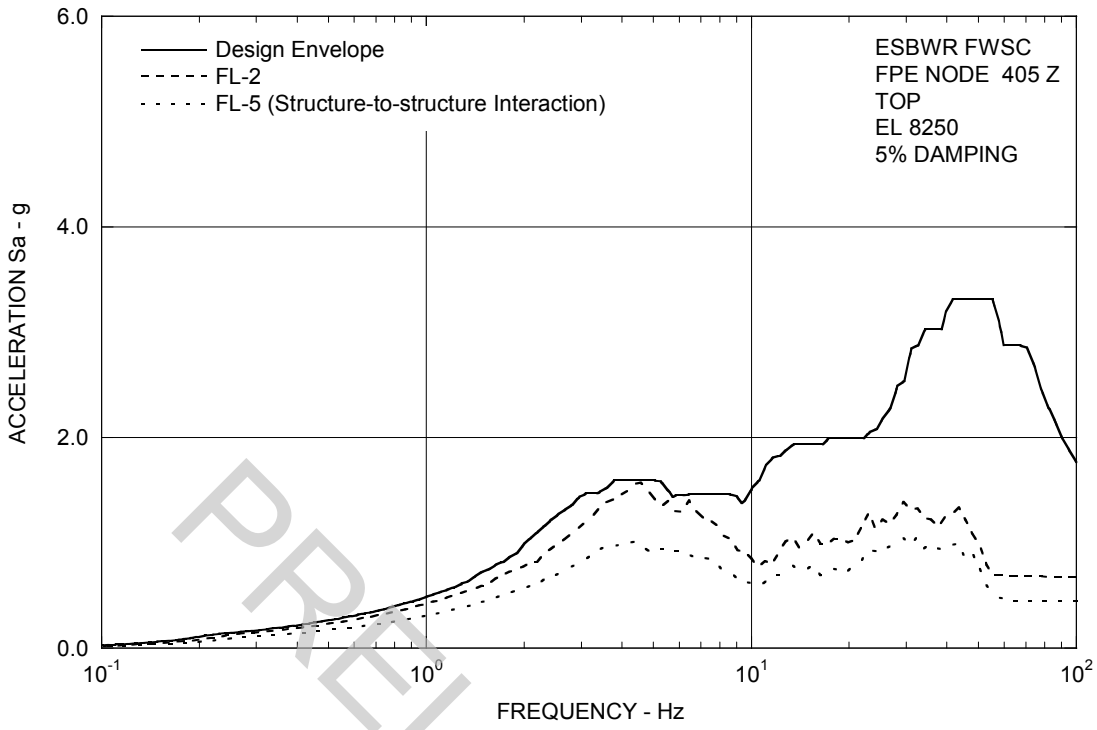

Figure 3A.8.11-23. FRS (Effect of Structure-Structure Interaction) – FPE Top Z

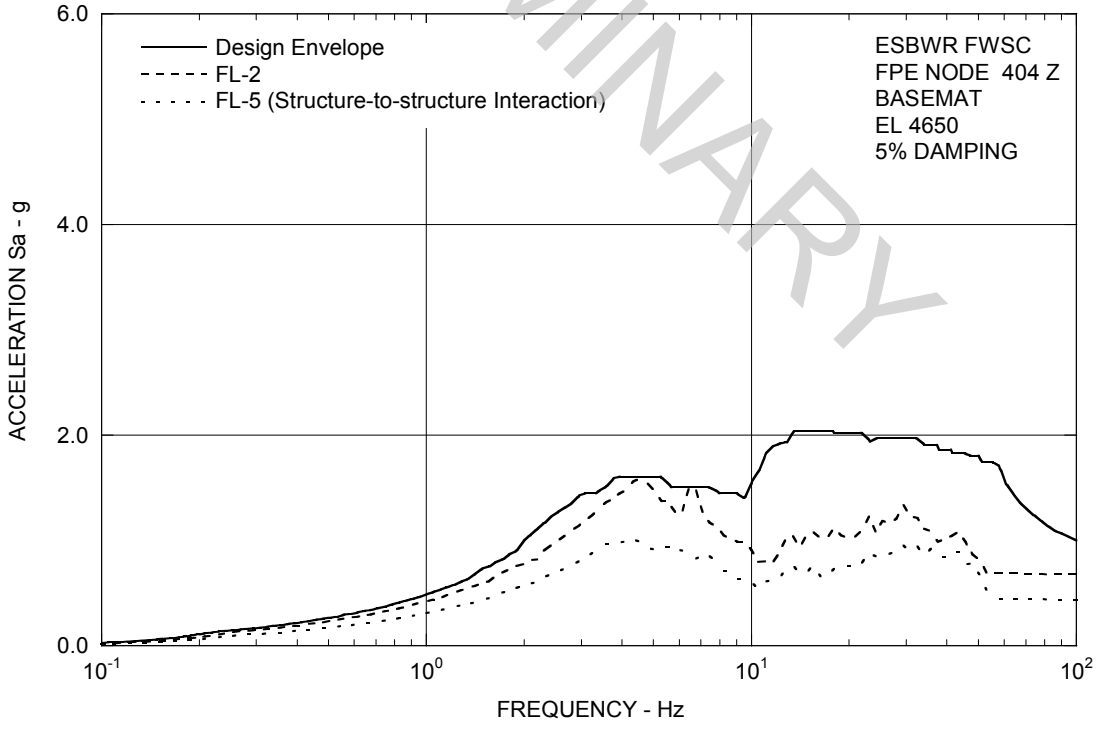

Figure 3A.8.11-24. FRS (Effect of Structure-Structure Interaction) – FPE Basemat Z

3A.9 SITE ENVELOPE SEISMIC RESPONSES

The site-envelope seismic loads are established from the envelopes of all analysis results from SSI cases summarized in Table 3A.6-1. The site-envelope seismic loads obtained are applicable for the design of Seismic Category I and II structures, systems and components housed in the ESBWR Standard Plant.

3A.9.1 Enveloping Maximum Structural Loads

The enveloping maximum shear and moment distributions along the RB/FB walls, RCCV, vent wall/pedestal, RSW, key RPV/internals, CB walls, and FWSC walls are shown in Tables 3A.9-1a through 3A.9-1h. These shears and moments are the envelope of all SSI cases, except for the LOCA flood case (RU-6). Tables 3A.9-2a through 3A.9-2e show enveloping maximum responses for the RB/FB LOCA flood case (RU-6). The torsional moments for building structures are due to geometric eccentricities only. Additional torsion due to an accidental eccentricity of 5% of maximum floor dimension under consideration is added for the design of building structures.

The vertical loads are expressed in terms of enveloping absolute acceleration. The enveloping maximum acceleration values are shown in Tables 3A.9-3a through 3A.9-3i for all cases except for LOCA flood case (RU-6). Tables 3A.9-4a through 3A.9-4e show enveloping maximum responses for LOCA flood case (RU-6). These acceleration values do not include the coupling effect and are only applicable for structural analysis in combination with the seismic loads due to horizontal shakings.

3A.9.2 Enveloping Floor Response Spectra

The site-envelope SSE floor response spectra are obtained according to the following steps:

- For each soil case analyzed, the calculated co-directional FRS in X, Y, and Z directions are combined by the SRSS method to obtain FRS at the building edges considering the coupling effects between vertical and rocking and between lateral and torsion motions.
- Individual site responses are enveloped to form the site-envelope response spectra in each of the 3 directions.
- The envelope spectra are subsequently peak broadened by ±15%.
- The spectral valleys are filled-in.

The site-envelope peak-broadened SSE floor response spectra at critical damping ratios 2, 3, 4, 5, 7, 10, and 20% for the RB/FB, CB and FWSC are shown in Figures 3A.9-1a through 3A.9-1l for the X direction, in Figures 3A.9-2a through 3A.9-2l for the Y direction, and in Figures 3A.9-3a through 3A.9-3l for the vertical direction. For seismic design of equipment and piping, the alternative seismic input can be the individual FRS of each site condition considered in generating the site-envelope spectra.

3A.9.3 Basemat Interface Loads with Foundation Medium for Foundation Stability Evaluation

The base shears, base moments and base vertical forces for consideration of foundation stability evaluation in Subsections 3G.1.5.5, 3G.2.5.5, 3G.3.5.5, and 3G.4.5.5 are the enveloping results of all cases except for the DAC3N cases for uniform sites (see Subsection 3A.8.7 for details).

Table 3A.9-1a

Enveloping Seismic Loads: RB/FB Stick

Elev. (m)	Node No.	Elem No.	Shear		Moment		Torsion (MN-m)
			X-Dir. (MN)	Y-Dir. (MN)	X-Dir. (MN-m)	Y-Dir. (MN-m)	
52.40*	110				1642	1808	
		1110	151.9	158.2	4303	4465	1379
34.00	109				5585	5522	
		1109	191.7	153.0	6477	6317	2405
27.00	108				7685	7106	
		1108	425.4	400.7	8964	8596	3333
22.50	107				9905	9193	
		1107	483.7	464.0	11464	11297	6093
17.50	106				12386	11935	
		1106	532.9	555.4	13778	13867	5068
13.57	105				14298	14377	
		1105	569.2	599.9	16593	16740	5245
9.06	104				16966	17191	
		1104	610.1	654.3	19378	19672	5985
4.65	103				19064	20192	
		1103	839.8	872.2	23163	24272	11425
-1.00	102				23673	24948	
		1102	871.4	938.5	27655	29263	11523
-6.40	101				28126	30038	
-11.50	2	1101	933.6	1029.7	32235	35275	11690

Note: Total torsional moments are obtained by the absolute sum of the accidental torsional moments and the values of the geometric torsional moments shown. The accidental torsional moment is the product of the horizontal force component and an eccentricity of 5% of the larger horizontal dimension at various elevations.

* The difference between the modeled elevation 52.4 m and the actual elevation 52.7 m at the RB roof is negligibly small.

Table 3A.9-1b

Enveloping Seismic Loads: RCCV Stick

Elev. (m)	Node No.	Elem No.	Shear		Moment		Torsion (MN-m)
			X-Dir. (MN)	Y-Dir. (MN)	X-Dir. (MN-m)	Y-Dir. (MN-m)	
34.00	209				195	581	
		1209	137.0	183.2	1057	1496	36
27.00	208				1708	2532	
		1208	164.9	248.5	2959	4368	1814
17.50	206				3315	4715	
		1206	230.2	290.2	4147	5761	1982
13.57	205				4327	5949	
		1205	263.4	326.2	5404	7264	2186
9.06	204				5628	7519	
		1204	304.2	365.8	6785	8909	2616
4.65	203				6992	9171	
		1203	227.3	289.4	7958	10581	2870
-1.00	202				8076	10738	
		1202	272.4	330.6	9417	12523	2926
-6.40	201				9534	12651	
-11.50	2	1201	261.7	303.5	10836	14200	1962

Note: Total torsional moments are obtained by the absolute sum of the accidental torsional moments and the values of the geometric torsional moments shown. The accidental torsional moment is the product of the horizontal force component and an eccentricity of 5% of the larger horizontal dimension at various elevations.

Table 3A.9-1c

Enveloping Seismic Loads: VW/Pedestal Stick

Elev. (m)	Node No.	Elem No.	Shear		Moment		Torsion (MN-m)
			X-Dir. (MN)	Y-Dir. (MN)	X-Dir. (MN-m)	Y-Dir. (MN-m)	
17.50	701				78	85	
		701	35.0	37.0	114	136	116
14.50	702				119	148	
		702	36.4	39.3	226	260	118
11.50	703				229	269	
		703	37.0	41.8	340	390	120
8.50	704				341	396	
		704	37.8	44.7	379	438	122
7.4625	705				359	438	
		705	40.7	40.5	456	525	101
4.65	706,303				581	621	
		1303	32.8	44.8	599	667	142
2.4165	377				732	817	
		1377	48.1	66.3	778	922	172
-1.00	302				839	959	
		1302	65.6	81.4	928	1050	146
-2.75	376				928	1050	
		1376	66.0	81.7	1116	1330	146
-6.40	301				1149	1346	
-11.50	2	1301	104.4	121.2	1655	1963	118

Note: Total torsional moments are obtained by the absolute sum of the accidental torsional moments and the values of the geometric torsional moments shown. The accidental torsional moment is the product of the horizontal force component and an eccentricity of 5% of the larger horizontal dimension at various elevations.

Table 3A.9-1d

Enveloping Seismic Loads: RSW Stick

Elev. (m)	Node No.	Elem No.	Shear		Moment		Torsion (MN-m)
			X-Dir. (MN)	Y-Dir. (MN)	X-Dir. (MN-m)	Y-Dir. (MN-m)	
24.18	707				2.1	1.7	
		707	3.0	2.7	13.2	12.4	0.4
20.20	708				18.4	16.8	
		708	14.6	12.3	79.0	68.4	1.4
15.775	709				81.9	71.0	
		709	17.3	14.4	158.4	133.6	1.9
11.35	710				159.1	136.4	
		710	19.9	16.6	236.2	198.7	2.4
7.4625	711				197.0	183.6	
		711	41.1	35.6	292.4	251.3	23.4
4.65	712				125.1	133.0	
		712	14.3	19.5	133.0	150.9	30.3
2.4165	713				3.6	3.2	
		713	1.5	1.3	2.9	2.7	0.2
1.96	714				2.7	2.4	
-0.80	715	714	0.9	0.7	0.5	0.5	0.1

Note: Total torsional moments are obtained by the absolute sum of the accidental torsional moments and the values of the geometric torsional moments shown. The accidental torsional moment is the product of the horizontal force component and an eccentricity of 5% of the larger horizontal dimension at various elevations.

Table 3A.9-1e

Enveloping Seismic Loads: RPV Stick

Elev. (m)	Node No.	Elem No.	Axial (MN)	Shear		Moment	
				X-Dir. (MN)	Y-Dir. (MN)	X-Dir. (MN-m)	Y-Dir. (MN-m)
Shroud	845		8.58			16.2	14.3
Bottom	846	844	8.58	7.2	7.0	21.3	17.3
RPV	815		25.26			143.8	135.8
Support	711	871	25.26	18.6	17.9	141.3	136.8

Table 3A.9-1f

Enveloping Seismic Loads: CB Stick

Elev. (m)	Node No.	Elem No.	Shear		Moment		Torsion (MN-m)
			X-Dir. (MN)	Y-Dir. (MN)	X-Dir. (MN-m)	Y-Dir. (MN-m)	
13.80	6				160	124	
		6	33.1	29.1	250	197	73.2
9.06	5				360	275	
		5	53.3	54.8	573	443	127.8
4.65	4				723	540	
		4	75.6	80.1	1136	988	178.2
-2.00	3				1232	1036	
-7.40	2	3	124.4	99.4	1570	1525	248.2

Note: Total torsional moments are obtained by the absolute sum of the accidental torsional moments and the values of the geometric torsional moments shown. The accidental torsional moment is the product of the horizontal force component and an eccentricity of 5% of the larger horizontal dimension at various elevations.

Table 3A.9-1g

Enveloping Seismic Loads: FWS Stick

Elev. (m)	Node No.	Elem No.	Shear		Moment		Torsion (MN-m)
			X-dir. (MN)	Y-dir. (MN)	X-dir. (MN-m)	Y-dir. (MN-m)	
19.70	10				4.3	7.0	
		9	4.6	5.1	14.2	19.3	0.7
17.25	9				22.1	26.7	
		8	11.1	12.1	39.0	46.9	2.2
15.53	8				45.4	57.2	
		7	15.5	16.5	70.7	84.4	3.6
13.81	7				76.1	92.3	
		6	19.3	20.1	107.5	124.5	4.9
12.10	6				111.3	128.4	
		5	22.8	23.8	133.8	152.9	5.8
11.00	5				136.4	157.0	
		4	24.6	25.3	163.4	184.2	6.4
9.90	4				165.6	187.5	
		3	26.1	26.6	194.2	216.5	6.9
8.81	3				197.0	220.6	
		2	43.3	45.5	278.9	295.0	7.5
6.73	2				280.9	298.7	
4.65	1	1	45.3	48.0	366.2	375.3	8.1

Note: Total torsional moments are obtained by the absolute sum of the accidental torsional moments and the values of the geometric torsional moments shown. The accidental torsional moment is the product of the horizontal force component and an eccentricity of 5% of the larger horizontal dimension at various elevations.

Table 3A.9-1h

Enveloping Seismic Loads: FPE Stick

Elev. (m)	Node No.	Elem No.	Shear		Moment		Torsion (MN-m)
			X-dir. (MN)	Y-dir. (MN)	X-dir. (MN-m)	Y-dir. (MN-m)	
8.25	405	402,			2.2	9.7	
4.65	404	401	8.1	7.4	27.7	27.0	15.1

Note: Total torsional moments are obtained by the absolute sum of the accidental torsional moments and the values of the geometric torsional moments shown. The accidental torsional moment is the product of the horizontal force component and an eccentricity of 5% of the larger horizontal dimension at various elevations.

Table 3A.9-2a

Enveloping Seismic Loads for LOCA Flooding: RB/FB Stick

Elev. (m)	Node No.	Elem No.	Shear		Moment		Torsion (MN-m)
			X-Dir. (MN)	Y-Dir. (MN)	X-Dir. (MN-m)	Y-Dir. (MN-m)	
52.40*	110				1588	1789	
		1110	129.4	159.9	3058	4465	1396
34.00	109				4290	5467	
		1109	189.5	150.2	4649	6094	2411
27.00	108				6201	7093	
		1108	420.7	356.7	7075	8018	3326
22.50	107				7903	8631	
		1107	472.9	398.8	8922	10425	5458
17.50	106				9973	11033	
		1106	507.1	471.9	11886	12690	4404
13.57	105				12494	13131	
		1105	536.2	506.5	14818	15142	4769
9.06	104				15328	15475	
		1104	574.7	548.2	17731	17564	5178
4.65	103				17613	17819	
		1103	813.1	723.7	21830	21065	10199
-1.00	102				22546	21467	
		1102	861.5	809.0	26988	25144	10689
-6.40	101				27557	25919	
-11.50	2	1101	938.7	914.9	31989	30136	11690

Note: Total torsional moments are obtained by the absolute sum of the accidental torsional moments and the values of the geometric torsional moments shown. The accidental torsional moment is the product of the horizontal force component and an eccentricity of 5% of the larger horizontal dimension at various elevations.

*: The difference between the modeled elevation 52.4 m and the actual elevation 52.7 m at the RB roof is negligibly small.

Table 3A.9-2b

Enveloping Seismic Loads for LOCA Flooding: RCCV Stick

Elev. (m)	Node No.	Elem No.	Shear		Moment		Torsion (MN-m)
			X-Dir. (MN)	Y-Dir. (MN)	X-Dir. (MN-m)	Y-Dir. (MN-m)	
34.00	209				189	567	
		1209	118.5	178.7	890	1429	36
27.00	208				1643	2508	
		1208	161.9	245.7	2818	4006	1669
17.50	206				3208	4341	
		1206	225.8	267.5	3848	5170	1735
13.57	205				4051	5339	
		1205	252.2	287.6	4885	6484	1988
9.06	204				5107	6740	
		1204	302.8	302.0	6319	7994	2263
4.65	203				6517	8244	
		1203	225.8	250.6	7575	9506	2562
-1.00	202				7716	9681	
		1202	272.0	289.8	9007	11082	2714
-6.40	201				9126	11219	
-11.50	2	1201	262.8	269.2	10336	12464	1962

Note: Total torsional moments are obtained by the absolute sum of the accidental torsional moments and the values of the geometric torsional moments shown. The accidental torsional moment is the product of the horizontal force component and an eccentricity of 5% of the larger horizontal dimension at various elevations.

Table 3A.9-2c

Enveloping Seismic Loads for LOCA Flooding: VW/Pedestal Stick

Elev. (m)	Node No.	Elem No.	Shear		Moment		Torsion (MN-m)
			X-Dir. (MN)	Y-Dir. (MN)	X-Dir. (MN-m)	Y-Dir. (MN-m)	
17.50	701				55	60	
		701	15.8	18.5	66	72	30
14.50	702				85	91	
		702	14.4	16.0	100	123	31
11.50	703				107	127	
		703	17.4	22.6	143	158	34
8.50	704				144	159	
		704	22.4	25.9	157	173	36
7.4625	705				187	207	
		705	18.9	14.6	232	238	20
4.65	706,303				483	477	
		1303	31.0	38.2	505	512	126
2.4165	377				618	631	
		1377	47.7	57.5	682	781	154
-1.00	302				733	833	
		1302	65.6	71.4	820	933	136
-2.75	376				820	933	
		1376	66.0	71.5	1018	1141	136
-6.40	301				1052	1175	
-11.50	2	1301	104.5	107.4	1556	1630	118

Note: Total torsional moments are obtained by the absolute sum of the accidental torsional moments and the values of the geometric torsional moments shown. The accidental torsional moment is the product of the horizontal force component and an eccentricity of 5% of the larger horizontal dimension at various elevations.

Table 3A.9-2d

Enveloping Seismic Loads for LOCA Flooding: RSW Stick

Elev. (m)	Node No.	Elem No.	Shear		Moment		Torsion (MN-m)
			X-Dir. (MN)	Y-Dir. (MN)	X-Dir. (MN-m)	Y-Dir. (MN-m)	
24.18	707				2.0	1.5	
		707	2.2	1.9	10.4	8.9	0.3
20.20	708				16.0	12.8	
		708	12.2	12.0	65.5	63.5	1.2
15.775	709				67.5	65.1	
		709	13.8	13.9	127.1	126.0	1.7
11.35	710				129.3	128.1	
		710	16.8	16.4	194.1	190.0	2.4
7.4625	711				153.8	174.2	
		711	43.6	33.8	252.5	247.3	18.7
4.65	712				103.2	102.9	
		712	13.5	16.6	113.1	119.1	27.0
2.4165	713				5.4	5.0	
		713	2.4	2.2	4.5	4.1	0.4
1.96	714				3.9	3.7	
-0.80	715	714	1.3	1.2	0.7	0.8	0.2

Note: Total torsional moments are obtained by the absolute sum of the accidental torsional moments and the values of the geometric torsional moments shown. The accidental torsional moment is the product of the horizontal force component and an eccentricity of 5% of the larger horizontal dimension at various elevations.

Table 3A.9-2e

Enveloping Seismic Loads for LOCA Flooding: RPV Stick

Elev. (m)	Node No.	Elem No.	Axial (MN)	Shear		Moment	
				X-Dir. (MN)	Y-Dir. (MN)	X-Dir. (MN-m)	Y-Dir. (MN-m)
Shroud	845		6.22			18.0	13.7
Bottom	846	844	6.22	9.0	5.3	25.2	16.4
RPV	815		21.34			121.2	130.8
Support	711	871	21.34	18.5	17.8	122.3	130.4

Table 3A.9-3a

Enveloping Maximum Vertical Acceleration: RB/FB

Elev. (m)	Node No.	Stick Model	Max. Vertical Acceleration (g)
52.40 *	110	RB/FB	1.27
34.00	109	RB/FB	0.83
27.00	108	RB/FB	0.73
22.50	107	RB/FB	0.73
17.50	106	RB/FB	0.73
13.57	105	RB/FB	0.74
9.06	104	RB/FB	0.73
4.65	103	RB/FB	0.78
-1.00	102	RB/FB	0.76
-6.40	101	RB/FB	0.68
-11.50	2	RB/FB	0.63
-15.50	1	RB/FB	0.51

Note: For structural design use only.

*: The difference between the modeled elevation 52.4 m and the actual elevation 52.7 m at the RB roof is negligibly small.

Table 3A.9-3b

Enveloping Maximum Vertical Acceleration: RCCV

Elev. (m)	Node No.	Stick Model	Max. Vertical Acceleration (g)
34.00	209	RCCV	0.90
27.00	208	RCCV	0.88
17.50	206	RCCV	0.73
13.57	205	RCCV	0.78
9.06	204	RCCV	0.65
4.65	203	RCCV	0.70
-1.00	202	RCCV	0.59
-6.40	201	RCCV	0.59

Note: For structural design use only.

Table 3A.9-3c

Enveloping Maximum Vertical Acceleration: VW/Pedestal

Elev. (m)	Node No.	Stick Model	Max. Vertical Acceleration (g)
17.50	701	VW	1.10
14.50	702	VW	1.04
11.50	703	VW	0.92
8.50	704	VW	0.77
7.4625	705	VW	0.70
4.65	706, 303	Pedestal	0.67
2.4165	377	Pedestal	0.64
-1.00	302	Pedestal	0.59
-2.753	376	Pedestal	0.51
-6.40	301	Pedestal	0.50

Note:For structural design use only.

Table 3A.9-3d

Enveloping Maximum Vertical Acceleration: RSW

Elev. (m)	Node No.	Stick Model	Max. Vertical Acceleration (g)
24.18	707	RSW	0.97
20.20	708	RSW	0.94
15.775	709	RSW	0.84
11.35	710	RSW	0.76
7.4625	711	RSW	0.70
4.65	712	RSW	0.67
2.4165	713	RSW	0.64
1.96	714	RSW	0.64
-0.80	715	RSW	0.65

Note:For structural design use only.

Table 3A.9-3e

Enveloping Maximum Vertical Acceleration: RB/FB Flexible Slab Oscillators

Elev. (m)	Node No.	Stick Model	Max. Vertical Acceleration (g)
52.40*	9101	Oscillator	1.20
	9102	Oscillator	1.82
	9103	Oscillator	3.14
	9104	Oscillator	2.45
	9105	Oscillator	2.32
	9106	Oscillator	2.99
	9107	Oscillator	2.80
	9108	Oscillator	2.61
34.00	9091	Oscillator	1.29
	9092	Oscillator	1.08
27.00	9081	Oscillator	1.16
	9082	Oscillator	0.99
	9083	Oscillator	1.09
	9084	Oscillator	1.32
	9085	Oscillator	0.97
22.50	9071	Oscillator	1.60
	9072	Oscillator	1.31
	9073	Oscillator	2.03
	9074	Oscillator	1.31
	9075	Oscillator	1.16
17.50	9061	Oscillator	1.79
	9062	Oscillator	1.49
	9063	Oscillator	0.82
	9064	Oscillator	1.84
	9065	Oscillator	1.42
	99064	Oscillator	1.07

Note: For structural design use only.

*: The difference between the modeled elevation 52.4 m and the actual elevation 52.7 m at the RB roof is negligibly small.

Table 3A.9-3e

Enveloping Maximum Vertical Acceleration: RB/FB Flexible Slab Oscillators (Continued)

Elev. (m)	Node No.	Stick Model	Max. Vertical Acceleration (g)
13.57	9051	Oscillator	0.81
	9052	Oscillator	1.46
9.06	9041	Oscillator	0.88
	9042	Oscillator	1.42
4.65	9031	Oscillator	1.17
	9032	Oscillator	0.97
	9033	Oscillator	1.02
	9034	Oscillator	1.51
	9035	Oscillator	1.38
-1.00	9021	Oscillator	1.12
	9022	Oscillator	1.45
	9023	Oscillator	1.01
	9024	Oscillator	0.89
	9025	Oscillator	1.34
	9026	Oscillator	1.57
	9027	Oscillator	0.88
-6.40	9011	Oscillator	0.92
	9012	Oscillator	0.92
	9013	Oscillator	1.35

Note: For structural design use only.

Table 3A.9-3f

Enveloping Maximum Horizontal Acceleration: RB/FB Wall Out-of-plane Oscillators

EL (m)	Node No.	Stick Model	Max. Horizontal Acceleration (g)
42.00	99981	Oscillator	1.54
(X-dir)	99982	Oscillator	1.30
42.00	99983	Oscillator	1.71
(Y-dir)	99984	Oscillator	1.56
	99985	Oscillator	1.25
13.57	99971	Oscillator	1.38
(X-dir)	99972	Oscillator	1.37
	99973	Oscillator	1.15
	99974	Oscillator	0.99
13.57	99975	Oscillator	1.28
(Y-dir)	99976	Oscillator	0.98

Note: For structural design use only.

Table 3A.9-3g

Enveloping Maximum Vertical Acceleration: CB

Elevation (m)	Node No.	Stick Model	Max. Vertical Acceleration (g)
13.80	6	CB	1.00
9.06	5	CB	0.86
4.65	4	CB	0.74
-2.00	3	CB	0.56
-7.40	2	CB	0.51
-10.40	1	CB	0.51
13.50	9001	Oscillator	2.19
	9002	Oscillator	1.34
	9003	Oscillator	1.43
9.06	9101	Oscillator	2.00
	9102	Oscillator	1.26
	9103	Oscillator	1.43
4.65	9201	Oscillator	1.30
	9202	Oscillator	1.43
-2.00	9301	Oscillator	1.39

Note:For structural design use only.

Table 3A.9-3h

Enveloping Maximum Vertical Acceleration: FWS

Elevation (m)	Node No.	Stick Model	Max. Vertical Acceleration (g)
19.70	10	FWS	1.69
17.25	9	FWS	1.64
15.53	8	FWS	1.58
13.81	7	FWS	1.58
12.10	6	FWS	1.43
11.00	5	FWS	1.23
9.90	4	FWS	1.13
8.81	3	FWS	1.05
6.73	2	FWS	1.00
4.65	8002	FWSC	0.78
2.15	8001	FWSC	0.78
19.70	11	Oscillator	3.26

Note: For structural design use only.

Table 3A.9-3i

Enveloping Maximum Vertical Acceleration: FPE

Elevation (m)	Node No.	Stick Model	Max. Vertical Acceleration (g)
8.25	405	FPE	1.12
6.45	402	FPE	1.09

Note: For structural design use only.

Table 3A.9-4a

Enveloping Maximum Vertical Acceleration for LOCA Flooding: RB/FB

Elev. (m)	Node No.	Stick Model	Max. Vertical Acceleration (g)
52.40*	110	RB/FB	1.18
34.00	109	RB/FB	0.82
27.00	108	RB/FB	0.72
22.50	107	RB/FB	0.66
17.50	106	RB/FB	0.66
13.57	105	RB/FB	0.65
9.06	104	RB/FB	0.65
4.65	103	RB/FB	0.69
-1.00	102	RB/FB	0.65
-6.40	101	RB/FB	0.56
-11.50	2	RB/FB	0.54
-15.50	1	RB/FB	0.51

Note: For structural design use only.

*: The difference between the modeled elevation 52.4 m and the actual elevation 52.7 m at the RB roof is negligibly small.

Table 3A.9-4b

Enveloping Maximum Vertical Acceleration for LOCA Flooding: RCCV

Elev. (m)	Node No.	Stick Model	Max. Vertical Acceleration (g)
34.00	209	RCCV	0.87
27.00	208	RCCV	0.86
17.50	206	RCCV	0.69
13.57	205	RCCV	0.62
9.06	204	RCCV	0.56
4.65	203	RCCV	0.52
-1.00	202	RCCV	0.50
-6.40	201	RCCV	0.49

Note: For structural design use only.

Table 3A.9-4c

Enveloping Maximum Vertical Acceleration for LOCA Flooding: VW/Pedestal

Elev. (m)	Node No.	Stick Model	Max. Vertical Acceleration (g)
17.50	701	VW	0.95
14.50	702	VW	0.87
11.50	703	VW	0.74
8.50	704	VW	0.62
7.4625	705	VW	0.62
4.65	706, 303	Pedestal	0.59
2.4165	377	Pedestal	0.56
-1.00	302	Pedestal	0.52
-2.753	376	Pedestal	0.50
-6.40	301	Pedestal	0.49

Note: For structural design use only.

Table 3A.9-4d

Enveloping Maximum Vertical Acceleration for LOCA Flooding: RSW

Elev. (m)	Node No.	Stick Model	Max. Vertical Acceleration (g)
24.18	707	RSW	0.84
20.20	708	RSW	0.82
15.775	709	RSW	0.74
11.35	710	RSW	0.63
7.4625	711	RSW	0.62
4.65	712	RSW	0.59
2.4615	713	RSW	0.56
1.96	714	RSW	0.56
-0.80	715	RSW	0.56

Note: For structural design use only.

Table 3A.9-4e

Enveloping Maximum Vertical Acceleration for LOCA Flooding: RB/FB Flexible Slab Oscillators

Elev. (m)	Node No.	Stick Model	Max. Vertical Acceleration (g)
52.40*	9101	Oscillator	1.02
	9102	Oscillator	1.53
	9103	Oscillator	3.08
	9104	Oscillator	2.32
	9105	Oscillator	2.29
	9106	Oscillator	2.82
	9107	Oscillator	2.76
	9108	Oscillator	2.61
34.00	9091	Oscillator	1.22
	9092	Oscillator	1.03
27.00	9081	Oscillator	1.15
	9082	Oscillator	0.97
	9083	Oscillator	1.06
	9084	Oscillator	1.27
	9085	Oscillator	0.95
22.50	9071	Oscillator	1.17
	9072	Oscillator	1.25
	9073	Oscillator	1.96
	9074	Oscillator	1.27
	9075	Oscillator	1.10
17.50	9061	Oscillator	1.75
	9062	Oscillator	1.40
	9063	Oscillator	0.79
	9064	Oscillator	1.51
	9065	Oscillator	1.38

Note: For structural design use only.

*: The difference between the modeled elevation 52.4 m and the actual elevation 52.7 m at the RB roof is negligibly small.

Table 3A.9-4e

Enveloping Maximum Vertical Acceleration for LOCA Flooding: RB/FB Flexible Slab Oscillators (Continued)

Elev. (m)	Node No.	Stick Model	Max. Vertical Acceleration (g)
13.57	9051	Oscillator	0.83
	9052	Oscillator	1.42
9.06	9041	Oscillator	0.90
	9042	Oscillator	1.37
4.65	9031	Oscillator	1.20
	9032	Oscillator	0.97
	9033	Oscillator	0.88
	9034	Oscillator	1.47
	9035	Oscillator	1.32
-1.00	9021	Oscillator	1.11
	9022	Oscillator	1.41
	9023	Oscillator	1.01
	9024	Oscillator	0.88
	9025	Oscillator	1.26
	9026	Oscillator	1.43
	9027	Oscillator	0.93
-6.40	9011	Oscillator	0.92
	9012	Oscillator	0.88
	9013	Oscillator	1.27

Note: For structural design use only.

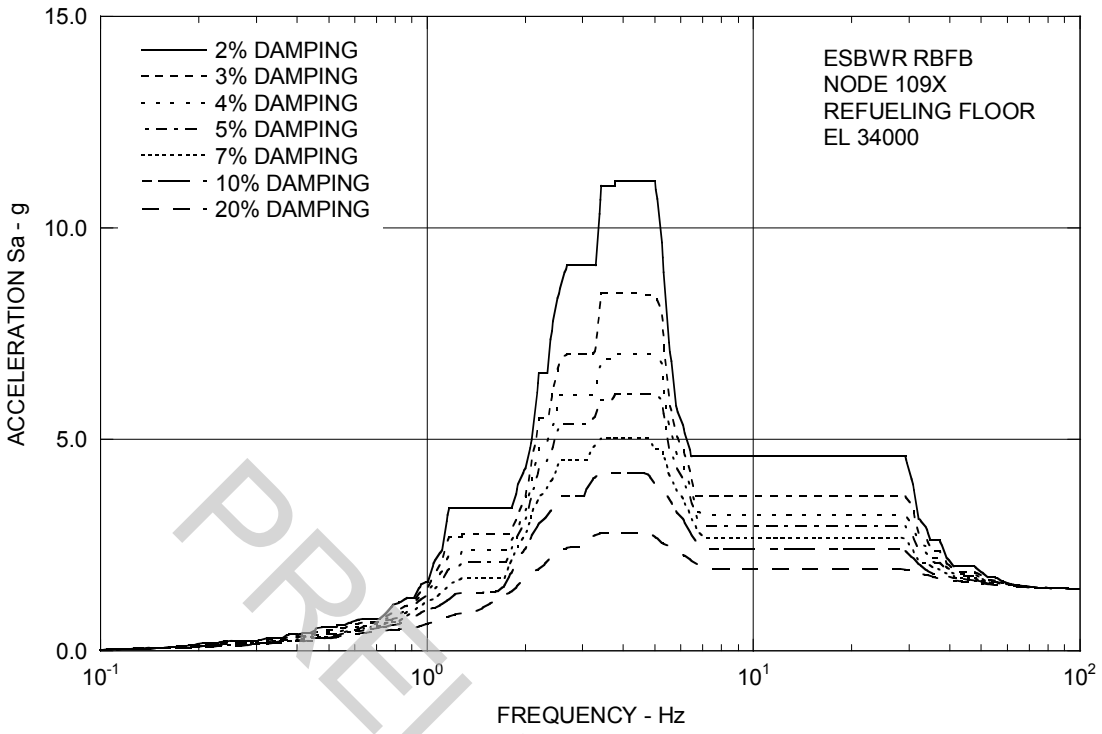

Figure 3A.9-1a. Enveloping Floor Response Spectra – RB/FB Refueling Floor X

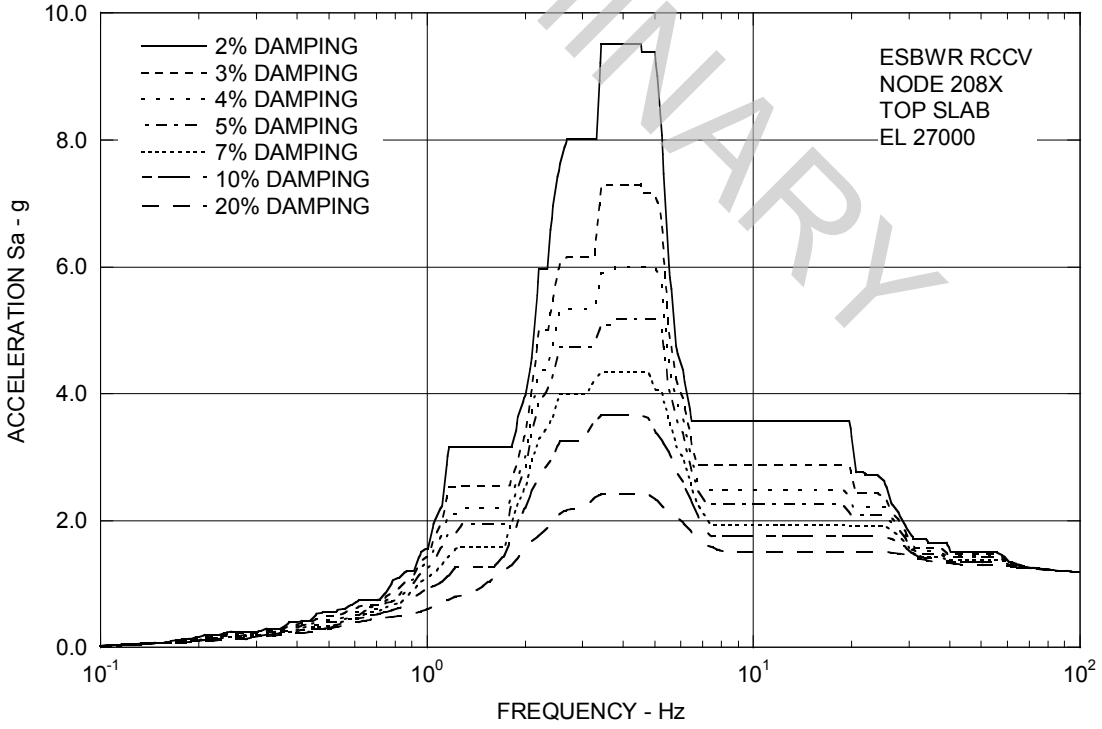

Figure 3A.9-1b. Enveloping Floor Response Spectra – RCCV Top Slab X

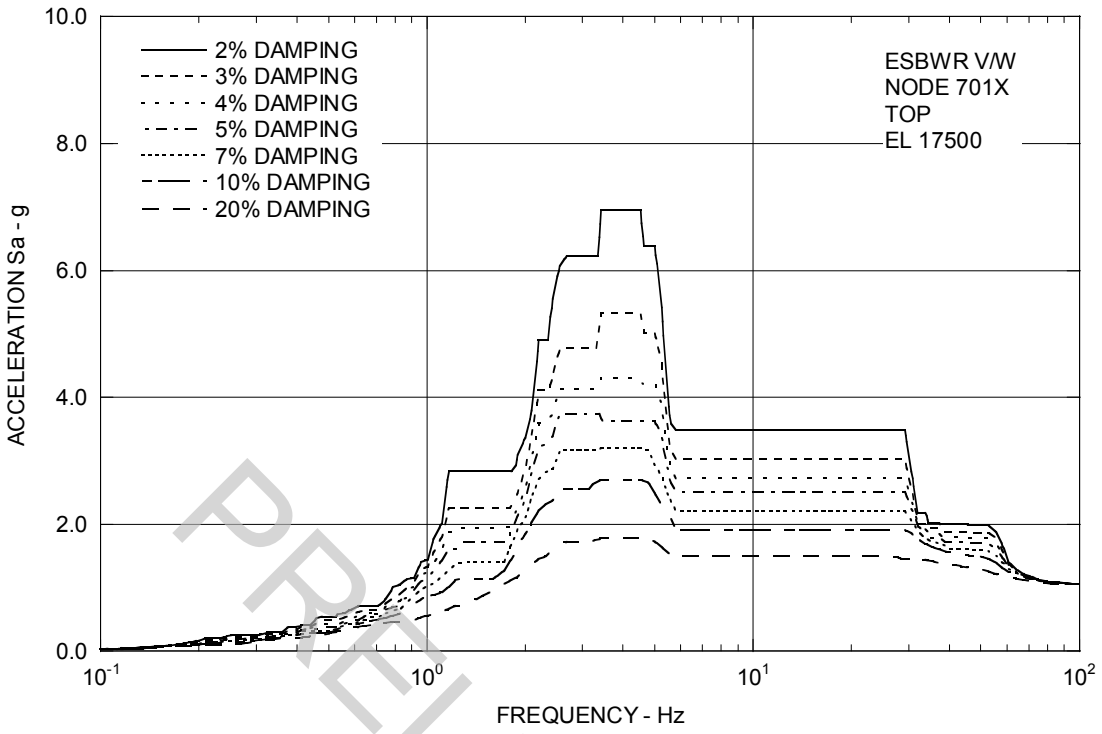

Figure 3A.9-1c. Enveloping Floor Response Spectra – Vent Wall Top X

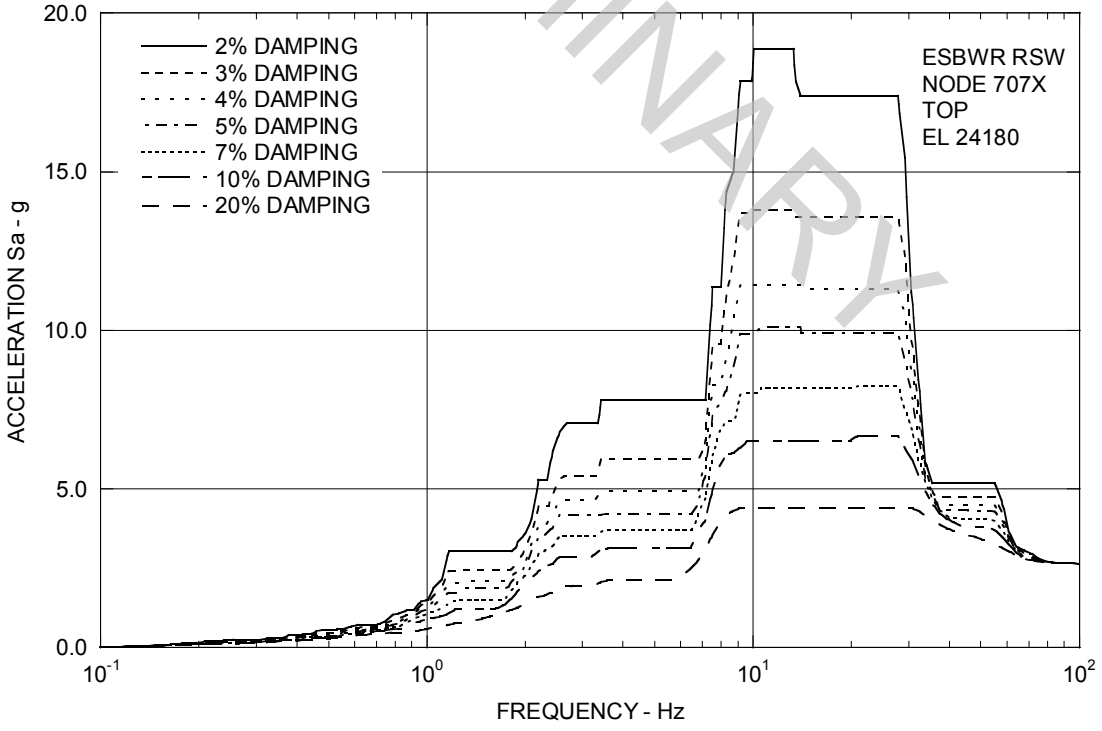

Figure 3A.9-1d. Enveloping Floor Response Spectra – RSW Top X

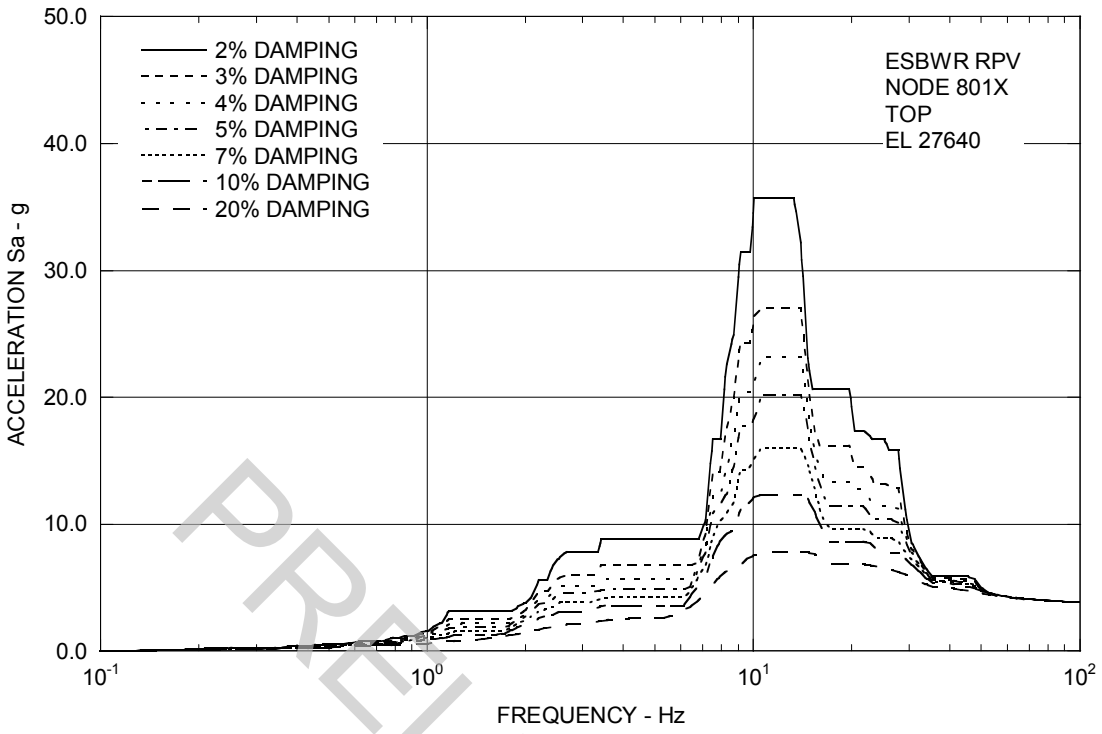

Figure 3A.9-1e. Enveloping Floor Response Spectra – RPV Top X

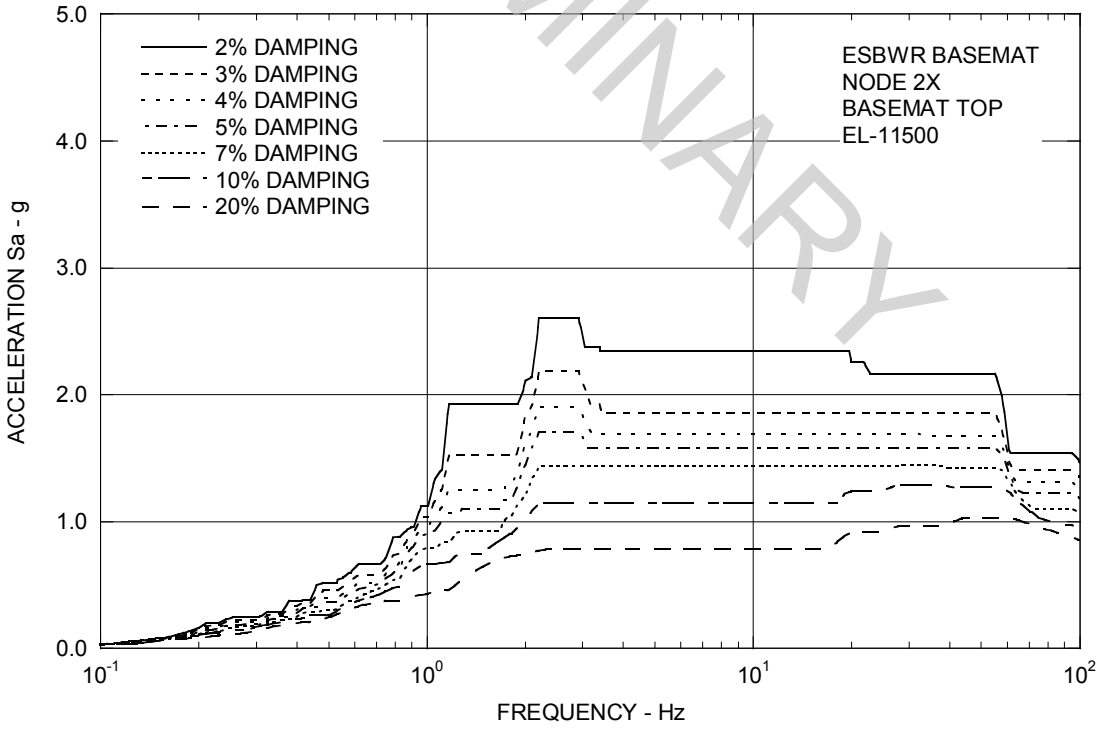

Figure 3A.9-1f. Enveloping Floor Response Spectra – RB/FB Basemat X

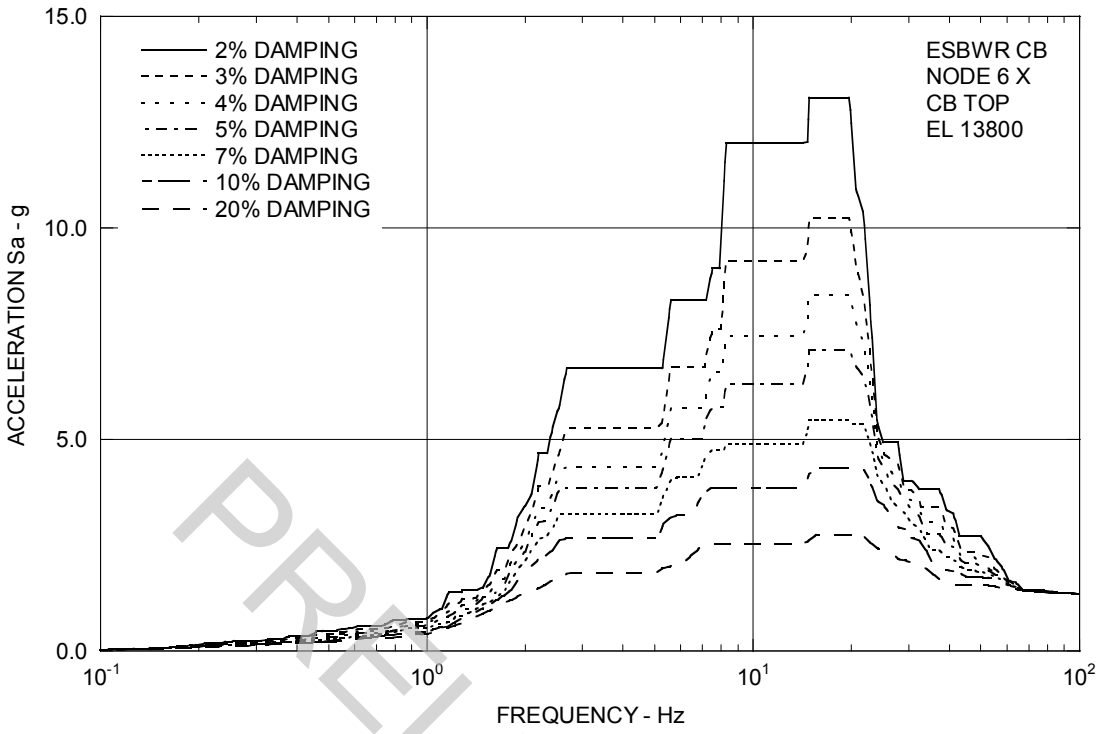

Figure 3A.9-1g. Enveloping Floor Response Spectra – CB Top X

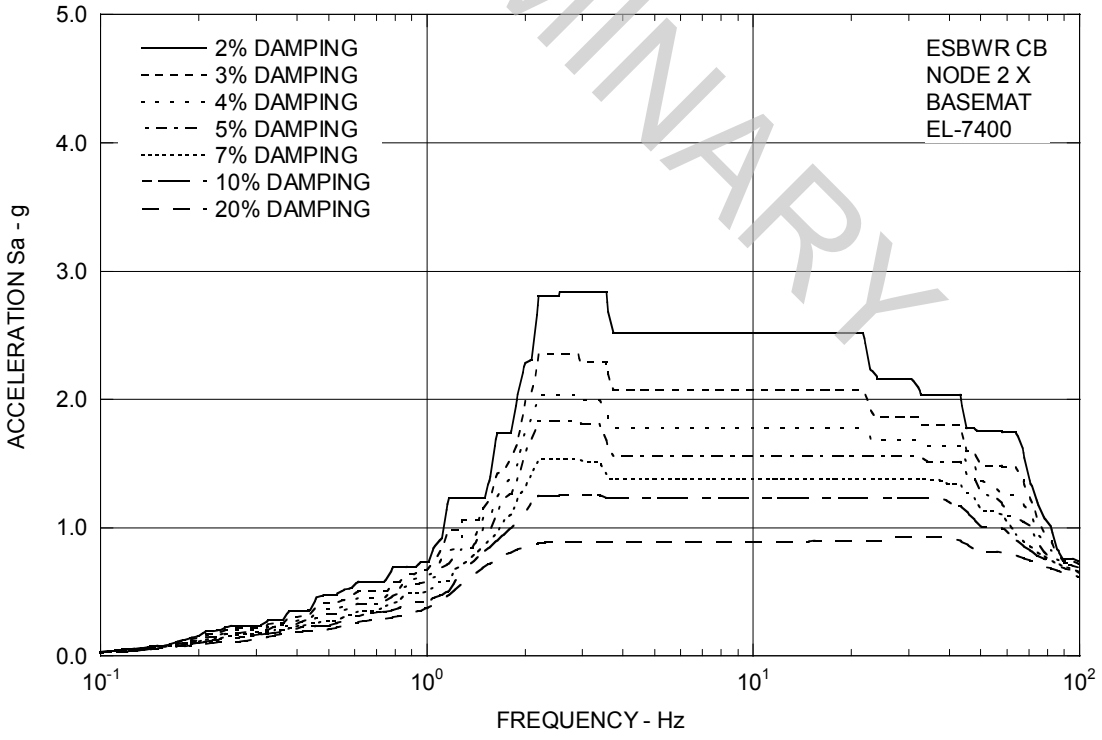

Figure 3A.9-1h. Enveloping Floor Response Spectra – CB Basemat X

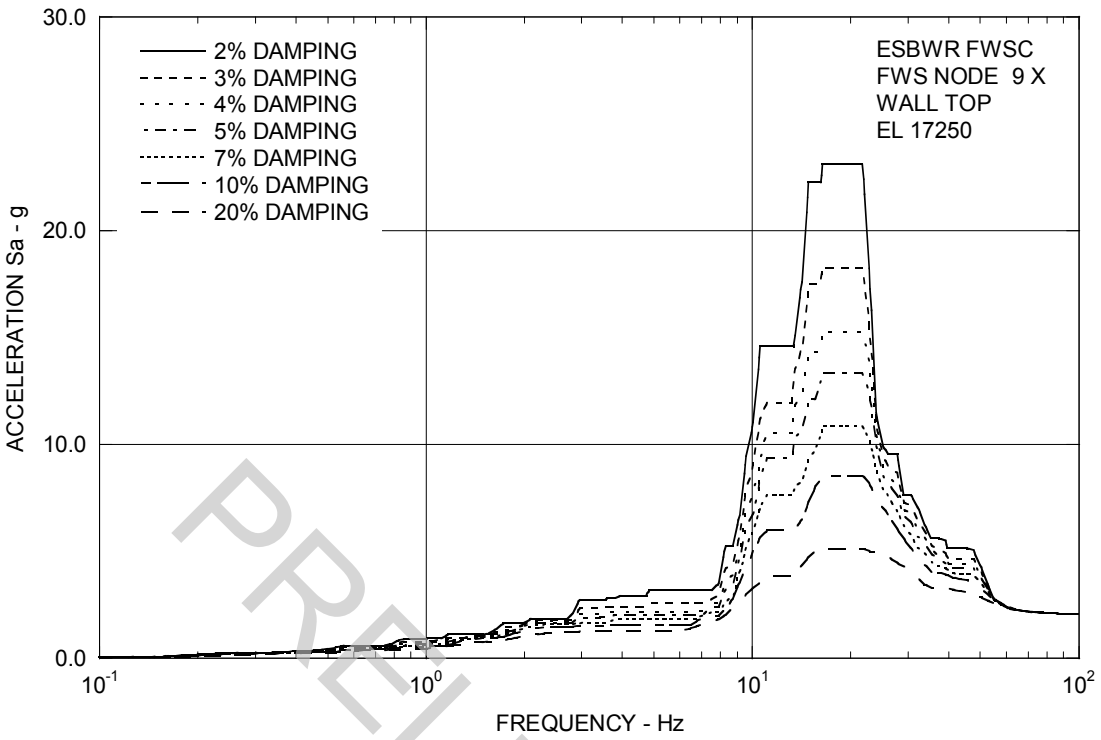

Figure 3A.9-1i. Enveloping Floor Response Spectra – FWS Wall Top X

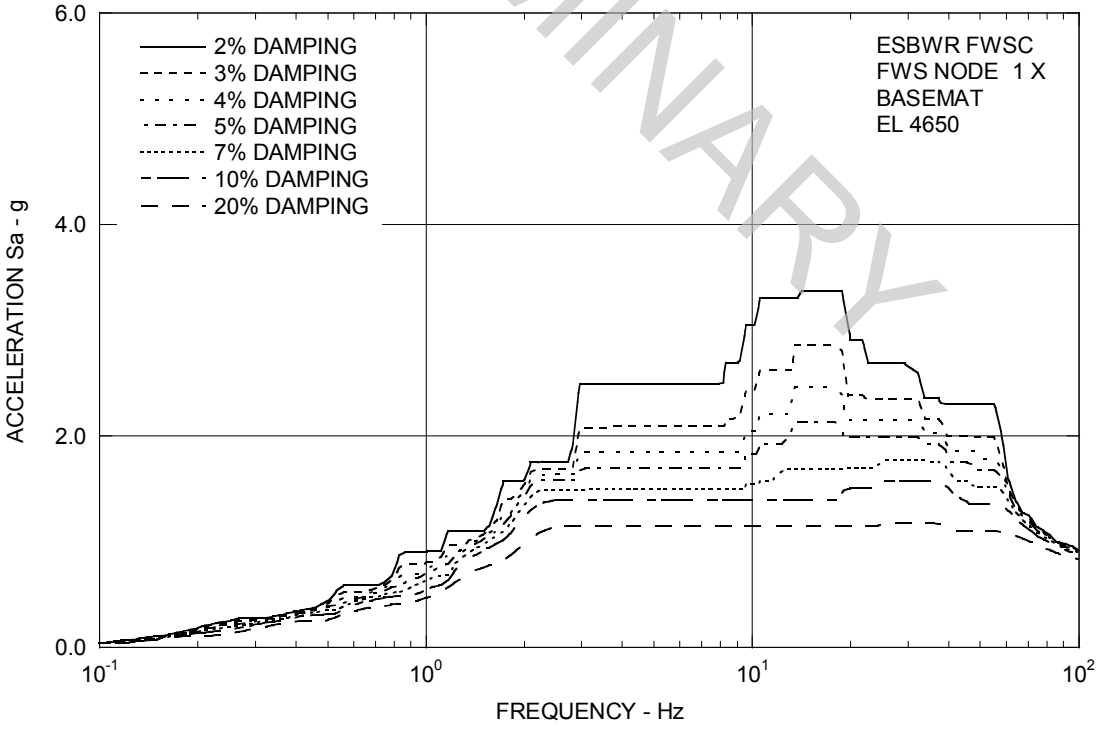

Figure 3A.9-1j. Enveloping Floor Response Spectra – FWS Basemat X

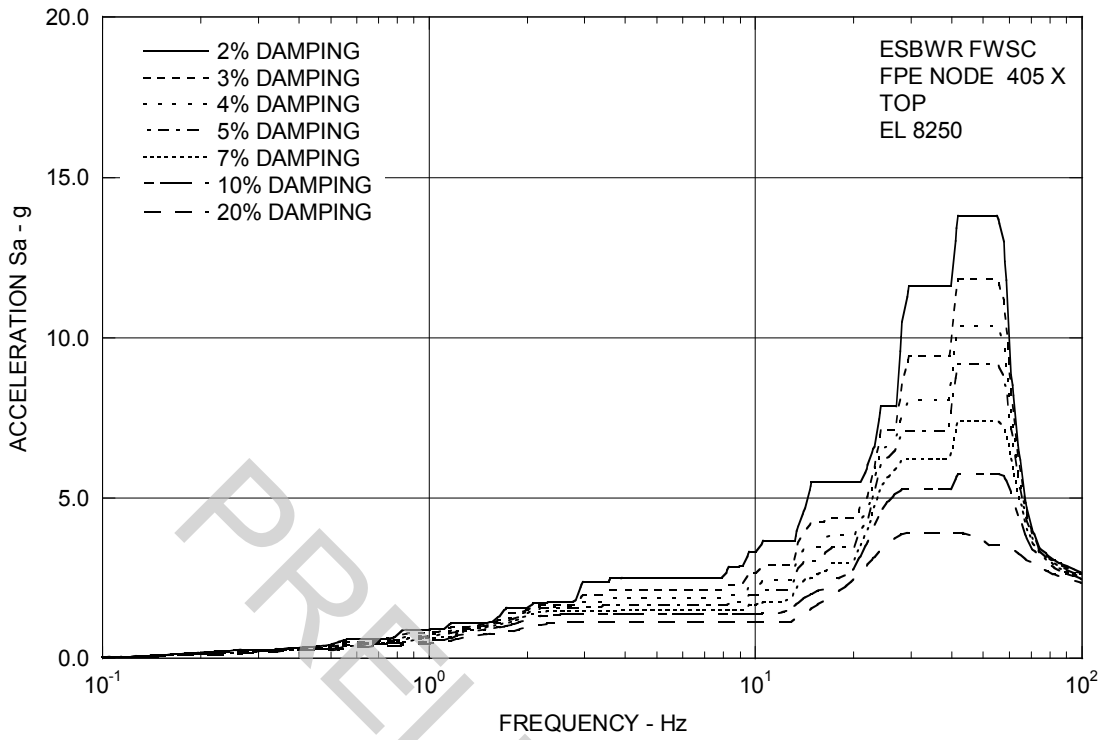

Figure 3A.9-1k. Enveloping Floor Response Spectra – FPE Top X

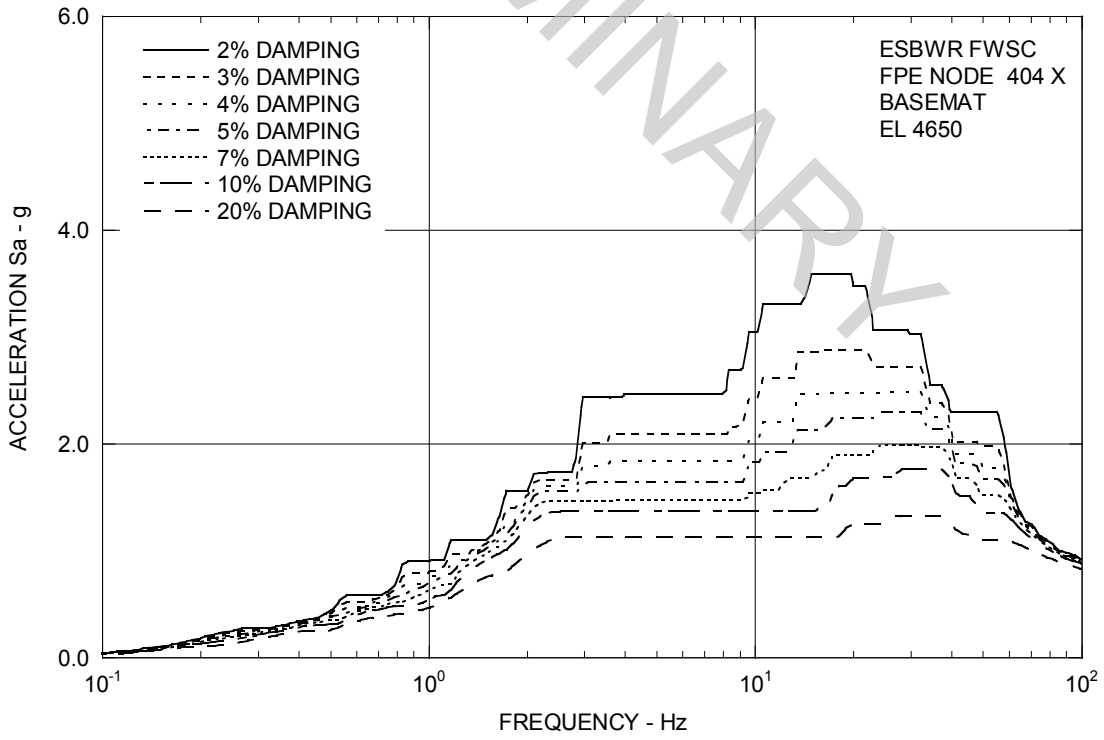

Figure 3A.9-1l. Enveloping Floor Response Spectra – FPE Basemat X

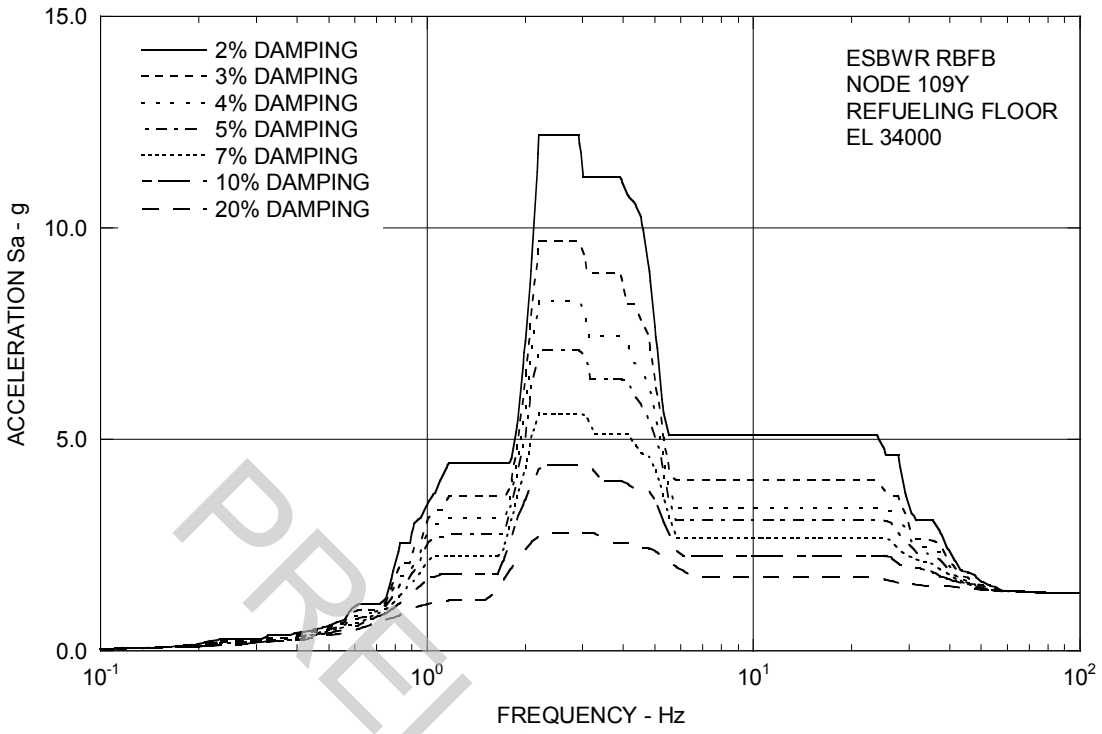

Figure 3A.9-2a. Enveloping Floor Response Spectra – RB/FB Refueling Floor Y

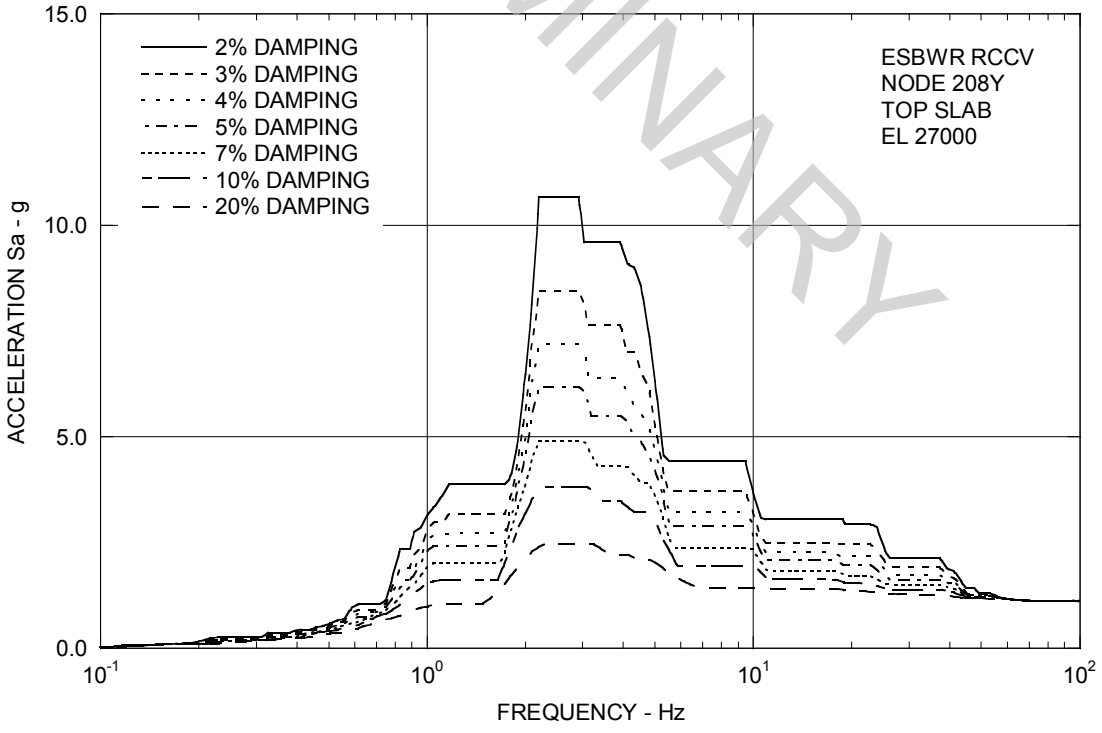

Figure 3A.9-2b. Enveloping Floor Response Spectra – RCCV Top Slab Y

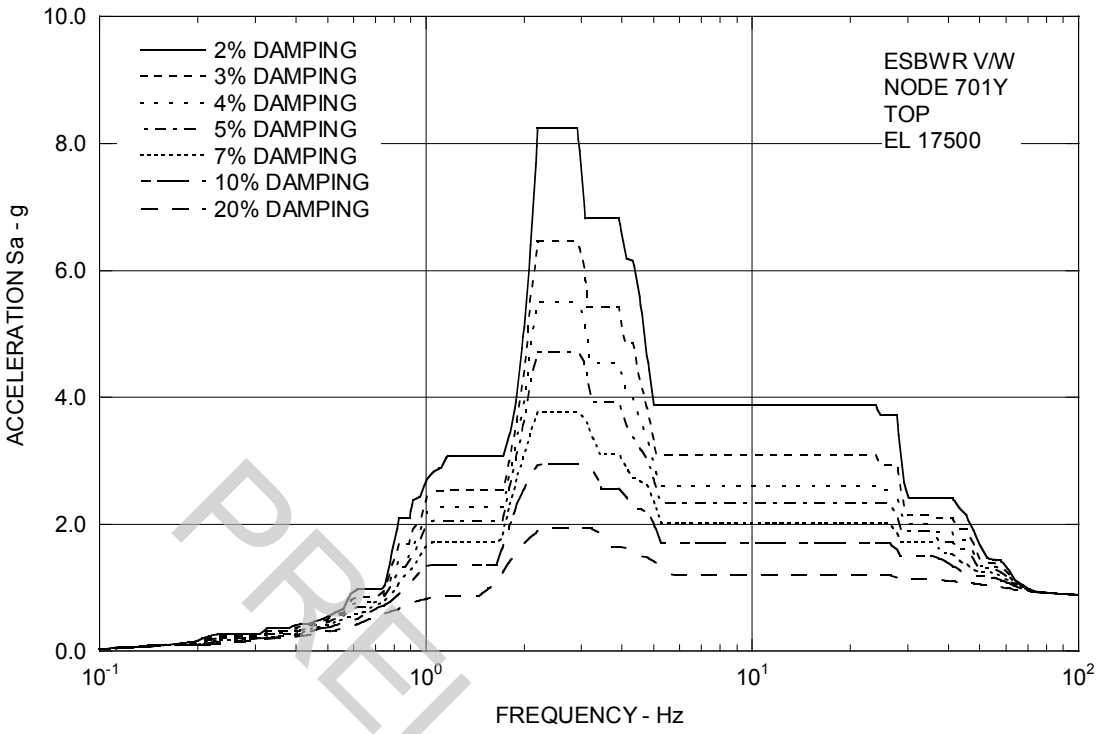

Figure 3A.9-2c. Enveloping Floor Response Spectra – Vent Wall Top Y

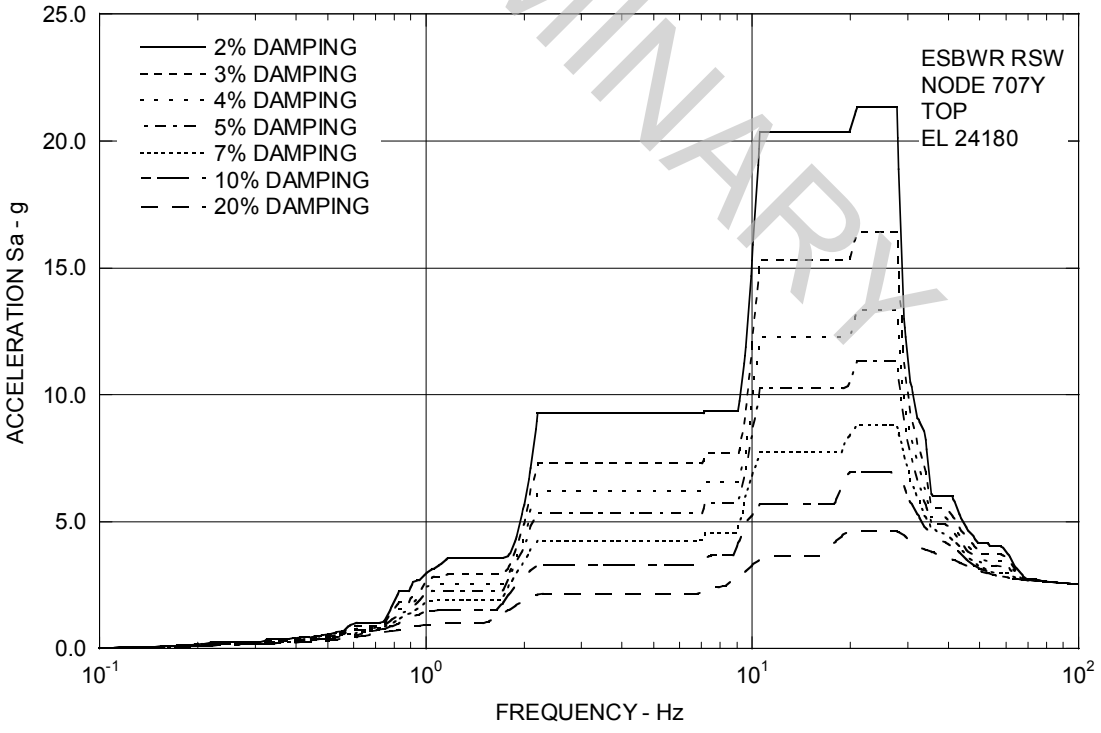

Figure 3A.9-2d. Enveloping Floor Response Spectra – RSW Top Y

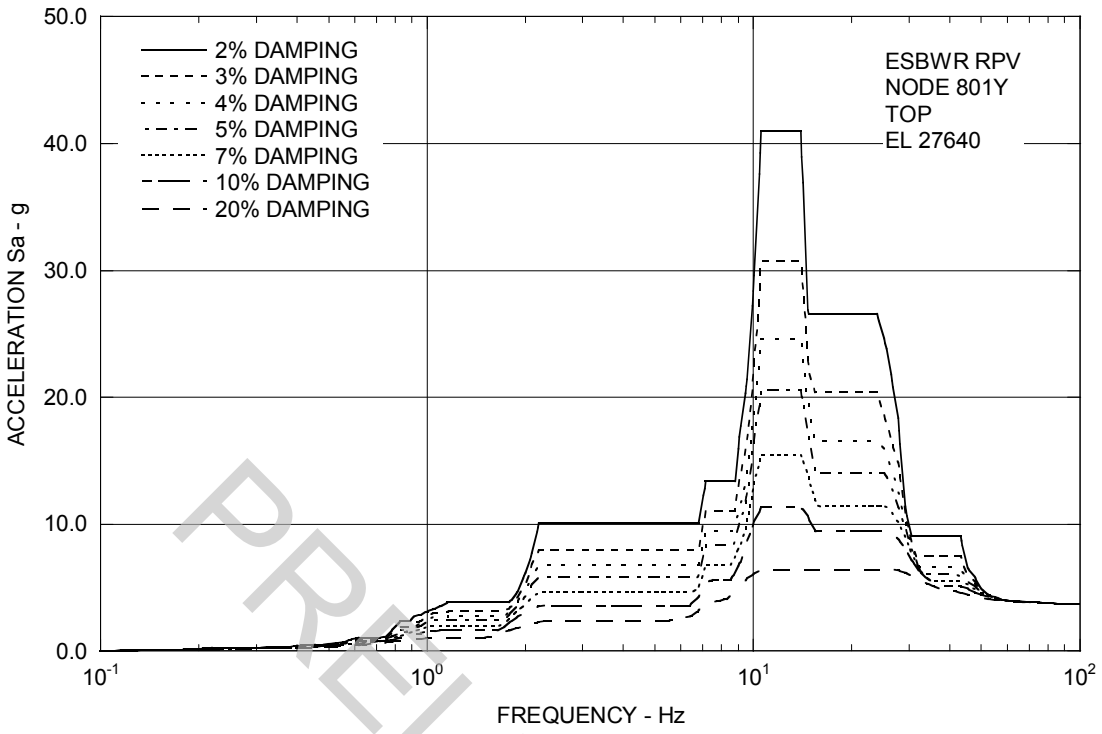

Figure 3A.9-2e. Enveloping Floor Response Spectra – RPV Top Y

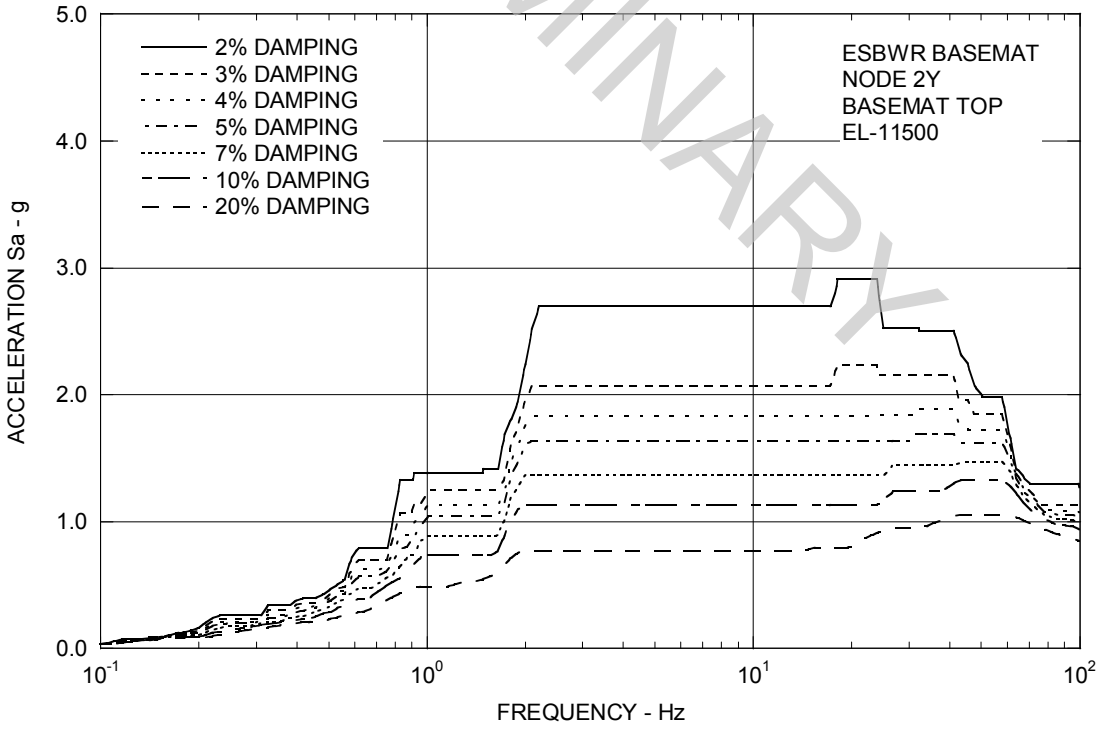

Figure 3A.9-2f. Enveloping Floor Response Spectra – RB/FB Basemat Y

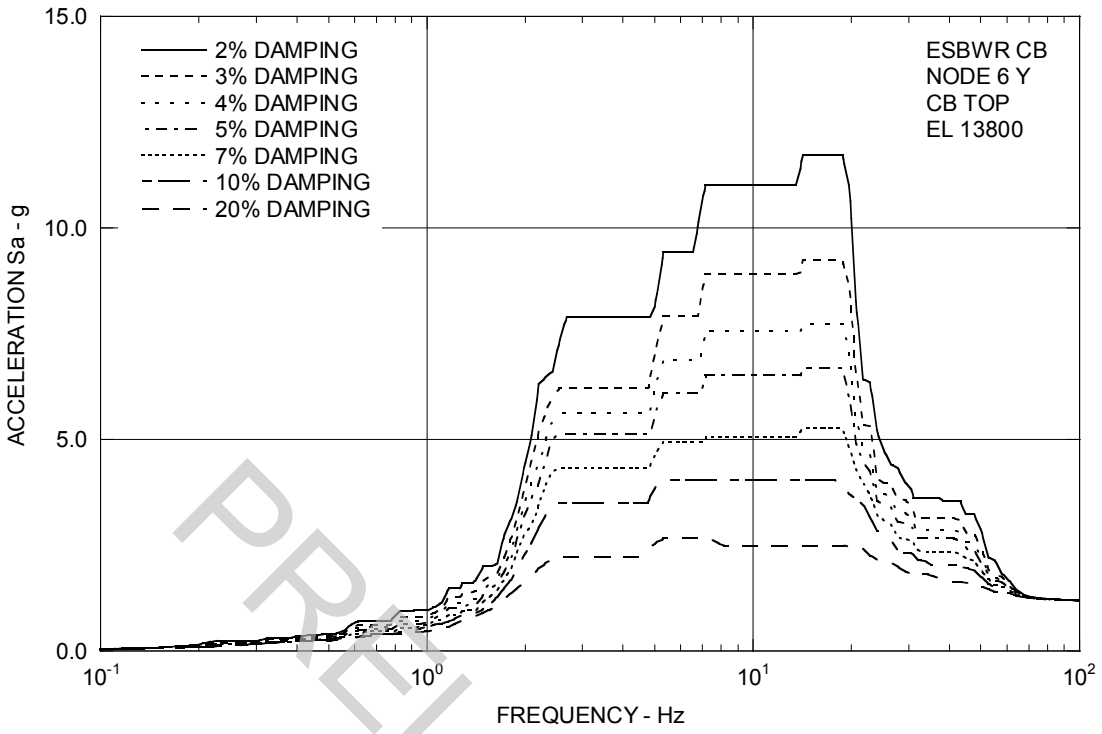

Figure 3A.9-2g. Enveloping Floor Response Spectra – CB Top Y

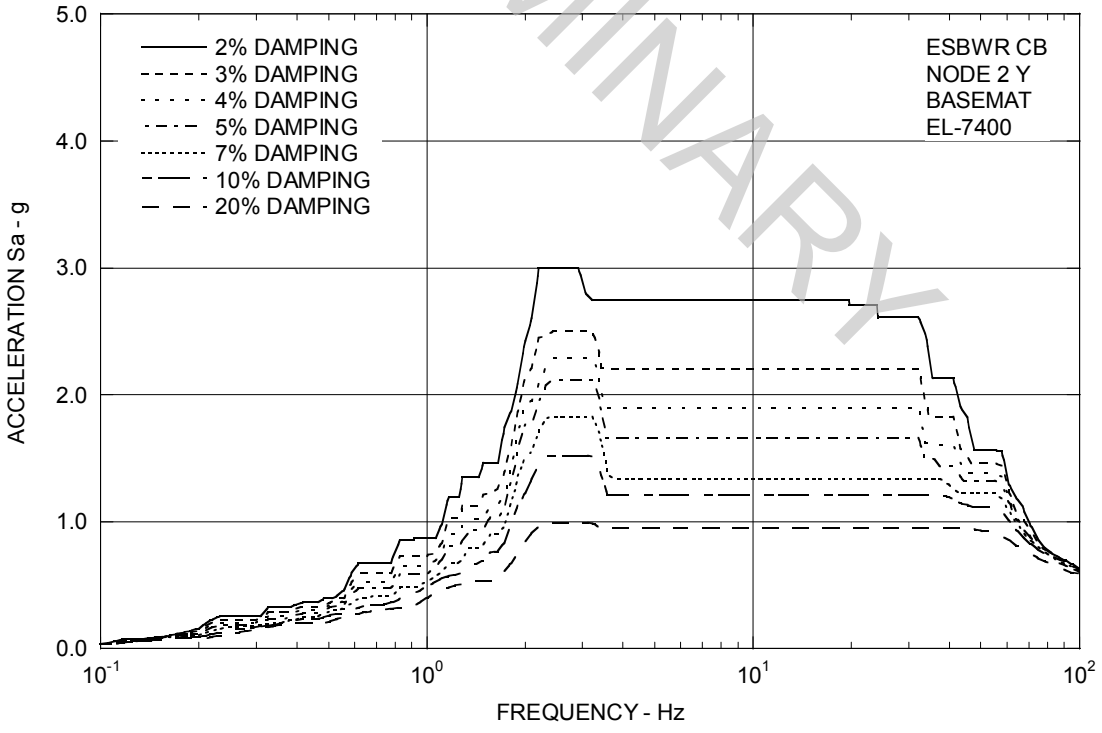

Figure 3A.9-2h. Enveloping Floor Response Spectra – CB Basemat Y

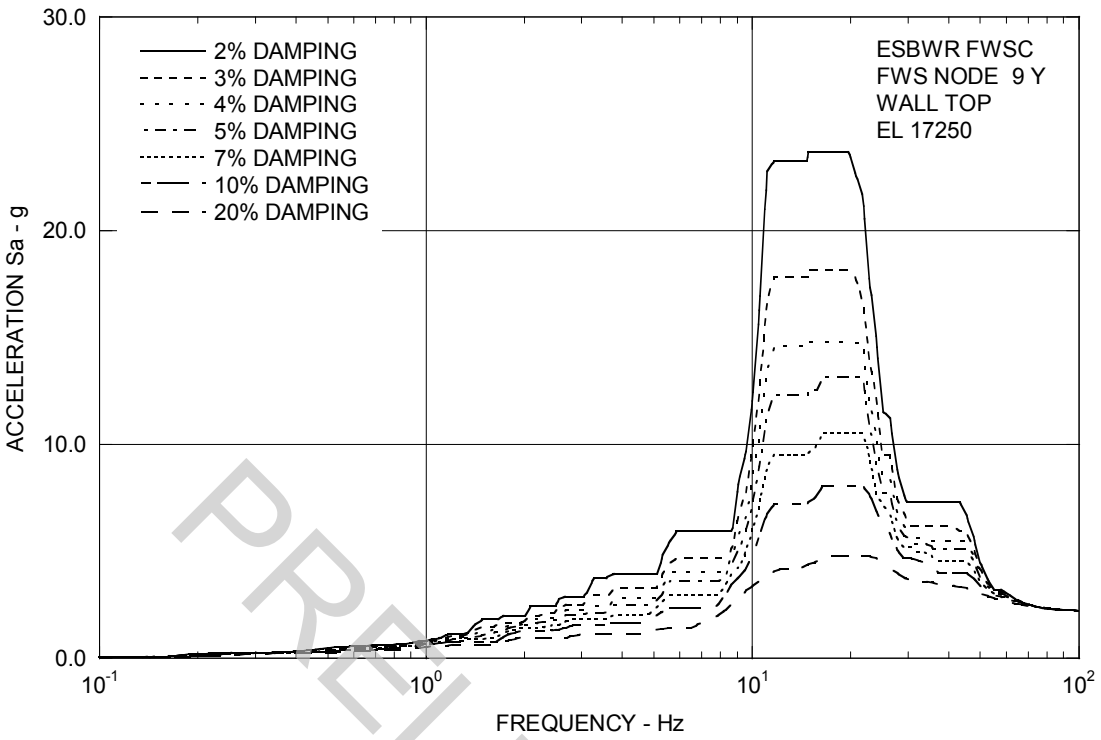

Figure 3A.9-2i. Enveloping Floor Response Spectra – FWS Wall Top Y

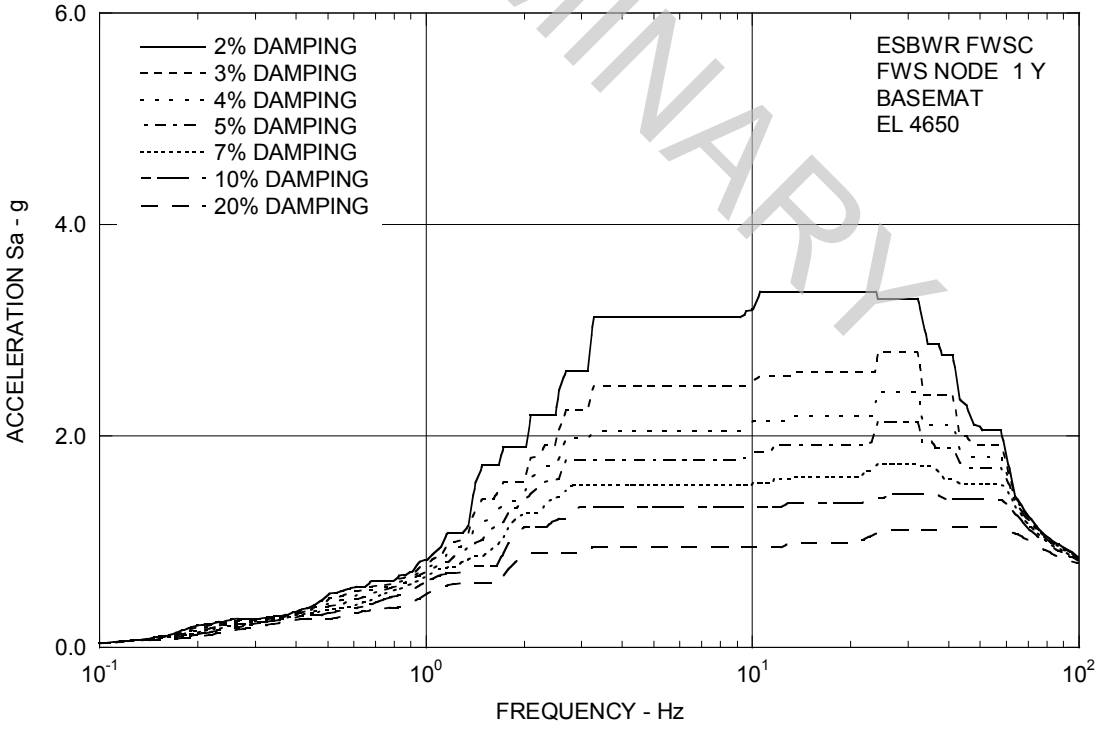

Figure 3A.9-2j. Enveloping Floor Response Spectra – FWS Basemat Y

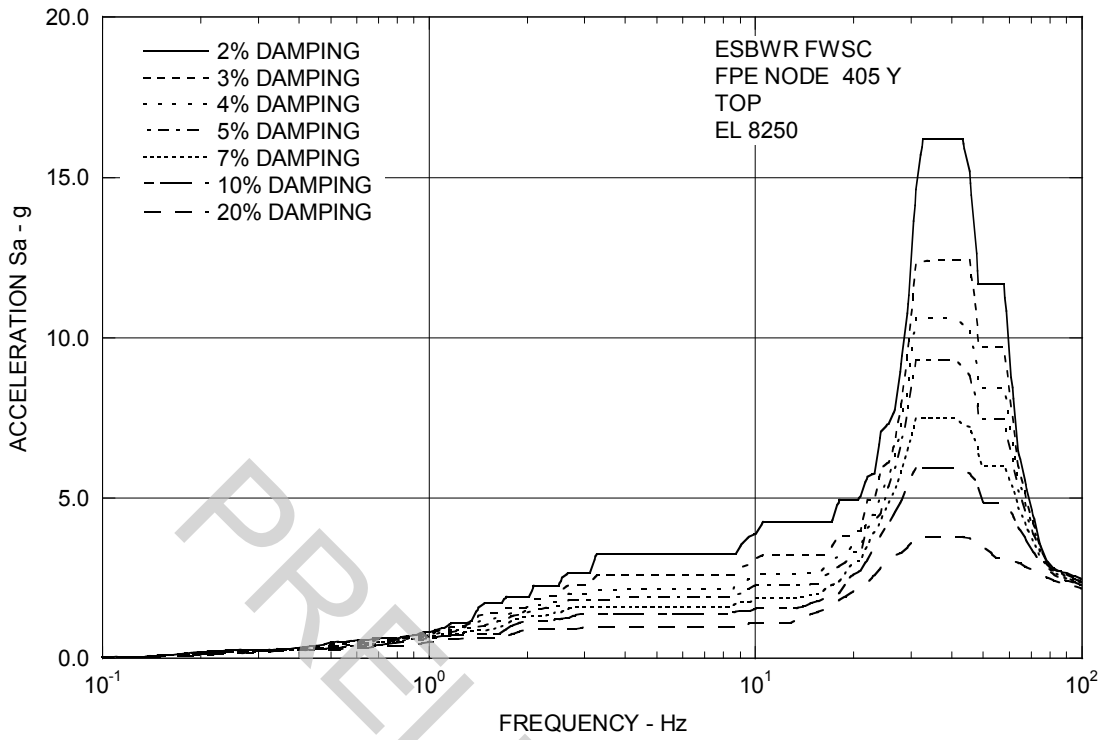

Figure 3A.9-2k. Enveloping Floor Response Spectra – FPE Top Y

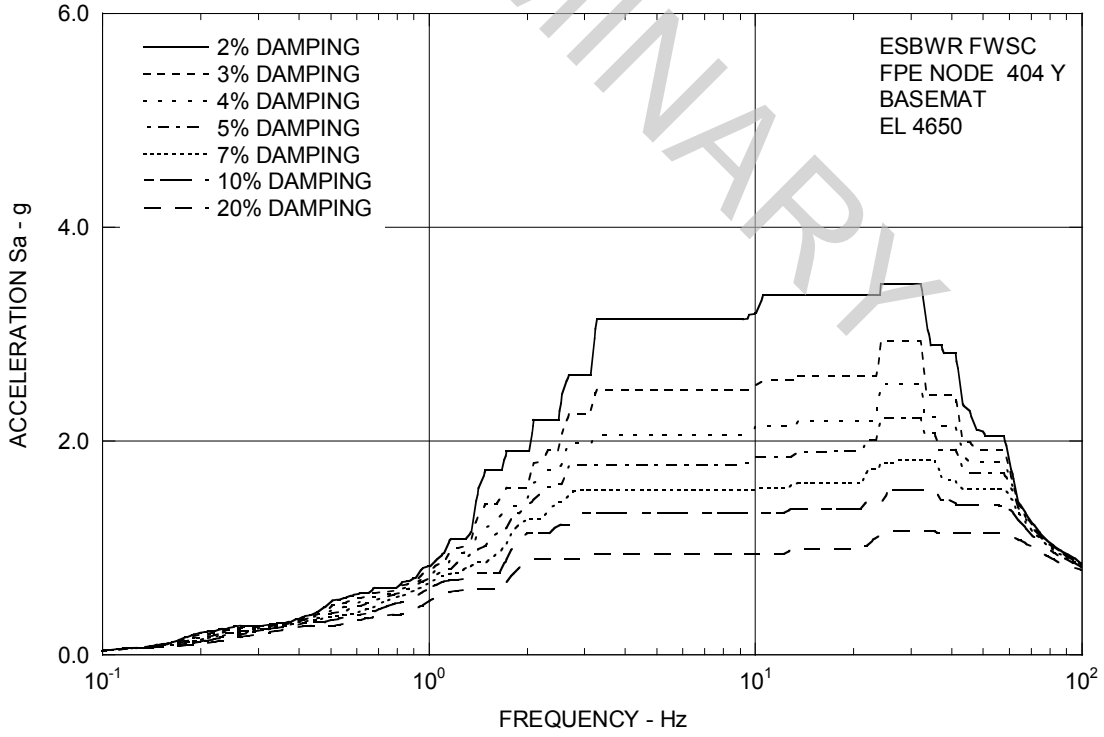

Figure 3A.9-2l. Enveloping Floor Response Spectra – FPE Basemat Y

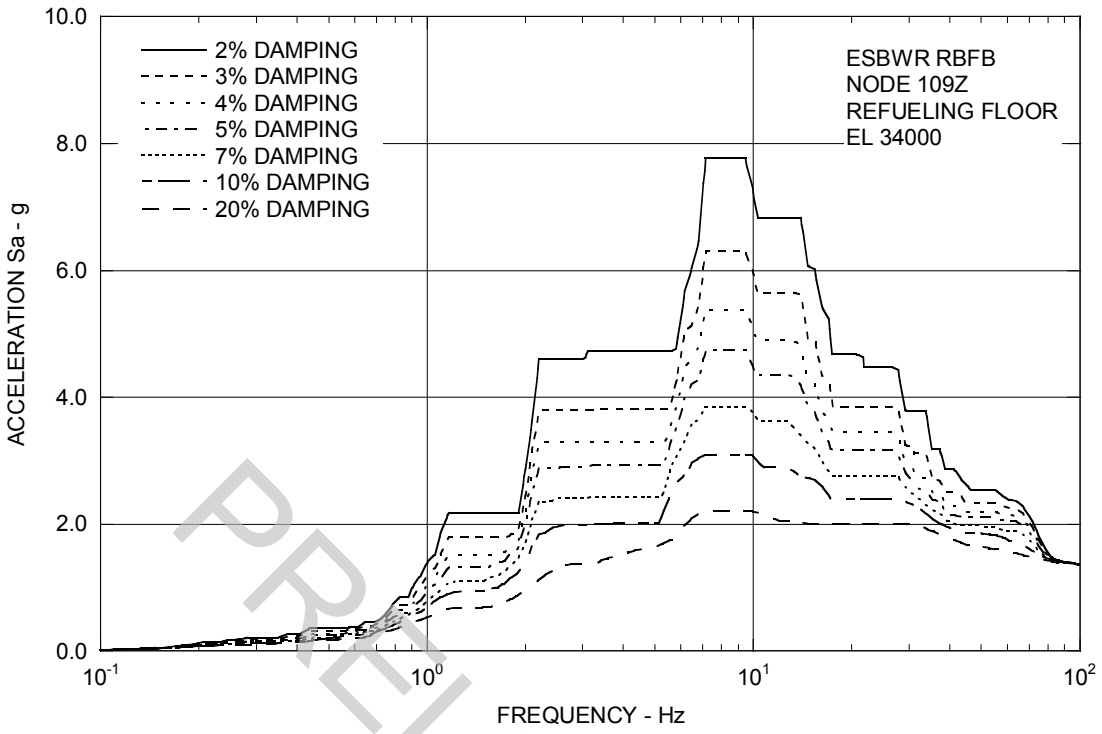

Figure 3A.9-3a. Enveloping Floor Response Spectra – RB/FB Refueling Floor Z

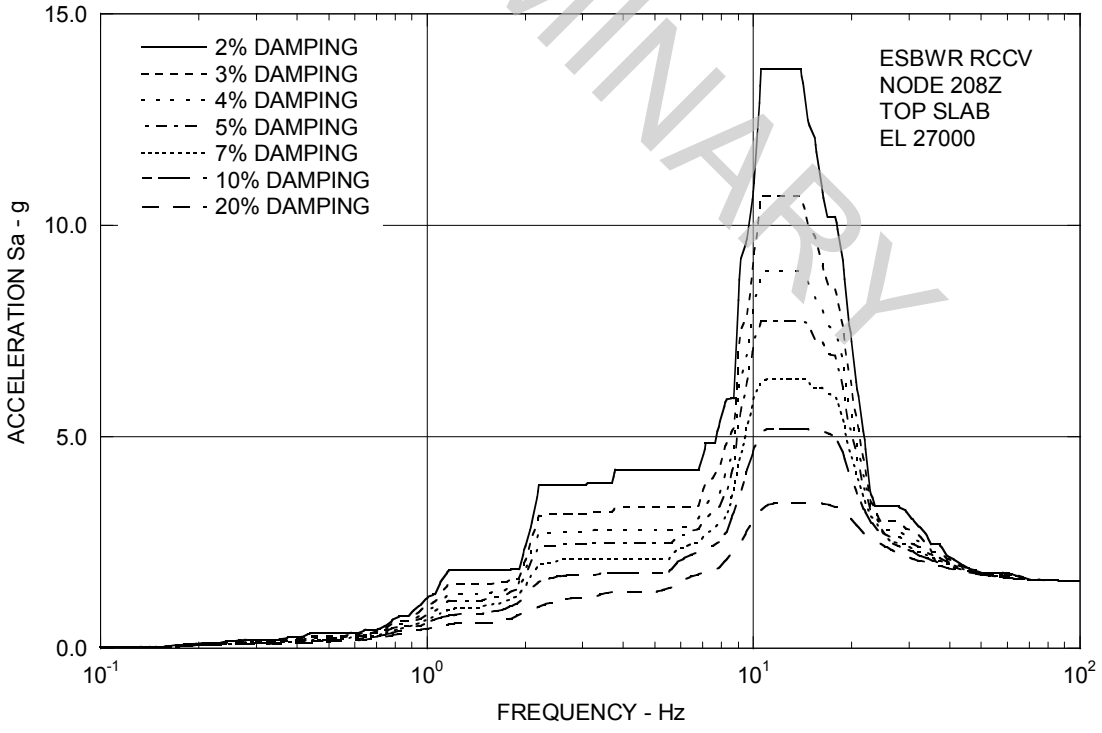

Figure 3A.9-3b. Enveloping Floor Response Spectra – RCCV Top Slab Z

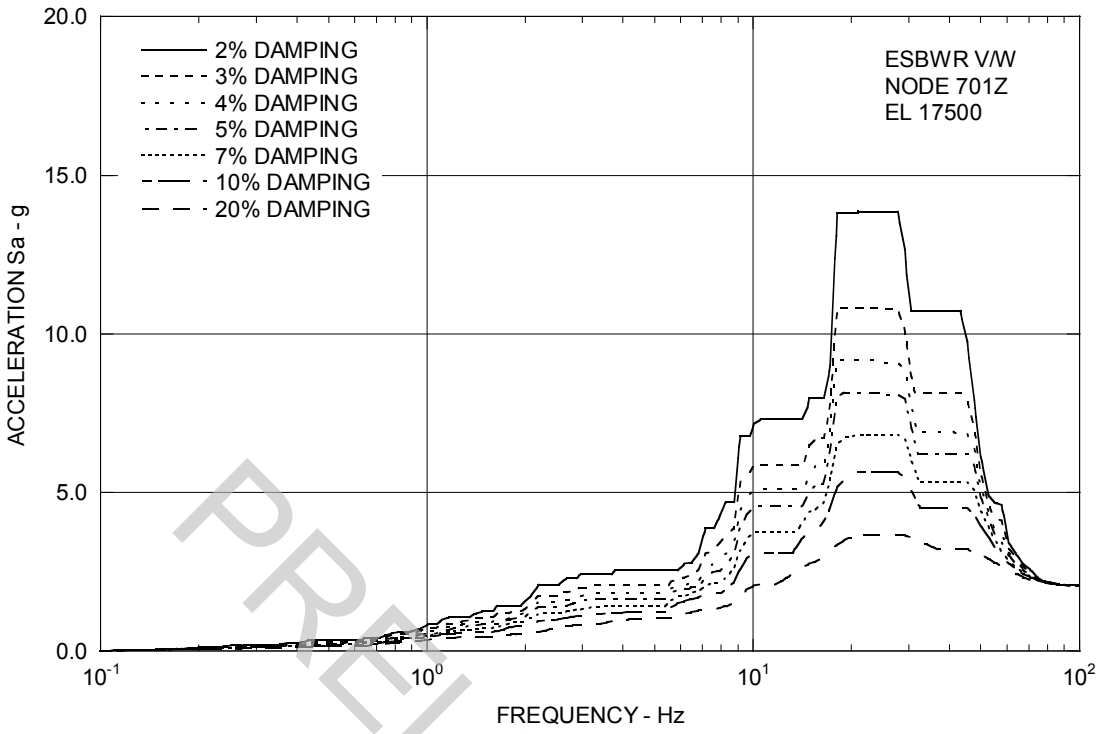

Figure 3A.9-3c. Enveloping Floor Response Spectra – Vent Wall Top Z

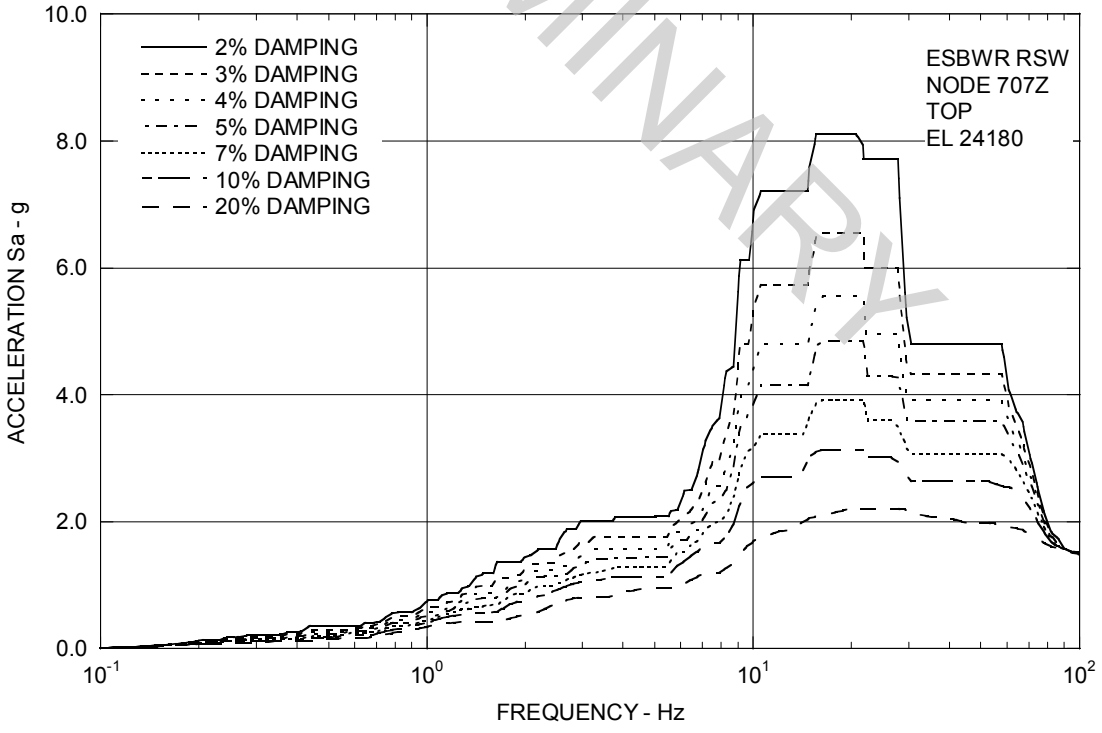

Figure 3A.9-3d. Enveloping Floor Response Spectra – RSW Top Z

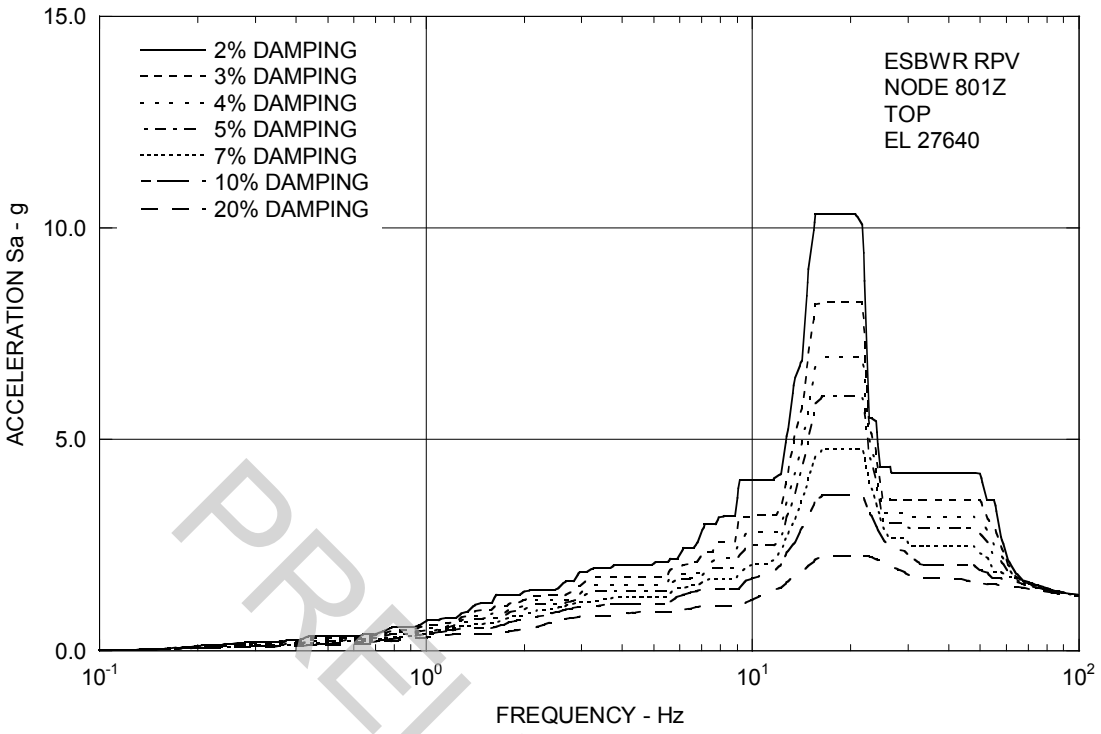

Figure 3A.9-3e. Enveloping Floor Response Spectra – RPV Top Z

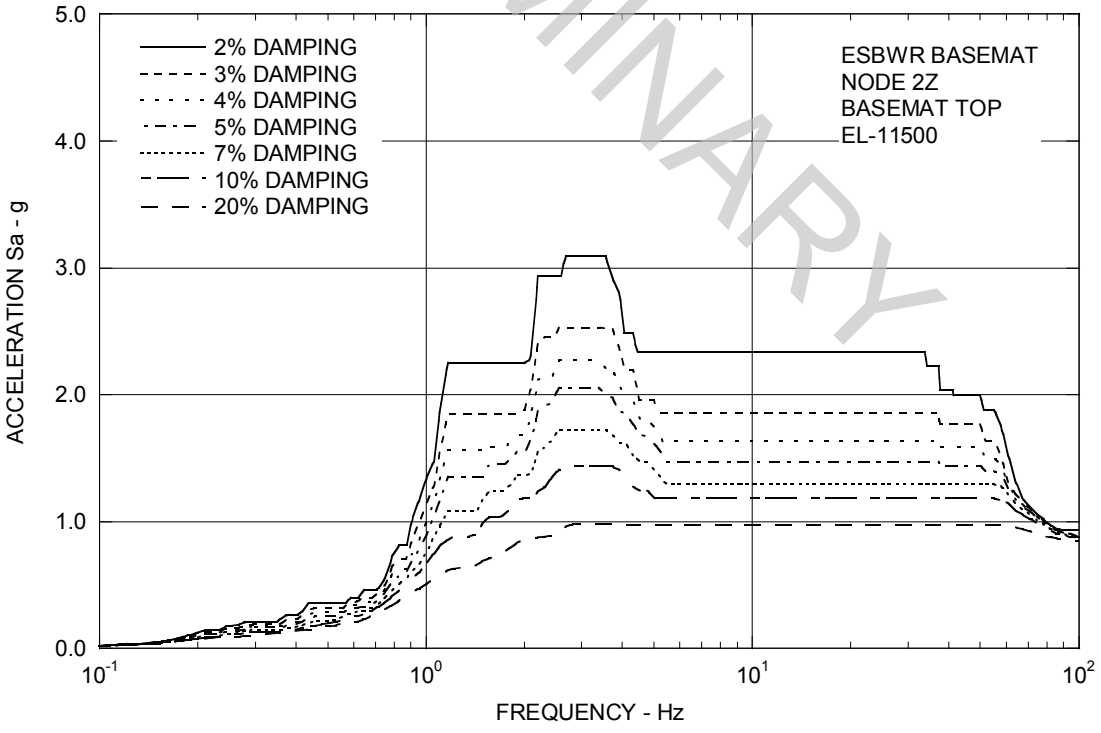

Figure 3A.9-3f. Enveloping Floor Response Spectra – RB/FB Basemat Z

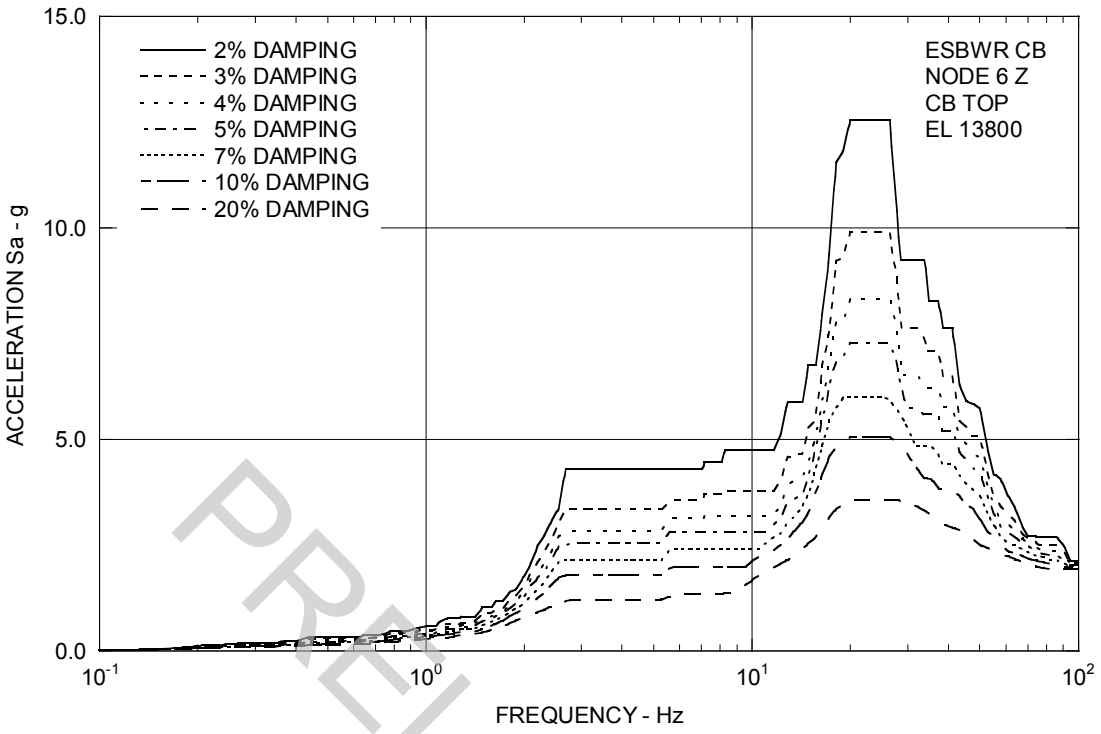

Figure 3A.9-3g. Enveloping Floor Response Spectra – CB Top Z

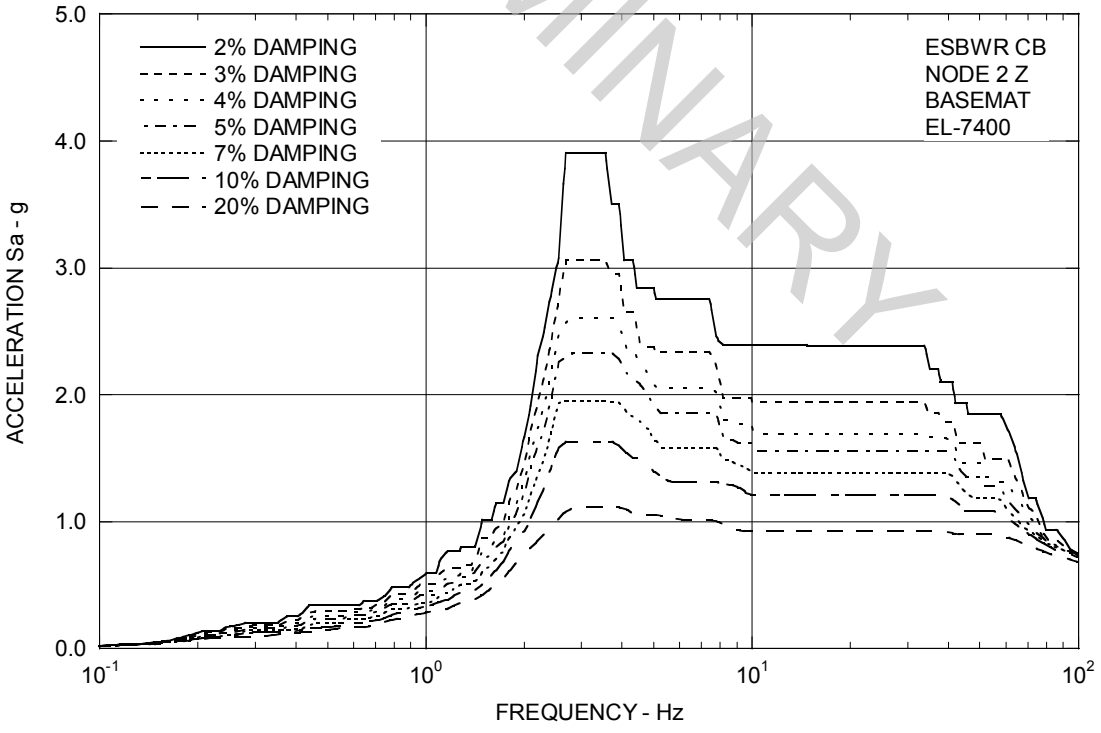

Figure 3A.9-3h. Enveloping Floor Response Spectra – CB Basemat Z

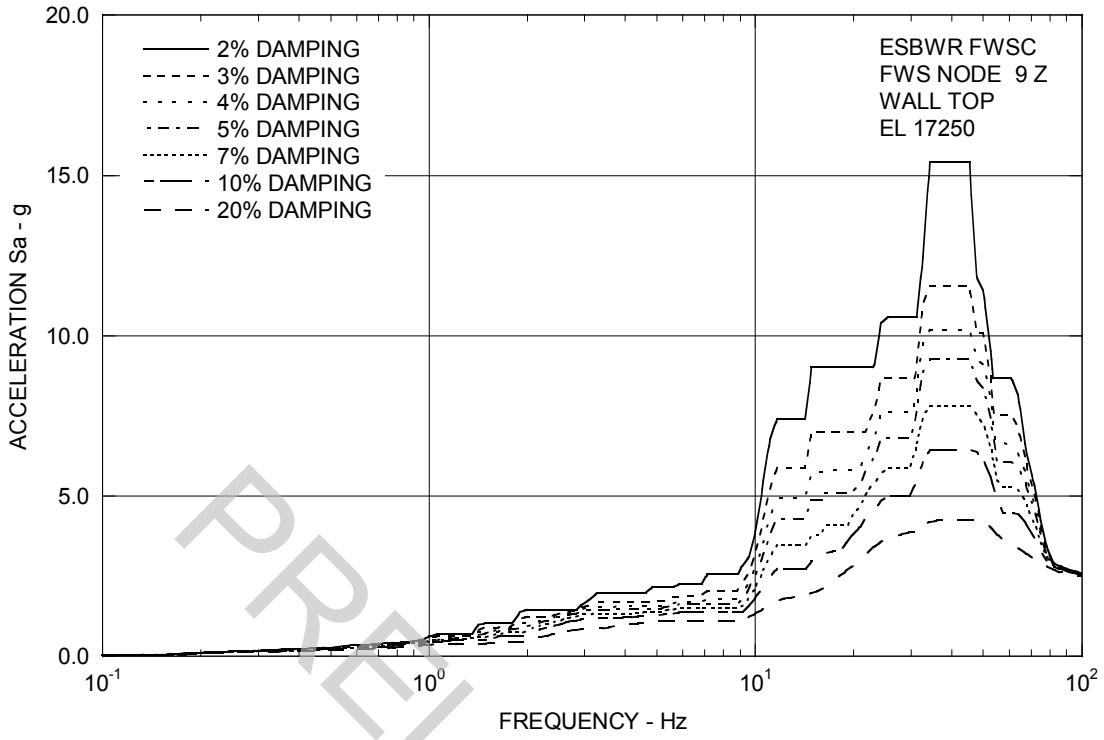

Figure 3A.9-3i. Enveloping Floor Response Spectra – FWS Wall Top Z

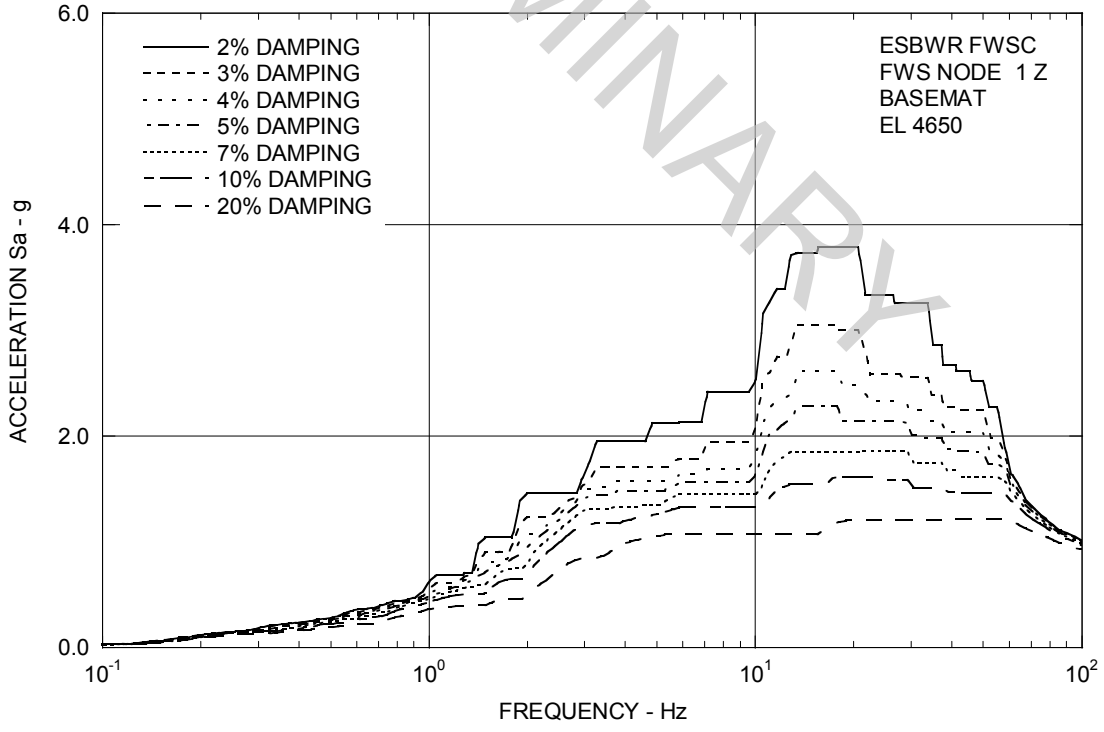

Figure 3A.9-3j. Enveloping Floor Response Spectra – FWS Basemat Z

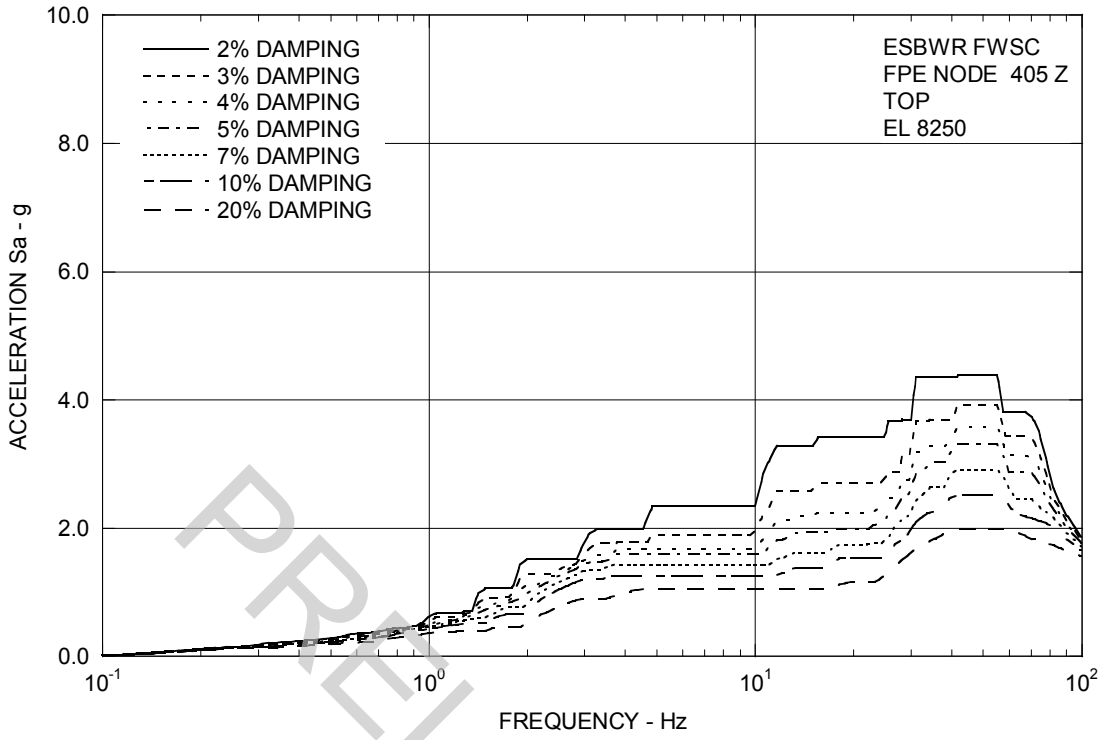

Figure 3A.9-3k. Enveloping Floor Response Spectra – FPE Top Z

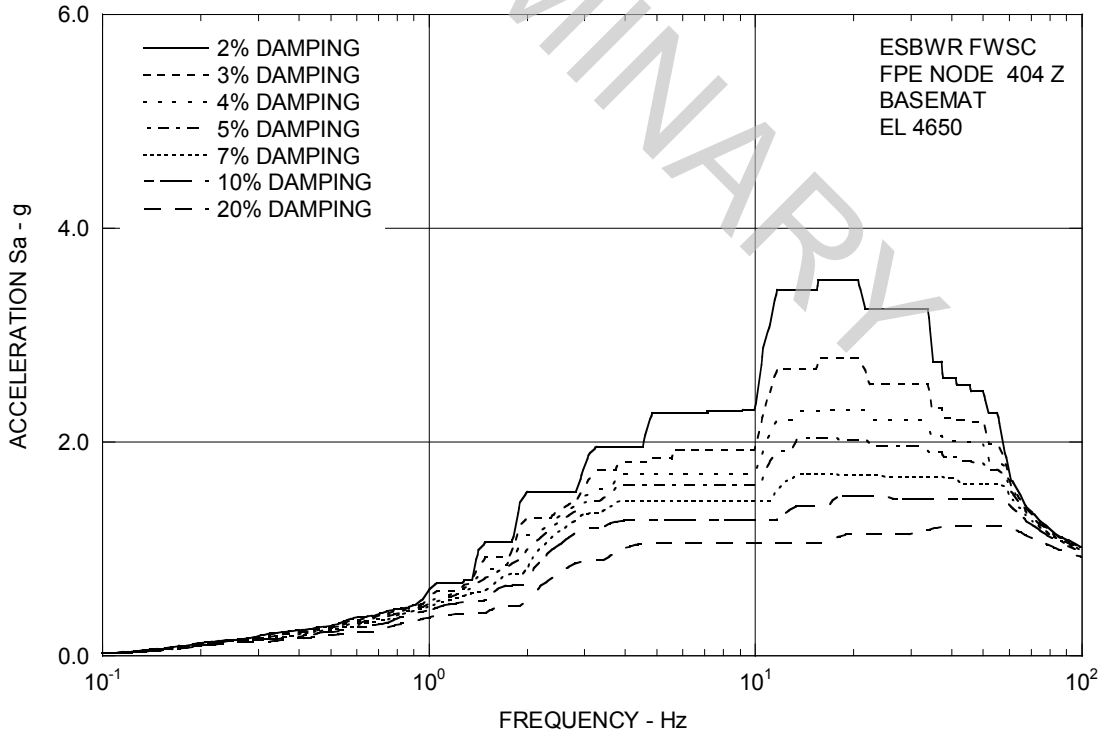

Figure 3A.9-3l. Enveloping Floor Response Spectra – FPE Basemat Z

3B. CONTAINMENT HYDRODYNAMIC LOAD DEFINITIONS

This appendix provides the hydrodynamic loads applied in structural evaluations of the primary containment. The methodology used to develop these load definitions, and the justification for their applicability to ESBWR is given in Reference 3B-1.

3B.1 SAFETY RELIEF VALVE LOADS

3B.1.1 Oscillating Pressure Load Into the Suppression Pool from Safety Relief Valves

The distributions of safety relief valve (SRV) loads applied to structural evaluation of the boundary of the suppression pool are shown in Reference 3B-1.

3B.1.2 Pressure Time History

For acceleration response spectra generation, time histories of SRV are needed. Reference 3B-1 shows a typical pressure history applied to structural evaluation that is normalized to the maximum pressure value, with a frequency of 8 Hz. This pressure time history profile can be used in digitizing the pressure amplitude variation with time for other frequencies varying from 5 to 12 Hz. It should be noted that the bubble pressure decays to 1/3 P_{max} with 5 cycles for any frequency between 5 and 12 Hz.

3B.2 ACCIDENT PRESSURE LOADS

During a loss-of-coolant-accident, the suppression pool boundary is subjected to hydrodynamic loads, such as pool swell (PS), condensation oscillation (CO) and chugging loads. These loads are not concurrent. The event-time relationship is shown in Reference 3B-1.

These PS boundary pressures are applied together with a drywell pressure of 345 kPaG (50 psig). The pressure distribution is shown in Reference 3B-1.

The spatial distribution of CO and chugging loads on the boundary of the suppression pool is shown in Reference 3B-1. Dynamic load factors to convert the dynamic loads to static equivalent loads are also included in the reinforced concrete containment vessel and liner design.

For response spectra generation, pressure-time histories of CO and chugging are described in Reference 3B-1.

Each CO load is considered symmetric (in-phase for all vents). Each chugging load is considered symmetric (in-phase for all vents) and asymmetric (half of vents out-of-phase with other half).

In addition to CO and chugging presented above, horizontal vent chugging and local CO loads are considered as follows:

- Horizontal Vent Chugging
  - Location: each of top horizontal vents
  - Loading: triangular pulse in the upward direction for global dynamic response analysis for vent pipe and pedestal design is shown in Reference 3B-1

  - Phasing: two cases, in-phase of all vents and half of vents 180° out-of phase with other half
  - Combination with pool Chugging: Square Root of the Sum of the Squares
- Local Condensation Oscillation
  - Location: within 2 vent diameters for each of the bottom horizontal vents
  - Loading: triangular pulses as shown in Reference 3B-1
  - Phasing: in-phase of all vents
  - Combination with pool CO: absolute sum

The CO and chugging load magnitudes are proprietary information. The proprietary magnitudes used are given in Reference 3B-1.

3B.3 COMBINED LICENSE (COL) INFORMATION

None.

3B.4 REFERENCES

3B-1 GE Hitachi Nuclear Energy, "ESBWR Containment Load Definition," NEDE-33261P, Class III (Proprietary), Revision 2, June 2008, and NEDO-33261, Class I (non-proprietary), Revision 2, June 2008.

3C. COMPUTER PROGRAMS USED IN THE DESIGN AND ANALYSIS OF SEISMIC CATEGORY I STRUCTURES

3C.1 INTRODUCTION

The following Seismic Category I structures and their foundations of the Nuclear Island are analyzed and/or designed using the computer programs described in this appendix:

(1) Concrete Containment Structure and Passive Containment Cooling System (PCCS) Condenser and Supports

(2) Reactor Building (RB)

(3) Fuel Building (FB)

(4) Control Building (CB)

(5) Firewater Service Complex (FWSC)

3C.2 STATIC AND DYNAMIC STRUCTURAL ANALYSIS PROGRAM (NASTRAN)

3C.2.1 Description

NASTRAN is a general purpose computer program for finite element analysis; its capabilities include: static response to concentrated and distributed loads; static response to thermal expansion; static response to enforced displacements; dynamic response to transient loads; dynamic response to steady-state sinusoidal loads; dynamic response to random excitation; and determination of eigenvalues for use in vibration analysis.

3C.2.2 Validation

The MSC Software Corporation of Santa Ana, California developed NASTRAN. The program validation documentation is available at MSC Software Corporation.

3C.2.3 Extent of Application

This program is used for the static and eigenvalue analysis of the concrete containment, RB, FB, CB and FWSC. This program is also used for the static and dynamic analysis of the Drywell Head and containment internal structures.

3C.3 ABAQUS AND ANACAP-U

3C.3.1 Description

ABAQUS/Standard is a widely used, commercially available finite-element program with a broad range of analysis capabilities. Implicit formulations for steady state solutions, transient thermal solutions and static stress analyses are employed using 3-dimensional models of continuum concrete elements, truss-type reinforcement sub-elements, and plate and membrane elements for liners and other steel components. Classical von Mises plasticity models and strength degradation with elevated temperature for the steel material are used for the nonlinear analyses. The ANACAP-U software is an advanced concrete constitutive model coupled to the ABAQUS software as a user subroutine. The ANACAP-U concrete material model provides

formulations for concrete cracking under tensile and shear loads, post-cracking shear stiffness and shear capacity as a function of crack width and shear deformations, with yielding and strain softening (crushing) under large compressive loads. Modulus of elasticity and strength degradation with increasing temperatures is also included for the concrete model.

3C.3.2 Validation

ABAQUS is written and maintained by ABAQUS, Inc. of Providence R.I., (formerly Hibbitt, Karlssen, and Sorensen, Inc.). The program has an extensive library of example problems that are used for verification and validation testing. Additional descriptions and information on the quality controls can be found on the ABAQUS web site, (www.abaqus.com). The ANACAP-U concrete material model for use with the ABAQUS program is written and maintained by ANATECH Corp, San Diego, CA. This software has been extensively verified with test problems and also validated against large-scale test results for the performance of reinforced concrete structures. ANACAP-U Program validation documentation is available at ANATECH Corp.

3C.3.3 Extent of Application

The ABAQUS/ANACAP-U software coupling is used in the nonlinear analyses for the structural performance of the reinforced concrete containment under loss-of-coolant-accident thermal conditions.

3C.4 CONCRETE ELEMENT CRACKING ANALYSIS PROGRAM (SSDP-2D)

3C.4.1 Description

SSDP-2D computes stresses in a thick concrete element under thermal and/or non-thermal (such as dead load, service loads) loads, and considers the effect of concrete cracking. The element that represents a section of a concrete shell or slab may include two layers of orthogonal reinforcing. It does not include the effect of the liner.

SSDP-2D calculates the stresses considering two-dimensional equilibrium conditions of section forces with the existence of thermal loads and concrete cracking. It is assumed in the code that concrete has an anisotropic property and that cracked concrete has reduced shear stiffness. Concrete is assumed to have no tensile strength.

3C.4.2 Validation

SSDP-2D is written and maintained by Shimizu Corporation of Tokyo, Japan. Program validation documentation is available at Shimizu Corporation.

3C.4.3 Extent of Application

This program is used for the analysis of the concrete containment, RB, FB, CB and FWSC.

3C.5 HEAT TRANSFER ANALYSIS PROGRAM (TEMCOM2)

3C.5.1 Description

TEMCOM2 solves a temperature distribution in a two-dimensional model based on a finite differential method. It performs analyses under the following conditions

- Element: triangle and quadrilateral elements
- Surface heat transfer: convection and radiation
- Temperature condition: steady-state and transient temperature conditions

3C.5.2 Validation

TEMCOM2 is written and maintained by Shimizu Corporation of Tokyo, Japan. Program validation documentation is available at Shimizu Corporation.

3C.5.3 Extent of Application

This program is used in the transient heat transfer analysis of the concrete containment and the RB.

3C.6 STATIC AND DYNAMIC STRUCTURAL ANALYSIS SYSTEMS: ANSYS

3C.6.1 Description

ANSYS is a large, finite element program for a broad range of analyses types. The structural analysis capabilities include material and geometric non-linear analysis, static analysis and a variety of dynamic analyses.

The element used in concrete cracking analysis allows for a full non-linear analysis of reinforced concrete with cracking and crushing of concrete.

3C.6.2 Validation

ANSYS is maintained by ANSYS INC., located at 275 Technology Drive, Canonsburg, PA, 15317.

3C.6.3 Extent of Application

This program is used for the containment dynamic analysis of containment loads, and for the static and dynamic analysis of the PCCS condenser.

3C.7 SOIL-STRUCTURE INTERACTION

3C.7.1 Dynamic Soil-Structure Interaction Analysis Program—DAC3N

3C.7.1.1 Description

DAC3N is a three-dimensional dynamic analysis program used for the seismic response analysis of a building structure considering soil-structure interaction (SSI). The response analysis is performed using the time history method solved by direct integration, Newmark's beta method. Eigenvalue analysis is performed using Subspace method.

In the DAC3N, the SSI system is modeled by the combination of soil spring and damping coefficient. Spring and damping coefficient are determined as frequency independent values, which fit the frequency dependent real and imaginary parts of soil spring obtained by the theoretical methods, such as vibration admittance theory based on three-dimensional wave propagation theory for uniform half space soil.

As mass elements, lumped masses and consistent masses are available. Structural elements, such as beams, trusses, dampers and direct input matrices are available in this program.

This program has nonlinear analytical capability.

3C.7.1.2 Validation

DAC3N is coded and maintained by Shimizu Corporation of Tokyo, Japan. Program validation documentation is available at Shimizu Corporation.

3C.7.1.3 Extent of Application

This program is used to perform the SSI analysis without embedment effect for Seismic Category I structures.

3C.7.2 Dynamic Soil-Structure Interaction Analysis Program – SASSI2000

3C.7.2.1 Description

SASSI2000 is used to solve a wide range of dynamic SSI problems in two or three dimensions. It was developed at the University of California, Berkeley in 1982 under the technical direction of John Lysmer. The program is based on the finite-element method formulated in the frequency domain using a substructuring technique.

3C.7.2.2 Validation

SASSI version 2000 was obtained from the University of California, Berkeley and implemented by Shimizu Corporation of Tokyo, Japan on the PC computer on Linux OS. Program validation documentation is available at UC Berkeley.

3C.7.2.3 Extent of Application

This program is used to perform the SSI analysis for Seismic Category I structures.

3C.7.3 Free-Field Site Response Analysis – SHAKE

3C.7.3.1 Description

SHAKE is a program, which can perform the free-field site response analysis. It was developed at the University of California, Berkeley by B. Schnabel, John Lysmer and H.B. Seed in 1972. The program is based on the theory of one-dimensional propagation of shear waves in the vertical direction in a horizontally-layered visco-elastic soils system overlying an elastic half-space medium.

SHAKE also has a function to account for non-linearities in soil shear modulus and hysteresis damping as functions of shear strain in soil by the use of equivalent-linear soil properties using

an iterative equivalent linearization procedure to obtain constant values of shear modulus and hysteresis damping ratio compatible with the effective shear strain in each soil layer.

3C.7.3.2 Validation

SHAKE was developed at the University of California, Berkeley and implemented by Shimizu Corporation of Tokyo, Japan on the Hewlett Packard computer workstation. Program validation documentation is available at UC Berkeley.

3C.7.3.3 Extent of Application

SHAKE is used to generate the free-field site response motions required in the seismic SSI analysis.

3D. COMPUTER PROGRAMS USED IN THE DESIGN OF COMPONENTS, EQUIPMENT, AND STRUCTURES

3D.1 INTRODUCTION

As discussed in Subsection 3.9.1.2, this appendix describes the major computer programs used in the analysis of the safety-related components, equipment, and structures. The quality of the programs and the computed results are controlled. The programs are verified for their application by appropriate methods, such as hand calculations, or comparison with results from similar programs, experimental tests, or published literature, including analytical results or numerical results to the benchmark problems. For computer program user details see Table 3D.1-1.

3D.2 FINE MOTION CONTROL ROD DRIVE (FMCRD)

3D.2.1 ABAQUS

3D.2.1.1 Description

See Subsection 3D.3.5.1.

3D.2.1.2 Validation

Hand calculations using theoretical equations published in literature are performed to demonstrate the program's applicability and validity.

3D.2.1.3 Extent of Application

This program is used for the elastic stress analysis and vibration analysis of the FMCRD. The program calculates elastic stresses for level D, faulted limits, but the ASME Code Section III, Appendix F limits are not within the program. Evaluation against level D limits is performed by hand calculation.

3D.2.2 ANSYS

3D.2.2.1 Description

See Subsection 3D.3.1.1.

3D.2.2.2 Validation

Hand calculations using theoretical equations published in literature are performed.

3D.2.2.3 Extent of Application

This program is used for the elastic stress analysis and vibration analysis of the FMCRD. The program calculates elastic stresses for level D, faulted limits, but the ASME Code Section III, Appendix F limits are not within the program. Comparison of calculated stresses to level D limits is performed by hand calculation.

3D.3 REACTOR PRESSURE VESSEL AND INTERNALS

Computer programs used in the analysis of the reactor pressure vessel (RPV), core support structures, and other safety-class reactor internals are described below and in Subsection 4.1.4.1.

3D.3.1 ANSYS

3D.3.1.1 Description

The ANSYS computer program is a finite element large-scale general-purpose program for the solution of several classes of engineering analysis problems. Analysis capabilities include static and dynamic, plastic, creep and swelling, small and large deflections, and other applications like thermal analysis, material non-linearities, contact analysis, etc.

3D.3.1.2 Validation

ANSYS applicability and validity are demonstrated by running a series of verification cases that exercise the elements and options used in the finite element code. The verification cases provided by ANSYS, Inc. are extracted from textbooks in which classical or theoretical solutions are published or can readily be obtained by simple hand calculations.

3D.3.1.3 Extent of Application

This program is used for the elastic and inelastic stress analysis and vibration analysis of the RPV and internals. The extent and limitation are determined by verification cases performed to qualify ANSYS as an Approved Production Program that is verified and documented for design applications or for all technical activities used in developing design-related information. The program calculates elastic and inelastic stresses for level D, faulted limits, but the ASME Code Section III, Appendix F limits are not within the program. Comparison of calculated stresses to ASME Code limits is performed in hand calculations. The computer program may be used for calculating stress and cumulative usage factors for Class 1, 2, or 3 components, but the environmental effects are addressed outside ANSYS in accordance with Regulatory Guide (RG) 1.207 and NUREG/CR-6909.

3D.3.2 Dynamic Stress Analysis of Axisymmetric Structures Under Arbitrary Loading - ASHSD2

3D.3.2.1 Description

This FORTRAN program was created at the Earthquake Engineering Research Center, University of California, Berkeley. A finite element method is presented for the dynamic analysis of complex axisymmetric structures subjected to any arbitrary static or dynamic loading or base acceleration. The three-dimensional axisymmetric continuum is represented either as an axisymmetric thin shell or as a solid of revolution or as a combination of both. The axisymmetric shell is discretized as a series of frustrums of cones, and the solid of revolution as triangular or quadrilateral “toroids” connected at their nodal point circles. Hamilton's variational principle is used to derive the equations of motion for this discrete structure. This leads to a mass matrix, stiffness matrix, and load vectors that are all consistent with the assumed displacement field. But to minimize computer storage and execution time, a diagonal mass matrix has been assumed in writing the computer program (with the input diagonalized

accordingly by coordinate system transform). These equations of motion are solved numerically through the time domain either by direct integration or by modal superposition. In both cases, a step-by-step integration procedure was used.

3D.3.2.2 Validation

Hand calculations using theoretical equations published in literature are performed to demonstrate the program's applicability and validity.

3D.3.2.3 Extent of Application

This program is used to calculate elastic stresses in the RPV and shroud support, using axisymmetric shell and solid elements for axisymmetric and non-axisymmetric static loading. The program calculates stresses for level D, faulted limits, but the ASME Code Section III, Appendix F limits are not within the program. Comparison of calculated stresses to ASME Code limits is performed in hand calculations.

3D.3.3 EVAST

3D.3.3.1 Description

This FORTRAN program was created by Babcock-Hitachi K.K. to calculate stress intensities, perform fatigue evaluation, and evaluate thermal ratcheting.

3D.3.3.2 Validation

Hand calculations are performed to demonstrate the program's applicability and validity.

3D.3.3.3 Extent of Application

This program is used to evaluate the primary stress intensities and fatigue and thermal ratcheting of the shroud support. Where fatigue curves are used, environmental effects are addressed outside EVAST in accordance with RG 1.207 and NUREG/CR-6909.

3D.3.4 TACF

3D.3.4.1 Description

This FORTRAN program was created by Babcock-Hitachi K.K. to evaluate temperature distribution.

3D.3.4.2 Validation

Hand calculations using theoretical equations published in literature are performed to demonstrate the program's applicability and validity.

3D.3.4.3 Extent of Application

This program is used to evaluate the steady and non-steady state axisymmetric thermal conduction of the RPV and shroud support.

3D.3.5 ABAQUS

3D.3.5.1 Description

This PC-based program was created by ABAQUS, Inc. ABAQUS solves traditional implicit finite element analyses, such as static, dynamics, and thermal, all powered with a wide range of contact and nonlinear material options. ABAQUS also has optional add-on and interface products that address design sensitivity analysis. ABAQUS enables a wide range of linear and nonlinear engineering simulations.

3D.3.5.2 Validation

Hand calculations using theoretical equations published in literature are performed to demonstrate the program's applicability and validity.

3D.3.5.3 Extent of Application

This program is used for elastic and plastic stress analysis in addition to temperature distribution analysis of the RPV. The program calculates stresses for level D, faulted limits, but the ASME Code Section III, Appendix F limits are not within the program. Comparison of calculated stresses to ASME Code limits is performed in hand calculations.

3D.3.6 FEMFL

3D.3.6.1 Description

This FORTRAN program was created by Babcock-Hitachi K.K. to evaluate elastic stresses.

3D.3.6.2 Validation

Hand calculations using theoretical equations published in literature are performed to demonstrate the program's applicability and validity.

3D.3.6.3 Extent of Application

This program is used for elastic stress analysis using axisymmetric structural shell and solid elements. The static loading may be axisymmetric or non-axisymmetric. The program is used in the analysis of the RPV. The program calculates stresses for level D, faulted limits, but the ASME Code Section III, Appendix F limits are not within the program. Comparison of calculated stresses to ASME Code limits is performed in hand calculations.

3D.3.7 SEISM

3D.3.7.1 Description

See Subsection 4.1.4.1.3.

3D.3.7.2 Validation

Test cases analyzed and compared with previous design problems are performed to demonstrate the program's applicability and validity.

3D.3.7.3 Extent of Application

In addition to those applications outlined in Chapter 4, this program is used to evaluate non-linear fuel lift analysis with spring, stop, and friction elements.

3D.3.8 PVElite

3D.3.8.1 Description

PVElite is a comprehensive program for the complete structural design or analysis of horizontal vessels and shell and tube heat exchangers. PVElite evaluates the entire vessel, analyzing the effects of weight and bending due to wind and seismic loads. It combines these overall loads with pressure to design and/or check vessel wall thickness.

3D.3.8.2 Validation

Hand calculations for a nozzle on a cylindrical vessel and a bracket or support on a cylindrical vessel are performed to validate the program.

3D.3.8.3 Extent of Application

This program is used to evaluate local stresses in the vessel wall due to externally applied loads on nozzles, supports and brackets.

3D.3.9 ANSYS Workbench

3D.3.9.1 Description

ANSYS Workbench is a unified working environment for developing and managing computer-aided engineering information and for setting up and working with finite element and computational fluid dynamics models.

3D.3.9.2 Validation

The program will be validated by implementing a series of verification test cases (provided with the program) and comparing the results to known results (provided with the program).

3D.3.9.3 Extent of Application

Workbench is used to condition models for design simulations, perform finite element analysis simulations and optimize designs.

3D.3.10 Structural Analysis Program - SAP4G

3D.3.10.1 Description

See Subsection 3D.5.1.1.

3D.3.10.2 Validation

Hand calculations and test cases are used to demonstrate the program's applicability and validity.

3D.3.10.3 Extent of Application

SAP4G is used to determine the dynamic response for the reactor vessel and internals.

3D.4 PIPING

3D.4.1 Piping Analysis Program – PISYS

3D.4.1.1 Description

PISYS is a computer code for analyzing piping systems subjected to both static and dynamic piping loads. Finite element models of a piping system formed by assembling stiffness matrices represent standard piping components. The piping elements are connected to each other via nodes called pipe joints. It is through these joints that the model interacts with the environment and loading of the piping system becomes possible. PISYS is based on the linear elastic analysis in which the resultant deformations, forces, moments, and accelerations at each joint are proportional to the loading and the superposition of loading is valid.

PISYS has a full range of static and dynamic load analysis options. Static analysis includes dead weight, uniformly distributed weight, thermal expansion, externally applied forces, moments, imposed displacements, and differential support movement (pseudo-static load case). Dynamic analysis includes mode shape extraction, response spectrum analysis, and time-history analysis by modal combination or direct integration. In the response spectrum analysis (i.e., uniform support motion [USM] response spectrum analysis or independent support motion [ISM] response spectrum analysis), modal response combination in accordance with RG 1.92 is performed. In the ground motion (uniform motion) or independent support time history analysis, the normal mode solution procedure is selected. In analysis involving time varying nodal loads, the step-by-step direct integration method is used.

3D.4.1.2 Validation

The PISYS program has been benchmarked against NRC piping models. The results are documented in Reference 3D-1 for mode shapes and USM response spectrum analysis options. The ISM option has been validated against NUREG/CR-1677.

Subsequently, the PISYS07 program, which is used for ESBWR piping analysis, has been benchmarked against NUREG/CR-6049.

3D.4.1.3 Extent of Application

This program is used for elastic stress analysis of piping systems.

3D.4.2 Component Analysis - ANSI7

3D.4.2.1 Description

ANSI7 is a computer code for calculating stresses and cumulative usage factors and to calculate combined stresses for service level A, B, C, and D loads in accordance with ASME Section III, article NB-3650. The program includes environmental fatigue effects on fatigue curves according to RG 1.207 and NUREG/CR-6909.

3D.4.2.2 Validation

Hand calculations are performed to demonstrate the program's applicability and validity.

3D.4.2.3 Extent of Application

This program is used for calculating stresses and cumulative usage factors for Class 1, 2, and 3 piping components in accordance with articles NB, NC, and ND-3650 of ASME Code Section III. ANSI7 is also used to combine loads and calculate combined service level A, B, C, and D loads on piping supports and pipe-mounted equipment. The program calculates elastic stresses for level D, faulted limits, but the ASME Code Section III, Appendix F limits are not within the computer program.

3D.4.3 (Deleted)

3D.4.4 Dynamic Forcing Functions

3D.4.4.1 Relief Valve Discharge Pipe Forces Computer Program – RVFOR

3D.4.4.1.1 Description

The relief valve discharge pipe connects the pressure-relief valve to the suppression pool. When the valve is opened, the transient fluid flow causes time-dependent forces to develop on the pipe wall. This General Electric (GE)-developed FORTRAN computer program computes the transient fluid mechanics and the resultant pipe forces using the method of characteristics.

3D.4.4.1.2 Validation

Hand calculations and experimental tests are used to demonstrate the program's applicability and validity.

3D.4.4.1.3 Extent of Application

This program is used to calculate the time-dependent forces on the wall of the discharge pipe.

3D.4.4.2 Turbine Stop Valve Closure – TSFOR

3D.4.4.2.1 Description

This GE-developed FORTRAN program utilizes the method of characteristics to compute fluid momentum and pressure loads at each change in pipe section or direction due to the fast closure of the turbine stop valve.

3D.4.4.2.2 Validation

Hand calculations are used to demonstrate the program's applicability and validity.

3D.4.4.2.3 Extent of Application

The TSFOR program computes the time-history forcing function in the main steam piping due to turbine stop valve closure.

3D.4.4.3 (Deleted)

3D.4.4.4 (Deleted)

3D.4.5 (Deleted)

3D.4.6 Response Spectra Generation

3D.4.6.1 ERSIN Computer Program

3D.4.6.1.1 Description

ERSIN is a computer code used to generate secondary response spectra for pipe-mounted and floor-mounted equipment. ERSIN provides direct generation of local or global acceleration response spectra.

3D.4.6.1.2 Validation

Hand calculations and test cases analyzed are used to demonstrate the program's applicability and validity.

3D.4.6.1.3 Extent of Application

Equipment control panels, local equipment racks, Main Steam Isolation Valves, Safety Relief Valves, and Hydraulic Control Units are some of the components analyzed using ERSIN computer code.

3D.4.6.2 RINEX Computer Program

3D.4.6.2.1 Description

RINEX is a computer code used to interpolate and extrapolate amplified response spectra used in the response spectrum method of dynamic analysis. RINEX is also used to generate response spectra with non-constant model damping. The non-constant model damping analysis option can calculate spectral acceleration at the discrete eigenvalues of a dynamic system using either the strain energy weighted modal damping or the ASME Code Class N-411-1 damping values.

3D.4.6.2.2 Validation

Hand calculations and test cases analyzed are used to demonstrate the program's applicability and validity.

3D.4.6.2.3 Extent of Application

This program is used to generate multiple damping spectra for piping.

3D.4.6.3 (Deleted)

3D.4.6.4 (Deleted)

3D.4.7 Pipe Dynamic Analysis (PDA) Program

3D.4.7.1 Description

PDA is a FORTRAN program used to determine the response of a pipe subjected to the thrust force occurring after a pipe break. It also is used to determine the pipe whip restraint design and capacity.

The program treats the situation in terms of generic pipe break configuration, which involves a straight, uniform pipe fixed (or pinned) at one end and subjected to a time-dependent thrust force at the other end. A typical restraint used to reduce the resulting deformation is also included at a location between the two ends. Nonlinear and time-independent stress-strain relations are used to model the pipe and the restraint. Using a plastic hinge concept, bending of the pipe is assumed to occur only at the fixed (or pinned) end and at the location supported by the restraint.

Effects of pipe shear deflection are considered negligible. The pipe-bending moment-deflection (or rotation) relation used for these locations is obtained from a static nonlinear cantilever beam analysis. Using moment angular rotation relations, nonlinear equations of motion are formulated using energy considerations, and the equations are numerically integrated in small time steps to yield the time-history of the pipe motion.

3D.4.7.2 Validation

PDA output pipe whip restraint force and displacement are benchmarked with ANSYS nonlinear time-history analysis results.

3D.4.7.3 Extent of Application

Pipe break analyses.

3D.4.8 Thermal Transient Program – LION

3D.4.8.1 Description

LION is a FORTRAN program used to compute radial and axial thermal gradients in piping. The program calculates a time-history of ΔT_1, ΔT_2, T_a, and T_b (defined in ASME Code Section III, Subsection NB) for uniform and tapered pipe wall thickness.

3D.4.8.2 Validation

LION was compared to analytical results published in literature.

3D.4.8.3 Extent of Application

Pipe thermal analyses.

3D.4.9 Engineering Analysis System - ANSYS

3D.4.9.1 Description

See Subsection 3D.3.1.1.

3D.4.9.2 Validation

See Subsection 3D.3.1.2.

3D.4.9.3 Extent of Application

This program is used to perform non-linear analysis of piping systems for time varying displacements and forces due to postulated pipe breaks. Also, this program is used to perform finite element analysis of pressure-retaining components and civil structures against the loads and events postulated in the design specifications.

3D.4.10 Piping Analysis Program – EZPYP

3D.4.10.1 Description

EZPYP is a GE FORTRAN program that links the ANSI7 and PISYS programs together. The EZPYP program can be used to run several PISYS cases by making user-specified changes to a basic PISYS pipe model. By controlling files and PISYS runs, the EZPYP program gives the analyst the ability to perform a complete piping analysis in one computer run.

3D.4.10.2 Validation

No calculations are performed in the program.

3D.4.10.3 Extent of Application

Sorting of data output from PISYS and ANSI7.

3D.4.11 Pipe Support Structural Analysis and Design Verification Computer Program – E/PD STRUDL

3D.4.11.1 Description

E/PD STRUDL is a safety-related computer program capable of performing a comprehensive structural analysis and design verification of pipe supports, including structural members, vendor components, welded pipe attachments, base plate, and anchor bolts. The program also can perform a base plate flexibility analysis by using a finite element analysis model for the base plate and anchor bolts with compression elements to represent concrete to generate stiffness and allowable forces and moments on the base plate. These allowable forces and moments are used to design-verify the anchorage components in compliance with NRC IE Bulletin 79.02. The stiffness values may be used in the structural analysis of the pipe supports. The non-nuclear support components are checked according to applicable AISC Code Edition. The structural capability includes, static, dynamic, and thermal analyses, as required.

The computer program is also designed to perform code-checking of nuclear support components according to ASME III NF Code. Vendor components are design-verified according to vendor allowable based on certified design reports provided by vendors. Structural components are verified based on applicable ASME III NF Code Edition, and the welds are verified according to AWS Standard.

3D.4.11.2 Validation

This program is a derivative of the original STRUDL computer program developed by MIT. Extensive enhancements for pipe support evaluations have been thoroughly verified and validated in accordance with the Washington Group Software Quality Assurance Program, which meets the requirements of Title 10, Code of Federal Regulations, Part 50 (10 CFR 50) Appendix B and ASME NQA-1.

3D.4.11.3 The Extent of Application

E/PD STRUDL is used for analysis and design of nuclear and non-nuclear pipe supports.

3D.4.12 ANSYS CFX COMPUTER PROGRAM

3D.4.12.1 Description

ANSYS CFX is a general purpose, finite volume Computational Fluid Dynamics software suite that combines an advanced solver with powerful pre- and post-processing tools. Analysis capabilities include: steady-state and transient flows, laminar and turbulent flows, subsonic, transonic and supersonic flows, heat transfer and thermal radiation, buoyancy, non-Newtonian flows, transport of non-reacting scalar components, multiphase flows, combustion, flows in multiple frames of reference and Lagrangian particle tracking.

3D.4.12.2 Validation

The applicability and validity of ANSYS CFX are demonstrated by running a test suite of cases that exercise the elements and options used in the finite volume code. The verification cases used for ANSYS CFX are extracted from textbooks in which classical or theoretical solutions are published or can readily be obtained by simple hand calculations.

3D.4.12.3 Extent of Application

This program is used to model the development of the blast wave inside the annulus between the RPV and the shield wall caused by the RPV Nozzle Terminal End Breaks. It is also used to model the blast wave development during the Main Steam Line Break event outside of the shield wall. The extent and limitation are determined by verification cases performed to qualify ANSYS CFX as an Approved Production Program that is verified and documented for design applications or for all technical activities used in developing design-related information.

3D.4.13 RELAP5/MOD3.3

3D.4.13.1 Description

The light water reactor (LWR) transient analysis code, RELAP5, was originally developed at the Idaho National Engineering Laboratory for the U.S. Nuclear Regulatory Commission (NRC). Code uses include analyses required to support rulemaking, licensing audit calculations, evaluation of accident mitigation strategies, evaluation of operator guidelines, and experiment planning analysis. RELAP5 has also been used as the basis for a nuclear plant analyzer. Specific applications have included simulations of transients in LWR systems such as loss of coolant, anticipated transients without scram (ATWS), and operational transients such as loss of

feedwater, loss of offsite power, station blackout, and turbine trip. RELAP5 is a highly generic code that, in addition to calculating the behavior of a reactor coolant system during a transient, can be used for simulation of a wide variety of hydraulic and thermal transients in both nuclear and nonnuclear systems involving mixtures of steam, water, noncondensable, and solute.

The MOD3 version of RELAP5 has been developed jointly by the NRC and a consortium consisting of several foreign and domestic organizations that were members of the International Code Assessment and Applications Program and its successor organization, the Code Applications and Maintenance Program. Credit also needs to be given to various Department of Energy sponsors, including the Idaho National Engineering Laboratory laboratory-directed discretionary funding program. The mission of the RELAP5/MOD3 development program was to develop a code version suitable for the analysis of all transients and postulated accidents in LWR systems, including both large- and small-break loss-of-coolant accidents (LOCAs) as well as the full range of operational transients.

The RELAP5/MOD3.3 code has been developed for best-estimate transient simulation of light water reactor coolant systems during postulated accidents. The code models the coupled behavior of the reactor coolant system and the core for loss-of-coolant accidents and operational transients such as anticipated transient without scram, loss of offsite power, loss of feedwater, and loss of flow. A generic modeling approach is used that permits simulating a variety of thermal hydraulic systems. Control system and secondary system components are included to permit modeling of plant controls, turbines, condensers, and secondary feedwater systems.

3D.4.13.2 Validation

The applications include results from ten phenomenological tests, nineteen separate effects tests, and five integral experiments. The phenomenological problems are primarily used to determine whether the code produces qualitatively correct results; however, two of the problems have analytical solutions that serve as quantitative tests as well. The separate effects problems all provide quantitative as well as qualitative tests for correct simulation. Each problem is selected to emphasize a particular physical effect that provides a test for correct functioning of a particular model or group of models. The integral problems provide tests for qualitative and, if data is available, quantitative correctness of all the code models working in concert.

3D.4.13.3 Extent of Application

RELAP5 is a generic transient analysis code for thermal-hydraulic systems using a fluid that may be a mixture of steam, water, noncondensables, and a nonvolatile solute. The fluid and energy flow paths are approximated by one-dimensional stream tube and conduction models. The code contains system component models applicable to LWRs. In particular, a point neutronics model, pumps, turbines, generator, valves, separator, and controls are included. The LWR applications for which the code is intended include accidents initiated from small break loss-of-coolant accidents, operational transients such as anticipated transients without SCRAM, loss of feed, loss-of-offsite power, and loss of flow transients. The reactor coolant system (RCS) behavior can be simulated up to and slightly beyond the point of fuel damage.

3D.5 PUMPS AND MOTORS

Following are the computer programs used in the dynamic analysis to ensure the structural and functional integrity of the ESBWR pump and motor assemblies.

3D.5.1 Structural Analysis Program - SAP4G

3D.5.1.1 Description

This program is a general structural analysis program for static and dynamic analysis of linear elastic complex structures. The finite-element displacement method is used to solve the displacement and stresses of each element of the structure. The structure can be composed of an unlimited number of three-dimensional truss, beam, plate, shell, solid, plane strain-plane stress and spring elements that are axisymmetric. The program can treat thermal and various forms of mechanical loading. The dynamic analysis includes mode superposition, time-history, and response spectrum analysis. Seismic loading and time-dependent pressure can be treated. The program is versatile and efficient in analyzing large and complex structural systems. The output contains displacement of each nodal point as well as stresses at the surface of each element.

3D.5.1.2 Validation

Hand calculations and test cases analyzed are used to demonstrate the program's applicability and validity.

3D.5.1.3 Extent of Application

SAP4G is used to analyze the structural and functional integrity of the pump/motor systems.

3D.5.2 (Deleted)

3D.6 COL INFORMATION

None.

3D.7 REFERENCES

3D-1 General Electric Co., "PISYS Analysis of NRC Benchmark Problems," NEDO-24210, August 1979.

3D-2 (Deleted)

Table 3D.1-1

Computer Program User Details

Program	Company – Location	Version(1)	Facility(1)
ANSYS	Hitachi – Japan	5.6	PC (WINDOWS 2000, XP)
ANSYS	GE – San Jose, Sunol	v8.1, v8.1A1, v9.0, v9.0A1, v10.0, and v10.0A1	SGI Server
ANSYS	GE – Wilmington	v8.1	LINUX server
ANSYS	ENSA – Spain	10	IBM Intellistation
ANSYS	EA	10	Workstation & PC
ASHSD2	Hitachi – Japan	0	Engineering Work Station 3050RX/230
EVAST	Hitachi – Japan	0	Engineering Work Station 3050RX/230
TACF	Hitachi – Japan	0	Engineering Work Station 3050RX/230
ABAQUS	Hitachi – Japan	6.5	PC (WINDOWS 2000, XP)
FEMFL	Hitachi – Japan	0	Engineering Work Station 3050RX/230
SEISM	GE – All locations	03V, October 1998	VAX Mainframe
PISYS	GE – All locations	08, July 2007	PC
PISYS	EA	May 2007	PC Windows 2000 & Windows XP
ANSI7	GE – All locations	14, September 2000	PC
ANSI7	EA	December 2006	PC Windows 2000 & Windows XP
RVFOR	GE – All locations	06D, January 1998	DEC Alpha workstation
TSFOR	GE – All locations	01D, January 1998	DEC Alpha workstation
ERSIN	GE – All locations	03V, October 1998	VAX Mainframe
RINEX	GE – All locations	01V, October 1998	VAX Mainframe
PDA	GE – All locations	01	PC
LION	GE – All locations	401, March 1994	Workstation and PC
EZPYP	GE – All locations	07D, January 1998	DEC Alpha workstation
E/PD STRUDL	WGI - Princeton	0707	PC
SAP4G	GE – All locations	07V, December 1995	VAX Mainframe
ABAQUS	Toshiba – Japan	6.5-1	Mainframe via PC
PVElite	ENSA – Spain	2008	IBM Intellistation
ANSYS Workbench	GE – All locations	11.0	LINUX Server
ANSYS CFX	GE – All locations	11.0	PC (WINDOWS 2000, XP), Linux
RELAP5/MOD3.3	EA-Spain	3.3	PC (WINDOWS 2000, XP)

(1) Later software versions and alternate facilities may be used as long as the software and facility are qualified for use.

3E. (DELETED)

3F. RESPONSE OF STRUCTURES TO CONTAINMENT LOADS

3F.1 SCOPE

This appendix specifies the design inputs, methodologies and responses of applicable safety-related structures, systems and components that receive dynamic excitation from primary containment operational-transient events or a loss-of-coolant-accident (LOCA) event. The input containment loads are described in Appendix 3B. The containment loads considered for structural dynamic response analysis are: (1) hydrodynamic loads which are condensation oscillation (CO), pool chugging, horizontal vent chugging (HVL), local CO and safety relief valve (SRV) discharge in the suppression pool, and (2) pipe break loads which consist of annulus pressurization in the annulus between the reactor shield wall (RSW) and reactor pressure vessel (RPV), nozzle jet, jet impingement and pipe whip restraint loads.

3F.2 DYNAMIC RESPONSE

3F.2.1 Classification of Analytical Procedure

Analytical procedure of containment loads is classified into the following two groups:

(1) Hydrodynamic loads in the suppression pool. The loads included in this group are SRV loads and LOCA related loads such as CO, pool chugging, HVL and local CO. Depending on the distribution of these loads in the pool, they can be further classified as:

- Symmetric loads in the suppression pool; or
- Asymmetric loads in the suppression pool

(2) Pipe break loads due to main steam (MS), reactor water cleanup (RWCU) or feedwater (FW) line break. The loads included in this group are pressure loads corresponding to annulus pressurization and concentrated loads, which are nozzle jet, jet impingement and pipe whip restraint loads.

3F.2.2 Analysis Models

(1) Analysis Model

The structural models used in the analyses represent a synthesis of the Reactor Building/Fuel Building (RB/FB) model and the RPV model. The beam model used for the pipe break load analysis is illustrated in Figure 3F-1. The hydrodynamic load analysis model of the RB/FB structure is a 3D finite element shell model for the entire 360 degrees as illustrated in Figure 3F-2. The cutaway view along the 0°-180° direction, designated as X (NS) axis, is shown in Figure 3F-3. The cutaway view along the 90°-270° direction, designated as Y (EW) axis, is shown in Figure 3F-4. The vertical direction of the model is the Z axis. This 3D building model is further coupled with the RPV beam model shown in Figure 3F-1. This coupled model is used for symmetric and asymmetric load cases.

The uncertainty associated with stiffness of the infill concrete in the vent wall (VW) and diaphragm floor (D/F) is considered with three models in the same manner as the seismic analysis:

a. No concrete stiffness, where E_c = 0 MPa (0 psi) for the infill concrete.

b. 50% concrete stiffness, where E_c = 13900 MPa (2.016×10^6 psi) for the infill concrete.

c. 100% concrete stiffness, where E_c = 27800 MPa (4.032×10^6 psi) for the infill concrete.

(2) Structural Damping

Material damping values used for SRV and LOCA analyses are in accordance with RG 1.61.

3F.2.3 Load Application

(1) Pipe Break Nozzle Load

The annulus pressurization pressures are converted to horizontal forces according to the following formula.

For RSW side:

$$Fj(t) = 2 \sum_{i=1}^{8} Pij(t) \int_{\theta=ai}^{\theta=bi} R\cos(\theta)d\theta \qquad \text{(3F-1)}$$

For RPV side:

$$Fj(t) = -2 \sum_{i=1}^{8} Pij(t) \int_{\theta=ai}^{\theta=bi} r\cos(\theta)d\theta \qquad \text{(3F-2)}$$

where:

Fj(t)	=	Force per unit height each level
Pij(t)	=	Pressure each level and angle
i	=	Cell Number
j	=	Level Number
R	=	RSW Inner Radius
r	=	RPV Outer Radius
θ	=	Angle (180°)
ai,bi	=	Extreme angles of the arc on which the load is applied

Jet reaction, jet impingement, and pipe whip reaction forces are considered as constant forces with a finite rise time of one millisecond. Pipe whip load is included as a transient load ending with a steady-state load.

(2) SRV Load

Symmetric SRV (all) response analysis is covered by a vertical load case simulating in-phase actuation of all valves. Asymmetric case of SRV (all) actuation is covered by two horizontal cases acting along 0°-180° direction (NS) and along 90°-270° direction (EW) simulating 180 degree out-of-phase actuation of all valves that maximizes the overturning effects. The SRV air bubble frequencies are expected to be within a range of 5 to 12 Hz. Ways of selecting the minimum number of bubble frequencies for dynamic analysis are selected as follows:

Frequency range of SRV Loads: $f_1 \leq f \leq f_2$ (f_1 = 5 Hz, f_2 = 12 Hz)

For vertical structural frequencies $(f_s)_v$:

a. If $(f_s)_v > f_2$ then use f_2

b. If $f_1 < (f_s)_v < f_2$ then use $(f_s)_v$

c. If $f_1 > (f_s)_v$ then use f_1

For horizontal structural frequencies $(f_s)_h$:

a. If $(f_s)_h > f_2$ then use f_2

b. If $f_1 < (f_s)_h < f_2$ then use $(f_s)_h$

c. If $f_1 > (f_s)_h$ then use f_1

Five vertical frequencies of 5 Hz, 6 Hz, 8 Hz, 10.2 Hz and 12 Hz are selected for the vertical direction analyses (symmetric load case) as well as for horizontal 0°-180° and 90°-270° analyses. Those frequencies cover the entire frequency range of bubble frequencies and capture the structure frequencies for any direction within the interval of 5 to 12 Hz.

(3) HVL Load

Both symmetric and non-symmetric upward loads are considered on the VW structure due to chugging in the top horizontal vents.

(4) Chugging and CO Loads

Sixteen critical pressure time histories for chugging and five for CO are selected for dynamic analysis. Furthermore, one local spike load is added in the CO response study.

3F.2.4 Analysis Method

(1) Pipe Break Load Analysis

For these analyses, multi-input excitation time history analyses are performed using a full transient analysis. The α mass matrix and β stiffness matrix multipliers are used for the damping matrix.

(2) Symmetric Load Analysis

For the dynamic response analyses of SRV and LOCA cases, the full transient analysis method is used. The stiffness matrix multiplier for each material is used to obtain the damping matrix as follows:

$$[C] = \sum_{j=1}^{Nm} \beta_j^m \left[K_j \right] \quad \text{(3F-3)}$$

where:

N_m = Number of materials

$[K_j]$ = structural stiffness matrix

[C] = structural damping matrix

β_j^m = stiffness matrix multiplier for material

(3) Asymmetric Load Analysis

The same analysis approach as symmetric loads is used.

3F.3 CONTAINMENT LOADS ANALYSIS RESULTS

The acceleration response spectra at selected locations for each loading event are presented in Figures 3F-5 through 3F-34. The maximum displacements and accelerations at selected locations for each loading event are presented in Tables 3F-1 through 3F-4.

The input excitation of suppression pool boundary horizontal loads (SRV, chugging, and HVL) is considered in two directions in the horizontal plane (0°-180° in X direction and 90°-270° in Y direction), and the annulus pressurization analysis is performed assuming that pipe break can be associated with any one of the vessel nozzles for each of the postulated line breaks.

The resulting responses to suppression pool loads are expressed in three directions, horizontal X (0°-180°), horizontal Y (90°-270°), and vertical Z. The horizontal responses to annulus pressurization loads are equally applicable to X (0°-180°) and Y (90°-270°) directions.

The results shown in Tables 3F-1 through 3F-4 and Figures 3F-5 through 3F-34 envelop the three models of VW and D/F infill concrete stiffness. As described in Subsection 3F.2.2, these are analysis models with (i) no stiffness, (ii) 50% stiffness and (iii) 100% stiffness.

Table 3F-1

Maximum Accelerations for Annulus Pressurization Loadings (g)

Location	Direction	Node	MS	RWCU	FW
Top of VW	Horizontal Vertical	701	0.0168 0.0361	0.0276 0.0692	0.0193 0.0569
Top of Pedestal	Horizontal Vertical	706	0.0076 0.0114	0.0134 0.0171	0.0104 0.0146
Upper Pool Slab	Horizontal Vertical	208	0.0055 0.0025	0.0125 0.0123	0.0094 0.0091

Table 3F-2

Maximum Accelerations for Hydrodynamic Loads (g)

Location	Direction	Node	SRV	HVL	Chugging	CO	Local CO
Top of VW	X (0º-180º) Y (90º-270º) Z (vertical)	1104	0.19 0.20 0.51	0.04 0.04 0.13	0.19 0.19 0.22	0.07 0.06 0.46	0.02 0.01 0.43
Suppression Pool Floor	X (0º-180º) Y (90º-270º) Z (vertical)	1254	0.12 0.12 0.77	0.01 0.01 0.01	0.09 0.08 0.85	0.09 0.08 1.22	0.09 0.09 0.37
RCCV Top Slab Side	X (0º-180º) Y (90º-270º) Z (vertical)	1119	0.06 0.08 0.10	0.000 0.000 0.000	0.02 0.01 0.02	0.04 0.01 0.21	0.01 0.00 0.02
RCCV Top Slab Center	X (0º-180º) Y (90º-270º) Z (vertical)	18P1	0.06 0.08 0.17	0.000 0.000 0.000	0.01 0.01 0.03	0.04 0.00 0.23	0.00 0.00 0.03

Table 3F-3

Maximum Displacements for Annulus Pressurization Loadings (mm)

Location	Direction	Node	MS	RWCU	FW
Top of VW	Horizontal Vertical	701	0.0155 0.0190	0.0200 0.0516	0.0163 0.0400
Top of Pedestal	Horizontal Vertical	706	0.0063 0.0097	0.0143 0.0175	0.0104 0.0129
Upper Pool Slab	Horizontal Vertical	208	0.0113 0.0109	0.0174 0.0174	0.0120 0.0019

Table 3F-4

Maximum Displacements for Hydrodynamic Loads (mm)

Location	Direction	Node	SRV	HVL	Chugging	CO	Local CO
Top of VW	X (0º-180º) Y (90º-270º) Z (vertical)	1104	0.85 1.50 1.76	0.00 0.00 0.00	0.06 0.06 0.15	2.96 0.12 7.30	0.07 0.01 0.24
Suppression Pool Floor	X (0º-180º) Y (90º-270º) Z (vertical)	1254	0.59 0.96 1.59	0.00 0.00 0.00	0.03 0.04 0.23	2.55 0.12 7.81	0.06 0.01 0.19
RCCV Top Slab Side	X (0º-180º) Y (90º-270º) Z (vertical)	1119	1.09 1.92 1.79	0.00 0.00 0.00	0.04 0.05 0.06	3.21 0.15 8.92	0.10 0.00 0.13
RCCV Top Slab Center	X (0º-180º) Y (90º-270º) Z (vertical)	18P1	1.09 1.87 1.64	0.00 0.00 0.00	0.04 0.05 0.06	3.19 0.09 8.20	0.10 0.00 0.14

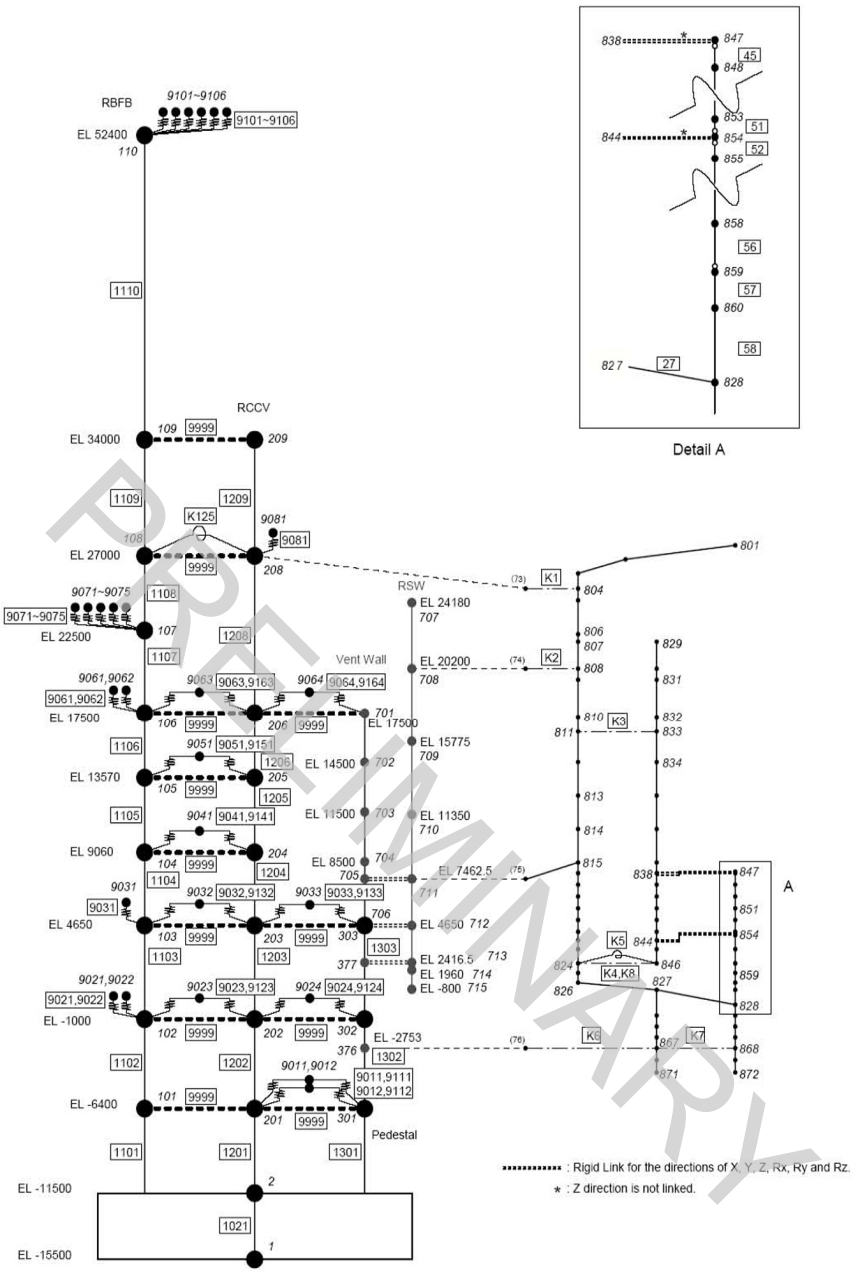

Figure 3F-1. Beam Model for Annulus Pressurization Load

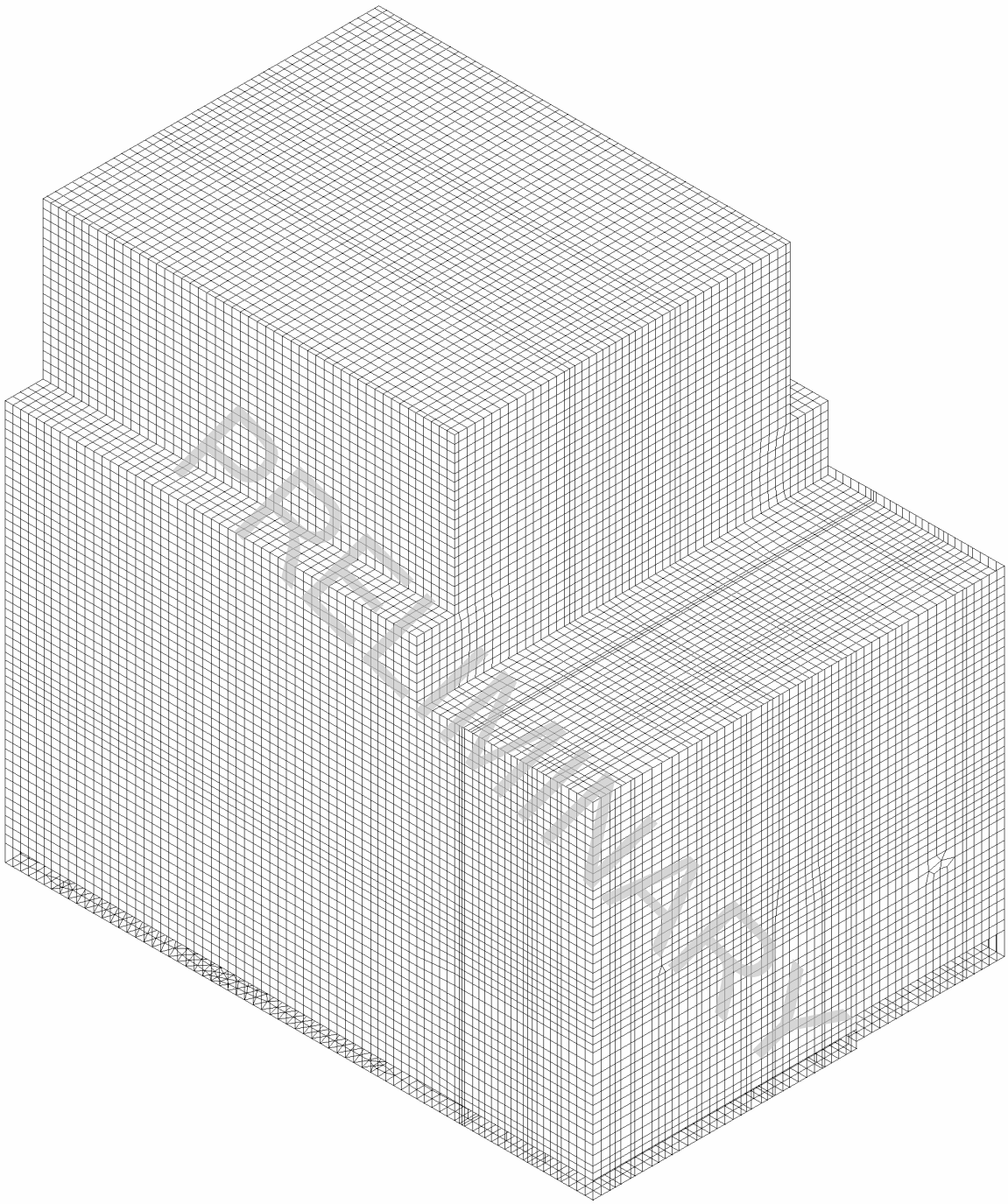

Figure 3F-2. RB/FB 3D Shell Model

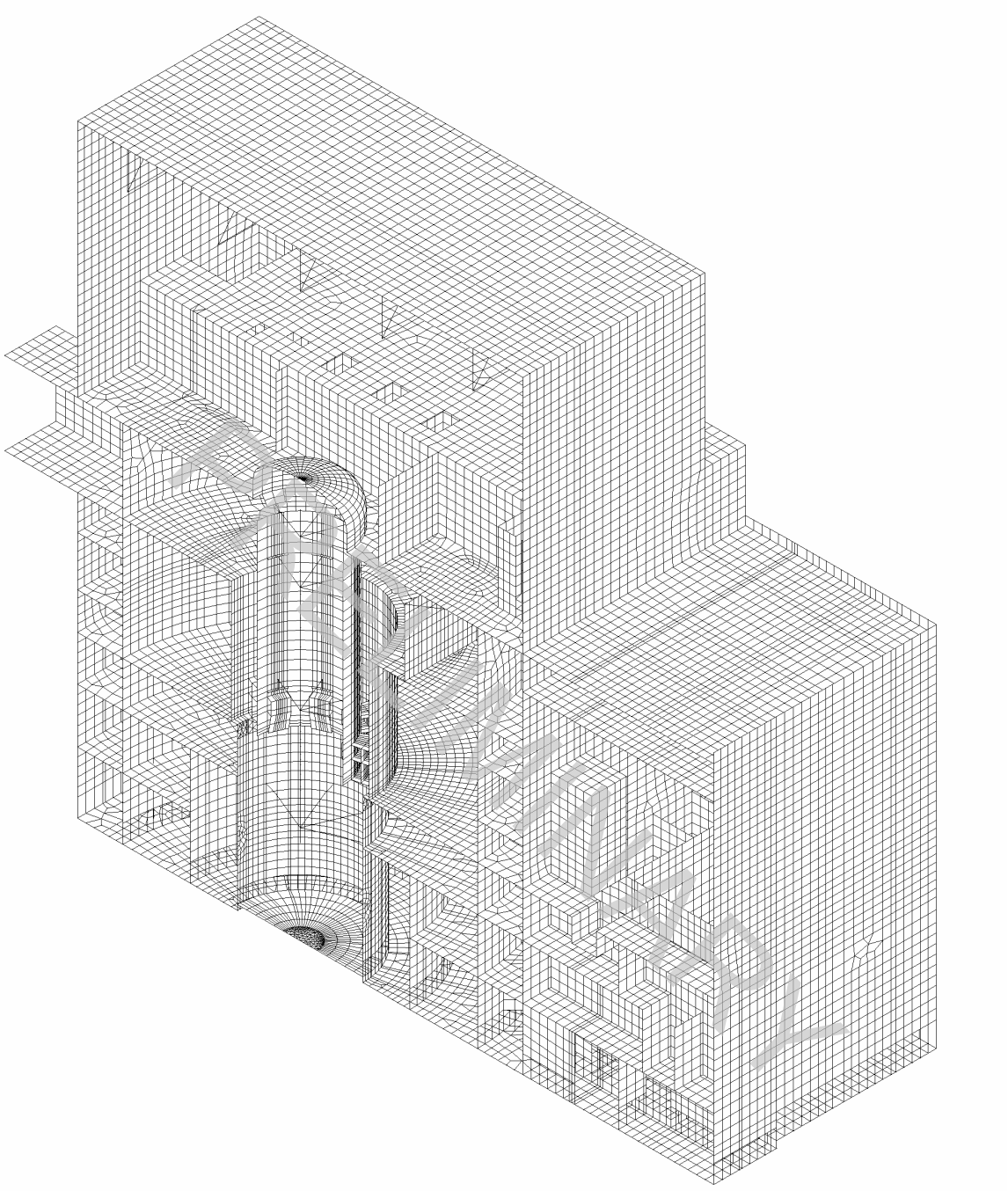

Figure 3F-3. RB/FB 3D Shell Model (0°-180° Direction)

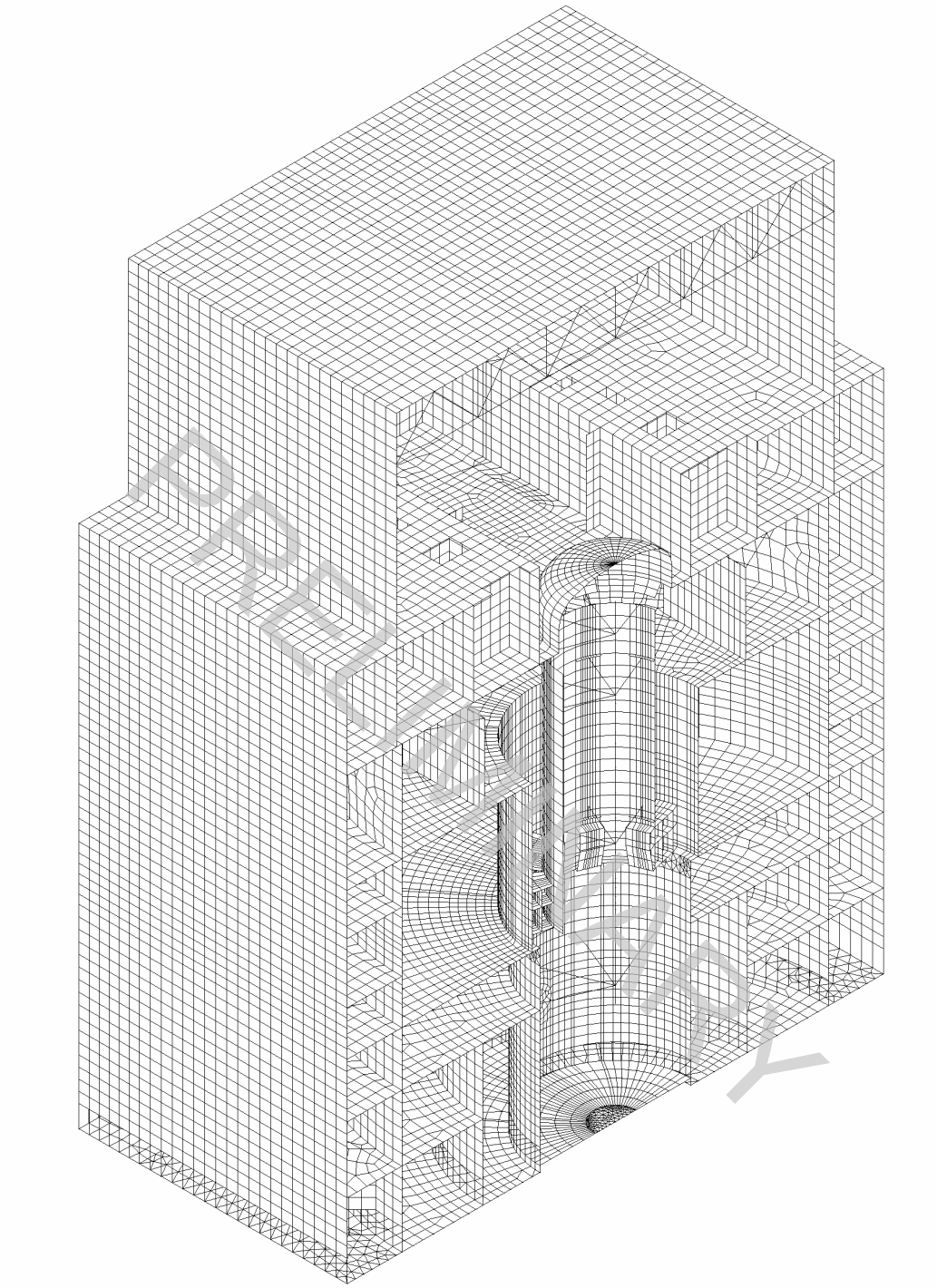

Figure 3F-4. RB/FB 3D Shell Model (90°-270° Direction)

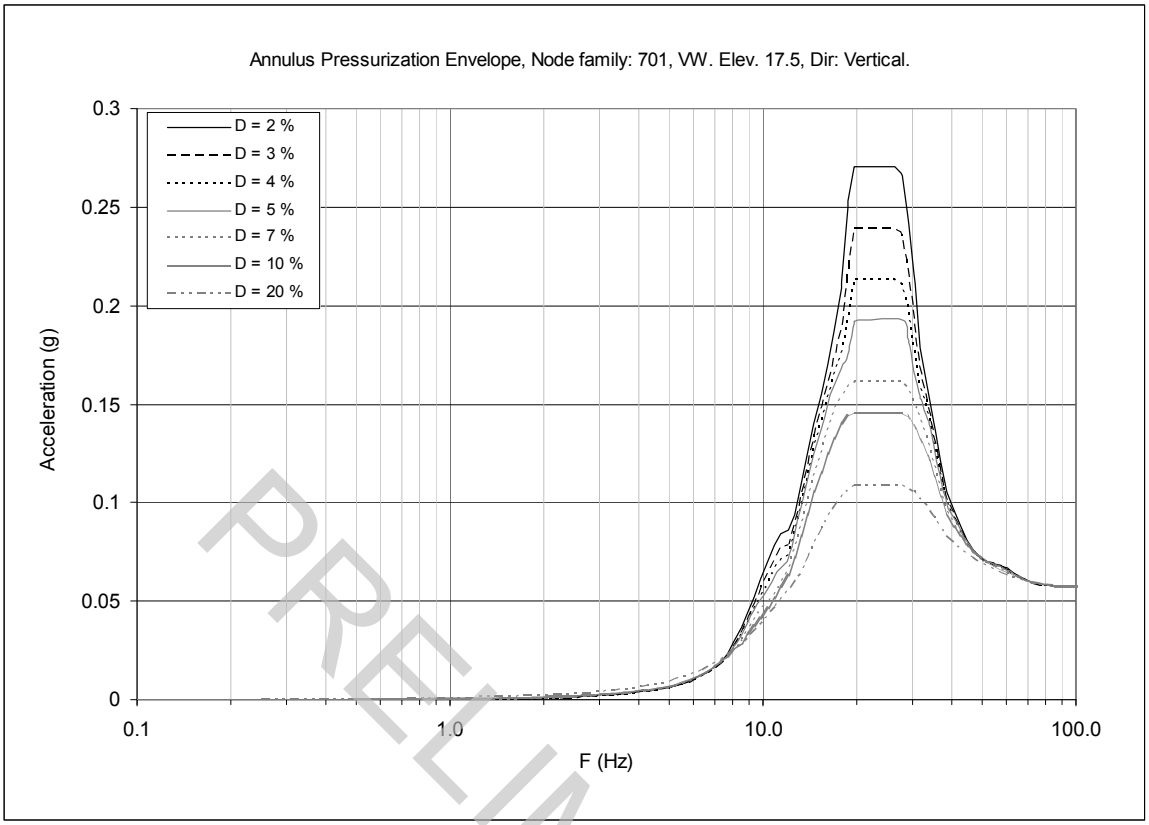

Figure 3F-5. Floor Response Spectrum—Annulus Pressurization Envelope, Node Family: 701, Vertical

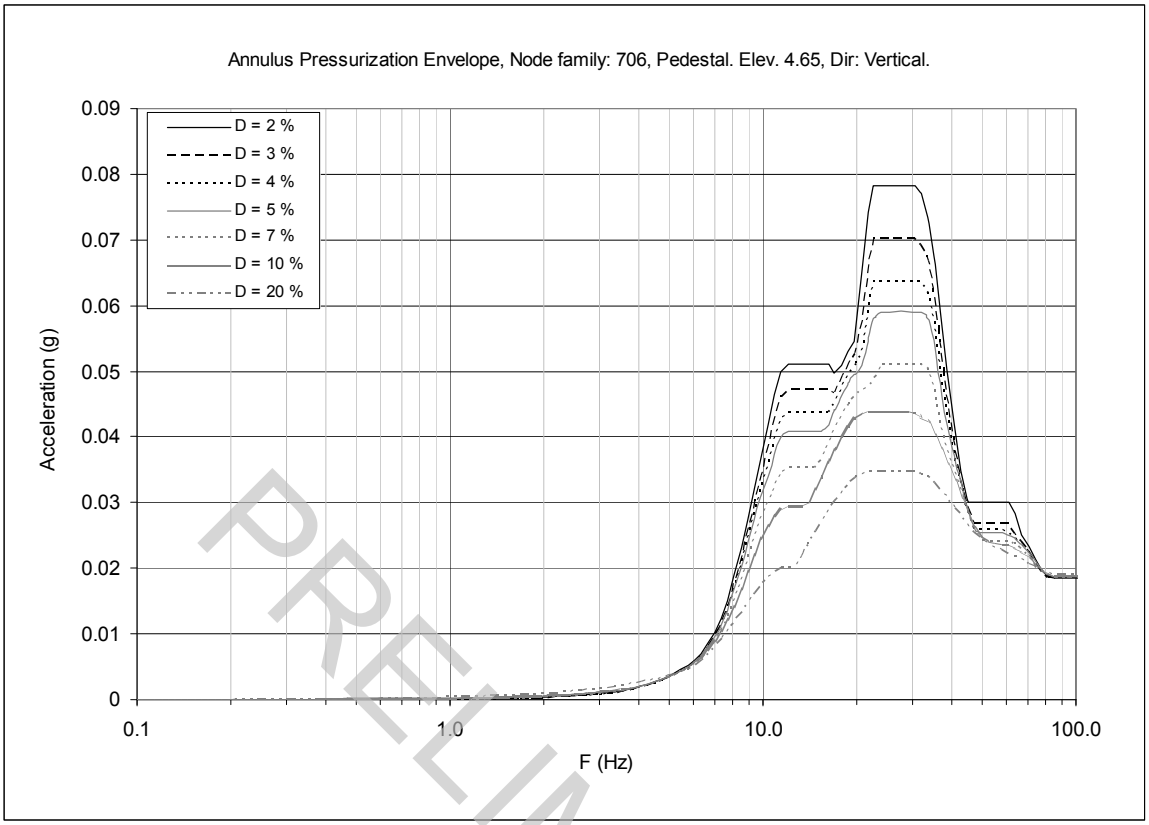

Figure 3F-6. Floor Response Spectrum-Annulus Pressurization Envelope, Node Family: 706, Vertical

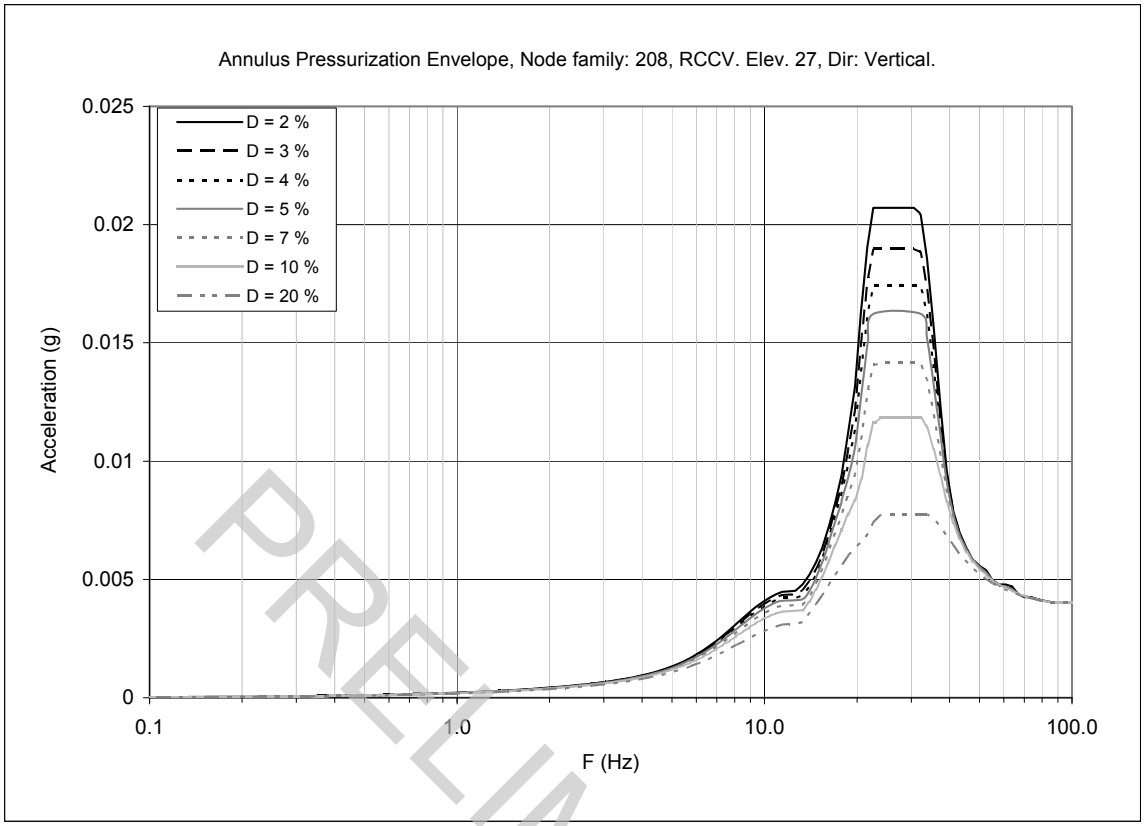

Figure 3F-7. Floor Response Spectrum-Annulus Pressurization Envelope, Node Family: 208, Vertical

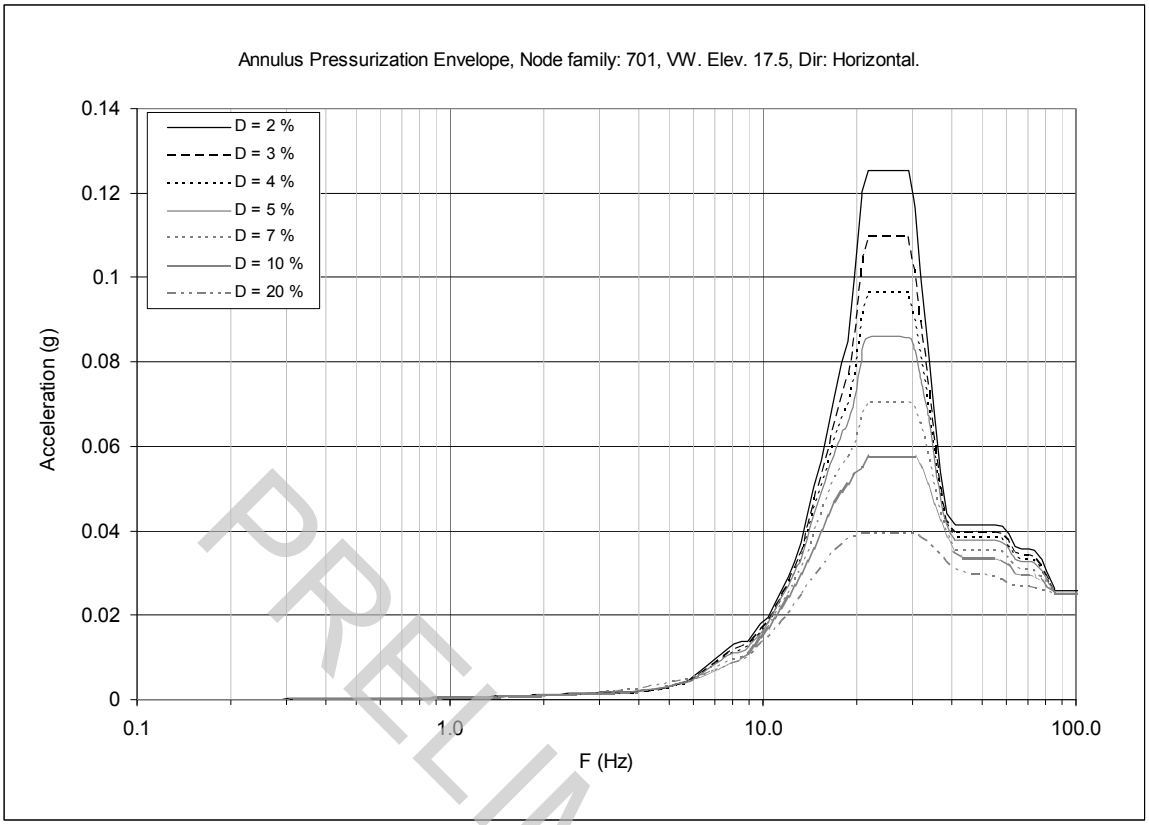

Figure 3F-8. Floor Response Spectrum—Annulus Pressurization Envelope, Node Family: 701, Horizontal

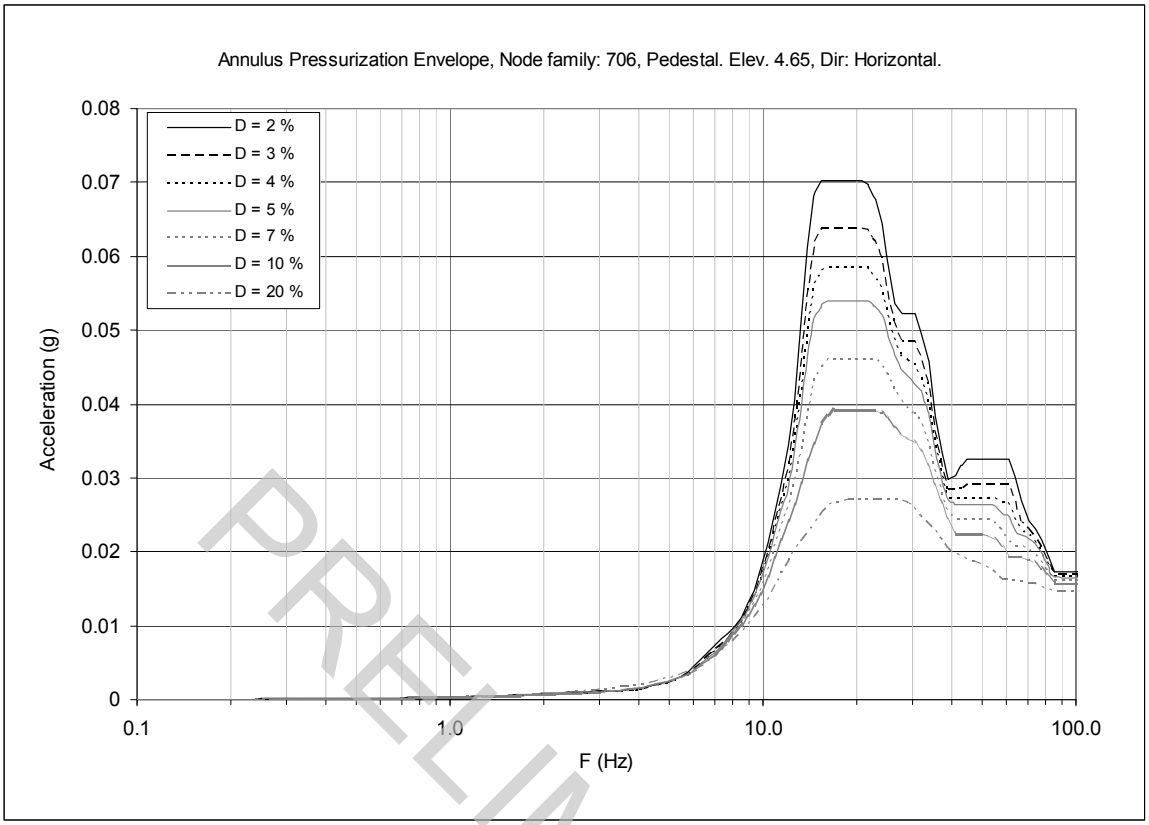

Figure 3F-9. Floor Response Spectrum—Annulus Pressurization Envelope, Node Family: 706, Horizontal

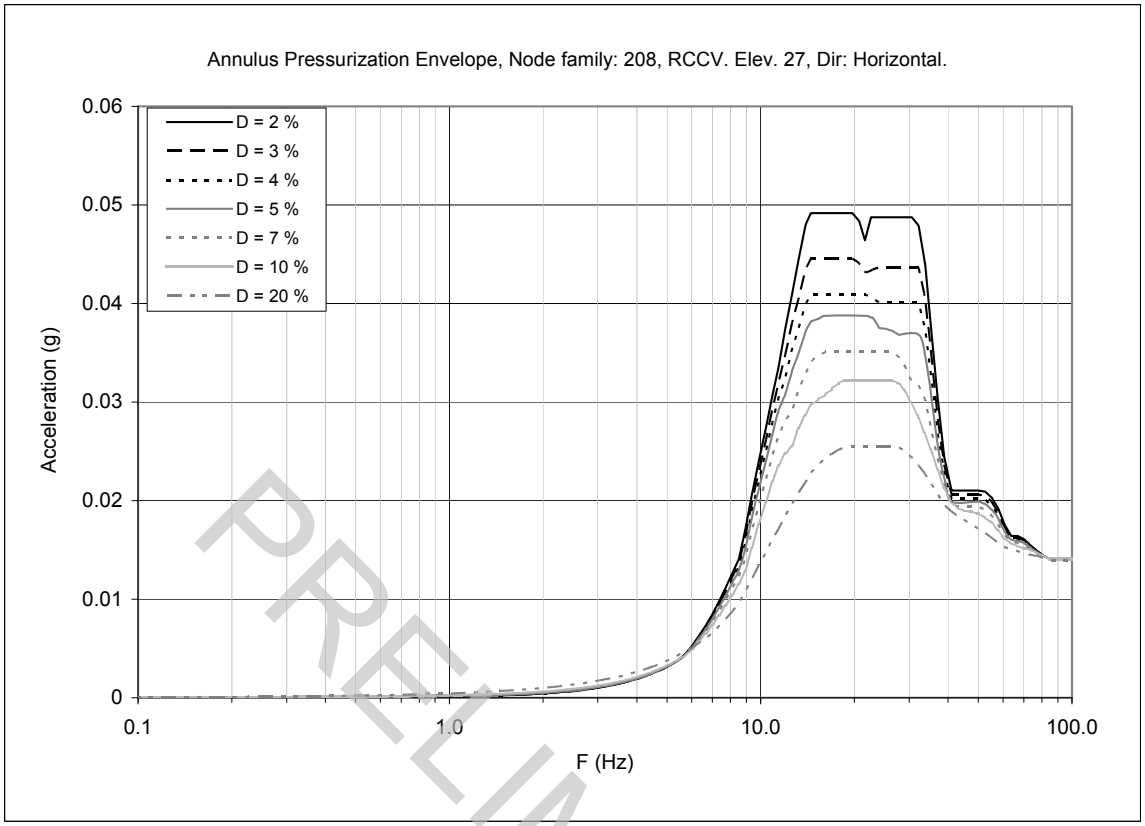

Figure 3F-10. Floor Response Spectrum—Annulus Pressurization Envelope, Node Family: 208, Horizontal

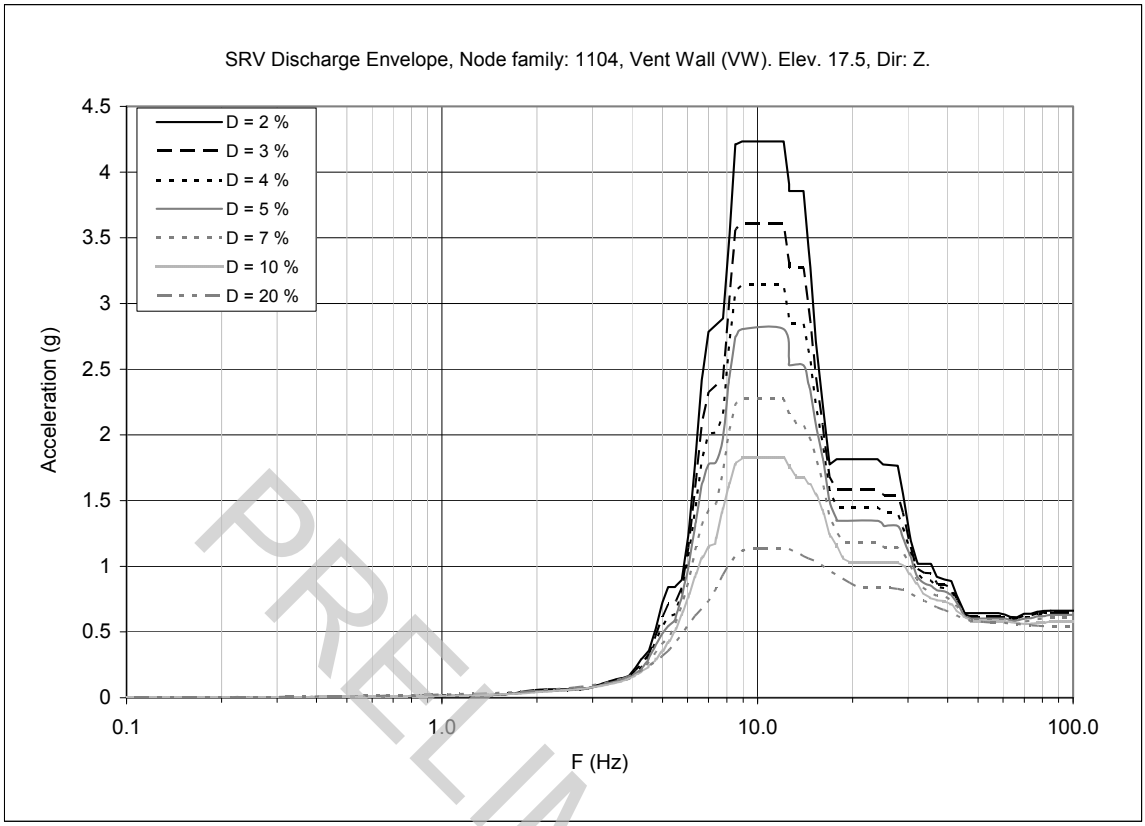

Figure 3F-11. Floor Response Spectrum—SRV Discharge Envelope, Node Family: 1104, Z-direction (Vertical)

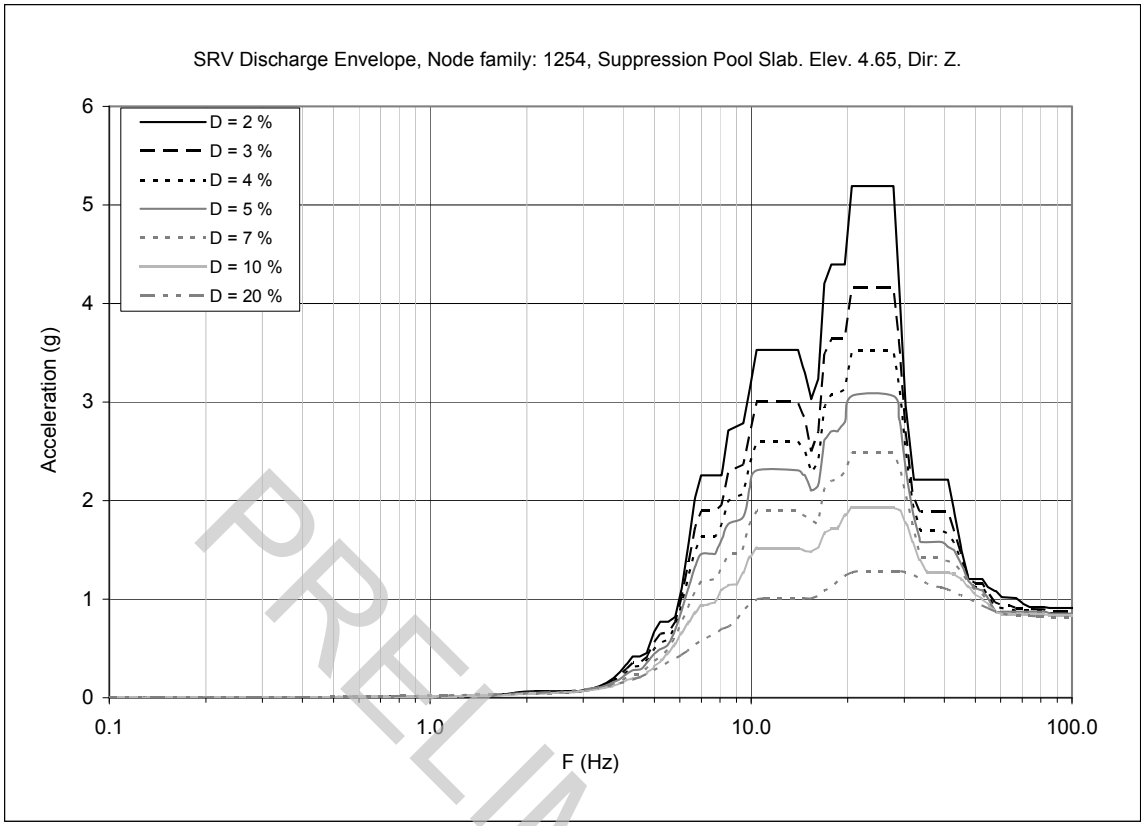

Figure 3F-12. Floor Response Spectrum—SRV Discharge Envelope, Node Family: 1254, Z-direction (Vertical)

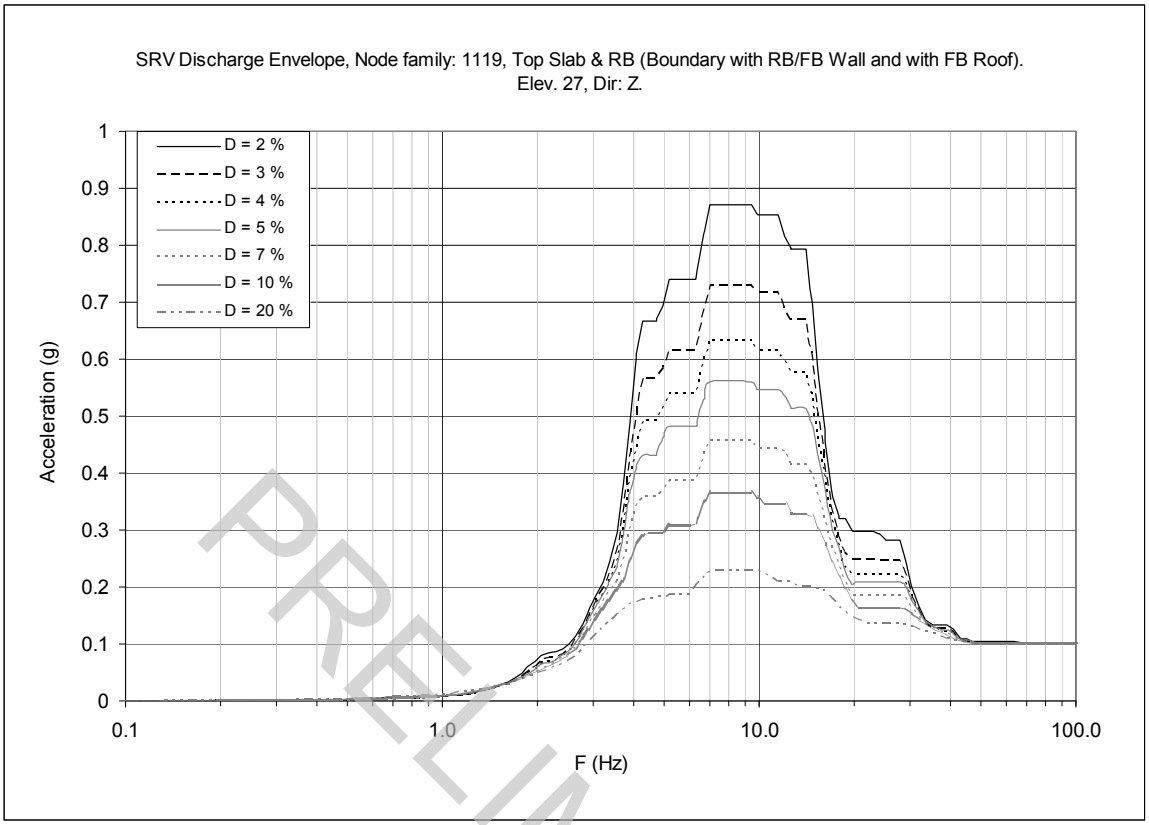

Figure 3F-13. Floor Response Spectrum—SRV Discharge Envelope, Node Family: 1119, Z-direction (Vertical)

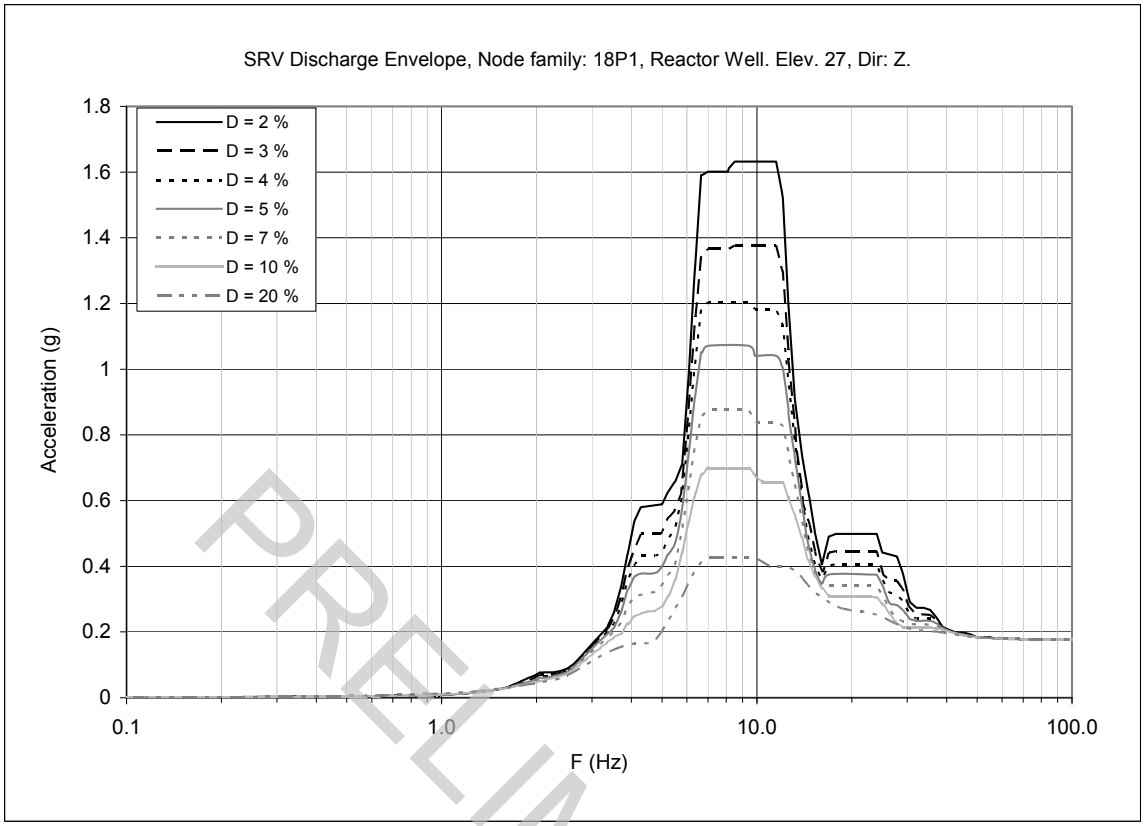

Figure 3F-14. Floor Response Spectrum—SRV Discharge Envelope, Node Family: 18P1, Z-direction (Vertical)

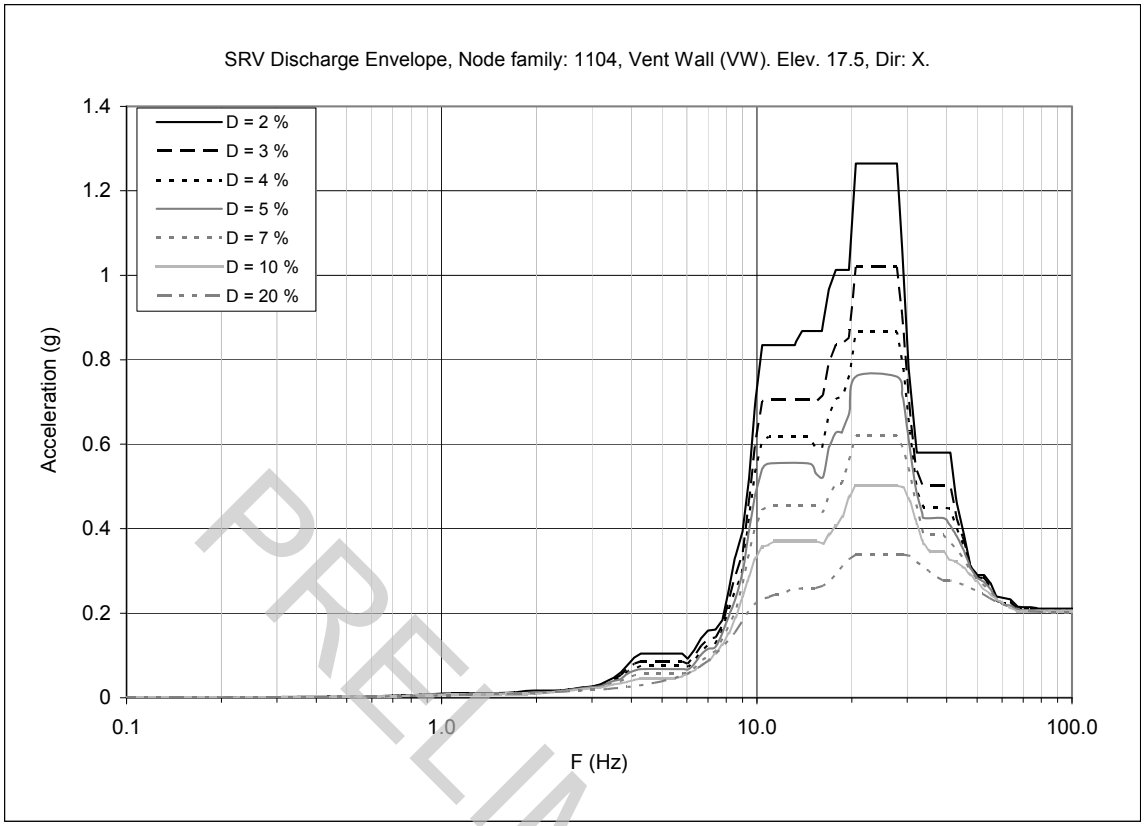

Figure 3F-15. Floor Response Spectrum—SRV Discharge Envelope, Node Family: 1104, X-direction (0°-180°)

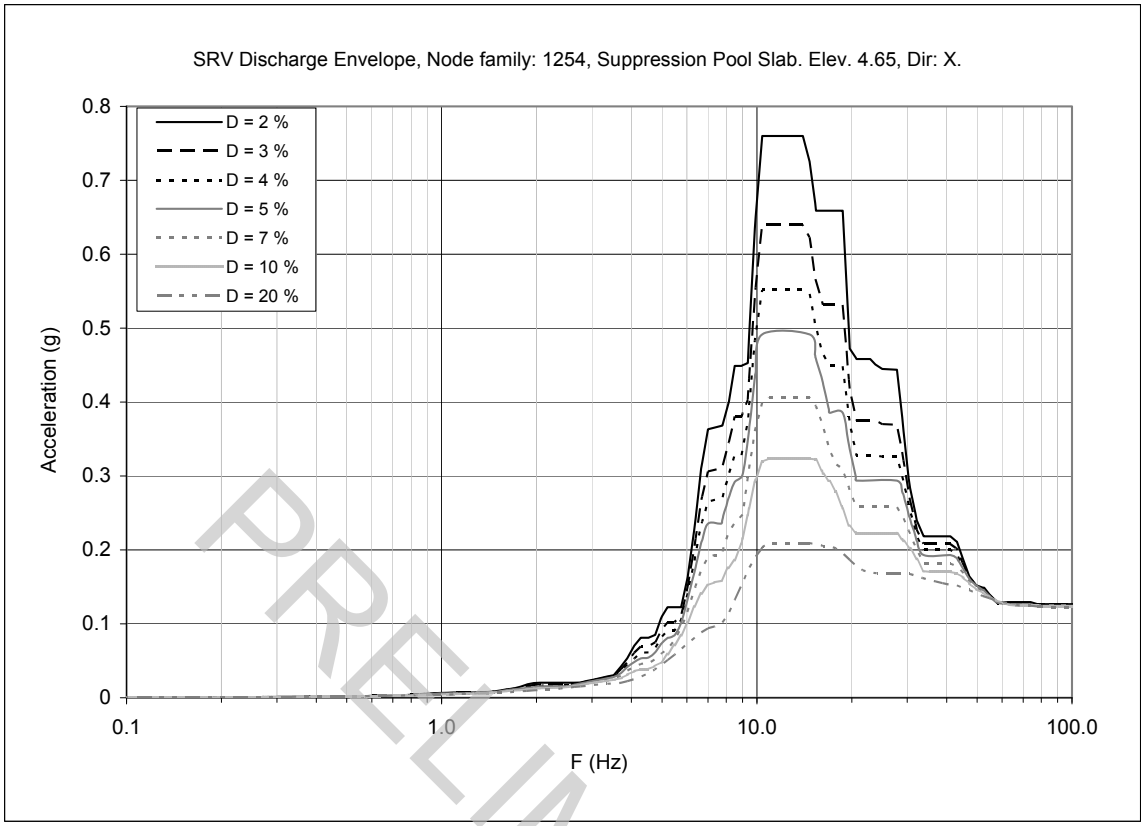

Figure 3F-16. Floor Response Spectrum—SRV Discharge Envelope, Node Family: 1254, X-direction (0°-180°)

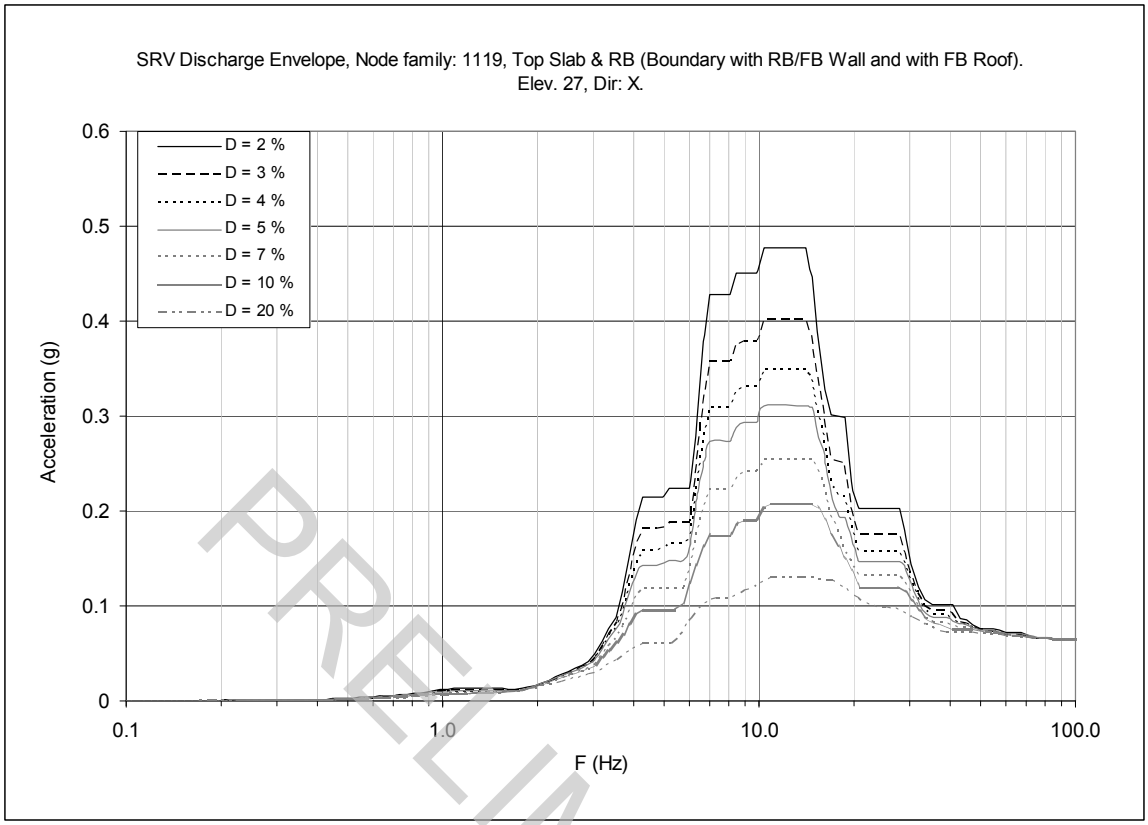

Figure 3F-17. Floor Response Spectrum—SRV Discharge Envelope, Node Family: 1119, X-direction (0°-180°)

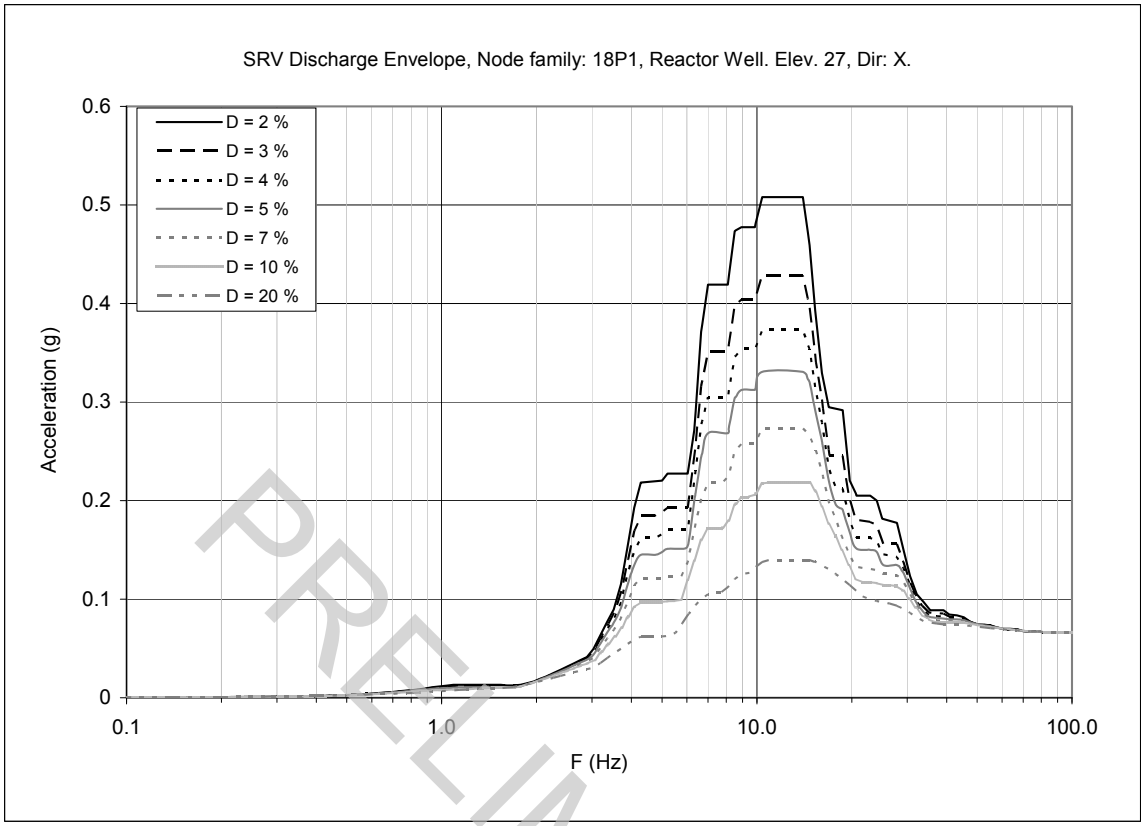

Figure 3F-18. Floor Response Spectrum—SRV Discharge Envelope, Node Family: 18P1, X-direction (0°-180°)

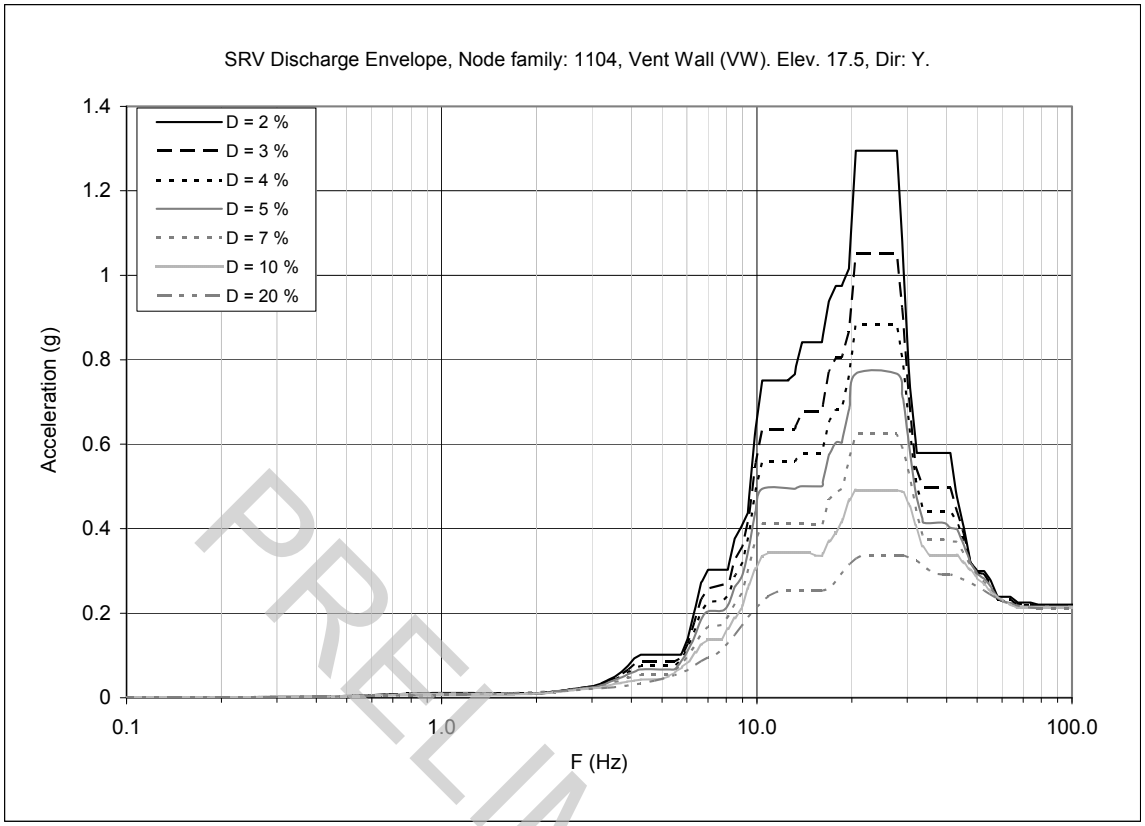

Figure 3F-19. Floor Response Spectrum—SRV Discharge Envelope, Node Family: 1104, Y-direction (90°-270°)

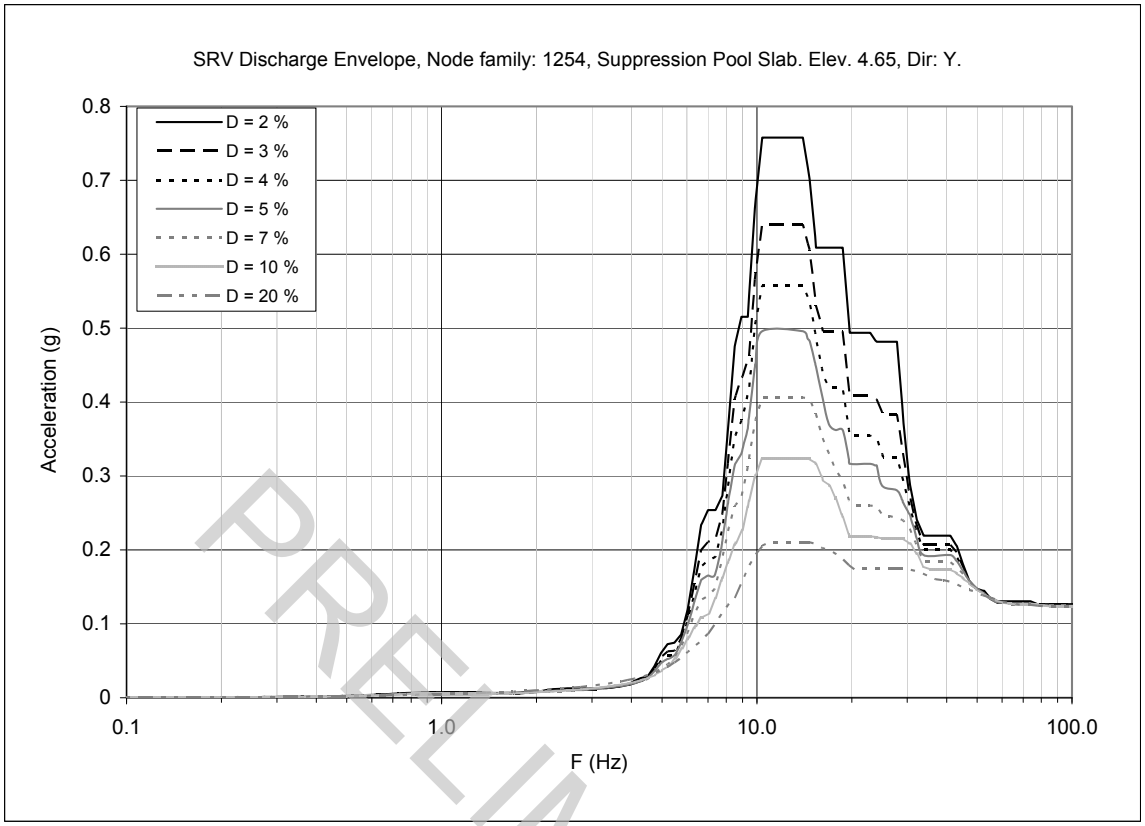

Figure 3F-20. Floor Response Spectrum—SRV Discharge Envelope, Node Family: 1254, Y-direction (90°-270°)

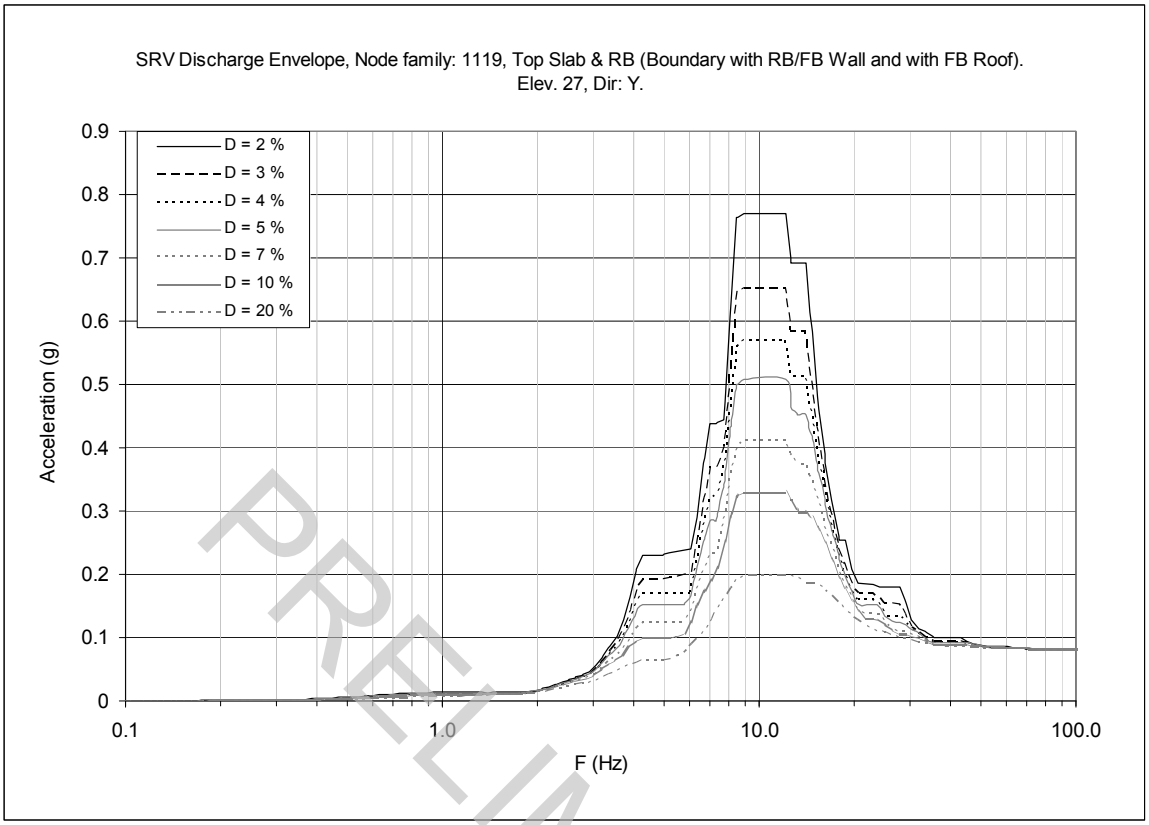

Figure 3F-21. Floor Response Spectrum—SRV Discharge Envelope, Node Family: 1119, Y-direction (90º-270º)

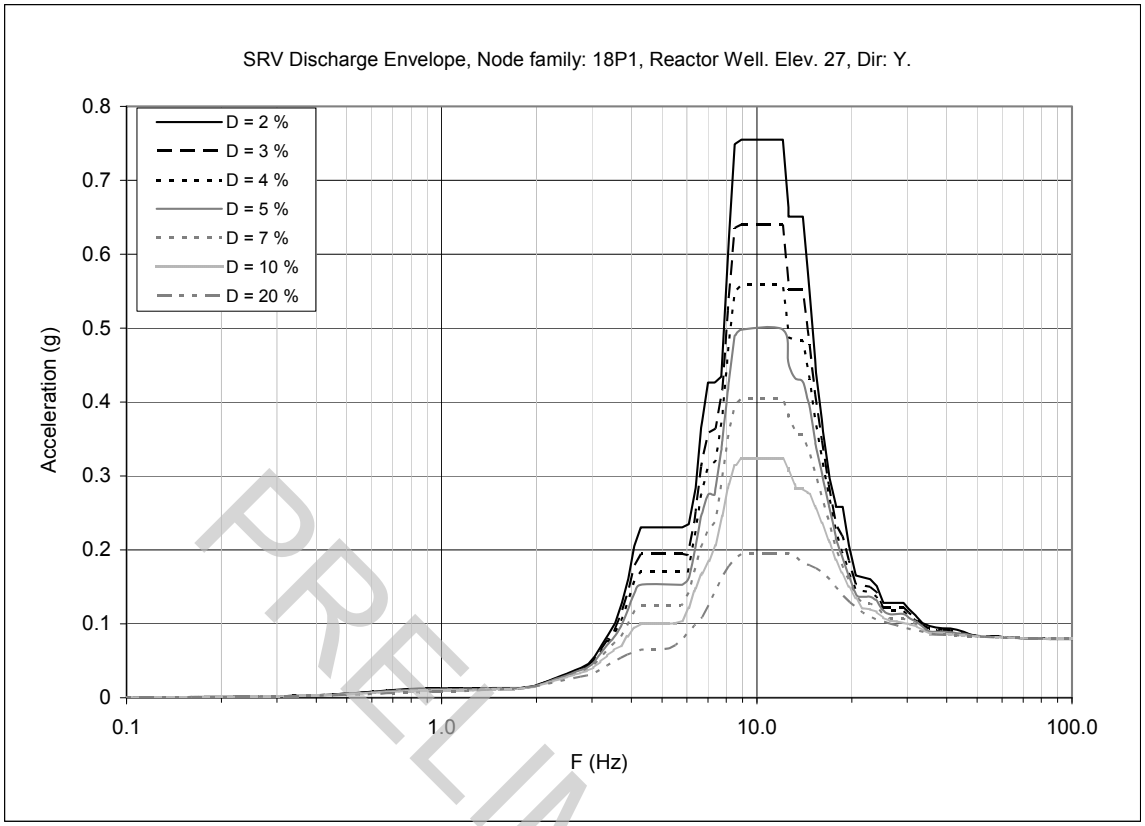

Figure 3F-22. Floor Response Spectrum—SRV Discharge Envelope, Node Family: 18P1, Y-direction (90°-270°)

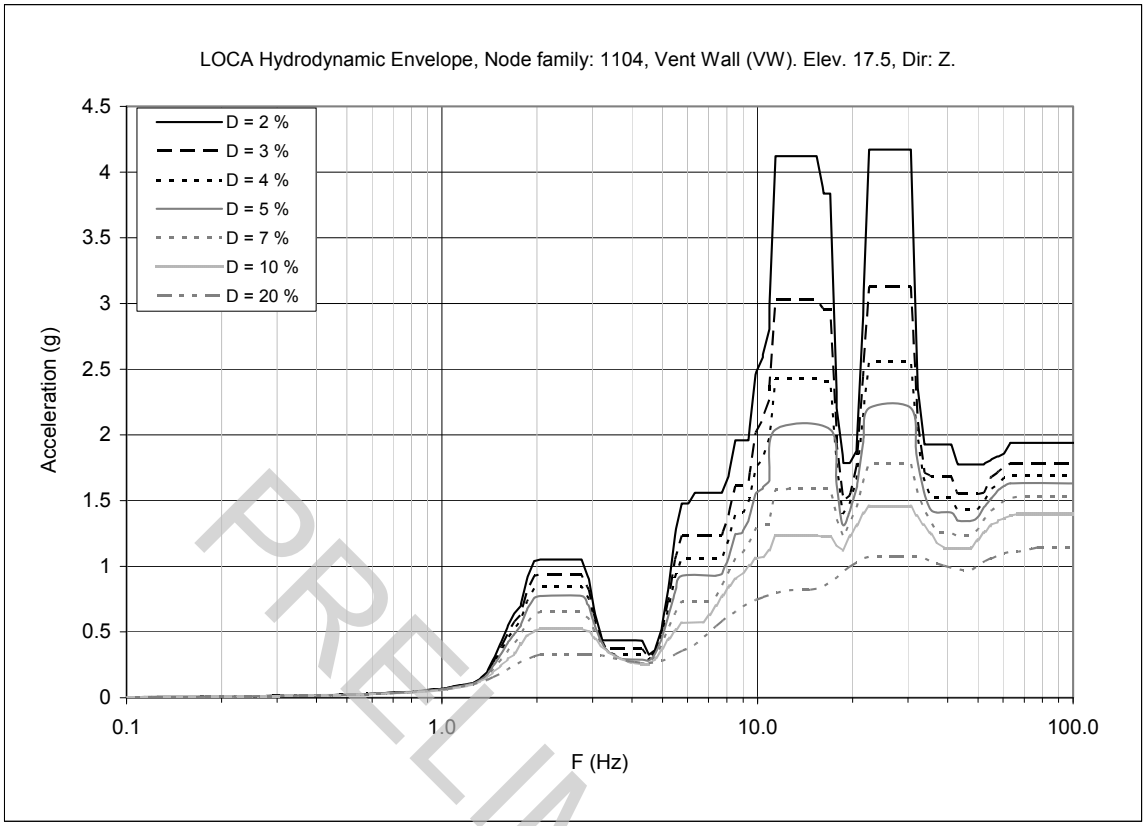

Figure 3F-23. Floor Response Spectrum—Chugging & CO Envelope, Node Family: 1104, Z-direction (Vertical)

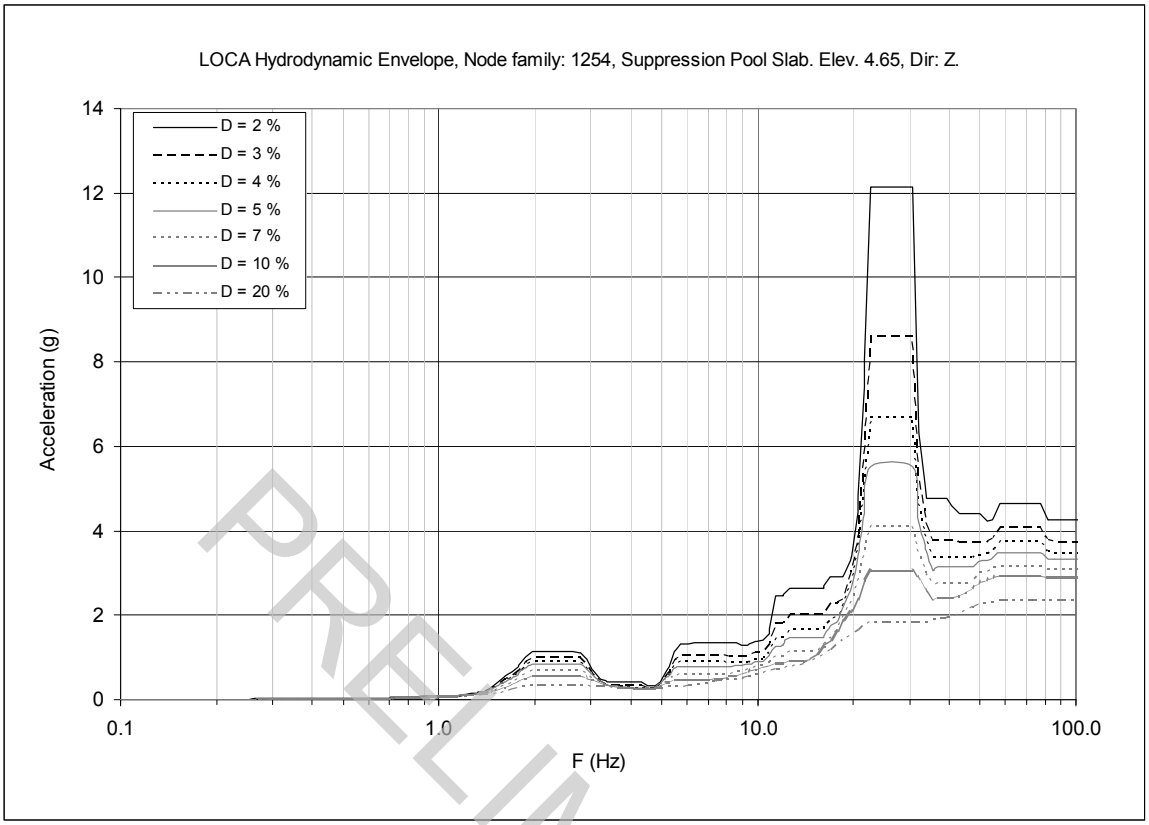

Figure 3F-24. Floor Response Spectrum—Chugging & CO Envelope, Node Family: 1254, Z-direction (Vertical)

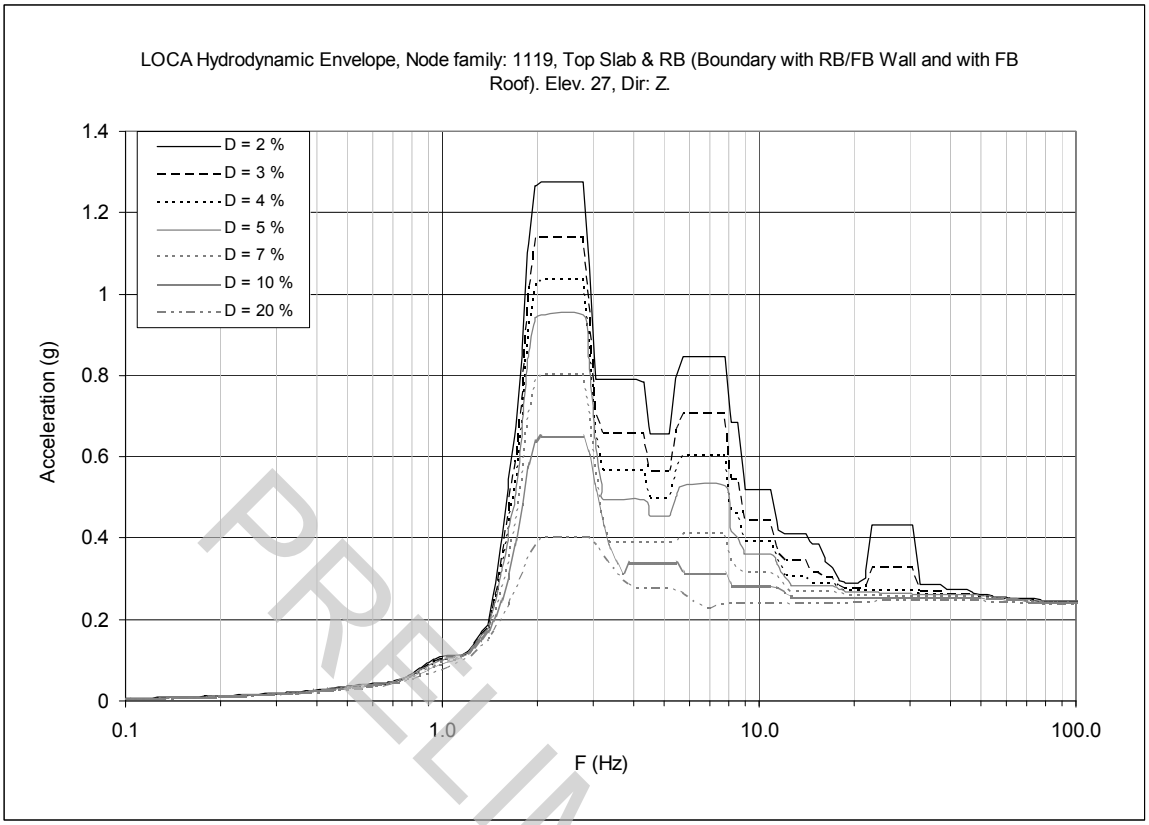

Figure 3F-25. Floor Response Spectrum—Chugging & CO Envelope, Node Family: 1119, Z-direction (Vertical)

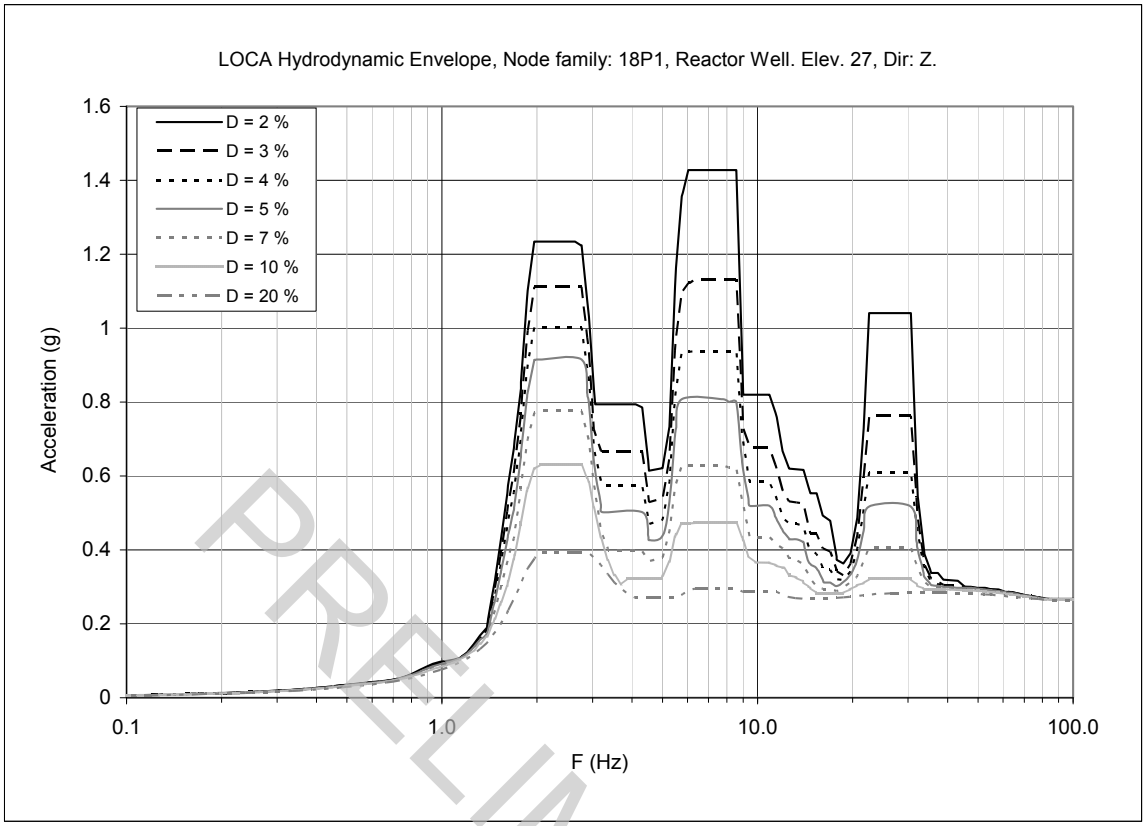

Figure 3F-26. Floor Response Spectrum—Chugging & CO Envelope, Node Family: 18P1, Z-direction (Vertical)

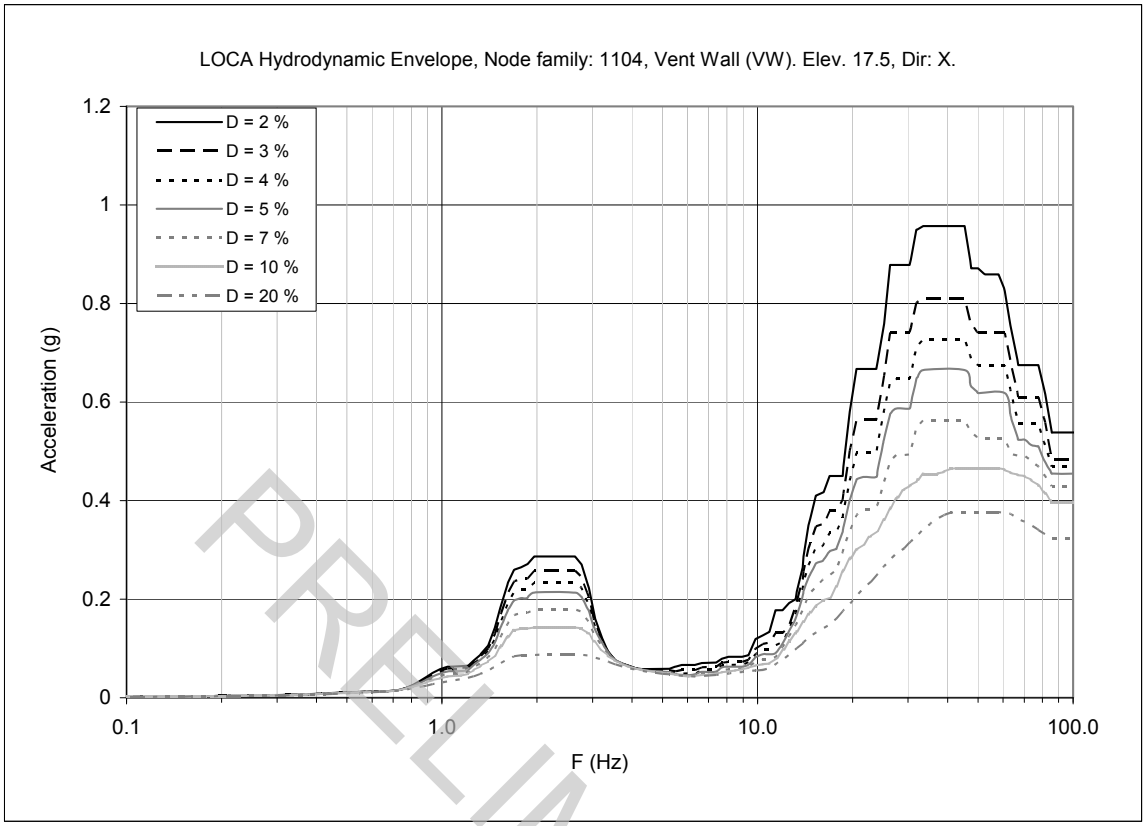

Figure 3F-27. Floor Response Spectrum—Chugging & CO Envelope, Node Family: 1104, X-direction (0°-180°)

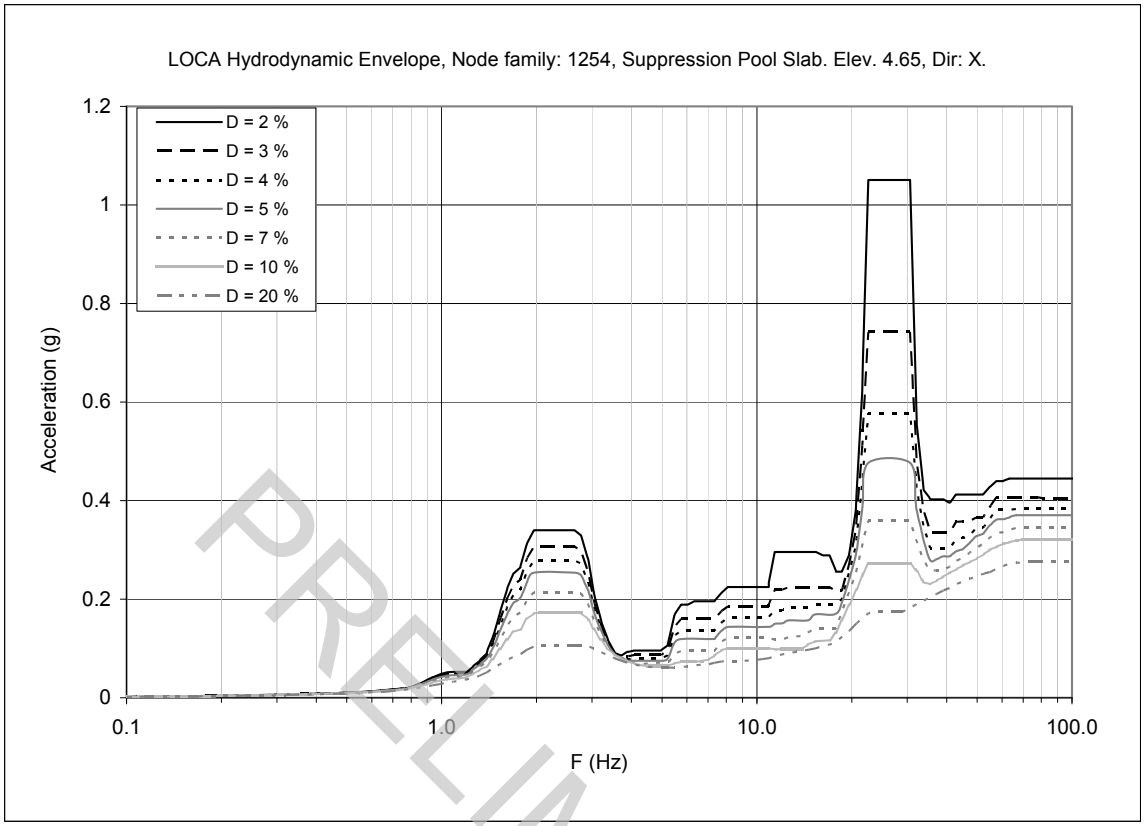

Figure 3F-28. Floor Response Spectrum—Chugging & CO Envelope, Node Family: 1254, X-direction (0°-180°)

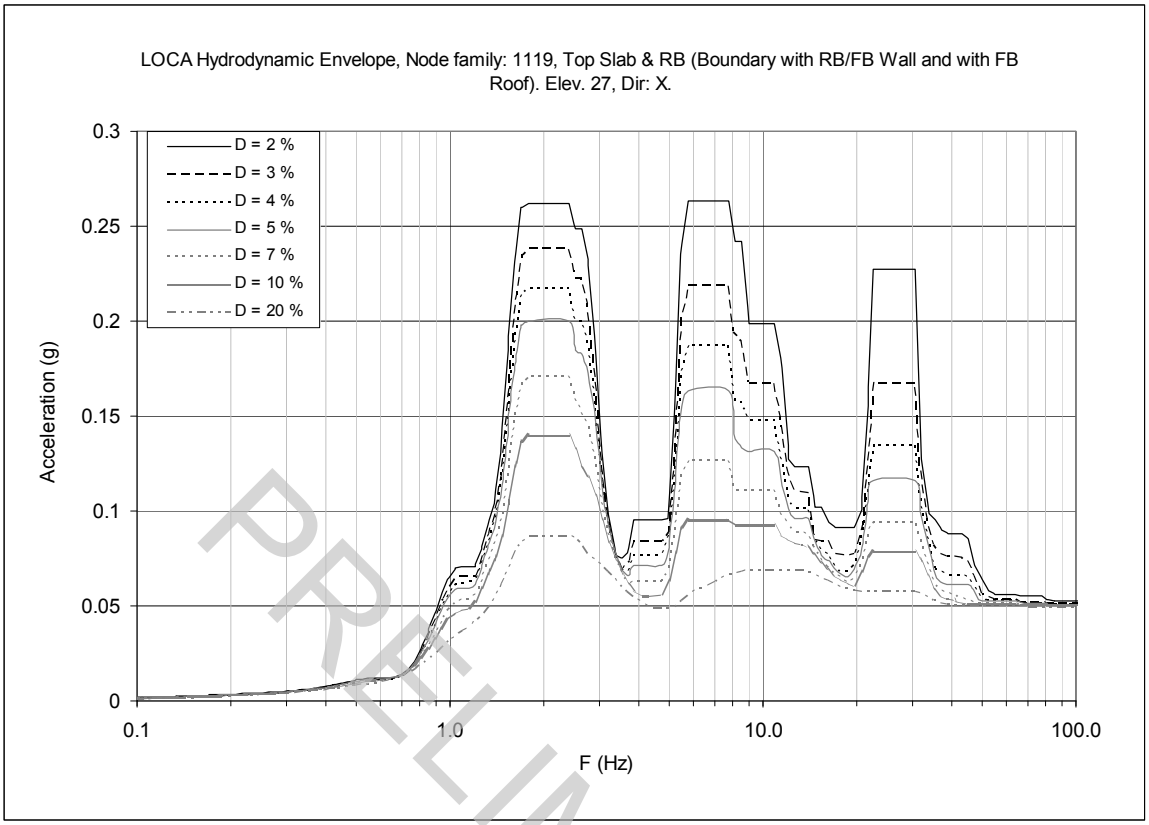

Figure 3F-29. Floor Response Spectrum—Chugging & CO Envelope, Node Family: 1119, X-direction (0°-180°)

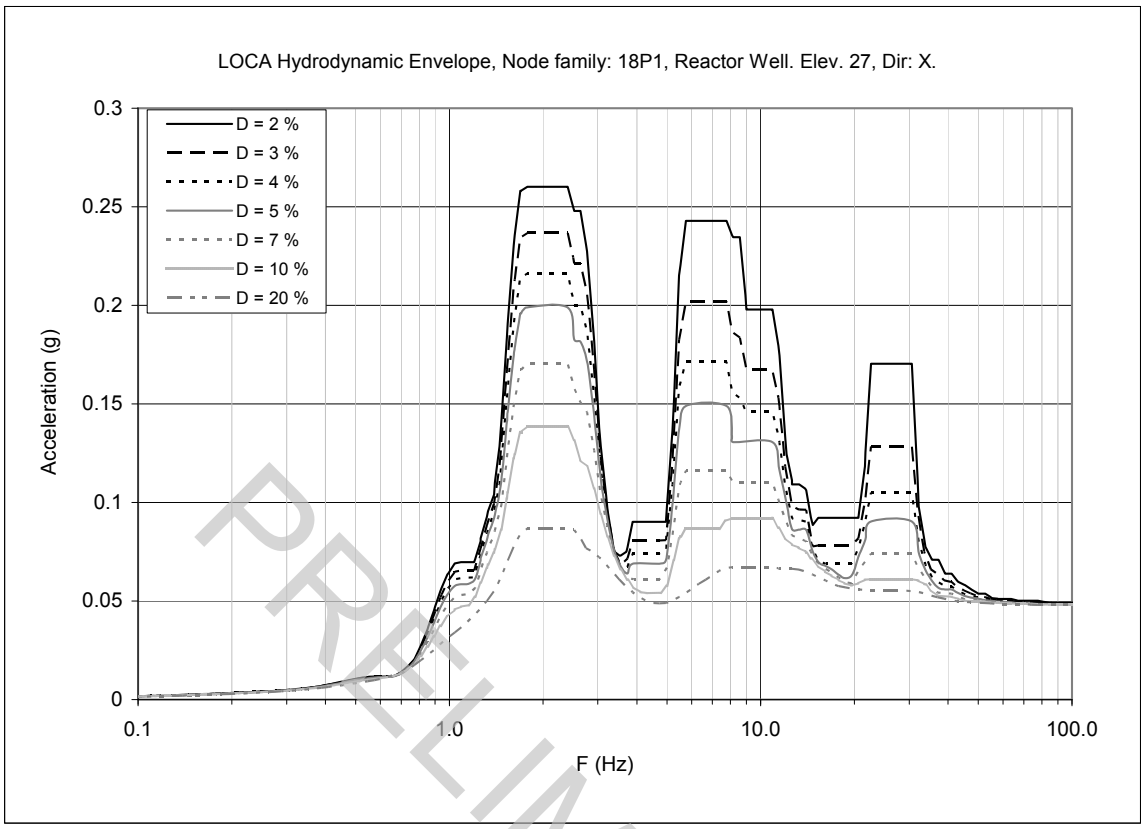

Figure 3F-30. Floor Response Spectrum—Chugging & CO Envelope, Node Family: 18P1, X-direction (0°-180°)

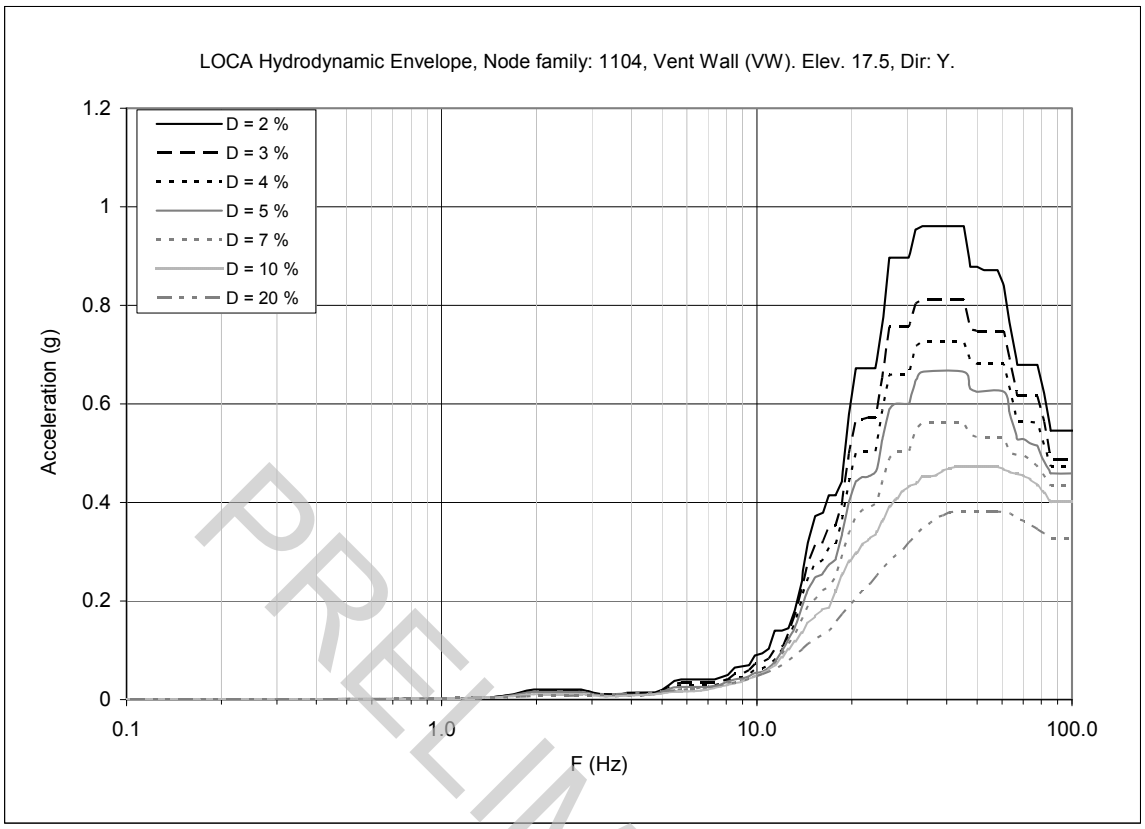

Figure 3F-31. Floor Response Spectrum—Chugging & CO Envelope, Node Family: 1104, Y-direction (90°-270°)

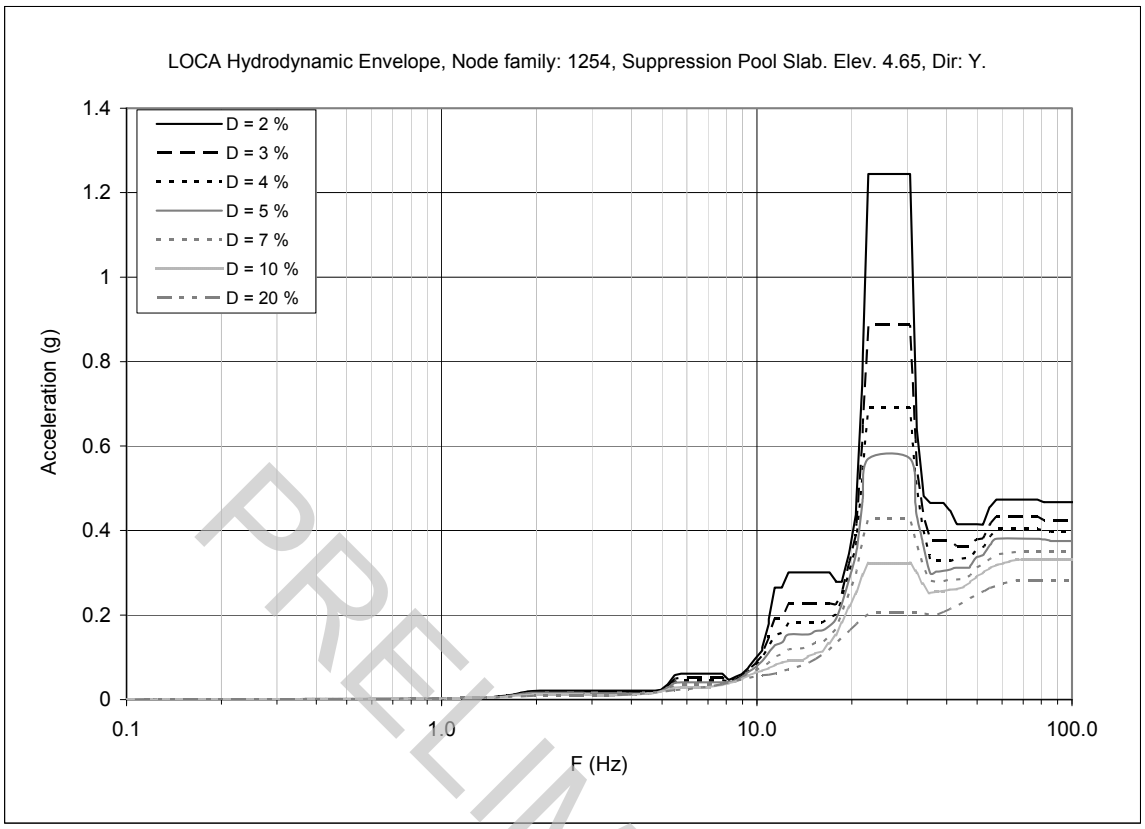

Figure 3F-32. Floor Response Spectrum—Chugging & CO Envelope, Node Family: 1254, Y-direction (90°-270°)

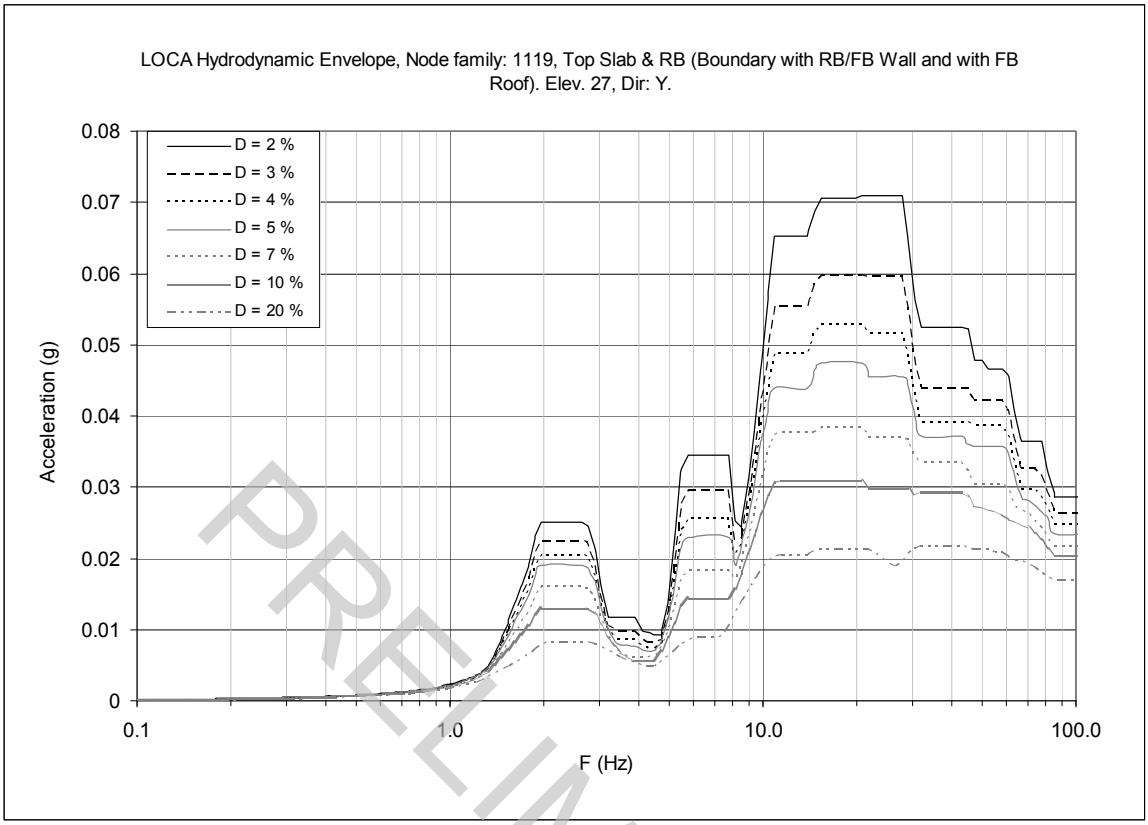

Figure 3F-33. Floor Response Spectrum—Chugging & CO Envelope, Node Family: 1119, Y-direction (90°-270°)

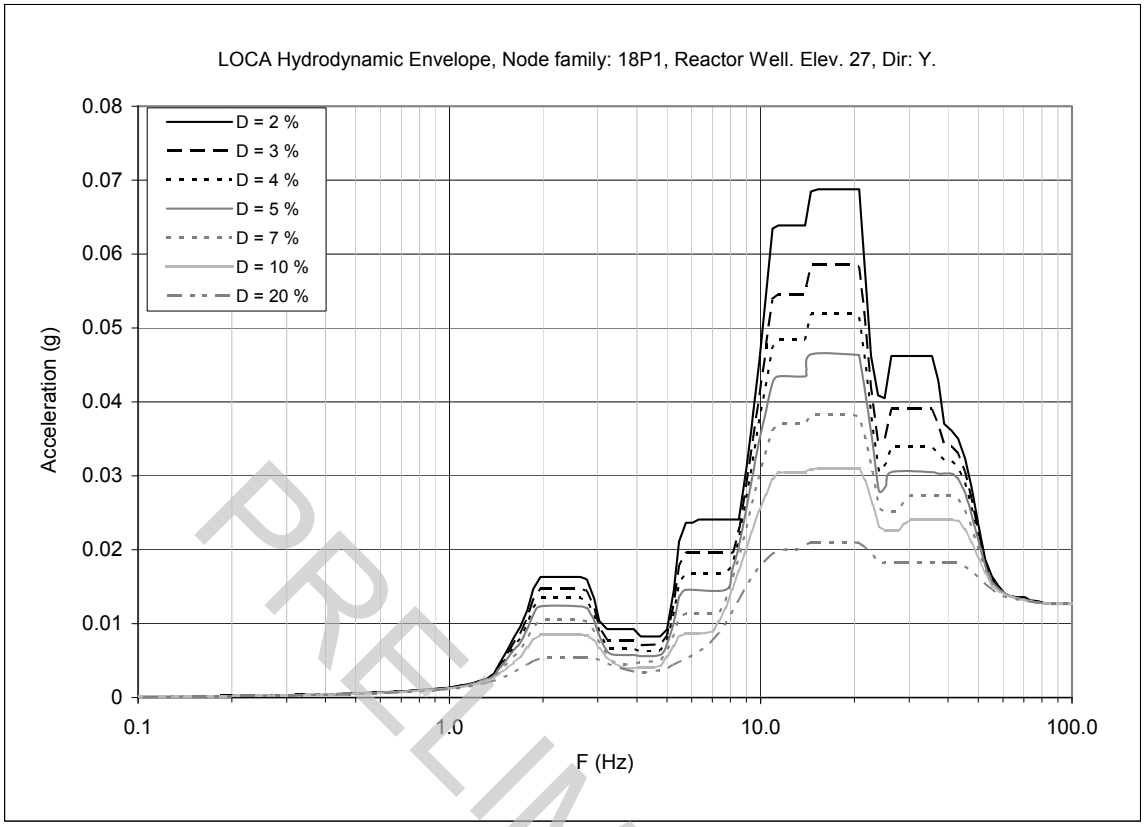

Figure 3F-34. Floor Response Spectrum—Chugging & CO Envelope, Node Family: 18P1, Y-direction (90°-270°)